

**RAD 7**



**BOOK OF  
ABSTRACTS**

SEVENTH  
INTERNATIONAL  
CONFERENCE  
ON RADIATION  
IN VARIOUS FIELDS  
OF RESEARCH

June 10-14, 2019  
Herceg Novi  
Montenegro



## TABLE OF CONTENTS

### A INVITED TALKS

Marina Frontasyeva	<b>Atmospheric deposition of radionuclides – Assessment based on passive moss biomonitoring</b>	2
Sebastien Incerti, Ivan Petrovic, Aleksandra Ristic-Fira	<b>Monte Carlo simulation of early biological damage induced by ionizing radiation at the DNA scale: Overview of the Geant4-DNA project</b>	3
Eiliv Steinnes	<b>Radioecological studies in Norway related to the fallout from the Chernobyl accident</b>	4
Kristina Gopcevic	<b>Matrix metalloproteinases: From structure to function</b>	5
Beata Brzozowska-Wardecka, Alice Sollazzo, Lei Cheng, Maciej Gałeczki, Adrianna Tartas, Lovisa Lundholm, Andrzej Wójcik	<b>Studies on DNA damage and repair in cells exposed to mixed beams of different ionising radiation qualities</b>	6
Igor Belyaev, Leonardo Makinistian	<b>Towards ELF magnetic fields for the treatment of cancer</b>	7

### B PLENARY TALK

Jelena Ajtić, Vladimir Djurdjevic, Darko Sarvan, Erika Brattich, Miguel-Angel Hernández-Ceballos, Benjamin Zorko, Dragana Todorović	<b>Temporal and spatial distribution of the beryllium-7 activity concentration in the surface air in Europe</b>	9
---	---	---

### 01 BIOCHEMISTRY

Šaćira Mandal, Adlija Čaušević, Sabina Semiz	<b>Free fatty acids and hepatic activity in Type 2 diabetes</b>	11
Sanja Petrovic, Jelena Zvezdanovic, Sasa Savic, Dragan Cvetkovic, Aleksandar Lazarevic, Dejan Markovic	<b>UVB irradiation impact on chlorophyll degradation in methanol/water solutions monitored by UHPLC/DAD-ESIMS analysis</b>	12

Nataša Avramović, Lidija Izrael-Zivković, Ivanka Karadžić	<b>Influence of different heavy metal ions on bacterial strain <i>P. aeruginosa san-ai</i> and correlation with produced exopolysaccharide biosurfactants</b>	13
Nataša Avramović, Lidija Izrael-Zivković, Ivanka Karadžić	<b>Combined effects of heavy metal ions and antibiotics on bacterial strain <i>P. aeruginosa san-ai</i></b>	14
Sasa Savic, Sanja Petrovic, Zivomir Petronijevic	<b>Identification of degradation products of quercetin in reaction with horseradish peroxidase by UHPLC-DAD-HESI-MS/MS method</b>	15

## 02 BIOINFORMATICS

Silviya Nikolova, Diana Toneva, Andrey Gizdov, Stanislav Harizanov, Ivan Georgiev	<b>Cross-sectional automatic assessment of the degree of sagittal suture closure on <math>\mu</math>CT volumetric images of dry skulls applying artificial neural network and machine learning techniques</b>	17
Diana Toneva, Silviya Nikolova, Gennady Agre, Ivan Georgiev, Nikolai Lazarov	<b>Excavation of the most distinctive characteristics in the metopic skull configuration by applying data mining techniques</b>	18
Joanna Czub	<b>“Matrix” – A robot control program to determine the ion beam profile</b>	19
Joanna Czub	<b>“Stolik” – A computer program to control the irradiation of biological material in HIL</b>	20

## 03 BIOMATERIALS

Katarzyna Roszek, Paulina Bolibok, Monika Bal, Artur Terzyk, Marek Wiśniewski	<b>Modern nanomaterials for cell protection from UV-initiated damage</b>	22
Paulina Bolibok, Katarzyna Roszek, Marek Wiśniewski	<b>Skin UV protection – new application of graphene oxide</b>	23
Jasna Vujin, Weixin Huang, Sylwia Ptasinska, Radmila Panajotovic	<b>Effects of water on thin films consisting of biomolecules and 2D-materials</b>	24
Jasna Vujin, Martina Gilić, Radmila Panajotović	<b>Application of 2D-materials in building biomolecular heterostructures</b>	25

## 04 BIOMEDICAL ENGINEERING

Remon Pop-Iliev, Pedram Karimipour Fard, Ghaus Rizvi	<b>Design of 3D polymeric bone tissue scaffolds for optimal degradation</b>	27
Dragos Manea, Mihaela Antonina Calin, Sorin Viorel Parasca, Andrei Museteanu	<b>Classification of the hyperspectral image of a basal cell carcinoma using artificial intelligence</b>	28

Mihaela Antonina Calin, Sorin Viorel Parasca, Ileana Carmen Boiangiu, Dragos Manea, Roxana Savastru	<b>Hyperspectral imaging for real-time detection and visualization of lip cancer: A pilot study</b>	29
---	---	----

## 05 BIOMEDICINE

Vladimir Jurišić	<b>Cell isolation with the help of immunomagnetic beads and labeling with monoclonal antibodies depending on the magnetic field strength</b>	31
Ekaterina Filippova	<b>Peripheral blood mononuclear cell application in the induced bullous keratopathy</b>	32
Olga Pechanova, Radoslava Rehakova, Michaela Kosutova, Martina Cebova	<b>Effects of statin and sesame oil therapy in experimental metabolic syndrome</b>	33
Stanislav Pavelka	<b>Radiometric studies of relations between leptin and thyroid hormones metabolism in white adipose tissue</b>	34
Stanislav Pavelka	<b>The influence of supplemental n-3 PUFA in diet and altered thyroid status of rats on their lipid metabolism</b>	35
Olga Molchan, Polina Shabunya, Svetlana Fatychava	<b>Effects of UV and green LED light on the photosynthesis, redox state and indole alkaloids biosynthesis in medicinal plants and <i>in vitro</i> cultures</b>	36
Fedor Jagla, Olga Pechanova	<b>Sensorimotor integration – Experimentally unkept expression of brain integration functions</b>	37
Anna A. Oleshkevich	<b>Threshold of safety of influence of continuous ultrasound on animal leukocytes</b>	38
Marta Poplawska, Olga Brzezinska, Grzegorz Galita, Joanna Makowska, Tomasz Poplawski	<b>Oxidative DNA damage and repair in rheumatoid arthritis – A correlation with the key BER genes polymorphisms</b>	39
Marta Poplawska, Olga Brzezinska, Grzegorz Galita, Joanna Makowska, Tomasz Poplawski	<b>Deficiency of the NHEJ and BER proteins is correlated with inefficient DNA repair in rheumatoid arthritis</b>	40
Edina Bilić-Komarica	<b>Risk factors and their impact on diabetes mellitus in elderly people</b>	41
Valeriy Zaporozhan, Andrey Ponomarenko	<b>Possible mechanism of immune response utilizing molecular probing of antigens by protein-miRNA complexes</b>	42

Marijana Stanojevic-Pirkovic, Marija Andjelkovic, Ivanka Zelen, Marina Mitrovic, Ivana Nikolic, Milan Zaric, Petar Canovic, Vladimir Jurisic, Olgica Mihaljevic, Dragan Milovanovic	<b>The importance of determining mineral bone density and vitamin D in schizophrenic patients treated with antipsychotics</b>	43
<b>06 BIOPHARMACEUTICALS</b>		
Anna Antsiferova, Marina Kopaeva, Vyacheslav Kochkin, Pavel Kashkarov, Mikhail Kovalchuk	<b>Influence of chronic low-dose administrations of silver nanoparticles on cognitive functions of mammals and identification of the effect reasons</b>	45
<b>07 BIOPHYSICS</b>		
Nadezda Sergeenko	<b>Influence of near earth electromagnetic resonances on human cerebrovascular system in time of heliogeophysical disturbances</b>	47
Yaroslav Bobitski, Iryna Yaremchuk, Tetiana Bulavinets	<b>Spectral characteristics of laser-irradiated micro and nanostructures on the base of nanoshells under plasmon resonance conditions</b>	48
Liliya Batyuk, Natalya Kizilova, Vladimir Berest, Oksana Muraveinik	<b>Hydration changes of the red blood cell membranes of gastric cancer patients evoked by radiation therapy</b>	49
Nadezhda Kudryasheva, Rosa Alieva, Tatiana Rozhko, Alena Olada, Ekaterina Kovel, Anna Sachkova	<b>Chemical and radiation toxicity via luminescent assay systems of different complexity: Bacterial cells, enzyme reactions, and fluorescent proteins</b>	50
Ekaterina Kovel, Nadezhda Kudryasheva, Anna Sachkova	<b>Biological activity of carbonic nano-structures of natural and artificial origin</b>	51
Roza Alieva, Nadezhda Kudryasheva	<b>Coelenteramide-containing fluorescent proteins as perspective bioassays for toxicity monitoring</b>	52
Anna A. Oleshkevich	<b>Co-directed influence of mitagenes and modulated ultrasound on cells of various origin</b>	53
Anna A. Oleshkevich, Svetlana A. Komarova, Anna V. Novikova	<b>Possibilities of mathematical non-linear-dynamics- method application in laboratory biophysical expertise</b>	54
Anna Sachkova, Ekaterina Kovel, Olga Nefedova, Nadezhda Kudryasheva	<b>Bioluminescent assays as sensitive sensors for evaluating the biological activity of humic substances</b>	55
Werner Hofmann, Renate Winkler-Heil, Herbert Lettner, Alexander Hubmer	<b>Simulation of radon transfer from thermal water through the skin in radon therapy</b>	56

## 08 BIOTECHNOLOGY

Violeta Jakovljevic, Natasa Djordjevic, Zana Dolicanin, Miroslav Vrvic	<b>The effect of a synthetic detergent on the production of some biotechnological useful metabolites by <i>Mucor racemosus</i></b>	58
Sang Hoon Kim, Yeong Deuk Jo, Jin-Baek Kim, Si-Yong Kang	<b>Optimal condition of gamma-rays, 45, and 100 MeV proton ions for mutation induction in <i>Cymbidium</i> hybrid, RBo03</b>	59
Sang Hoon Kim, Yeong Deuk Jo, Jin-Baek Kim, Si-Yong Kang	<b>Mutation frequency and spectrum of the <i>Cymbidium</i> hybrid, RBo03, according to diverse gamma-ray treatments</b>	60
Violeta Jakovljevic, Natasa Djordjevic, Zana Dolocanin, Miroslav Vrvic	<b>Synergistic effect of <i>Penicillium verrucosum</i> and <i>Geotrichum candidum</i> on enhanced protease production by submerged fermentation</b>	61

## 09 CANCER RESEARCH

Radostina Alexandrova, Lora Dyakova, Tanya Zhivkova, Zdravka Petrova, Milena Glavcheva, Boyka Andonova-Lilova, Abudulkadir Abudalleh, Rossen Spasov, Gabriela Marinescu, Daniela-Cristina Culita, Luminita Patron	<b>3D cancer cell colonies as reliable model systems in the search for new antitumor agents</b>	63
Elena Gershtein, Irina Goryatcheva, Denis Naberezhnov, Nikolay Kushlinskii	<b>Soluble forms of the immune check-point receptor PD-1 and its ligand PD-L1 in peripheral blood of patients with various tumors: Clinical and pathologic correlations and prospect</b>	64
Kamila Butowska, Witold Kozak, Janusz Rak, Jacek Piosik	<b>Synthesis and characterization of conjugated doxorubicin for drug delivery</b>	65
Edina Bilić-Komarica	<b>Causes of hepatocellular cancer in same number of women and man who have chronic hepatitis B and C etiology</b>	66
Radostina Alexandrova, Zdravka Petrova, Desislav Dinev, Boyka Andonova-Lilova, Rossen Spasov, Gabriela Marinescu, Daniela-Cristina Culita, Luminita Patron	<b>Ru(III) complexes with schiff bases effectively inhibit 2D and 3D growth of cultured human and animal tumor cells</b>	67
Svetlana Vasilievna Chulkova, Evgeny Vyacheslavovich Glukhov, Lyudmila Yuryevna Gritsova, Elena Nikolaevna Sholokhova, Nikolay Nikolayevich Tupitsyn	<b>Humoral immunity in patients with gastric cancer: The role of B-1 lymphocytes in the antitumor immunity</b>	68

Svetlana Vasilievna Chulkova,  
Natalya Vasilyevna Lepkova,  
Angelina Vladimirovna Egorova

**Clinical and biological factors forecast metachronous breast cancer**

69

**10 ENVIRONMENTAL CHEMISTRY**

Yulia Vosel, Sergey Vosel, Irina Makarova, Mikhail Melgunov

**Geochemistry of  $^{234}$ , $^{238}$ U isotopes in modern carbonate sediments of small lakes (Baikal Region)**

71

Ivan Pozdnyakov, Yuliya Tyutereva, Ekaterina Mordvinova, Victoria Salomatova, Petr Sherin, Marina Parkhats, Yong Chen, Zizheng Liu

**Photodegradation of selected micropollutants stimulated by photolysis of natural humic substances: A mechanistic study**

72

Jong-Myoung Lim, Ji-Young Park, Hyuncheol Kim, Mee Jang, Won-Young Kim, Wan-Ro Lee

**Rapid analysis of uranium and plutonium isotopes in environmental samples using inductively coupled plasma mass spectrometry**

73

Inga Zinicovscaia, Rodica Sturza, Irina Gurmeza, Konstantin Vergel, Svetlana Gundorina, Marina Frontasyeva

**Study of metal accumulation in the soil–leaf–fruit system using neutron activation analysis**

74

Dmitrii Grozdov, Inga Zinicovscaia, Liliana Cepoi, Tatiana Chiriac, Tatiana Mitina

**Silver removal from batch systems using *Arthrospira (spirulina) platensis* biomass**

75

Tatjana Trtić-Petrović, Otilia Ana Culicov, Roman Balvanović, Andjelka Petković

**Instrumental neutron activation for analysis of spatial distribution of heavy metals in surface sediments of the Danube River**

76

Branka Petković, Larisa Ilijin, Dajana Todorović, Marija Mrdaković, Milena Vlahović, Anja Grčić, Vesna Perić-Mataruga

**Motor behaviour and energy metabolism of *Blaptica dubia* in artificial magnetic fields**

77

Marija Šljivić-Ivanović, Mihajlo Jović, Slavko Dimović, Ivana Smičiklas

**Optimization of Sr-ion extraction from the contaminated soil using Box-Benken design**

78

Juan F. Facetti–Masulli, Peter Kump, Mirna Delgado

**Trace and minor elements in bottom sediments of selected rivers and brooks from Eastern Paraguay by X-ray fluoresce**

79

Otilia Culicov, Marina Frontasyeva, Inga Zinicovscaia

**Some applications of neutron activation analysis: An updated review of investigations at IBR-2 reactor**

80

Grzegorz Boczkaj, Michał Gałgól, Elvana Cako, Kirill Fedorov

**Sonocavitation and hydrodynamic cavitation based advanced oxidation processes (AOPs) for water and wastewater treatment**

81

Evgeny Gerber, Anna Romanchuk, Ivan Pidchenko, Christoph Hennig, Alexander Trigub, Stephan Weiss, Andreas Scheinost, Andre Rossberg, Stepan Kalmykov, Kristina Kvashnina	<b>Probing plutonium dioxide nanoparticles with various synchrotron methods</b>	82
Kseniya Mezina, Yulia Vosel, Mikhail Melgunov, Dmitrii Belyanin, Boris Shcherbov, Inna Zhurkova, Maksim Rubanov	<b><math>^7\text{Be}</math>, <math>^{210}\text{Pb}</math> and <math>^{137}\text{Cs}</math> in the biogeocenosis components of the Arctic and southern zones of Western Siberia</b>	83
Yulia Vosel, Sergey Vosel, Irina Makarova, Mikhail Melgunov	<b>Geochemistry of <math>^{234}\text{U}</math>, <math>^{238}\text{U}</math> isotopes in modern carbonate sediments of small lakes (Baikal Region)</b>	84
Nikolai Alov, Pavel Sharanov	<b>Total reflection X-ray fluorescence analysis of copper and copper-zinc ores from South Ural mountains</b>	85
Nikolai Alov, Pavel Sharanov	<b>Using totally reflected X-ray radiation for environmental monitoring of Moscow small river waters</b>	86
Anna Goi	<b>Removal of natural radioactivity from groundwater used as a drinking water source</b>	87

## 11 ENVIRONMENTAL PHYSICS

Aleksandra Mihailović, Ivana Lončarević, Nebojša M. Ralević, Selena Samardžić, Ljuba Budinski-Petković, Jordana Ninkov, Ljubo Nedović	<b>Correlation of available and total lead content in urban soil</b>	89
Biljana Vuckovic, Natasa Todorovic, Jovana Nikolov, Jelena Zivkovic Radovanovic, Ljiljana Gulan	<b>Radon measurement in water from public fountains in rural areas in northern part of Kosovo and Metohija</b>	90
Olga Maltseva	<b>The total electron content of the ionosphere as the witness and object of space weather influence</b>	91
Slavica Brkić, Blanka Tuka	<b>Empirical model for estimating solar radiation based on air temperature for Sarajevo area, Bosnia and Herzegovina</b>	92
Blagorodka Veleva, Elena Hristova, Lyuben Dobrev, Stefan Georgiev, Nastya Vankova	<b>Recent results of atmospheric radioactivity measurements in Bulgaria based on NIMH activity</b>	93
Selena Samaradžić, Uranija Kozmidis Luburić, Milan Cvijanović, Robert Lakatoš, Aleksandra Mihailović, Tomas Nemeš, Milka Veselinović	<b>Analysis of the measured noise values in different types of industrial processes and the potential risk of NIHL</b>	94

Gordana Žauhar, Marija Čargonja, Darko Mekterović, Paula Žurga, Jagoda Ravlič Gulan	<b>Application of X-ray fluorescence technique (XRF) for determination of heavy metal concentrations in hair of workers at metal workshop</b>	95
Dora Krezhova, Kalinka Velichkova	<b>Hyperspectral leaf reflectance and red edge position as indicators of diseases in plants</b>	96
<b>12 ENVIRONMENTAL POLLUTION</b>		
Maja Turk Sekulić, Maja Brborić, Borivoje Stepanov, Sabolč Pap, Jelena Radonić	<b>Supporting climate change vulnerability and adaptation assessments at the Danube River: DDT impact</b>	98
Maja Turk Sekulic, Olivera Paunovic, Sabolc Pap, Sanja Radovic	<b>Functionalisation of biochar derived from lignocellulosic biomass using microwave technology for application in wastewater treatment</b>	99
<b>13 MATERIALS SCIENCE</b>		
Ivana Lončarević, Ljuba Budinski-Petković, Aleksandra Mihailović, Zorica Jakšić, Slobodan Vrhovac	<b>Reversible random sequential adsorption of polydisperse mixtures on a triangular lattice</b>	101
R. Lok, U. Gurer, O. Yilmaz, A. Varol, H. Karacali, A. Aktağ, E. Yilmaz	<b>Smart mask designs and electrical properties of platinum temperature sensors</b>	102
R. Lok, H. Karacali, A. Aktağ, E. Yilmaz	<b>Examination of Pt/Al<sub>2</sub>O<sub>3</sub>/p-Si/Al MOS capacitors under different temperatures</b>	103
<b>14 MEDICAL DEVICES</b>		
Ekaterina Filippova	<b>Structural changes of the cornea after the intrastromal implantation of plasma modified PET track-etched membrane</b>	105
Evgeniya Gorbunova, Ekaterina Filippova	<b>Morphological features of the musculoskeletal stump eye formation using titanium nickelide construction</b>	106
Yongseok Lee, Shiva Abbaszadeh	<b>Translating high spatial resolution detector based on cadmium zinc telluride to clinical positron emission tomography</b>	107
Anatoliy Korobov, Vsevolod Korobov, Oksana Shevchenko, Yulia Ivanova, Andrey Mandryka	<b>A. Korobov – V. Korobov phototherapeutic device “BARVA-SDS” for treatment and prevention of diabetic foot</b>	108
Yuriy Kovalenko, Sergei Miroshnychenko, Andrei Nevhasymy	<b>A digital basic X-ray system with tomosynthesis – New possibilities of the X-ray machine of the World Health Organization</b>	109

Irina M. Yeshchina, Irina N. Kodinec, Dinara J. Nurbaeva	<b>Specific changes of ultrasound scan of organs and blood biochemical indicators in vinyl chloride production workers: Dose-dependent interrelationship</b>	110
--	--	-----

## 15 MEDICAL IMAGING

Holger Stephan	<b>Development of nuclear and optical dual-labelled agents for cancer imaging</b>	112
Milica Jeremic Knezevic, Aleksandar Knezevic, Daniela Djurovic Koprivica, Bojana Milekic, Dubravka Markovic, Tatjana Puskar, Jasmina Boban	<b>Magnetic resonance evaluation of the temporomandibular joint disc shape</b>	113
Yuriy Kovalenko	<b>Improvement of primary level X-ray diagnostics for the purpose of raising primary care efficiency</b>	114
Dora Zlatareva, Diana Toneva, Silvia Nikolova, Vasil Hadjidekov	<b>Application of medical CT imaging for investigation of sex differences in facial soft tissue thicknesses</b>	115
Dora Zlatareva, Violeta Groudeva	<b>Brain, head and neck vascular malformations diagnosed by magnetic resonance and computed tomography angiography</b>	116
Boyana Deneva, Katja Roemer, Guntram Pausch, Andreas Wagner, Wolfgang Enhardt, Toni Koegler	<b>Single Plane Compton Imaging</b>	117
Olena Sharmazanova, Hanna Kirik	<b>Diaphyseal fracture of the X-ray scoring healing of the tibia</b>	118
Olena Sharmazanova, Yuriy Kovalenko, Larisa Urina	<b>Application of digital tomosynthesis in lung pathology</b>	119
Aleksandar Pavlović, Vladimir Ostojić, Vladimir Petrović	<b>Image based estimation of absorbed patient dose in radiography</b>	120
Z. Idiri, K. Boukefoussa, M. Belaabed, S. Bitam	<b>Simulation and optimization of a first generation gamma transmission computed tomography using MCNP5 code</b>	121

## 16 MEDICAL PHYSICS

Irena Muçollari, Rejnardo Tafaj, Bledar Cullhaj, Blerina Myzeqari, Valbona Bali	<b>Isocentric accuracy with Winston–Lutz test for LINAC-based stereotactic radiosurgery treatments</b>	123
Liudmyla Aslamova, Ielyzaveta Kulich, Nadiia Melenevska	<b>Reasons and basis for implementation of medical physicists certification in Ukraine</b>	124

Liudmyla Aslamova, Ielyzaveta Kulich, Nadiia Melenevska	<b>Safety culture in syllabus on medical physics in Ukraine</b>	125
Taylan Tuğrul, Osman Eroğul	<b>Determination of initial electron parameters by means of Monte Carlo simulations for the siemens artiste Linac 6 MV photon beam</b>	126
Vladimir Panteleev, Anatoly Barzakh, Leonid Batist, Dmitry Fedorov, Victor Ivanov, Pavel Molkanov, Stanislav Orlov, Maxim Seliverstov, Yuri Volkov	<b>A new method for production of radionuclide-generator <math>^{212}\text{Pb}/^{212}\text{Bi}</math></b>	127
Giuseppe Palma, Laura Cella	<b>A new formalism of dose-surface histograms for robust modeling of skin toxicity in radiation therapy</b>	128
Sohyun Ahn, Min-Joo Kim, Sanghyuk Song, Inyoung Wang, Junetaek Sin	<b>Measurement of output factor for small radiation field using solid water phantom</b>	129
Sohyun Ahn, Sanghyuk Song, Inyoung Wang, Junetaek Sin	<b>Monte Carlo simulation and measurement for improving dose uniformity of total skin electron beam therapy with three ports</b>	130
Ana Diklić, Doris Šegota, Slaven Jurković	<b>Investigation of dose indicators for breast cancer CT localization procedures in radiation therapy in Croatia</b>	131
Marina Troshina, Sergey Dyuzhenko, Ekaterina Koryakina, Vladimir Potetnya, Olga Golovanova, Sergey Koryakin, Stepan Ulyanenko	<b>Treatment plan verification in proton therapy using the FBX chemical dosimeter</b>	132
Yaroslav Bobitski, Adriana Barylyak, Igor Demkovich	<b>Theoretical substantiation of the protocol of laser thermal disinfection of the root canal system of the tooth</b>	133
Vladimir Klimanov, Maria Kolyvanova, Janneta Galjautdinova	<b>Small fields and non-equilibrium condition for 6 and 18 MV photon beam dosimetry</b>	134
Sergei Akulinichev, Ivan Yakovlev, Dmitry Kokoncev, Arkadiy Yuris, Anton Nikitenkov	<b>Advantages of ytterbium sources for HDR brachytherapy</b>	135
Doris Segota, Ana Diklic, Maja Karic, Slaven Jurkovic	<b>Assessment of radiation doses to neonates from chest radiography at University Hospital Rijeka</b>	136
Kerem Duruer, Durmuş Etiz, Haluk Yücel	<b>Investigation of EBT3 radiochromic film behaviour in high dose range of 6 MV photon and 6 MeV electron beams by employing the most suitable scanning channel of three-color flatbed scanner</b>	137

## 17 MEDICINAL CHEMISTRY

Anife Ahmedova, Boyan Todorov	<b>Radiopharmaceuticals for theranostic applications</b>	139
Miroslava Stankovic, Igor Stojanovic, Ivana Zlatanovic, Vesna Milovanovic, Gordana Stojanovic	<b>An overview of the effect of <i>Hypogimnia physodes</i>, <i>Hypogimnia tubulosa</i>, <i>Umbilicaria crustulosa</i> and <i>Umbilicaria cylindrica</i> acetone extracts on frequencies and distribution of micronucleus in human lymphocytes</b>	140
Safija Herenda, Edhem Hasković, Denis Hasković	<b>Determination of the redox potential of drugs for cardiovascular diseases</b>	141
M. Cvijović, Z. Nedić, P. Đurđević, V. di Marco	<b>ATR–FTIR spectroscopy in chlorpyrifos residue investigation</b>	142
Galya K. Toncheva, Nikolina P. Milcheva, Siana K. Chobanova, Mariela G. Kalendarska, Kiril B. Gavazov	<b>Complex formation in a low toxic organic solvent-based liquid-liquid extraction-chromogenic system for vanadium(V), nickel(II) and copper(II)</b>	143

## 18 MICROWAVE, LASER, RF, UV AND SOLAR RADIATIONS

Natalya Chueshova, Frantishek Vismont, Igor Cheshik	<b>Reproductive system of male rats at the post-natal stage of development under the influence of electromagnetic radiation from a mobile phone (1745 MHz)</b>	145
Marek Wiśniewski, Paulina Bolibok, Monika Bal, Wojciech Zięba, Katarzyna Roszek	<b>Mechanistic aspects of GO sandwich formation due to UV radiation</b>	146
Michel Israel, Petya Ivanova, Tsvetelina Shalamanova, Mihaela Ivanova, Victoria Zaryabova	<b>Exposure and risk assessment connected to the health and safety of workers in the production of electricity</b>	147
Victoria Zaryabova, Tsvetelina Shalamanova, Michel Israel, Hristina Petkova	<b>Public concern of electromagnetic exposure in Bulgaria – A case study of overexposure</b>	148
Mihaela Ivanova, Michel Israel, Mariyana Stoynovska	<b>Measurement, exposure and risk assessment of sources of optical radiation in working environment</b>	149
Jelena Jovanovic, Borivoj Adnadjevic	<b>A rapid and efficient microwave method to prepare graphene foam</b>	150
Borivoj Adnadjevic, Jelena Jovanovic	<b>Novel microwave assisted synthesis of fullerene</b>	151
Paula Corte-Leon, Aleksandra Allue, Koldo Gondra, Valentina Zhukova, Mihail Ipatov, Juan Maria Blanco, Arkady Zhukov	<b>Smart composites with embedded magnetic microwire inclusions allowing non-contact stresses and temperature monitoring</b>	152

Arcady Zhukov, Mihail Ipatov, Paula Corte-Leon, Juan Maria Blanco, Valentina Zhukova	<b>Giant magnetoimpedance effect at GHz frequencies in amorphous microwires</b>	153
Nurhan Türker Tokan, Sultan Aldirmaz Çolak, Muhammet Donmez	<b>Complete analysis of Vivaldi antennas</b>	154
Fikret Tokan, Mücahit Alçep	<b>Perforated narrow-band dielectric lens antenna design</b>	155
Petr Skorobogatov, Konstantin Epifantsev, Alexander Shemohaev, Vitalij Telets	<b>Method and mean of IC's testing under multiple electrical overstresses</b>	156
Zorica Podrascanin, Zoran Mijatovic, Ana Firanj Sremac	<b>Comparison of ground-based and OMI satellite UVI measurements in Novi Sad</b>	157
Andriy Kovalskiy, Maria White, Joshua Allen, Justin Oelgoetz, Roman Golovchak, Oleh Shpotyuk, Karel Palka, Stanislav Slang, Miroslav Vlcek	<b>Transient optical effects in spin-coated chalcogenide glass thin films induced by UV radiation</b>	158
B. Gustavino, V. Maselli, L. Salvi, G. Paoluzzi, E. Santovetti, S. Filippi, R. Meschini	<b>DNA-damage induced in human lymphocytes by exposure to 915 MHz mobile-phone radiation: Does smoking habit modulate its genotoxicity?</b>	159
Bianca Gustavino, Federica Maruccia, Gabriele Gentile	<b>Induction of DNA damage by UVB radiation in erythrocytes of scaly reptiles and protective role of skin pigmentation</b>	160

## 19 NEUTRON AND HEAVY ION RADIATIONS

Roberto Bedogni, Katia Alikaniotis, Marco Costa, Valeria Monti, Elisabetta Durisi, Oriol Sans-Planell, Jose-Maria Gomez-Ros	<b>Radiation resistant compact sensors for multipurpose neutron diagnostics</b>	162
Adrian Florinel Bucsa	<b>Neutron activation analysis – <i>ko</i> standardization applied on Gen IV nuclear materials</b>	163
Renat Ibragimov, Ilia Urupa, Evgeny Tyurin, Elena Ryabeva	<b>Spectrometry of fast neutrons with energy value of around 14 MeV produced in the d-t reaction in a gas filled neutron tube by using a radiation diamond detector</b>	164
Sergey Kulikov, Maksim Bulavin	<b>The irradiation facility at the IBR-2 research reactor</b>	165
Kiril Krezhov	<b>Neutron diffraction study of <math>\text{La}_{0.6}\text{Ca}_{0.4}\text{CoO}_{3-d}</math> as a promising zinc-air rechargeable battery material</b>	166

Kiril Krezhov, Tatyana Koutzarova, Svetoslav Kolev, Petya Peneva	<b>Structure and magnetic properties of nanosized Al-substituted barium hexaferrite powders</b>	167
<b>20 NUCLEAR MEDICINE</b>		
Turan Şahmaran, Salih Sinan Gültekin	<b>Compliance and reproducibility of radioiodine I-131 uptake test measurements</b>	169
Oleg Kochnov, Natalia Zorina	<b>Production of medical radionuclide Mo-99 from low-enriched uranium</b>	170
Turan Şahmaran, Mehmet Bayburt	<b>Determination of the radiation dose received by the patient during positron emission tomography – computed tomography (PET – CT) procedures</b>	171
Michael Zhukovsky, Hesham M.H. Zakaly, Mostafa Y. A. Mostafa, Darya Deryabina	<b>A possible use of <sup>177</sup>Lu based radiopharmaceuticals for palliative therapy of bone metastases</b>	172
Esra Arslan, Tamer Aksoy	<b>Quantitative 18 FDG PET CT metabolic parameters and overall survival in small cell lung cancer (SCLC)</b>	173
Esra Arslan, Tamer Aksoy	<b>Is there any benefit to screening prone position versus supine breast 18 FDG PET CT?</b>	174
Tamer Aksoy, Ozlem Erez, Cihan Gundogan	<b>Impact of different vendors on SPECT-CT dosimetry for hepatic transarterial radioembolization</b>	175
Tamer Aksoy, Esra Arslan	<b>PET/CT findings of a soft tissue tumor elastofibroma dorsi</b>	176
Vojislav Antic, Mirjana Petrovic, Zivorad Savic	<b>Software evaluation of possible incidents and nearmisses in nuclear medicine</b>	177
Silvija Lučić, Andrea Peter, Dolores Srbovan, Milena Spirovski	<b>Lutetium DOTATATE dual time post therapy scintigraphy</b>	178
<b>21 PHARMACEUTICAL SCIENCES</b>		
Marina Filimonova, Lyudmila Shevchenko, Alina Samsonova, Tatiana Podosinnikova, Victoria Makarchuk, Alexander Filimonov	<b>Nitric oxide as a basis for the creation of new promising drugs</b>	180
Branka Dražić, Slađana Tanasković, Mirjana Antonijević-Nikolić	<b>Preparation and study of two new mixed ligand Cu(II) complexes</b>	181

## 22 RADIATION CHEMISTRY

Marcin Kozanecki, Paulina Maczugowska, Piotr Sawicki, Sebastian Sowinski, Krzysztof Halagan, Piotr Ulanski, Slawomir Kadlubowski	<b>An initiation process in radiation induced polymerization in an aqueous solution – Simulations and experiments</b>	183
Karina Falkiewicz, Witold Kozak, Janusz Rak	<b>Can 6-substituted pyrimidine nucleosides sensitize DNA damage induced by ionizing radiation?</b>	184
Sergey Bazhukov, Marina Pervova, Irina Bazhukova	<b>Radiolysis of organic compounds under electron beam irradiation during radiation sterilization</b>	185
Zaiana Dzhivanova, Elena Belova, Mikhail Kadyko	<b>Regeneration of radiation-degraded extraction systems used in the reprocessing of spent nuclear fuel (SNF)</b>	186
Zaiana Dzhivanova, Elena Belova, Ivan Skvortsov	<b>Radiation-thermal stability of extraction systems based on diamides of heterocyclic dicarboxylic acids in diluents F-3 and FS-13</b>	187
Slawomira Janiak, Henryk Bem	<b>The correlation between radon in soil and indoor radon concentrations in houses in the City of Kalisz, Poland</b>	188
Daria Mazurek, Slawomira Janiak, Henryk Bem	<b><math>^{222}\text{Rn}</math> and <math>^{226}\text{Ra}</math> radionuclides in drinking water in the Kalisz Area of Poland</b>	189
Krzysztof Piechocki, Marcin Kozanecki, Slawomir Kadlubowski	<b>Radiation Induced Polymerisation and Crosslinking as an effective method for poly(olygoether methacrylates) smart materials synthesis</b>	190
Krzysztof Piechocki, Marcin Kozanecki	<b>POEGMAs based smart drug delivery systems prepared by Radiation Induced Polymerization and Crosslinking</b>	191
Aleksandar Lazarević, Sanja Petrović, Jelena Stanojević, Dragan Cvetković, Jelena Zvezdanović	<b>Irreversible bacteriochlorophyll a degradation induced by visible light in methanol solutions</b>	192
Huanhuan Liu	<b>Radiation induced drug release from PCL-PEO micelles</b>	193
Radosław Wach	<b>Radiation reactions in polysaccharides: Crosslinking vs. scission</b>	194

## 23 RADIATION DOSIMETERS

Matanat Mehrabova, Hidayat Nuriyev, Huseyn Orujov, Niyazi Hasanov, Aybeniz Abdullayeva	<b>Electrical and photoelectrical properties of CdTe/CdMn(Fe)Te thin-film heterojunctions</b>	196
--	---	-----

Srboljub Stanković, Aleksandar Jakšić, Boris Lončar, Dragana Nikolić, Mirjana Radenković	<b>One numerical method for determining the absorbed dose of gamma and X radiation in the ZrO<sub>2</sub> dielectric within the MOS capacitor</b>	197
Markéta Koplová, David Zoul, Vít Rosnecký, Helena Štěpánková, Václav Římal, Josef Štěpánek	<b>Study of molecular mechanisms of radiochromic phenomenon in polycarbonate</b>	198
Slavica Porobić, Milena Marinović-Cincović, Dragana Jovanović, Dušan Mijin	<b>Radiation, thermal and optical properties of PVA films containing arylazo pyridone dyes</b>	199
Aleksandra Sokić, Luka Perazić, Jovana Knežević	<b>Measurement of ambient dose equivalent H*(10) in the surroundings of nuclear facilities in Serbia and abandoned uranium mine in Kalna via OSL dosimetry</b>	200
Krzysztof Chelminski, Wojciech Bulski	<b>The comparison of sensitivity of gafchromic EBT film types</b>	201
G. Kramberger, V. Cindro, D. Flores, S. Hidalgo, B. Hiti, M. Manna, I. Mandić, M. Mikuž, M. Mikuž, D. Quirion, G. Pellegrini, M. Zavrtnik	<b>Simulation and measurements of 3D silicon detectors timing performance</b>	202
Stefan Ilić, Aleksandar Jevtić, Nikola Đikić, Goran Ristić	<b>Smart Geiger Muller counter</b>	203

## 24 RADIATION EFFECTS

Paulina Filipczak, Piotr Chudobinski, Szymon Bres, Malgorzata Matusiak, Slawomir Kadlubowski, Marcin Kozanecki	<b>An impact of electron-beam and laser irradiations on Ag nanoparticles stabilized by sodium tricitrate</b>	205
Valentyn Laguta, Maksym Buryi, Martin Nikl	<b>Trapped-electron and trapped-hole centers in oxide scintillators</b>	206
Maksym Buryi, Valentyn Laguta, Akira Yoshikawa, Martin Nikl	<b>Point defect origin and local structure in LiCaAlF<sub>6</sub> single crystals</b>	207
Oleh Shpotyuk, Valentina Balitska, Mykhaylo Shpotyuk	<b>On the phenomenological identity of radiation-induced effects in glassy chalcogenides under a prism of unified configuration-enthalpy model</b>	208
Suzana Samaržija-Jovanović, Vojislav Jovanović, Branka Petković, Slaviša Jovanović, Gordana Marković, Milena Marinović-Cincović, Jaroslava Budinski-Simendić	<b>The effect of UV irradiation on hydrolytic stability of urea-formaldehyde resins filled with thermally modified montmorillonite</b>	209

Juan Antonio Garcia Pascual	<b>Operational experience and performance with the ATLAS pixel detector at the large hadron collider at CERN</b>	210
Wojciech Migdał, Urszula Gryczka, Sylwester Bułka, Dagmara Chmielewska-Śmietanko, Magdalena Ptaszek, Anna Jarecka-Boncela	<b>Application of low energy electron beam for surface treatment of agricultural products</b>	211
Dagmara Chmielewska-Śmietanko, Urszula Gryczka, Wojciech Migdał, Jarosław Sadło, Kamil Kopeć	<b>Effect of electron beam irradiation on paper-based materials</b>	212
Afrodita Ramos, Blagica Cekova	<b>Safety features of irradiated food</b>	213
Sergey Stefanovsky, Olga Stefanovsky, Michael Kadyko, Jana Glazkova	<b>The effect of irradiation with accelerated electrons and gamma-rays on the oxidation state and structure of sodium-aluminum-iron-phosphate glasses</b>	214
Denis Ukolov, Roman Mozhaev, Maxim Cherniak, Alexander Pechenkin	<b>Radiation hardness estimation method of complex optoelectronic devices on YB:YAG laser with semiconductor laser pump</b>	215
Slaviša Jovanović, Jaroslava Budinski-Simendić, Milena Marinović-Cincović, Gordana Marković, Vesna Teofilović, Dejan Kojić, Nevena Vukić, Vojislav Jovanović	<b>The influence of network precursor ratio on the crosslinking and radiation resistance of hybrid elastomeric materials</b>	216
Anna V. Novikova, Viktor E. Novikov, Anna A. Oleshkevich	<b>Possible role of intravascular hemolysis in the pathogenesis of oxidant stress after sublethal ionizing and non-ionising radiation dose effect</b>	217
Mikhail Ksendzuk, Marina Filimonova, Valentina Surinova, Alexander Filimonov, Tatyana Podosinnikova, Alina Samsonova	<b>Nitrogen monoxide metabolites as the marker of acute radiation syndrome</b>	218
Andrey Tugai, Tetiana Tugai, Viktor Zheltonozhsky, Marina Zheltonozhskaya, Olena Polischuk, Leinid Sadovnikov, Natalia Sergeichuk	<b>Activation of lipid peroxidation (LPO) is one of the universal effects of chronic radiation exposure</b>	219
Narendra Jain	<b>Age associated tritium vulnerability in postnatally developing Swiss albino mouse cerebellum</b>	220
Mirella Tanori, Arianna Casciati, Barbara Tanno, Paola Giardullo, Alessandro Zambotti, Carmela Marino, Caterina Merla, Mariateresa Mancuso	<b>New therapeutic strategy for medulloblastoma: <math>\mu</math>S-Pulse Electric Field exposure targeting cancer stem cells to promote radiosensitization</b>	221

Ilaria De Stefano, Barbara Tanno, Simona Leonardi, Emanuela Pasquali, Francesca Antonelli, Paola Giardullo, Arianna Casciati, Mirella Tanorin, Gabriele Babini, LDLensRad Consortium, Simonetta Pazzaglia, Mariateresa Mancuso	<b>Radiation-induced cataract in <i>Ptch1</i><sup>+/-</sup> mice: Exploring the role of age, dose, dose rate and genetic background</b>	222
Marko Milovanovic, Maciej Trzebinski, Michael Rijssenbeek, Karlheinz Hiller, Patrick Fassnacht, Tomas Sykora, Sebastian Grinstein, Marco Bruschi, Hasko Stenzel	<b>Effects of radiation damage in ATLAS Roman Pots (ALFA &amp; AFP)</b>	223
Miroslav Vlcek, Karel Palka, Stanislav Slang, Liudmila Loghina, Anastasia Iakovleva	<b>Radiation induced 3D structuring of chalcogenide glass thin films</b>	224
Galina P. Zhurakovskaya, Svetlana V. Belkina	<b>The influence of pharmaceuticals on the ionization and excitation of molecules while exposed to ionizing radiation</b>	225

## 25 RADIATION IN MEDICINE

Mirjana M. Petrović, Živorad N. Savić, Katarina Ž. Savić, Sofija Ž. Savić, Aleksandra R. Vasiljević, Dušanka R. Petrović, Dragana D. Brakočević, Danica M. Kovljanić, Valentina S. Radunović, Vanja Puletić, Drina Lj. Janković, Aleksandar A. Vukadinović, Vojislav Antić, Vladimir Jurišić	<b>Clinical significance of radioimmunoassay (RIA) and immunoradiometric assay (IRMA) in endocrinology</b>	227
Ekaterina Shleenkova, George Kaidanovsky, Stepan Bazhin, Vladimir Iliyn	<b>On the issue of control of equivalent doses of radiation for the eye lens for medical personnel</b>	228
Đurđica Milković, Danica Batinić	<b>Radiologic examination of urinary tract in children with special reference to ionizing radiation</b>	229
Francisco Cutanda-Henriquez, Silvia Vargas Castrillon	<b>Assessment of volume averaging effects in thimble ion chambers for flattening filter free photon beams</b>	230
Darka Hadnađev Šimonji, Olivera Nikolić, Marijana Basta Nikolić, Olivera Ciraj Bjelac, Sanja Stojanović, Mirela Juković	<b>Evaluation of radiation dose at optimized protocols for some standard MDCT examinations in a large university hospital</b>	231

Monica Cavallari, Laura Mantovani, Loredana D'Ercole, Nicoletta Paruccini, Raffaele Villa, Raffaella Soavi	<b>Image quality and delivered dose in neuroradiological procedures</b>	232
Luisa Alunni Solestizi	<b>Possible use of CMOS image sensors in radioguided surgery with <math>\beta</math> emitters</b>	233
Jan Slezak	<b>New approach for prevention and treatment of radiation induced heart disease: Molecular hydrogen significantly reduces the effects of oxidative stress</b>	234
Magdalena Długosz-Lisiecka, Teresa Jakubowska, Magdalena Zbrojewska	<b>Activation of cyclotron construction elements</b>	235
Narcisa Tribulova, Csilla Vicenczova, Barbara Szeiffova Bacova, Tamara Egan Benova, Branislav Kura, Chang Yin, Rakesh Kukreja	<b>Myocardial connexin-43 and PKC signaling are involved in adaptation of the heart to irradiation-induced injury: Implication of miR-1 and miR-21</b>	236
Barbara Szeiffova Bacova, Csilla Vicenczova, Branislav Kura, Tamara Egan Benova, Chang Yin, Rakesh C. Kukreja, Jan Slezak, Narcisa Tribulova	<b>Irradiation-induced cardiac connexin-43 and miR-21 responses are hampered by treatment with atorvastatin and aspirin</b>	237
Mihon Mirela, Ilie Simona, Carmen Manea <sup>1</sup> , Chilug Livia	<b>Improved radioanalytical methods for quality control of [<sup>18</sup>F]NaF</b>	238

## 26 RADIATION MEASUREMENTS

Sung-Hee Jung, Ji-Ho Yoon	<b>A study on preparation of HQ clathrate as gaseous radiotracer carrier</b>	240
Jovana Nikolov, Natasa Todorovic, Andrej Vranicar, Péter Völgyesi, Éva Kovács-Széles	<b>Comparison of non-destructive nuclear forensics methods for analysis of nuclear material</b>	241
Michal Cieslak, Kelum A.A. Gamage, James Taylor	<b>Study of modulation properties of tungsten-based coded-aperture</b>	242
Taylan Tuğrul	<b>Absorption ratio of treatment couch and effect on surface and build-up region doses</b>	243
Mariia Pyshkina, Michael Zhukovsky, Alexey Ekidin	<b>Testing of RAM ION dosimeter in operational fields</b>	244
Magdalena Długosz-Lisiecka, Marcin Krystek, Michał Barasiński	<b>Radiation monitoring report from sailing around the Antarctic continent, along and south of the 60<sup>th</sup> parallel</b>	245
Tomas Nemes, Dusan Mrdja, Istvan Bikit	<b>Random coincidences in the sum-peak method</b>	246

Elena Shishkina, Alexandra Volchkova, Denis Ivanov, Yurii Timofeev, Bruce Napier	<b>Ensuring the effectiveness of extensive EPR dosimetry study of combined radiation exposure</b>	247
Natasa Todorovic, Jovana Nikolov, Ivana Stojkovic	<b>Determination of <math>^{210}\text{Pb}</math> in water by Cherenkov counting</b>	248
Simona Ilie, Calin Alexandru Ur, Octavian Sima, Gabriel Suliman	<b>Determination of the Co-60 source activity by using the sum-peak method</b>	249
Ivana Stojković, Nataša Todorović, Jovana Nikolov	<b>LSC screening of wastewater samples</b>	250
Hana Assmann Vratiská, Jaroslav Šoltés, Pavel Kůs, Hana Kořenková	<b>Development of short-lived radioactive tracers for the description of processes influencing the migration of contaminants in the environment</b>	251
Manssour Fadil, Ngoc-Duy Trinh, Marek Lewitowicz	<b>Thick target neutron yields: Experimental program in GANIL to measure the double differential neutron fluxes generated by the interaction of heavy ions with thick targets</b>	252
Deniz Bender, Rasit Turan, Merve Genc Unalan, Mustafa Unal, Özden Basar Balbasi, Ercan Yilmaz	<b>A study on the performance the CdZnXTe1-X radiation detectors grown by Vertical Gradient Freeze (VGF) technique</b>	253
Michael Schubert, Jürgen Kopitz, Kay Knoeller	<b>Improved approach for LSC detection of <math>^{35}\text{S}</math> aiming at its application as tracer for short groundwater residence times</b>	254
Elena Katamanova, Elena Beigel, Kseniya Panchukova, Oksana Kalinina, Evgeniya Zayka	<b>Use of contemporary diagnostic radiography methods in occupational diseases</b>	255
Iurii Simirskii, Alexey Stepanov, Ilia Semin, Anatoly Volkovich	<b>Radiation survey during research reactor dismantling</b>	256
Andrej Vraničar, Nataša Todorović, Jovana Nikolov, Ivana Stojković, Jan Hansman, Branislava Tenjović, Miloš Travar, Miodrag Krmar	<b><math>^{226}\text{Ra}</math> in water measurement by non-Marinelli geometry and gamma spectrometry</b>	257
Miloš Travar, Jovana Nikolov, Nataša Todorović, Andrej Vraničar, Jan Hansman, Dušan Mrđa	<b>The <math>^{210}\text{Pb}</math> correction for the self-absorption effect in EFFTRAN and Angle software</b>	258
Ufuk Paksu, Birol Engin	<b>ESR spectroscopy study of gamma irradiated dry yeast</b>	259
Ana Sofia Silva, Maria de Lurdes Dinis	<b>Distribution of the gamma dose rate measured in 15 Portuguese thermal establishments</b>	260
Toshiyuki Onodera, Keitaro Hitomi	<b>Photoresist on thallium bromide crystals for gamma-ray detector fabrication</b>	261

Tariq F. Hailat, Molham M. Eyadeh, Khalid A. Rabaeh, Balázs G. Madas, Feras M. Aldweri	<b>Dosimetric characterization of Methylthymol blue Fricke gel dosimeters using nuclear magnetic resonance and optical techniques</b>	262
Seung Kyu Lee, Sang In Kim, Jungil Lee, Insu Chang, Jang-Lyul Kim, Hyoungtaek Kim, Min Chae Kim	<b>Design and performance testing of the neutron detection module based on an inorganic scintillator for the neutron dosimetry</b>	263
Alfonso Compagno, Nadia Cherubini, Maria Letizia Cozzella, Alessandro Lago, Luigi Lepore	<b>ISOCS measurements: A way to improve radioactive waste characterization</b>	264
Dusan Mrdja, Rade Marjanovic, Kristina Bikit-Schroeder, Istvan Bikit, Jaroslav Slivka, Sofija Forkapic, Tomas Nemes	<b>Monte-Carlo simulation of coincidence background spectrum of large-volume NaI(Tl) detector</b>	265
Kristina Bikit-Schroeder, Dusan Mrdja, Istvan Bikit, Jaroslav Slivka, Gergő Hamar, Gábor Galgóczi, Dezső Varga	<b>Monte-Carlo simulation of the MUCA imaging system</b>	266
Anna Bianchi, Valeria Conte, Anna Selva, Paolo Colautti, Alessio Parisi, Brigitte Reniers, Filip Vanhavere	<b>Microdosimetry with a sealed mini-TEPC at the SOBP of CATANA</b>	267
Elio Tomarchio	<b>On the feasibility of dating the age of a nuclear incidental event by gamma-ray spectrometry of environmental samples</b>	268
Monika Mietelska, Marcin Pietrzak, Aliaksandr Bantsar, Zygmunt Szepliński	<b>Overview of recent nanodosimetric experiments with Jet Counter device</b>	269
Alexey Stepanov, Iurii Simirskii, Nikolay Gromov, Iliia Semin, Vyachaslav Stepanov, Anatoly Volkovich	<b>Survey of soil radioactive contamination in the basement premises of the reactor MR</b>	270
Kristina Bikit-Schroeder, Dusan Mrdja, Istvan Bikit, Jaroslav Slivka, Gergő Hamar, Gábor Galgóczi, Dezső Varga	<b>Investigation of light collection efficiency in plastic scintillators</b>	271
Agata Walencik-Łata, Danuta Smółka-Danielowska	<b>Analysis of radioactivity content in hard coal and products of coal combustion</b>	272
Vyacheslav Stepanov, Oleg Ivanov, Sergey Smirnov, Victor Potapov, Alexey Danilovich	<b>Application of remotely controlled collimated spectrometric systems in the works on dismantling the MR reactor and rehabilitation of the territory of NRC Kurchatov Institute</b>	273

Stepan Bazhin, Ekaterina Shleenkova, George Kaidanovsky, Vladimir Iliyn	<b>Comparative assessment of individual doses of radiation of personnel in Russia and the European countries</b>	274
Gintautas Tamulaitis, Saulius Nargelas, Augustas Vaitkevicius, Alberto Gola, Alberto Mazzi, Mikhail Korjik	<b>Influence of Mg codoping on carrier dynamics in GAGG:Ce scintillation crystals</b>	275
Jan Kisiel	<b>Natural radiation background measured within the BSUIN (Baltic Sea Underground Innovation Network) project</b>	276
Jordanka Semkova, Rositza Koleva, Victor Benghin, Krasimir Krastev, Yuri Matviichuk, Borislav Tomov, Tsvetan Dachev, Stephan Maltchev, Plamen Dimitrov, Igor Mitrofanov, Alexey Malakhov, Dmitry Golovin, Maxim Mokrousov, Anton Sanin, Maxim Litvak, Andrey Kozyrev, Vladislav Tretyakov, Sergey Nikiforov, Andrey Vostrukhin, Vyacheslav Shurshakov, Sergey Drobyshhev	<b>New results for the space radiation environment aboard the ExoMars Trace Gas Orbiter during the transit to Mars and in Mars orbit</b>	277
Mikhail Petrichenkov, Vladimir Chudaev, Anatoliy Repkov, Vladimir Eksta, Nataliya Shamakina, Sergey Melnik	<b>Neutron dosimetry at BINP using TLDs with LiF and portable devices</b>	278
Nevenka M. Antović, Nikola R. Svrkota, Sergey K. Andrukhovich	<b>Registration of gamma-gamma coincidences from Ba-133 decay</b>	279
Zbigniew Tymiński, Paweł Saganowski, Tomasz Dziel, Anna Listkowska, Edyta Lech, Ewa Kołakowska, Tomasz Ziemek, Daniel Cacko, Ryszard Broda	<b>Quality assurance of gamma ray measurements with HPGc detectors used in radiopharmaceutical production</b>	280
Dmitry Spassky, Sergey Omelkov, Vitali Nagirnyi, Nina Kozlova, Nataliya Krutyak, Alice Ukhanova, Oleg Buzanov, Mikhail Korjik	<b>Study of luminescence properties of <math>Gd_3(Ga,Al,Sc)_5O_{12}:Ce^{3+},Ca^{2+}</math> scintillating single crystals under UV and electron beam excitation</b>	281
Georgi Gorine, Jacopo Bronuzzi, Giuseppe Pezzullo, Isidre Mateu, Blerina Gkotse, Maurice Glaser, Didier Bouvet, Alessandro Mapelli, Federico Ravotti, Jean-Michel Sallese	<b>Low-mass radiation-hard beam profile monitors for high energy protons using microfabricated metal thin-films</b>	282

Diego Sanz, Harris Kagan, William Trischuk	<b>Development of polycrystalline chemical vapor deposition diamond detectors for radiation monitoring</b>	283
Vojislav Antic, Olivera Ciraj- Bjelac, Predrag Bozovic, Otas Durutovic	<b>Assessment of the occupational exposure of urologists during percutaneous nephrolithotomy surgical interventions</b>	284
V.V. Zabrodskii, S.V. Bobashev, A.V. Nikolaev, A.G. Alekseev, P.N. Aruev, E.V. Sherstnev	<b>A 2×32-format hybrid matrix high-speed XUV- detector</b>	285

## 27 RADIATION ONCOLOGY

Igor Stojkovski, Violeta Klisarovska, Petar Chakalaroski	<b>Radiation dose to the brain in postoperative radiation and impact on survival of patients with glioblastoma multiformae</b>	287
Evgenija Kuzmina, Tatiana Mushkarina, Tatiana Konstantinova, Tatiana Bogatyreva, Ludmila Grivtsova	<b>Reaction of peripheral blood's regulatory suppressor T-lymphocytes to components of chemoradiation therapy of Hodgkin's lymphoma</b>	288
Ioana-Carmen Brie, Maria Perde-Schrepler, Pirooska Virag, Eva Fischer-Fodor, Olga Soritau	<b>Combined immune and radiation therapy in the management of poor prognostic cancers</b>	289
Mateusz Bilski, Karolina Brzozowska, Kamila Masłowska, Monika Bilaska, Ludmiła Grzybowska- Szatkowska	<b>Radiation induced bystander effect – Pros and cons</b>	290
Mateusz Bilski, Anna Rycyk, Piotr Kozłowski, Karolina Szymańska, Ludmiła Grzybowska-Szatkowska	<b>High fraction doses for glioma treatment – An alternative for selected patients</b>	291
Violeta Klisarowska, Petar Chakalaroski, Igor Stojkovski	<b>Acute toxicity in standard treatment of cervical cancer</b>	292
Özlem Mermut, Esra Arslan	<b>Sinonasal intestinal-type adenocarcinoma</b>	293
Özlem Mermut	<b>Pelvic insufficiency fracture (PIF)</b>	294
Adam Spyra	<b>Monte Carlo simulations of radioembolization in various human organs</b>	295
Olena Safronova, Tetyana Udatova, Yaroslav Kmetuyk	<b>Determination of optimal safety margins using image- guided radiotherapy for prostate cancer</b>	296
Olena Safronva	<b>Evaluation of radiation doses to organs at risk with application of 3D-conformal radiotherapy and intensity-modulated radiotherapy for treatment of patients with breast cancer</b>	297

Petar Chakalaroski, Violeta Klisarovska, Igor Stojkovski, Lenche Kostadinova, Bojana Petreska	<b>Organ wall as a superior volume in presenting the absorbed dose compared to the whole organ volume in intensity-modulated irradiation therapy-treated gynecological malignancies</b>	298
Songül Barlaz Us, Özden Vezir, Ülkü Çömelekoğlu	<b>Protective effects of N-acetylcysteine on acute radiotherapy-induced cardiotoxicity in rats: An electrophysiological evaluation</b>	299
Serap Ketenci, Ayşe Dağlı Değerli, Funda Öztürk, Mustafa Özer, Tarık Sütçü, Beste M. Atasoy	<b>Dosimetric results of two different planning systems for craniospinal irradiation with VMAT techniques</b>	300
Dejan Trbojevic	<b>Hadron radiation in cancer therapy</b>	301
Berrin Inanc	<b>A dosimetric comparison of single arc and double arc therapy in the treatment of high-risk prostate cancer with pelvic nodal radiation therapy</b>	302
Svetlana V. Belkina, Galina P. Zhurakovskaya, Olga A. Vorobey	<b>Hyperthermic sensitization of tumour cells to radiation or chemicals: Optimization of the efficiency</b>	303

## 28 RADIATION PHYSICS

Matanat Mehrabova, Niyazi Hasanov, Aygun Kazimova, Aygul Hasanli	<b>Ab initio calculations of electronic structure of defects in <math>Cd_{1-x}Mn_xTe(Se)</math> and impact of <math>\gamma</math>-irradiation on optical properties of their epitaxial films</b>	305
Tomasz Wasowicz, Marta Łabuda, Boguslaw Pranszke	<b>Collisions of low-energy helium cations with furan molecules</b>	306
Anatoly Titov, Iurii Lomachuk, Daniil Maltsev, Nikolai Mosyagin, Sergei Semenov, Leonid Skripnikov	<b>Concept of clusters embedded in a crystal: Study of properties of point defects in xenotime and monazite containing actinides</b>	307
Anna Zakharova, Marina Bedrina, Sergei Semenov	<b>Quantum-chemical modeling of gadolinium endocomplexes with fullerenes</b>	308
Daniil Maltsev, Yuriy Lomachuk, Nikolai Mosyagin, Leonid Skripnikov, Anatoly Titov	<b>Embedding a potential method for the cluster modeling of solids and its application to the study niobate minerals as actinide immobilization matrices</b>	309
Renat Ibragimov, Natalia Khatina, Evgeny Klopikov, Svyatoslav Kolesnikov, Elena Ryabeva	<b>Analytical model for calculating the energy spectra of neutron radiation produced in d-t reactions for neutron generators with gas-filled or vacuum neutron tubes</b>	310
Irina Bazhukova, Sergey Sokovnin, Alexandra Myshkina, Valentina Kasyanova, Sergey Bazhukov	<b>Irradiation of cerium oxide nanoparticles by fast electrons</b>	311

David Zoul, Pavel Zháňal, Ladislav Viererbl, Antonín Kolros, Milan Zuna, Václava Havlová	<b>Computed gamma tomography of radioactive metallurgical and geological samples</b>	312
Leena Diehl, Riccardo Mori, Marc Hauser, Karl Jakobs, Ulrich Parzefall, Liv Wiik-Fuchs	<b>Investigation of charge multiplication in irradiated p- type silicon sensors designed for the ATLAS Phase II Strip Tracker</b>	313
Dragana Krstic, Dragoslav Nikezic	<b>Application of Monte Carlo software for calculation of efficiency of semiconductor germanium detector</b>	314
Arif Maharramov, Ulker Samedova, Musa Nuriyev, Mazahir Bayramov, Amdulla Mekhrabov	<b>Microwave absorbance properties of Fe<sub>3</sub>O<sub>4</sub>+epoxy resin and Fe<sub>3</sub>O<sub>4</sub>+bentonite/epoxy resin nanocomposites</b>	315
Tomasz Wasowicz, Annti Kivimaki, Robert Richter	<b>Fragmentation of molecules into neutral high- Rydberg fragments after core excitation and core ionization using soft X-ray synchrotron radiation</b>	316
Alexandr Belousov, Vladimir Morozov, Grigorii Krusanov, Andrey Davydov, Maria Kolyvanova, Alexander Shtil, Vladimir Klimanov, Alexander Samoylov	<b>Repartition of the secondary particles contributions into the absorbed dose of proton radiation behind the Bragg peak in the presence of gold nanoparticles</b>	317
Giuseppe Lorusso, Alberto Boso, Peter Ivanov, Ana Denis- Bacelar, Andrew Pollard, Hiroshita Haba	<b>Auger electron spectroscopy studies at the National Physical Laboratory for medical applications</b>	318
Michal Piasecki	<b>The TlPb<sub>2</sub>Br<sub>5-x</sub>I<sub>x</sub> system as potential detectors for X- ray and γ-ray at ambient temperature</b>	319
Heidi Nettelbeck, Carmen Villagrasa, Marion Bug, Hans Rabus	<b>Nanodosimetry: Estimating radiation damage to DNA with Monte Carlo track structure simulation</b>	320

## 29 RADIATION PROTECTION

Harmen Bijwaard, Ischa de Waard	<b>Current state of medical diagnostic reference levels and possibilities for improvements in the Netherlands</b>	322
Alexandru Pavelescu, Carmen Tuca, Radu Deju	<b>Modelling of a radiological incident in the intermediary storage of activated wastes from VVR-S nuclear research reactor decommissioning</b>	323
Charlotte Duchemin, Matteo Magistris, Marco Silari, Biagio Zaffora	<b>Clearance from regulatory control in Switzerland of CERN's radioactive waste</b>	324
Radu Deju, Carmen Tuca, Monica Mincu	<b>Radiological monitoring approach for dismantling of the fuel assembly separator from VVR-S nuclear research reactor</b>	325

Vlado Valkovic	<b>Terrorists and “dirty bomb”</b>	326
Chris Theis, Fernando Pereira, Helmut Vincke	<b>PyActiWiz – A massively parallel scripting environment to calculate radionuclide inventories for radiation protection purposes</b>	327
Nataliya Maznyk, Franz Fehringer, Christian Johannes, Tetiana Sypko, Nataliia Bohatyrenko, Wolfgang-Ulrich Müller	<b>Virtual biodosimetry laboratory as a small network for radiation emergencies</b>	328
Vijay Singh	<b>Biomarkers for assessing radiation injury identified using large animal model</b>	329
Alexander Grebenyuk, Alexander Starkov, Olga Strelova, Alexey Miliaev, Kamil Mamedov	<b>Health protection measures for major radiation accidents</b>	330
Alain Niba Ngwa, Steffen Kerker	<b>Radon measurements in big buildings</b>	331
Mee Jang, Chang Jong Kim, Won Woo Choi, Jong Myoung Lim	<b>Development of an in-situ radioactivity screening method for building materials using XRF and radioactivity index</b>	332
Marina Maslova, Lidia Gerasimova	<b>Synthesis and adsorption properties of <math>\text{TiO}(\text{OH})\text{H}_2\text{PO}_4 \cdot \text{H}_2\text{O}</math> titanium phosphate</b>	333
Lidia Gerasimova, Marina Maslova, Shchukina Ekaterina, Anatoly Nikolaev	<b>Ion-exchange behavior of titanosilicate ivanukite framework in relation to nuclear wastes treatment</b>	334
Pavel Sharagin, Elena Shishkina, Evgenia Tolstykh, Alexandra Volchkova, Michael Smith, Bruce Napier, Marina Degteva	<b>Comparison of <math>^{90}\text{Sr}</math> dose factors for active bone marrow of adult males and females</b>	335
Evgeniy Nazarov, Alexey Ekinin, Alexey Vasilyev	<b>Compilation of available information on carbon-14 releases from different types of nuclear reactors</b>	336
Carmen Tuca, Alexandru Pavelescu	<b>Dose assessment in decontamination process of hot cells from VVR-S nuclear research reactor under decommissioning</b>	337
Zoran Mirkov	<b>The level of patient doses in intraoral and panoramic radiography in Serbia</b>	338
Elimkhan Jafarov, Haydar Piriye	<b>Are there alternatives to nuclear power?</b>	339
Sergei Akhromeev, Sergei Kiselev, Vladimir Shlygin, Tatyana Lashchenova, Natalya Shandala	<b>Comprehensive study of environmental contamination at nuclear legacy sites in the Russian Far East</b>	340

Wangkyu Choi, Seungeun Kim, Seonbyeong Kim	<b>Removal of radioactive contaminants incorporated in corrosion oxide film using decontamination foams</b>	341
Sergei Kiselev, Vladimir Shlygin, Sergei Akhromeev, Tatyana Lashchenova, Renata Starinskaya, Tamara Gimadova, Julia Zozul, Natalia Shandala	<b>Regulatory supervision during decommissioning &amp; dismantling of nuclear submarines in the Russian Northwest</b>	342
Jozef Sabol, Jana Hudzietzová	<b>Problems in meeting regulatory requirements related to the skin dose</b>	343
Denis Komarov, Olga Komova, Viktoriya Gavrilova	<b>The scavengers of reactive oxygen species TEMPOL and reactive nitrogen species cPTIO enhance chromosome aberrations induced by low-dose <math>\gamma</math>-irradiation</b>	344
Dejan Vasovic, Goran Janackovic, Stevan Musicki	<b>Occupational health and safety considerations within CBRN area</b>	345
Petr Kuča, Jan Helebrant, Irena Češpírová, Jiří Hůlka	<b>RAMESIS project aimed at supporting citizen monitoring network in the Czech Republic – Final report</b>	346
Nataliya Shandala, Sergei Kiselev, Vitaly Starinskiy, Dmitrii Isaev, Yrii Belskih, Vladimir Shlugin, Alexey Titov	<b>30 years following the accident at the Chazhma Bay (Primorsky Territory): Environmental assessment of the contaminated areas</b>	347
Inge Schmitz-Feuerhake	<b>Dose estimations for Chernobyl contaminations by UNSCEAR: Neglected lessons from cytogenetic studies</b>	348
Stevan Musicki, Sladjan Hristov, Dejan Vasovic	<b>Review of SAF CBRN equipment and personnel: Expectations, advantages and constrains</b>	349
Vitaly Starinskiy, Nataliya Shandala, Sergey Kiselev, Alexey Titov, Anna Filonova, Sergey Ahromeev	<b>Study of environmental contamination and the health status of the population living in the vicinity of uranium legacy sites in the Central Asia countries</b>	350
Snežana Stankovic <sup>1</sup> , Dušan Popović <sup>2</sup> , Matejka Bizjak <sup>3</sup> , Ana Kocić <sup>1</sup> , Dragana Grujić <sup>4</sup> , Goran Poparić	<b>UV protection offered by textile fabrics</b>	351
Jozef Sabol, Bedřich Šesták	<b>A need for a simplified system in radiation protection</b>	352
Milos Mladenovic, Ivana Maksimovic, Miodrag Milenovic, Dalibor Arbutina, Stevan Karimanovic, Danijela Soldatović, Nebojša Bilanović	<b>Nuclear safety and nuclear security – Integrated approach (PC NFS experience)</b>	353
Sixuan Li, Qiuju Guo, Youyi Ni	<b>Study on plutonium in seawater collected around several nuclear power plants in China</b>	354

Sebastian Pflugbeil, Inge Schmitz-Feuerhake	<b>Radiation effects in occupationally exposed persons: Who cares for the adoption of the state of knowledge in compensation cases?</b>	355
Elio Tomarchio, Mariarosa Giardina, Daniele Greco	<b>Measurement of long-lived radionuclide activity induced in target components of a cyclotron used for [<sup>18</sup>F]-[FDG] production</b>	356
Nikola Svrkota, Jelena Popović, Nevenka M. Antović	<b>Occupational exposures in the Centre for Nuclear Medicine, Clinical Centre of Montenegro</b>	357
Anna Cimmino, Robert Froeschl, Heinz Vincke	<b>Analysis of the radiological risks associated with the installation, extraction, and long-time storage of the CASTOR detector at the CMS experiment</b>	358

### 30 RADIOBIOLOGY

Ihar Cheshyk, Natallia Puzan, Alexander Nikitin	<b>Study of radioprotective properties of microbiological preparations EM-1 and EMX-Gold</b>	360
Tariq Hailat, Emese Drozdik, Balázs Madas	<b>Computational cell dosimetry for alpha-particle exposure by Monte-Carlo methods</b>	361
Nataliya Maznyk, Tetiana Sypko, Nataliia Bohatyrenko, Olena Sukhina, Irina Krugova, Viktor Starenkiy	<b>Cytogenetic effects in lymphocytes of cancer patients with different tumor localizations on early and late stages of radiotherapy treatment</b>	362
Soile Tapio, Zohaib Nisar Khan, Omid Azimzadeh, Fabian Metzger, Munira Kadhim, Fiona Lyng, Simonetta Pazzaglia, Mariateresa Mancuso, Anna Saran	<b>“Out-of-target” effects in the murine hippocampus after partial body irradiation</b>	363
A. Ristić-Fira, O. Keta, V. Petković, G.A.P. Cirrone, G. Petringa, G. Cuttone, I. Petrović	<b>On formation of DNA double strand breaks after irradiation of human malignant cells with therapeutic proton and carbon ion beams</b>	364
I. Petrović, S. Incerti, V. Petković, O. Keta, G.A.P. Cirrone, G. Petringa, G. Cuttone, A. Ristić-Fira	<b>Radiobiological validation of the GEANT4-DNA simulation toolkit through evaluation of DNA DSBs</b>	365
Ulyana Bliznyuk, Valentina Avduhina, Alexander Belousov, Polina Borschegovskaya, Alexander Chernyaev, Irina Gordonova, Victoria Ipatova, Zoya Nikitina, Felix Studenikin, Dmitry Yurov	<b>The influence of accelerated 1 MeV electron beam on microbiological and organoleptic parameters of a chilled rainbow trout</b>	366

Nely Metlyayeva, Valery Krasnyuk, Boris Kukhta, Vladimir Yatsenko, Vyacheslav Korenkov, Lyubov Yunanova	<b>Human acute stress response to entry of cesium and strontium into an organism as a result of an unfortunate event in the manufacture</b>	367
Tatiana Mushkarina, Evgenija Kuzmina, Tatiana Konstantinova	<b>Reaction to gamma irradiation at in vitro studies of regulatory suppressor T cells (T<sub>reg</sub>) of healthy donors</b>	368
Simone Moertl, Lisa Mutschelknaus, Michael Schneider, Omid Azimzadeh, Michael Atkinson	<b>Exosomes are communicators of prosurvival signals during radiation response</b>	369
Fulger Ciupagea, Nuta Niculaie, Gabriela Rosca Fartat, Constantin Ghioca	<b>Health study of industrial radiography of occupationally exposed workers</b>	370
Elimkhan Jafarov, Mehriban Velijanov, Jamala Orujova	<b>Effect of pre-sowing irradiation of chickpea seeds on the content of low molecular weight antioxidants under salt stress</b>	371
Coretchi Liuba, Gincu Mariana	<b>Microdosimetry investigations as a dosimetric tool to explore the radiation cellular mechanism</b>	372
Kei Wakimura, Mikio Kato	<b>Motility and chemotactic response of <i>Escherichia coli</i> mutant strains and gamma-irradiated cells</b>	373
Jin Kyu Kim, Mi Young Kang, Jin-Hong Kim, Seungsik Lee	<b>Molecular dosimetry with gamma-H2AX Foci in MCF7 cells</b>	374
Larisa Andronic	<b>Comparative evidence of meiotic rearrangements in gamma irradiated and virus infected tomato plants</b>	375
Alina Glazunova, Firdaus Hazieva	<b>The application of electromagnetic radiation in the development of <i>Polemonium caeruleum</i> varieties</b>	376
Natalia Koltovaya, Nadya Zhuchkina, Ksenia Lyubimova	<b>Gene mutations induced by gamma-rays in haploid and diploid yeast cells</b>	377
Zacharenia G. Nikitaki, Ifigenia V. Mavragani, Spyridon A. Kalospyros, Alexandros G. Georgakilas	<b>Clustered DNA damage: A severe biological triggering effect with challenging detection</b>	378
Iurii Severiukhin	<b>Assessment of visual behavior and optomotor response of rats after irradiation with 5 Gy protons</b>	379
Andreyan Osipov, Margarita Pustovalova, Anna Grekhova, Petr Eremin, Natalia Vorobyeva	<b>Low-dose X-ray irradiation does not cause detrimental effects in the progeny of irradiated mesenchymal stem cells</b>	380
Tadashi Hongyo, Yukimitsu Sawai, Hirofumi Kuchino, Itsuki Seki, Kentaro Yamamura, Shota Hirose, Io Ishibashi, Yasuyuki Ueda	<b>Thyroid dysfunction of a child who was born after a radiological examination of its mother by oil-soluble iodinated contrast medium (Lipiodol)</b>	381

Adrianna Tartas, Maciej Galecki, Mateusz Filipek, Werner Friedland, Andrzej Wójcik, Beata Brzozowska-Wardecka	<b>Modeling of chromosome aberrations induced in cells exposed to mixed beams of ionizing radiation</b>	382
Ekaterina Koryakina, Vladimir Potetnya, Marina Troshina, Maria Efimova, Raisa Baykuzina, Anatoliy Lychagin, Alexey Solovev, Sergey Koryakin, Stepan Ulyanenko	<b>RBE of accelerated carbon ions and of neutron-produced heavy-charged particles in Chinese hamster cells</b>	383
Vladimir Potetnya, Ekaterina Koryakina, Marina Troshina, Nina Boldueva, Sergey Koryakin, Stepan Ulyanenko	<b>Dosimetric and radiobiological aspects of cell monolayer irradiation with 14 MeV neutrons in the presence and absence of proton equilibrium</b>	384
Mateusz Filipek, Beata Brzozowska-Wardecka, Maciej Galecki, Adrianna Tartas	<b>DNA damage in cancer cells exposed to beta radiation measured experimentally and modeled in Monte Carlo simulations</b>	385
Eszter Persa, Tünde Szatmári, Nikolett Sándor, Géza Sáfrány, Katalin Lumniczky	<b>Pitfalls in isolation and characterisation of bone marrow extracellular vesicles mediating radiation-induced bystander effects in mice</b>	386
Tetiana Andriichuk, Natalia Raksha, Sergii Vakal, Ludmyla Ostapchenko	<b>Some aspects of nuclear-mediated pathway of radiation-induced apoptosis</b>	387
Valérie Van Eesbeeck, Ruben Props, Mohamed Mysara, Rob Van Houdt, Pauline Petit, Corinne Rivasseau, Jean Armengaud, Pieter Monsieurs, Jacques Mahillon, Natalie Leys	<b>Effect of radiation and temperature on the microbial community in the cooling water of a nuclear reactor</b>	388
V. V. Panfilova, O. I. Kolganova, O. F. Chibisova	<b>Higher brain functions of the offsprings of irradiated animals</b>	389
Natalia Vorobyeva, Oleg Kochetkov, Margarita Pustovalova, Anna Grekhova, Taisia Blokhina, Elizaveta Yashkina, Andrey Osipov, Dmitry Kabanov, Pavel Surin, Valeryi Barchukov, Andreyan Osipov	<b>Comparative study of DNA double-strand breaks formation in human mesenchymal stem cells exposed to organically bound tritium vs tritiated water, and X-rays</b>	390
Dariya Babina, Vladislav Petin, Victoria Panfilova	<b>Exposure of yeast cells with different repair efficiency to densely ionizing radiation</b>	391
Nadezhda Shimalina, Makar Modorov, Elena Antonova, Vera Pozolotina	<b>Genetic diversity in <i>Plantago major</i> L. populations growing under conditions of radioactive and chemical contamination</b>	392

### 31 RADIOCHEMISTRY

Ingrid Lehman-Andino, Evgen V. Govor, Alexander N. Morozov, Alexander M. Mebel, Christopher J. Dares, Raphael G. Raptis, Konstantinos Kavallieratos	<b>Ligands for extraction of actinides from alkaline high-level waste and from acidic used nuclear fuel. Theoretical and experimental studies of the effect of soft-donors in binding and extraction selectivity</b>	394
Piotr Szajerski, Agnieszka Bogobowicz, Andrzej Gasiorowski	<b>Leaching behavior of Cs-137, Sr-90, Co-60 and Am-241 isotopes from native and radiation-degraded sulfur polymer concrete (SPC) composites</b>	395
Sergey Kulyukhin, Igor Rumer, Elena Krasavina, Andrey Gordeev	<b>Sorption of U(VI) onto Mg-Al layered double hydroxides and oxides from aqueous solutions</b>	396
Svyatoslav Vuchkan, Ihor Syika, Yuriy Kylivnyk	<b>Adsorption of heavy metal ions onto titanium silicate</b>	397
Alexei A. Bessonov, Iraida A. Charushnikova, Alexander M. Fedosseev	<b>Cation-cation interaction of <math>N_pO_2^+</math> ions in double neptunium(V) nitrate crystal complexes</b>	398
Dagmara Chmielewska-Śmietanko, Marek Henczka, Pavel Apel, Oleg Orelovich, Marina Gustova	<b>Application of nanocomposite sorbent SiEA-KNiFe in the process of water purification from radioactive isotopes</b>	399
Hanna Vasylyeva, Ivan Myroniuk, Igor Myktytn	<b>Adsorption of <math>Y^{3+}</math> ions from aqueous solutions by neodymium-supported titanium dioxide</b>	400
Vladimir Kulemin, Aleksandr Veleshko, Sergey Kulyukhin	<b>Plutonium and uranium concentration from sea water</b>	401
Elena Belova, Mikhail Kadyko, Yulia Nikitina, Ivan Skvortsov	<b>The products of radiolysis of extraction systems based on TODGA in 1-decanol with Isopar-M and TODGA in 1-nonanol with Isopar-M</b>	402
Maria Angela Menezes, Paula Salles, Márcia Sathler, Hellen Oliveira, Radojko Jaćimović	<b>An action towards food safety: Evaluation of chemical impurities in sugar by neutron activation analysis</b>	403
Juan F. Facetti-Masulli, Hector D. Colman	<b>Effects of gamma irradiation on cassava flour from Paraguay</b>	404
Paula Salles, Márcia Sathler, Cláudia Ferreira, Maria Ângela Menezes, Radojko Jaćimović	<b>Elemental composition of hair in individuals with sedentary lifestyle from Belo Horizonte, Brazil, analysed by ko-INAA</b>	405
Konstantin Dvoeglazov, Ekaterina Pavlukevich, Lubov Podrezova, Tatyana Podimova, Yelizaveta Filimonova	<b>Study of Tc(VII) ions reduction by diformylhydrazine in nitric acid solutions</b>	406

Ekaterina Pavlyukevich, Konstantin Dvoeglazov, Polina Mitrças	<b>Kinetics of Np(VI) and Pu(VI) reduction with diformylhydrazine in nitric acid</b>	407
Andrei Ivanets, Irina Shashkova, Natalja Kitikova, Artem Radkevich, Tatiana Stepanchuk, Marina Maslova, Natalia Mudruk	<b>New Ti-Ca-Mg phosphate sorbents for removal of <sup>137</sup>Cs, <sup>60</sup>Co and <sup>85</sup>Sr from multicomponent liquid radioactive waste</b>	408
Mirza Nuhanovic, Mirza Nuhanovic, Nusret Dreskovic, Samir Đug, Narcisa Smječanin	<b>Investigation of the natural radioactivity of the sediment samples from the area of Una River</b>	409
Vladimir Petrov, Anastasiya Smirnova, Petr Matveev, Artem Mitrofanov, Igor Rodin, Timur Baygildiev, Stepan Kalmykov	<b>Experimental and theoretical study of gamma- radiolysis of diamides of N-heterocyclic acids promising for separation of trivalent f-elements</b>	410
Petr Matveev, Vladimir Petrov, Nickolay Andreadi, Natalia Borisova, Gladis Zakirova, Elena Belova, Boris Myasoedov, Stepan Kalmykov	<b>New pyridine-based phosphine oxides for liquid extraction of Am(III), Cm(III) and Ln(III)</b>	411
Aliaksandr Zaruba, Artsiom Radkevich, Olga Korenkova, Nadzeia Voronik	<b>Study of radionuclide speciation in spent fuel pool model solutions</b>	412
Iurii Nevolin, Sergey Kulyukhin, Vladimir Petrov, Stepan Kalmykov	<b>Gas-phase conversion of UPd<sub>3</sub>, URu<sub>3</sub> and URh<sub>3</sub> intermetallides into water-soluble uranium compounds</b>	413
Elena Belova, Alexey Rodin, Georgy Thorzhnitskiy, Mikhail Kadyko, Zayana Dzhivanova, Ivan Skvortsov, Anton Smirnov, Yulia Nikitina	<b>Exothermic processes in extraction systems during the reprocessing of spent nuclear fuel</b>	414

## 32 RADIOECOLOGY

S.V. Ostakh	<b>The label method for the assessment of the technical feasibility waste management of the oil and gas industry</b>	416
Konrad Wysogład	<b>Environmental studies of the radioisotope concentration in coal mine waste in Silesian and Lubelskie Province – Poland</b>	417
Lydia Bondareva, Nataliya Fedorova	<b>Environmental risks for the freshwater ecosystem of the Yenisei River and health risks for humans</b>	418
M. Radenković, S. Milošević, S. Stanković, J. Joksić, A. Onjia	<b>Airborne uranium assessment by epiphytic lichen species in contaminated areas</b>	419

Hing Ming Hung	<b>The impact of high energy X-ray and <math>\beta</math>-ray irradiation on the germination of rice seed</b>	420
Mihajlo Vićentijević, Dubravka Vuković, Vujadin Vuković, Branislava Mitrović, Dragan Živanov, Jasna Kureljušić	<b>RH control Cs<sup>137</sup> in fito-sanitary supervision</b>	421
Ludmila Mikhailovskaya, Vera Pozolotina	<b>The spatial distribution of radionuclides in the soils of the Urals contaminated from different sources</b>	422
Dmitry Manakhov, Elena Alekhina, Denis Lipatov, Sergrey Mamikhin	<b>Speciation of <sup>226</sup>Ra and <sup>232</sup>Th in Albic Stagnic Retisol</b>	423
Liliana Petrenko	<b>Geological and non-geological aspects in the context of geological radioactive waste disposal</b>	424
Mikhail Melgunov, Kseniya Mezina, Boris Shcherbov, Yulia Vosel, Inna Zhurkova, Maksim Rubanov	<b>Pb-210, Be-7 and Cs-137 in lichens, mosses and pine needles of the south of Western Siberia</b>	425
Fabio Girardi, Maria Letizia Cozzella, Donatella Ferri, Nadia Cherubini	<b>Optimization of nutrient ratio in Hoagland solution to improve the capability of rapeseed (<i>Brassica napus</i> L) to decontaminate water from pollution of radioactive cesium isotopes in hydroponic condition</b>	426
Osman Günay, Serpil Aközcan	<b>Measurements of natural radioactivity in soil of Buyukcekmece (Istanbul-Turkey)</b>	427
Marya Kropacheva	<b>The artificial isotope distribution in substrate–plant system: The design of rhizobox for laboratory and nature experiments</b>	428
Alexander A. Dvornik, Alexander M. Dvornik, Sergey Gaponenko, Natalia Shamal, Raisa Korol, Alesya Bardyukova, Veronika Seglin	<b>Decision support system on radioactive consequences of wildfires in Chernobyl Exclusion Zone (Belarus)</b>	429
Dmitri Gudkov, Alexander Kaglyan, Sergey Kireev, Ludmila Yurchuk, Vladimir Belyaev, Alexander Nazarov	<b>Estimation of radiation dose rate to fish occupying different ecological zones in water bodies within the Chernobyl Exclusion Zone</b>	430
Christina Ganzha, Dmitri Gudkov, Igor Abramiuk, Vladyslav Pavlovsky, Oleksandr Kaglyan	<b>Abnormalities of the postcranium skeleton of juvenile fish from lakes within the Chernobyl Exclusion Zone</b>	431
Vesna Radumilo, Ivan Knežević, Dalibor Arbutina, Boris Lončar	<b>Atmospheric dispersion modeling of radionuclides around nuclear facilities in Serbia</b>	432
Shafiga Topchiyeva, Matanat Mehrabova	<b>Definition of air pollution</b>	433

Christo Angelov, Ilia Penev, Todor Arsov, Stefan Georgiev	<b>Natural and man-made aerosol activity observation at Moussala BEO</b>	434
Marija Lekić, Nataša Lazarević, Nevena Zdjelarević, Dalibor Arbutina, Boris Lončar	<b>Determination of gamma-emitting radionuclides in soil sample for the purposes of proficiency test IAEA- TEL-2018-04 ALMERA</b>	435
Tetiana Tugai, Lubov Zelena, Andrey Tugai, Olena Polischuk, Natalia Sergeichuk	<b>Evaluation of genomic alterations in <i>Cladosporium cladosporioides</i> with radioadaptive properties</b>	436
Ivanka Antović, Nikola Svrkota, Nevenka Antović	<b>Beryllium-7 in six fish species from the Bay of Boka Kotorska</b>	437
Robert-Csaba Begy, Daniel S. Veres, Szabolcs Kelemen	<b>Climate change reconstruction for modern warm period in north of Romania by using <sup>210</sup>Pb chronology</b>	438
Robert-Csaba Begy, Szabolcs Kelemen, Daniel S. Veres, Timea Sandor-Nagy	<b>Studies on the effects of land use changes on soil erosion and increased sedimentation using radionuclides</b>	439
Milan Tanić, Denis Dinić, Željko Mihaljev, Brankica Kartalović, Marko Daković	<b>Natural and artificial radionuclides in the soil of public parks and playgrounds in Kruševac, Serbia</b>	440
N. Pomortseva, D. Gudkov, A. Kaglyan	<b>Effects of long-term irradiation on cytogenetic characteristics of the common roach (<i>Rutilus rutilus</i> L.) from water bodies within the Chernobyl Exclusion Zone</b>	441
Vladimir I. Ivanenko, Roman I. Korneikov	<b>Extraction of cesium, strontium and cobalt radionuclides by titanium phosphate adsorbents from NPP complex solutions</b>	442
Milda Peciuliene, Vaida Vasiliauskiene, Vigilija Cidzikiene, Dainius Jasaitis	<b>Natural radionuclides in soil and evaluation of their exposure in specific areas on the territory of Lithuania</b>	443
Sanja Bijelović, Nataša Dragić, Emil Živadinović, Tanja Likić, Nataša Todorović, Jovana Nikolov	<b>Is there a health risk of radionuclides in drinking water from districts in Vojvodina?</b>	444

### 33 RADIOLOGY

Živorad N. Savić, Katarina Ž. Savić, Sofija Ž. Savić, Mirjana M. Petrović, Vladimir S. Radak, Srbislav S. Pajić, Vojislav M. Antić	<b>CT perfusion of endocranium</b>	446
Milan Mijailović, Snežana Lukić	<b>Comparing kinetic imaging with conventional DSA - 55% X-ray dose reduction in angiography</b>	447

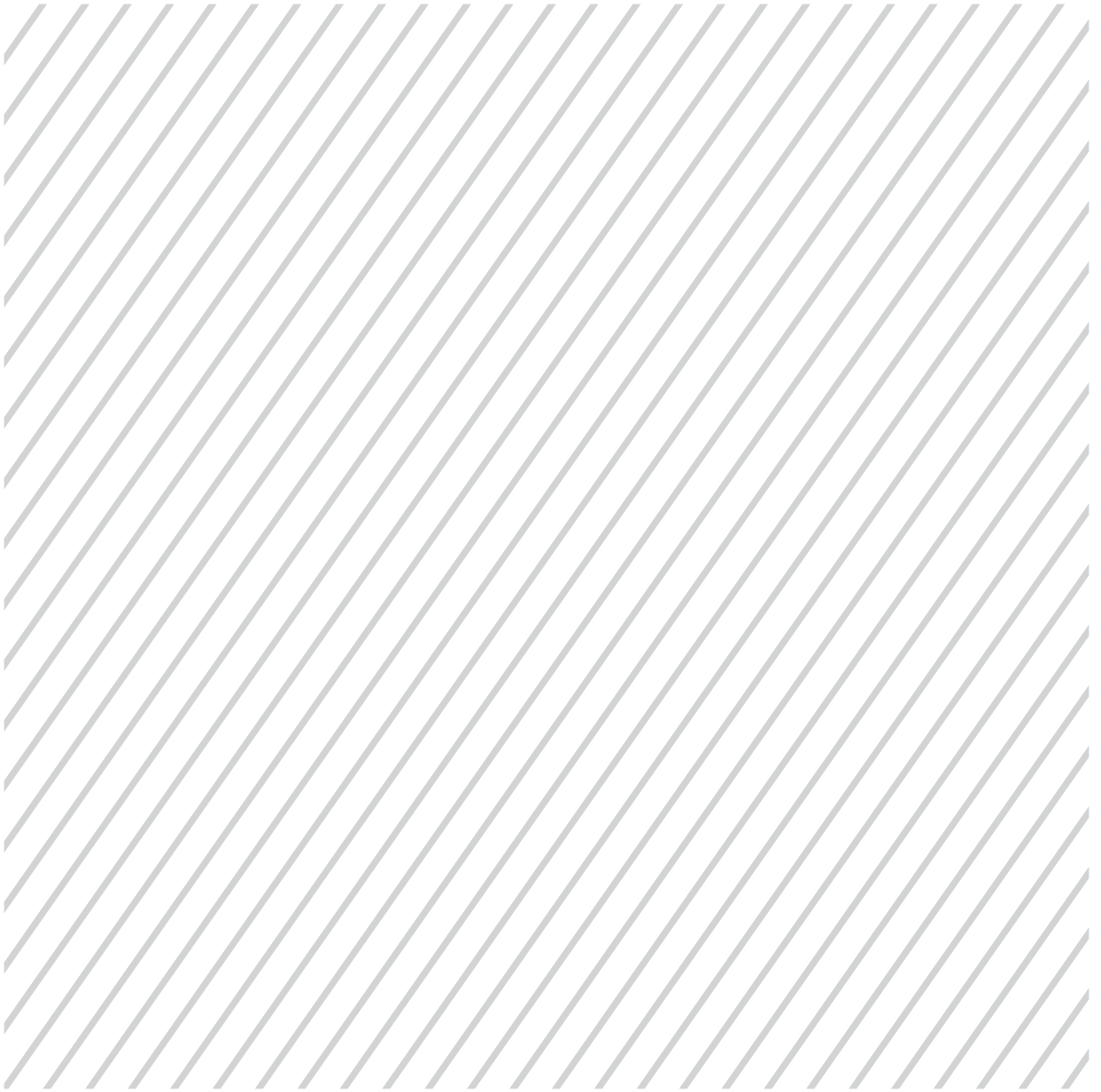
Snežana Lukić, Milan Mijailović	<b>MR lower limb angiography, alternative to reduce radiation dose</b>	448
Magdalena Radović	<b>The role of strain sonoelastography in evaluation of breast lesions - Physics, indications and diagnostic performance</b>	449
<b>34 RADIOPHARMACOLOGY</b>		
Boyan Todorov, Iva Belovezhdova, Outi Keinänen, Anu J. Airaksinen	<b>2-deoxy-2-[<sup>18</sup>F]fluoro-D-glucose glycoconjugates via oxime formation</b>	451
Olha Storchylo	<b>Mechanisms of the implementation of damage to the functions of the small intestine in two generations of posterity of irradiated rats</b>	452
<b>35 RADIOTHERAPY</b>		
Yong Nam Kim, Hyeong-min Joo	<b>Development of inverse planning strategy using volumetric arc therapy for intensity-modulated radiation treatment for prostate cancer</b>	454
Francisco Cutanda Henriquez, Silvia Vargas Castrillon	<b>The value of robust statistics in the analysis of linac quality assurance images</b>	455
Andrey Vertinskiy, Evgeniya Sukhikh, Leonid Sukhikh	<b>The cylindrical dosimeter for 3D verification of high-modulated radiation therapy plans</b>	456
Dražan Jaroš, Goran Kolarević, Bojan Pavičar	<b>Accuracy of intensity-modulated radiation therapy treatment planning and delivery</b>	457
Violeta Acovska, Dragan Nikolovski	<b>Comparison of 3D-CRT vs IMRT for anal cancer treatment planning</b>	458
Songül Barlaz Us, Eda Bengi Yilmaz	<b>Evaluation of tomotherapy HDA beam parameters</b>	459
Hargita Hegyesi, Nikolett Sándor, Balázs Hornyák, Szabina Mecsei, Lilla Turiák, Ágnes Kittel, Géza Sáfrány, Lóránd Bertók, Edit I Buzás	<b>Proteomic signature of bone marrow-derived small extracellular vesicles in heart-irradiated radiotherapy model</b>	460
Nazar Bartosik	<b>Study of nuclear fragmentation in particle therapy with the FOOT experiment</b>	461
Marcello Serra, Gianluca Ametrano, Borzillo Valentina, Rossella Di Franco, Paolo Muto, Maria Quarto, Giuseppe Roberti, Federica Savino	<b>A dosimetric comparison between cyberknife and intensity/volumetric modulated techniques in stereotactic radiosurgery (SRS)</b>	462

Federica Savino, Gianluca Ametrano, Maria Quarto, Marcello Serra, Cecilia Arrichiello, Leonardo Baldassarre, Fabrizio Cammarota, Giuseppe Roberti, Paolo Muto	<b>Evaluation of the additional dose delivered to the patient during imaging procedures in image-guided radiotherapy through in vivo measurements: Preliminary results</b>	463
Irena Muçollari, Artur Xhumari, Aurora Aliraj, Anastela Mano, Gramoz Braçe, Rejnardo Tafaj, Ejona Lilamani, Bledar Cullhaj, Blerina Myzeqari, Erald Karaulli	<b>Stereotactic radiosurgery for small volume intracranial meningiomas: Plan quality</b>	464
Lenche Kostadinova, Petar Chakalaroski, Marina S. Vukashinovic	<b>Adaptive radiotherapy in advanced nasopharyngeal carcinoma - Case report</b>	465

### 36 RADON AND THORON

Piotr Szajerski, Maciej Jura	<b>Low radon exhalation rate composites based on NORM residues</b>	467
Perko Vukotic, Ranko Zekic, Tomislav Andjelic, Nikola Svrkota, Marija Bogicevic, Aleksandar Dlabac	<b>Radon in Montenegrin schools and kindergartens – Preliminary results</b>	468
Karel Jilek	<b>The NRPI low-level continuous radon gas monitor for measurement below 1 Bq/m<sup>3</sup></b>	469
Igor Čeliković, Gordana Pantelić, Ivana Vukanac, Jelena Krneta-Nikolić, Miloš Živanović, Aleksandar Kandić, Boris Lončar	<b><sup>222</sup>Rn and <sup>220</sup>Rn exhalation rate and natural radionuclide content in different granites used in Serbia</b>	470
Hüseyin Ali Yalim, Ayla Gümüş	<b>Soil gas radon concentration and terrestrial radioactivity correlations in Afyonkarahisar</b>	471
Hüseyin Ali Yalim, Ayla Gümüş, Ridvan Ünal	<b>Indoor radon concentrations and related dose rates at the houses of Afyonkarahisar</b>	472
Anita Csordás, Katalin Zsuzsanna Szabó, Zoltán Sas, Erika Kocsis, Tibor Kovács	<b>Indoor radon survey in Hungarian kindergartens</b>	473
Michael Zhukovsky, Hyam Nazmy, Mostafa Y. A. Mostafa, Vladislav Semyannikov	<b>A combined system for the measurements of aerosol size distribution</b>	474
Coretchi Liuba	<b>National radon survey in Moldova Republic</b>	475

Gordana Pantelic, Ivana Vukanac, Jelena Krneta Nikolic, Milos Zivanovic, Igor Celikovic, Milica Rajacic	<b>Uncertainty evaluation in radon concentration measurement in soil using NAI detectors</b>	476
Yunxiang Wang, Lei Zhang, Qiuju Guo	<b>Long-term observation and analysis of atmospheric radon and its short-life progeny</b>	477
Kremena Ivanova, Zdenka Stojanovska, Jana Djounova, Bistra Kunovska, Nina Chobanova, Decislava Djunakova	<b>Sample design for radon concentration investigation in Bulgarian caves</b>	478
Bistra Kunovska, Kremena Ivanova, Zdenka Stojanovska, Nina Chobanova, Decislava Djunakova, Jana Djounova	<b>The sampling frame definition of the buildings with public access to radon concentration surveys</b>	479
Nina Chobanova, Jana Djounova, Kremena Ivanova, Bistra Kunovska	<b>Radon risk communication program for buildings with public access</b>	480
Yucai Mao, Yunxiang Wang, Lei Zhang, Qiuju Guo	<b>Influence of humidity on an electrostatic radon monitor with 16.8L volume</b>	481
Yunxiang Wang, Lei Zhang, Qiuju Guo	<b>Determination of relative degassing rate of an extraction membrane based on a radon-in-water source</b>	482
Robert Lakatoš, Sofija Forkapić, Selena Samardžić, Kristina Bikit-Schroeder, Dušan Mrđa	<b>Statistical analysis of naturally occurring predictors affecting radon concentration in indoor air</b>	483
Ljiljana Gulan, Gordana Milic, Zora Zunic, Bajram Jakupi	<b>Correlation between indoor radon/thoron activity concentrations and gamma dose rates in Central Kosovo and Metohija</b>	484
Ljiljana Gulan, Gordana Milić, Biljana Vučković, Jelena Živković Radovanović, Boris Drobac	<b>Case study of indoor radon measurements in one building</b>	485



**Invited  
Talks**

**A**

## Atmospheric deposition of radionuclides – Assessment based on passive moss biomonitoring

**Marina Frontasyeva**

Joint Institute for Nuclear Research, Dubna, Russia

Terrestrial moss has been used for the monitoring of atmospheric deposition of radionuclides since the late 50s of the last century, mostly for tracing deposition patterns of radionuclides due to technological accidents [1-3]. However, until recent time this aspect of investigations was absent in the UNECE ICP Vegetation (<http://icpvegetation.ceh.ac.uk/>) in spite of the great importance of knowledge on global mixing of long-lived radionuclides in the atmosphere and their deposition after the Chernobyl and Fukushima disasters. In the moss survey 2015/2016, an optional assessment of long-lived radionuclides such as  $^{137}\text{Cs}$  and  $^{210}\text{Pb}$  was suggested [4]. Low background gamma ray spectrometry is provided by several interested laboratories in Russia, Slovakia, Kazakhstan and Serbia, the JINR member-states. The feasibility of moss sampling to assess the atmospheric deposition of radionuclides is discussed and examples from the literature are reviewed.

**Keywords:** Moss, biomonitor, atmospheric deposition, radionuclides, nuclear accidents

### References

1. Svensson, G. K., & Liden, K. (1965). The quantitative accumulation of  $^{95}\text{Zr}$  +  $^{95}\text{Nb}$  and  $^{140}\text{Ba}$  +  $^{140}\text{La}$  in carpets of forest moss. *Health Physics* 11, 1033-1042.
2. Steinnes, E., & Njastad, O. (1993). Use of mosses and lichens for regional mapping of  $^{137}\text{Cs}$  fallout from the Chernobyl Accident. *Journal of Environmental Radioactivity* 21, 65-73.
3. Aleksiyayenak, Yu.V., Frontasyeva, M.V., Florek, M., Sykora, I., Holy, K., Masarik, J., Brestakova, L., Jeskovsky, M., Steinnes, E., Faanhof, A. & Ramatlhabe, K.I. (2013). Distributions of  $^{137}\text{Cs}$  in moss collected from Belarus and Slovakia. *Journal of Environmental Radioactivity* 117, 19-24.
4. <http://icpvegetation.ceh.ac.uk/publications/documents/MosssmonitoringMANUAL-2015-17.07.14.pdf>

## Monte Carlo simulation of early biological damage induced by ionizing radiation at the DNA scale: Overview of the Geant4-DNA project

**Sebastien Incerti<sup>1</sup>, Ivan Petrovic<sup>2</sup>, Aleksandra Ristic-Fira<sup>2</sup>**

<sup>1</sup> CNRS, Bordeaux, France

<sup>2</sup> Vinca Institute of Nuclear Sciences, Belgrade, Serbia

Modeling accurately biological damage induced by ionizing radiation at the scale of the DNA molecule remains a major challenge of today's radiobiology research (1). In order to provide the community with an easily accessible mechanistic simulation platform, the general purpose and open source "Geant4" particle-matter Monte Carlo simulation toolkit (2) is being extended in the framework of the "Geant4-DNA" project (3-7) with a set of functionalities allowing the detailed simulation of particle-matter interactions in biological medium. These functionalities include physical, physico-chemical and chemical processes that can be combined with nanometer size geometries of biological targets in order to predict early DNA damage. We will present an overview of the Geant4-DNA project and discuss on-going developments.

### References

1. "Monte Carlo role in radiobiological modelling of radiotherapy outcomes," Phys. Med. Biol. 57 (2012) R75-R97
2. <http://geant4.org>
3. <http://geant4-dna.org>
4. "Geant4-DNA example applications for track structure simulations in liquid water: a report from the Geant4-DNA Project", Med. Phys. 45 (2018) e722-e739
5. "Track structure modeling in liquid water: A review of the Geant4-DNA very low energy extension of the Geant4 Monte Carlo simulation toolkit," Phys. Med. 31 (2015) 861-874
6. "Comparison of Geant4 very low energy cross section models with experimental data in water," Med. Phys. 37 (2010) 4692-4708
7. "The Geant4-DNA project," Int. J. Model. Simul. Sci. Comput. 1 (2010) 157-178

## Radioecological studies in Norway related to the fallout from the Chernobyl accident

**Eiliv Steinnes**

Norwegian University of Science and Technology, Trondheim, Norway

Precipitation chemistry may vary substantially over short distances, particularly in countries with a complex topography. Not only is the amount of precipitation critically dependent on topography and meteorological factors, but the chemical composition of the falling precipitation may also vary substantially with distance to the ocean. In territories close to the coast the content of elements released from the ocean either as sea salt particles or by biogenic gaseous emission may be orders of magnitude higher in falling precipitation than what is the case in territories situated far from the ocean. Thus the atmospheric deposition of radionuclides at a given site does not only depend on the amount and frequency of precipitation, but perhaps even more on the chemical composition of the precipitation. After the radionuclide reaches the ground, other chemical substances supplied by precipitation may continue to influence its further mobility and biological uptake. Norway is a country where the amount as well as the chemical composition of the precipitation varies substantially over its territory, depending on topography as well as distance from the ocean. This does not only strongly influence the atmospheric supply of chemical substances originating from the ocean, but also the mobility and hence the plant availability of other substances already present in the soil. This may influence the mobility and plant availability of several important radionuclides. Research in Norway has shown that the mobility of  $^{137}\text{Cs}$  from the Chernobyl accident in natural surface soil showed considerable variation over many years following the accident (Gjelsvik and Steinnes, 2013 [1]). Studies of marine influence of surface soil chemistry show that the atmospheric deposition of iodine in Norway and hence the availability of iodine in the soil varies by more than a factor of 10 over a 250-km transect from the ocean (Steinnes and Frontasyeva, 2002 [2]). Although not studied so far, this is likely to affect the fate of newly fallen  $^{131}\text{I}$  fallout and subsequent doses to humans and other biota, and should be considered in case of future nuclear accidents. More over soil chemistry studies in Norway involving strontium indicate that the fate of  $^{89}\text{Sr}$ - $^{90}\text{Sr}$  fallout after a nuclear accident and the resulting radiation doses to humans and other biota may also depend on precipitation chemistry.

**Keywords:** Radionuclides, precipitation chemistry, boreal forest, soil, vegetation

### References

1. Gjelsvik, R., Steinnes, E., 2013. Geographical trends in  $^{137}\text{Cs}$  fallout from the Chernobyl accident and leaching from natural soil in Norway. *Journal of Environmental Radioactivity* 126, 99-103.
2. Steinnes, E., Frontasyeva, M., 2002. Marine gradients of halogens in soil studied by epithermal neutron activation analysis. *Journal of Radioanalytical and Nuclear Chemistry* 253, 173-177.

## Matrix metalloproteinases: From structure to function

**Kristina Gopcevic**

Department of Chemistry, Faculty of Medicine, University of Belgrade, Belgrade, Serbia

Matrix metalloproteinases (MMPs) are calcium-dependent endopeptidases which require coordination of a zinc ion to mediate catalysis and are responsible for remodeling the extracellular matrix (ECM). Such remodeling processes are necessary for a vast and varied array of physiological events, such as wound repair, organismal growth and development, and mediation of immune responses. They have been extensively investigated to decrypt their real pathological role and to design inhibitors as potential drug candidates since the discovery of their involvement in cancer progression about 30 years ago. Dysregulation of MMPs has been observed in an equally diverse index of diseases. From pulmonary disorders to autoimmune diseases to cancer, MMPs have been found to directly contribute to disease progression. Cancer research has traditionally focused largely on cancer cell mutations that confer either proliferative or survival advantages. The tumor microenvironment, particularly the extracellular matrix, is now emerging as a key player in influence cancer progression. MMPs are present in nearly all human cancers; they can be expressed by healthy fibroblasts in the adjacent stroma, cancer-associated fibroblasts, and/or by non-fibroblastic cancer cells. This is of great significance, as MMPs can influence the tumor environment by promoting angiogenesis, tumor growth, and metastasis. Accordingly, MMP expression is tied to tumor aggressiveness, stage, and patient prognosis. Transcription of MMPs is tightly regulated and expression is generally very low. Further regulation of MMP activity occurs by post-translational modification, production of the enzymes as zymogens requiring activation, and coexpression of tissue inhibitors of metalloproteinases (TIMPs). Dysregulation of any of these regulatory mechanisms during pathological conditions may contribute to worsening of disease. Increased expression of MMPs is correlated to increased cancer cell proliferation and an increase in tumor size. Several MMPs have been shown to drive cell migration and invasion through the basement membrane. MMPs have been shown to contribute to angiogenesis by degrading basement membranes, allowing for endothelial cell invasion. Nearly every member of the MMP family has been found to be dysregulated in human cancers, with MMP-1,-2,-7,-9,-13, and -14 at the top of this list. Together, these factors all point to MMPs as attractive targets for therapeutics. The dysregulation of MMP activities, especially in early cancer stages, still raises great interest for MMPs as therapeutic targets, despite the failure of the early clinical trials using broad spectrum MMP inhibitors. This review will focus on the role of MMPase in breast cancer and colorectal cancer.

## Studies on DNA damage and repair in cells exposed to mixed beams of different ionising radiation qualities

**Beata Brzozowska-Wardecka<sup>1</sup>, Alice Sollazzo<sup>2</sup>, Lei Cheng<sup>2</sup>,  
Maciej Galecki<sup>1</sup>, Adrianna Tartas<sup>1</sup>, Lovisa Lundholm<sup>2</sup>, Andrzej Wójcik<sup>2,3</sup>**

<sup>1</sup> Biomedical Physics Division, Faculty of Physics, University of Warsaw, Poland

<sup>2</sup> Department of Molecular Bioscience, Centre for Radiation Protection Research, The Wenner-Gren Institute, Stockholm University, Sweden

<sup>3</sup> Department of Radiobiology and Immunology, Institute of Biology, Jan Kochanowski University, Kielce, Poland

A particular problem of modern external beam radiotherapy like IMRT and proton therapy is exposure of patients to scattered neutrons with a relative biological effectiveness (RBE) higher than X-rays. The interesting question is if there is an additive or synergistic effect of high and low linear energy transfer (LET) radiations when given together. If they act additively, then the risk of cancer can be deduced from the results of exposure to the single agents. Otherwise, RBE values must be generated for the mixed exposure scenarios or corrected to account for the synergism.

The goal of this study was to analyse the kinetics of formation and repair of ionising radiation-induced foci (IRIF) in cells exposed to alpha particles, X-rays and a mixed beam of both radiations. To this end human cells were transfected with plasmids coding for the DNA repair protein 53BP1 that are tagged with the green fluorescent protein (GFP). Cells were exposed to mixed beams in a dedicated exposure facility built at Stockholm University (SU). The facility is composed of a 50 MBq Am-241 alpha source and an YXLON 200 X-rays source. The alpha source is mounted on an inverted plate in a custom-designed irradiator which is kept inside a 37°C cell incubator.

Spatiotemporal dynamics of 53BP1 foci formation and repair were recorded by time-lapse photography and image analysis. The distributions of cell frequencies with the specific size of foci and the size of foci itself were analysed. Moreover, Monte Carlo simulations (the PARTRAC code) were used not only for calculating radiation hits, but also for the biological damage in the DNA in terms of single and double strand breaks.

Exposure to a mixed beam induces complex DNA damage above the level expected from the additive action of both radiations. Clustered DNA damage poses serious problems for the DNA repair and error-prone repair of DNA damage is associated with cancer induction. Increased damage complexity following exposure to mixed beams will suggest a higher than expected risk of cancer induction in modern radiotherapy. The results are consistent with the previous studies carried out at SU with different cell types and different biological assays. A synergistic interaction of the beam components was observed at the level of micronuclei, gammaH2AX foci and chromosomal aberrations.

## Towards ELF magnetic fields for the treatment of cancer

Igor Belyaev<sup>1</sup>, Leonardo Makinistian<sup>2</sup>

<sup>1</sup> Department of Radiobiology, Cancer Research Institute, Biomedical Research Center, Slovak Academy of Sciences, Bratislava, Slovakia

<sup>2</sup> Department of Physics and Instituto de Física Aplicada, Universidad Nacional de San Luis-CONICET, San Luis, Argentina

Responses of living systems to weak electromagnetic fields (EMF) of extremely low frequencies (ELF, 1-300 Hz) have been investigated for decades. In 2002, ELF was classified as possibly carcinogenic to humans, Group 2B, by the International Agency for Research on Cancer (IARC). ELF fields higher than 0.3  $\mu\text{T}$  consistently correlated with increased risks of childhood leukemia. Recent data indicated an increased risk in late stage (promotion/progression) of astrocytoma grade IV for occupational ELF exposure. On the other hand, numerous studies performed in the former Soviet Union countries and Eastern Europe have shown that ELF can be used as a therapeutic modality. A variety of diseases, including cancer, have been treated with ELF in these countries. In the USA, the usage of ELF has been approved and used for bone healing.

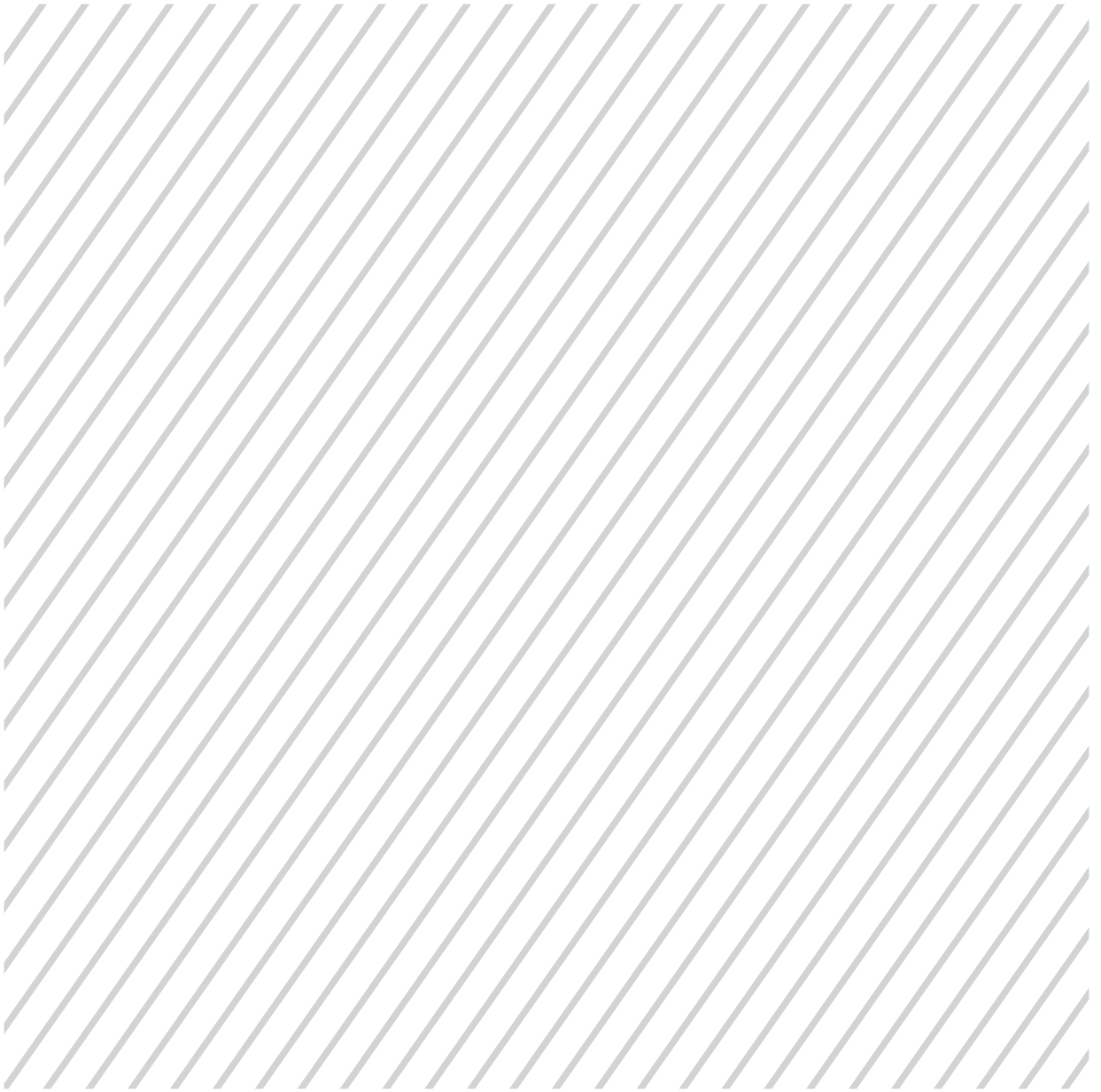
The body of data obtained by different research groups over the world clearly shows that weak ELF result in biological effects only under specific conditions of exposure. This specificity deals with both physical and biological variables. All these conditions must be controlled in replication studies; otherwise reproducibility of ELF effects can be very poor.

It was found in a number of studies that growth of human cancer cells of different origin can be inhibited by weak ELF under specific conditions of exposure. Moreover, inhibition of tumor growth was reported in animal studies and a synergy of ELF exposure with standard therapeutic modalities was observed both in vitro and in vivo. Importantly, normal cells were significantly less responsive to ELF than cancer cells suggesting a clear advantage for minimizing side-effects.

Several physical mechanisms were suggested to explain the observed dependence of ELF effects on physical variables. However, these mechanisms do not provide exact values of amplitude and frequency windows, in which the ELF effects are often observed. Thus, screening through the different parameters of exposure remains an important issue.

Based on our studies and data available in the literature we conclude that weak ELF can affect biological systems in dependence on a number of variables. These variables define the value of the ELF effect and its biological significance resulting in either detrimental or beneficial outcome. Our analysis of the available studies suggests the convenience of screening for the search of effective ELF parameters for further application in cancer treatments.

**Acknowledgments:** LM thanks financial support from the Universidad Nacional de San Luis, Argentina (grant PROICO 02-0518). IB was supported by the Structural Funds of EU (Protonbeam, ITMS: 26220220200), the Slovak Research and Development Agency (APVV-15-0250), the Scientific Grant Agency (VEGA 2/0089/18) of Slovak Republic.



**Plenary  
Talk**

**B**

## Temporal and spatial distribution of the beryllium-7 activity concentration in the surface air in Europe

**Jelena Ajtić<sup>1</sup>, Vladimir Djurdjevic<sup>2</sup>, Darko Sarvan<sup>1</sup>, Erika Brattich<sup>3</sup>, Miguel-Angel Hernández-Ceballos<sup>4</sup>, Benjamin Zorko<sup>5</sup>, Dragana Todorović<sup>6</sup>**

1 University of Belgrade, Faculty of Veterinary Medicine, Belgrade, Serbia

2 University of Belgrade, Faculty of Physics, Institute of Meteorology, Belgrade, Serbia

3 Alma Mater Studiorum University of Bologna, Department of Physics and Astronomy, Bologna, Italy

4 European Commission, Joint Research Centre, Knowledge for Nuclear Security and Safety Unit

Radioactivity Environmental Monitoring Group, Ispra, Italy

5 Jožef Stefan Institute, Ljubljana, Slovenia

6 University of Belgrade, Vinča Institute of Nuclear Sciences, Belgrade, Serbia

Since 2015, a scientific collaboration network between the University of Belgrade, the University of Bologna and the Radioactive Monitoring Environmental (REM) group of the European Commission Joint Research Centre – Ispra, has addressed the characterisation of the beryllium-7 concentration in the surface air recorded across Europe, and its link with meteorological conditions. A set of studies carried out over this period has been based on the beryllium-7 activity measurements collected and validated by the Radioactivity Monitoring Environmental Data Bank (REMdb) (<https://rem.jrc.ec.europa.eu/RemWeb/Index.aspx>). REMdb makes accessible and understandable to a wider audience radioactivity measurements made by all European Member States in the air, water, milk, and mixed diet. Thus, the scientific community is given research opportunities to exploit a unique collection of almost 5 million environmental radioactivity measurements taken across Europe since 1988. Our collaboration has also investigated other sets of multidecadal beryllium-7 activity concentrations: 1) sampled in Serbia and measured at the Vinča Institute of Nuclear Sciences, and 2) sampled in Slovenia and measured at the Jožef Stefan Institute.

This paper compiles our current understanding of the abundance of beryllium-7, which is a naturally occurring radionuclide, in the surface air in Europe. Beryllium-7 is produced in the upper troposphere-lower stratosphere (UT-LS) region, where it attaches to fine aerosols and is then transported through the atmosphere. Due to its origin, it is considered a good tracer of air mass history, and it can be used as an indicator of different processes in the atmosphere, such as vertical exchange across the UT-LS region. Based on a number of our previous studies, we here give an overall picture of the beryllium-7 activity concentration distribution in Europe. We describe its general decrease from the south of the continent towards the polar region, different periodicities and outliers identified in the time series, and we make an effort to identify the underlying driving mechanisms that give rise to this distribution. We also look into temporal trends that show a statistically significant increase in the beryllium-7 surface concentration. Since temperature is one of the major factors that influence this radionuclide's abundance in the air, we speculate that the trends are affected by the global increase in temperature. For that reason, we intend to further inquire into the possibility of using the beryllium-7 surface concentration as an indicator of climate change.



**Biochemistry**  
**01**

## Free fatty acids and hepatic activity in Type 2 diabetes

Šaćira Mandal<sup>1</sup>, Adlija Čaušević<sup>1</sup>, Sabina Semiz<sup>2</sup>

<sup>1</sup> University of Sarajevo, Faculty of Pharmacy, Sarajevo, Bosnia and Herzegovina

<sup>2</sup> Faculty of Engineering and Natural Sciences, International University of Sarajevo, Sarajevo, Bosnia and Herzegovina

Metabolic derangements in Type 2 diabetes mellitus (T2D) are associated primarily with the carbohydrate and lipid levels disturbances. Increased flow of free fatty acids (FFAs) into the blood that is coming from the adipocytes as well as an elevated flux of FFAs from de novo lipid synthesis in the liver contribute to these metabolic disturbances. Previous studies suggested a strong association of the hepatic activity of certain enzymes, such as aspartate and alanine transferase (AST, ALT), gamma glutamyl transpeptidase (GGT), and alkaline phosphatase (AP) with the progression of T2D. In this study, we examined the potential association of the hepatic activities of the liver enzymes and FFAs levels in T2D. Analysis of the activities of ALT, AST, GGT and AP, as well levels of FFAs, fasting plasma glucose (FPG), and lipid profile was performed in 40 healthy control and 71 age-matched diabetic subjects. All participants were free of hepatitis, viral infections or active liver damage. Our results showed a positive association between levels of palmitic and oleic acids with ALT activity ( $p < 0.05$ ), while the activity of GGT was significantly associated with the levels of palmitic, stearic, and oleic fatty acids ( $p < 0.01$ ). Our data suggest that an elevation of free fatty acid levels and the hepatic fat accumulation in insulin-resistant conditions affect the hepatic enzymes activities, which might contribute further to the progression of Type 2 diabetes and its complications.

## UVB irradiation impact on chlorophyll degradation in methanol/water solutions monitored by UHPLCDAD-ESIMS analysis

**Sanja Petrovic, Jelena Zvezdanovic, Sasa Savic,  
Dragan Cvetkovic, Aleksandar Lazarevic, Dejan Markovic**

Faculty of Technology, University of Niš, Leskovac, Serbia

Chlorophylls - photosynthetic pigments are involved in collection and light conversion processes in photosynthetic organisms. Chlorophylls primarily absorb in the Vis region and their composition is significantly altered (e.g. photodegraded) when exposed to UV-light in vivo and in vitro. In this work, chlorophyll degradation induced by continuous UV-B irradiation in the aqueous mediums (with 10%, 30% and 50% of methanol) was investigated using the ultrahigh liquid chromatography coupled with diode array and electrospray ionization mass spectrometry detectors (UHPLCDAD-ESIMS). Continuous UV-B irradiation of chlorophylls in aqueous mediums (10%, 30% and 50% methanol) was performed in cylindrical photochemical reactor "Rayonnet", with 9 symmetrically placed lamps, with emission maximum in UV-B subrange at 300 nm. The total emitted measured energy flux was 14 W/m<sup>2</sup>. The degradation was governed in the period of 30 minutes: longer UV-B irradiation induced higher chlorophyll degradation and accordingly higher amounts of products formation. Main UV-B-induced products of chlorophyll in the aqueous mediums were hydroxy-pheophytin a, pheophytin a and hydroxy-lactone-pheophytin a, accompanied with the corresponding epimers. Degradation of chlorophylls after 30 minutes of UVB irradiation was 50, 34 and 24%, at the methanol/water solutions ratio of 10/90, 30/70 and 50/50, respectively. Chlorophylls aggregation dominant in the aqueous medium with the highest methanol content (50%) play a protective role against the UV-B irradiation.

**Keywords:** Chlorophyll, UVB, irradiation, UHPLCDAD-ESIMS

**Acknowledgments:** This work was supported under the Project of the Ministry of Education, Science and Technological Development of the Republic of Serbia no. TR-34012.

## Influence of different heavy metal ions on bacterial strain *P. aeruginosa san-ai* and correlation with produced exopolysaccharide biosurfactants

**Nataša Avramović, Lidija Izrael-Zivković, Ivanka Karadžić**

Faculty of Medicine, Department of Chemistry in Medicine, University of Belgrade, Belgrade, Serbia

*P. aeruginosa san-ai* strain was isolated from water-soluble, mineral cutting oil (San-ai oil-Tokyo) and it can ability to survive the extreme conditions such as high pH (pH=10) and high temperature (>40 °C). Environmental adaptability of *P. aeruginosa san-ai* to extreme conditions shows its potential for heavy metals tolerance and exopolysaccharide (EPS) biosurfactant production with possible application in heavy metal bioremediation. *P. aeruginosa san-ai* produces diverse secondary metabolites including exopolysaccharides (EPSs), rhamnolipids (RLs), enzymes, siderophores.

*P. aeruginosa san-ai* produces alginate as the main acidic EPS. Alginate is a polymeric high-molecular mass biosurfactant containing large number of disaccharide units composed of  $\beta$ -1,4-D-mannuronic and L-guluronic acids linked via  $\beta$ -1,4-glycosidic bonds. This polysaccharide is O-acetylated at some of the C-2 and C-3 carbons of the mannuronic acid residues.

Toxicity of heavy metal ions for humans and microorganisms originates from their high solubility, rapid transport through the biological membranes, possibility to bind with intracellular proteins and nucleic acids by coordination in complexes, ability to disturb redox homeostasis and to induce oxidative stress. Some microorganisms can tolerate heavy metal ions using plasmid mediated efflux system, absorbing heavy metals to their cell wall in the form of insoluble salts by precipitation and binding metal ions to biological complexing agents such as exopolysaccharides (EPS) biosurfactants. The goal of this work was study the toxic effect of different heavy metal ions (Pb(II), Cr(VI), Cu(II), Zn(II) and Hg(II)) on bacterial strain *P. aeruginosa san-ai* and correlation with of its naturally produced exopolysaccharide biosurfactants (EPS) that can find potential application in bioremediation.

Influence of different concentrations of heavy metal ions (0.1-7 mM) on *P. aeruginosa san-ai* grown in LB medium compared to control (LB medium) were studied by MIC determination in the following order: Pb (II) (>6 mM) > Cr(VI) (>5 mM)  $\cong$  Cu(II) (>5 mM)  $\cong$  Zn(II) (>5 mM) > Hg(II) (>0.1 mM). EPS production by *P. aeruginosa san-ai* in the presence of sublethal heavy metal ions concentrations compared to control (LB medium) showed a correlation with their toxicity showing maximum of EPS production for the most toxic Hg(II) and minimum for the least toxic Pb(II) ions. IR spectra of EPS of control and sublethal heavy metal ions-amended samples obtained by *P. aeruginosa san-ai* grown in LB medium indicate potential application of EPS in heavy metals bioremediation due to the splitting of both  $\nu_{s}(\text{COO})$  and  $\nu_{as}(\text{COO})$  bands in heavy metals-amended samples into two new bands indicating coordination of heavy metal ions to carboxylic groups of EPS.

## Combined effects of heavy metal ions and antibiotics on bacterial strain *P. aeruginosa san-ai*

Nataša Avramović, Lidija Izrael-Zivković, Ivanka Karadžić

Faculty of Medicine, Department of Chemistry in Medicine, University of Belgrade, Belgrade, Serbia

*P. aeruginosa san-ai* strain belongs to extreme diverse bacterial genus *Pseudomonas* and it is common in wide range of environmental habitats. *P. aeruginosa san-ai* has ability to adapt, survive and growth in extreme environmental conditions due to its metabolic diversity. Enzymes, exopolysaccharides (EPSs), rhamnolipids (RLs), siderophores are diverse secondary metabolites of *P. aeruginosa san-ai* and these virulence factors are responsible for bacterial adherence, biofilm formation and maintenance, infection development and antibiotic resistance. Siderophores (pyoverdine, pyocyanin, pyochelin) are small molecules with important role as metal chelators. Beside their essential function to transport iron, their functions are antibiotic activity, ability to bind variety of other metals, especially heavy metals, act as signaling molecules and regulation of oxidative stress.

There are three basic mechanisms by which bacterial strain *P.aeruginosa san-ai* resist the action of antimicrobial agents: restricted uptake and efflux, drug inactivation and changes in targets. The innate resistance of *P. aeruginosa san-ai* to all classes of antibiotics has generally been attributed to the low permeability of cell wall. Failure of antibiotics to accumulate within the organism is due to a combination of restricted permeability of the outer membrane and the efficient removal of antibiotic molecules that do penetrate by the action of efflux pumps. The aminoglycosides (e.g. amikacin) inhibit protein synthesis by binding to the 30S subunit of the ribosome while  $\beta$ -lactams (e.g. amoxicillin, ceftazidime) inhibit the peptidoglycan-assembling transpeptidases located on the outer cytoplasmic membrane. Antibiotics and heavy metals are two common environmental pollutants, hazardous to health and ecological safety. Although their individual effects on organisms were well known in many studies, there is still not enough information about their combined effects.

In this work, we have studied resistance of *P. aeruginosa san-ai* to four antibiotics (amikacin, ceftazidime, amoxicillin and tetracycline) and six heavy metal ions (Pb(II), Cu(II), Zn(II), Cr(VI), Cd(II) and Hg(II)) used different concentrations. Bacterial growth of *P. aeruginosa san-ai* in LB medium without heavy metals (control) shows intermediate sensitivity to antibiotics amikacin and ceftazidime and resistance to antibiotics amoxicillin and tetracycline. Compared to control, presence of all these heavy metals showed synergistic effects on bacterial sensitivity to antibiotics amikacin and ceftazidime (increase of inhibition zone diameter) in dependence of metal concentrations as well as resistance to antibiotics amoxicillin and tetracycline, except in the presence of Pb(II) ions. Actually, in the presence of different concentrations of Pb(II) ions (2-100 mg/L), it is observed a small positive effect on bacterial antibiotic sensitivity to antibiotics amoxicillin and tetracycline with an increased inhibition zone compared to control. Siderophores (pyoverdine, pyocyanin, pyochelin) produced by *P. aeruginosa san-ai* in the presence sublethal concentrations of these six heavy metal ions (Pb(II), Cu(II), Zn(II), Cr(VI), Cd(II) and Hg(II)) were determined and it is observed the down-regulation of all siderophores except in the presence of Pb(II) ions. Up-regulation of all siderophores can be correlated with observed bacterial sensitivity to antibiotics amoxicillin and tetracycline in the presence of Pb(II) ions due to the impact of siderophores in antibiotic activity.

## Identification of degradation products of quercetin in reaction with horseradish peroxidase by UHPLC-DAD-HESI-MS/MS method

**Sasa Savic, Sanja Petrovic, Zivomir Petronijevic**

University of Nis, Faculty of Technology, Leskovac, Serbia

Quercetin (3,3',4',5,7-pentahydroxyflavone) is one of the most known polyphenols of plant origin, widely used in human nutrition. Due to its antioxidant properties, quercetin is usually used as a food supplement and it is recommended for the prevention and suppression of many diseases that are closely related to oxidative stress. However, although quercetin has high antioxidant activity, in some cases, oxidation of quercetin, as well as other phenolic compounds, in plants by some oxydases (e.g. peroxidase and polyphenol oxydases) can take very easily. Obtained products of flavonoid oxidation are often highly reactive species (semiquinones and quinones) that could oxidase other polyphenols, leading to the heterogenous polymers formation. Bearing in mind that all reactive oxygen species (ROS) represent a risk for live systems, it seems nesesity to identify products of degradation. Therefore, the aim of present study was to investigate in vitro quercetin oxidation by horseradish peroxidase and to identify obtained degradation products. For identification of degradation products in reaction of quercetin and peroxidase liquid chromatography tandem mass spectrometry was used. The completly new method was developed. The main degradation products identified were: quercetin quinones and their derivatives, phloroglucinol carboxylic acid, protocatechuic acid, quercetin heterodimer and its derivatives.



**Bioinformatics**

**02**

## Cross-sectional automatic assessment of the degree of sagittal suture closure on $\mu$ CT volumetric images of dry skulls applying artificial neural network and machine learning techniques

Silviya Nikolova<sup>1</sup>, Diana Toneva<sup>1</sup>,  
Andrey Gizdov<sup>2</sup>, Stanislav Harizanov<sup>3,4</sup>, Ivan Georgiev<sup>3,4</sup>

<sup>1</sup> Institute of Experimental Morphology, Pathology and Anthropology with Museum, Bulgarian Academy of Sciences, Sofia, Bulgaria

<sup>2</sup> National High School of Mathematics and Natural Sciences, Sofia, Bulgaria

<sup>3</sup> Institute of Information and Communication Technologies, Bulgarian Academy of Sciences, Sofia, Bulgaria

<sup>4</sup> Institute of Mathematics and Informatics, Bulgarian Academy of Sciences, Sofia, Bulgaria

**Background.** The sagittal suture (SS) is a midline suture overlaying the midline dural fiber tract. The SS is considered as the initial site where suture closure commences, as well as the most frequent initial spot for isolated craniosynostosis resulting in scaphocephaly. In this study we aim to develop and implement an algorithm for unbiased automatic assessment of the SS closure degree. Our further goal is to apply this algorithm on larger sample in order to objectively assess the relation of SS closure to aging.

**Materials and Methods.** For the purpose of the study, we generated volumetric images of 9 skulls of contemporary adult Bulgarian males with known age-at-death (21 ÷ 58 years, average 37 years) using industrial  $\mu$ CT system Nikon XT H 225. The scanning parameters were adjusted using the Inspect-X software. The obtained spatial resolution was 97.5  $\mu$ m as the voxels were isotropic. The reconstruction was performed using CT Pro 3D software. Volumetric rendering and further exportation as TIFF series were accomplished on VG Studio Max 2.2. software. The algorithm for automatic assessment of the SS closure degree consisted of several stages realized in MatLab. The first one was generation of downscaled, triangulated version of the skull surface, centered at the SS. For this purpose a set of 350 points along the SS were manually defined and those points were joined in a “smallest cost path” with respect to a given criteria. Next, the normal vector to the skull surface at each marking point was calculated and the generated local cross-sectional image was oriented in the normal plane. The SS was manually outlined on cross-sectional tomograms of 4 skulls (4 x 350 = 1400 in number), which were used as a dictionary for training an artificial neural network for SS detection. The other 5 skulls were used for algorithm verification. The average SS width for the detected pixels was calculated representing the amount of gray pixels (sutural space) towards the white ones (sutural edges). The two phases were generated, using fuzzy K-means clustering. Further information for the SS closure was assessed by “bone cross ratio” measuring the projection of detected suture towards the whole bone thickness.

**Results and Conclusion.** The clear view and measurable distance between the sutural edges are important for an accurate analysis. Industrial  $\mu$ CT generates volumetric images with high resolution, which makes the data extraction relatively easy, and does not require additional image processing to improve the data quality. The developed algorithm for automatic assessment of the SS closure on such images proved to be useful and reliable. It is a fundamental step for further unbiased assessment of relation between SS closure and aging.

**Acknowledgments:** This study was supported by the National Science Fund of Bulgaria, grant DN01/15-20.12.2016.

## Excavation of the most distinctive characteristics in the metopic skull configuration by applying data mining techniques

Diana Toneva<sup>1</sup>, Silviya Nikolova<sup>1</sup>,  
Gennady Agre<sup>2</sup>, Ivan Georgiev<sup>2,3</sup>, Nikolai Lazarov<sup>4,5</sup>

1 Institute of Experimental Morphology, Pathology and Anthropology with Museum, Bulgarian Academy of Sciences, Sofia, Bulgaria

2 Institute of Information and Communication Technologies, Bulgarian Academy of Sciences, Sofia, Bulgaria

3 Institute of Mathematics and Informatics, Bulgarian Academy of Sciences, Sofia, Bulgaria

4 Medical University of Sofia, Sofia, Bulgaria

5 Institute of Neurobiology, Bulgarian Academy of Sciences, Sofia, Bulgaria

**Background.** The metopic suture is determined by the anterior dural fibre tract and forms during the uterine development between the growing halves of the frontal bones. It runs from *nasion* to anterior fontanelle and allows frontal part of the neurocranium to grow in width. The metopic suture is the first suture to close physiologically usually to the end of the first or second postnatal year. The non-fusion leads to condition known as *metopism*, in which metopic suture persists in adulthood preserving the bipartition of the frontal bone. The *metopism* is also reported to be related to specific construction of the neurocranium. In this study we aimed to excavate the most distinctive characteristics in the metopic skull configuration, applying data mining techniques. Therefore, we generated volumetric images of skulls in order to record external and internal variables.

**Materials and Methods.** A total of 175 contemporary skulls of adult Bulgarian males were studied. The skulls were divided into two series based on persistence of metopic suture, which was set as a class attribute: control series (n = 100, class 0) and metopic series (n = 75, class 1). All of the skulls were scanned with a hand-held laser scanner CreaformVIUscan and polygonal models were generated. For 150 of the skulls, an industrial  $\mu$ CT scanning using Nikon XT H 225 system was performed and volumetric images were generated. The obtained spatial resolution was 97.5  $\mu$ m as the voxels were isotropic. The digital morphometry was accomplished both on polygonal models and on cross-sectional tomograms. A decision tree model was generated by means of J48 algorithm, a Weka implementation of the version 8 of C4.5 algorithm.

**Results and Conclusion.** Mining the collected data showed that the major distinctive peculiarities in the configuration of the metopic skull are related to the dimensions of the frontal bone, which was considerably wider but shorter.

**Acknowledgments:** This work was supported by the Bulgarian National Science Fund, Grant DN11/09-15.12.2017.

## **“Matrix” – A robot control program to determine the ion beam profile**

**Joanna Czub**

Jan Kochanowski University, Kielce, Poland

The robot with the semiconductor detector which is used to record the intensity of the ion beam, is a part of the experimental system existing in the Heavy Ion Laboratory at University of Warsaw, Warsaw, Poland designed to irradiation of live biological cells. The robot's standard task is to change the position of the semiconductor detector attached to it. The position change occurs within the size of the ion beam and is called the beam profile measurement. A computer program, using LabWindows software, was written to correctly control the robot movements. The program called “Matrix” allows to enter measurement positions within the size of the beam with any step value, graphical visualization of measured and unmeasured positions, presentation of the speed value, presenting the current position of robot in both numerical and graphical form.

## **“Stolik” – A computer program to control the irradiation of biological material in HIL**

**Joanna Czub**

Jan Kochanowski University, Kielce, Poland

The experimental system for radiobiological purposes, using the ion beams which are accelerated by the U200P cyclotron, is located in the Heavy Ion Laboratory (HIL) at the University of Warsaw, Warsaw, Poland. In this system, the ion beam has the size of a square with dimensions: 1 cm by 1 cm, while the Petri dish with cells has a diameter of 4.8 cm. This mismatch of two sizes forced the solution to move the Petri dish relative to the stable ion beam. This movement is carried out by an electronically controlled robot. The change of position occurs as a result of the robot's registration of the electronic pulse which is emitted by the beam intensity detection system. “Stolik” is self-developed computer program written in the LabWindows development environment. The goal of the program is to manage all robot activities. Thanks to the program one can enter basic parameters initiating the robot operation, setting in the position considered to be the beginning of movement, setting the trajectory of the robot movement with its graphic visualization and uploading it into the robot's memory, stopping the robot at any time.



**Biomaterials**

**03**

## Modern nanomaterials for cell protection from UV-initiated damage

**Katarzyna Roszek<sup>1</sup>, Paulina Bolibok<sup>2</sup>,  
Monika Bal<sup>2</sup>, Artur Terzyk<sup>2</sup>, Marek Wiśniewski<sup>2</sup>**

<sup>1</sup> Department of Biochemistry, Faculty of Biology and Environmental Protection, Nicolaus Copernicus University in Torun, Torun, Poland

<sup>2</sup> Faculty of Chemistry, Physicochemistry of Carbon Materials Research Group, Nicolaus Copernicus University in Torun, Torun, Poland

UV-mediated damage in different cell types includes generation of reactive oxygen species (ROS) that oxidize cell proteins and lipids, and creation of variety of mutagenic and cytotoxic DNA lesions. When unrepaired, lesions contribute to mutations and cancer cell development.

The intensifying production of modern nanomaterials results in their numerous novel applications. We have compared three nanostructured materials: graphene oxide (GO), titanium dioxide (TiO<sub>2</sub>) and cysteine-based metal-biomolecules frameworks (MBioFs) in terms of their anti-oxidative and anti-UV properties. GO seems to be most promising due to its multifaceted action as physical barrier, ROS-scavenger and biological defense activator. On the other hand, MBioFs can serve as inducers of biological response, *inter alia* increasing the enzymatic and non-enzymatic anti-oxidative potential of cells. We have tested their unique properties in mouse 3T3 fibroblasts *in vitro* culture exposed to UV radiation. Treatment of cultured fibroblasts with GO, TiO<sub>2</sub> and MBioFs at concentration 100 µg/mL resulted in increasing the cell viability after UV exposure by 15 to even 80 %, when compared to the untreated cells. In general, these effects were time- and concentration-dependent. We have also compared the total anti-oxidative capacity of fibroblasts and the activity of anti-oxidative enzymes, including catalase.

Our results shed more light on anti-oxidative and anti-UV properties of nanostructured materials and will facilitate their future biomedical applications for cell protection from UV-mediated damage.

**Acknowledgments:** This work was supported by the Polish National Science Centre (NCN) grant OPUS 9 no. 2015/17/B/ST5/01446, and PRELUDIUM 14 no. 2017/27/N/ST5/02696

## Skin UV protection – new application of graphene oxide

**Paulina Bolibok<sup>1</sup>, Katarzyna Roszek<sup>2</sup>, Marek Wiśniewski<sup>1</sup>**

<sup>1</sup> Faculty of Chemistry, Physicochemistry of Carbon Materials Research Group, Nicolaus Copernicus University in Toruń, Toruń, Poland

<sup>2</sup> Department of Biochemistry, Faculty of Biology and Environmental Protection, Nicolaus Copernicus University in Toruń, Toruń, Poland

Although the photoprotection is not a new problem, the perfect UV filter (the compound, the material or the substance) has not yet been discovered. Due to its high biocompatibility, carbonaceous materials are increasingly common ingredients in cosmetic products.

The aim of the presented studies was determination of graphene oxide (GO) photoprotective properties.

First, the synthesis of GO was performed. After the characterization of obtained material, the determination of its spectroscopic properties due to the irradiation process, was carried out. Based on these, the hypothesis suggested triple mechanisms of photoprotection, was formulated:

- physical (physical barrier that disperse and absorb UV radiation);
- biological (to stimulate the cells for increased defense);
- chemical (antioxidant, free radical scavenger).

The studies were executed in different variants (three irradiation times, three GO concentration and addition of GO at different stages of the experiment). In most of the cases, a noticeable increase of cells proliferation (relative to control) was observed. The obtained results showed that GO is promising material for the UV protection.

**Acknowledgments:** This work was supported by the Polish National Science Centre (NCN) grant PRELUDIUM 14 no. 2017/27/N/ST5/02696.

## Effects of water on thin films consisting of biomolecules and 2D-materials

**Jasna Vujin<sup>1</sup>, Weixin Huang<sup>2</sup>, Sylwia Ptasinska<sup>3</sup>, Radmila Panajotovic<sup>1</sup>**

<sup>1</sup> Institute of Physics, Belgrade, Serbia

<sup>2</sup> Stanford University, Stanford, United States

<sup>3</sup> University of Notre Dame, South Bend, United States

One of the hottest research topics in the field of 2D-materials is the one concerning their heterostructures with biomolecules. They can serve as scaffolds for growing cells, or bio-chemical sensors, for example. The most popular 2D-material, graphene, and transition metal dichalogenides( $WS_2$ ) in combination with various biomolecules (lipids, biopolymers, amino acid, protein...) attracted considerable attention as active components of organic electronic devices. A relatively simple and cheap method of producing thin graphene films is from the liquid phase. The ever present question of how water/humidity from air or biomolecule aqueous solution affects the properties of these heterostructures is very difficult to answer because of the complicated interplay between these components.

In our experiment, we first exposed bare graphene and  $WS_2$  thin films to water in the controlled environment. Then we did the same experiment with the lipid layer (DPPC dipalmitoyl-sn-glycero-phosphotidilcholine), by collecting the XPS (X-ray Photo-Electron) spectra. In order to examine electrical properties of such heterostructures in ambient condition, we measured the current-voltage response after the deposition of aqueous solution of amino acids, protein and cell culture. In addition, we collected the information about the topography of our heterostructures and Raman.

## Application of 2D-materials in building biomolecular heterostructures

**Jasna Vujin<sup>1</sup>, Martina Gilić<sup>2</sup>, Radmila Panajotović<sup>1</sup>**

<sup>1</sup> Laboratory for Graphene, Other 2D-Materials and Ordered Nanostructures, Institute of Physics, Belgrade, Serbia

<sup>2</sup> Laboratory for Electronic Materials, Institute of Physics, Belgrade, Serbia

A quest for non-toxic, easily produced and inexpensive materials with satisfactory chemical (inertness, resistance to degradation) and physical (mechanical robustness, flexibility) properties, that can be used in combination with biological molecules and cells, was greatly accomplished by the discovery of atomically thin 2D-materials. Their exceptional mechanical and tunable electrical properties offer an excellent base for building various types of bio-chemical sensors, growth of self-assembled bio-membranes, and scaffolds for biological tissue engineering. As the most popular of these materials, graphene has become widely used, in various forms – as nanotubes, nanoflakes, nanopaticles, etc. Others, like MoS<sub>2</sub> and WS<sub>2</sub>, have gained their popularity as active elements of biochemical sensors, mostly due to their tunable (semi) conductivity after physi- or chemisorption on their surface. In both conductive (graphene) and semi-conductive (MoS<sub>2</sub> and WS<sub>2</sub>) thin films of 2D-materials it is necessary to assess their surface morphology, and the chemical and physical changes in combination with water, and biological molecules, such as aminoacids, proteins, lipids, etc. In order to do this, we used several experimental methods – AFM, KPFM Raman and FT-IR spectroscopy. We used graphene and WS<sub>2</sub> thin films for deposition of two different amino acids – cystein, arginine – and sphingomyelin – playing an important role in neuro-signalling and in the structure of neuron's axon sheath.



**Biomedical  
Engineering**

**04**

## **Design of 3D polymeric bone tissue scaffolds for optimal degradation**

**Remon Pop-Iliev, Pedram Karimipour Fard, Ghaus Rizvi**

UOIT – University of Ontario Institute of Technology, Oshawa, Canada

Artificial polymeric biodegradable bone tissue scaffolds are deliberately designed to acquire a 3D structure that mimics the characteristics of natural tissue analogs. Multiple Polylactic acid (PLA) based 3D structures were manufactured to mimic a spongy bone tissue. A mammalian cell line in a proper medium was employed inside a carbon dioxide incubator by using 5% CO<sub>2</sub> to simulate in-vitro environment and assess cell attachment to the scaffold. Mammalian cells are traveling through the 3D scaffolds and attach to its internal structure as well as the surface of the pores. Conventional methods to assess biodegradation rate patterns and cell attachment of 2D structures exist, however they lack the ability to assess the internal structure degradation rate patterns of 3D printed scaffolds. This paper focuses on evaluating the structure, the cell attachment, and the biodegradation rate patterns of 3D polymeric bone tissue scaffolds made by additive manufacturing methods through visualization and structure assessment utilizing the micro computed tomography technique. The respective experimental results improved significantly the understanding of the governing variables and parameters for designing a 3D bone tissue scaffold that would degrade in the most optimal rate and pattern.

## Classification of the hyperspectral image of a basal cell carcinoma using artificial intelligence

**Dragos Manea<sup>1,2</sup>, Mihaela Antonina Calin<sup>1</sup>,  
Sorin Viorel Parasca<sup>3</sup>, Andrei Museteanu<sup>3</sup>**

1 National Institute of Research and Development for Optoelectronics – INOE 2000, Magurele, Romania

2 The University of Bucharest, Faculty of Physics, Magurele, Romania

3 Emergency Clinical Hospital for Plastic, Reconstructive Surgery, and Burns, Bucharest, Romania

One of the most common human malignancy is skin cancer, diagnosed primarily visually, starting with an initial clinical examination, followed by dermoscopic analysis, a biopsy and histopathological examination. Automatic classification of skin lesions using images is a difficult task due to the fine variability of skin lesions. However optical diagnosis evolution climbed vertiginously in the past decade due to the advances in imaging sensors technology and increased computational performances. The techniques that took the most advantage from this increased imaging quality and computational power were the technique based on artificial intelligence. Neural Networks are a class of algorithms based on artificial intelligence, loosely modeled after the neuronal structure of the human brain that improves its performance without being explicitly instructed on how to do so. When designing the architecture of a neural network one has to take into consideration certain aspects, such as: the way the layers are arranged, which layers are used, the number of neurons used in each layer and many more things. Architectural design is a rather complicated subject and requires a lot of research. However, the use of neural networks for the automatic processing of medical images could substantially improve the diagnosis process, both in terms of accuracy and time requirement, by automatically differentiating between benign and malignant tissues. In this paper, a method of content-based hyperspectral image classification using neural networks algorithm is proposed. The method consist of three steps: selection of the object region using watershed segmentation technique, spectral features extraction using wavelet-transform, and image processing with neural networks.

The method was tested on a hyperspectral image of a patient with basal cell carcinoma located on the nose. The performance of the proposed method was assessed using confusion matrix. The results showed that using a neuronal weight of 0.2, the overall accuracy of the method is 85% while the kappa coefficient is 0.82. In conclusion, the proposed method seems to be promising and could be used successfully in the classification of skin affected by basal cell carcinoma. Additional studies are needed to increase its performance as well as test it on large groups of patients to confirm the results.

## Hyperspectral imaging for real-time detection and visualization of lip cancer: A pilot study

**Mihaela Antonina Calin<sup>1</sup>, Sorin Viorel Parasca<sup>2</sup>,  
Ileana Carmen Boiangiu<sup>2</sup>, Dragos Manea<sup>1,3</sup>, Roxana Savastru<sup>1</sup>**

<sup>1</sup> National Institute of Research and Development for Optoelectronics – INOE 2000, Magurele, Romania

<sup>2</sup> Emergency Clinical Hospital for Plastic, Reconstructive Surgery, and Burns, Bucharest, Romania

<sup>3</sup> The University of Bucharest, Faculty of Physics, Magurele, Romania

Hyperspectral imaging, recognized as an important tool for remote sensing, has recently entered into the field of biomedical research and applications. This technique integrates conventional imaging and spectroscopy to simultaneously provide both spatial and spectral information about a scene under investigation. This unique feature makes hyperspectral imaging a particularly useful tool in the biomedical field for diagnosing and monitoring medical treatments. On the other hand, early recognition of malignant or pre-malignant lesions in risk populations is a prerequisite for successful treatment. While expert clinical examination and subsequent pathological diagnosis is the current way of identifying skin cancer, various imagistic methods are tested in order to speed up the diagnostic algorithm. Given its capacity of providing a large amount of objective data, hyperspectral imaging might have a place in early detection of dangerous skin lesions. In this study, the ability of hyperspectral imaging to detect lip cancer in the complex background of the face with no a priori spectral information about the specific content of the investigated region was evaluated. Two anomaly detection algorithms, namely Reed-Xiaoli anomaly detector and Reed-Xiaoli/ Uniform Target hybrid detector were used to identify spectral differences between pathological and normal tissues. The study was performed on a presumed (clinical exam) basal cell carcinoma in the upper lip. Hyperspectral images of the face were acquired using a pushbroom hyperspectral imaging system covering a (400-800) nm spectral range. The detection performance was quantitatively evaluated based on the area under the curve (AUC) calculated from the receiver operating characteristic (ROC) curve for hyperspectral data. The results revealed that the detection performance of Reed-Xiaoli/Uniform Target hybrid detector is superior to that of the Reed-Xiaoli detector. In conclusion, these preliminary data suggest that hyperspectral imaging combined with Reed-Xiaoli/Uniform Target hybrid detector could play an important role in lip cancer detection and biopsy site selection. While the current study is based on only one case on a single area, the method could be extended, based on further studies, to larger areas, like the whole face.



**Biomedicine**

**05**

## **Cell isolation with the help of immunomagnetic beads and labeling with monoclonal antibodies depending on the magnetic field strength**

**Vladimir Jurišić**

University of Kragujevac, Faculty of Medical Sciences, Kragujevac, Serbia

Isolation of peripheral blood cells or cells from the bone marrow in patients with tumors are very important for evaluating the immune system. These analyses also include their functional activity in-vitro and complex molecular and gene analyzes. For these analyzes, a large number of purified cells are needed.

In this paper, we compared the cellular yield of CD56 + NK cells depending on the type of magnet used for cell separation. In the research, we used monoclonal antibodies labeled with Miltenyi magnetic beads for cell separation. The effect and influence of the strength of the magnetic field on the yield of isolated cells was studied in particular with the help of two types of magnets of BioLegens and Dynabeads companies used for cellular isolation. The measurement of the field produced by a ring magnet of the outer radius R1 and an inner radius R2 made in a laboratory of electromagnetic of the Institute of Physics at the Faculty of Science in Kragujevac. We measured the magnetic field using a gaussmeter with estimated precision of  $\pm 5\%$ . From the direct measurement technique we obtained a magnetization value of 0.6740 T for the MojoSort™ Magnet from a Biolegends company and 0.2748 T for a magnet from Dynabeads and MagniSort Technology.

The results showed that the yield of the cell was directly dependent on the strength of the magnet and the type of magnetic field by using identical antibodies. With a magnet more powerful and with a cylindrical magnetic field, certainly more CD56 + cells are isolated, which is important for further research and cell culture estimation, since we need optimal cell account.

## Peripheral blood mononuclear cell application in the induced bullous keratopathy

**Ekaterina Filippova**

Tomsk Polytechnic University, Tomsk, Russia

Bullous keratopathy is one of the leading causes of chronic corneal edema and visual loss among corneal diseases. Cell-based therapies may be an alternative to radical surgery. Peripheral blood mononuclear cells (PBMCs) are identified as blood cells with a round nucleus and are presented by lymphocytes, monocytes, natural killer cells, dendritic cells and fraction of stem cells and also being leukocytes and mesenchymal stem cells secrete cytokines.

**The aim of this research** is the study of peripheral blood mononuclear cells applying on the corneal endothelium in a condition of the induced bullous keratopathy *in vivo*.

**Materials and methods.** 48 pubescent male Wistar rats weighing 250 g were used. The animals were divided into 2 groups: 1 group - main group – 24 rats (24 eyes) with bullous keratopathy and after layering PBMCs suspension to the interior surface of the cornea. PBMCs were obtained from heparinized venous blood from rats and by Ficoll- Verografin centrifugation. The viability of PBMCs was measured by trypan blue dye exclusion and was consistently greater than 98%. 2 group – control group – 24 rats (24 eyes) with the bullous keratopathy and received a traditional treatment (metabolic modulators, keratoprotectors). The overall duration of the experiment comprised 31 days. Sampling was performed on days 7, 10, 17, 24, and 31 after the start of the experiment for morphology studying.

**Results.** Statistically significant gaps reduction area (up to  $475 \pm 23 \mu\text{m}^2$ ) was observed with the main group animals on day 3 from the start of the treatment. The area reduced by 1.7, 3 and 13 times on days 7, 14 and 21 correspondingly. The given value reduced by 1.4 times in the control group on day 14. It reduced by 2.0 times from the initial value and reached its lowest:  $290 \pm 19 \mu\text{m}^2$  on day 21. In the meantime, the overall tissue gaps area on day 21 comprised  $45 \pm 10 \mu\text{m}^2$ .

The epithelium thickness reduced by 1.2 times (which corresponds with 20%) from the initial value. However, no differences were noted in the control group. The thickness reached its normal value of 30.8 in the main group on day 21. It reduced to 35.7 in the control group.

The cornea thickness in the main group reached its normal value for the Wistar rats of  $258 \pm 29 \mu\text{m}$  on day 21. It comprised  $301 \pm 19 \mu\text{m}$  in the control group.

**Conclusion.** Injecting suspension of PBMCs into the anterior chamber of an eyeball provides a proved faster (by 3.0 times) reduction of the stroma hydration, which helps to restore its transparency, when treating experimentally modeled bullous keratopathy.

**Sources of funding.** The research was conducted with the financial support of the Russian Foundation for Basic Research (RFBR) as part of the project № 18-315-00048.

## Effects of statin and sesame oil therapy in experimental metabolic syndrome

**Olga Pechanova, Radoslava Rehakova, Michaela Kosutova, Martina Cebova**

Centre of Experimental Medicine, Slovak Academy of Sciences, Bratislava, Slovakia

Statin therapy for cardiovascular and obesity-associated diseases may be associated with several side effects. Products from food sources with polyphenolic compounds may represent promising supplementary agents in the treatment of cardiovascular and metabolic diseases with minimal side effects. Thus, we aimed to study the effect of sesame oil and simvastatin treatment on plasma lipid profile, nitric oxide generation, and oxidative load in obese Zucker rats. 12-week-old male Zucker rats were divided into the control and sesame oil- (1.25 ml/kg/day) treated Zucker lean groups, the control and sesame oil (1.25 ml/kg/day), or simvastatin (15 mg/kg/day) together with sesame oil-treated Zucker fa/fa groups,  $n = 6$  in each group. The treatment lasted for 6 weeks. Sesame oil composition and plasma lipid profile were analyzed. Nitric oxide synthase (NOS) activity, endothelial NOS (eNOS), phosphorylated eNOS, and inducible NOS (iNOS) protein expressions were determined in the left ventricle and aorta. Total NOS activity was measured by conversion of  $^3\text{H}$ Arginine to  $^3\text{H}$  Citrulline and NOS isoforms were analyzed by Western blot. Oxidative load, measured as conjugated diene (CD) and thiobarbituric acid reactive substance (TBARS) concentrations, was detected in the liver. Neither sesame oil nor cotreatment with simvastatin affected plasma lipid profile in Zucker fa/fa rats. Sesame oil and similarly cotreatment with simvastatin markedly increased NOS activity and phosphorylated eNOS protein expressions in the left ventricle and aorta of Zucker fa/fa rats. There were no changes in eNOS and iNOS protein expressions within the groups and tissues investigated. Hepatic CD concentration was higher in Zucker fa/fa comparing Zucker lean rats, and sesame oil treatment decreased it significantly. Interestingly, this decrease was not seen after cotreatment with simvastatin. In conclusion, phosphorylation of eNOS and decreased oxidative load may significantly contribute to increase in total NOS activity with potential beneficial properties. Interestingly, simvastatin did not affect NO generation already increased by sesame oil in obese Zucker rats.

**Acknowledgments:** The study was supported by APVV [No. APVV-14-0932] and VEGA [No. 2/0195/15, 2/0137/16, 2/0170/17, 2/0165/15].

## Radiometric studies of relations between leptin and thyroid hormones metabolism in white adipose tissue

Stanislav Pavelka

Institute of Physiology, Department of Radiometry, Czech Academy of Sciences, Prague, Czech Republic

**Common introduction.** White adipose tissue (WAT) represents an important target for regulating actions of thyroid hormones (THs) thyroxine ( $T_4$ ) and triiodothyronine ( $T_3$ ). However, data about local transformations of THs in WAT are still scarce. Adipokine leptin, secreted by adipose tissue, serves as an important signaling molecule that affects the activity of hypothalamic centers, while decreasing food intake. Several results of our previous studies indicate that THs and leptin may share some common downstream action sites and could act additively to enhance energy expenditure in adipose tissue. Nevertheless, the possible interplay between THs and leptin in the control of metabolism and weight of adipose tissue remains to be characterized.

**Aims of the study.** Using our newly developed advanced radiometric enzyme assays, we assessed changes in activities of the key enzymes of THs metabolism, the three known iodothyronine deiodinases (IDs) of types 1, 2 and 3 (D1, D2 and D3) in several depots of WAT and in brown adipose tissue (BAT), as well as in the liver of experimental mice. The obesity-prone male C57BL/6J mice were maintained under the conditions that promoted either adipose tissue hypertrophy (i.e., during obesogenic treatment) or involution (after mild caloric restriction). Determined were also changes in IDs activities in response to leptin administration.

**Main conclusions.** 1) Special high-fat diet (HF-diet) feeding of the mice resulted in increased plasma levels of leptin, as well as of total  $T_4$  and  $T_3$ . 2) Development of HF-diet-induced obesity in the mice was associated with an enhancement of D1 activity in WAT. 3) Mild (10 %) caloric restriction decreased D1 activity in WAT and reduced leptin plasma levels. 4) Administered leptin increased D1, but not D2 and D3 activities in WAT. 5) Demonstrated changes in D1 activity in WAT under the conditions of changing adiposity, and a stimulatory effect of leptin on D1 activity, suggest a functional role for D1 in WAT. 6) Possibly, D1 might be involved in the control of metabolism of adipose tissue and/or of its accumulation.

## The influence of supplemental n-3 PUFA in diet and altered thyroid status of rats on their lipid metabolism

Stanislav Pavelka

Institute of Physiology, Department of Radiometry, Czech Academy of Sciences, Prague, Czech Republic

**Common introduction.** Thyroid dysfunction, confirmed for instance by RIA determination of plasma concentrations of thyroid hormones (THs), is known to produce many alterations in lipid metabolism, for THs affect the intermediary metabolism of carbohydrates, lipids and proteins in most tissues. Several experimental studies and clinical trials have shown that n-3 polyunsaturated fatty acids (n-3 PUFA) improve hyperlipidemia, reduce inflammation, attenuate blood coagulation and decrease reactive oxygen species (ROS) generation in mitochondria. Especially marine n-3 PUFA that are rich in eicosapentaenoic acid (EPA) and docosahexaenoic acid (DHA) are well known food components recommended for the prevention of cardiovascular diseases, atherosclerosis, and for the management of hyperlipidemia. However, an imbalance of dietary n-6 to n-3 PUFAs ratio may result in altered gene regulation that can negatively affect cell membrane composition and organ functions.

**Aims of the study.** There are some indications of a possible existence of a cross talk between n-3 PUFA and THs receptor. Therefore, the aims of our study were to test whether and in what way n-3 PUFA supplementation in diet could affect changes of lipid metabolism, induced in rats by experimental alteration of their thyroid status.

**Experimental conditions.** 36 inbred male Lewis rats aged 4 months were randomly divided into 3 groups, and were maintained for 6 weeks in experimentally evoked and confirmed (by RIA of THs concentration) hypothyroid (HY) or hyperthyroid (TH), and control euthyroid (EU) status. Furthermore, n-3 PUFA preparation of Vesteralens, Norway was administered orally, in the dose of 200 mg/kg b.w./day for 6 weeks, to a half of the rats from each experimental group.

**Main conclusions.** Our preliminary results suggest that n-3 PUFA supplementation under used conditions did not significantly modify either serum concentrations of glucose and triglycerides or total cholesterol, high-density lipoprotein and low-density lipoprotein cholesterol levels in experimental animals that were chronically maintained in any thyroid status.

## Effects of UV and green LED light on the photosynthesis, redox state and indole alkaloids biosynthesis in medicinal plants and *in vitro* cultures

Olga Molchan<sup>1</sup>, Polina Shabunya<sup>2</sup>, Svetlana Fatychava<sup>2</sup>

<sup>1</sup> The Institute of Experimental Botany of the National Academy of Sciences of Belarus, Minsk, Belarus

<sup>2</sup> The Institute of Bioorganic Chemistry of the National Academy of Sciences of Belarus, Minsk, Belarus

Light-Emitting Diodes (LED) are modern innovative sources of energy producing the light with different emission wavelengths from UV-C (250 nm) to infrared (1000 nm). LED is the first light sources to allow of real spectral control and creation of any preset spectrum. There are many advantages of LED to plant lighting: energy efficiency, ecological safety, absence of the considerable thermal radiation and small size, etc. Major advantage is the possibility to produce the any preset light wavelengths stimulating plants photosynthesis, photomorphogenesis and biosynthesis. Therefore, the influence of LED lighting on the growth and development of plants today is intensively studied.

Plant growth and development are strongly controlled by specific light wavelengths. Secondary metabolite biosynthesis and accumulation in medicinal plants are also regulated by light. However to date it remains unclear how changes in spectral content and intensity of light regulate biomass and important terpenoid indole alkaloids (TIA) accumulation in medicinal plant. The aim of this study is to study LED light regimes effects on photosynthesis, growth, yield, redox state and secondary metabolite accumulation in medicinal plants producing TIA and to present LED spectrum for medicinal plant cultivation and drug production.

*Catharanthus roseus*, *Vinca minor*, *Aerva lanata* are medicinal plants accumulating pharmacologically significant TIA. Some of them are antineoplastic drugs used in chemotherapy of cancer diseases, in arterial hypertension treatment, etc. Plants were cultivated in growth chamber divided into isolated compartments under the climatic control and artificial illumination using LED sources with different regimes (spectrum and photon flux density).

Red and blue light are usually basal in the LED lighting spectra. In our preliminary tests, it was shown that red and blue lighting only are not optimal for biosynthesis and pharmacologically valuable metabolites accumulation in plants. It is advisable to include green and UV wavelength in the plant lighting spectrum. Theoretically unprofitable wavelengths as green also showed significant physiological effects on investigated plants. UV and green lighting lead to the increase in the amount of the pigments, photosynthesis intensity, redox state and levels of secondary metabolite biosynthesis. Our experiments showed that some LEDs light regimes strongly stimulated plant growth and biomass production, roots and flower formation. We found different effects of LED's light spectrum on TIA and phenolic compounds accumulation in plant tissues. It was discovered LED lighting regime stimulating the catharanthine, vindoline and ajmalicine accumulation, biosynthesis of vincamine in plant leaves and tissue cultures.

The influence of LED lighting on redox-active compounds content in plant cells were also measure. It was obtained evidences for the participation of redox state in the UV light mediated vinblastine biosynthesis in leaves and in the green light mediated vincamine biosynthesis in callus tissues. The correlation between various light regimes, biomass and TIA accumulation in different organs of plants is discussed. According to the results of present studies the LED light effect on photosynthesis, redox state and biosynthetic potential are species specific.

The results of this work can use in development of techniques for optimization of medicinal plants cultivation and drug production.

## **Sensorimotor integration – Experimentally unkept expression of brain integration functions**

**Fedor Jagla, Olga Pechanova**

Centre of Experimental Medicine, Slovak Academy of Sciences, Institute of Normal and Pathological Physiology, Bratislava, Slovakia

It is well known that the several hierarchical levels of interactions between the brain neuronal organization and the other human body systems exist. There is one special and unique integration which sub serve the interindividual communication as well as the communications between men and his/her environment – sensorimotor integration (SMI). On the other side, the all external as well as internal information can affect the generation of specific type of the SMI. The control mechanism of a given SMI may include either intentional or reflex type process.

The special type of the sensorimotor integration, as also the most precise and tight one is the visual-oculomotor. Its following two characteristics should be remembered. First, the eye movements organize our visual perception and second, they may be executed as a reflex movement or as an intentional focussing of our glance. We will present the use of the electrophysiological measurements – electroencephalography and electrooculography - used regularly in neuro/psychophysiology and the results of the change in sensorimotor response (eye movement characteristics) to external stimuli in psychophysiological research in human experiments concerned with the possible brain activation and change in cognitive functions.

## Threshold of safety of influence of continuous ultrasound on animal leukocytes

**Anna A. Oleshkevich**

Moscow State Academy of Veterinary Medicine and Biotechnology, Moscow, Russia

From dogs, cats, horses of different gender, age and breeds, groups were formed in accordance with age and state of health according to the principle of physiological analogues. It was found that the morphological changes in leukocytes are associated with a dose of continuous ultrasound (US) exposure occurring against the background of a decrease in viability. The threshold values of a safe *in-vitro* acoustic wave impact on the blood of animals were found — minimal US-intensity to be lower  $0.05 \text{ W/cm}^2$  with an exposure time of less than 30 sec.

A gradual increase in the percentage composition of agranulocytes, deformation and a change in permeability of cytoplasmic membrane ( $p < 0.05$ ) were revealed. The effect, starting with granulocytes, in all types of leukocytes was simultaneously registered at an irradiation time of 30 sec and higher.

It was shown that US-intensity of  $0.05\text{--}0.1 \text{ W/cm}^2$  is “safe” for the blood cells of healthy animals, but it changes the leukogram and reduces the number of viable blood cells from sick animals. The severity of the changes depends mainly on the intensity of the ultrasonic wave, the exposure time and the state of health. The etiology of the disease does not affect the features of the cellular response. The results of regression and correlation analysis between changes in the physiological cells' state, US-exposure and the viability of the blood cells showed close ( $|r| > 0.69$ ) and medium ( $0.3 < |r| < 0.69$ ) negative correlations ( $p < 0.001$ ). Mathematical patterns of changes in the viability of leukocytes within 3 min of treatment with continuous ultrasound confirmed this conclusion.

## Oxidative DNA damage and repair in rheumatoid arthritis – A correlation with the key BER genes polymorphisms

**Marta Poplawska<sup>1</sup>, Olga Brzezinska<sup>2</sup>,  
Grzegorz Galita<sup>3</sup>, Joanna Makowska<sup>2</sup>, Tomasz Poplawski<sup>3</sup>**

1 Biobank, Department of Immunology and Allergy, Medical University of Lodz, Lodz, Poland

2 Department of Rheumatology, Medical University of Lodz, Lodz, Poland

3 Department of Molecular Genetics, University of Lodz, Lodz, Poland

Rheumatoid arthritis (RA) is a systemic, inflammatory disease of the joints and surrounding tissues. RA manifests itself with severe joint pain, articular inflammation and oxidative stress. RA is associated with certain types of cancer. We have assumed that increased susceptibility to cancer of RA patients may be linked with genomic instability induced by disturbed DNA repair of oxidative DNA lesions by BER. In the present work we determined the level of basal and oxidative DNA damage and the kinetics of removal of DNA damage induced by tert-butyl hydroperoxide in peripheral blood mononuclear cells (PBMC) of 30 RA patients and 30 healthy individuals. The data from DNA damage and repair study were correlated with the genotypes of functional polymorphisms of the key BER genes including XRCC1, hOGG1, UNG, SMUG1, TDG, MBD4, MUTYH. DNA damage and repair were evaluated by alkaline single cell gel electrophoresis (comet assay). The genotypes of the polymorphism were determined by TaqMan SNP Genotyping Assays. We observed an association between RA occurrence, impaired DNA repair in PBMC and the polymorphisms of XRCC1, and hOGG1 genes. Therefore, our result suggest that polymorphism of the XRCC1, and hOGG1 genes may be linked with RA by the modulation of the cellular response to oxidative stress and these polymorphisms may be a useful additional marker in this disease along with the genetic or/and environmental indicators of oxidative stress.

**Acknowledgments:** This work was supported by the National Science Center (Poland) – UMO-2017/25/B/NZ6/01358.

## Deficiency of the NHEJ and BER proteins is correlated with inefficient DNA repair in rheumatoid arthritis

**Marta Poplawska<sup>1</sup>, Olga Brzezinska<sup>2</sup>,  
Grzegorz Galita<sup>3</sup>, Joanna Makowska<sup>2</sup>, Tomasz Poplawski<sup>3</sup>**

<sup>1</sup> Biobank, Department of Immunology and Allergy, Medical University of Lodz, Lodz, Poland

<sup>2</sup> Department of Rheumatology, Medical University of Lodz, Lodz, Poland

<sup>3</sup> Department of Molecular Genetics, University of Lodz, Lodz, Poland

Rapidly expanding evidence suggests that reduced activity of the DNA repair in patients with rheumatoid arthritis (RA) promotes lymphocytes ageing and destructive inflammation in synovial tissue. We analyzed the sensitivity of the peripheral blood mononuclear cells (PBMC) isolated from 30 RA patients and 30 healthy individuals to DNA damaging agents: tert-Butyl hydroperoxide (TBH) and bleomycin and calculate the repair efficiency. The metrics from DNA damage and repair study were correlated with profiles of the expression of 30 genes related to the maintenance of genome stability. DNA damage and repair were evaluated by alkaline single cell gel electrophoresis (comet assay). The expression of DNA repair genes were analyzed by the The Oligo GEArray Human Genome Stability and DNA Repair Microarray. We observed delayed oxidative and bleomycin DNA lesions repair in PBMC isolated from RA patients as compared with healthy subjects. RA PBMC cells also failed to produce sufficient transcripts of key proteins involved in the BER and NHEJ pathways. Therefore, our results suggest that decreased expression of DNA repair proteins may be responsible for inefficient DNA repair in RA.

**Acknowledgments:** This work was supported by the National Science Center (Poland) – UMO-2017/25/B/NZ6/01358.

## Risk factors and their impact on diabetes mellitus in elderly people

**Edina Bilić-Komarica**

UKCS, Sarajevo, Bosnia and Herzegovina

Diabetes mellitus is a group of metabolic diseases characterized by chronic hyperglycemia due to defects in insulin secretion or defect in its action, or due to the existence of both of these disorders. In addition to glucose metabolism disorders, the metabolism of fat and protein is disturbed in diabetes. Diabetes mellitus is the main growing problem of all age groups in Bosnia and Herzegovina. Precise data on prevalence are not known. The largest number of patients was registered in the 7th decade of life. Particularly type 2 diabetes is a growing problem with an accelerated increase in prevalence due to an increased number of elderly people in the overall population and an increasing presence of obesity. Type 2 diabetes is a disease that arises as a result of the interaction of genetic factors and environmental factors. The aim of this study was to investigate risk factors that influence the onset of type 2 diabetes in older people. The study included 108 patients from the Clinical Center in Sarajevo, of which 88 were female and 20 male. Based on data on sex, age, hyperlipidemia, adiposity, genetic components, smoking, hypertension, and fibrinogen, we have identified the number of risk factors that have affected the onset of the disease. The study aims to present recommendations for the diagnosis and treatment of diabetes mellitus based on relevant evidence to the individual with the intention of helping the doctor to apply the best possible treatment strategy for a particular patient.

**Keywords:** Diabetes mellitus, risk factors, elderly people, genetic factors, environmental factors, obesity

## Possible mechanism of immune response utilizing molecular probing of antigens by protein-miRNA complexes

Valeriy Zaporozhan, Andrey Ponomarenko

Odessa National Medical University, Odessa, Ukraine

Since 1957, when Burnet's Clonal selection Theory of Immune response was proposed, there was a significant progress in molecular biology and genetics. Thus, it is time for the reconsideration of possible mechanisms of immunity. It is obvious that an instructive immunological mechanism based on molecular recognition would be much more practical in comparison with the preexisting cell clones selection. We suggest that the pivotal role in the adaptive immunity fulfils recently discovered small interfering RNAs (**siRNA**) and microRNA (**miRNA**).

It is known that the siRNA and miRNA in cells exist in the form of miRNA-protein complex. The siRNA and miRNA are able to exert both gene expression-silencing and gene expression-activation functions. We propose that:

- 1) miRNA-associated polypeptides are extremely variable, similar (or identical) to variable regions of the heavy ( $V_H$ ) and light chains ( $V_L$ ) of immunoglobulins;
- 2) "Immune" miRNA represent itself the matrix RNA (mRNA) for the associated polypeptides, so that the miRNA-polypeptide complex is something like polymeric transfer RNA (**tRNA**): a complex of the variable region of future antibody with its coding nucleotide sequence (the miRNA itself);
- 3) Immune cells contain an extensive repertoire of the miRNA-polypeptide complexes able to specifically attach to various antigens (electrostatic interactions);
- 4) Upon the specific attachment of the miRNA-peptides with potential antigen, the newly formed complex move to the plasma membrane of the immune cell were is expressed with costimulatory molecules (the antigen presentation); the miRNA separates from the complex, is transported to nucleus and activate expression of corresponding specific Ig-gene segments: the V, D and J gene segments on 2, 14 or 22 chromosome. In case of the binding with an auto-antigen, the miRNA transforms to siRNA and block possible autologous antibody synthesis;
- 5) Activated in the described way, immune cells start antigen presentation or antibody secretion depending on the immune cell type.

The immune cells contain active reverse transcriptase (for example – telomerase reverse transcriptase (**TERT**) which possibly participates in the proposed mechanism.

We predict that the genetic fragments (miRNA or DNA) coding necessary variable fragments of specific antibody to corresponding (invading) antigens are able to actively disseminate between the immune cells inside the body (priming of the naive immune cells) and initiate in this way the orchestrated immune response to foreign antigens. This process may involve retrotransposones and other gene mobile elements which permits target-priming and genetic sequence insertion throughout the chromosome interior.

Described Hypothesis of the instructive immunological mechanism based on molecular recognition conforms to current concept of "Read-Write Genomes" which implies that genome is the subject to accidental modification and is capable to be rapidly restructuring.

## The importance of determining mineral bone density and vitamin D in schizophrenic patients treated with antipsychotics

**Marijana Stanojevic-Pirkovic<sup>1,2</sup>, Marija Andjelkovic<sup>1,2</sup>, Ivanka Zelen<sup>1</sup>,  
Marina Mitrovic<sup>1</sup>, Ivana Nikolic<sup>1</sup>, Milan Zaric<sup>1</sup>, Petar Canovic<sup>1</sup>,  
Vladimir Jurisic<sup>3</sup>, Olgica Mihaljevic<sup>3</sup>, Dragan Milovanovic<sup>2,4</sup>**

1 University of Kragujevac, Faculty of Medical Sciences, Department of Biochemistry, Kragujevac, Serbia

2 Clinical Center Kragujevac, Department of Laboratory Diagnostics, Kragujevac, Serbia

3 University of Kragujevac, Faculty of Medical Sciences, Department of Pathophysiology, Kragujevac, Serbia

4 University of Kragujevac, Faculty of Medical Sciences, Department of Pharmacology, Toxicology and Clinical Pharmacology, Kragujevac, Serbia

**Introduction.** Osteoporosis is a metabolic disease of bone tissue with significant medical, social and economic consequences. Literary data indicate the linkage of osteoporosis on the one hand and schizophrenia and other psychotic disorders on the other. The decrease in mineral bone density in schizophrenic patients is most likely due to the cumulative effect of numerous factors, including the antipsychotic medication itself.

**Aim.** The aim of this study was to identify and quantify the risk factors associated with the disturbance of bone marrow homeostasis in patients with psychotic disorders.

**Methods.** This study included 45 subjects of both sexes who were diagnosed with schizophrenia, bipolar disorder with psychotic characteristics or other psychotic entities and who were treated at the Clinic for Psychiatry of KC "Kragujevac" in Kragujevac from a newly-acquired illness or in the stage of exacerbation of a chronic illness. All the subjects were taken anamnestic data and risk factors for the disturbance of bone tissue homeostasis were identified. For the purpose of assessing bone density, a diagnostic examination of DXA (double energetic x-ray absorption spectrometry) was performed in all subjects. Mineral bone density was measured at the level of the lumbar vertebrae (L1-L4) and the neck of the femur, on the device Horizon DXA System, (Hologic). The method is based on measuring the size of the radioactive beam that passes through the target tissue. For the evaluation of bone metabolism all the subjects were determined serum concentrations of vitamin D (25(OH)D<sub>3</sub>) and total calcium, in the course of five measurements. The first sample was collected before the introduction of pharmacotherapy, and the remaining four after the introduction of the medication, at intervals of seven days. The serum concentration of vitamin 25(OH)D<sub>3</sub> was measured on the Cobas e 411 (Roche Diagnostics GmbH, Mannheim, Germany) by electrochemiluminescence method, and the serum calcium concentration on the biochemical analyzer Olympus AU400 (Beckman Coulter Inc., Brea, USA) by a photometric color test. In order to get the statistical analysis of the obtained data, Student's t-test for independent samples for estimating difference significance was used, whereas the relationship between the tested variables was analyzed by Pearson method of linear correlation.

**Results.** In 16 patients (36%), based on the DEXA test, the presence of a decrease in mineral bone density was determined, whether there was osteoporosis or osteopenia. The mean values of vitamin D were within the reference limits and there were no statistically significant differences in values at five different times, ( $F = 0.337$ ,  $df = 4$ ,  $p = 0.853$ ). However, in 15 patients at the beginning of treatment, vitamin D values below 20ng/mL were detected. The mean value of vitamin D from a total of 179 samples was 21.4 +/- 8.46. There was no statistically significant correlation between the values of vitamin D in the blood and sampling time during the study, although a trend of overall decline in concentration was determined (Pearson  $r^2 = -0.015$ ,  $p = 0.837$ ). Although the values of calcemia were within the reference range, generally speaking, statistically significant differences yet occurred in five different periods during treatment ( $F = 2.92$ ,  $df = 4$ ;  $p = 0.023$ ). A statistically significant difference was determined between the pre-treatment value compared to the values measured after the first cycle of therapy ( $t = 2.14$ ,  $df = 68$ ,  $p = 0.035$ ), the second cycle ( $t = 2.03$ ,  $df = 81$ ,  $p = 0.046$ ) and especially the fourth cycle of therapy ( $t = 2.23$ ,  $df = 58$ ,  $p = 0.029$ ). The mean value of calcemia, from a total of 185 samples was 2.402 +/- 0.163mmol/L. Between the values of calcium in the blood and sample taking time during the study there was not only a slight but statistically significant negative correlation (Pearson  $r^2 = -0.203$ ,  $p = 0.006$ ) but also a negative linear regression ( $F = 7.87$ ,  $df = 1$ ,  $p = 0.006$ ).

**Conclusion.** The results of our study have shown that antipsychotics, during the initial phase of the treatment of psychotic disorders, cause a progressive, mild and statistically significant decrease in the concentration of calcium in the serum. However, an additional risk factor for the disturbance of bone marrow homeostasis in the examined population was certainly a vitamin D deficiency, present among one third of patients before the introduction of pharmacotherapy. The present factors are not independent factors for the development of osteoporosis.



**Biopharmaceuticals**

**06**

## **Influence of chronic low-dose administrations of silver nanoparticles on cognitive functions of mammals and identification of the effect reasons**

**Anna Antsiferova, Marina Kopaeva,  
Vyacheslav Kochkin, Pavel Kashkarov, Mikhail Kovalchuk**

National Research Center Kurchatov Institute, Moscow, Russia

Since the beginning of the 2000s silver nanoparticles (Ag-NPs) have been used in various applications from pharmaceuticals to textile and from hygiene products, packing materials to daily food supplements [1,2]. Undoubtedly, Ag possesses unique antiseptic properties that were known since antiquity. Therefore, people in the past successfully used silver dishes as antiseptics.

Nowadays silver is not forgotten and still competes with the modern antibiotics, however, usually in nanoform.

In some cases Ag-NPs can accumulate in different organs such as liver, kidney, blood and brain of mammals. Several works showed that all tissues except the brain easily remove silver and some scientific researches reliably demonstrate the penetration of Ag-NPs via the blood-brain barrier and their jamming in the nerve tissue [3]. Therefore, brain can be regarded as a target organ for Ag-NPs.

There is a lot of scientific research that show toxicity of Ag-NPs to nerve cells as, at first, neurons, astrocytes and glial cells. Of course, the toxic effect is almost straightly proportional to the doses of Ag-NPs and the exposure time.

Due to the accumulation of Ag-NPs in the brain and their toxicity to brain cells some of the recent works are devoted to study of the influence of Ag-NPs on cognitive and behavioral functions of model mammals such as rats and mice. Usually such researches are conducted for no more than 30 days and the doses of Ag-NPs are able to poison animals without acting on the brain.

In the present research the influence of the daily prolonged (30, 60, 120 and 180 days) administration of silver nanoparticles on cognitive functions of model mammals was studied. The accumulation of silver in whole brain, hippocampus, cerebellum, cortex and residual part of mice brain was investigated by highly precise and representative Neutron Activation Analysis and the histological studies were conducted.

Some of the main results of the comprehensive study are the description of the biokinetics of silver in the hippocampus, cerebellum and cortex, the finding of the jump increase of silver in the hippocampus and cerebellum after the period of administration of 120 days. Accumulation of silver in the mice brain and hippocampus itself as well as the integrity violation of the CA2 subregion caused long-term contextual memory impairment at 180 days of silver nanoparticle exposure. However, destruction of CA2 had started 60 days before the visible changes in behavior appeared.

### **References**

1. Morones J.R., et al, The bactericidal effect of silver nanoparticles, *Nanotechnology*, 16, 2346–2353 (2005).
2. Antsiferova A., Kopaeva M., Kashkarov P. Effects of prolonged silver nanoparticle exposure on the contextual cognition and behavior of mammals, *Materials*, 11, 4, 558 (2018).
3. Antsiferova A.A., et al, Extremely low level of Ag nanoparticle excretion from mice brain in in vivo experiments. *IOP Conf. Series: Materials Science and Engineering*, 98 (2015).



**Biophysics**

**07**

## **Influence of near earth electromagnetic resonances on human cerebrovascular system in time of heliogeophysical disturbances**

**Nadezda Sergeenko**

Pushkov Institute of Terrestrial Magnetism, Ionosphere and Radio Wave Propagation (IZMIRAN) RAS,  
Moscow, Troitsk, Russia

Problems of adaptation of the person are current in the conditions of heliogeophysical disturbances at its life-support, both on the Earth, and in space. Changes of fluidity of blood, levels of catecholamins of blood on different phases of heliogeomagnetic disturbances are analyzed.

The physical processes influencing on cerebrovascular shifts at people during indignations are discussed. Physical characteristics of environment (bioeffective frequencies of ionospheric resonators) are compared with own frequencies human body. It is supposed, that the human body is the difficult nonlinear self-oscillatory system exposed to resonant influence. It is supposed, that in a storm initial stage the stochastic resonance can be one of physical mechanisms of influence of external weak periodic signals against noise. External electromagnetic fluctuations can synchronize or desynchronize rhythms of electromagnetic fluctuations of cells of a brain and blood. Ionosphere disturbances lead to fluctuations of frequencies and the periods of the ionosphere Alfen's resonator which, in turn, can influence on rhythms of components of an organism, first of all on a brain and rheological properties of blood, as in experiences in vitro, and in vivo.

Also possibility of direct influence of geomagnetic variations during storms on a brain and the system of blood connected with influence of an electromagnetic field on dynamics of process of aggregation - disaggregation of erythrocytes and ADF (an adenosinediphosphatase acid) - induced platelet aggregation in a blood stream is discussed.

The found out effects are statistically authentic and specify presence of direct influences of physical processes during indignations on blood cells.

The received results allow to assume, that, one of leading mechanisms of influence of indignations on cerebrovascular system of the person are their effects on rheological properties of blood.

The prediction of the biotropic effects of electromagnetic disturbances during the active Sun, as well as the geophysical forecast, is largely determined by empirical regularities and is probabilistic. To implement a probabilistic forecast, an adequate statistical model must be developed. This problem was solved in the framework of this work. Time series of the number of strokes in Moscow were subject to trend processing. The obtained samples were sorted according to the state of the heliogeophysical situation and statistical distributions and invariants were calculated. An attempt was made to describe the statistical variability of variations in the number of strokes based on the Poisson model. For the studied samples, the characteristic function of the exponential type was chosen under the assumption that the time series are a superposition of some deterministic and random process. Through the Fourier transform, the characteristic function is transformed into a probability density function.

## **Spectral characteristics of laser-irradiated micro and nanostructures on the base of nanoshells under plasmon resonance conditions**

**Yaroslav Bobitski<sup>1</sup>, Iryna Yaremchuk<sup>2</sup>, Tetiana Bulavinets<sup>2</sup>**

<sup>1</sup> Faculty of Mathematics and Natural Sciences, University of Rzeszow, Department of Photonics, Lviv Polytechnic National University, Rzeszow, Lviv, Poland

<sup>2</sup> Department of Photonics, Lviv Polytechnic National University, Lviv, Ukraine

Intensive theoretical and experimental studies of laser-irradiated micro and nanostructures on base of nanoshells, found wide application in physics, chemistry, biomedicine and other. Nanoshells form a separate class of materials with unique physical and chemical properties whose research is of great scientific and practical value, due to a wide range of possible applications of such materials as sensitive elements, in particular sensors, filters, chemical catalysts, photovoltaic devices and photo-thermal therapy, etc. It is possible to accurately control the spectral position of the surface plasmon resonance by changing their spatial geometry and the ratio core/shell dimensions. In addition, the nanoshells are more sensitive to changes in the dielectric medium and are characterized by multiband surface plasmon resonance.

In this work, the spectral characteristics of nanoshells, namely silver-gold, silver-copper, silver-titanium dioxide and titanium dioxide -silver in the conditions of localized plasmon resonance have been theoretically researched for the purpose of their further photonics and plasmonics applications. It is shown that by changing the thickness of the shell on the metal or semiconductor core, one can shift the spectral position of the surface plasmon absorption peak in the visible spectral region and evaluate the influence of deformation of nanostructures on their optical characteristics.

It is indicated that in the case of bimetallic structures, the spectral position of the absorption and scattering cross sections peaks is not sensitive to changes in the thickness of the shell, only their amplitude changes.

In the case of nanostructures such as silver-titanium dioxide there is a clearly pronounced additional peak in the spectra of absorption and scattering cross sections. Such a two-band nature can be explained by the excitation of localized plasmons on two interfaces titanium dioxide/silver and silver/environments. The spectral position of the both peaks of absorption and scattering cross sections is shifted to the long-wave region of the spectrum, when the shell thickness changes and when the nanostructure is deformed (extended) for such type of the nanoshells.

The structure of titanium dioxide-silver is characterized by a shift of the second peak into the short-wave region of the spectrum when shell thickness increases and when there are deformations. And the first one is practically not sensitive to such changes. It should be noted that with a certain shell thickness, such structure will have characteristics similar to those of a silver nanoparticle.

## Hydration changes of the red blood cell membranes of gastric cancer patients evoked by radiation therapy

Liliya Batyuk<sup>1</sup>, Natalya Kizilova<sup>2</sup>, Vladimir Berest<sup>3</sup>, Oksana Muraveinik<sup>4</sup>

1 Kharkiv National Medical University, Kharkiv, Ukraine

2 Warsaw University of Technology, Warsaw, Poland

3 V. N. Karazin Kharkiv National University, Kharkiv, Ukraine

4 Kharkiv City Clinical Hospital No. 7, Kharkiv, Ukraine

Cancer is one of the most essential medical and social problems in the world due to its significant prevalence and serious consequences: the loss of efficiency, disability and the high percentage of death. One of the leading therapeutic methods for malignant tumors is radiation therapy [1]. The heterogeneity of the red blood cell (RBC) membrane composition, its ability to quickly change the nature of the interaction between the components determine the presence of a wide range of structural and functional reactions of the cell to its adaptation to environmental conditions. Analysis of the dielectric characteristics of the RBC in cancer patients provides additional information on the tumor development and treatment processes that is of great interest in connection with elaboration of more efficient methods for the early diagnosis of cancer [2]. In the present study the suspensions of red blood cells (RBC) and RBC shadows of gastric cancer patients (20 people) have been used. The control group consisted of 25 healthy donors. According to the international classification system TNM (tumor, nodus and metastasis), the patients were distributed as follows: T<sub>2</sub>N<sub>1</sub>O (second stage of the disease without signs of distant metastases) – 45% and T<sub>3</sub>N<sub>1</sub>M<sub>0</sub> (third stage, without signs of distant metastases) – 55%. The median age was 47 years. A group of patients received radiotherapy as an independent treatment course in the mode of classical fractionation, with a total focal dose of 45 Gy. Blood sampling was driven by a vein puncture after irradiation. The dielectric properties of the RBC have been studied by microwave dielectrometry at the frequency  $f=9.2$  GHz in the wide temperature range  $T=0-46^{\circ}\text{C}$ . The dielectric relaxation time of water molecules, the change in the free energy of activation of the dipole relaxation of water molecules were study and the hydration of cells before and after radiation therapy was evaluated. Since the obtained data showed a non-parametric nature of the distribution, the Wilcoxon criterion was used to estimate the significant difference in the results of treatment, and Fisher's exact method was used for the data analysis with  $p < 0.05$ .

The results of the study indicate the existence of a thick layer of hydrated water over the surface of RBC in cancer patients with gastric cancer. It has been shown by numerical estimations that each water molecule in the layer forms up to two hydration bonds, approximately. Probably bound water fills the entire space between the glycoproteins of the cell receptors. A number of structural transitions in RBC membranes in the 6, 8-15, 15-20, 36-40 and 42-46° C temperature ranges have been observed. These transitions are accompanied by a change in the activation energy of the dielectric relaxation of water molecules. Similar changes have been detected on the RBC ghosts. Therefore, the observed effect is mostly connected with cellular membrane, not with haemoglobin solution.

Radiotherapy leads to a decrease in the concentration of strongly bound water. Probably, as a result of therapy, the irreversible adsorption of glycoproteins that are part of cellular receptors occurs; this may partially lead to loss of integrity of the cell membranes and cell rupture. Therefore, dielectric parameters of the RBC membranes can be used for quantitative estimation of the stage of disease and control over the anticancer radiation therapy.

### References

1. Kizilova N. Review on modern techniques in diagnostic and planning radiology. *Int. J. Biosen. Bioelectron.* 2018;4(6):242-247.
2. Batyuk L., Kizilova N. Dielectric properties of red blood cells for cancer diagnostics and treatment. *AS Cancer Biology.* 2018; 2(10):55-60.

## Chemical and radiation toxicity via luminescent assay systems of different complexity: Bacterial cells, enzyme reactions, and fluorescent proteins

Nadezhda Kudryasheva<sup>1</sup>, Rosa Alieva<sup>1</sup>, Tatiana Rozhko<sup>2</sup>,  
Alena Olada<sup>3</sup>, Ekaterina Kovel<sup>1</sup>, Anna Sachkova<sup>4</sup>

1 Institute of Biophysics FRC KSC SB RAS, Krasnoyarsk, Russia

2 Krasnoyarsk State Medical Academy, Krasnoyarsk, Russia

3 Krasnoyarsk State Agrarian University, Krasnoyarsk, Russia

4 National Research Tomsk Polytechnic University, Tomsk, Russia

Luminescence of living systems is a convenient parameter to monitor environmental toxicity. Luminescent systems of different complexity – luminous marine bacteria, their enzyme reactions, and coelenteramide-containing fluorescent proteins (CLM-CFPs) were used as bioassays to monitor toxicity of water solutions under model conditions; toxic effects were compared at cellular, biochemical and protein' structure levels, respectively. Organic compounds, metallic salts, and radioactive elements (under conditions of low-dose irradiation) were applied to vary toxicity of media. Luminescence inhibition (toxic) and activation (adaptive response) effects were evaluated and discussed. Application of CLM-CFPs as toxicity bioassays of a new type is justified, they can serve as a proper tool for study efficiency of primary physicochemical processes in organisms under external exposures. Coelenteramide (CLM), fluorophore of CLM-CFPs, is a photochemically active molecule; it acts as a proton donor in its electron-excited states, generating several forms of different fluorescent state energy and, hence, different fluorescence color, from violet to green. Contributions of the forms to the visible fluorescence depend on the CLM microenvironment in proteins. Hence, CLM-CFPs can serve as fluorescence biomarkers with color differentiation to monitor results of destructive biomolecule exposures. Variations of spectral-luminescent and photochemical properties of CLM-CFPs under different exposures – chemicals (1), temperature (1), and ionizing radiation (2-3) is considered.

Application of the luminescent bioassays of different complexity for detoxification efficiency evaluation is discussed. Natural and artificial bioactive compounds, humic substances (4) and fullerenols (5-6), are used as detoxifying agents. Detoxification mechanisms were revealed to be complex, with chemical, biochemical, and cellular aspects conditioning those. Active role of the bioassay systems in the detoxification processes was demonstrated.

**Acknowledgments:** This work was supported by RFBR and the government of Krasnoyarsk region, projects N18-44-242002 and 18-44-240004; PRAN-32.

### References

1. Alieva R., Kudryasheva N. *Talanta*, 2017, 170, 425.
2. Petrova A., et al. *Anal&Bioanal. Chem*, 2017, 409(18), 4377.
3. Petrova A., et al. *Anal&Bioanal. Chem*, 2018, 410(26), 6837.
4. Kudryasheva N., Tarasova A. *Environ. Sci. Pollut. Res.*, 2015, 22(1), 155.
5. Kudryasheva N., et al. *Photochemistry and Photobiology*. 2017, 93(2), 536.
6. Sachkova A., et al. *Biochemistry and Biophysics Reports*. 2017, 9, 1-8.

## Biological activity of carbonic nano-structures of natural and artificial origin

Ekaterina Kovel<sup>1</sup>, Nadezhda Kudryasheva<sup>1</sup>, Anna Sachkova<sup>2</sup>

<sup>1</sup> Institute of Biophysics SB RAS, Federal Research Center Krasnoyarsk Science Center SB RAS, Krasnoyarsk, Russia

<sup>2</sup> Tomsk Polytechnic University, Tomsk, Russia

The aim of the work is to compare the biological activity of carbonic nano-structures of natural and artificial origin, namely, humic substances (*HS*) and fullerenols. Enzyme-based luminescent bioassay was applied to evaluate toxicity and antioxidant properties these compounds; chemiluminescent lumonol method was used to study a content of reactive oxygen species (*ROS*) in the solutions. The representative of the fullereneol group,  $C_{60}O_y(OH)_x$  where  $y=2-4$ ,  $x=22-24$ , was chosen. Toxicity of the bioactive compounds was evaluated using effective concentrations  $EC_{50}$ ; detoxification coefficients ( $D_{OxT}$ ) were applied to study and compare antioxidant activity of the compounds. Antioxidant activity and ranges of active concentrations of the bioactive compounds were determined in model solutions of organic and inorganic oxidizers – 1,4-benzoquinone and potassium ferricyanide. Values of  $EC_{50}$  revealed higher toxicity of *HS* than fullereneol (0.005 and 0.108 g L<sup>-1</sup>, respectively); detoxifying concentrations of fullereneol were found to be lower. Antioxidant ability of *HS* was demonstrated to be time- dependent; the 50-min preliminary incubation in oxidizer solutions was suggested as optimal for the detoxification procedure. On the contrary, fullereneol' antioxidant effect demonstrated independency on time. Antioxidant effect of *HS* did not depend on amphiphilic characteristics of the media (values of  $D_{OxT}$  were 1.3 in the solutions of organic and inorganic oxidizers), while this of fullereneol was found to depend: it was maximal ( $D_{OxT} = 2.0$ ) in solutions of organic oxidizer (1,4-benzoquinone). Hence, both *HS* and fullereneol demonstrated toxic and antioxidant properties; however quantitative characteristics of these effects were different. The difference in toxicities was explained with (1) flexibility of fragments of *HS*, (2) their higher ability to decrease *ROS* content. The difference in antioxidant activity was attributed to flexibility of *HS* macromolecules. The paper demonstrates a high potential of luminescent enzymatic bioassay to study biological activity of nano-structures of natural and artificial origin.

**Acknowledgments:** The work was supported by the PRAN-32, grant of RFBR N18-29-19003mk.

## Coelenteramide-containing fluorescent proteins as perspective bioassays for toxicity monitoring

**Roza Alieva, Nadezhda Kudryasheva**

Institute of Biophysics SB RAS, Federal Research Center 'Krasnoyarsk Science Center SB RAS', Krasnoyarsk, Russia

Nowadays, physicochemical approach to understanding the mode of action of toxic substances in organisms remains flawed and controversial. A good solution here would be the use of simplest bioassay systems. Coelenteramide-Containing Fluorescent Proteins (CLM-CFPs) can serve as proper tools for study primary physicochemical processes in organisms under external exposures. CLM-CFPs are products of bioluminescent reactions of marine coelenterates. As opposed to Green Fluorescent Proteins, the CLM-CFPs are not widely applied in biomedical research, and their potential as colored biomarkers is undervalued now. Coelenteramide, fluorophore of CLM-CFPs, is a photochemically active molecule; it acts as a proton donor in its electron-excited states, generating several forms of different fluorescent state energy and, hence, different fluorescence color, from violet to green. Contributions of the forms to the visible fluorescence depend on the coelenteramide microenvironment in proteins. Hence, CLM-CFPs can serve as fluorescence biomarkers with color indication to monitor results of destructive biomolecule exposures.

Discharged photoprotein obelin from *Obelia longissima* was chosen as a representative of the CLM-CFP group. Light-induced fluorescence spectra of the discharged obelin exposed chronically to (1) exogenous compounds (alcohols), and (2) higher temperature (40°C) were recorded and studied. Fluorescence intensity and contributions of "violet" (neutral CLM structure) and "blue-green" (ionized CLM structure) forms to the overall visible emission were analyzed for all the exposures. It was found that the destructive exposures result in a decrease of the maximal fluorescent intensity and rise of contribution of the "violet" fluorescent component in the overall fluorescence spectrum. The effect was related to changes of proton transfer efficiency in a fluorescent state of CLM in the obelin active center.

**Acknowledgments:** The study was funded by RFBR and the government of Krasnoyarsk region, project N 18-44-242002.

## Co-directed influence of mitagens and modulated ultrasound on cells of various origin

Anna A. Oleshkevich

Moscow State Academy of Veterinary Medicine and Biotechnology, Moscow, Russia

To study the *in-vitro* effects of low therapeutic intensity ultrasound (US) in animal cells, a 3-day transplanted MDBK cell culture was employed. For *in vivo* exposure, outbred adult male mice of 10–12 weeks of age, weighing 24–26 g, were applied. Irradiation of mice was carried out in a thermostatic cuvette (25°C); the testicles of US-treated mice were at the beginning of the far zone of the emitter. The passed into tissue US-intensity was 90 % of the nominal intensity. On the third day after irradiation, the cellular (stage 7 of the cell cycle) elements of the seminiferous tubules of the testes of experimental animals were counted. The US-exposure varied within the following limits: time from 1 to 300 sec, SATA-intensity 0.01–2.0 W/cm<sup>2</sup>, generative frequency was 0.88 MHz, modulation – from 10 to 1000 Hz. Devices: UZT-1-01F; UZT-5 and UZT-1.02S.

Plant mitagens Concanavalin A (Cohn A) and phytohemagglutinin (PHA) were tested in concentrations from  $1 \times 10^{-4}$  to 10 mg per 1 ml of suspension. The multiplicity of mitagen adding into the suspension of transplantable cell culture was 1:5. The MDBK culture cells were grown by the traditional method in 50 ml mattresses. A monolayer in the control was formed for 2–3 days. Cultivation of the treated with stimulants and control cells was carried out at a temperature of 37°C in the Eagle's medium with 10% of bovine serum, with antibiotics (100 µg/ml) lincomycin or kanamycin, with 5% of glutamine and sodium bicarbonate until neutral pH. The initial planting concentration of cells was  $8.0 \times 10^4$ – $1.0 \times 10^5$  per 1 ml. For studies, the suspension of synchronized cell cultures at different stages of the cell cycle was explored. The initial number of cells with an intact membrane in the control and experience was at least 80 %. The integrate membrane of the tested cells was determined by the absence of trypan blue-staining. Stimulation of the cell growth was initiated by US-intensity of 0.03–0.05 W/cm<sup>2</sup> with an exposure time of 5–30 sec. The increase of cell mass was 65–130% in compare with control & depended on both the duration of exposure and the stage of cell cycle. The maximum stimulating effect was registered after single “preplant” US-continuous treatment of cells (0.05 W/cm<sup>2</sup>, exposure time 10 sec). The cell growth in control did not exceed  $3.1 \times 10^5$  per 1 ml. The proliferation index increased as a result of US-stimulation from 3.8 to 9.0. Cohn A in optimal concentration of 1.0 mg/ml increased the “yield” of cells to  $1.1 \times 10^6$  per 1 ml. With an optimal PHA concentration of 0.01 mg/ml, the average cell growth was  $9.6 \times 10^5$  per 1 ml. Also, in “experimental” cultures, an increase in the rate of proliferation was recorded – the monolayer was finally formed 10–12 h faster than in the control. The largest increase in MDBK-harvest was obtained, as well as in experiments with US, with a single “preplant” cell treatment. In the case of treatment with cell stimulants at the monolayer formation stage, no positive effect was observed. A similar pattern was also observed in *in vivo* experiments. Stimulation of cells of the seed epithelium, which are only in the early stages of maturation at the time of irradiation, has been revealed. A positive effect was obtained after US-irradiating of the testes with intensity of 1.0 W/cm<sup>2</sup> for 5 min: a significant increase ( $p < 0.05$ ) in the number of spermatids and spermatozoa was recorded at US-modulative frequency of 250 Hz. It should be noted that the maximum proliferation index (9.1–13.7) in all cases of the use of stimulants was observed in cultures with minimal proliferative activity in the control (2.7–3.0).

## **Possibilities of mathematical non-linear-dynamics-method application in laboratory biophysical expertise**

**Anna A. Oleshkevich, Svetlana A. Komarova, Anna V. Novikova**

Moscow State Academy of Veterinary Medicine and Biotechnology, Moscow, Russia

The aim of the work was to study the perspectivity of experimental biophysical methods' attracting for the solving the problems of wool examination.

The authors explored the possibility of fluorescence microscopy methods using in conjunction with the methods of mathematical non-linear dynamics to determine the species of animal hair. The objects of the study were native animal hair (goats). The investigation was subjected to both guard and down hair, cut with scissors at the level of leather, which ensured the presence of all parts of the hair in the object.

In the software package "*HarFA*", by determining the regression equations and constructing the corresponding graphs and histograms, we conducted a fractal analysis of the images of animal hair using the method of A. A. Oleshkevich and co-authors [RF patent for invention № 2640177]. This method allows to take micrographs of hair and to carry out their fractal analysis using the "*HarFA 5.1*" software package. Comparison of the analysis of hair in reflected light with the results of fractal analysis revealed great information content of the method. The best results are given by a combination of studies in the "*HarFA*" software package with fluorescence microscopy methods.

## Bioluminescent assays as sensitive sensors for evaluating the biological activity of humic substances

Anna Sachkova<sup>1</sup>, Ekaterina Kovel<sup>2</sup>, Olga Nefedova<sup>3</sup>, Nadezhda Kudryasheva<sup>2</sup>

<sup>1</sup> National Research Tomsk Polytechnic University, Tomsk, Russia

<sup>2</sup> Institute of Biophysics FRC KSC SB RAS, Krasnoyarsk, Russia

<sup>3</sup> National Research Tomsk State University, Tomsk, Russia

The elaboration of the reliable approaches to the evaluation of the activity of bioactive compounds in toxic solutions is of special interest. Bioluminescent assays are great tools for it, due to high rates of the assay procedure, simple registration of the luminescent signal and high sensitivity. Humic substances are products of natural transformation of organic matter in soil. They are polymeric molecule, include a lot of functional groups and, hence, are characterized by a lot of chemical and physico-chemical properties. The purpose of this work was to analyze the influence of Humic Substances on chemical and biochemical processes taking place in bioluminescent systems in present of toxic compounds. In our work we used the Gumat-80 preparation (Gumat, Russia). It was produced by non-extracting treatment of coal with alkali (KOH and NaOH). This work includes the results of research on the mechanisms of action of HS on living cells of *Photobacterium phosphoreum*. The effect of Humic Substances on bacterial cells in solutions of toxic compounds (CrCl<sub>3</sub> and benzoquinone) was studied by electron microscopy. It was found that in the presence of Humic Substances in the majority of cells, the amorphous substance of average electron density was observed outside of cell walls. It seems to represent the remains of a mucous layer fixed by HS. The remains of a mucous capsule were not observed in toxic solutions without HS or in the solutions of Humic Substances. Probably, the Humic Substances macromolecules enhance and stabilize the mucous capsule, thus intensifying the protective response of cells. The enzyme-based assay was used to demonstrate a decrease in biochemical toxicity. We studied rates of oxidation of organic reduce, NADH, in the presence of FMN, endogenous oxidizer, or toxic compounds (CuSO<sub>4</sub> and K<sub>3</sub>[Fe(CN)<sub>6</sub>]). It was shown that HS increase rates NADH oxidation by FMN, and they didn't change rates of NADH oxidation by toxic compounds. This means that Humic Substances make endogenous reactions more competitive, it can be a result of an amphiphilic nature of Humic Substances, which promote combining biological molecules that are of amphiphilic nature, too. Our work demonstrates a high potential of the bioluminescent assay systems to evaluate the biological activity of Humic Substances.

## Simulation of radon transfer from thermal water through the skin in radon therapy

**Werner Hofmann, Renate Winkler-Heil, Herbert Lettner, Alexander Hubmer**

Department of Chemistry and Physics of Materials, University of Salzburg, Salzburg, Austria

The transfer of radon from thermal water through the skin and the subsequent distribution among different organs of the human body via the blood can experimentally only be determined by measuring the radon activity concentration in the exhaled air. In this study, six test persons were exposed to radon rich thermal water in a bathtub in a radon therapy facility in Badgastein, Austria. The time-dependent exhaled activity concentration was continuously measured during the 20 minutes bathing and resting phases. Recorded exhaled radon activity concentrations for the test persons were normalized to the corresponding radon activity concentrations in water and to the individual body surface areas.

The simulation of the transport of radon through the skin, the exhalation via the lungs and the distribution among the organs is based on the biokinetic model of Leggett et al. (2013), extended by an additional skin compartment. In this model, human organs and tissues are represented by eight compartments, three of them, i.e. fat, bone and breast, are further divided into two sub-compartments, which are connected with the arterial and venous blood compartments. As a result of the diffusional transport through the skin, radon is first transferred to the venous blood compartment and subsequently to the pulmonary blood, and finally exhaled due to the exchange between pulmonary blood and lung air. The radon transfer coefficients from organs or tissues to venous blood are determined by the blood perfusion rates, the volume of the organs, and the tissue-to-blood partition coefficients.

The radon activity concentrations in different organs and tissues, resulting from the transfer from arterial blood, absorption in the organ, transfer to venous and uptake through the skin blood can be described with a differential mass balance equation. The coupled linear differential equations describing the radon activity concentrations in each compartment as a function of time during and after radon exposure in the thermal bath were solved numerically with the program package Mathcad. Consistent with the measured exhalation curves, the radon activity concentration in the exhaled breath rapidly increases in a nearly linear manner, eventually reaching a saturation value at the end of the exposure, and then decreases rapidly in an exponential fashion within a few minutes in the subsequent resting phase. While the radon activity concentrations in most organs follow the same pattern as for radon exhalation, activities in tissues with a higher fat content, such as the red bone marrow, decay much slower, thereby still receiving a radiation dose even a couple of hours after the end of exposure.



**Biotechnology**

**08**

## The effect of a synthetic detergent on the production of some biotechnological useful metabolites by *Mucor racemosus*

Violeta Jakovljević<sup>1</sup>, Natasa Djordjević<sup>1</sup>, Zana Dolicanin<sup>1</sup>, Miroslav Vrvic<sup>2</sup>

<sup>1</sup> Department of Biomedical Sciences, State University of Novi Pazar, Novi Pazar, Serbia

<sup>2</sup> Department for Biochemistry, Faculty of Chemistry, University of Belgrade, Belgrade, Serbia

Filamentous fungi represent an incredibly rich and rather overlooked reservoir of natural products, which various applications in different fields. Numerous fungal products such as enzymes, alcohols, organic acids and pharmaceuticals have a central role to the development of modern biotechnology.

The current study investigated the production of some potentially useful metabolites of *Mucor racemosus* in a liquid Czapek-Dox medium (CDM) supplemented with powder detergent MERIX (Henkel, Serbia) at concentrations of 0.3% and 0.5%. The fungal isolate used in the current study originated from water samples of Rasina River (Kruševac, Serbia). The monosporial culture of fungus was determined using Systematic key, at Institute for Biology and Ecology, Faculty of Science, Kragujevac. One mL suspension of spores ( $1 \times 10^7$  spores per mL) was introduced in sterile CDM comprising (g/l) of: 3 NaNO<sub>3</sub>, 1 K<sub>2</sub>HPO<sub>4</sub>, 0.25 MgSO<sub>4</sub>, 0.01 FeSO<sub>4</sub>, 30 sucrose, distilled water up to 1000 ml (control) and in same medium with addition of detergent mentioned concentrations. The fungus was growing in shake flask condition (150 rpm) at room temperature during 16 days. The  $\alpha$ -amylase activity was determined according to Bernfeld method. Amino acid content of fermentation broth of the control and both detergents' media was analyzed by anion-exchange chromatographic method in the Laboratory Sojaprotein (Bečej, Serbia). The activity of  $\alpha$ -amylase of fermentation broths was examined at 3<sup>rd</sup>, 6<sup>th</sup>, 9<sup>th</sup>, 12<sup>th</sup> and 16<sup>th</sup> day of cultivation. Besides, the qualitative and quantitative amino acids content of 16-days-old fermentation broth was determined by HPLC. The obtained results showed that detergent at concentration of 0.3% considerable enhanced the  $\alpha$ -amylase activity (for 48.55%) and the quantity of arginine (for 40.38%) compared to control. The detergent at concentration of 0.5% significantly enhanced the quantity of arginine (119.09%) and alanine (192.79%), whereas  $\alpha$ -amylase retained 100% of its activity in this medium.

Based on the presented results it could be concluded addition of commercial detergent in applied concentrations in Czapek-Dox liquid medium cultivated with *M. racemosus* could be useful strategy for the production of various metabolites with potentially practical application in different industrial areas.

## Optimal condition of gamma-rays, 45, and 100 MeV proton ions for mutation induction in *Cymbidium* hybrid, RBo03

**Sang Hoon Kim, Yeong Deuk Jo, Jin-Baek Kim, Si-Yong Kang**

Advanced Radiation Technology Institute, Korea Atomic Energy Research Institute, Jeongeup, South Korea

In Asian countries, *Cymbidium* species have been one of the most favored orchid species. Mutation breeding using ionizing radiation such as gamma-rays or X-rays is a useful method to broaden the genetic diversity for the limited resources. Recently, plant breeding using heavy ions has been attempted mainly in Japan and China. Protons have intermediate physical properties between heavy ions and gamma-rays, and are therefore expected to have distinct mutation effects for plants. The purpose of this study is to detect the optimal condition of the gamma-rays, 45, and 100 MeV proton ions for mutation induction in a *Cymbidium* hybrid, RBo03 (*Cymbidium sinensis* × *C. goeringii*). The rhizomes of RBo03 were irradiated with gamma-rays and 45 MeV proton ions using a spread-out Bragg peak (SOBP) technology at doses of 20, 40, 60, 80, and 100 Gy, 100 MeV proton ions at doses of 10, 15, 20, 30, and 40 Gy. The relative weight, survival, multiplication, and regeneration rate were scored at 3 and 6 months after irradiation of gamma-rays and proton ions. As a result, the optimal treatment conditions of proton ions were identified as 25 and 35 Gy, reduction dose 50 ( $RD_{50}$ ), for 45 and 100 MeV without application of SOBP technology, respectively. When SOBP is applied at 45 MeV proton ions, the biological responses of RBo03 are not clear with increasing doses. The  $RD_{50}$  of the RBo03 to gamma-rays was 50 Gy. Therefore, the biological effects of 45 and 100 MeV proton ions to the rhizomes of RBo03 were identified as more severe than gamma-rays. These results can be used as user guidelines of proton ions for mutation induction in *Cymbidium*.

## Mutation frequency and spectrum of the *Cymbidium* hybrid, RBo03, according to diverse gamma-ray treatments

**Sang Hoon Kim, Yeong Deuk Jo, Jin-Baek Kim, Si-Yong Kang**

Advanced Radiation Technology Institute, Korea Atomic Energy Research Institute, Jeongeup, South Korea

This study is focused on comparing the mutation frequency and spectrum on diverse gamma-ray treatments and detecting the optimal condition for mutation induction in *Cymbidium* hybrid, RBo03. In the first study, rhizomes of RBo03 (*Cymbidium sinensis* × *C. goeringii*) were irradiated at 20-100 Gy for 24 h. In the second, rhizomes of RBo03 were irradiated using diverse gamma-ray treatments (25 Gy/1 h, 35 Gy/4 h, 50 Gy/8 h, 50 Gy/16 h, and 50 Gy/24 h), which were doses showing similar biological responses to diverse irradiation times (1, 4, 8, 16, and 24 h). The relative weight, survival, multiplication, and regeneration rate of the rhizomes were evaluated at 3 and 6 months after irradiation of gamma-rays. As a result of the first study, RD<sub>50</sub> (reduction dose 50) of RBo03 was identified as a 50 Gy dose at an irradiation of 24 h. The second study indicated that the regeneration ratio of RBo03 was overall decreased by gamma-ray treatment compared to the control, and mostly reduced at an irradiation of 24 h. The mutation frequency of RBo03 was identified to be high at an irradiation of less than 8 h and was the highest as 4.22% at 35 Gy/4 h treatment. The mutation spectrum of RBo03 was evaluated as the mutation index and was identified similarly for three different gamma-ray treatments (25 Gy/1 h, 35 Gy/4 h, and 50 Gy/8 h). Finally, the optimal gamma-ray treatment condition for mutation induction in *Cymbidium* hybrid, RBo03, was 35 Gy/4 h or 50 Gy/8 h treatment, and irradiation of less than 8 h was more efficient than that of more than 16 h. These results can be used as user guidelines for mutation breeding using gamma-rays in *Cymbidium* species.

## **Synergistic effect of *Penicillium verrucosum* and *Geotrichum candidum* on enhanced protease production by submerged fermentation**

**Violeta Jakovljevic<sup>1</sup>, Natasa Djordjevic<sup>1</sup>, Zana Dolocanin<sup>1</sup>, Miroslav Vrvic<sup>2</sup>**

<sup>1</sup> Department of Biomedical Sciences, State University of Novi Pazar, Novi Pazar, Serbia

<sup>2</sup> Department for Biochemistry, Faculty of Chemistry, University of Belgrade, Belgrade, Serbia

Proteases are one of the largest groups of hydrolytic enzymes having 60% share in world enzyme market and among them, 35% consists of alkaline proteases. Alkaline proteases have the applications in industries like laundry detergents, pharmaceutical, leather, food processing and proteinaceous waste bioremediation. Proteases of fungal origin have an advantage over bacterial protease as mycelium can be easily removed by filtration. Detergent industry requires efficient, environmental friendly and economical strategies for unwanted protein degradation. The stability and compatibility of proteases with surfactants and detergents are necessary for their practical application in detergent formulation.

The current study investigated the production of alkaline protease by mixed culture composted from two native isolates: *Penicillium verrucosum* and *Geotrichum candidum* by submerged fermentation. The fungi were isolated from man-made contaminated wastewater (Lepenica River, Kragujevac, Serbia). The monosporial cultures of fungi were determined using Systematic key, at Institute for Biology and Ecology, Faculty of Science, Kragujevac. The equal amount of spore suspension of fungi was introduced in sterile Czapek-Dox liquid medium comprising (g/l) of: 3 NaNO<sub>3</sub>, 1 K<sub>2</sub>HPO<sub>4</sub>, 0.25 MgSO<sub>4</sub>, 0.01 FeSO<sub>4</sub>, 30 sucrose, distilled water up to 1000 ml (control). Parallel, the same medium was prepared with addition of 0.5% ethoxylated oleyl-cetyl alcohol (EOCA). The mixed culture was growing in shake flask condition (orbital shaker 150 rpm) at room temperature during 19 days. The proteolytic activity of fermentation broth was determined periodically, at 4<sup>th</sup>, 7<sup>th</sup>, 10, 14<sup>th</sup> and 19<sup>th</sup> day by Anson's method. After 19 days of incubation, the total dry weight biomass was determined gravimetrically.

Based on results, the maximum proteolytic activity in control and EOCA medium was 0.32 IU/mL and 0.57 IU/mL, respectively. In both media, the maximal enzyme activity was produced in early growth phase of mycelia, at 4<sup>th</sup> day. With culture aging, proteolytic activity was decreased. The addition of surfactant in growth medium had not significant influence on production biomass dry weight. Nevertheless, the best enzyme activity obtained in medium with surfactant (enhanced for 77.98%) indicates the potential application of mixed culture in production of protease in green detergents.



**Cancer  
Research**

**09**

## 3D cancer cell colonies as reliable model systems in the search for new antitumor agents

**Radostina Alexandrova<sup>1</sup>, Lora Dyakova<sup>2</sup>, Tanya Zhivkova<sup>1</sup>, Zdravka Petrova<sup>1</sup>,  
Milena Glavcheva<sup>1</sup>, Boyka Andonova-Lilova<sup>1</sup>, Abudulkadir Abudalleh<sup>1</sup>, Rossen  
Spasov<sup>3</sup>, Gabriela Marinescu<sup>4</sup>, Daniela-Cristina Culita<sup>4</sup>, Luminita Pattron<sup>4</sup>**

1 Institute of Experimental Morphology, Pathology and Anthropology with Museum, Bulgarian Academy of Sciences, Sofia, Bulgaria

2 Institute of Neurobiology, Bulgarian Academy of Sciences, Sofia, Bulgaria

3 Medical Faculty, Sofia University "St. Kliment Ohridski, Sofia, Bulgaria

4 Institute of Physical Chemistry "Ilie Murgulescu", Romanian Academy, Bucharest, Romania

Three-dimensional (3D) cell cultures have been suggested to provide more biologically *relevant information and more predictive data for in vivo tests* and are recognized as suitable model systems for drug discovery and development.

The aim of our study was to apply 3D cancer cell colony method (3D-CFM) for the evaluation of cytotoxic activity of a wide range of compounds (antitumor agents, non-steroidal anti-inflammatory drugs, metal complexes with various ligands).

The investigations were performed with permanent cell lines established from human (breast cancer – MCF-7 and MDA-MB-231; carcinoma of the uterine cervix – HeLa) and animal (rat sarcoma – LSR-SF-SR; chicken hepatoma – LSCC-SF-Mc29) tumors.

In addition to the long-term experiments (14-45 days; with 3D cancer cell colonies) realized by 3D-CFM, short-term experiments (24-72h; with monolayer cell cultures) were also carried out by thiazolyl blue tetrazolium bromide (MTT) test, neutral red uptake cytotoxicity assay, crystal violet staining, Annexin V/FITC method, double staining with acridine orange and propidium iodide, hematoxylin and eosin staining.

The results obtained revealed that all examined compounds decreased to varying degrees viability and/or proliferation of the treated cells. Zn(II)/Au(I) complexes with Schiff bases were found to express the most promising cytotoxic activity.

Whereas short-term experiments assess the ability of the compounds tested to kill quickly tumor cells, 3D-CFM allows prolonged monitoring of the cytotoxic effect of the compounds studied, as well as evaluation of the reversibility of their action. Combined application of short-term experiments with monolayer (2D) cell cultures and long-term experiments with 3D cancer cell colonies can be accepted as a reliable model system for the needs of experimental oncopharmacology.

**Key words:** 2D and 3D cell cultures, cancer cell lines, cytotoxic activity, antitumor agents

**Acknowledgments:** This study was supported by COST Action CA16119 ("CellFit"); Grant ДКОСТ № 01/10 from 22.10.2018 and Grant № DFNI Б0230 from 12.12.2014, National Science Fund, Bulgarian Ministry of Education and Science; a bilateral project between Bulgarian Academy of Sciences and Romanian Academy

## **Soluble forms of the immune check-point receptor PD-1 and its ligand PD-L1 in peripheral blood of patients with various tumors: Clinical and pathologic correlations and prospect**

**Elena Gershtein, Irina Goryatcheva, Denis Naberezhnov, Nikolay Kushlinskii**

N.N. Blokhin National Medical Research Center of Oncology, Moscow, Russia

**Background.** Ability to withstand the immune response of the organism is one of the key features of malignant tumor. Among various possibilities of escaping from antitumor immunity an important role belongs to modification of PD-1/PD-L immune check-point signaling pathway that in normal physiologic conditions controls autoimmune reactions. Tumor PD-1 and/or PD-L1 expression is investigated both as a predictor of corresponding immunotherapy efficiency, and as molecular markers of overall prognosis and patients' survival. This goal could be also attained by the measurement of soluble forms of these proteins (sPD-1 and sPD-L1) in blood serum.

**Objective.** comparative evaluation of sPD-1 and sPD-L1 content in blood serum or plasma of practically healthy persons and patients with various benign and malignant tumors; analysis of the associations between these markers and clinical and pathologic characteristics in order to assess their clinical value.

**Design.** 117 patients with renal tumors, 121 with ovarian tumors, 70 – with gastric cancer and 58 with bone sarcomas were enclosed. Control group comprised 74 practically healthy persons. sPD-L1 and sPD-1 concentrations were measured using standard enzyme immunoassay kits (Affimetrix, eBioscience, USA).

**Results.** sPD-L1 levels in blood serum of patients with renal cancer and benign tumors were significantly higher than in control ( $p < 0.0001$  and  $p < 0.05$  respectively). sPD-L1 level significantly increased with disease stage ( $p < 0.001$ ) and T index, was significantly higher in patients with lymph node metastases (both  $N_1$ , and  $N_2$ ) than in those with  $N_0$ ; it was also increased in  $M+$  patients, and in patients with G III-IV in comparison to G I-II tumors. It also was positively associated with VEGF ( $R=0.26$ ;  $p < 0.01$ ), VEGFR1 ( $R=0.30$ ;  $p < 0.01$ ), MMP-7 ( $R=0.45$ ;  $p < 0.0001$ ), MMP-8 ( $R=0.44$ ;  $p < 0.0001$ ) and TIMP-1 ( $R=0.44$ ;  $p < 0.0001$ ) serum levels. sPD-1 concentrations did not differ significantly between study groups. In gastric cancer and bone sarcomas patients sPD-L1, but not sPD-1 levels were also increased as compared to control. In ovarian cancer patients both sPD-L1 and sPD-1 did not differ from control, but sPD-L1 significantly increased with disease stage and was higher in patients with ascites than in those without it.

**Conclusions.** sPD-L1 level is increased in peripheral blood of patients with various malignant tumors, correlates with disease progression and tumor grade, and can be regarded as promising marker for monitoring of anti-PD1/PD-L treatment efficiency. Potential clinical implications of sPD-1 require further investigations and analysis.

**Acknowledgments:** Supported by RFBR grant 18-03-00793.

## Synthesis and characterization of conjugated doxorubicin for drug delivery

**Kamila Butowska<sup>1,2</sup>, Witold Kozak<sup>3</sup>, Janusz Rak<sup>3</sup>, Jacek Piosik<sup>1,2</sup>**

1 Intercollegiate Faculty of Biotechnology of the University of Gdańsk, Gdańsk, Poland

2 Medical University of Gdańsk, Gdańsk, Poland

3 University of Gdańsk, Gdańsk, Poland

New materials, platforms and drug delivery systems play an important role in cancer treatment. Today chemotherapy is a combination of anticancer drug with different kinds of monoclonal antibody, liposomes and polymeric or nanoscale platforms that improve selectivity and decrease side effects of therapy.[1]Doxorubicin belongs to the group of chemotherapeutics commonly used in patients with cancer diseases.[2]

In this study, doxorubicin (DOX) was conjugated with the C<sub>60</sub>fullerene (Ful-DOX) [3]as well as with a polyethylene chain (Methano-DOX). The obtained conjugates were comprehensively characterized using <sup>1</sup>H NMR and MALDI TOF/TOF and triple TOF mass spectrometry. Moreover, the absorption and fluorescence spectra of compounds were measured. In order to compare the cytotoxic effects of free DOX, Ful-DOX and Methano-DOX, MTT and WST-1 assays were employed using several types of breast cancer cell lines.

In summary, we successfully synthesized and characterized Ful-DOX and Methano-DOX conjugates and demonstrated that transforming DOX into its conjugates dramatically diminishes the cytotoxicity of the drug.

**Acknowledgments:** This work was supported by the Polish Ministry of Science and Higher Education under the Grant Nos. DS/530-Mo45-D674-17 (Jacek Piosik) and DS/530-8227-D494-18 (JanuszRak).

### References

- [1] Y. You, Z. Xu, Y. Chen, Doxorubicin conjugated with a trastuzumab epitope and an MMP-2 sensitive peptide linker for the treatment of HER2-positive breast cancer, *Drug Deliv.*, 25, 448-460, 2018.
- [2] S.G. Creemers, L.J. Hofland, E. Korpershoek, G.J.H. Franssen, F.J. van Kemenade, W.W. de Herder, R.A. Feelders, Future directions in the diagnosis and medical treatment of adrenocortical carcinoma, *Endocr.Relat. Cancer*, 23, R43-R69, 2016.
- [3] F. Lu, S.A. Haque, S-T. Yang, P.G. Luo, L. Gu, A. Kitaygorodskiy, H. Li, S. Lacher, Y-P. Sun, Aqueous Compatible Fullerene-Doxorubicin Conjugates, *J. Phys. Chem. C*, 113, 17768-17773, 2009.

## Causes of hepatocellular cancer in same number of women and man who have chronic hepatitis B and C etiology

**Edina Bilić-Komarica**

UKCS, Sarajevo, Bosnia and Herzegovina

Hepatocellular liver cancer (HCC) is associated with a high incidence of chronic hepatitis B and C etiology. Hepatocellular cancer must not always be preceded by cirrhotic liver disease. In the pathogenesis of cirrhosis, the liver is dominated by three pathological processes, including hepatocyte necrosis (cell death), fibrosis and regeneration. Cirrhosis, with its histological characteristics, is a precancerous condition that leads to the development of cancer. Viruses B or C in their presence in the liver parenchyma trigger an inflammatory process followed by hepatocyte necrosis. Chronic active hepatitis B and C etiology is a major medical problem since viruses by their presence and incorporation in the hepatocyte genome trigger the pathological process leading to HCC. Alfa-fetoprotein (AFP) is the most important diagnostic marker for HCC. It has relatively high specificity and sensitivity and is widely applied in practice. With this research, we will point out all known facts about the increase of Hepatocellular carcinoma (HCC) in men and women with hepatitis B and C etiology. The research highlights the diagnosis of hepatitis, the polymerized chain reaction, and the serological reaction very important for the quantification of the virus in the serum of the diseased, then the histological finding of the liver obtained by taking a bioptic sample by percutaneous liver biopsy. A particular review is given on the epidemiological significance of hepatitis, as viral infections spread throughout the Earth's sphere, as well as viruses declared to be biological carcinogens. Also, the research has given great importance to AFP as a significant carcinoma antigen in proving HCC.

**Keywords:** HCC, viruses, hepatitis B, hepatitis C, cancer, liver, cirrhosis

## **Ru(III) complexes with schiff bases effectively inhibit 2D and 3D growth of cultured human and animal tumor cells**

**Radostina Alexandrova<sup>1</sup>, Zdravka Petrova<sup>1</sup>, Desislav Dinev<sup>1</sup>,  
Boyka Andonova-Lilova<sup>1</sup>, Rossen Spasov<sup>2</sup>, Gabriela Marinescu<sup>3</sup>,  
Daniela-Cristina Culita<sup>3</sup>, Luminita Patron<sup>3</sup>**

<sup>1</sup> Institute of Experimental Morphology, Pathology and Anthropology with Museum, Bulgarian Academy of Sciences, Sofia, Bulgaria

<sup>2</sup> Medical Faculty, Sofia University "St. Kliment Ohridski", Sofia, Bulgaria

<sup>3</sup> Institute of Physical Chemistry "Ilie Murgulescu", Romanian Academy, Bucharest, Romania

Searching for new effective anticancer agents is among the most important challenges facing modern biomedicine and medicinal chemistry.

Various Ru(II) and Ru(III) complexes have been found to express encouraging antitumor properties in model systems in vitro and in vivo. On the other hand many Schiff bases and especially their metal complexes have been reported to exhibit promising anticancer potential.

The aim of our study was to evaluate the cytotoxic activity of three newly synthesized ruthenium(III) complexes with Schiff bases resulted from the condensation reaction between salicylaldehyde and ethylenediamine (Salen), 1,3-diaminopropane (Salpn) and 1,2-phenylenediamine (Salphen), respectively.

Cell lines established from human breast cancer (MCF-7, MDA-MB-231), cervical carcinoma (HeLa), non-small cell lung cancer (A549) and glioblastoma multiforme (8MG-BA) as well as from transplantable sarcoma in rat induced by Rous sarcoma virus strain Schmidt-Ruppin (LSR-SF-SR) were used as model systems in our investigations. Non-tumor human Lep-3 cells were used for comparative purposes. The effect of the compounds on cell viability and proliferation was examined by thiazolyl blue tetrazolium bromide (MTT) test, neutral red uptake cytotoxicity assay, crystal violet staining, Annexin V/FITC method, double staining with acridine orange and propidium iodide, hematoxylin and eosin staining, 3D colony-forming method. The compounds were applied at a concentration range of 5-100 µg/ml for 24-72 h (in short-term experiments, with monolayer cultures) and 25-30 days (in long-term experiments, with 3D cancer cell colonies).

The results obtained revealed that all examined metal complexes reduced significantly viability and/or proliferation of the treated cells in a time- and concentration-dependent manner. Tested independently, the ligand Salen did not decrease cancer cell growth.

In conclusion, the investigated newly synthesized Ru(III) complexes with Schiff bases Salen, Salpn or Salphen express promising cytotoxic activity against human and animal tumor cells that has been proved in short-term and long-term experiments using monolayer (2D) and 3D cell cultures and methods with different molecular / cellular targets and mechanisms of action.

**Keywords:** Metal complexes, schiff bases, ruthenium(iii), cancer, cell lines, cytotoxic activity

**Acknowledgments:** This study was supported by COST Action CA15135 ("MuTaLig"); Grant ДКОСТ 01/16 from 17.08.2017, Fund "Scientific Research", Bulgarian Ministry of Education and Science; a bilateral project between Bulgarian Academy of Sciences and Romanian Academy.

## Humoral immunity in patients with gastric cancer: The role of B-1 lymphocytes in the antitumor immunity

Svetlana Vasilievna Chulkova<sup>1,2</sup>, Evgeny Vyacheslavovich Glukhov<sup>1</sup>,  
Lyudmila Yuryevna Grivtsova<sup>1</sup>, Elena Nikolaevna Sholokhova<sup>1</sup>,  
Nikolay Nikolayevich Tupitsyn<sup>1</sup>

<sup>1</sup> N.N.Blokhin National Medical Research Center of Oncology, Ministry of Health of Russia, Moscow, Russia

<sup>2</sup> N.I.Pirogov Russian National Research Institute, Ministry of Health of Russia, Moscow, Russia

**Introduction.** A small number of B1-lymphocytes, mainly cells secreting antibodies, are detected in the spleen, where they account for up to 5% of the number of B-cells. Splenectomy for the purpose of adequate lymphodissection in stomach cancer causes pronounced and long-term dysfunction of the various parts of the immune system.

**Purpose.** To study the B-cell humoral immunity in patients with gastric cancer.

**Materials and methods.** The study included 50 patients with gastric cancer. Group 1 - patients with gastrectomy and spleno-protective D2-lymphodissection, 2-nd group - patients with gastrectomy, D2-lymphodissection and splenectomy. Subpopulations of B-cells: CD20, CD21, CD23, CD38, HLA-DR, CD71, CD10, CD95, CD25, CD5, CD56 and IgG- and IgG- light chain immunoglobulins.

**Results and discussion.** In the evaluation of subpopulations of B-cells before surgical treatment a significant number of B-cells with a low level of CD21+ expression, a prominent proportion CD23+ number and clonal B-cells cases were detected. In this case, as a rule, CD23+ B-cells had a weaker expression of the antigen of mature B-cells CD20. The number of CD19+CD5+B-cells on average was 17.7% and in 3 patients more than 40%. It was found that some of these cells demonstrate the CD38+ and CD25+ activation antigens. In the first group of patients reliable correlations (before and after the operation) between the relative and absolute number of CD19+B cells, as well as CD19+CD21+cells, were obtained. In the 2-nd group, the relative number of B-lymphocytes, CD5+B-cells, CD19+CD38+ cells was reliably correlated. Since 3 months after surgical treatment, the percentage of cells with CD5+antigen expression significantly increased ( $t = -6.015$  sig<0.0001,  $p = 0.013$ ), and the relative number of CD19+ lymphocytes and CD19+CD21+B-cells decreased ( $p = 0.08$ ). After the operation a high percentage of CD19+CD5+B-cells was found in the group of patients with splenectomy ( $p=0.049$ ), which are precursors of functionally more perfect, clonally more diverse true B-cells.

**Conclusion.** CD5+ B-lymphocytes percentage increased significantly from 12.9 to 21.8% in the group of patients with standard D2-lymphodissection and splenectomy, while the total number of CD19 + lymphocytes and CD19+ CD21+ cells decreased. Thus, in patients of the experimental group, there may be a decrease in antibody production, a weakening of both general and antitumor immunity.

**Keywords:** B- lymphocytes, humoral immunity, stomach cancer, splenectomy, D2-lymphodissection

## Clinical and biological factors forecast metachronous breast cancer

**Svetlana Vasilievna Chulkova<sup>1,2</sup>,  
Natalya Vasilyevna Lepkova<sup>2</sup>, Angelina Vladimirovna Egorova<sup>2</sup>**

1 N.N.Blokhin National Medical Research Center of Oncology, Ministry of Health of Russia, Moscow, Russia

2 N.I.Pirogov Russian National Research Institute, Ministry of Health of Russia, Moscow, Russia

**Objective.** To study the clinical and biological predictive factors for metachronous breast cancer.

**Materials and methods.** The study included 210 patients with metachronous breast cancer. With the primary tumor, 22.9% of patients, 19.4% were patients, with the second tumor - 31.9%. In primary breast cancer, 18.1% of patients received surgical treatment, 27.6% combined treatment (surgical treatment, radiotherapy, chemo- or chemo-radiation therapy).

**Results and discussion.** Survival in the group of breast cancer patients in whom the metachronous tumor appeared in the first 3 years after treatment was 58%, and the mortality rate was 3.03, while in the group in which the second tumor was detected after 5 years of treatment, 100% and 0.33, respectively. Patients younger than 50 years old: in most of these patients, the tumor is receptor-positive, and the survival rate is 91.7%. In patients with stages T1-2N1-3 – T1-2N0, a high survival rate is noted compared to others, and this is certainly due to the fact that metachronous cancer more often occurs after 5 years after treatment. When assessing lesions of the lymphatic apparatus, it was found that with primary breast cancer, and with a metachronous tumor, the total 5-year survival in the presence of 1 metastatic lymph node is 89.5%, whereas in a lesion of more than 3 lymph nodes only 68.5%. 91.9% of patients are dominated by aneuploid tumors, and they are associated with the early stages of the process, are observed mainly in women younger than 50 years and in 35.2% of cases are combined with the loss of chromosomal material. Diplomas with a set of chromosomes occurred at the age of over 50 years and with locally advanced stages. Tetraploid tumors were detected in almost 3% of cases. In determining the degree of malignancy of the tumor, it was established that in metachronous cancer, the overwhelming percentage of tumors has a degree of malignancy II.

**Conclusion.** Thus, during our study, important prognostic signs of metachronous breast cancer were established: the time of occurrence of a metachronous tumor, the age of patients, ovarian-menstrual function, the level of steroid hormone receptors, the stage of the process, the number of metastases in regional lymph nodes. According to the results of multivariate analyzes (Shannons), the risk of developing metachronic breast cancer is made up of young women, with intact menstrual function, in the early stages, the tumor in which is aneuploid with a loss of chromosomal material.

**Keywords:** Breast cancer, metachronous cancer, predictive factors, DNA cytofluorimetry, ploidy activity of tumor



**Environmental  
Chemistry**

**10**

## Geochemistry of $^{234,238}\text{U}$ isotopes in modern carbonate sediments of small lakes (Baikal Region)

Yulia Vosel<sup>1</sup>, Sergey Vosel<sup>2,3</sup>, Irina Makarova<sup>1</sup>, Mikhail Melgunov<sup>1,3</sup>

<sup>1</sup> The V.S. Sobolev Institute of Geology and Mineralogy of the Russian Academy of Sciences, Novosibirsk, Russia

<sup>2</sup> The Voevodsky Institute of Chemical Kinetics and Combustion Siberian Branch of the Russian Academy of Sciences, Novosibirsk, Russia

<sup>3</sup> Novosibirsk State University, Novosibirsk, Russia

The processes of diagenesis play a significant role in the redistribution of the elements in aquatic sediments. Our work is devoted to study of lake sediments diagenetic processes involving U and Mn in order, to obtain evidence of the U (IV) phases formation.

The freshwater lake Alaty (53° 12' 51.65" N, 102° 11' 43.66" E) and saline Tsagan-Tyrm (52° 51' 59.52" N, 106° 35' 33.47" E) were studied. The main method of the study was the sequential extraction method [Tessier et al., 1979]. The method allows to separate the lithogenic phases from the chemogenic and to measure  $^{234,238}\text{U}$  isotope activity in all phases. In the lithogenic phases, the isotopic ratio is  $^{234}\text{U}/^{238}\text{U} = 1$ . In surface waters, this ratio is usually much more [Chalov, 1975]. The Tessier method do not interact with the U (IV) phases and they must remain in the residues.  $^{234}\text{U}$  and  $^{238}\text{U}$  isotopes in the samples was measured by  $\alpha$ -spectrometry. The measurements of Ca, Sr, Mn are made by the atomic adsorption method.

The concentration of  $\text{Mn}^{2+}$  ions in carbonates was measured by electron paramagnetic resonance. The amount of  $\text{MnOx}$  in the upper sediment horizons, in a layer of 0-30 cm, increases sharply towards the sediment-water boundary. The main amount of U in the bottom sediments of both lakes is the authigenic U. Throughout the sediment core of Alaty  $^{234}\text{U}/^{238}\text{U}$  in authigenic fractions is approximately  $1.7 \pm 0.3$  and close to that in the lake water ( $1.66 \pm 0.27$ ). In the upper half of the section 0-42 cm in the residue  $^{234}\text{U}/^{238}\text{U} = 1.0 \pm 0.15$ . At the same time, at a great depth (93 cm) in the residue  $^{234}\text{U} / ^{238}\text{U} = 1.5 \pm 0.29$ . This directly shows that, in addition to the terrigenous U, the newly formed phases of U (IV) exist. In all authigenic fractions throughout the sediment core of the lake Tsagan-Tyrm  $^{234}\text{U}/^{238}\text{U} = 2.7 \pm 0.15$  and fully corresponds to water ( $2.6 \pm 0.13$ ). The lake is very shallow, with high salinity. In winter, the lake waters are almost completely freezing, which leads to sharply reducing conditions. Measurements carried out for horizons of 0-3, 6-9 and 33-35 cm show that in their residue  $^{234}\text{U}/^{238}\text{U} > 2$ , and accordingly there is a chemogenic U, i.e. there may be phases U (IV). A large number of U (IV) phases is found in the horizon of 3-6 cm. At the same time, it has been shown that Mn oxide are completely absent in the upper layers, they appear only at a depth of 12 cm and below. Such distribution of U and Mn is completely explained by the sharply reducing environment in the upper horizons of the sediment of the lake Tsagan-Tyrm. The conducted study confirms the hypothesis of the formation of U (IV) phases in lake sediments.

**Acknowledgments:** The work was carried out within the framework of state task No.0330-216-0011, with partial financial support of RFBR grant 18-05-00953\_a. Analytical studies were carried out in the Center for Multielement and Isotope Studies of the SB RAS.

## Photodegradation of selected micropollutants stimulated by photolysis of natural humic substances: A mechanistic study

Ivan Pozdnyakov<sup>1,2</sup>, Yuliya Tyutereva<sup>1,2</sup>, Ekaterina Mordvinova<sup>1,2</sup>, Victoria Salomatova<sup>1,2</sup>, Petr Sherin<sup>2,3</sup>, Marina Parkhats<sup>4</sup>, Yong Chen<sup>5</sup>, Zizheng Liu<sup>6</sup>

1 Voevodsky Institute of Chemical Kinetics and Combustion, Novosibirsk, Russia

2 Novosibirsk State University, Novosibirsk, Russia

3 International Tomography Center, Novosibirsk, Russia

4 B.I. Stepanov Institute of Physics National Academy of Sciences of Belarus, Minsk, Belarus

5 School of Environmental Science and Engineering, Huazhong University of Science and Technology, Wuhan, China

6 School of Civil Engineering, Wuhan University, Wuhan, China

Humic substances (HS, including humic and fulvic acids) are naturally photoactive components, which widely present in surface waters. HS are able to generate reactive oxygen species (ROS) under solar irradiation, which can react with dissolved organic pollutants initiating their degradation and mineralization. That is why much attention is paid nowadays to investigation of HS photochemistry and to development of approaches to water treatment based on generation of ROS [1].

The talk exhibits several examples of mechanistic study of emerging micropollutants (herbicides, phenylarsonic feed additives and PPCP) UV photooxidation by humic substances (IHSS standards and fulvic acids of ChangSheng and Aladdin companies). Some of these results have been published recently [2,3]. Main information was obtained by combination of steady-state and flash photolysis, time resolved luminescence with LC and LC/MS techniques. Main attention was paid to:

- i. identification of active short-lived transient species (including ROS, triplet states and organic radicals)
- ii. nature of final photoproducts
- iii. quantum yields of photoreactions
- iv. construction of whole mechanism of photodegradation of target compounds

**Acknowledgments:** The work was financially supported by Russian Science Foundation (18-13-00246), Russian Foundation for Basic Research (18-53-00002\_BEL, 18-53-53006\_GFEN) and the Belarusian Republican Foundation for Fundamental Research (grant N<sup>o</sup> F18R-140). HPLC and HPLC-MS measurements were supported by FASO Russia (project 0333-2018-0003).

### References

1. K. McNeill, S. Canonica, Triplet state dissolved organic matter in aquatic photochemistry: reaction mechanisms, substrate scope, and photophysical properties, *Environ. Sci.: Processes Impacts*, 18 (2016) 1381-1399.
2. I.P. Pozdnyakov, P.S. Sherin, V.A. Salomatova, M.V. Parkhats, V.P. Grivin, B.M. Dzhagarov, N.M. Bazhin, V.F. Plyusnin, Photooxidation of herbicide Amitrole in the presence of fulvic acid, *Env. Sci. Pollut. Res.*, 25 (2018) 20320-20327
3. Y. Chen, J. Liang, L. Liu, X. Lu, J. Deng, I.P. Pozdnyakov, and Y. Zuo, Photosensitized Degradation of Amitriptyline and Its Active Metabolite Nortriptyline in Aqueous Fulvic Acid Solution, *J. Environ. Quality*, 46 (2017) 1081-1087

## **Rapid analysis of uranium and plutonium isotopes in environmental samples using inductively coupled plasma mass spectrometry**

**Jong-Myoung Lim, Ji-Young Park, Hyuncheol Kim,  
Mee Jang, Won-Young Kim, Wan-Ro Lee**

Korea Atomic Energy Research Institute, Daejeon, South Korea

Plutonium and uranium in the environment are known to have a relatively high toxicity. Thus these nuclides have been a focus of interest not only in environmental studies for the origin of the nuclear materials, but also in waste management field from nuclear power plants. Moreover, the isotopic composition of actinides (Pu and U) provides the source information of nuclear and radiological materials used during illegal activities. For emergency preparedness for nuclear accidents, as an attempt to reduce the social costs and apprehension arising from radioactivity in the environment, an accurate and rapid assessment of actinide radionuclide deposition levels or contamination is highly desirable. Thus a rapid and accurate analytical method that can be used to evaluate the radioactivity of actinides (e.g.,  $^{238}\text{U}$ ,  $^{235}\text{U}$ ,  $^{239}\text{Pu}$ , and  $^{240}\text{Pu}$ ) should be developed and validated. While  $\alpha$ -spectrometry has a prominent measurement capability at a very low activity level of  $^{238}\text{U}$ ,  $^{235}\text{U}$ ,  $^{239}\text{Pu}$ , and  $^{240}\text{Pu}$ , it has a major disadvantage of a long counting time for the determination of  $\alpha$ -nuclide activity, and cannot separate Pu nuclides. Contrary to the  $\alpha$ -spectrometry method, a measurement technique using ICP-MS with an advanced sample introduction and mass counting system allows radioactivity in many samples to be measured with a short time period with a high degree of accuracy and precision. Both methods also encounter the most significant difficulties during pretreatment (e.g., purification, speciation, and dilution/enrichment). Since the pretreatment process consequently plays an important role in the measurement uncertainty, a method of development and validation should be performed. In this study, a rapid digestion and separation method for U and Pu radionuclides was developed in soil and ground water samples. The soil and ground water samples were digested using  $\text{LiBO}_2$  fusion and concentrated on the hot plate, respectively. The target nuclides (e.g., U and Pu) were separated and concentrated using TRU and UTEVA resin. Finally, the mass concentrations of U and Pu isotopes were determined using Quadrupole ICP-MS system with an APEX nebulizer. For an evaluation of the accuracy and precision of evaluated method, various reference materials (RMs) from IAEA and NIST were analyzed.

## Study of metal accumulation in the soil–leaf–fruit system using neutron activation analysis

**Inga Zinicovscaia<sup>1,2,3</sup>, Rodica Sturza<sup>4</sup>, Irina Gurmeza<sup>4</sup>,  
Konstantin Vergel<sup>1</sup>, Svetlana Gundorina<sup>1</sup>, Marina Frontasyeva<sup>1</sup>**

1 Joint Institute for Nuclear Research, Dubna, Russia

2 Horia Hulubei National Institute for R&D in Physics and Nuclear Engineering, Bucharest – Magurele, Romania

3 The Institute of Chemistry of the Academy of Sciences of Moldova, Chisinau, Moldova

4 Technical University of Moldova, Chisinau, Moldova

The determination of macro- and microelements in soil-leaf-fruit systems is extremely important for assessing the quality of the fruits and for consumer's health. The content of major and trace elements in selected varieties of fruits (apple, plum, and grape) as well as in leaves and soils samples collected in the Republic of Moldova was determined using neutron activation analysis. Content of trace elements determined in analyzed soil corresponds to average values obtained for microelements in the Republic of Moldova. The majority of elements in apple fruits were higher in comparison with plum and grape fruits. The highest concentration in case of all fruits was obtained for K: 14500 µg/g (grape), 21600 µg/g (plum) and 23700 µg/g (apple). Transfer factors from soils to leaves and fruits as well as from leaves to fruits, the daily intake of metals, and the hazard quotient indices were calculated. The transfer factor calculated for different systems showed large differences between metals. The values for the estimated dietary intakes and hazard quotients for toxic elements (Cr, Co, Fe, Mn, Ni, V, and Zn) were lower than the recommended safety limits by Food and Nutrition Board. Therefore, the analyzed fruits were considered to be safe for human consumption.

## Silver removal from batch systems using *Arthrospira (spirulina) platensis* biomass

Dmitrii Grozdov<sup>1</sup>, Inga Zinicovscaia<sup>1</sup>,  
Liliana Cepoi<sup>2</sup>, Tatiana Chiriac<sup>2</sup>, Tatiana Mitina<sup>3</sup>

1 Joint Institute for Nuclear Research, Dubna, Russia

2 Institute of Microbiology and Biotechnology, Chisinau, Moldova

3 The Institute of Chemistry, Chisinau, Moldova

The cyanobacterium *Arthrospira (Spirulina) platensis* was used to study the process of silver biosorption. Effects of various parameters such as contact time, dosage of biosorbent, initial pH, temperature, and initial concentration of Ag(I) were investigated for a batch adsorption system. The optimal biosorption conditions were determined as pH 5.0, biosorbent dosage of 0.4 g, and initial silver concentration of 30 mg/L. Equilibrium adsorption data were analyzed by the Langmuir and Freundlich models – however the Freundlich model provided a better fit with the experimental data. The kinetic data fit well into the pseudo-second-order model, with a correlation coefficient 0.99. The analysis of thermodynamic parameters ( $\Delta G^\circ$ ,  $\Delta H^\circ$  and  $\Delta S^\circ$ ) revealed that the nature of adsorption was feasible, spontaneous ( $\Delta G^\circ < 0$ ) and exothermic ( $\Delta H^\circ < 0$ ) process. The biosorption capacity of biomass *Arthrospira platensis* serves as a basis for the development of green technology for environmental remediation.

## Instrumental neutron activation for analysis of spatial distribution of heavy metals in surface sediments of the Danube River

**Tatjana Trtić-Petrović<sup>1</sup>, Otilia Ana Culicov<sup>2,3</sup>,  
Roman Balvanović<sup>1</sup>, Andjelka Petković<sup>4</sup>**

<sup>1</sup> Laboratory of Physics, Vinča Institute of Nuclear Sciences, University of Belgrade, Belgrade, Serbia

<sup>2</sup> Frank Laboratory of Neutron Physics, Joint Institute for Nuclear Research, Dubna, Russia

<sup>3</sup> National Institute for R&D in Electrical Engineering ICPE-CA, Bucharest, Romania

<sup>4</sup> "Jaroslav Černi" Institute for the Development of Water Resources, Belgrade, Serbia, Belgrade, Serbia

In this paper, the spatial distribution of the heavy metals including technology-critical elements (TCE) in the surface river sediments was investigated. The surface sediments of the Danube River in the Republic of Serbia, as well as three tributaries were analysed. Instrumental neutron activation analysis (INNA) has been applied for quantification of the selected element in the samples. The main features of INAA are: simultaneously determining more than 40 elements with high sensitivity and low detection limit, high selectivity due to specific nuclear reaction for each element, the nondestructive method, the sample stays intact and no chemical separation treatment is involved, simple sample preparation step, especially solid samples, a small quantity of sample ( $\approx 200 \mu\text{g}$ ) and determination of the total element concentration independent of chemical species, real total analysis since the test portion does not have to be dissolved. The heavy metal concentration in the sediments connected with hydropower dam and accumulation of sediments in the reservoir systems Iron gate I and Iron gate II were discussed.

Surface river sediments were collected from the river bottom at the central and the deepest part using an Ekman grab sampler and air-dried in a thin layer in the dark at room temperature ( $23 \pm 1$  °C). Also, deep river sediments (1.5 and 7 m) were collected and used for comparison purpose. After drying, the samples were homogenized using a pestle and mortar and sieved through a 1-mm sieve to ensure sample homogeneity. INAA were used to quantify following elements: Na, K, Rb, Cs, Mg, Ca, Sr, Ba, Al, Sc, Ti, V, Cr, Mn, Fe, Co, Ni, Zn, Ga, As, Se, Yr, Ag, Cd, Sb, La, Ce, Nd, Sm, Eu, Gd, Tb, Dy, Tm, Yb, Th, Hf, Ta, W, Au, Hg and U. Irradiations were performed at the pulsed reactor IBR 2 (Frank Laboratory of Neutron Physics, JINR, Dubna, Russian Federation) using epithermal neutrons. Principal Component Analysis (PCA) and Power transformation as a pretreatment method were applied for analysis of experimental data.

It was found that the increase in the amount of sediment in the reservoir prior to the dam Iron gate I was accompanied by an increase in the concentration of the following metals: antimony, arsenic, chromium, europium, neodymium and samarium.

## Motor behaviour and energy metabolism of *Blaptica dubia* in artificial magnetic fields

**Branka Petković, Larisa Ilijin, Dajana Todorović,  
Marija Mrdaković, Milena Vlahović, Anja Grčić, Vesna Perić-Mataruga**

Institute for Biological Research “Siniša Stanković”, University of Belgrade, Belgrade, Serbia

During the evolution, all organisms are exposed to the constant action of different environmental factors, biotic and abiotic, which are variable in time and space. Life on Earth is formed in a natural magnetic field (geomagnetic field). Therefore, magnetic field (MF) is classified as abiotic factor that help maintain different life processes of plants, animals and humans, as well as their biological and physiological functions. Organisms are exposed to new type of artificial MFs, due to the increasing electrification and technological development. So, MF is growing environmental pollutant and as a consequence of response and/or adaptation of organisms on new, stressful conditions, changes could be observed on all levels of the biological organization. So, the aim of this study was to evaluate the long – term effect of a static MF (SMF) and an extremely low frequency MF (ELF MF) on the motor behaviour in *Blaptica dubia* nymphs, as well as on their fat body glycogen concentration and total lipid content. One month old nymphs were randomly divided into three experimental groups: control, exposed to SMF (110 mT) and exposed to ELF MF (50 Hz, 10 mT). The cockroaches were exposed to these MFs for 5 months, while the control ones were kept outside the reach of the magnetic field. Fat body glycogen concentration, as well as total lipid content, was measured spectrophotometrically according to Wyatt and Kalf (1957) and Stone and Mordue (1980), respectively. Also, we monitored nymphal behaviour for 10 minutes in “open – field” test and analyzed several behavioural parameters (travel distance, average speed while in motion, time mobile, travel distance of the head, number of body rotations, immobility time) using ANY – maze software. Exposure to SMF and ELF MF affected the all examined behavioural parameters. Namely, in comparison to control cockroaches, all parameters, except immobility time, were significantly higher in *B. dubia* nymphs exposed to both MFs. The difference between the MF groups was no statistically significant. In SMF and ELF MF groups, fat body glycogen concentration was significantly lower compared to control group. Between the MF groups significant differences were not observed. The lipid concentration in the fatty body of *B. dubia* nymphs depended on the applied MF. In nymphs exposed to SMF, total lipid content was significantly higher compared to control. ELF MF caused its decrease compared to control and SMF group. These differences were significant only for SMF group. This study provides evidences that long – term exposure of *B. dubia* nymphs to magnetic fields induces important alterations in their motor behaviour, and consequently examined parameters of carbohydrate and lipid metabolism.

**Acknowledgments:** This study was supported by the Serbian Ministry of Education, Science and Technological Development (grant No. 173027).

## Optimization of Sr-ion extraction from the contaminated soil using Box-Benken design

**Marija Šljivić-Ivanović, Mihajlo Jović, Slavko Dimović, Ivana Smičiklas**

University of Belgrade, Vinča Institute of Nuclear Sciences, Belgrade, Serbia

Among the factors that affect the degradation of soil quality, contamination with radioactive substances has gained significance due to the fast development and exploitation of nuclear energy. The remediation measures based on physical, chemical and biological principles aim to reduce the adverse effects of ionizing radiation on the ecosystem as a whole, either by radionuclide separation from the soil matrix or by their solidification/stabilization. The selection of suitable method is carried out for each individual case of contamination, as it depends on the soil type, the pollutant type, distribution, and the level of contamination, area that needs to be treated, overall cost, etc. In order to develop a site-specific treatment, optimization of the method performance is required through the extensive research on the effects of a large number of variables. In such cases, experimental design methodology (DOE) represents a useful approach for the comparison of different treatments and their optimization. In contrast to the conventional strategy of varying one factor at the time, DOE implies a simultaneous variation of all factors in order to disclose the most influential factors, the significant interactions between the factors, and the optimal levels of the factors. In the present study, the problem of soil contamination with  $^{90}\text{Sr}$  was addressed. Previous investigations on Sr-ions distribution in the soil have revealed their preferential association with the ion-exchangeable sites, regardless of the soil type, contamination level and aging time. High mobility of Sr in the soil is, therefore, the property that makes the separation by chemical extraction a simple and economical option since the effects can be achieved using solutions of competing cations. The soil, sampled at the site of the Vinča Institute of Nuclear Science and the Public Company Nuclear Facilities of Serbia, was artificially contaminated with Sr-ions. The Box-Benken design was used for the analysis of soil remediation efficiency using  $\text{Ca}(\text{NO}_3)_2$  as an extracting agent. Reagent concentration, soil/liquid ratio and contact time were considered as process variables, whereas the amounts of extracted cations and the final pH values were monitored as the response functions. The applicability of different mathematical models, with the inclusion of linear or quadratic terms, was tested for the description of experimental results. Analysis of variance of the chosen responses showed that Sr extraction efficiency was primarily affected by the variation of the reagent concentration. By proper selection of the levels of investigated factors, complete removal of Sr was achieved. Furthermore, DOE enabled the prediction of system responses, which makes it a significant tool in practical applications.

## Trace and minor elements in bottom sediments of selected rivers and brooks from Eastern Paraguay by X-ray fluorescence

**Juan F. Facetti–Masulli<sup>1</sup>, Peter Kump<sup>2</sup>, Mirna Delgado<sup>3</sup>**

<sup>1</sup> National University of Asuncion, Asunción, Paraguay

<sup>2</sup> Josef Stefan Institute, Ljubljana, Slovenia

<sup>3</sup> Hydroconsult SRL, Asunción, Paraguay

Selected minor and trace elements in bottom sediments from the Tebicuary River, a tributary of the Paraguay River, as well as from Tapiracuai and Kuarepoti Brooks on the left side of the later large basin, have been investigated by X-Ray Fluorescence (XRF) techniques to determine their correlation as well as provenance. The analysis of complex spectra was performed by the AXIL software and the quantitative analysis by the QAES software. Analyzed trace and minor elements were the refractory Rb, Sr, Y, Zr, Nb, Ba, La, Ce, Nd as well as Ti, Cr, V, Mn, Fe, Cu and Zn from the 3d series and Cd and Pb both of known toxicity. The spidergrams of refractory elements normalized to Primordial Mantle (PM) and Upper Crust (UC) values suggest the recycling of materials of the sediments ie, they have been subjected to weathering cycles. Spidergrams of the 3d elements normalized to UC and comparing with current Sediment Quality Guidelines (SQG) indicate that the normalized values are low and no harmful effects should be expected.

## Some applications of neutron activation analysis: An updated review of investigations at IBR-2 reactor

**Otilia Culicov<sup>1,2</sup>, Marina Frontasyeva<sup>1</sup>, Inga Zinicovscaia<sup>1,3</sup>**

1 Joint Institute for Nuclear Research, Dubna, Russia

2 National Institute for R&D in Electrical Engineering (ICPE-CA), Bucharest, Romania

3 Horia Hulubei National Institute for R&D in Physics and Nuclear Engineering (IFIN-HH), Bucharest, Romania

Since 1936, when it was discovered, the neutron activation analysis is a sensitive multi-element analytical technique used both for quantitative and qualitative analysis of a large spectra of major, minor, trace and rare elements. In spite of the fact that a variety of highly sensitive methods of multi-element analysis has been developing during the last decades, NAA remains essential as a highly reliable and accurate reference method.

Pulsed fast reactor IBR-2 of the Joint Institute for Nuclear Research, equipped with pneumatic system REGATA for instrumental neutron activation analysis provides activation with thermal, epithermal and fast neutrons for determination of both short and long-lived isotopes.

The presented results are the fruit of the international collaboration between educational and research institutions from the eighteen JINR member states and other countries. Experience of the FLNP JINR in employing instrumental neutron activation analysis in air, soil and water pollution studies performed in various geographic and climatic areas is summarized. Results of INAA application in investigation of unique geological objects, in development of green technologies for wastewater purification and new functional materials, as well as heritage investigations are presented.

# Sonocavitation and hydrodynamic cavitation based advanced oxidation processes (AOPs) for water and wastewater treatment

**Grzegorz Boczkaj, Michał Gągol, Elvana Cako, Kirill Fedorov**

Gdansk University of Technology, Faculty of Chemistry, Department of Process Engineering and Chemical Technology, Gdansk, Poland

Cavitation combined with advanced oxidation processes (AOPs), is a promising alternative to the technologies of wastewater treatment technologies in use today [1-2]. One of the most interesting types of cavitation is sonocavitation (acoustic cavitation) induced by ultrasound radiation.

The paper discusses a state of the art of cavitation based AOPs, including sonocavitation as well as presents recent developments in this field of our research group. The principles of cavitation combined with AOPs will be presented followed by evaluation of their effectiveness in oxidation of organic contaminants.

An examples of degraded particular pollutants will include *p*-nitrotoluene, *p*-aminophenol, 1,4-dioxane, alachlor, chloroform, trichloroethylene, sodium pentachlorophenate and carbon tetrachloride. Applications for disinfection of water will be also addressed. The paper will present also results of studies on pre-treatment of real post-oxidative effluents formed during bitumen production as an example of possible implementation of cavitation based processes in real industrial scenario [3-5].

The fundamentals and recent developments of the cavitation reactors design as well as the effect of process parameters (including pH, temperature, concentration and kind of contaminants) on the effectiveness of oxidation will be also presented. The oxidation effectiveness for individual treatment methods will be compared and their advantages and limitations discussed, including economical aspects of the processes and possibility of their scale-up.

## References

1. G. Boczkaj, A. Fernandes, 2017, Wastewater treatment by means of Advanced Oxidation Processes at basic pH conditions: A review, Chem. Eng. J. 320, 608-633.
2. M. Gągol, A. Przyjazny, G. Boczkaj, 2018, Wastewater treatment by means of advanced oxidation processes based on cavitation – A review, Chem. Eng. J. 338, 599-627.
3. M. Gągol, A. Przyjazny, G. Boczkaj, 2018, Highly effective degradation of selected groups of organic compounds by cavitation based AOPs under basic pH conditions, Ultrason. Sonochem. 45, 257-266.
4. M. Gągol, A. Przyjazny, G. Boczkaj, 2018, Effective method of treatment of industrial effluents under basic pH conditions using acoustic cavitation – a comprehensive comparison with hydrodynamic cavitation processes, Chem. Eng. Process. 128, 103-113.
5. G. Boczkaj, M. Gągol, M. Klein, A. Przyjazny, 2018, Effective method of treatment of effluents from production of bitumens under basic pH conditions using hydrodynamic cavitation aided by external oxidants, Ultrason. Sonochem. 40, 969-979.

## Probing plutonium dioxide nanoparticles with various synchrotron methods

**Evgeny Gerber<sup>1,2,3</sup>, Anna Romanchuk<sup>3</sup>, Ivan Pidchenko<sup>1,2</sup>, Christoph Hennig<sup>1,2</sup>,  
Alexander Trigub<sup>4</sup>, Stephan Weiss<sup>2</sup>, Andreas Scheinost<sup>1,2</sup>, Andre Rossberg<sup>1,2</sup>,  
Stepan Kalmykov<sup>3</sup>, Kristina Kvashnina<sup>1,2</sup>**

1 Rossendorf Beamline at ESRF – The European Synchrotron, Grenoble, France

2 Helmholtz Zentrum Dresden-Rossendorf (HZDR), Institute of Resource Ecology, Dresden, Germany

3 Lomonosov Moscow State University, Department of Chemistry, Moscow, Russia

4 National Research Centre “Kurchatov Institute”, Moscow, Russia

Plutonium is one of the most complicated elements among actinides. It can exist in four different oxidation states (III, IV, V, VI) under environmental conditions. Due to the small value of standard electrode potentials among these linked oxidation states plutonium can change its oxidation state easily. Moreover, plutonium may exist in several oxidation states simultaneously, which makes its chemistry even more complex.

It was previously shown that plutonium migrates in colloidal form in the subsurface environment with the distance of several kilometers. It turned out that so called “colloidal Pu(IV) polymers” are in fact aggregates of PuO<sub>2</sub> nanoparticles with diameters ~ 2 nm. However, the certain structure and stoichiometry of these colloids, as well as presence of other oxidation states but Pu(IV) is still debated.

This contribution will show results of plutonium oxide nanoparticle studies at the large-scale facility – The European Synchrotron (ESRF) by complementary methods that used X-rays in different regimes to probe the Pu oxide nanoparticles. Samples were prepared by rapid chemical precipitation using precursors in the different oxidation states (Pu(III), Pu(IV), Pu(V) and Pu(VI)). These precursors were obtained by chemical reduction or oxidation of Pu stock solution. The obtained nanoparticles were characterized at the different beamlines at the ESRF. It gives the opportunity to study our samples with various techniques: X-ray diffraction (XRD), pair distribution function analysis (PDF), and several types of spectroscopies: high energy resolution fluorescence detection (HERFD) at L<sub>3</sub> and M<sub>5</sub>-edges, X-ray emission spectroscopy (XES) and extended X-ray absorption fine structure (EXAFS) spectroscopy. The applying multifold synchrotron methods benefits to discover features, which may be unclear or even indistinguishable, these approach is also crucial to confirm results, obtained with individual methods.

It was found that small (2 nm) nanoparticles are formed from the Pu(III), Pu(IV), Pu(V) aqueous solutions, with the crystal structure close to PuO<sub>2</sub>, without any other Pu-O contributions or oxidation states of Pu except Pu(IV).

## $^7\text{Be}$ , $^{210}\text{Pb}$ and $^{137}\text{Cs}$ in the biogeocenosis components of the Arctic and southern zones of Western Siberia

**Kseniya Mezina<sup>1</sup>, Yulia Vosel<sup>1</sup>, Mikhail Melgunov<sup>1,2</sup>,  
Dmitrii Belyanin<sup>1,2</sup>, Boris Shcherbov<sup>1</sup>, Inna Zhurkova<sup>1</sup>, Maksim Rubanov<sup>1</sup>**

1 Sobolev Institute of Geology and Mineralogy, Siberian Branch of the Russian Academy of Sciences, Novosibirsk, Russia

2 Novosibirsk State University, Novosibirsk, Russia

Natural origin radioactive isotopes  $^7\text{Be}$  and  $^{210}\text{Pb}$  in significant quantities flow from the atmosphere on the earth's surface. The sources of the radionuclides are different. In modern studies, "atmospheric"  $^7\text{Be}$  and  $^{210}\text{Pb}$  are often used as tracers of various natural processes [Baskaran M., 1993, 2001; Branford D., 2004; Gourdin E., 2014; Renfro A. A., 2013].

There are lack of well-known data on the atmospheric influx of  $^7\text{Be}$  and  $^{210}\text{Pb}$  in the Arctic and southern zones of Western Siberia in the literature. The aim of the work is to make a comparative intake nature analysis of the  $^7\text{Be}$ ,  $^{210}\text{Pb}$  and  $^{137}\text{Cs}$  into the biogeocenosis components in the Tundra zones (Arctic and southern (highland zone)) of Western Siberia.

The biogeocenosis components (mosses, lichens, cedar and larch needles) of the Western Siberia Arctic zone were sampled from 20 to 22 September 2018 and of the south part of Western Siberia (the highland zone of the Gorny Altai) from 11 to 18 June 2018. Measurements of the  $^7\text{Be}$ ,  $^{210}\text{Pb}$  and  $^{137}\text{Cs}$  activities in the prepared samples were carried out using semiconductor gamma spectrometry.

The average concentrations of  $^7\text{Be}$ ,  $^{210}\text{Pb}$  and  $^{137}\text{Cs}$  in the larch needles are 207, 106 and 5  $\text{Bq}\cdot\text{kg}^{-1}$ , respectively, for the Arctic zone of Western Siberia. In the cedar needles, their content is different from larch needle and are  $^7\text{Be}$  – 46,  $^{210}\text{Pb}$  – 18 and  $^{137}\text{Cs}$  – 44  $\text{Bq}\cdot\text{kg}^{-1}$ . In mosses contents are  $^7\text{Be}$  – 317,  $^{210}\text{Pb}$  – 909 and  $^{137}\text{Cs}$  – 27  $\text{Bq}\cdot\text{m}^{-2}$ , and in lichens are  $^7\text{Be}$  – 307,  $^{210}\text{Pb}$  – 705 and  $^{137}\text{Cs}$  – 36  $\text{Bq}\cdot\text{m}^{-2}$ .

For the south of Western Siberia, contents are the following: in the larch needles are  $^7\text{Be}$  – 65,  $^{210}\text{Pb}$  – 52 and  $^{137}\text{Cs}$  – 2  $\text{Bq}\cdot\text{kg}^{-1}$ . In the cedar needles are  $^7\text{Be}$  – 51,  $^{210}\text{Pb}$  – 26 and  $^{137}\text{Cs}$  – 8  $\text{Bq}\cdot\text{kg}^{-1}$ . In mosses are  $^7\text{Be}$  – 167,  $^{210}\text{Pb}$  – 653 and  $^{137}\text{Cs}$  – 15  $\text{Bq}\cdot\text{m}^{-2}$ , and in lichens are  $^7\text{Be}$  – 208,  $^{210}\text{Pb}$  – 568 and  $^{137}\text{Cs}$  – 10  $\text{Bq}\cdot\text{m}^{-2}$ .

A comparative analysis of the data shows:

In the Arctic zone of Western Siberia, high concentrations of  $^7\text{Be}$  and  $^{210}\text{Pb}$  are observed in the larch needles, and they are significantly higher than in the south of Western Siberia (Gorny Altai).

In both studied areas for cedar and larch needles there is a dependence. The larch needles are enriched with natural radionuclides, but are depleted of  $^{137}\text{Cs}$ , and for cedar needles there is an inverse relationship.

In the mosses and lichens of Gorny Altai,  $^7\text{Be}$ ,  $^{210}\text{Pb}$  and  $^{137}\text{Cs}$  are less than in mosses and lichens of the Arctic zone of Western Siberia.

**Acknowledgments:** The work in Arctic zone supported by the Russian Science Foundation project 18-77-10039 and the work in Altai mountainous supported by the Russian Foundation for Basic Research grant 17-05-41076 RGO\_a. Analytical studies were carried out in the Analytical Center for multi-elemental and isotope research SB RAS.

## Geochemistry of $^{234,238}\text{U}$ isotopes in modern carbonate sediments of small lakes (Baikal Region)

Yulia Vosel<sup>1</sup>, Sergey Vosel<sup>2,3</sup>, Irina Makarova<sup>1</sup>, Mikhail Melgunov<sup>1,3</sup>

<sup>1</sup> The V.S. Sobolev Institute of Geology and Mineralogy of the Russian Academy of Sciences, Novosibirsk, Russia

<sup>2</sup> The Voevodsky Institute of Chemical Kinetics and Combustion Siberian Branch of the Russian Academy of Sciences, Novosibirsk, Russia

<sup>3</sup> Novosibirsk State University, Novosibirsk, Russia

The processes of diagenesis play a significant role in the redistribution of the elements in aquatic sediments. Our work is devoted to study of lake sediments diagenetic processes involving U and Mn in order, to obtain evidence of the U (IV) phases formation.

The freshwater lake Alaty (53° 12' 51.65" N, 102° 11' 43.66" E) and saline Tsagan-Tyrm (52° 51' 59.52" N, 106° 35' 33.47" E) were studied. The main method of the study was the sequential extraction method [Tessier et al., 1979]. The method allows to separate the lithogenic phases from the chemogenic and to measure  $^{234,238}\text{U}$  isotope activity in all phases. In the lithogenic phases, the isotopic ratio is  $^{234}\text{U}/^{238}\text{U} = 1$ . In surface waters, this ratio is usually much more [Chalov, 1975]. The Tessier method does not interact with the U (IV) phases and they must remain in the residues.  $^{234}\text{U}$  and  $^{238}\text{U}$  isotopes in the samples were measured by  $\alpha$ -spectrometry. The measurements of Ca, Sr, Mn are made by the atomic adsorption method.

The concentration of  $\text{Mn}^{2+}$  ions in carbonates was measured by electron paramagnetic resonance. The amount of  $\text{MnOx}$  in the upper sediment horizons, in a layer of 0-30 cm, increases sharply towards the sediment-water boundary. The main amount of U in the bottom sediments of both lakes is the authigenic U. Throughout the sediment core of Alaty  $^{234}\text{U}/^{238}\text{U}$  in authigenic fractions is approximately  $1.7 \pm 0.3$  and close to that in the lake water ( $1.66 \pm 0.27$ ). In the upper half of the section 0-42 cm in the residue  $^{234}\text{U}/^{238}\text{U} = 1.0 \pm 0.15$ . At the same time, at a great depth (93 cm) in the residue  $^{234}\text{U} / ^{238}\text{U} = 1.5 \pm 0.29$ . This directly shows that, in addition to the terrigenous U, the newly formed phases of U (IV) exist. In all authigenic fractions throughout the sediment core of the lake Tsagan-Tyrm  $^{234}\text{U}/^{238}\text{U} = 2.7 \pm 0.15$  and fully corresponds to water ( $2.6 \pm 0.13$ ). The lake is very shallow, with high salinity. In winter, the lake waters almost completely freeze, which leads to sharply reducing conditions. Measurements carried out for horizons of 0-3, 6-9 and 33-35 cm show that in their residue  $^{234}\text{U}/^{238}\text{U} > 2$ , and accordingly there is a chemogenic U, i.e. there may be phases U (IV). A large number of U (IV) phases is found in the horizon of 3-6 cm. At the same time, it has been shown that Mn oxide are completely absent in the upper layers, they appear only at a depth of 12 cm and below. Such distribution of U and Mn is completely explained by the sharply reducing environment in the upper horizons of the sediment of the lake Tsagan-Tyrm. The conducted study confirms the hypothesis of the formation of U (IV) phases in lake sediments.

**Acknowledgments:** The work was carried out within the framework of state task No.0330-216-0011, with partial financial support of RFBR grant 19-05-00267\_a. Analytical studies were carried out in the Center for Multielement and Isotope Studies of the SB RAS.

## Total reflection X-ray fluorescence analysis of copper and copper-zinc ores from South Ural mountains

**Nikolai Alov, Pavel Sharanov**

Lomonosov Moscow State University, Faculty of Chemistry, Department of Analytical Chemistry, Moscow, Russia

Determination of elemental composition of ores is an important technological task. Obtaining the operative information on the elemental composition during the process of ore extraction and enrichment allows optimizing technological processes and increasing the efficiency of production. Receiving the information about the toxic elements is also important for the environment protection.

Unfortunately, considerable part of analysis time is spent on sample preparation, in particular for its dissolution. In our work we propose to use the method of Total Reflection X-ray Fluorescence analysis (TXRF) for rapid direct determination of elemental composition of ores. TXRF is a modern method of determination of elemental composition which is able to analyze solid and liquid (after drying) state samples.

In present work the following analysis sequence is proposed. Sample picked up from conveyor belt is successively grounded along with mass decreasing by using jaw crusher, rod mill and iron mortar until 1-2 mm fragments are obtained. This fraction is milled by Pulverisette 7 (Fritsch, Germany) planetary mill using 10 mm zirconium oxide balls in zirconium oxide bowl. A 5-6 mg portion of finely milled ore sample is placed into the polyethylene vial and filled with ethylene glycol and shaken. We propose to use ethylene glycol as a dispersion medium in order to provide necessary stability of obtained suspension. A nickel internal standard is added and the suspension is treated by ultrasonic radiation to destroy ore agglomerates. The vial is finally shaken to obtain homogeneous suspension and a droplet rapidly sampled by micropipette and placed onto quartz reflector. The droplet is being dried on electrical hot plate at 70-80 °C during 1-2 min. Measurements are carried out with energy-dispersive TXRF spectrometer S2 PICOFOX (Bruker Nano, Germany) with Mo K $\alpha$  (17.5 keV) excitation during 500 s.

Samples from Uchaly (South Ural Mountains, Bashkortostan, Russia) and from Gai (Orenburg district, Russia) copper-zinc ore deposits were analyzed by proposed technique. Concentration of 13 elements (Al, S, K, Ca, Mn, Fe, Cu, Zn, As, Rb, Sr, Ba, Pb) were determined simultaneously. The relative standard deviation of measurements does not exceed 10%. It was found that copper concentration in Uchaly samples varies between 0.5-4 mass.% and zinc concentration varies between 2-3 mass.%. All of the ore samples contain high amount of iron (20-25 mass %) and sulfur (15-20 %, 13% in one of the samples), so that can be classified as sulfide ores (FeS<sub>2</sub> matrix) which is the most widespread copper ore. Samples from Gai deposit have higher variation in the matrix composition. Concentration of Fe is in 9-45 mass% range and S is in 5-35 mass% range. This ore deposit can be classified as quartz-sulfide lode ores.

## Using totally reflected X-ray radiation for environmental monitoring of Moscow small river waters

**Nikolai Alov, Pavel Sharanov**

Lomonosov Moscow State University, Faculty of Chemistry, Department of Analytical Chemistry, Moscow, Russia

The human impact on the environment leads to a change in the chemical composition of water used in everyday life, compared with its natural composition. Water is used by humankind everywhere, including cooking and drinking, so attention should be paid to water analysis. One of the most effective modern methods for determining the elemental composition of water is Total Reflection X-ray Fluorescence Analysis (TXRF). The method allows determine small amounts of substance (less pg in absolute values) with low detection limits (down to ng/l for liquid samples). In present work we used TXRF technique to determine elemental composition of the natural waters of the southwest district of Moscow: Ramenka and Rogachevka rivers and the drinking water source in the park of the 50th anniversary of the October using the TXRF method, as well as comparing the data obtained with the Russian sanitary standards.

Several samples from water system of Moscow southwest district were taken for the analysis. Samples were acquired in plastic bottles. The measurements were carried out on the TXRF spectrometer S2 PICOFOX (Bruker Nano GmbH, Germany) using quartz reflectors. The excitation was performed by Mo K $\alpha$  (17.5 keV) radiation. The time of the spectrum acquisition is 250 s. Gallium solution with the concentration 1000 mg/l is used as an internal standard. This element is easily detected by TXRF. It does not present in sample and does not cause spectral interference with elements in sample.

In water samples S, Cl, K, Ca macroelements, Fe, Cu, Zn, Br, Sr microelements and trace elements Ti, Mn, Ba, Pb were detected. Analysis of water reservoirs shows that water from Ramenka River has the highest mineralization of all investigated water samples. The highest concentration of such elements as S, Cl, K, Ca, Cu, Zn, Br was found in this sample. At the same time the content of same elements is much lower in the pond from which the river flows. It is presumably due to the sedimentation of water followed by transition of elements to muddy sediment at the bottom of the reservoir. In the confluent of the Ramenka river – Rogachevka river, the content of elements of S, Cl, K, Ca, Cu, Zn, Br is also lower than in Ramenka. The mineralization of water after confluence of Rogachevka to Ramenka decreases due to dilution. Waters investigated meet the standards set for a household water, with the exception of the Ramenka river (sample 2), in which chlorine content exceeds the maximum allowed concentration (488 mg/l).

## Removal of natural radioactivity from groundwater used as a drinking water source

**Anna Goi**

Tallinn University of Technology, Tallinn, Estonia

The concentration of some natural water constituents, as iron, manganese, ammonium and radiological parameters in the groundwater of Estonia from Cambrian-Vendian aquifer used as a drinking water source exceed the threshold limits and indicative dose of 0.1 mSv per year for radiological parameter set in the Council Directives of the European Union and in the Estonian Radiation Act. In order to satisfy the demands for safe and reliable quality of potable water comprehensive and complex combined technology based on the Hydrous Manganese Oxide (HMO) oxidation-filtration process was tested.

Aeration was found to be effective for the iron removal at natural water pH of 7.8, but it was not effective for the manganese removal that requires pH higher than 9.5. The aeration-filtration using sand-dolomite resulted in the substantial increase of the pH from 7.8 to 9.1 leading to the improved removal of manganese. Pre-aeration was applied for the removal of aggressive CO<sub>2</sub> that otherwise reacts with the solid CaCO<sub>3</sub> or Mg(OH)<sub>2</sub> re-carbonising the water. Calcium that is in the water in the form of Ca(HCO<sub>3</sub>)<sub>2</sub> reacting with Ca(OH)<sub>2</sub> (formed due to CaO in contact with H<sub>2</sub>O) gives solid CaCO<sub>3</sub>. Thus, 50% removal of calcium ion in water was achieved by the dolomite-sand filtration.

The HMO-accumulated quartz sand filtration (the periodic HMO-dosing) was able to achieve the threshold limits for Mn, Fe and Ra-228 set for the drinking water quality. Some increase (by 21%) in the ammonium removal using the sand-anthracite filter bed comparing to that obtained by the sand filter bed alone was achieved. Aeration results in the microbial growth in the filter bed leading to the biological oxidation of ammonium.

Complete removal of ammonium and radium was achieved only in the combined aeration, the HMO-oxidation and the multimedia bed sand-zeolite filtration technological scheme due to the zeolite addition. Zeolite is an ion-exchangeable material that accumulates radionuclides in its structure and needs the chemical regeneration to avoid the creation of NORM-waste (Goi et al., 2018).

**Acknowledgments:** The study was realized in the framework of the LIFE ALCHEMIA project – LIFE16 ENV/ES/000437 (the TalTech project ID VEU17119) which was financial supported by the LIFE Programme of the European Union ([www.lifealchemy.eu](http://www.lifealchemy.eu)). The project partners from Viimsi Vesi AS for providing the samples and the University of Tartu, Institute of Physics for the radioactivity analyses as well as PhD Juri Bolobajev for the experimental assistance are gratefully acknowledged. This publication reflects only the author's view. The European Commission/Agency is not responsible for any use that may be made of the information it contains.

### References

- A. Goi, N. Nilb, S. Suursoo, K. Putk, M. Kiisk, J. Bolobajev, Regeneration of filter materials contaminated by naturally occurring radioactive compounds in drinking water treatment plant, Journal of Water Process Engineering, 2018, in press.



**Environmental  
Physics**

**11**

## Correlation of available and total lead content in urban soil

**Aleksandra Mihailović<sup>1</sup>, Ivana Lončarević<sup>1</sup>, Nebojša M. Ralević<sup>1</sup>, Selena Samardžić<sup>1</sup>, Ljuba Budinski-Petković<sup>1</sup>, Jordana Ninkov<sup>2</sup>, Ljubo Nedović<sup>1</sup>**

<sup>1</sup> Faculty of Technical Sciences, University of Novi Sad, Novi Sad, Serbia

<sup>2</sup> Institute of Field and Vegetable Crops Novi Sad, Novi Sad, Serbia

Most of Pb prevailing in the environment is mainly related to anthropogenic sources such as: automobile exhaust products, metalliferous mining activities, Pb smelter emission, battery stores, leaded paints, coal combustion. Lead and its compounds tend to accumulate in soils where, due to their low solubility and non-biodegradable nature, they will remain bioavailable for many years. The aims of the present study were: to measure the available and total concentrations of Pb in urban soil of Novi Sad, to determine availability ratio (AR) and to estimate pollution sources.

Over a hundred of surface soil samples (0 -10 cm depth) were collected in the vicinity of busy and less busy roads. The soil samples were air-dried at room temperature and milled to a particle size of < 2 mm. The samples were analyzed for available lead content after extraction with 0.05 mol/l EDTA (pH = 7.00) and for “pseudo-total” content after digesting the soil in concentrated HNO<sub>3</sub> and H<sub>2</sub>O<sub>2</sub>. The concentrations of Pb were determined by ICP-AES technique. The limits of detection for available lead concentration was 0.5 and for pseudo-total 5 mg/kg

The obtained results showed a large variability of available lead levels in soil samples and the relative standard deviation (RSD) value (2.24) exceeded those for total metal content (1.35). The available Pb concentrations ranged from 2.5 to 665.6 mg/kg with the mean value 28.3 mg/kg. The total Pb concentrations varied from 8.9 – 999 mg/kg and the mean value was 82.3 mg/kg. Higher Pb levels were measured at the locations near busy roads. Following values of available Pb ratio (AR) were obtained: 1/2 of the samples were within the interval 0.2 – 0.3, for 1/3 of the samples percentage of soil samples ranged from 0.3 – 0.4 and for one sample the value was > 0.67. According to Pearson’s correlation analysis, strong positive correlation exists between available and total lead content:  $r = 0.936$  at the level of significance 0.01. High value of RSD for available lead content in the samples and increased ratio of available Pb points to anthropogenic pollution. On the basis of these findings, we conclude that Pb in urban soils in Novi Sad originated from anthropogenic sources (mainly traffic).

**Acknowledgments:** The research is supported by the Project of the Ministry of Education, Science and Technological Development, Republic of Serbia, No. TR34014.

## **Radon measurement in water from public fountains in rural areas in northern part of Kosovo and Metohija**

**Biljana Vuckovic<sup>1</sup>, Natasa Todorovic<sup>2</sup>,  
Jovana Nikolov<sup>2</sup>, Jelena Zivkovic Radovanovic<sup>1</sup>, Ljiljana Gulan<sup>1</sup>**

<sup>1</sup> University of Pristina, Faculty of Natural Sciences, Kosovska Mitrovica, Serbia

<sup>2</sup> University of Novi Sad, Faculty of Sciences, Department of Physics, Novi Sad, Serbia

Radon is a natural colourless, odourless and tasteless radioactive gas and in nature it can be found in soil, water and underground rocks. His presence is directly related to the presence of uranium. Radon is ingested by inhalation, which makes it the second most important cause of lung cancer, right after smoking. Drinking water which is abundant in radon can also cause cancer, which is the goal of this research. This research was conducted in rural areas of the counties Zvečan (10 locations) and Zubin Potok (10 locations) in the northern part of Kosovo and Metohija. Radon concentration in water was measured by RAD7 (DURRIDGE Co.). During the sampling water temperature and its pH value were also measured. Radon concentrations in water at investigation areas were from 2.2 Bq/l to 46.3 Bq/l, with its mean value of 10.6 Bq/l, and standard deviation of 12 Bq/l. Annual effective doses of ingestion and inhalation were determined as well.

## The total electron content of the ionosphere as the witness and object of space weather influence

**Olga Maltseva**

Institute for Physics Southern Federal University, Rostov-on-Don, Russia

The ionosphere is the environment of a near Earth space through which radio-waves propagate, ensuring functioning of various land and satellite technological systems. The main parameter of the ionosphere is the critical frequency measured by a network of ground-base ionosondes, which is rare enough to provide the sufficient resolution of parameters on a global scale. The situation has changed with the advent of systems GNSS and measurement of the total electron content TEC. However, as orbit latitudes of satellites of these systems are limited, behavior of TEC and possibilities of its use in high latitudes is insufficiently studied. One of the important problems is a study of TEC changes connected with influence of Space Weather (SW). Other problem is the obtaining of the critical frequency foF2 with use of TEC. In the given work, these problems are solving by means of experimental data of foF2 and TEC for the station Longyearbyen (78.2°N, 15.9°E) during period (2011-2014) of foF2 data availability in SPIDR base. Data of TEC were calculated from IONEX files of the global map JPL. For solving the first problem link of TEC with parameters of SW (index of sunlight F10.7, intensity of interplanetary magnetic field IMF and density of protons of solar wind Np) and index Dst of geomagnetic activity is investigated. The role of each factor is estimated by means of linear correlation. The most expressed are daily and seasonal variations. Correlation of TEC and foF2 with F10.7 is positive and strong (~0.6-0.9) in summertime, and the maximum coefficients for TEC decrease with growth of solar activity, and increase for foF2. For the Dst index, correlation is positive from March till September with the maximum coefficients 0.8 for TEC and 0.8-1.0 for foF2, during winter time coefficients are negative with small values. For parameter IMF, during winter time when factors for Dst are negative, positive and maximum coefficients for IMF reach the values 0.6-0.7 for TEC and 0.8-1.0 for foF2. During other period factors are positive and small. For parameter Np, seasonal dependences for each hour have the character of fluctuations concerning a time axis with prevalence of positive, small values. It specifies that the behavior of the ionosphere in auroral latitudes is operated by a magnetic field (both internal, and external). For solving the second problem, values of foF2 are obtained during the periods of geomagnetic disturbances when very often there are no experimental data of foF2, but TEC is measured and there are values of the International Reference Ionosphere model IRI. Results of the TEC use to obtain foF2 are compared to the model IRI results by means of absolute and relative deviations of the calculated values from experimental foF2. Comparison is carried out for median, instant values and the values calculated with the TEC use. It is shown, that the TEC usage increases conformity with experimental data in 1.5-2.0 times in comparison with the IRI model.

## **Empirical model for estimating solar radiation based on air temperature for Sarajevo area, Bosnia and Herzegovina**

**Slavica Brkić, Blanka Tuka**

University of Mostar, Mostar, Bosnia and Herzegovina

There are numerous correlations and methods that have been developed to estimate global solar radiation (GSR) based on the readily available meteorological parameters like sunshine duration, temperature and relative humidity which are used as the input for radiation models at any location.

The most widely used parameter to estimate GSR is sunshine duration. But sunshine data and cloud observations are not easily available in all locations. There are number of mathematical and Clear sky models are available which are not suitable to estimate the GSR during foggy months or cloudy sky. In Sarajevo area around three months in a year are polluted, foggy and cloudy. It is very difficult to estimate the accurate results of solar radiation using a clear sky model. Therefore it is necessary to develop some precise solar radiation model which use commonly available measured parameter such as air temperature. The temperature based models can be used to estimate monthly average daily GSR for Sarajevo area.

## Recent results of atmospheric radioactivity measurements in Bulgaria based on NIMH activity

**Blagorodka Veleva<sup>1</sup>, Elena Hristova<sup>1</sup>,  
Lyuben Dobrev<sup>2</sup>, Stefan Georgiev<sup>2</sup>, Nastya Vankova<sup>3</sup>**

<sup>1</sup> National Institute of Meteorology and Hydrology, Sofia, Bulgaria

<sup>2</sup> Institute of Nuclear Research and Nuclear Engineering, Sofia, Bulgaria

<sup>3</sup> National Institute of Meteorology and Hydrology – Varna branch, Varna, Bulgaria

There is an extended experience in atmospheric radioactivity monitoring and studies in National Institute of Meteorology and Hydrology (NIMH) since the period of global nuclear fallout. The radioactivity of aerosol and atmospheric deposition samples is measured daily by beta radiometry in 4 regional radiometric laboratories placed in Sofia, Pleven, Varna and Burgas. Filter samples of Total Suspended particulate (TSP) taken in these laboratories are measured for short lived gross beta activity, 5<sup>th</sup> minute after end of sampling and after 120 h for so called long live beta activity, when the radon daughters are decayed. Three types of atmospheric deposition samples are collected, pre-concentrated and measured in our network: i) total monthly deposition, collected in cylindrical container over the distilled water layer in 19 meteorological stations; ii) 24 hours planshet samples at 1m above ground in 7 stations; iii) daily precipitation samples in 8 stations. Aliquots from all liquid samples are pre-concentrated by evaporation and transfer to aluminum plates for beta radiometry. The daily planshet samples are ashed at ~400°C and also measured for beta radionuclides. If the activity is above the set alarm levels the samples are measured for gamma emitting radionuclides by low level gamma spectrometry in own gamma-spectrometry lab in Pleven and in the INRNE gamma-spectrometry labs with whom there is a long lasting collaboration.

In this study the work of the network for atmospheric radioactivity as time series, mean and maximum values of concentration and deposition for the period 2010-2018 are presented. Two episodes of transboundary transport and deposition of man-made radionuclides was recorded in Bulgaria during this period. The Fukushima NPP accident in March 2011 did not affect much the long lived gross beta activity in filter and deposition samples, but <sup>131</sup>I, <sup>137</sup>Cs and <sup>134</sup>Cs were detected in weekly precipitation samples in Sofia, Burgas and some other stations in Northern Bulgaria. In the end of September and in the beginning of October 2017 well distinguished signal of gross beta activity increase was measured first in coastal stations in Varna and Burgas and then in Sofia and Plovdiv. The increase of gross beta was due to contamination with <sup>106</sup>Ru as proved by gamma spectrometry. The obtained concentration and deposition are compared to the available data from other European regions, bulletins of ROSGIDROMET and CTBTO database. The trajectory model HYSPLIT was successfully used in order to look for the source of contamination. These results can be considered as relevant and useful for environmental radioactivity monitoring in the country and the Balkan region.

## Analysis of the measured noise values in different types of industrial processes and the potential risk of NIHL

**Selena Samaradžić<sup>1</sup>, Uranija Kozmidis Luburić<sup>1</sup>, Milan Cvijanović<sup>2</sup>, Robert Lakatoš<sup>1</sup>, Aleksandra Mihailović<sup>1</sup>, Tomas Nemeš<sup>1</sup>, Milka Veselinović<sup>1</sup>**

<sup>1</sup> Faculty of Technical Sciences, Novi Sad, Serbia

<sup>2</sup> Clinical Centre of Vojvodina, Faculty of Medicine, Novi Sad, Serbia

Noise is one of the outcomes of rapid urbanization and technological development. In industrial settings, in most machines, there is a continual and sometimes also intermittent type of noise. The sources are all moving parts of the machines and the elements of the machinery drive such as motors, compressors and vacuum pumps, which supply mechanical energy, air under pressure or vacuum. Noise in the work environment is the major cause of concern for safety and health of the industrial workers. The impact of noise will primarily be localized on hearing damage called noise induced hearing loss (NIHL), which has profound social and occupational impact on affected individuals and substantially reduces quality of life. Hearing damages from excessive noise are usually generated when noise exceeds permanently 85 dBA and the workers reject or misuse personal hearing protectors. The aim of this investigation was to determine noise level and noise spectrum of some machines in four different types of industry: printing, textile, electro and footwear industry, during certain production processes. The  $L_{eq}$ ,  $L_{min}$  and  $L_{max}$  and dBA means of  $L_{eq}$  at 1/1 octave band was measured using TES-1358A Sound Level Meter. Results showed that 60% machines produced  $L_{eq}$  levels which exceed the limiting threshold level of 85 dB in footwear industry, 40% in printing, 60% in electro and 16% in textile industry. The predominant sources were grinding machine with the mean of  $L_{eq}$  of  $111.7 \pm 2.5$  dB, VF pump with  $L_{eq}$  of  $90.8 \pm 3$  dB, pounding machine with  $L_{eq}$  of  $96.7 \pm 1.5$  dB and folders with  $L_{eq}$  of  $87.7 \pm 3.14$  dB. The frequency analysis at 1/1 octave bands revealed for most of the machines that the noise was dominated by higher frequency noise from 1000 Hz to 4000 Hz. It was also observed that the means of  $L_{eq}$  levels exceeded the permissible levels given by NR-80 curve at higher frequencies. The high levels of noise suggest that hearing conservation program to protect workers from the effects of hazardous noise exposure in the workplace must be integrated into industrial companies. This study has shown that some workers are at the risk of developing noise induced hearing loss due to excessive occupational exposure to noise.

**Keywords:** Noise level, industry, sound level meter, NIHL

## **Application of X-ray fluorescence technique (XRF) for determination of heavy metal concentrations in hair of workers at metal workshop**

**Gordana Žauhar<sup>1,2</sup>, Marija Čargonja<sup>2</sup>, Darko Mekterović<sup>2</sup>, Paula Žurga<sup>3</sup>,  
Jagoda Ravlić Gulan<sup>1</sup>**

1 University of Rijeka, Faculty of Medicine, Rijeka, Croatia

2 University of Rijeka, Department of Physics, Rijeka, Croatia

3 Teaching Institute for Public Health of Primorsko-Goranska County, Rijeka, Croatia

Workers in metal workshop are exposed to metals as an occupational hazard, and by breathing, touching, or ingesting, they mostly undergo long-term low level or accidentally short-term high-level exposures. Metal processing such as welding, cutting, grinding and turning can be very important source of particulate matter in metal workshops. Hence, it is necessary to quantify exposure by monitoring workers and to control exposure to metals.

Possible impacts of particulate matter on human health were estimated by analysing hair samples of the workers included in the study. Employees from University of Rijeka were used as a control group.

The hair samples were washed, dried, and the levels of 18 elements (S to Pb) were determined with an X-Ray Fluorescence technique at the Laboratory for Elemental Microanalysis at the Department of Physics, University of Rijeka. The element levels of hair were compared between the male controls (employees from University of Rijeka) and the workers from metal workshop. Results of analysis obtained with XRF technique were compared with results obtained with Inductively Coupled Plasma Mass Spectrometry (ICP-MS).

Our results have shown that workers in metal workshop have higher levels of Al, Cr, Mn and Fe in their hair when compared to controls.

## Hyperspectral leaf reflectance and red edge position as indicators of diseases in plants

**Dora Krezhova<sup>1</sup>, Kalinka Velichkova<sup>2</sup>**

<sup>1</sup> Space Research and Technology Institute, Bulgarian Academy of Sciences, Sofia, Bulgaria

<sup>2</sup> University of Mining and Geology, Sofia, Bulgaria

The availability of remotely-sensed data from different sensors of various platforms with a wide range of spatiotemporal and spectral resolutions makes remote sensing the best source of data for large scale applications and study. Remote sensing technique, based on hyperspectral reflectance measurements, opens new ways for plant monitoring. Leaf spectral reflectance is a sensitive indicator for a variety of environmental factors affecting plants such as stress, diseases, drought and senescence. The red edge position (REP) is strongly correlated with the foliar chlorophyll content thereby it is a good estimator for vegetation health. The accurate estimation of the REP (the inflection point of slope on the reflectance spectrum of vegetation between 680 nm and 760 nm) is dependent upon sensor band positions, widths and sensor type. Various techniques have been developed to minimize the error in estimating the REP. The aim of this report is to assess different REP extraction techniques for disease detection (viral infection) of young potato plants using hyperspectral data and to test which one is best. Leaf reflectance data from two groups of plants, healthy and infected with Potato Virus Y (PVY), were collected by a portable fiber-optics spectrometer in the visible and near infrared spectral ranges (450-1000 nm) with a spectral resolution of 1.5 nm. Five REP extraction techniques (maximum of first derivative, four-point linear interpolation, polynomial fitting, linear extrapolation, and inverted Gaussian modelling) were tested and compared. The results from all of them have shown that the wavelength and reflectance of REP for infected plants were shifted towards the shorter wavelengths in comparison with healthy plants that indicated the presence of a viral infection. The polynomial fitting and inverted Gaussian modelling techniques generated close results for the estimated REPs (the shifts are 5.3 nm and 4.8 nm, respectively).



**Environmental  
Pollution**

**12**

## Supporting climate change vulnerability and adaptation assessments at the Danube River: DDT impact

Maja Turk Sekulić<sup>1</sup>, Maja Brborić<sup>1</sup>,  
Borivoje Stepanov<sup>1</sup>, Sabolč Pap<sup>2</sup>, Jelena Radonić<sup>1</sup>

<sup>1</sup> University of Novi Sad, Faculty of Technical Sciences, Department of Environmental Engineering and Occupational Safety and Health, Novi Sad, Serbia

<sup>2</sup> University of the Highlands and Islands, North Highland College, Environmental Research Institute, Thurso, United Kingdom

The organochlorine pesticide DDTs (Dihlor-difenil-trihloretan) and its degradates are among the most lipophilic, persistent and abundant organochlorine contaminants in the environment. The discovery of the ubiquitous distribution of DDTs in environmental matrices and its severe effects on wildlife ultimately led to the ban of DDT in most industrialized countries in the early 1970s. However, not all uses ended with the restrictions; in fact, DDT is under current usage as vector control in numerous developing countries. In order to estimate the level of contamination of the aquatic sediment, during 2012 at the ten target locations along the Danube River through the territory of the Republic of Serbia, the monitoring of the organochlorine pesticides (DDT and its metabolites DDE and DDD) was carried out. The sampled sediments were extracted with dichloromethane by the Soxhlet extraction method, and final extracts were analyzed by gas chromatography-mass spectrometry. Target organochlorine pesticides were quantitated at all sites. The mean concentrations of  $\Sigma$ DDE,  $\Sigma$ DDD and  $\Sigma$ DDT (sum of p.p. and p.p.) ranged from 0.25 to 4.76, 0.31 to 2.86 and 0.16 to 9.84  $\mu\text{g}\cdot\text{kg}^{-1}$ , respectively, while total values  $\Sigma$ DDT ranged from 0.70 to 16  $\mu\text{g}\cdot\text{kg}^{-1}$  with a mean value of 5.08  $\mu\text{g}\cdot\text{kg}^{-1}$  and a median of 3.00  $\mu\text{g}\cdot\text{kg}^{-1}$ . The classification of data by Kohonen's self-organizing maps (SOM) allowed understanding and visualizing the spatial distribution of samples. Correlations and relationships between the samples and the variables can be easily visualized using the viewing of SOM planes of components. The results have highlighted the dependencies between the different DDTs and the classification of studied sediments into three classes into the function of ten stations coring and their pollution levels. By comparing the obtained values of the concentration of DDT and its metabolites with the values prescribed by the Regulation on threshold values of pollutants in surface and groundwaters and sediment and deadlines for their achievement ("RS Official Gazette", No. 50/2012), it can be concluded that at the site Ritopek the values of  $\Sigma$ DDT,  $\Sigma$ DDE, and  $\Sigma$ DDD exceed a considerable degree of maximum permissible concentrations. On the basis of the obtained results, it can be concluded that along the Danube River flow in the territory of Serbia there are still significant potential sources of pollution of aquatic systems with organochlorine pesticides, which is necessary to detect and prevent the further use of adequate pesticide control currently imported and produced in our country, thus reducing the extremely negative ecotoxicological effects currently present in the aquatic system. The results of this study add new data to the international database of the river Danube producing comparable and reliable information on sediment and water quality.

**Keywords:** DDTs, Kohonen's self-organizing maps, sediment, Danube River

**Acknowledgments:** This research was supported by City administration for environmental protection, Novi Sad, Republic of Serbia (01-209/439-3), Ministry of Education, Science and Technological Development, Republic of Serbia (III46009).

## Functionalisation of biochar derived from lignocellulosic biomass using microwave technology for application in wastewater treatment

Maja Turk Sekulic<sup>1</sup>, Olivera Paunovic<sup>1</sup>,  
Sabolec Pap<sup>1,2</sup>, Sanja Radovic<sup>1</sup>

<sup>1</sup> University of Novi Sad, Faculty of Technical Sciences, Department of Environmental Engineering and Occupational Safety and Health, Novi Sad, Serbia

<sup>2</sup> Environmental Research Institute, North Highland College, University of the Highlands and Islands, Thurso, United Kingdom

Pharmaceutical pollution contributes to a severe public health crisis responsible for over 25,000 deaths a year across the EU and an annual cost of more than €1.5 billion to the economy (Burke, 2019). Water treatments that can be used to remove pharmaceuticals from wastewater include: adsorption (Turk Sekulic et al., 2019), advanced oxidation processes, ultrasonic treatment, carbon nanotube membranes, biological processes and photocatalysis, as well as various combinations of these. However, these may have disadvantages, i.e., high operational costs, toxic by-product production, or, the application may be overly complex (Turk Sekulic et al., 2018). A study to produce an efficient biochar to be used for pharmaceutical wastewater remediation was carried out introducing potassium hydroxide in biochar using a microwave heating/radiation. The aim of the study was to make a highly efficient and low-cost biochar (WpOH) derived from wild plum kernels (*Prunus cerasifera* – Ehrh) as a common Serbian waste material (Paunovic et al., 2019). Optimisation study of naproxen (NPX) removal from aqueous solutions by adsorption onto synthesised biochar has been investigated in batch adsorption experiments. The maximum adsorption capacity (73.14 mg/g) occurred between pH 5 and 7 through electrostatic attraction between the negatively charged NPX and the positively charged WpOH functional groups. Time dependent assays show rapid and spontaneous uptake of NPX within the first 5-10 minutes. According to initial adsorbate concentration data, the results showed that adsorption was highly dependent on initial NPX concentration. The percentage of NPX adsorption is reduced when the initial NPX concentration is increased from 3.1 to 125.3 mg/L due to the limited availability of active binding sites on the WpOH surface. The experimental results indicated that the use of wild plum kernel as a precursor material for the preparation of efficient biochar was feasible. Overall, cheap and abundant production, rapid and facile preparation, fast and efficient adsorption of NPX can make the WpOH a preferred adsorbent for pharmaceutical removal from wastewater.

**Acknowledgments:** This research was supported by City administration for environmental protection, Novi Sad, Republic of Serbia (01-209/439-3), Ministry of Education, Science and Technological Development, Republic of Serbia (III46009).

### References

1. Burke, M., 2019. EU sets goal of tackling pharmaceutical pollution in the environment. Chem. World.
2. Paunovic, O., Pap, S., Maletic, S., Taggart, M.A., Boskovic, N., Turk Sekulic, M., 2019. J. Colloid Interface Sci. 547, 350–360.
3. Turk Sekulic, M., Boskovic, N., Slavkovic, A., Garunovic, J., Kolakovic, S., Pap, S., 2019. Process Saf. Environ. Prot. 125, 50–63.
4. Turk Sekulic, M., Pap, S., Stojanovic, Z., Bošković, N., Radonić, J., Šolević Knudsen, T., 2018. Sci. Total Environ. 613–614, 736–750.



**Materials  
Science**

**13**

## Reversible random sequential adsorption of polydisperse mixtures on a triangular lattice

Ivana Lončarević<sup>1</sup>, Ljuba Budinski-Petković<sup>1</sup>,  
Aleksandra Mihailović<sup>1</sup>, Zorica Jakšić<sup>2</sup>, Slobodan Vrhovac<sup>2</sup>

<sup>1</sup> Faculty of Technical Sciences, University of Novi Sad, Novi Sad, Serbia

<sup>2</sup> Institute of Physics, Zemun, Beograd, Serbia

We have studied the reversible RSA of polydisperse mixtures on a triangular lattice numerically by means of Monte Carlo simulations. Mixtures are composed of shapes of different numbers of segments and rotational symmetries. We concentrate here on the influence of the number of mixture components and the length of the shapes making the mixture on the kinetics of the deposition process. Despite the complexity of the adsorption-desorption processes of polydisperse mixtures, above the jamming limit, the time evolution of the total coverage of a mixture can be described by the Mittag-Leffler function for all the mixtures we have examined. Our results show that the equilibrium coverage decreases with the number of components making the mixture and also with the desorption probability, via corresponding stretched exponential laws. Special attention has been paid to the mixtures containing objects of various shapes, but made of the same number of segments. We have proposed a simple formula that can be used to predict the value of a steady-state coverage fraction of a mixture knowing the steady-state coverage fractions of the pure component shapes. Such a formula could be used to avoid the time-consuming simulations of the reversible RSA of mixtures.

## Smart mask designs and electrical properties of platinum temperature sensors

**R. Lok<sup>1,2</sup>, U. Gurer<sup>1</sup>, O. Yilmaz<sup>1</sup>, A. Varol<sup>3</sup>, H. Karacali<sup>2</sup>, A. Aktağ<sup>1,2</sup>, E. Yilmaz<sup>1,2</sup>**

1 Center for Nuclear Radiation Detectors Research and Applications, AIBU, Bolu, Turkey

2 Physics Department, Abant İzzet Baysal University, Bolu, Turkey

3 Arcelik A.S Cooking Appliances Plant, Bolu, Turkey

Temperature is the most frequently measured environmental value because physical, electronic, chemical, mechanical and biological systems are affected by temperature. For this reason, it is important to measure the temperature and keep it at certain values in the control systems. Using highly expensive materials such as platinum, the sensors made are really difficult to produce according to the desired resistance value. Therefore, lithography masks prepared for the temperature sensors to be produced gain importance. Especially in the production stages of platinum temperature sensors, chemical etching can be quite difficult. Therefore, you need to design smart masks to control production stages. Hence, when you prepare a mask, the points called trimming will make it easier for you to adjust the resistance you want to set. So, resistors are normally fabricated to lower resistance value than needed trimmed by cutting holes in them with lasers to increase their resistance value.

**Keywords:** Platinum temperature sensor, mask design, trimming

**Acknowledgments:** This work is supported by the Scientific and Technological Research Council of Turkey (TUBİTAK) and Arcelik A.Ş under the contract number TEYDEB 1505- 5170059. This work is also partially supported by the Presidency of Turkey, Presidency of Strategy and Budget under Contract Number: 2016K121110.

## Examination of Pt/Al<sub>2</sub>O<sub>3</sub>/p-Si/Al MOS capacitors under different temperatures

R. Lok<sup>1,2</sup>, H. Karacali<sup>2</sup>, A. Aktağ<sup>1,2</sup>, E. Yilmaz<sup>1,2</sup>

1 Center for Nuclear Radiation Detectors Research and Applications, AIBU, Bolu, Turkey

2 Physics Department, Abant İzzet Baysal University, Bolu, Turkey

In this study, the electrical characteristics of the Pt/Al<sub>2</sub>O<sub>3</sub>/p-Si/Al MOS capacitors were determined by using C–V and G/ω–V measurements for several frequencies from 100 kHz to 1 MHz and different temperatures from 40 °C to 100 °C. With rising temperature during bias temperature stress, a dramatic deterioration was observed in the C–V and G/ω–V characteristics at the measuring temperature of 120° C / device which was caused by the increased effective oxide thickness, oxide trapped charge density, and interfacial density of states (*Dit*). Specifically, no deterioration was observed in the C–V and G/ω–V characteristics below 100 °C. Our results show that the Pt/Al<sub>2</sub>O<sub>3</sub>/p-Si/Al MOS capacitors can be used as temperature sensors at low temperatures. Measurements were taken 5 times on different days. As a result, this MOS capacitor can be used for temperature measurements at a value of 100 °C or less.

**Keywords:** Pt/Al<sub>2</sub>O<sub>3</sub>/p-Si/Al MOS capacitors, interface states, oxide traps

**Acknowledgments:** This work is supported by the Presidency of Turkey, Presidency of Strategy and Budget under Contract Number: 2016K121110



**Medical  
Devices**

**14**

## Structural changes of the cornea after the intrastromal implantation of plasma modified PET track-etched membrane

Ekaterina Filippova

Tomsk Polytechnic University, Tomsk, Russia

Track-etched membranes have a good opportunity to be using as implants for ophthalmology. However, the track-etched membrane has limited wettability of the surface. One of the modern methods of modifying the polymers surface and of properties changes is the low-temperature plasma modification. So it is necessary to know corneal stroma changes after the plasma modified PET track-etched membrane implantation.

**The aim of this research** is the studying of corneal stroma changes after the plasma modified PET track-etched membrane implantation.

**Materials and methods.** The PET track-etched membranes were done by the PET film irradiating by  $^{40}\text{Ar}^{+8}$  with 41 MeV energy and chemical treatment in NaOH solution. The plasma modification of PET track-etched membranes was done with using the experimental low temperature plasma device. The plasma treatment time of each membrane surface was 30 seconds. The steam sterilization of modified PET track-etched membranes was conducted at a temperature of 132°C and pressure of 0.2 MPa.

12 pubescent male Chinchilla rabbits weighing 3.5 – 4.0 kg were used for in vivo experiments. The plasma modified PET track-etched membrane was implanted in the deep layers of cornea stroma near the Descemet membrane. The overall duration of the experiment comprised 8 weeks. Such methods as visual check, optical coherent tomography (OCT) of cornea and photographic registration were also used in course of the experiment. After 8 weeks from the in vivo experiment start cornea was performed for morphology studying.

**Results.** Morphology results showed that the epithelium thickness of animals was  $30.8 \pm 1.9 \mu\text{m}$  on day 31 from the start of the experiment. The epithelium consisted of 4-5 layers of squamous cells. Bowman's membrane differentiated along the entire length. The stroma of the cornea contained packed collagen fibers. Edema area of  $45 \pm 10 \mu\text{m}^2$  was found. Descemet's membrane visualized well and was homogeneous along the whole length. Endothelium consisted of the one cells layer.

It is established that the implantation of the PET track-etched membrane is accompanied by inflammatory infiltration of the corneal stroma. The inflammatory infiltration was represented mainly by lymphocytes ( $50.01\% \pm 3.14$ ), macrophages ( $41.71\% \pm 2.31$ ) and neutrophils ( $8.94\% \pm 2.82$ ). The loose tissue had newly formed small blood vessels ( $16.29\% \pm 5.18$ ).

**Conclusion.** The research showed that the plasma modified PET track-etched membrane in the corneal stroma is accompanied by the development of a moderately pronounced inflammatory response.

**Acknowledgments:** The research was conducted with the financial support of the Russian Foundation for Basic Research (RFBR) as part of the project № 18-315-00048.

## Morphological features of the musculoskeletal stump eye formation using titanium nickelide construction

Evgeniya Gorbunova<sup>1</sup>, Ekaterina Filippova<sup>2</sup>

<sup>1</sup> Siberian State Medical University, Tomsk, Russia

<sup>2</sup> Tomsk Polytechnic University, Tomsk, Russia

Eye trauma leads to conditions that require removal of the eyeball. It is known the main method of anophthalmia treatment is medical implants implantation. There are several medical implants used for the anophthalmia treatment such as hydroxyapatite, carbon compositions, tantalum, ceramics, injection hydrogel and monolithic silicone. However they can cause the transplant rejection and have the high price. The titanium nickelide implantation is the new and interesting method for the anophthalmia treatment because it leads the high connective tissue proliferation and firm implant fixation in orbit.

**The aim of this research** is the studying of morphological features of the musculoskeletal stump eye formation after titanium nickelide implantation.

**Materials and methods.** 18 pubescent male Wistar rats weighing 200-250 g were used for *in vivo* experiments. The animals were eviscerated and implanted the titanium nickelide implant into the scleral sac. The titanium nickelide implant is made of a filament of porous titanium nickelide of the TN-10 brand with a thickness of 100 microns. Before implantation the implants were sterilized by ethylene oxide. The overall duration of the experiment comprised 21 days. Such methods as visual check and photographic registration were used in course of the experiment. After 21 days after implantation the implant was removed for morphological research.

**Results.** Visual check showed that the animals had moderate edema and hyperemia of the conjunctiva 1 day after implantation. The formed stump of the eyeball had a rounded shape and was moderately mobile.

Morphological research showed that the titanium nickelide implantation contributed the loose connective tissue with blood vessels development. There were cells infiltration ( $2020.6 \pm 562.8$  cells) and newly formed blood vessels ( $5.3\% \pm 1.9$ ) between collagen fibers.

**Conclusion.** The implantation of titanium nickelide (repeated 2 times) into the scleral sac after evisceration is accompanied by development of the connective tissue and high vascularization, which provides a strong fixation of the implant and reduces the risk of its rejection.

**Acknowledgments:** This research was supported by Tomsk Polytechnic University Competitiveness Enhancement Program project VIU-SEC B.P. Veinberg-210/2018.

## Translating high spatial resolution detector based on cadmium zinc telluride to clinical positron emission tomography

**Yongseok Lee, Shiva Abbaszadeh**

University of Illinois at Urbana Champaign, Urbana, United States

Current head and neck cancer diagnosis and treatment planning suffers from poor spatial resolution of whole-body positron emission tomography (WB-PET) scans. In the neck, where tissue layers are thin, the spatial resolution of WB-PET (4-6 mm) is not sufficient to evaluate small lymph nodes (<5 mm), establish how far the tumor has invaded locally, and guide the decision to respect a tumor rather than irradiate and deliver chemotherapy. This work elaborates on the design, development, optimization, characterization, and validation of a dedicated head and neck PET scanner. The proposed system will be the first head and neck scanner to exhibit features as small as 1 mm with high photon sensitivity, enabled by the use of high energy and spatial resolution properties of cadmium zinc telluride (CZT) crystals. This system will be integrated into a transportable stage and is designed to not interfere with the conventional workflow of the WB-PET scan procedure, and has the additional attraction of being used for dynamic PET studies. We expect that this dedicated head and neck PET imaging system will deliver the following new capabilities: i) detection and evaluation of small lymph nodes, ii) improved treatment planning and determining the extent of the tumor growth, and iii) improved confidence in differentiating post-treatment change from tumor recurrence. The system will consist of two panels and have an adjustment for panel-to-panel separation distance. Each panel contains 150,  $4 \times 4 \times 0.5$  cm<sup>3</sup> cross-strip CZT crystals covering a  $20 \times 15$  cm<sup>2</sup> panel area. The crystals will be mounted in an edge-on configuration for increased photon detection efficiency. A novel event recovery scheme based on the 3D position sensitive cross-strip crystals will be developed to recover multiple interaction photon events, reject random events, and significantly increase the photon sensitivity of the system.

## **A. Korobov – V. Korobov phototherapeutic device “BARVA-SDS” for treatment and prevention of diabetic foot**

**Anatoliy Korobov<sup>1</sup>, Vsevolod Korobov<sup>1</sup>,  
Oksana Shevchenko<sup>1</sup>, Yulia Ivanova<sup>2</sup>, Andrey Mandryka<sup>3</sup>**

1 VN Karazin Kharkiv National University, Kharkiv, Ukraine

2 State Institution “VT Zaytsev Institute of General and Emergency Surgery of NAMSU”, Kharkiv, Ukraine

3 Clinical Health Resort “Beriozovy Gay”, Mirgorod, Ukraine

**Relevance.** Threatening epidemiology (one amputation of the lower limb is performed in patients with diabetes mellitus every 40 seconds).

**Purpose.** Development of a stationary device for treatment and prevention of diabetic foot by application of low-intensity optical radiation.

**Results.** The developed phototherapeutic device is a two-section chamber for simultaneous irradiation of both patients' limbs. The chamber has a base, a back wall, two outer and two inner side walls, as well as a front wall. The front wall has a turning axis. The listed parts compose two sections. The base and walls of the chamber are equipped with boards with LEDs emitting inside the sections, providing uniform irradiation of patient's legs and feet. The devices use LEDs that emit in two or six spectral ranges. The half-intensity emission bandwidth of each LED 25-30 nm. The radiation power of the LEDs is in the range of 2-5 mW (depending on the spectral range). LED power is supplied from an external power supply and control unit. The supply voltage of boards with LEDs is 14 V.

**Conclusion.** For several years, the developed devices of the described design have been used with high efficiency for the prevention and treatment of diabetic foot in Ukrainian health resorts and clinics. Outcome of treatment performed in Health Resort “Beriozovy Gay”, specializing in diabetes mellitus, and State Institution “VT Zaytsev Institute of General and Emergency Surgery of NAMSU”, allow prediction of significant (by 3-5 times) decrease in number of lower limb amputations in patients with diabetes mellitus subject to the wide use of the developed A. Korobov – V. Korobov phototherapeutic device “BARVA-SDS”.

**Keywords:** Diabetic foot syndrome, A. Korobov – V. Korobov phototherapeutic device “Barvasds”, prevention, treatment

## A digital basic X-ray system with tomosynthesis – New possibilities of the X-ray machine of the World Health Organization

Yuriy Kovalenko<sup>1</sup>, Sergei Miroschnyenko<sup>2</sup>, Andrei Nevhasymy<sup>3</sup>

<sup>1</sup> P.L. Shupyk National Medical Academy of Postgraduate Education, Kiev, Ukraine

<sup>2</sup> National Aviation University, Kiev, Ukraine

<sup>3</sup> Teleoptic PRC LLC, Kiev, Ukraine

**Objective.** At the end of the 20<sup>th</sup> century, the World Health Organization recommended the basic X-ray system as main roentgen machine for X-ray diagnostics. This easy to use and reliable X-ray diagnostic system allows stably obtaining good quality roentgenograms even when using film technologies of X-ray images visualization.

The objective of the work is to show new possibilities of a basic roentgenographic system after applying 21<sup>st</sup> century technologies to its design.

**Materials and methods.** The design of basic roentgenographic system is added by high-frequency X-ray generator with “pulse-fluoro” mode and capacitor storage to provide to provide power supply from conventional single-phase 220V power network, dynamic digital receiver with software for reconstruction of the slices of X-ray images and the robotic system for the movement of X-ray tube, allowing to rotate the X-ray tube by 40 deg in 4-6 seconds using a preset algorithm.

**Results.** The simple and universal X-ray system is realized allowing performing roentgenographic, fluoroscopic and tomographic (tomosynthesis) examinations on one and the same work station with patient in standing, sitting or recumbent position.

In roentgenography mode, the resolution of 43x 60 cm digital images obtained in 10 seconds after the exposure exceeds 4.0 line pairs per millimeter.

In fluoroscopy mode image frequency of up to 20 per second is provided with image pixel size low 350x300 micron.

In tomosynthesis mode, the resolution of up to 2.0 l.p./mm is achieved in the received slices of the examined object with not less than 200 slices obtained. According to the literature the use of tomosynthesis allows to increase in 1.3-1.6 times the sensitivity of diagnostics in detecting chest organs pathology and pathology of skeletomuscular system.

**Conclusion.** The possibility to perform roentgenography, fluoroscopy and tomosynthesis using basic X-ray system significantly expands the range of diagnostic possibilities of the X-ray machine of World Health Organization.

## **Specific changes of ultrasound scan of organs and blood biochemical indicators in vinyl chloride production workers: Dose-dependent interrelationship**

**Irina M. Yeshchina, Irina N. Kodinec, Dinara J. Nurbaeva**

Federal State Budgetary Scientific Institution "East-Siberian Institute of Medical and Ecological Research", Angarsk, Russia

The ultrasound scan of the liver, pancreas, biliary tract, and blood biochemical indicators results depending on the toxic load dose are presented. The aim was to determine the informative value of ultrasound scan, which is a screening test for diagnosis of abdominal pathology, in conjunction with the biochemical indicators of blood, most sensitive to the pathological process, against the background of occupational intoxication caused by low doses of vinyl chloride. Forty two vinyl chloride production workers were examined. Depending on the exposure load, the subjects were divided into two groups. Thirty one employees with a high degree of the toxic load (exceeding up toxic load to 4 times, average age -  $50.48 \pm 0.96$  years, experience of work in harmful conditions -  $24.24 \pm 1.20$  years) were enrolled in the first group. The second group included eleven workers with an extremely high degree of the toxic load (exceeding of toxic load more than 4 times, average age -  $46.77 \pm 1.86$  years, experience of work -  $22.33 \pm 2.11$  years). Ultrasound scan of the abdominal organs was performed by Ultrasonic diagnostic system Voluson E8 Expert using 4.5 MHz, 12 MHz sensors. Blood was collected from the cubital vein using vacuum systems such as Vaccuet. Statistical processing was carried out with the program "Statistica 10.0".

Ultrasound scan results revealed a clear dependence of the severity of the changes in the organs - lipomatosis, fatty hepatitis, diffuse changes in the liver and pancreas - on the toxic load vinyl chloride degree. In addition, deviations of biochemical blood tests were established depending on the degree of the toxic load of vinyl chloride - increase of alkaline phosphatase, gamma-glutamyl transferase, very low-density lipoprotein, atherogenic index, and triglycerides.

The obtained data will simplify the volume of examinations in vinyl chloride production workers to determine occupational nature of the disease and the severity of pathological changes.



**Medical  
Imaging**

**15**

## Development of nuclear and optical dual-labelled agents for cancer imaging

**Holger Stephan**

HZDR Institute of Radiopharmaceutical Cancer Research, Dresden, Germany

For the past decade, nuclear and optical dual-labelled imaging agents have attracted enormous attention. Applied to cancer imaging, tumours can be tracked down by nuclear techniques such as single-photon emission tomography (SPECT) and positron emission tomography (PET), and subsequently resected using image-guided surgery with the appropriate fluorophores. Moreover, the high spatial resolution of fluorescence imaging permits the elucidation of cell-biological events and thereby gaining a deeper insight into *in vitro* and *in vivo* processes. The development of dual imaging probes can be achieved using sophisticated low-molecular compounds that combine moieties for the desired imaging modalities, *e.g.* dyes for fluorescence optical imaging, and appropriate bifunctional chelator agents (BFCAs) for radiometals enabling SPECT or PET. We have developed BFCAs based on bis(2-pyridylmethyl)-1,4,7-triazacyclononane (DMPTACN) and 3,7-diazabicyclo[3.3.1]nonane (bispidine) that rapidly form stable  $^{64}\text{Cu}^{\text{II}}$  complexes under mild conditions. These BFCAs are well-suited for *in vivo* application in cancer imaging. Since they are also relatively easy to functionalize with multiple modalities, they are ideal chelators for the design of targeted dual-labelled imaging agents (PET, fluorescence imaging). Moreover, these chelating agents can be easily grafted on the surface of nanomaterials that are equipped with a multitude of different functionalities, such as targeting units, solubility enhancer and fluorescent tags. Hence, higher sensitivity can be achieved compared to small molecules, and there is an almost infinite variability regarding the surface functionalization.

Examples of target-specific peptides and bio(nano)materials equipped with DMPTACN/bispidine ligands for labelling with  $^{64}\text{Cu}$  as an ideal positron emitter are discussed. This enables tumour imaging and the biodistribution of materials can be studied over a period of days *via* positron emission tomography (PET). The additional introduction of fluorescence labels allows for optical imaging with high spatial resolution, and offers the possibility to visualize cellular processes by fluorescence microscopy.

## **Magnetic resonance evaluation of the temporomandibular joint disc shape**

**Milica Jeremic Knezevic<sup>1</sup>, Aleksandar Knezevic<sup>2</sup>, Daniela Djurovic Koprivica<sup>1</sup>,  
Bojana Milekic<sup>1</sup>, Dubravka Markovic<sup>1</sup>, Tatjana Puskar<sup>1</sup>, Jasmina Boban<sup>3</sup>**

1 University of Novi Sad, Faculty of Medicine, Department of Dentistry, Novi Sad, Serbia

2 University of Novi Sad, Faculty of Medicine, Clinic for Physical Medicine and Rehabilitation, Novi Sad, Serbia

3 University of Novi Sad, Faculty of Medicine, Department of Radiology, Novi Sad, Serbia

The temporomandibular joint (TMJ) is the critical load-bearing joint in the human body, with articular disc acting as a stress absorber during everyday orofacial activity. The TMJ disc increases the contact area between opposing articulating surfaces and, thus, distributes lower magnitude stress to a larger surface area of the joint.

Normal shape of the TMJ articular disc is biconcave and has a bow-tie configuration. The disc will have biconcave shape during all the movements and positions of the lower jaw. It should be located between the condyle and the posterior slope of the articular eminence. During disorder progression, the disc becomes deformed, the anterior and intermediate zones become thinner, and the posterior zone thickens. This all leads to changes of disc shape and length, which becomes rounded or elongated and deformed.

According to these characteristics, Murakami divided the shape of articular disc into biconcave, biconvex, biplanar, hemiconvex, and folded. Biconcave disc has concave both upper and lower surfaces; biplanar, the whole disc is of even thickness; hemiconvex has only upper surface concave, while the lower is convex; biconvex disc has convex both upper and lower surfaces and folded disc is folded at the centre.

Without ionizing radiation and invasion, MRI is considered suitable and internationally recognized standard for analyzing the TMJ disc position, morphology and mobility as well as surrounding anatomical structures in normal and pathologic conditions.

## Improvement of primary level X-ray diagnostics for the purpose of raising primary care efficiency

**Yuriy Kovalenko**

P.L. Shupyk National Medical Academy of Postgraduate Education, Kiev, Ukraine

**Objective.** Currently, in Ukraine, only 20% of medical aid is provided at primary care level while in most of European countries this indicator exceeds 70%. One of the reasons is continuous decrease of access to high quality X-ray diagnostics for the population, used for establishment of up to 80 % of clinical diagnoses.

The objective of the work is the analysis of possibility for bringing high quality X-ray diagnostics closer to primary care physicians by using novel technologies and for increasing population access to it so to be able promptly obtaining diagnostic information and timely providing the treatment.

**Materials and methods.** The work analyses possibility and expediency of installing modern X-ray equipment in primary care units (PCU) or near to them. The possibilities of reception of high quality diagnostic radiological information and of its fast use are assessed; material and time expenses for different options of diagnostic service provision to the population are compared.

**Discussion.** For the last seven years near one thousand of new primary care units were open, most of them remotely from medical entities with X-ray offices, that considerably (by several hours, and in some cases by several days) increases the time needed for getting a diagnosis for the patient. It significantly decreases the efficiency of treatment. Also, in prevailing number of cases the patient is forced to receive the conclusion of diagnostic examination by the nearest radiologist independently from the level of qualification of the latter. Use of lightweight digital x-ray units which can be easily transported by usual car, in combination with the use of information technology allows bringing X-ray diagnostics closer to PCUs, and telecommunication networks allow for engaging the best experts to remote consultations on a specific clinical situation. As a result, the time to get the correct diagnosis for the patient is 15-30 minutes.

**Conclusion.** Performing X-ray examinations at PCUs allows reducing in times the time required for establishment of the diagnosis to patients, and the use of remote expert consultations increases the probability of diagnosis correctness

## Application of medical CT imaging for investigation of sex differences in facial soft tissue thicknesses

**Dora Zlatareva<sup>1</sup>, Diana Toneva<sup>2</sup>, Silvia Nikolova<sup>2</sup>, Vasil Hadjidekov<sup>1</sup>**

<sup>1</sup> Department of Diagnostic Imaging, Medical University, Sofia, Bulgaria

<sup>2</sup> Department of Anthropology and Anatomy, Institute of Experimental Morphology, Pathology and Anthropology with Museum, Bulgarian Academy of Sciences, Sofia, Bulgaria

The soft tissue thickness represents the amount of soft tissue that overlies a definite landmark of the skull. Knowing the amounts of soft tissue in a set of anatomical points is crucial for a realistic facial reconstruction i.e. the recreation of an individual's face based on the skull for forensic and bioarchaeological purposes. In this study we aim to use volumetric images generated by computed tomography (CT) in order to investigate the sex differences in the facial soft tissue thicknesses. The images were generated using a medical CT system Toshiba Aquilion 64. The CT scans were performed on patients for diagnostic purposes and the obtained DICOM series were anonymized. In this study head CT scans of 74 adult Bulgarians were used. According to the body-mass index values of the males and females, they were divided into two groups: normal and overweight. The soft tissue thicknesses were measured at 16 (7 midline and 9 bilateral) anatomical landmarks. The measurements were performed using the free software InVesalius. The thicknesses were measured in the axial and sagittal views, perpendicular to the bone surface. The statistical significance of the sex differences was assessed using the independent t-test or Mann-Whitney test, depending on the results of the normality test.

The mean values of the soft tissue thicknesses in all landmarks were reported according to the sex and body mass index category of the individuals. For both normal and overweight body-mass index categories, males had more soft tissue at the majority of facial points than females. The only exceptions were observed in the cheek zone, where females had thicker soft tissues. The significant sex differences did not follow the same pattern in the normal and overweight category.

**Acknowledgments:** This study was supported by the National Science Fund of Bulgaria, grant DN01/15-20.12.2016.

## Brain, head and neck vascular malformations diagnosed by magnetic resonance and computed tomography angiography

Dora Zlatareva, Violeta Groudeva

Department of Diagnostic Imaging, Medical University, Sofia, Bulgaria

**Aim.** Non-invasive imaging of suspected vascular malformations within the brain, head and neck is mainly performed by multidetector computed tomographic (MDCT) angiography. The advances of magnetic resonance (MR) imaging allow not only detailed characterization of these abnormalities but also could replace some methods using ionizing radiation. The classification of vascular malformations of the brain and soft tissue has changed over the past years. The aim of this study is to characterize and describe magnetic resonance and computed tomography (CT) imaging findings of vascular malformations of the brain, head and neck.

**Materials and methods.** We examined 30 patients with head and neck vascular malformation and 45 patients with brain vascular malformations. Magnetic resonance imaging has been performed on 3Tesla MR unit with standard protocol including gadolinium contrast material and CT angiography (CTA) on 64 slices tomograph.

**Results.** Eighteen out of 30 patients were with head and neck hemangiomas, 7 patients with venous malformations, 2 patients with capillary malformations and 3 with lymphatic malformation. In 20 patients we diagnosed brain cavernomas, 3 out of 20 were multiple. Brain venous malformations were detected in 8 patients and arteriovenous malformations in 11. Six patients have been diagnosed as Vein of Galen aneurysmal malformation. The most frequent location for cavernomas was temporal and frontal region, while arteriovenous malformations have a common parietal and temporal location in our cohort of patients. The most common clinical symptoms for brain imaging were headache and seizure, while head and neck regions are referred by vascular surgeon due to skin changes and local tumour.

**Conclusion.** The proper clinical referral and imaging protocol in combination with good knowledge of MR and CT imaging findings of vascular malformations are mandatory conditions for precise imaging diagnosis and monitoring.

## Single Plane Compton Imaging

**Boyana Deneva<sup>1</sup>, Katja Roemer<sup>1</sup>, Guntram Pausch<sup>2,3</sup>,  
Andreas Wagner<sup>1</sup>, Wolfgang Enghardt<sup>2,3,4</sup>, Toni Koegler<sup>2,3</sup>**

<sup>1</sup> Helmholtz-Zentrum Dresden-Rossendorf, Institute of Radiation Physics, Dresden, Germany

<sup>2</sup> Helmholtz-Zentrum Dresden-Rossendorf, Institute of Radiooncology – OncoRay, Dresden, Germany

<sup>3</sup> OncoRay – National Center for Radiation Research in Oncology, Dresden, Germany

<sup>4</sup> German Cancer Consortium (DKTK), partner site Dresden, Dresden, Germany

Nuclear medicine is nowadays a vital branch of the medical imaging modalities for diagnostic purposes, as well as a powerful tool among the therapeutic procedures. The use of radioactive tracers inhaled, swallowed or directly injected in the bloodstream of the patient enables real-time monitoring of metabolic processes in the body. To fulfil its task, the nuclear medicine needs high quality imaging techniques. The gamma camera and its utilization in SPECT have established themselves as important technologies for radionuclide imaging. Despite the immense improvement of the imaging techniques, there are still physical limits to the camera performance manifested mainly by the constant trade-off between spatial resolution and detection efficiency due to the used collimator. In order to overcome these limitations, the concept of the “Single Plane Compton Imaging” was developed, based on the idea of the “Directional Gamma Radiation Detector”, published in Ref. [1] and [2].

A setup for the investigation of this novel concept was developed at the Helmholtz-Zentrum Dresden – Rossendorf. Consisting of an inorganic scintillator crystal (4x4 GAGG:Ce, as well as 4x4 CsI+CaF<sub>2</sub> checkboard) array, read out by a Philips digital silicon photomultiplier and mounted on a moveable x-y table, the setup is intended to reconstruct arbitrary activity distributions.

Data acquired in a proof-of-principle experiment will be presented. Also, preliminary reconstructions of measured activity distribution using the MLEM method will be shown and compared to predictions obtained from particle transport calculations performed with Geant 4.

### References

[1] G. Kraft et al., U.S. patent no. 8030617 B2, granted in Oct. 2011

[2] A. Gueorguiev et al. U.S. patent no. 8299441 B2, granted in Oct. 2012

## Diaphyseal fracture of the X-ray scoring healing of the tibia

**Olena Sharmazanova, Hanna Kirik**

Kharkov Medical Academy of Postgraduate Education, Kharkov, Ukraine

**Introduction.** The radiographic union score for tibia (RUST, 2014), which is used for intramedullary fixation of fractures, is known.

**The purpose:** to study the X-ray score assessment of the degree of healing of diaphyseal tibial fracture (DTF) in the treatment of external fixation devices.

**Materials and methods.** The results of clinical and radiographic examination of 78 patients (56.5% of men and 43.5% of women) in the age from 18 to 60 years at different times after receiving acute injury of the shin with the use of external fixation devices were analyzed. For reproduction of the evaluation of DTF healing, the “radiographic union score for tibia” (RUST, 2014) indices (fracture line and bone callus) were supplemented by an evaluation of the characteristics of the bone callus (its intensity and connection with the cortical layer), each attribute was evaluated at 4 points on 4 bone surfaces, therefore the minimum score was 4, maximal – 16.

**Results.** Complete aggregation of DTF in the treatment of external fixation devices in 3 months was noted in 11.2% for 4 months – in 28.8%, in 6 months – in 27.7%. Slow fusion of fractures with complications is set at 32.3%.

In case of timely healing of DTF, the number of points of RUST is equal to: in 2 months. 4-8; after 3 months – 8-10; after 4 months – 11-13 points.

**Conclusion.** The ball assessment of healing of diaphyseal fractures of the tibia can be used in the treatment of external fixation devices, which allows standardizing the results of the X-ray conclusion.

## Application of digital tomosynthesis in lung pathology

Olena Sharmazanova<sup>1</sup>, Yuriy Kovalenko<sup>2</sup>, Larisa Urina<sup>3</sup>

<sup>1</sup> Kharkov Medical Academy of Postgraduate Education, Kharkov, Ukraine

<sup>2</sup> Center of X-ray technologies of the Association of Radiologists of Ukraine, Kyiv, Ukraine

<sup>3</sup> Department of Radiology, Children's Clinical Hospital № 3, Kyiv, Ukraine

**Objective.** To determine the potential of digital tomosynthesis (DT) in lung pathology in adults.

**Materials and methods.** Digital tomosynthesis of the chest organs was performed for 50 patients (mean age –  $38.8 \pm 12.6$  years). Among them, 14 (35.0%) had a diagnosis of acute congestive pneumonia, 6 (15.0%) had focal and disseminated pulmonary tuberculosis, 8 (20.0%) had pulmonary tumors, 22 (55.5%) were the chronic obstructive pulmonary disease. DT was performed on a domestic digital X-ray diagnostic complex with a digital tomosynthesis mode after performing digital radiographs.

**Results.** The use of DT made it possible to clarify the radiograph of the pathology in 42.0% of cases in 6 (12.0%) patients, the radiological data were changed: in 4 with the norm for chronic obstructive pulmonary disease, 2 with pneumonia for tuberculosis. In 2 patients, a small lesion in the lungs (size of lesions is from points up to 1-2 mm) and the cavity using DT chest.

**Conclusions.** Digital tomosynthesis can be considered as an alternative to computed tomography in the primary diagnosis of pulmonary pathology, during screening studies and monitoring of treatment.

## Image based estimation of absorbed patient dose in radiography

**Aleksandar Pavlović, Vladimir Ostojić, Vladimir Petrović**

Faculty of Technical Sciences, Novi Sad, Serbia

It is of significant importance to radiologists to use radiation dose responsibly and not to risk the health of the patient. Therefore, there is a need for a method that could estimate how much of the radiation dose the patient absorbed. This paper describes the method for estimation of absorbed patient dose, based on the radiography image.

The mathematical model connecting detected radiation dose and pixel values of radiography image is made and described. The connection is found to be linear. The way the linear coefficient changes with variation of applied voltage is also given.

Measuring of radiation dose was done with several values of filtration used, in order to determine the way applied filtration affects the dose that comes to the digital detector. It is found that the radiation dose drops exponentially with the rise of applied filtration.

It is experimentally confirmed that the dose is inversely proportional to the squared distance from the source of radiation and the detector. It is also shown how presence of the anti-scatter grid attenuates the radiation dose.

In the end, all the collected data and mathematical relations are used for estimation of absorbed patient dose. The main idea is that the difference between calculated radiation dose and the actual radiation dose that came to the digital detector represents the absorbed patient dose that needs to be estimated.

## Simulation and optimization of a first generation gamma transmission computed tomography using MCNP5 code

**Z. Idiri<sup>1</sup>, K.Boukefoussa<sup>1</sup>, M.Belaabed<sup>2</sup>, S.Bitam<sup>2</sup>**

<sup>1</sup> Centre de Recherche Nucléaire d'Alger, Alger-Gare, Algeria

<sup>2</sup> Université Hadj Lakhdar de Batna, Batna, Algeria

Before realizing a first generation gamma transmission computed tomograph dedicated to soil studies, a simulation of the system has been carried out using the Monte Carlo Neutron and Photon transport code (MCNP5). This tomograph is mainly composed of a <sup>137</sup>Cs source and a 3-inch NaI(Tl) gamma detector, the two are collimated. In the modeling of the system, the scanned sample is taken as universal soil and represented in cylindrical form. In the first step, the collimators apertures, the sample diameter and the source-detector were optimized using calculated linear and mass attenuation coefficients. In the second step, we introduced a cylindrical void of 6 mm diameter in the sample and we simulated the scan by calculating the linear attenuation coefficient for all the geometries encountered during a normal scan, i.e. moving the pair source-detector and rotating the sample with steps of 1mm and 2° respectively. As the calculations require long time, only a small projection matrix is obtained. This latter is then used in iGorbit software for image reconstruction. In the obtained image, the introduced porosity is significantly visible demonstrating then the viability of the modeled gamma transmission tomograph.



**Medical  
Physics**

**16**

## Isocentric accuracy with Winston–Lutz test for LINAC-based stereotactic radiosurgery treatments

**Irena Muçollari, Rejnardo Tafaj,  
Bledar Cullhaj, Blerina Myzeqari, Valbona Bali**

University Hospital Center, Tirana, Albania

Stereotactic radiosurgery requires three-dimensional planning with computerized and delivering a high single dose through stereotactic convergent beams, which could be originate from: cobalt convergent sources (gamma knife); proton; static or dynamic coplanar and non- coplanar arcs (Xknife, LINAC); or robotic equipment like Cyberknife. The “stereotaxy” describes a procedure in which a “target lesion” is localized against a fixed reference system in three dimensional such as a rigid head frame. To assure high accuracy in radiation delivery during linear accelerator based stereotactic radiosurgery procedures, a Winston-Lutz test is performed to measure the effective isocenter over a range of gantry and couch angles employed. In this work will be reviewed the Winston –Lutz tests with gafchromic film which has been performed as quality assurance for different treatment plans for patient with brain tumors. This procedure provides the safety of a SRS treatment plan executed with an Oncor Siemens accelerator with tertiary cones and Brown-Robert-Wells frame by Radionics. The results of this study indicate that Linac including the BRW stereotactic frame is optimal for SRS treatment of patients with intracranial tumors.

**Keywords:** Brain, tumor, frame, stereotactic radiosurgery, SRS

## **Reasons and basis for implementation of medical physicists certification in Ukraine**

**Liudmyla Aslamova, Ielyzaveta Kulich, Nadiia Melenevska**

Taras Shevchenko National University of Kyiv, Kyiv, Ukraine

All over the world high technologies are used and implemented in medicine. Ukraine is not an exception. For example, up-to-date there are 24 linear accelerators and 2 PET centers. The amount of high-tech equipment will be increasing to provide needs of more than 42 million people in the country. Such equipment needs first and foremost quality assurance by certified personal.

Ukraine selected one of ten principles of “Further generations protection”, namely not to accumulate radioactive waste. Therefore, on one hand, equipment with radionuclides should be replaced by the one with generating ionizing radiation sources. On the other hand, radiation protection and safety procedures, safety culture should be affectively introduced during the use of high technologies in medical activities with ionizing radiation sources. This is described in international standards stated in the IAEA Basic Safety Standards and progressively implemented in Ukraine. At the same time there are some difficulties with standards implementation. Today definition of “medical physicist” is absent in Ukrainian legislation base as well as his/her duties and functions. However, a certain part of medical personal is performing medical physicist’s functions in part. National system regulated for registration and tracing of patient’s exposure dose is absent.

It is an evidence to implement national education system for medical physicists interconnected with formal certification schemes for the recognition of the expertise and competence. Such a certification scheme could either be directly under the control of the regulatory body, or operated by a non-governmental not-for-profit organization. IRPA Guidance 2016 recommends that it can be an associate society, under an approval from the regulatory body, or its activity is regulated by national legislation.

Taras Shevchenko National University of Kyiv has a successful experience of cooperation with Swedish regulatory authority in the frames of project “Quality Assurance and Quality Control in medical radiology in Ukraine” connected with education and training of medical physicists. Faculty of Radio Physics, Electronics and Computer Systems is educating magisters on specialties “medical physics”, “biomedical physics, engineering and informatics”. Training and Research Center for Radiation Safety successfully carries out refresher courses and examination on “Radiation safety for certain activities related to nuclear energy use” more than 14 years. The center has certificate ISO 9001:2008. Base on long years of experience, the university together with non-governmental not-for-profit organization Ukrainian Association of Medical Physicists and Engineers looking for a possibility to introduce certification scheme for radiation protection and medical physics experts.

## **Safety culture in syllabus on medical physics in Ukraine**

**Liudmyla Aslamova, Ielyzaveta Kulich, Nadiia Melenevska**

Taras Shevchenko National University of Kyiv, Kyiv, Ukraine

Nowadays safety culture concept is considered a mechanism to identify latent deficiencies of safety and to bring the latter beyond the standards laid down in the legislation and required by the regulators. When the concept of safety culture is applied to activities with nuclear energy use in medicine, it calls for the enhancement of protection system for patients, personnel and environment. For instance, it should be understood on all levels that nuclear technologies require special attitude to radiation protection and safety. Everyone should remain vigilant when working with ionizing radiation sources.

Sufficient attention must be paid to safety culture in education, training and continuous professional development of medical physicists. Nowadays, in Ukraine safety culture principles are incorporated into the education and training system for specialists on nuclear energy. In medicine with nuclear energy use, medical physicist performs quality assurance and quality control of medical procedure, ensures radiation protection and safety for the patient, personnel and environment. Thus, special training for all mentioned roles and functions is expected, and daily practices should be performed in accordance with the safety culture principles. It is very important for medical physicists' community in Ukraine to be exposed to international experience and best practices, so as to raise their awareness and improve qualification. Some specialists participate in international events like conferences, trainings, workshops etc, of course, but there is no common practice of sharing the knowledge gained therein in place. Awareness could also be considerably raised through participation in international interactive projects, for example, project of International Atomic Energy Agency named Radiation Protection of Patients. There is a very useful data base called Safety Reporting and Learning System for Radiotherapy concerning incidents with nuclear energy use in medicine. Any medical institution can access it. Anyone can obtain and study a range of reports, graphs, statistics etc. Recent times few medical institutions joined to the data bases in the frame of the IAEA Regional project RER9147 "Enhancing Member States' Capabilities for Ensuring Radiation Protection of Individuals Undergoing Medical Exposure".

The present paper is an attempt to collect together all different ways to implement safety culture principle for medical physicists' education and to give some recommendations of common use for the principle in syllabus on medical physics.

## Determination of initial electron parameters by means of Monte Carlo simulations for the siemens artiste Linac 6 MV photon beam

Taylan Tuğrul<sup>1</sup>, Osman Eroğul<sup>2</sup>

<sup>1</sup> Yüzüncü Yıl University, Medicine Faculty, Radiation Oncology Department, Van, Turkey

<sup>2</sup> TOBB University of Economics and Technology, Department of Biomedical Engineering, Ankara, Turkey

**Introduction.** It is essential to define all the characteristics of initial electrons hitting the target i.e. mean energy and full width of half maximum (FWHM) of the spatial distribution intensity, which is needed to run Monte Carlo simulations. In this study, we have investigated initial electron parameters of Siemens Artiste Linac with 6 MV photon beam using the Monte Carlo method.

**Methods.** At the first step, Siemens Artiste Linac head geometry was modeled using BEAMnrc code after the specifications of linac obtained from the manufacturer. The BEAMnrc of linac head components include the exit window, target, primary collimator, flattening filter, monitor chamber, Y Jaws and X MLC. PEGS4 (EGS preprocessor) cross-section data for specific materials in the accelerator were obtained from 700icru.pegs4data file. This data file contains cross-section data for particles with kinetic energy as low as 0.01 MeV and physical density such as mass density, atomic number and electron density for all the different materials used in the accelerator. In all simulations the electron cut-off energy (ECUT) was defined 0.7 MeV and the photon cut-off energy (PCUT) was defined 0.01 MeV. UBS was used (Splitting factor is 20 and Russian Roulette is off) as the variance reduction parameters. In BEAMnrc, the number of history of Monte Carlo calculation was  $6 \times 10^8$  particles (Total particles in phase space file are nearly 25 million). Monte Carlo simulations were performed for monoenergetic beams ranging from 6 to 6.4 MeV and FWHM varied from 0.28 to 0.32 cm for 6 MV beam. The phase space files were used as input file to DOSXYZnrc simulation to determine the dose distribution in water phantom. We have obtained percent depth dose curves and the lateral dose profile. All the results were obtained at 100 cm of SSD and for 10 x 10 cm<sup>2</sup> field. For correct PDD and lateral dose profile; Quality Index (QI), gamma index criteria and maximum dose depth have considered.

**Results.** We concluded that there existed a good conformity between Monte Carlo simulation and measurement data when we used electron mean energy 6.3 MeV and 0.30 cm FWHM value as initial parameters. We have observed that FWHM values effect very little on PDD and we see the electron mean energy and FWHM values effect on lateral dose profile. However, these effects are between tolerance values.

**Conclusion.** In this study, the important components were defined about Siemens Artiste Linac head. Then, the significant parameters were obtained. A small change in electron parameters creates strong effects on the dose. The phase space file which was obtained from Monte Carlo Simulation for linac can be used as calculation of scattering, MLC leakage, to compare dose distribution on patients and in various researches.

## **A new method for production of radionuclide-generator $^{212}\text{Pb}/^{212}\text{Bi}$**

**Vladimir Pantelev, Anatoly Barzakh, Leonid Batist, Dmitry Fedorov, Victor Ivanov, Pavel Molkanov, Stanislav Orlov, Maxim Seliverstov, Yuri Volkov**

Petersburg Nuclear Physics Institute, Gatchina, Russia

The radionuclides decaying by alpha particle emission are very effective tools for therapy of different malignant tumors at a very early stage of their formation. One of the general advantages of alpha particle is its very short range (60-80  $\mu\text{m}$ ) in a biological tissue. The action of a radionuclide, decaying by alpha particles, is very effective, as it is very local and does not destroy the surrounding healthy tissues. One of the goals of radioisotope complex RIC-80, which is presently constructed at the beam of C-80 cyclotron, is the production of high purity alpha-particle emitters  $^{223,224}\text{Ra}$  and  $^{225}\text{Ac}$ . For the purpose of medical, high purity radionuclide production at one of the target stations of RIC-80 the electromagnetic mass-separator will be installed. The presented work is devoted to R@D of a high temperature method of  $^{212}\text{Pb}$  and  $^{224}\text{Ra}$  extraction from a high density thorium carbide target which is kept in a high vacuum. This target is a prototype of presently developed mass-separator target unit for RIC-80 facility. The results of effective separate extraction of  $^{212}\text{Pb}$  and  $^{224}\text{Ra}$  from the tested target material at different temperatures have been obtained, that gives the possibility of  $^{212}\text{Pb}/^{212}\text{Bi}$  generator construction. The perspective of the developed method utilization for production of other medical radionuclides is discussed.

## **A new formalism of dose-surface histograms for robust modeling of skin toxicity in radiation therapy**

**Giuseppe Palma, Laura Cella**

CNR-IBB, Napoli, Italy

In modern radiation therapy (RT), technological advances have increased user control over healthy tissues dose distributions. In this framework, mathematical models of radiobiological effects potentially play an essential role and Normal Tissue Complication Probability (NTCP) modeling may help to identify the optimal plan that minimizes radiation-induced side effects for individual patients. Lyman-Kutcher-Burman (LKB) approach to NTCP modeling has widely been applied for the toxicity prediction as a function of radiation dose distribution. It relies on the extraction of the dose-volume histogram (DVH) of an organ as dose summary function of a given radiation-induced morbidity endpoint.

In this study, we lay the theoretical groundwork for a novel approach to LKB NTCP modeling to account for surface effects in radiation induced toxicity phenomena of hollow organs.

A key element of the proposed formalism is represented by the definition used for the extraction of dose-surface histograms (DSHs). In this respect, we propose a new recipe that computes the DVH on a 3D structure in the limit of vanishing thickness to approach the two-dimensional space for DSH. This allows for refashioning the concept of generalized equivalent uniform dose (gEUD). A refashioned LKB NTCP model is accordingly derived for surface or hollow organs, following the general theory of nested models for fitting the values of its parameters (and deriving the associated confidence intervals) that best capture a given radiation induced toxicity endpoint in a cohort of cancer patient.

In conclusion, the DSH represents a natural tool for describing radiation-induced morbidity for hollow organs. In this work, we formally defined a new way for robust DSH computation and, accordingly, provided a re-definition of gEUD that could allow for a DSH-based LKB NTCP for the description of surface toxicity phenomena. We believe that this formalism – easily implementable within commercial treatment planning systems – might improve the knowledge on toxicity endpoints that are supposed to be related to surface effects.

## Measurement of output factor for small radiation field using solid water phantom

**Sohyun Ahn<sup>1</sup>, Min-Joo Kim<sup>2</sup>, Sanghyuk Song<sup>1</sup>, Inyoung Wang<sup>3</sup>, Junetaek Sin<sup>3</sup>**

<sup>1</sup> Department of Radiation Oncology, Kangwon National University Hospital, Chuncheon-si, South Korea

<sup>2</sup> Department of Radiation Oncology, Yonsei Cancer Center, Yonsei University College of Medicine, Yonsei University Health System, Seoul, South Korea

<sup>3</sup> Kangwon National University Hospital, Chuncheon-si, South Korea

Measurement of small field must be performed with appropriately designed detectors and careful attention to prevent geometric misalignment of detector during setup and measurement process. Also, several challenging physical parameters for electronic equilibrium, invalidating the Bragg-Gray conditions, source occlusion could be a problematic issues and various detector-specific effects such as the volume averaging effect, the fluence/dose perturbations has remained as a controversial issue. Most of guidance for small field dosimetry had recommended utilizing water-filled phantom and those phantoms required to spend time about 20 to 40 minutes for phantom setup. The small field dosimetry based on the general method is required to perform after MLC-related maintenance, but could be a troublesome process because of time spent and required to streamline the measurement procedures or methods. The current study presents the simplified measurement method for output factor of small field by utilizing commercialized solid water phantom and various ionization chambers for 6 and 10 MV X-ray energies. The measurement result was quantified and compared with conventional measurement method and the feasibility of the simplified measurement method has been discussed.

The output factor (OF) is defined as  $DFS/D_{10 \times 10}$ , the ratio of dose at given field size (DFS) to the dose at  $10 \times 10$  cm<sup>2</sup>. Measurement was performed on available photon beam energies used (6 and 10 MV) for IMRT/VMAT. Applied small field size was  $1 \times 1$ ,  $2 \times 2$ ,  $3 \times 3$ ,  $4 \times 4$ ,  $5 \times 5$  cm<sup>2</sup> and  $8 \times 8$  cm<sup>2</sup> as a regular field size and  $10 \times 10$  cm<sup>2</sup> for reference field size with 90 cm SSD at gantry angle  $100^\circ$ . The OFs for small field, under  $5 \times 5$  cm<sup>2</sup>, were measured by MicroDiamond 60019 (MD), Pinpoint3D 31016 (PP3D, PTW, PTW-Freiburg, Germany), Extradin A16 (A16, Standard Imaging, Madison, WI, USA) using Elekta Infinity (Elekta, Stockholm, Sweden) that included an MLC and had utilized clinical purpose of IMRT/VMAT. As a conventional measurement methodology, the MP3-XS (PTW, PTW-Freiburg, Germany) as a water-filled phantom, three different chambers (MD, PP3D, and A16) was used in conjunction with the associated software, MEPHYSTOmC2, and UniDos electrometer (PTW, PTW-Freiburg, Germany). The simplified measurement method, suggested in this study, utilized the Blue Water phantom (BW in the following, Standard Imaging, Middleton, WI, USA). As a reference data, the output factor calculated in MONACO TPS (version 1.6, Elekta AB, Stockholm, Sweden) was applied. As a result, output factors with two different measurement conditions were in good agreement at less than 2%. The result has demonstrated that small field output factor could be measured in BW phantom or solid water phantom, alternatively for water phantom. Although the measurement of small field output factor in solid water phantom could not be a best solution, easy and quick setup using solid water phantom for measurement of small field output factor could be helpful.

## Monte Carlo simulation and measurement for improving dose uniformity of total skin electron beam therapy with three ports

Sohyun Ahn<sup>1</sup>, Sanghyuk Song<sup>1</sup>, Inyoung Wang<sup>2</sup>, Junetaek Sin<sup>2</sup>

<sup>1</sup> Department of Radiation Oncology, Kangwon National University Hospital, Chuncheon-si, South Korea

<sup>2</sup> Kangwon National University Hospital, Chuncheon-si, South Korea

**Purpose/Objective(s).** TSEB has been used in the treatment of cutaneous T-cell lymphoma or mycosis fungoides. The Stanford technique or six-dual field technique is to irradiate the entire skin by irradiating six ports electron beams while changing the body direction, positions of arms and legs while the patient is standing. This method is by far the most commonly used method, but it is difficult for the patient to maintain the same posture for a fairly long period of time. As noted in several papers, the reason for maintaining dose uniformity is due to the nature of TSEB. It is not easy to use the latest treatment techniques to investigate uniform doses of irregular whole body skin of a patient while minimizing dose to the internal organ. It is certain that if the patient is in a lying position, he or she can make treatment possible for patients with mobility discomfort. On the other hand, it is difficult to ensure dose uniformity of areas where radiation is difficult to be irradiated unless artificially placed arms and legs such as between arm and body (underarm), between legs and legs (groin). In this study, we tried to improve the dose uniformity of TSEB patients using 3 ports instead of 6 ports.

**Materials/Methods.** We performed TSEBT using Elekta Infinity LINAC and High dose rate electron (HDRE) mode was used to shorten treatment time. To improve the rotation and position accuracy of patients during TSEBT, a dedicated patient set up system for TSEBT was also used. The effect of X-ray on spoiler on dose uniformity was quantitatively evaluated by Monte Carlo simulation. Since we use only 3 ports, we used a human phantom to optimize the incidence angle of MUs and LPO and RPO beam for each beam port. In-vivo dosimetry was performed while applying the optimized treatment set up with Monte Carlo simulation and phantom experiment.

**Results.** We distinguished dose distribution by the X-ray distribution from the acryl spoiler and by the primary electron distribution with Monte Carlo simulation. In the experiment using the anthropomorphic phantom, it was verified that 84 ~ 112 cGy was contained in the field area including the side when PA 100 MU and 60 LPO / RPO 1400 MU were irradiated. The shield was installed on the acryl panel to cover the field above and below the light field interface. Based on the results of MC simulation and phantom measurement, we performed the first treatment according to MU and set up per port, and performed in vivo dosimetry. The dose distribution was 91.5 ~ 117.8 cGy, showing dose uniformity within 10% during treatment.

**Conclusion.** We performed TSEBT on the limited region using 3 ports instead of the traditional 6 ports and found the optimized set up condition through MC simulation and phantom experiment to maintain dose uniformity that is clinically usable.

## **Investigation of dose indicators for breast cancer CT localization procedures in radiation therapy in Croatia**

**Ana Diklić, Doris Šegota, Slaven Jurković**

University Hospital Rijeka, Rijeka, Croatia

Computed tomography (CT) has become an integral component of modern radiotherapy. CT data obtained is used for individual treatment planning and accurate localization. However, there is a growing awareness of the dose delivered to the part of the body outside the target volume. Ionizing radiation carries a stochastic risk of malignancy; therefore, doses should be kept as low as reasonably achievable in order to provide an adequate information needed for radiotherapy planning. The aim of this study was to investigate the variation in CT localization scanning protocols for breast cancer patients between radiotherapy centers in Croatia. Data collection sheets were distributed to all institutions performing this type of procedure. All of them responded and a retrospective data collection was performed. Computed Tomography Dose Index volumetric, Dose-Length Product and scan length were recorded and statistically analyzed. The national diagnostic reference level for breast cancer CT protocol in radiation therapy is proposed and compared to other seldom published data. This study provides a platform for dose comparison and optimisation of planning CT protocols in breast cancer. Results will be presented.

## Treatment plan verification in proton therapy using the FBX chemical dosimeter

**Marina Troshina, Sergey Dyuzhenko, Ekaterina Koryakina,  
Vladimir Potetnya, Olga Golovanova, Sergey Koryakin, Stepan Ulyanenko**

A. Tsyb Medical Radiological Research Center – branch of the National Medical Research Radiological Center of the Ministry of Health of the Russian Federation, Obninsk, Russia

Scanning beam technique in proton therapy allows the improvement of the irradiation conformity of tumors differing in shapes, sizes, and localizations. This method was implemented at the proton therapeutic complex “Prometheus” (ZAO Protom) at the MRRC, Obninsk. Slight variation in delivered dose distributions for the same treatment plan is characteristic of the plan execution despite the high proton irradiation accuracy. So measurements at different points of the irradiated volume must be carried out several times to determine whether dose distribution is correctly delivered. This procedure takes a lot of time of the accelerator operation. To solve this problem the dosimetry system which is able to measure the average dose for the entire volume of interest for one execution of the plan might be used.

A modified ferrous sulfate FBX dosimeter was used in the study. Aqueous FBX solution can be irradiated in the vials of arbitrary shape. The vials for the chemical dosimeter were prepared from thermoplastic by means of 3D-printing. The shapes of vial replicated that of PTV for a patient treated by protons at MRRC. For each vial multiple scans were performed at the cone tomography machine built in the proton therapy complex, the vial being filled with water and installed in the water phantom. Then the vial scans were superimposed on the patient tomogram and the resulting file was used to calculate the irradiation plan. The exposure directions and the proton energy range were similar to the treatment plan.

The vials were filled with a dosimetric solution just before irradiation. Optical density measurements were performed in an hour after exposure. FBX-dosimeter calibration curves for standard gamma radiation and for scanning proton beam were obtained previously. Two types of vials were used, two PTV volume models and two PTV models with nearby critical structures. Each experiment was repeated three times or more.

The average doses in the PTV measured by FBX dosimeter were differed from treatment plan values not more than 10%. For a critical structure located approximately 10 mm away from PTV the optical density of FBX solution did not differ from the unirradiated control. When irradiated volumes were close to each other, the dose in the critical organ model determined by FBX was 25% of the dose measured in PTV model vial and 32% of the planned dose. This study is the first step towards development of personalized phantoms for quick verification of irradiation plans for proton scanning beam.

## Theoretical substantiation of the protocol of laser thermal disinfection of the root canal system of the tooth

**Yaroslav Bobitski<sup>1,2</sup>, Adriana Barylyak<sup>3</sup>, Igor Demkovich<sup>2</sup>**

1 Faculty of Mathematics and Natural Sciences, University of Rzeszow, Rzeszow, Poland

2 Department of Photonics, Lviv Polytechnic National University, Lviv, Ukraine

3 Department of Therapeutic Dentistry, Danylo Halytsky Lviv National Medical University, Lviv, Ukraine

The success of endodontic treatment in modern dentistry depends on the effectiveness of root macrocanal disinfection and system of dentinal microcanals, since bacteria are the main cause of periapical infections. The growing resistance of bacterial microflora limits traditional antibiotic therapy. Among the alternative physical methods of the tooth root system disinfection, laser technologies are one of the most promising ones, with its selective thermal effect on the pathogenic agent.

Preliminary experimental data indicate the infection of dentin through the dentinal tubules at a distance up to 800  $\mu\text{m}$  from the surface of the macrocanal. It has been proved that laser irradiation in certain modes can cause a bactericidal effect at a depth up to 1000  $\mu\text{m}$ .

However, with laser bacterial thermal disinfection, it is necessary to balance the temperature rise in deep dentin to achieve the effect of disinfection and to exclude the critical thermal growth to the adjacent zones to the hard tissue of the tooth – periodontal and bone.

The purpose of this study is theoretical calculation of temperature fields in the root dentin and the surrounding tissues of the tooth, depending on the energy and time and spectral irradiation regimes to obtain effective protocols for laser disinfection of the root canal system.

For a theoretical study, a geometric model of the average tooth structure was constructed and chosen method of delivering laser radiation along the root canal through an optical fiber was constructed. The following cases were considered: the use of Er, Cr: YSGG laser (2780 nm); Nd: YAG laser (1060 nm) and simultaneous exposure with two Laser Er, Cr: YSGG (2780 nm) and diode (980 nm) lasers. For each case, we calculated the volume distribution of the energy at the end of the optical fiber along the macrocanal. We obtained protocols to achieve bacterial disinfection in dentin at a depth of 800  $\mu\text{m}$ , with the condition that the temperature exceeds 47° C with a minimum duration absorbed in the dentin and the surrounding tissue by the Monte Carlo method. In addition, the temperature fields in the heterogeneous zone of the structure, depending on the movement speed of n of 10 seconds and avoiding the thermal trauma of periodontal and bone tissue.

It is proved that the minimum time of 36 sec of the endodontic procedure of deep dentin disinfection, excluding the excess of a critical temperature of 47 C in periodontium, provides only a protocol using a laser device with a simultaneous generation at a wavelength of 2780 nm (Er, Cr: YSGG laser) and 980 nm (diode laser).

## Small fields and non-equilibrium condition for 6 and 18 MV photon beam dosimetry

Vladimir Klimanov, Maria Kolyvanova, Janneta Galjautdinova

State Research Center – Burnasyan Federal Medical Biophysical Center of Federal Medical Biological Agency,  
Moscow, Russia

**Introduction.** The relationships between the absorbed dose (D), kerma (K) and the ionization kerma ( $K_{col}$ ) for photon radiation in different media are of fundamental importance in radiation dosimetry. The transfer of secondary electrons produced in the medium as photons interact with matter has a decisive influence on these relations. Under conditions of charged particles equilibrium (CPE), the absorbed dose and ionization kerma are equal. However, when the medium is irradiated with external beams, CPE practically does not exist. Square radiation fields with sizes from  $4 \times 4$  to  $40 \times 40$  cm<sup>2</sup> are usually used in conventional radiotherapy. For such fields, the ratio between the depth distributions of D and  $K_{col}$  for megavolt beams has a typical form. The region where the D and  $K_{col}$  curves run almost parallel to each other is called the region of dynamic equilibrium or quasi-electron equilibrium conditions (quasi- CPE). The purpose of this work was to calculate the dependence of the ratio between D, K and  $K_{col}$  on the transverse dimensions of the fields in build-up region for 6 MV and 18 MV photons beams with small circular cross sections in water.

**Material and methods.** In the work using the Monte Carlo method of EGSnrc and MCNP4C2 codes, distributions were calculated in a water phantom for beams with a radius on the phantom surface from 0.1 to 3.0 cm and for depths from 0 up to 40 cm. The build-up region was particularly studied.

**Results.** The calculation results show that the ratio of ionization kerma to kerma for both beams at depths up to 40 cm is almost constant and is equal to  $0.993 \pm 0.0005$  for 6 MV and  $0.975 \pm 0.001$  for 18 MV spectrum of photon beam. The ratio of absorbed dose to ionization kerma, in contrast to conventional square beams with an area of 20 cm<sup>2</sup>, is substantially less than 1 with a radius of beam  $\leq 1.5$  cm for 6 MV and  $\leq 2.5$  cm for 18 MV spectrum of photon beam at all considered depths in a water phantom.

**Conclusion.** The data indicate that the ratio between the absorbed dose, kerma and ionization kerma for photon fields produced by beams of small cross-sections are very different from those of traditional beams. This fact should be considered in the dosimetry of small fields.

**Keywords:** Small field dosimetry, radiation therapy, clinical dosimetry, Kerma, ionization kerma, absorbed dose

**Acknowledgments:** The reported study was funded by RFBR and CITMA according to the research project №18-52-34008

## Advantages of ytterbium sources for HDR brachytherapy

**Sergei Akulinichev<sup>1</sup>, Ivan Yakovlev<sup>1</sup>,  
Dmitry Kokoncev<sup>1</sup>, Arkadiy Yuris<sup>2</sup>, Anton Nikitenkov<sup>2</sup>**

<sup>1</sup> Institute for Nuclear Research of RAS, Moscow, Russia

<sup>2</sup> Obninsk Institute for Nuclear Power Engineering, Obninsk, Russia

Compared to other isotopes for HDR brachytherapy, the isotope Yb-169 requires a much lighter shielding. For example, the tungsten shield of only 1-2 cm makes the HDR therapeutic ytterbium source harmless for the personnel. Therefore, the source loader with ytterbium sources may be a compact and cheap desktop device. Moreover, the treatment quality may be significantly improved by means of ytterbium radiation collimation. This is particularly important for the intracavitary treatment of vaginal tumors because the neighbor critical organs, especially bladder and rectum, are very radiosensitive. We found that a layer of only 1 mm of tungsten makes it possible to sufficiently collimate the ytterbium photon emission, sparing the neighbor critical organs. We have designed a simple and cheap construction of applicators for intracavitary treatment of cancer, allowing to significantly raise the quality of brachytherapy by directing the main photon emission to a tumor. We have carried out calculations of dose distributions in tissue using different Monte-Carlo programs (Geant-4 and FOTELP) and compared the results for different isotopes and different design of sources. These results show that ytterbium sources open new perspectives for HDR brachytherapy. Earlier we have developed a new technology for manufacturing high-density ceramic cores of ytterbium oxide. Source cores made from ceramics have high mechanical characteristics and a glassy surface. The use of ceramics makes it possible to increase source activity without changing the external dimensions of the source.

## **Assessment of radiation doses to neonates from chest radiography at University Hospital Rijeka**

**Doris Segota, Ana Diklic, Maja Karic, Slaven Jurkovic**

University Hospital Rijeka, Rijeka, Croatia

Radiosensitivity of a newborn is greater than a mature child or an adult. Therefore, X-ray examinations of this population must be optimized rigorously and the doses to the patient must not be higher than needed for achieving required diagnostic information. Optimization is very important since most of those neonates will require multiple X-ray examinations during their neonatal course.

The aim of this study was to investigate and assess the radiation doses to neonates from chest radiography procedure at our institution. X-ray examinations in neonatal intensive care unit at University Hospital Rijeka are performed on a mobile X-ray machine using CR plates. Quality Control procedures are performed regularly.

Data for assessing radiation dose was collected during period of six months. Radiographic parameters such as applied potential, current-time product, film to focus distance and patient data were recorded. Diagnostic reference level was calculated in terms of Entrance Skin Air Kerma (ESAK). The number of procedures per neonate patient before leaving the intensive care unit was also investigated. Results will be presented.

## Investigation of EBT<sub>3</sub> radiochromic film behaviour in high dose range of 6 MV photon and 6 MeV electron beams by employing the most suitable scanning channel of three-color flatbed scanner

**Kerem Duruer<sup>1</sup>, Durmuş Etiz<sup>1</sup>, Haluk Yücel<sup>2</sup>**

<sup>1</sup> Eskişehir Osmangazi University, Faculty of Medicine, Department of Radiation Oncology, Ankara, Turkey

<sup>2</sup> Ankara University, Institute of Nuclear Sciences, Ankara, Turkey

Radiochromic film dosimetry has been commonly used for determination of dose measurement in radiotherapy for many years because of their high spatial resolution, low energy dependence and its approximate tissue equivalent. Additionally it has other advantages, e.g. a water resistance material and a relatively insensitive to visible light. Hence they are very useful and practical for clinical applications such as brachytherapy, electron therapy and skin dose measurements. Among them, the dynamic dose range of EBT<sub>3</sub> radiochromic films are generally recommended for the dose range of 0.1 to 20 Gy. However, in this study, it is aimed to observe the behavior of EBT<sub>3</sub> films in high dose range of up to 90 Gy under the irradiations. For this aim, the net optical outputs were obtained with increasing dose values under photon and electron beams by employing three colors scanning channels (red-green-blue). Thus, for making calibration curves, it was decided which color channel for EBT<sub>3</sub> radiochromic film would be the most suitable one in different dose ranges.

In the setup, the reference conditions were first established and dose calibration procedure was carried out in RW<sub>3</sub> phantom. Then the irradiated films were cut into 2x2.5 cm<sup>2</sup> pieces and they were grouped into 2 as irradiation and control groups. The control group wasn't irradiated. Before the irradiation, two groups of films have been scanned in flatbed scanner. After that, the irradiation group films were placed to align the exact place of effective point of ionization chamber under the reference condition. Later, they were irradiated one by one to up to 90 Gy with using 6 MV and 6 MeV beam qualities, respectively. Subsequently, both of film groups were again scanned in flatbed scanner.

Optical densities and their standard deviations corresponding to the chosen dose values were obtained from the scanned films. Thus calibration curves were plotted for all three colors channels according to two different beam conditions. The results obtained for 6 MV beam quality showed that if red color channel is selected for the dose range of 0.8 Gy-7.3 Gy, and green color channel is selected for 7.3 Gy-42 Gy, and blue color channel is selected for 42 Gy-90 Gy the percentage errors in the obtained results are minimal.

In conclusion, the percentage errors for the obtained results were evaluated for 6 MV photon and 6 MeV electron energies by using different scanning channels of EBT<sub>3</sub> radiochromic film. It has been found that measurements having low percentage error values can be achieved by using the scanning channels of their proper combinations with increasing doses for both energies. The study also shows that EBT<sub>3</sub> radiochromic films can be used at lower error values at doses higher than the recommended dose range values.

**Acknowledgments:** This work was supported by TUBITAK Project No: 118S616. This work is also a part of PhD. dissertation study of Mr. Kerem Duruer in Ankara University, Turkey.



**Medicinal  
Chemistry**

**17**

## Radiopharmaceuticals for theranostic applications

**Anife Ahmedova, Boyan Todorov**

Faculty of Chemistry and Pharmacy, Sofia University, Sofia, Bulgaria

The growing advancement in nuclear medicine challenges researchers from several different fields to integrate imaging and therapeutic modalities in a theranostic radiopharmaceutical, which can be defined as a molecular entity with readily replaceable radioisotope to provide easy switch between diagnostic and therapeutic applications for efficient and patient-friendly treatment of diseases. For such a reason, the diagnostic and therapeutic potential of all five medical radionuclides of copper have thoroughly been investigated as they boost the hope for development of successful radiotheranostics. To facilitate the mutual understanding between all different specialists working on this multidisciplinary field, we summarized the recent updates in copper-based nuclear medicine, with specific attention to the potential theranostic applications. Thereby, we focus on the current achievements in the copper-related complementary fields, such as synthetic and nuclear chemistry, biological assessment of radiopharmaceuticals, design and development of nanomaterials for multimodal theranostic implications.

This work includes: i) description of available copper radionuclide production methods; ii) analyses of the synthetic strategies for development of improved copper radiopharmaceuticals; iii) summary of reported clinical data and recent preclinical studies from the last five years on biological applicability of copper radiopharmaceuticals; and iv) illustration of some sophisticated multimodal nanotheranostic agents that comprise several imaging and therapeutic modalities. Significant advancement can be seen in the synthetic procedures, which enables the broader implication of pretargeting approaches via bioorthogonal click reactions, as well as in the nanotechnology methods for biomimetic construction of biocompatible multimodal copper theranostics. All this gives the hope that personalized treatment of various diseases can be achieved by copper theranostics in the near future.

**Acknowledgments:** Authors are grateful to NSFB (contract KP-06-N29/4) for the financial support.

## **An overview of the effect of *Hypogimnia physodes*, *Hypogimnia tubulosa*, *Umbilicaria crustulosa* and *Umbilicaria cylindrica* acetone extracts on frequencies and distribution of micronucleus in human lymphocytes**

**Miroslava Stankovic<sup>1</sup>, Igor Stojanovic<sup>2</sup>,  
Ivana Zlatanovic<sup>3</sup>, Vesna Milovanovic<sup>4</sup>, Gordana Stojanovic<sup>3</sup>**

<sup>1</sup> Nuclear Facilities of Serbia, Vinca, Serbia

<sup>2</sup> Zegin Pharmacy, Aleksinac, Serbia

<sup>3</sup> Department of Chemistry, Faculty of Science and Mathematics, University of Nis, Nis, Serbia

<sup>4</sup> Technical High School, Krusevac, Serbia

The *Hypogimnia physodes*, *Hypogimnia tubulosa*, *Umbilicaria crustulosa* and *Umbilicaria cylindrical* acetone extracts were tested for *in vitro* protective effect on chromosome aberrations in peripheral human lymphocytes using cytochalasin-B blocked MN assay at concentrations of 1.0 and 2.0  $\mu\text{g mL}^{-1}$ . At the concentration of 1.0  $\mu\text{g/mL}$  *H. physodes*, *H. tubulosa*, *U. crustulosa* and *U. cylindrical* extracts caused a decrease on the micronucleus frequency of 5.4 %, 4.2 %, 10.8% and 5.3%, respectively, comparing to the control cell cultures. Treatment of the cell cultures with acetone extract of *H. tubulosa*, *U. crustulosa* and *U. cylindrical* extracts at concentration of 2  $\mu\text{g/mL}$  showed a decrease in the frequency of MN of 4.2 %, 16.8 % and 11.0% respectively while *H. physodes* extract at concentration of 2  $\mu\text{g/mL}$  gave increases in MN frequency of 3.3 % (Stojanovic et al., 2013; Zlatanović et al. 2017; Stojanović et al., 2017).

Only *U. crustulosa* extract at concentration of 2  $\mu\text{g/mL}$  showed higher reduction of MN than amifostine (radioprotectant, previously known as WR- 2721) at concentration of 1  $\mu\text{g mL}^{-1}$  which gave a decrease in the MN frequency of 11.4% comparing to control cell cultures.

**Acknowledgments:** The authors acknowledge the Ministry of Education, Science and Technological Development of Serbia for the financial support (Grant No 172047).

## Determination of the redox potential of drugs for cardiovascular diseases

**Safija Herenda<sup>1</sup>, Edhem Hasković<sup>2</sup>, Denis Hasković<sup>3</sup>**

<sup>1</sup> Department of Chemistry, Faculty of Science, University of Sarajevo, Sarajevo, Bosnia and Herzegovina

<sup>2</sup> Department of Biology, Faculty of Science, University of Sarajevo, Sarajevo, Bosnia and Herzegovina

<sup>3</sup> Clinical Center of the University of Sarajevo, Organizational Unit Clinical Chemistry and Biochemistry, Sarajevo, Bosnia and Herzegovina

Hypertension is the most common cardiovascular disease associated with an increased incidence of stroke and coronary heart disease. Several types of antihypertensive drugs are used to control risk factors in the world. Perindoril is one of the drugs used to treat high blood pressure, heart failure or stable coronary heart disease, while Metoprolol is a cardioselective blocker of beta<sub>1</sub>-adrenergic receptors in the heart. In this paper, the electrochemical processes of selected drugs on glassy carbon electrodes (GC) were examined using the cyclic voltammetry method, with the aim of determining the redox potential of perindopril and metoprolol. With the cyclic voltammetry technique, the influence of different substrate concentrations was monitored, and the influence of different scanning rates on the look of the voltamogram was examined. Cyclic voltammetry provides basic information on redox potentials, it allows qualitative and quantitative monitoring of the redox process within the substrate itself and allows determination of surface charge concentration. Cyclic voltamograms can also provide information on charge transfer rates, charge transfer processes, and interactions between enzymatic segments in specific locations. We have come to the conclusion that with the increase in the concentration of a particular drug, there is an increase in the current in the area of reduction, that is, the obtained reduction potentials for both drugs are about 0.015 mV. It was found that the concentration of investigated drugs had a significant effect on kinetic and redox characteristics.

## ATR-FTIR spectroscopy in chlorpyrifos residue investigation

M. Cvijović<sup>1</sup>, Z. Nedić<sup>2</sup>, P. Đurđević<sup>3</sup>, V. di Marco<sup>4</sup>

<sup>1</sup> Faculty of Medicine, University of Belgrade, Belgrade, Serbia

<sup>2</sup> Faculty of Physical Chemistry, University of Belgrade, Belgrade, Serbia

<sup>3</sup> Faculty of Science, University of Kragujevac, Kragujevac, Serbia

<sup>4</sup> Dipartimento di Scienze Chimiche, University of Padova, Padova, Italy

Food of plant origin treated by pesticide formulations (emulsifiable concentrate-EC and emulsion in water-EW) based on chlorpyrifos (CPS) is investigated by infra red (IR), infra red with Fourier transform (FTIR) and attenuated total reflection-Fourier transform with infra red spectroscopy (ATR-FTIR). These techniques are used for samples with no special preparation.

CPS pesticide and its metabolites are very persistent and can be chosen after many years in the food, water, soil, body fluids as residual. Chlorpyrifos-oxon (CPO) is the most toxic metabolite of CPS to humans.

The FT-IR spectra were recorded with a resolution of 2 cm<sup>-1</sup>, 32 scans on a Thermo Nicolet 6700 FT-IR spectrometer and on an attenuated total reflection Fourier transform infrared in aim to analyze the chemical changes of the samples before and after treatment. FT-IR spectra of CPS and CPO standards have been recorded firstly. The P=O stretch vibration,  $\nu=537.12$  cm<sup>-1</sup> originated from chlorpyrifos-oxon and the P=S vibration,  $\nu=634.59$  cm<sup>-1</sup> originated from CPS, both in fingerprint area in IR spectrum. The intensities of these vibrations bands are monitored in EC and EW formulations and samples. The samples have been untreated apple, apple treated by EC formulations with different concentration calculated to chlorpyrifos, apple that are rinsed with water after EC treatment and apple that are after rinsing with water, treated by dishtowel. These samples are prepared as dry skin and were recorded by an attenuated total reflection Fourier transform infrared spectrometer (ATR-FTIR) in order to see how change CPS and CPO characteristic vibration.

The samples treated by dishtowel show still noticeable P=S vibration,  $\nu=634.59$  cm<sup>-1</sup> from CPS, that indicated decrease of pesticide amount 10 times in comparison to band intensity in sample treated by EC formulations with same concentration. In this case not all CPS was removed from the apple skin, maybe because of concentration overdose.

ATR-FTIR spectra, consists of four wavenumber intervals: (3100-3400) cm<sup>-1</sup> typical for water, (2700-3600) cm<sup>-1</sup> typical for compound with carbonyl group, (2100-2700) cm<sup>-1</sup>, area without significant compound and (450-1700) cm<sup>-1</sup> characteristic for esters.

In further investigations, data from ATR FTIR spectra should be used as base for mathematical calculations by genic algorithms and artificial neural network for quantitative pesticide determination.

## Complex formation in a low toxic organic solvent-based liquid-liquid extraction-chromogenic system for vanadium(V), nickel(II) and copper(II)

**Galya K. Toncheva<sup>1</sup>, Nikolina P. Milcheva<sup>2</sup>,  
Siana K. Chobanova<sup>1</sup>, Mariela G. Kalendarska<sup>1</sup>, Kiril B. Gavazov<sup>2</sup>**

<sup>1</sup> Faculty of Chemistry, Department of General and Inorganic Chemistry with Methodology of Chemical Education, University of Plovdiv "Paissii Hilendarski", Plovdiv, Bulgaria

<sup>2</sup> Faculty of Pharmacy, Department of Chemical Sciences, Medical University of Plovdiv, Plovdiv, Bulgaria

Liquid-liquid extraction-chromogenic systems for vanadium(V), nickel(II) and copper(II) containing azo dye {4-(2-thiazolylazo)orcinol, TAO}, quaternary ammonium salt (Aliquat 336) and low-toxic organic solvent (isobutanol) were studied. The optimum conditions for extraction of the mentioned metal ions were found. The following extraction and spectrophotometric characteristics were determined: absorption maxima, molar absorptivities, Sandell's sensitivities, constants of extraction, constants of distribution, fractions extracted, and Beer's law limits. The stoichiometry of the extracted binary and ternary complexes was established by different methods.

**Acknowledgments:** This work was supported by the Plovdiv University Scientific Fund (grant No SP19-009).



**Microwave  
Laser  
RF  
UV  
and  
Solar  
radiations**

**18**

## **Reproductive system of male rats at the post-natal stage of development under the influence of electromagnetic radiation from a mobile phone (1745 MHz)**

**Natalya Chueshova<sup>1</sup>, Frantishek Vismont<sup>2</sup>, Igor Cheshik<sup>1</sup>**

<sup>1</sup> Institute of Radiobiology of National Academy of Sciences of Belarus, Gomel, Belarus

<sup>2</sup> Belarusian State Medical University, Minsk, Belarus

A complex assessment of morphofunctional changes in the reproductive system of male rats has been carried out, beginning with the period of its formation and development (50-52 days) and reaching the age of sexual maturity (4.5 months), under low-intensity electromagnetic radiation from a mobile phone (EMR MP, 1745 MHz, daily, 8 hours/day by fractions of 30 minutes with an interval of 5 minutes, power density  $0.2-20 \mu\text{W}/\text{cm}^2$ ,  $= 7.5 \pm 0.34 \mu\text{W}/\text{cm}^2$ ).

The evaluation of the reproductive system was carried out on the 1st and 30th days after cessation of the effects during 1, 7, 30, 60 and 90 days. The mass of organs of the reproductive system (testes, epididymis, seminal vesicles) was estimated, the number of spermatogenic cells at different stages of differentiation (cycle of spermatogenesis), and the total number and viability of epididymal spermatozoa. Serum testosterone concentration was measured.

The character of the revealed morphofunctional changes in the reproductive system of male rats under conditions of low-intensity EMR from MP is largely dependent on the duration of exposure and the age of the animals.

The impact of EMR from MP on the body of male rats during puberty leads to morphofunctional changes in the developing reproductive system, characterized by an increase in the mass of epididymis and seminal vesicles. The development of degenerative changes in testes is revealed, which manifests itself in oppression of proliferative activity and in the activation of differentiation of cells of spermatogenic epithelium – spermatids, accompanied by a significant increase in the number of epididymal spermatozoa (early puberty) with a decrease in their viability on the background of a drop in testosterone concentration in the blood serum.

Long-term (during the 60<sup>th</sup> and 90<sup>th</sup> days) the effect of EMR from MP on the body of male rats is characterized by a weakly expressed reaction of the spermatogenic epithelium. The most characteristic disorders with prolonged influence of EMR from MP are manifested in a decrease in the number and viability of spermatozoa, as well as in increasing the concentration of testosterone in the blood serum.

Thus, the character of morphofunctional changes in the reproductive system of male rats testifies to the inhibition of the generative function under conditions of low-intensity EM from MP.

## Mechanistic aspects of GO sandwich formation due to UV radiation

Marek Wiśniewski<sup>1</sup>, Paulina Bolibok<sup>1</sup>,  
Monika Bał<sup>1</sup>, Wojciech Zięba<sup>1</sup>, Katarzyna Roszek<sup>2</sup>

<sup>1</sup> Faculty of Chemistry, Physicochemistry of Carbon Materials Research Group, Nicolaus Copernicus University in Toruń, Toruń, Poland

<sup>2</sup> Department of Biochemistry, Faculty of Biology and Environmental Protection, Nicolaus Copernicus University in Toruń, Toruń, Poland

A novel conductive carbon paper based on reduced graphene oxide (RGO) with a sandwich structure was successfully prepared through step-by-step UV-induced reduction process in which an inner – oxidized layer – is sandwiched between two thin RGO layers. This unique design strategy not only provides a highly conductive network for its surface but also maintains the structural integrity of the composite. The sandwich-structured paper exhibits a significant conductive anisotropy. The high electrical conductivity is equivalent to the most of the graphene composite papers obtained by the conventional processes. However, compared with the similar layer-by-layer assembly technique, the present method is more feasible and time saving. Moreover, the sandwich structured paper shows excellent mechanical strength and good flexibility, which may facilitate its applications in future flexible electronics.

In order to look closer into the observed phenomena, the Raman and FT-IR spectroscopy (in transmission as well as in drift modes) was applied to monitor possible changes in the surface and bulk chemistry. The analysis of the carbon fingerprint region of 1700–1000 1/cm gives unique information on the UVB radiation influence on the GO structure.

Interestingly, the results from Raman measurements are ambiguous. From the  $I_D/I_G$  ratio analysis (ca. 1.14) one can conclude that there were almost no changes in the sample as the ratio remains at the same level. However, the quantitative analysis show that both G and D bands increase equally in intensity and this could be misleading and misinterpreted as the UVB-exposure causes both oxidation and C=C network formation.

The similar conclusions may be drawn from FTIR results. The spectral changes, during small doses ( $0.1 \text{ W}\cdot\text{cm}^{-2}$ ) UVB radiation, revealed clearly that GO undergoes oxidation. The increase in the radiation time causes the rise in the concentration of  $\cdot\text{OH}$  radicals, on the GO surface. Due to presence of such strong oxidizing agent, the characteristic bands of C=O, and other surface oxygen-containing functionalities increase in the intensity. On the other hand the appearance of the band, with a maximum near 1600  $\sim 1/\text{cm}$ , usually attributed to C=C stretching vibration, was also observed, means that the carbon surface undergoes reduction process. The observed spectral changes coincide perfectly with the Raman results, and mean that the tested material surface rebuilds the  $\text{sp}^2$  network and parallelly has been oxidized.

**Acknowledgments:** This work was supported by the Polish National Science Centre (NCN) grant PRELUDIUM 14 no. 2017/27/N/ST5/o2696.

## **Exposure and risk assessment connected to the health and safety of workers in the production of electricity**

**Michel Israel<sup>1</sup>, Petya Ivanova<sup>2</sup>,  
Tsvetelina Shalamanova<sup>2</sup>, Mihaela Ivanova<sup>2</sup>, Victoria Zaryabova<sup>2</sup>**

<sup>1</sup> Medical University Pleven, National Center of Public Health and Analyses, Sofia, Sofia, Bulgaria

<sup>2</sup> National Centre of Public Health and Analyses, Sofia, Bulgaria

The aim of the study is to perform exposure and risk assessment of electromagnetic fields (EMF) at workplaces connected with electricity production according to the requirements of Directive 2013/35/ EU. The study covers the following sets of workplaces:

- Workplaces in power distribution systems (indoor and outdoor distribution systems);
- Workplaces with metalworking machines: lathes, mills, electric welding.

Measurements are made using a frequency non-selective method, based on: “Non-binding guide to good practice for implementing Directive 2013/35/EU Electromagnetic Fields Vol. 1 – Practical guide”.

Exposure and risk assessment have been performed by comparing the measured values with action values (ALs) and the exposure limit values (ELVs) according to the requirements of Directive 2013/35/EU, as well as with the reference values adopted by the Council Recommendation 1999/519/EC for persons at “specific risk”.

The results of the exposure and risk assessment show the following:

Electric field strength for the power frequency field (50 Hz) does not exceed the high ALs for non-thermal effects; low ALs are not exceeded except for single points in outdoor high voltage substations. In cases where the low ALs for non-thermal effects are exceeded, the reference levels according to Recommendation 1999/519 / EC are exceeded as well.

There are not measured values of the field strength above the reference levels according to Council Recommendation 1999/519/EC at the remaining workplaces.

The results show compliance with the ELVs with respect to the health and sensory effects.

Magnetic flux density values of power frequency fields’ do not exceed the ALs for non-thermal effects. Measured values show also compliance with the ELVs for health and sensory effects. The magnetic flux densities do not exceed the reference levels according to Council Recommendation 1999/519/EC.

From the results obtained, it can be concluded that no risk can be expected for the workers’ health from the EMFs exposure except for those defined as persons at a specific risk. For persons at a specific risk, appropriate recommendations for the employer have been proposed for health and safety practices at work.

## Public concern of electromagnetic exposure in Bulgaria – A case study of overexposure

**Victoria Zaryabova<sup>1</sup>, Tsvetelina Shalamanova<sup>1</sup>,  
Michel Israel<sup>2</sup>, Hristina Petkova<sup>1</sup>**

<sup>1</sup> National Center of Public Health and Analyses, Sofia, Bulgaria

<sup>2</sup> Medical University-Pleven, National Center of Public Health and Analyses, Sofia, Bulgaria

Risk management in the precautionary framework proposed by the World Health Organization (WHO) concerning public health is an interactive process and it encourages the development of new information and understanding, as well as a review of the measures in the context of existing uncertainty. By including a wide range of stakeholders in the process, the framework requires clarification of their interests, as well as transparency about the way of taking decisions. The framework related to the protection of human beings against electromagnetic fields (EMF) exposures is an upgrading approach that encompasses procedures for managing human health risks that are either unknown or insecure. The framework assists for:

- Development and evaluation of the opportunities to reduce the electromagnetic exposure;
- Choice of action/actions appropriate to the risk under consideration;
- Assessment and supervision of the chosen action/actions.

The WHO proposes the “Precautionary Principle/Approach” to be applied for cases when uncertainty of research is great, and when there are serious problems with the implementation of new technologies for which there is insufficient information on their harmful effects.

At the same time, the WHO suggests communication strategies to be applied after analyses and evaluation of the exposure to reduce the public concern (EMF Risk Perception... WHO 1998, Risk Perception...ICNIRP 1997, Establishing a Dialogue...WHO 2002).

Here, we would like to present a case study of public concern in connection with EMF exposure from base station for mobile communication situated in urban area, and the way of solving the problem. Different approaches for exposure assessment have been applied, as follows:

- measuring methods: point measurements; monitoring measurements over a long period of time (monitoring for more than 24 hours); spectrum analyses
- analytical methods: exposure assessment through processing data of measurements; and/or evaluation of the safety zones around “sensitive” buildings by calculation/modeling.

A communication strategy with the general population has been chosen and applied on the basis of the analyses of the results of evaluation of the exposure. This communication strategy is specific and effective, and it refers to all stakeholders, including administration, mobile operators, local authorities, regional control bodies of the Ministry of Health, and others.

The main purpose of this paper is connected to the methodology of the processes presenting our model for effective solving a problem of public concern connected with EMF exposure.

## Measurement, exposure and risk assessment of sources of optical radiation in working environment

Mihaela Ivanova<sup>1</sup>, Michel Israel<sup>1,2</sup>, Mariyana Stoynovska<sup>2</sup>

<sup>1</sup> National Center of Public Health and Analyses, Sofia, Bulgaria

<sup>2</sup> Medical University–Pleven, Pleven, Bulgaria

The report presents results of measurement, exposure and risk assessment of optical radiation sources in an industrial unit: electric welding, oxygene and plasma cutting machines.

Measurements of the optical radiation parameters are performed over the entire optical range within the scope of Directive 2006/25/EC (transposed in Bulgarian legislation with Ordinance No 5 /2010). They are made at the level of the exposed eyes and skin of workers having activities or stay in the source area.

The studied sources emit mainly in the ultraviolet (UV) and visible range of the optical spectrum, therefore the applicable exposure limit values (ELVs) correspond to the two ranges.

Although the highest exposure to optical radiation is to the workers who directly handle the source, the exposure and risk assessment refers more to other workers indirectly involved in the activities with sources of optical radiation. The reason is that first group of directly exposed workers is protected by personal protective equipment (PPE) so the radiation does not reach them up to the maximal radiation levels.

The exposure assessment results show an exceeding of the ELVs for the visible and UV range in the vicinity of the electric welding and plasma cutting machine and ELVs for the visible range for the oxygene.

The risk assessment for workers has taken into account that the risk of exposure of the eye to visible light is high, but exposure to visible radiation is unlikely to occur due to the aversion to bright light and involuntary turning the head away from the source.

This is not the case with exposure to UV radiation, which is invisible to the eye and no natural mechanisms for protection. So, high levels of exposure and risk to the cornea and the lens of the eye are possible.

This means that the risk of exposure to visible optical radiation is high, but the probability of exposure is medium to low. In the ultraviolet range the risk and the likelihood of exposure is high. There is a health risk to persons who are particularly sensitive to exposure to optical radiation as well.

In addition, effects on the health and safety of workers are possible as a result of the interaction between optical radiation and photosensitising substances at the workplace or medications and/or food.

## A rapid and efficient microwave method to prepare graphene foam

**Jelena Jovanovic, Borivoj Adnadjevic**

University of Belgrade, Faculty of Physical Chemistry, Belgrade, Serbia

Graphene is two-dimensional monolayer carbon sheet, has shown great potential for application in various technological fields (hydrogen storage, molecular sensors, artificial muscle actuators, lithium ion batteries, reinforcing fillers) due to its high surface area, high thermal conductivity and excellent mechanical strength (1). The various methods are reported for graphene preparation: micromechanical exfoliation of graphite (2), chemical vapor deposition(3) and chemical reduction of graphene oxide (4).

In this work, a novel, rapid and eco-friendly method for graphene synthesizing is presented. The method is based on the ability of graphite to selectively absorb microwave irradiation and adequate selection of reactants (hydrogen peroxide ( $H_2O_2$ ) and ammonium-persulfate (APS). This enables simultaneous reactions:  $H_2O_2$  decomposition which is intercalated into the inter-layer graphite, rapid expansion of graphite layers and oxygen removal.

In this work the effects of : a) composition of reaction mixture (hydrodynamically cavitation activated graphite,  $H_2O_2$ , APS); b) inlet power of microwave irradiation and c) duration of action of microwave field were investigated on: the degree of conversion of graphite into graphene, the degree of expansion of the obtained products and absorption properties of the products against the diesel oil.

The degree of conversion of graphite into graphene (DCG) was determined by using the XRD and Raman spectroscopy methods. The degree of expansion (DE) was determined by comparison the volume of the obtained product against the volume of initially used graphite. The specific absorption capacity (SAC) of the obtained graphene was determined by gravimetric method.

Based on the obtained results it was concluded the following: a) by applying the novel method it is possible to synthesize graphene from graphite in short time (60 s), with following characteristic: DSG > 95% and SAC > 350 g/g; b) the optimal conditions for graphene obtaining are: the reaction mixture content (65% graphite; 32%  $H_2O_2$ ; 3% APS); P=650W and t=70 s; c) under the MWI power lower than  $P \leq 400W$  and time lower than  $t \leq 5$  s there is no conversion of graphite into graphene; d) the increase in the power of MW field leads to the decrease in the duration of the process.

### References

1. K.S. Novoselov, A.K. Geim, S.V. Morozov, D. Jiang, Y. Zhang, S.V. Dubonos, I.V. Crigorieva, A.A. Firsov, *Science* 306 (2004) 666.
2. M.D. Stoller, S.J. Park, Y.W. Zhu, J.H. An, R.S. Ruoff, *Nano Lett.* 8 (2008) 3498.
3. A. Reina, X.T. Jia, J. Ho, D. Nezich, H.B. Son, V. Bulovic, M.S. Dresselhaus, J. Kong, *Nano Lett.* 9 (2009) 30.
4. S. Park, R.S. Ruoff, *Nat. Nanotechnol.* 4 (2009) 217.

## Novel microwave assisted synthesis of fullerene

**Borivoj Adnadjevic, Jelena Jovanovic**

University of Belgrade, Faculty of Physical Chemistry, Belgrade, Serbia

Fullerene (C<sub>60</sub>) presents a specific allotropic form of carbon. Fullerene has spherical shape and consists of 60 carbon atoms arranged in stable structure where its 32 faces include 12 pentagons and 20 hexagons (1). Due to its extraordinary physico-chemical properties, fullerene found wide range of applications and it is the subject of numerous investigations (2).

In the literature are described several procedures for C<sub>60</sub> synthesis: graphite vaporization (3) at low pressure and sooting flame of benzene and acetylene at controlled pressure and temperature (4) and arching between graphite rods in helium atmosphere (5).

In this investigation is presented a novel, fast and inexpensive method for C<sub>60</sub> synthesis by applying hydrodynamic cavitation to activate graphite (HDC) and using microwave irradiation. The method is based on the ability of cavitation bubbles to destroy graphite layers and on the high selectivity of that activated graphite to absorb microwave irradiation and rapidly heat the obtained material until high temperatures. In this work is investigated the influence of: a) duration of HDC activation of graphite (1-5 min), b) power of the microwave field within range of P=150-300 W and c) duration of irradiation within range from t= 1-10 min on the degree of graphite conversion into C<sub>60</sub> (SC) and solubility of the obtained product in toluene. The SC was determined by XRD method and for the product solubility in toluene gravimetric method was used.

Based on the obtained results it was concluded that: a) by applying the suggested method it is obtain C<sub>60</sub> with SC >95%, fully soluble in toluene, under the microwave field power of 300W in very short time (3 min), b) activated graphite can be converted into C<sub>60</sub> under the power of microwave field higher than 220W, c) SC increase with the increase in the duration of irradiation, d) the content of C<sub>70</sub> increase with the increase in the power of microwave field and the duration of irradiation.

### References

1. Schein, S. and Friedrich, T. A geometric constraint, the head-to-tail exclusion rule, may be the basis for the isolated-pentagon rule in fullerenes with more than 60 vertices. *PNAS* 2008, 105: 19142-19147.
2. Mateo-Alonso A., Tagmatarchis N., Prato M., Fullerenes and Their Derivatives in: Carbon nanomaterials (Yury Gogotsi, editor), Taylor and Francis Group, 2006, 1.
3. Kroto, H. W., Heath, J. R., O'Brien, S. C., Curl, R. F. and Smalley, R. E. (1985) C<sub>60</sub>: Buckminsterfullerene. *Nature*, 318: 162-164.
4. Mckinnon, J. T. and William, L. B. (1992) Combustion synthesis of fullerenes. *Combustion and Flame*, 88: 102-112.
5. Haufler, R. E., Chai, Y., Chibante, L. P. F., Conceicao, J., Jin, C., Wang, L. S., Maruyama, S., and Smalley, R. E. (1991) Carbon arc generation of C<sub>60</sub>. *Mat. Res. Soc. Symp. Proc.*, 206: 627-637

## Smart composites with embedded magnetic microwire inclusions allowing non-contact stresses and temperature monitoring

**Paula Corte-Leon<sup>1</sup>, Aleksandra Allue<sup>2</sup>, Koldo Gondra<sup>2</sup>,  
Valentina Zhukova<sup>1</sup>, Mihail Ipatov<sup>1</sup>, Juan Maria Blanco<sup>3</sup>, Arkady Zhukov<sup>1</sup>**

<sup>1</sup> Dpto. Fisica de Materiales, Univ. Basque Country, San Sebastian, Spain

<sup>2</sup> Gaiker Technological Centre, Zamudio, Spain

<sup>3</sup> Dpto. Fisica Aplicada, EUITI; Univ. Basque Country, San Sebastian, Spain

Amorphous magnetic wires can present excellent magnetic properties (e.g. high magnetic permeability, giant magnetoimpedance, GMI, effect and fast domain wall dynamics) and good mechanical properties (plasticity, flexibility) are suitable for many technological applications, such as magnetic sensors, magnetic memories and logics, transformers, etc [1]. The thinnest amorphous microwires with metallic nucleus diameters of 0.5-40  $\mu\text{m}$  coated by a thin insulating and flexible glass-coating can be prepared using the Taylor-Ulitovsky method [2]. Thin and flexible glass-coating provides new functionalities such as improved mechanical and corrosive properties, adherence with polymeric matrices and biocompatibility [2]. These mentioned features of glass-coated microwires are beneficial for a number of emerging applications opening new opportunities for development of novel applications, such as non-destructive stresses monitoring, biomedical applications, magnetoelastic sensors and smart composites with tunable magnetic permittivity [3].

A novel sensing technique for non-destructive and non-contact monitoring of the composites utilizing ferromagnetic glass-coated microwire inclusions with magnetic properties sensitive to tensile stress and temperature is proposed. We provide in-situ studies of the evolution of transmission and reflection parameters of the composites with microwire inclusions during the composites matrix polymerization. Using the free space technique we observed considerable variation of the reflection in the range of 4-7 GHz and transmission upon the matrix polymerization. Observed dependencies are discussed considering variation of temperature and stresses during the thermoset matrix polymerization and their influence on magnetic properties of glass-coated microwires.

### References

- [1] K. Mohri, T. Uchiyama, L. P. Shen, C. M. Cai, L. V. Panina, Amorphous wire and CMOS IC-based sensitive micro-magnetic sensors (MI sensor and SI sensor) for intelligent measurements and controls, *J. Magn. Magn. Mater.*, 249 (2001) pp. 351-356.
- [2] A. Zhukov, M. Ipatov, M. Churyukanova, A. Talaat, J. M. Blanco and V. Zhukova, Trends in optimization of giant magnetoimpedance effect in amorphous and nanocrystalline materials, *J. Alloys Compd.*, 727 (2017) pp. 887-901.
- [3] A. Talaat, J. Alonso, V. Zhukova, E. Garaio, J. A. García, H. Srikanth, M. H. Phan and A. Zhukov, Ferromagnetic glass-coated microwires with good heating properties for magnetic hyperthermia, *Sci. Reports*, 6 (2016) 39300.

## Giant magnetoimpedance effect at GHz frequencies in amorphous microwires

Arcady Zhukov<sup>1</sup>, Mihail Ipatov<sup>1</sup>,  
Paula Corte-Leon<sup>1</sup>, Juan Maria Blanco<sup>2</sup>, Valentina Zhukova<sup>1</sup>

1 Dpto. Fisica de Materiales, Univ. Basque Country, San Sebastian, Spain

2 Dpto. Fisica Aplicada, EUPDS Basque Country University, San Sebastian, Spain

Studies of Giant Magnetoimpedance (GMI) effect in different kind of magnetic materials have attracted considerable attention from the point of view of various technological applications as well as from the point of view of basic research [1,2]. One of the main tasks in this field is the achievement of the highest GMI effect that will allow improvement of the sensitivity of the magnetic sensors and devices utilizing GMI effect. Moreover one of the main advantages of the magnetic sensors utilizing GMI effect is a small size. In particularly small size and high magnetic field resolution are the features of magnetic field sensors made from thin magnetically soft microwires that have been proposed for magnetic compass applications in Cell phones [2]. Additionally, high frequency GMI effect is suitable for development of smart composites with tunable magnetic permittivity [3].

Accordingly, development of thin magnetically soft wires is a key for GMI applications. It must be underlined that the diameter reduction must be associated with the increasing of the resonance frequency and therefore in increasing of the optimal GMI frequency range: a tradeoff between dimension and frequency is required in order to obtain a maximum effect [4]. Consequently development of thin soft magnetic materials required for miniaturization of the sensors and devices requires an extension of the frequency range for the impedance toward the higher frequencies (GHz range).

Accordingly, the purpose of this paper is to study the GMI effect in thin amorphous magnetically soft microwires extending the frequency range up to GHz band. Studies of magnetic properties and GMI effect of amorphous Co-Fe rich microwires reveals that they present GMI effect at GHz frequencies. Magnetic field dependences of GMI effect are affected by the microwires composition and geometry. We discussed observed experimental dependences considering both different magnetic structure and the anisotropy in the bulk and near the surface and close analogy between giant magnetoimpedance and ferromagnetic resonance. Features of high frequency GMI effect can be described using FMR-like approximation.

### References

- [1] T. Uchiyama, K. Mohri, and Sh. Nakayama, Measurement of Spontaneous Oscillatory Magnetic Field of Guinea-Pig Smooth Muscle Preparation Using Pico-Tesla Resolution Amorphous Wire Magneto-Impedance Sensor, *IEEE Trans. Magn.*, 47, No 10 (2011) pp. 3070-3073
- [2] A. Zhukov, M. Ipatov, M. Churyukanova, A. Talaat, J. M. Blanco and V. Zhukova, Trends in optimization of giant magnetoimpedance effect in amorphous and nanocrystalline materials, *J. Alloys Compd.*, 727 (2017) pp. 887-901.
- [3] F.Qin, H.-X. Peng, Ferromagnetic microwires enabled multifunctional composite materials, *Progress in Materials Science* 58 (2013) 183–259
- [4] D. Ménard, M. Britel, P. Ciureanu and A. Yelon, "Giant magnetoimpedance in a cylindrical conductor," *J. Appl. Phys.* 84, (1998) pp. 2805–2814.

## Complete analysis of Vivaldi antennas

**Nurhan Türker Tokan<sup>1</sup>, Sultan Aldirmaz Çolak<sup>2</sup>, Muhammet Donmez<sup>1</sup>**

<sup>1</sup> Yıldız Technical University, İstanbul, Turkey

<sup>2</sup> Kocaeli University, Kocaeli, Turkey

In ultra-wideband applications, mostly the performance of the antenna is investigated in terms of the frequency domain parameters such as gain, group delay. These parameters are not sufficient to prove the performance of the antenna. Besides frequency domain analysis, a time domain analysis is required to characterize the transient behavior of UWB antennas for pulsed operations. Vivaldi antennas are widely used in UWB applications, especially in radar and microwave imaging applications. In recent works, gain of Vivaldi antennas are enhanced by adding corrugation on the edge of exponential flaring and/or grating elements on the slot area. In these works, the frequency domain parameters are demonstrated but pulse preserving capabilities of these modified structures are not investigated.

With this contribution, analysis of the two different kinds of Vivaldi antennas is performed in time domain and their time domain characteristics are compared with that of standard Vivaldi antenna. Vivaldi antenna, Vivaldi antenna with corrugation and Vivaldi antenna with corrugation and strips operating in the 3.1–10.6 GHz ISM band is designed using Rogers RT/Duroid 5870 substrate with 0.51 mm dielectric thickness. The dielectric constant of the dielectric material is 2.33. Chemical etching technique with photolithography is employed for the manufacturing. Standard Fourier transform relationship is used to recover time domain waveforms from  $S_{21}$  measurements. Pulse width extension and fidelity factor parameters for the time domain signal are derived. These parameters are quantified by comparing standard deviations of three Vivaldi antennas to that of the ideal delayed signal. The results proved even better pulse preserving capability of modified Vivaldi corrugation and strips.

## Perforated narrow-band dielectric lens antenna design

**Fikret Tokan, Mücahit Alçep**

Yıldız Technical University, İstanbul, Turkey

Dielectric lens antennas fabricated with a dense dielectric material, allow good power transfer efficiency through the lens and enable fabrication of low-cost and compact-size lens antennas. Dielectric lens antennas are inexpensive solutions for beam steering applications with their capability of being integrated to millimeter and sub-millimeter planar feeding structures. Low-permittivity (dielectric constant  $< 3$ ), low-loss materials are affordable solutions for dielectric lenses, which can be easily manufactured with standard tools.

Typically, when the relative permittivity of the selected lens material is higher than three, considerable amount of internal reflections occur at the dielectric-air interface. The amount of internal reflections due to the dielectric contrast with free space, increase dramatically with the increment of dielectric constant.

These internal reflections deteriorate not only return loss but also the radiation characteristics of the antenna. Most common way of reducing the internal reflections is using matching layers made of homogeneous dielectric materials on the lens surface.

In this paper, a low-cost alternative method, creating perforated structure on the top of the lens in order to obtain equivalent relative permittivity value is applied to a narrow band dielectric lens antenna. The results emphasize that perforated lens structure has similar return loss value and radiation characteristics with the lens antenna having matching layers.

**Acknowledgments:** This work was supported by Research Fund of the Yildiz Technical University. Project Number: FBA-2017-3070.

## **Method and mean of IC's testing under multiple electrical overstresses**

**Petr Skorobogatov, Konstantin Epifantsev,  
Alexander Shemohaev, Vitalij Telets**

Moscow Engineering Physical Institute, Moscow, Russia

Sources of interference for on-board electronics of supersonic aircrafts are electrostatic discharges. The surface differential charging the reversible and irreversible failures of onboard electronic equipment may be in the result. Such a strong impact of discharges on the operation of on-board electronics is due to both the parameters of discharge pulses (the rate of increase of the discharge current reaches at  $10^{10}$  A/s) and the increased sensitivity of electronics to such influences.

Exposure to repetitive electrical overstresses may be more dangerous for solid-state electronics than exposure to a single voltage pulse of a very high level. Indeed, an electronic device with a high level of resistance to electrical overstress (EOS) pulses may be unreliable if it has some probability of failure under repeated stresses with a lower voltage electrostatic discharge. This indicates that repetitive stress is an important problem of reliability in special applications.

The EOS pulses have values from volts to kilovolts amplitude and from tens of nanosecond to several of microsecond in duration. The purpose of the work was to develop and produce a new generator of EOS pulses with extended characteristics and increased technical and monitoring capabilities. The goals and the purposes of the generator creation with the declared parameters are specified. This article shows the main methods and ways of obtaining ultra-short high voltage pulses. The problems encountered by the developer when creating the equipment and the ways of solving are shown.

The generator was used for the influence of a pulse train with an energy lower than the threshold failure, which leads to the accumulation of damage effect inside the components (additive effect). Consequently, a failure occurs during the influence of the pulse with an energy lower than the threshold. The paper analyses the existing experimental results on revealing the additive effect. The influence of a voltage pulse train of subthreshold energies, which were affected on different semiconductor devices including IC's are given. The obtained experimental results prove the presence of the additive effect in IC's which were influenced by the voltage pulse sequence of subthreshold energies and make it possible to derive a dependence describing the character of the accumulation of damage effect in the devices under test. The derived dependence correlates well with the Arrhenius equation. It is the evidence that the failure in IC's under the influence of a voltage pulse of subthreshold energies has thermal behavior.

Based on this dependence, it is suggested a method of testing procedure of IC's electronic components to the influence of the voltage pulse sequences.

## Comparison of ground-based and OMI satellite UVI measurements in Novi Sad

**Zorica Podrascanin<sup>1</sup>, Zoran Mijatovic<sup>1</sup>, Ana Firanj Sremac<sup>2</sup>**

<sup>1</sup> Faculty of Sciences, University of Novi Sad, Novi Sad, Serbia

<sup>2</sup> Faculty of Agriculture, University of Novi Sad, Novi Sad, Serbia

The satellite measurements offer nearly global coverage of erythemal dose rate or the UV index (UVI) on daily basis. Those measurements are very important since those are the only measurements in some regions. However, the spatial and temporal variability of surface UV irradiance is very high and ground-based measurements are very important for better understanding of UVI effects on human health. In this paper we compared the satellite measurements with the ground-based measurements of UVI in Novi Sad. For that purpose we used Level-3 daily global gridded Aura-OMI Spectral Surface erythemal dose rates. Those erythemal dose rates cover the globe at 1.0x1.0 deg grids at local solar noon from November 2004 until now. The ground-based measurements were measured by a Yankee Environmental Systems (YES) UVB-1 pyranometer since 2003. Ground-based UVI values in Novi Sad were compared with the satellite data using statistic measures such as correlation coefficient, root mean square error and bias.

## Transient optical effects in spin-coated chalcogenide glass thin films induced by UV radiation

**Andriy Kovalskiy<sup>1</sup>, Maria White<sup>1</sup>, Joshua Allen<sup>1</sup>, Justin Oelgoetz<sup>1</sup>, Roman Golovchak<sup>1</sup>, Oleh Shpotyuk<sup>2</sup>, Karel Palka<sup>3</sup>, Stanislav Slang<sup>3</sup>, Miroslav Vlcek<sup>3</sup>**

<sup>1</sup> Austin Peay State University, Clarksville, United States

<sup>2</sup> Jan Długosz University, Częstochowa, Poland

<sup>3</sup> University of Pardubice - CEMNAT, Pardubice, Czech Republic

Thermally evaporated thin films of chalcogenide glasses are known to be highly photosensitive to bandgap and super-bandgap radiation. However, their practical application is limited because of long-term structural relaxation accompanied the photoinduced changes. Spin-coating is one of the alternative methods of thin film preparation which mostly eliminates photosensitivity to bandgap radiation and removes metastable component of photoinduced changes caused by super-band gap (mostly UV) light. Such films are usually manufactured through chemical dissolution of bulk glasses in different amine-based solvents with subsequent spin-coating of the liquid onto silica substrate and appropriate one-stage or multi-stage thermal treatment. Such photostability can be very useful, especially for the nonlinear optical applications, which require high transparency in IR spectral region and minimum sensitivity to the high energy light radiation.

Structure of thermally stabilized spin-coated films can, in general, be considered as consisting of fragments of bulk glass connected through the residual units of organic solvents. However, increase of annealing temperature promotes direct connections between the glass fragments (through chalcogen atom or newly formed appropriate structural units). The decrease in photosensitivity relatively to the evaporated thin films is linked to the lack of excessive concentration of homopolar bonds in the film structure. At the same time, noticeable transient red shift of optical absorption edge (photodarkening) is still observed at irradiation of the spin-coated thin films with super-bandgap UV light. It is shown that by changing post-synthesis annealing conditions it is possible to control the transient optical switching effect.

Kinetics of the transient photoinduced optical changes demonstrates significant deviation from the exponential behavior. Mechanisms of the transient effects are debated based on parameters of fitting of the kinetic curves with stretched exponential function. Possible applications of the observed effects are discussed.

**Acknowledgments:** APSU team acknowledges financial support from NSF grant DMR-1409160.

## **DNA-damage induced in human lymphocytes by exposure to 915 MHz mobile-phone radiation: Does smoking habit modulate its genotoxicity?**

**B. Gustavino<sup>1</sup>, V. Maselli<sup>1</sup>, L. Salvi<sup>1</sup>,  
G. Paoluzzi<sup>2</sup>, E. Santovetti<sup>3</sup>, S. Filippi<sup>4</sup>, R. Meschini<sup>4</sup>**

<sup>1</sup> Department of Biology, University of Tor Vergata, Rome, Italy

<sup>2</sup> INFN-Rome, Tor Vergata, Rome, Italy

<sup>3</sup> Department of Physics, University of Tor Vergata, Rome, Italy

<sup>4</sup> Department of Ecological and Biological Science, Tuscia University, Viterbo, Italy

Mobile and wireless technologies are the main source of exposure to radiofrequency (RF) electromagnetic fields (EMF), which have demonstrated to cause crucial changes and deleterious effects in biological systems even under non-thermal conditions. Growing supportive evidence of increased risk for head and brain tumors associated with the use of mobile and cordless phones emerge from epidemiological studies.

While the majority of studies in plants and invertebrates have proven the induction of oxidative stress, DNA-damage and mutations, results from mammalian cells still appear to be controversial. In particular, experimental exposure of human lymphocytes to mobile-phone RF seems to demonstrate absence of genotoxic effects or ambiguous results.

In our work the genotoxic and mutagenic potential of 915 MHz mobile-phone radiations were studied in human lymphocytes from 12 healthy donors aged 22 to 30 years, equally divided by sex and smoking habits. A total of 10 hours exposure was administered to blood sample cultures using a Transverse Electromagnetic (TEM) cell in non-thermal conditions (SAR <2W/Kg). The effects of continuous (C-RF) and fractionate (F-RF) exposures were tested, the latter consisting of four 2.5h exposure cycles with a 10-minute interval. X-rays (3Gy) were used as positive control. The alkaline Comet assay and the CBMN test were used to estimate the induction of DNA-damage and the mutagenic effects, respectively.

The CBMN-test showed a significant MN increase in cells exposed to C-RF and a significant increase of MN in smoking donors. Comparison between sexes showed a significant MN increase in the female group, smokers showing higher frequencies than the non-smokers in F-RF exposed samples. The Comet assay evidenced: i) a statistically significant increase of DNA-damage after F-RF exposure, with a slight yet significant difference between sexes, females showing greater amounts of DNA damage than males after each fraction; ii) a significant increase of DNA damage in smokers compared to non-smokers, in each fraction, both inside sex-groups and in the overall donor sample; iii) significant sex differences in the samples of smoking donors, females showing a larger DNA damage in every fraction. Our data indicate that *in vitro* exposure to 915 MHz mobile-phone can induce genotoxic and mutagenic effects in human lymphocytes RF, the genotoxic effect resulting particularly evident. The higher level of DNA-damage induced by the F-RF mode of exposure compared to the C-RF one is supported by data from other authors who invoke a role of adaptation mechanisms taking place in the presence of constant fields. The unexpected differences between the sexes and particularly the influence of smoking habits enhancing the level of DNA damage deserve to be further investigated.

## Induction of DNA damage by UVB radiation in erythrocytes of scaly reptiles and protective role of skin pigmentation

**Bianca Gustavino, Federica Maruccia, Gabriele Gentile**

Department of Biology, University of Tor Vergata, Rome, Italy

The protective role of skin pigmentation against genotoxic effects of UV solar irradiation is studied in peripheral blood erythrocytes sampled from individuals belonging to different species of Galápagos iguanas living at the equatorial line in the Isabela Island i.e., two land Iguana species, *Conolophus marthae* (*Cm*) which has a reduced skin pigmentation, and *Conolophus subcristatus* (*Cs*), plus a marine species, *Amblyrhynchus cristatus* (*Ac*). The two land species share the same habitat on the Volcano Wolf at 1707m of altitude, thus exposed to the same maximum level of solar UV irradiation (UVI=16+), which is in apparent contrast to the reduced pigmentation level of *Cm*. In contrast, the marine iguana (*Ac*) has an intense black pigmentation which, in combination with the altitude at sea level and the time spent in the water, suggests that it is less compromised by such a high level of UVB radiation.

The mutagenic baseline level was therefore studied in circulating erythrocytes of *Cm* specimens (n=22), *Cs* (n=13) and *Ac* (n=13), by the micronucleus (MN) test. The frequency of nuclear anomalies (AN) has also been studied, which represent the expression of gene amplification activation. The statistically significant increases ( $p < 10^{-3}$ ) of both MN and AN frequencies in *Cm* erythrocytes compared to those found in individuals of *Cs* and *Ac* indicates that *Cm* is more susceptible than *Cs* to the UV-induced DNA damage; also, the lowest frequency of MN and AN detected in the marine iguanas supports the hypothesis that the intense skin pigmentation, in addition to the shielding effect of aquatic environment, provides an efficient protection from UV-induced genotoxic effects. On this basis, we performed *in vitro* exposures to UVB radiation of blood samples from a healthy *Pogona vitticeps* (bearded dragon) donor, analysing the induction of DNA damage (Comet assay) immediately after treatment, and that of MN and AN at increasing times after it. Single and fractionate UVB exposures (1,2 mW/cm<sup>2</sup>) were carried out (total exposure time lasting from 60" up to 40'). UVC radiation (2 mW/cm<sup>2</sup>) was used as a positive control. A slight and dose-dependent DNA-damage increase was detected after UVB and UVC irradiation, which confirmed the genotoxicity of the treatments. Increased MN frequencies were also found 10 days after UVB and UVC treatments, while a general increase of AN frequencies was detected irrespective of type and mode of exposure, compared to untreated control values. Results from *in vitro* experiments (Comet and MN tests) confirm the genotoxic and mutagenic effects of UVB exposures and are in agreement to those obtained on Galápagos iguanas. By comparing AN induction from *in vitro* exposures to those from the three species of iguanas, it can be speculated that gene amplification could be a response mechanism to UV exposure as an environmental stressor, the intensity of which might be independent by stress severity, but possibly related to the genetic background.



**Neutron  
and  
Heavy  
Ion  
Radiations**

**19**

## **Radiation resistant compact sensors for multipurpose neutron diagnostics**

**Roberto Bedogni<sup>1</sup>, Katia Alikaniotis<sup>1</sup>, Marco Costa<sup>2</sup>, Valeria Monti<sup>2</sup>,  
Elisabetta Durisi<sup>2</sup>, Oriol Sans-Planell<sup>2</sup>, Jose-Maria Gomez-Ros<sup>3</sup>**

<sup>1</sup> INFN-LNF, Frascati, Italy

<sup>2</sup> Università di Torino, Torino, Italy

<sup>3</sup> CIEMAT, Madrid, Spain

New types of radiation resistant, semiconductor-based, compact size, low-cost and nearly gamma insensitive thermal neutron sensors were developed by an INFN-based collaboration. Commercially available windowless Silicon carbide photodiodes of different sensitive area were identified as suitable devices. These are sensitized to thermal neutrons through in-house evaporation-based deposition of <sup>6</sup>LiF. Whilst the radiation resistance is ensured by the large value of energy gap (three times higher than silicon), the very thin depleted layer at standard operating voltages (2-3  $\mu\text{m}$ ) promotes very low gamma sensitivity. This communication describes the performance of these sensors, relying on irradiation tests in radionuclide, accelerator or reactor-based neutron and photon fields.

## **Neutron activation analysis – $k_0$ standardization applied on Gen IV nuclear materials**

**Adrian Florinel Bucsa**

Politehnica University of Bucharest, Institute for Nuclear Research Pitesti, Pitesti, Romania

Gen IV nuclear materials represent an advanced class of materials used in lead or lead-bismuth eutectic cooled power reactors. Titanium alloys are part of this class. Our study shows the results of characterization of  $^{15}\text{-}^{15}\text{Ti}$  from the point of view of elemental concentration using the NAA- $k_0$  method, after irradiation of a sample of this special steel in reflector location of TRIGA SSR 14 MW reactor from Institute for Nuclear Research Pitesti – Romania. The study was meant to emphasize the importance of knowing the elemental concentration of  $^{15}\text{-}^{15}\text{Ti}$  alloy and the interpretation of the data obtained related to the behaviour of these elements in high neutron flux and in lead or lead-bismuth corrosive environment.

## **Spectrometry of fast neutrons with energy value of around 14 MeV produced in the d-t reaction in a gas filled neutron tube by using a radiation diamond detector**

**Renat Ibragimov, Iliia Urupa, Evgeny Tyurin, Elena Ryabeva**

National Research Nuclear University MEPhI (Moscow Engineering Physics Institute), Moscow, Russia

The results of experimental studies of the using diamond radiation detector for spectrometry fast neutrons with energy value around 14 MeV arising from the d-t reaction in a gas-filled neutron tube have presented in this work.

Listed experimental results was achieved by using the radiation diamond detector and spectrometry electronic devices that provide value of Full Wide on Half High (FWHH) less than 1% at energy of alpha particle 7.6 MeV. For FWHH estimation, isotope Ra-226 source of alpha particles with several different energies was used.

The least squares method was used to restore the energy spectrum of d-t neutrons detected by a radiation diamond detector. After comparing the experimental data and simulation results, we calculated the ratio of contributions to the final spectrum from neutrons formed under different conditions (from atomic (D +) or molecular (D<sub>2</sub> +) deuterium ions, atomic (T +) or molecular (T<sub>2</sub> +) tritium ions, or molecular ions DT + incident on a target containing atoms D and T).

In this study also was measured the dependence of energy and neutron intensity from angle between neutron and ions beam, that irradiate the neutron tube target.

In addition, in the course of the experiments, the effect of the polarization effect on the operation of a diamond detector, as well as the sensitivity of the detector and electronics to accompanying X-rays, have studied. It have been established that the polarization effect does not have any effect on the detector output data when the flux of fast neutrons with an energy value of about 14 MeV is up to  $1.7 \times 10^7$  n/sm<sup>2</sup>s. The diamond detector was operating continuously under irradiation for several hours. It has also been shown that the contribution of X-ray and gamma radiation to the work of the diamond detector and the associated electronics (a charge-sensitive amplifier) could be eliminated by amplitude discrimination without losing useful signals from 14-MeV neutrons.

## The irradiation facility at the IBR-2 research reactor

**Sergey Kulikov, Maksim Bulavin**

Joint Institute for Nuclear Research, Dubna, Russia

The irradiation facility at the IBR-2 fast pulsed research reactor is located at the beamline No.3. It allows to carry out irradiation of samples with fast neutrons and gamma quanta at a distance of a few dozen centimeters from the reactor core, which will make possible to achieve a large neutron fluence on the sample (materials) tested in a wide energy range and implement online measurements on fault tolerance of electronic components. Experiments on the irradiation of materials are carried out in the framework of FLNP JINR cooperation with other centers for such projects, as LHC (the detectors ATLAS and CMS) and TOKAMAK (the projects ITER and DEMO), as well as in the framework of cooperation with scientific organizations of JINR member-states. A wide range of materials under study on the irradiation facility of the IBR-2 reactor includes the radiation resistance research of printed circuit boards and other elements of detectors, the magnetic field sensors, scintillators, new perspective materials for neutron guide glasses, test experiments on radiation coloring of topazes and production of medical radioisotopes of molybdenum, technetium and others.

The neutron flux density with an energy of  $25 \text{ meV} \div 10 \text{ MeV}$  is from  $5 \cdot 10^5 \text{ n/cm}^2 \cdot \text{s}$  to  $2 \cdot 10^{12} \text{ n/cm}^2 \cdot \text{s}$ , which provides the neutron fluence on the sample in one standard reactor operation cycle (11 days) from  $5 \cdot 10^{11} \text{ n/cm}^2$  to  $2 \cdot 10^{18} \text{ n/cm}^2$ . At the same time, the temperature on the sample during irradiation at the closest to the core point is below  $50^\circ\text{C}$ . The report gives a brief overview of experiments, results and their discussion.

## Neutron diffraction study of $\text{La}_{0.6}\text{Ca}_{0.4}\text{CoO}_{3-d}$ as a promising zinc-air rechargeable battery material

**Kiril Krezhov**

Bulgarian Academy of Sciences, Sofia, Bulgaria

A metal-air battery is a type of battery or fuel cell that uses the oxidation of a metal with oxygen from atmospheric air to produce electricity. It is furnished with an anode prepared from pure metals, such as lithium or zinc, and an air cathode, which is connected to a source of air. The catalysts in the air cathode support the electrochemical reaction with the oxygen gas. Lately, metal-air batteries have attracted considerable research attention as the new generation of high-performance batteries as they feature simple design structure, very high energy density, and a relatively inexpensive production. Large-capacity rechargeable batteries are becoming increasingly necessary for mobile devices, and the metal-air battery is currently the most promising for this application. Among various metal-air rechargeable battery designs the zinc-air rechargeable battery model, although known long ago, has been revived in the last decade as one of the most viable future options due to its very high theoretical energy density, environmental-friendliness, affordability, and safety. It has the potential to outperform existing lithium-ion batteries in terms of higher energy density, lower cost, longer cycle life, and higher safety. However, one has to overcome the slow oxygen reduction reaction and oxygen evolution reaction kinetics representing a limiting factor for the energy conversion efficiency and the poor charge-discharge cycle life of state-of-the-art zinc-air battery. One reason for this is the low stability of the air electrode against reversible operation. The latest advances in developing non-precious metal catalysts are achieved by utilizing of bifunctional catalysts based on transition metal oxides (single/mixed-metal oxides, spinels and perovskites), transition metals, carbon-based materials and precious metals/alloys. Of the various catalysts that have been developed to date for high performance, perovskite oxides have attracted attention due to their inherent catalytic activity as well as structural flexibility. Particularly, the perovskite  $\text{La}_{0.6}\text{Ca}_{0.4}\text{CoO}_{3-d}$  has been of interest as a bifunctional catalyst for the bifunctional air electrode. In an effort for improving fundamental understanding of material properties relevant to the rechargeable zinc and air electrodes we have investigated the structural details in dependence on preparation of powder samples of  $\text{La}_{0.6}\text{Ca}_{0.4}\text{CoO}_{3-d}$  using full profile analysis of neutron and x-ray diffraction patterns. Oxygen vacancies remain random at room temperature. The neutron diffraction data collected at different temperatures down to 4.2 K show that the crystal structure of the samples adopts orthorhombic symmetry independently of their porosity and preparation technological conditions.

## Structure and magnetic properties of nanosized Al-substituted barium hexaferrite powders

**Kiril Krezhov<sup>1</sup>, Tatyana Koutzarova<sup>2</sup>, Svetoslav Kolev<sup>2</sup>, Petya Peneva<sup>2</sup>**

<sup>1</sup> Bulgarian Academy of Sciences, Sofia, Bulgaria

<sup>2</sup> Institute of Electronics, Bulgarian Academy of Sciences, Sofia, Bulgaria

BaFe<sub>12</sub>O<sub>19</sub> is among the most important hard magnetic materials and is widely used as permanent magnets, a magnetic recording material, as well as in microwave components and devices, such as circulators and absorbers. It is known that substituting the iron cations in BaFe<sub>12</sub>O<sub>19</sub> with the non-magnetic Al<sup>3+</sup> alters its magnetic structure (the magneto-crystalline anisotropy) and, thus, leads to changes in the hexaferrite's magnetic characteristics.

We report studies on the correlation between the microstructure, crystalline structure and magnetic properties of nanosized monodomain Al-substituted barium hexaferrite (BaFe<sub>10</sub>Al<sub>2</sub>O<sub>19</sub>) powders obtained by the single microemulsion method. The powders were characterized using X-ray diffraction analysis with Cu-K<sub>α</sub> radiation, scanning electron microscopy (Philips ESEM XL30 FEG) and transmission electron microscopy (TEM).



**Nuclear  
Medicine**

**20**

## Compliance and reproducibility of radioiodine I-131 uptake test measurements

Turan Şahmaran<sup>1</sup>, Salih Sinan Gültekin<sup>2</sup>

<sup>1</sup> Hatay Mustafa Kemal University, Hatay, Turkey

<sup>2</sup> Health Sciences University, Ankara Dışkapı Yıldırım Beyazıt Training and Research Hospital, Ankara, Turkey

**Aim.** Radioiodine I-131 uptake (RAIU) test is one of the important tests performed by nuclear medicine departments. A RAIU value measured at 4th and 24th hours has been widely used for differential diagnosis and treatment dose calculation. In this study, for the RAIU test, we aimed to evaluate the compliance of repeated measurements, to define practical methods for reproducibility and to assess the reliability of use.

**Materials and methods.** Study group consists of consecutively on one hundred nineteen patients (65 females, 54 males, age ranging;  $55 \pm 12$  years, TSH level;  $2.07 \pm 6.74$  uIU/mL). Each measurement of all participants was repeated twice at 4th and 24th hours under equal geometry and stable counting conditions using a standard procedure. All measurements were obtained using the same thyroid uptake system consisting of NaI crystal, photomultiplier tube and multi-channel analyzer. Data were evaluated by statistical methods. For assessment of the reproducibility, we used two different method covering three parameters; reproducibility coefficient (RC), the root-mean-square standard deviation (SDRMS) and the lowest significant change (LSC) values.

**Results.** The average RAIU values of the first and second measurements were  $23.71 \pm 16.52$  and  $23.94 \pm 16.64$  at 4th hour ( $p > 0.05$ ), and  $35.33 \pm 19.22$  and  $35.49 \pm 19.19$  at 24th hour ( $p > 0.05$ ), respectively. We found a statistically significant difference between both repeated measurement pairs when they were evaluated according to their differences ( $p < 0.05$ ). Between repeated measurements there was a mean difference of  $-0.24 \pm 0.62$  at 4th hour (limits of agreement; 0.97 to -1.44), and a difference of  $-0.16 \pm 0.44$  at 24th hour (limits of agreement; 0.70 to -1.02). When we investigated the correlation between the repeated RAIU measurements, considering differences and averages; Negative correlation was found for 4th hour measurements ( $r = -0.203$ ,  $p < 0.05$ ), no significant correlation was found for 24th hour measurements ( $r = 0.074$ ,  $p > 0.05$ ). For both the 4th hour and 24th hour measurement pairs, compliance values were within the limits of agreement. RA, SDRMS and LSC were calculated as 1.23%, 0.37% and 1.02% for the 4th hour measurements and 0.88%, 0.40% and 1.11% for the 24th hour measurements, respectively.

**Conclusion.** It is important to define the reproducibility of tests in laboratories. We notice two practical methods for reproducibility of probe-based RAIU test that can be used in a typical nuclear medicine department and presented their findings here. Our compliance values were within acceptable limits. Although we found a statistically significant difference in the reproducibility of the measurements, we think that it may be not cause apparent effect in the clinical setting.

## Production of medical radionuclide Mo-99 from low-enriched uranium

Oleg Kochnov, Natalia Zorina

Karpov Institute of Physical Chemistry, Obninsk, Russia

**Introduction.** Tc-99m is the most widely used radionuclide in nuclear medicine for diagnostics (about 30 millions of medical procedures in the world). It is obtained from the maternity radionuclide Mo-99 which can be produced by different methods. The most common method is fission method when Mo-99 is obtained from U-235 fission products of high-enriched uranium (HEU) in research reactors. Such Mo-99 is also called “fission”.

The proposed solution of replacement HEU with LEU is the first step on the road to manufacture scaling which requires the minimal expenses for reconstruction of the existing line for Mo-99 production.

**Research objective.** HEU-LEU conversion of Mo-99 production is quiet complicated process as both Mo-99 producers and Mo-99 consumers face several technical problems related to preparation of LEU targets and their irradiation, radiochemical separation of Mo-99, radioactive wastes treatment, and LEU Mo-99 delivery to consumers. Global Mo-99 producers have spent 6-9 years for such a conversion. It turned out that HEU-LEU conversion is very expensive and complicated process. Besides, operational costs while producing Mo-99 from LEU targets are significantly higher as compared to manufacturing from HEU targets, while the product cost of LEU Mo-99 is the same as the cost of HEU Mo-99.

The necessity of the project execution is defined by the reservation of Russia export potential in LEU Mo-99 supplies.

To compare neutronic characteristics of targets for Molybdenum production made of high-enriched and low-enriched (19.7% of  $^{235}\text{U}$ ) fuel the comparative calculating by Monte-Carlo method were made.

**Results.** Based on the results of performed calculating the following conclusions can be made:

1. It is possible to use LEU targets (enrichment is 19.7% of U-235) of flow-through tube-in-tube type in loop facilities without exceeding the limits and conditions for safe operation.
2. The difference in energy release in targets (90% and 19.7% enrichment of U-235) does not exceed 3.3% and has no effect on capability of loop facilities to perform the effective heat removal.
3. Maximum temperature of coolant in near-wall region in targets 90% and 19.7% enrichment of U-235) is 96.6 °C and 97.3 °C correspondingly and does not cause near-wall boiling.

## **Determination of the radiation dose received by the patient during positron emission tomography – computed tomography (PET – CT) procedures**

**Turan Şahmaran<sup>1</sup>, Mehmet Bayburt<sup>2</sup>**

1 Hatay Mustafa Kemal University, Kirikhan Vocational High School, Hatay, Turkey

2 Ege University, Institute of Nuclear Sciences (Retired), İzmir, Turkey

Positron emission tomography/computed tomography (PET / CT) is an imaging modality that acquires functional (PET) and anatomical (CT) information of a patient within a single examination. Amongst all the radiopharmaceuticals developed so far for PET imaging, <sup>18</sup>F-fluorodeoxyglucose has widespread application and is most commonly used.

This study can be examined in three parts. In the first part, the calibration of Thermoluminescence Dosimeters (TLD) has been done. The lithium fluoride TLD chips (3.2× 3.2× 0.9 mm) (Model 100: Harshaw Chemical, Solon, Ohio, USA) were used to measure each patient and Model 3500 Reader (Harshaw Chemical, Solon, Ohio, USA) was used for TLD readout. TLDs was calibrated initially and variations of the sensitivities were kept within ±5%. Later these dosimeters have been made ready for irradiation by placing them between special black bands that do not receive any light.

In the second part, TLD was placed in the bladder, heart, thyroid and brain regions of voluntary PET patients before injection. TLD dosimeters remained on patients until PET / CT examinations were completed, and thus dosimeters were irradiated. Irradiated dosimeters were read at the luminescence laboratory of Ege University Institute of Nuclear Sciences.

In the third part, every value elicited has been compared with the values in the international commission and committees International Commission on Radiological Protection (ICRP), U. S. Nuclear Regulatory Commission (Nureg/CR) and Committee on Medical Internal Radiation Dose (MIRD) reports and the calculated results have been observed to be in accordance with the recommended values.

## A possible use of $^{177}\text{Lu}$ based radiopharmaceuticals for palliative therapy of bone metastases

**Michael Zhukovsky<sup>1</sup>, Hesham M.H. Zakaly<sup>2</sup>,  
Mostafa Y. A. Mostafa<sup>2</sup>, Darya Deryabina<sup>2</sup>**

<sup>1</sup> Institute of Industrial Ecology UB RAS, Ekaterinburg, Russia

<sup>2</sup> Ural Federal University, Ekaterinburg, Russia

In recent years, such a radionuclide, as  $^{177}\text{Lu}$  is considered as a promising material for the creation of therapeutic radiopharmaceuticals. With the therapeutic use of radiopharmaceuticals, the absorbed doses per tumor may exceed 10 Gy. In this case, it is extremely important that the absorbed doses to healthy organs and tissues do not exceed the threshold for the incidence of deterministic effects. Possible use of radionuclide  $^{177}\text{Lu}$  for the palliative treatment of pain in the formation of bone metastases is analyzed. Radionuclide  $^{177}\text{Lu}$  is a beta-emitting nuclide with maximal energy of 0.49 MeV and a half-life of 6.6 days (161 h). Two therapeutic agents were considered: methylene diphosphonate (MDP) and ethylenediamine tetramethylene phosphonic acid (EDTMP). Both drugs contain phosphorus compounds in their composition, which ensures a high tropism to bone tissue. For both drugs, biokinetic models of  $^{177}\text{Lu}$  behavior in the human body are created. Because a number of studies have shown that the radiochemical stability of drugs is about 99%; separately, the calculations took into account the presence of a free radionuclide  $^{177}\text{Lu}$  in each of the solutions. Absorbed doses in organs and tissues when using radiopharmaceuticals  $^{177}\text{Lu}$ -MDP,  $^{177}\text{Lu}$ -EDTMP, as well as already used drugs  $^{153}\text{Sm}$ -EDTMP and  $^{89}\text{SrCl}_2$  are compared. In order to assess the risk of exposure of a patient to a radiopharmaceutical, the absorbed doses are calculated for each organ where the radioactive label is mainly deposited: in the kidneys, red bone marrow, liver and bone surface. The intensity of dose accumulation when using different drugs in the pathological focus is different. The drug  $^{177}\text{Lu}$ -MDP faster than other drugs leads to the full realization of the expected dose, therefore, when it is used, the therapeutic effect is achieved faster. The slowest absorbed dose accumulates when strontium chloride is used. To compare the effectiveness of preparations based on the  $^{177}\text{Lu}$  radionuclide, the analysis of radiopharmaceuticals currently used for palliative therapy of bone metastases was performed:  $^{89}\text{SrCl}_2$  and  $^{153}\text{Sm}$ -EDTMP. The most exposed organs are: for  $^{89}\text{Sr}$  – the kidneys, red bone marrow and liver, for  $^{153}\text{Sm}$ -EDTMP – red marrow. For radiopharmaceuticals based on the  $^{177}\text{Lu}$  radionuclide, the most exposed organs are the kidneys, liver and red bone marrow. When using the radiopharmaceutical  $^{153}\text{Sm}$ -EDTMP, the absorbed dose in the red bone marrow is almost twice the value for the drugs based on the  $^{177}\text{Lu}$  radionuclide. This proves the effectiveness of the radiopharmaceutical  $^{177}\text{Lu}$ -MDP and  $^{177}\text{Lu}$ -EDTMP. In medical practice, methylene diphosphonate is used as a diagnostic drug; however, according to the results of the calculation, it is  $^{177}\text{Lu}$ -MDP that demonstrates the best results for palliative therapy of bone metastases.

## Quantitative 18 FDG PET CT metabolic parameters and overall survival in small cell lung cancer (SCLC)

Esra Arslan, Tamer Aksoy

Health Sciences University, Istanbul Training and Research Hospital, Clinic of Nuclear Medicine, Istanbul, Turkey

**Purpose.** The aim of this study to detect the prognostic significance of 18 FDG PET-CT metabolic parameters in small cell lung carcinoma

**Methods.** Tumor localisation, tumor size, distant organ metastasis, metabolic parameters detected with 18 FDG PET-CT including primary tumor SUVmax analyzed in totally 244 patients and SUV peak, SUVmean 40%, metabolic tumor volume (MTV)40%, TLG40(total lesion glycolysis) SUVmean70%, (MTV)70%, TLG70 were evaluated in 31 patients for survival analyses.

**Results.** Totally 244 cases diagnosed with small cell lung carcinoma(SCLC) retrospectively analyzed between years 2010-2018. 230 were male, 14 were female. Mean  $\pm$ STD age was 65.95 $\pm$ 9.98. Mean $\pm$ STD primary tumor SUV max 19.74 $\pm$ 8.71. 82 cases have distant organ metastasis mean $\pm$ STD primary tumor SUV max 20 $\pm$ 8.69 and 162 case has no distant organ metastasis mean $\pm$ STD primary tumor SUV max 19.74 $\pm$ 8.71. 182 cases died mean survival: 15.52 $\pm$ 15.77 months, median: 10.42 months. 31 case parameters calculated MTV40% and MTV70%. MTV40% values smaller 20 cases mean OS is significantly higher than higher 20 cases.

**Conclusion.** There is a relationship between 18FDG PET-CT parameters and small cell lung cancer survival. Highest correlation has been found MTV40% and OS time in SCLC.18 FDG PET-CT parameters may predict the tumor biology and survival expectancy in SCLC.

## Is there any benefit to screening prone position versus supine breast 18 FDG PET CT?

**Esra Arslan, Tamer Aksoy**

Health Sciences University, Istanbul Training and Research Hospital, Clinic of Nuclear Medicine, Istanbul, Turkey

**Objectives.** Prone position 18F fluorodeoxyglucose positron emission tomography/computed tomography (FDG-PET/CT) may improve the localisation of the tumor and separation of deep anatomic parts especially axillary lymph nodes. The aim of this study was to compare the PET CT metabolic and anatomic parameters by prone versus supine 18 FDG-PET in newly diagnosed breast cancer.

**Materials and methods.** Locally Institutional Review Board approved this prospective study. 39 breast cancer patients whom newly diagnosed underwent both prone and supine FDG-PET/CT at the same scanning session. Two readers performed an independent review of all scans. Differences between the observers were resolved at a consensus reading session. Primary tumor SUV<sub>max</sub>, SUV<sub>peak</sub> and SUV<sub>mean</sub> 40%, MTV<sub>40%</sub>, TLG 40, Thresh 40, SUV<sub>mean</sub> 70%, MTV<sub>70%</sub> TLG<sub>70</sub> Thresh 70 has been calculated both supine and prone position.

**Results.** Prone position mean primary tumor SUV<sub>max</sub>±STD :12.78±8.91, supine position mean primary tumor SUV<sub>max</sub> ±STD :13.26±9.73. Categorization of anatomic disease distribution has concordant between prone and supine scanning in 35 patients. In the 27 patients with breast and axillary disease, equal numbers of metastatic lymph nodes were identified on prone and supine scanning in 15 patients, whereas in the remaining 12 patients, prone scanning diagnosed in a higher number of visualized lymph nodes. Prone position; mean 40% MTV±STD:13±25 and mean 70%MTV±STD:1.98±2.53. Supine position; mean 40% MTV±STD: 13.87±25.54 and mean 70% MTV±STD:2.26±2.85

**Conclusion.** Prone and supine position FDG-PET/CT scanning gives identical information on locoregional disease distribution in Locally Advanced Breast Cancer. But prone position scanning may perform better than supine for assessing the number of metastatic lymph nodes. Prone position FDG-PET/CT may be useful in future clinical and research studies, including PET and magnetic resonance imaging (MRI) fusion applications.

## **Impact of different vendors on SPECT-CT dosimetry for hepatic transarterial radioembolization**

**Tamer Aksoy, Ozlem Erez, Cihan Gundogan**

University of Health Sciences, Istanbul Training and Research Hospital, Clinic of Nuclear Medicine, Istanbul, Turkey

Radioembolization with (90)Y-loaded microspheres is increasingly used in the treatment of primary and secondary liver cancer. Technetium-99 m macroaggregated albumin (MAA) scintigraphy, which is used as a surrogate of microsphere distribution to assess lung or digestive shunting prior to therapy, based on tumoral targeting and also for dosimetry. Here, in this study, we aim to see if there are any differences between two different vendor's programs design to measure liver volume and hepatic Tc99m MAA uptake.

Ten Tc99m MAA scintigraphies of 9 patients, which were all acquired in the same device, with in 2 hours after angiographies. All scintigraphies were evaluated separately by two dedicated nuclear medicine workers (a nuclear medicine specialist and a health physicist) with two different vendor's volume measuring programs. Separate region of interests (ROI's) were drawn on CT images around liver parenchyma for measuring liver volume and ROI's were drawn on SPECT-CT fusion images for measuring tumors MAA uptake ratio and volume and also for total liver parenchyma's MAA uptake value and volume. All parameters were evaluated within each volumes and counts, and also for ease of use.

Although we had studied very small patient group this study guides us about the effects of different vendors programs and differences between their abilities and ease to measure volumes.

## **PET/CT findings of a soft tissue tumor elastofibroma dorsi**

**Tamer Aksoy, Esra Arslan**

University of Health Sciences, Istanbul Training and Research Hospital, Clinic of Nuclear Medicine, Istanbul, Turkey

Elastofibroma dorsi (ED) is a rare, benign, slowly-growing connective-tissue tumor that occurs most often at the infrascapular area and seen in elderly people. It can be detected with various imaging modalities, like CT, MRI, USG and PET.

This benign but painful tumor might show increased metabolic activity which may be confused with other benign or malignant tumors. It was also shown that elastofibroma dorsi might express increased somatostatin receptor expression.

In this study, we are going to present our experience in elastofibroma dorsi with F-18 FDG PET/CT and Ga-68 DOTATATE PET-CT with various case examples. And also according to our knowledge second case in the literature which shows somatostatin receptor expression in elastofibroma dorsi.

## **Software evaluation of possible incidents and nearmisses in nuclear medicine**

**Vojislav Antic, Mirjana Petrovic, Zivorad Savic**

Clinical Centre of Serbia, Belgrade, Serbia

This paper presents a product which has a goal to make, as much as possible, the transformation from unpredictable to foreseeable, through experience based on long-standing practice in monitoring all phases of the nuclear-medicine process, as well as external factors, that can cause incidents in nuclear medicine.

Namely, there is already dedicated nuclear medicine software on the market, which primarily deals with the traceability of the nuclear-medical process (etc. IBC Clinic – Management Process and BioDose/NMIS). The authors have designed a concept for software add-on, that should, in their opinion, in a isolate and comprehensive way, handle all incidental situations and nearmisses in nuclear medicine practice, in the sense that it includes and records problems related to the particularities: 1) Local rules and procedures; 2) Production, separation and application of radiopharmaceuticals; 3) Radiation safety; 4) Quality assurance of nuclear-medical diagnostic devices, IT equipment, devices for radiation measurement; 5) Application and control of radiation protection equipment and means; 6) Non-standardized compression and accumulation of radioactive waste; 7) Mechanical injuries (patient, employee); 8) Errors in the administration of radiopharmaceuticals (wrong patient, inadequate dosage, pregnant / breastfeeding patients); 9) Patient's health status and 10) Patient's influence in the creation or escalation of incidents.

In this way, by memorizing and continuously monitoring the evaluation of practical local cognition, in the opinion of the authors, incident situations would be minimized, and it would be strong basis for establishment of the most efficient system for the development of a safety culture in nuclear medicine organization.

## Lutetium DOTATATE dual time post therapy scintigraphy

**Silvija Lučić<sup>1,2</sup>, Andrea Peter<sup>2</sup>, Dolores Srbovan<sup>2</sup>, Milena Spirovski<sup>1,2</sup>**

<sup>1</sup> Medical Faculty, University of Novi Sad, Novi Sad, Serbia

<sup>2</sup> Oncology Institute of Vojvodina, Novi Sad, Serbia

Radiolabeled somatostatin analogs are used for diagnostic purposes and afterward possible radionuclide therapy mainly for metastatic neuroendocrine tumors but also can be indicated as radionuclide therapy in dedifferentiated metastatic thyroid cancer patients. The most important criteria in planning the application of peptide receptor radionuclide therapy (PRRT) is to demonstrate somatostatin receptor positivity of the tumor cell. Another factor is the various types of somatostatin receptors (SSSTR 2-5) and the affinity of the radiolabeled somatostatin analog to the particular SSTR. Well established radiopharmaceuticals for somatostatin receptor scintigraphy (SRS) are <sup>111</sup>Indium Octreotide (OctreoScan) and <sup>68</sup>Gallium labeled somatostatin analogs but also <sup>99m</sup>Tc-EDDA/ HYNIC-Tyr3-octreotide (*tectrotid*). Scintigraphy with *tectrotid* was used for determination of the presence of SSTR positivity in metastatic follicular thyroid cancer patient in whom the radioiodine therapy possibilities were exhausted. With the presence of SRS positivity scan with metastatic deposits affinity marked as grade 3, the radiolabeled somatostatin analogs radionuclide therapy with <sup>177</sup>Lu-DOTATATE was applied. The radionuclide <sup>177</sup>Lu is both beta and gamma emitter, which allows imaging after therapy.

Accepted protocols for PRRT posttherapy scintigraphy suggest dual phase post therapy scanning early as soon as 4 hours after the treatment, 24h and 48h afterwards. Due to our local schedule possibilities an early 4hour whole body scintigraphy was done with two different collimators high energy and low energy-high sensitivity with acquisition parameters on dual-headed Siemens E CAM gamma camera with dual window of 113 KeV and 208 KeV (20% windowing) 10cm/minute speed of the table. And a late whole body scintigraphy was done 72hours after the therapy with high energy, medium energy and low energy collimators respectfully with the same dual windowing, and at 8cm/minute speed of the table for medium and low energy collimator, and 3cm/minute bed speed for high energy collimator.

The early whole body <sup>177</sup>Lu-DOTATATE whole body scan with high energy collimator demonstrated visualization of normal physiological distribution and abnormal increased uptakes in most of the lesions seen in *tectrotid* scan with a disappointing degree of uptake grade. Whole body scan with low energy collimator were too distorted. In contrast, late whole body scan with low energy collimator as well with medium energy collimator showed an excellent visualization of abnormal increased uptake in all of the lesions seen in *tectrotid* scintigraphy, with high degree of uptake and good target to background ratio. As expected, the medium energy collimator showed the best resolution and the higher target to background ratio.

Our delayed whole body scans showed that early 4-hour scanning could be avoided and that the late, as late as 72 hours after therapy scans are useful and have an excellent diagnostic value.



**Pharmaceutical  
Sciences**

**21**

## Nitric oxide as a basis for the creation of new promising drugs

**Marina Filimonova, Lyudmila Shevchenko, Alina Samsonova,  
Tatiana Podosinnikova, Victoria Makarchuk, Alexander Filimonov**

A. Tsyb Medical Radiological Research Center – branch of the National Medical Research Center of Radiology of the Ministry of Health of the Russian Federation, Obninsk, Russia

Nitric oxide, NO – a new “guiding star” in medicine, indicating the direction of the search for drugs against many diseases. That is what most researchers now consider. The avalanche-like increase in the number of publications about the nitric oxide role in biological objects led the American Association for the Advancement of Science and the authoritative scientific journal “Science” to call nitrogen oxide the molecule of the year in 1992. It turned out that nitric oxide controls both intracellular and extracellular processes in living organisms. This includes such different processes, as well as mental activity, vascular tone, heat shock protein synthesis, immune response and even genome functioning. Many diseases – hypertension, myocardial ischemia, thrombosis, cancer – are caused by a violation of the physiological processes that are regulated by nitric oxide. It is for this reason that nitric oxide is of great interest to biologists and physicians of various specialties. For the discovery of the role of nitric oxide in biology and medicine, several scientists were awarded the Nobel Prize in Physiology and Medicine in 1998. In this regard, the development of potential drugs that can modify the content of nitric oxide in organs and tissues is very promising. For instance, NO donors, such as nitroglycerin, have long been used in cardiology. Interestingly, NO-reducing agents – inhibitors of NO synthases – are nowadays also developed as potential drugs by leading research centers. Thus, the drug L-NNA, a competitive inhibitor of eNOS, is currently undergoing clinical trials as an antitumor agent.

We have shown that selective competitive reversible NOS inhibitors can be widely used in extreme medicine, as antishock, as well as in nuclear medicine and oncology. Thus, in our laboratory, original NOS inhibitor was created, which, when administered by a course, is able to inhibit tumor growth, metastasis and metastatic growth. We also create new compounds, NOS inhibitors, which are able to significantly limit the complications of tumor radiotherapy, if applied before each session of local irradiation of the tumor. It is important that these compounds with this method of application are safe for the oncologic patients and do not reduce the effectiveness of antitumor therapy. Moreover, on the basis of NOS inhibitors, we have created a new drug that is highly effective in various types of shock. The results of official preclinical trials are highly rated and now the drug is ready for clinical trials.

Thus, our results confirm the multifaceted role of nitric oxide in the metabolism and the high availability of its modifiers as a basis for the creation of new drugs.

## Preparation and study of two new mixed ligand Cu(II) complexes

Branka Dražić<sup>1</sup>, Slađana Tanasković<sup>1</sup>, Mirjana Antonijević-Nikolić<sup>2</sup>

<sup>1</sup> Faculty of Pharmacy, University of Belgrade, Belgrade, Serbia

<sup>2</sup> Higher Medical and Business-technological School of Applied Studies, Šabac, Serbia

**Objective.** The aim of the present study was to prepare and investigate structural characteristics of two new Cu(II) octaazamacrocyclic complexes with ibuprofen and its derivatives belonging to the aryl-propanoic acid class of compounds, structurally similar to the commercially available non-steroidal anti-inflammatory drugs (NSAIDs). This class of drugs is used to treat fever, pain and inflammation and belong to one of the most prescribed class of compounds. The studies were carried out using elemental analysis, UV/Vis and IR spectra and molar conductivity. New synthesized complexes with formulas:  $[\text{Cu}_2\text{Ltpmc}](\text{ClO}_4)_3 \cdot 6\text{H}_2\text{O}$  (LH = ibuprofen = 2-(4-(2-methylpropyl)phenyl)propanoic acid) (1) and  $[\text{Cu}_2\text{Ltpmc}](\text{ClO}_4)_3 \cdot 4\text{H}_2\text{O}$  (LH = 3-hydroxy-3-(4-isobutylphenyl)butanoic acid) (2) are insoluble in  $\text{CH}_3\text{OH}$  and cold distilled water. Molar electrical conductivity in  $\text{CH}_3\text{CN}$  of  $950/870 \text{ S cm}^2 \text{ mol}^{-1}$  is very high, but corresponding with the results of the elemental analysis. The large value obtained for complexes could be a consequence of the crystal bonded molecules of  $\text{H}_2\text{O}$ . UV/VIS spectra of the complexes is typical for a high-spin Cu(II) complex exhibiting maxima at 648 nm (1) and 660 nm (2). The position of the absorption peaks corresponded to d-d transitions in Cu(II) complexes and assigned to  $\text{CuN}_4\text{O}$  chromophore. In the IR spectra of the complexes, can observed following characteristic bands belonging to:  $\nu(\text{O-H})$  in the range  $3650\text{-}3350 \text{ cm}^{-1}$  (broad, medium) from the crystal bonded molecules of  $\text{H}_2\text{O}$ ,  $2987 \text{ cm}^{-1}\text{-}2872 \text{ cm}^{-1}$  (medium) saturated  $\text{sp}^3$  carbon stretching,  $1550\text{cm}^{-1}\text{-}1609 \text{ cm}^{-1}$  of skeletal  $\nu(\text{C}=\text{C})$  of ring from coligand and at  $1609 \text{ cm}^{-1}$  (sharp, medium) of skeletal  $\nu(\text{C-N})$  of pyridine ring from macrocyclic ligand. In the spectra of complexes there is a band around  $465/468 \text{ cm}^{-1}$  which is origin from  $\nu(\text{C-N})$  and a band about  $410/413 \text{ cm}^{-1}$  from  $\nu(\text{Cu-O})$ . The comparison of the spectra of the complexes and corresponding ligands in the range  $1750\text{-}1350 \text{ cm}^{-1}$ , can observed the change of the  $\Delta\nu$  value ( $\nu_{\text{asym}} - \nu_{\text{sym}}$ ) of the complex which confirms that the ligand is coordinated to the metal through  $\text{COO}^-$  groups. The proposed coordination mode of the ligands in complexes: oxygen atoms of  $\text{COO}^-$  are engaged in coordination thus forming a bridge between two Cu(II) from the same tpmc unit. Also  $\nu(\text{ClO}_4^-)$  at  $1094.5 \text{ cm}^{-1}$  (strong, sharp) and  $\delta(\text{ClO}_4^-)$  at  $622.6 \text{ cm}^{-1}$  (medium) the presence of  $\text{ClO}_4^-$  as counter ion.

**Conclusion.** Based on the results of applied methods we proposed that the complexes are binuclear, same exo coordination of each Cu(II) ion with azamacrocyclic ligand engaging two pyridine nitrogens and two cyclam's N atoms, and  $\mu\text{-O,O'}$  coordinated  $\text{COO}^-$  group from co-ligand.



**Radiation  
Chemistry**

**22**

## An initiation process in radiation induced polymerization in an aqueous solution – Simulations and experiments

**Marcin Kozanecki<sup>1</sup>, Paulina Maczugowska<sup>1</sup>, Piotr Sawicki<sup>2</sup>, Sebastian Sowinski<sup>2</sup>, Krzysztof Halagan<sup>1</sup>, Piotr Ulanski<sup>2</sup>, Slawomir Kadlubowski<sup>2</sup>**

<sup>1</sup> Department of Molecular Physics Lodz University of Technology, Lodz, Poland

<sup>2</sup> Institute of Applied Radiation Chemistry Lodz University of Technology, Lodz, Poland

Develop of medicine, pharmacy, electronics, optics, micromechanics and many other branches leads to increasing interest in polymer-based smart and functional materials with tailored architecture. Synthesis of the macromolecules with precisely controlled structure have been still challenging despite of a strong development of advanced methods of polymer synthesis, such as Controlled Radical Polymerization or Polymerization-Induced Self-Assembly. Radiation induced polymerization and/or crosslinking offers additional possibility for simultaneous sterilization of the products, what is especially important for medical applications. Independently of the mechanism of polymerization process, to control structure of produced polymer the kinetics of occurring reactions should be well known. In case of polymer systems kinetics is commonly interweaves with diffusion, which strongly changes upon monomer conversion. The main problem originates from the growth of macromolecules changing not only its own mobility, but also reduces the diffusivity of neighboring low-molecular-weight species (solvent molecules, monomers, catalysts, etc.). The broad distribution of time-scales which should be taken into account to describe an impact of molecular mobility on kinetics of polymerization processes is the next challenge.

Presented herein study is a first step of a project focused on a development of simulation tools based on cooperative dynamics such as Dynamic Liquid Lattice (DLL) model or Cooperative Motion Algorithm (CMA), for analyzing induced by ionizing radiation synthesis of complex crosslinked polymer systems in aqueous environment including conventional hydrogels as well as micro- and nanogels. The goal of presented herein investigation is to demonstrate possibility of use of simulations based on DLL model to describe correctly kinetics of the first step of radical polymerization – initiation. It was found that the DLL model well reflects the 2<sup>nd</sup>-order kinetics of water radiolysis (the simplest model system) and is also useful to study more complex systems such as irradiated by ionizing radiation aqueous solutions of free radical scavengers. The transfer of radicals from products of water hydrolysis to scavenger molecules is a simple model of the initiation of polymerization simplified by an elimination of propagation and termination processes.

**Acknowledgments:** This project was supported by Polish National Science Center grants no. 2017/25/B/ST4/01110.

## Can 6-substituted pyrimidine nucleosides sensitize DNA damage induced by ionizing radiation?

**Karina Falkiewicz, Witold Kozak, Janusz Rak**

University of Gdańsk, Gdańsk, Poland

Radiotherapy is one of the most commonly used modalities for anticancer treatment. During such a treatment, cancer cells are exposed to ionizing radiation (IR), which however exerts dangerous side effects. Furthermore, hypoxia characteristic for solid tumor cells induces resistance to ionizing radiation. These problems call for the application of radiosensitizers, besides IR, that increase cancer cells radiosensitivity.

Modified nucleosides are a promising group of radiosensitizers. They easily penetrate a cell membrane, are phosphorylated in the cytoplasm and processed by DNA polymerases, which ultimately leads to their incorporation into the newly biosynthesized DNA. The most thoroughly studied analogs of this type are 5-bromo and 5-iodo-2'-deoxyuridine. Recently, it has been postulated that 6-substituted uridine and cytidine could work as DNA radiosensitizers. Indeed, computational studies demonstrated that the low-activation barrier of dissociative electron attachment to these pyrimidine nucleosides produces the uridin-6-yl radical that is able to abstract a hydrogen atom not only from the sugar moiety of adjacent nucleoside in DNA, but also from its own 2'-deoxyribose. The latter process should substantially increase the amount of strand breaks in DNA labeled with 6-substituted pyrimidines.

With such attractive computational characteristics, we decided to synthesize 6I-dU and test its reactivity toward hydrated electron in radiolytic studies. However, the compound turned out to be quite instable in a neutral water solution. Surprisingly, the presence of the iodine atom in the 5<sup>th</sup> position of 2'-deoxyuridine or the 2'-hydroxyl group in 6-iodouridine makes the compound stable.

In the current work, we present a density functional theory (DFT) study on the mechanism of hydrolysis of 6-iodo-2'-deoxyuridine. For comparison, the hydrolysis of 5-iodo-2'-deoxyuridine and 6-iodouridine has been characterized at the same level of theory. The thermodynamic and activation barriers were calculated at the B3LYP/DGDZVP++ level, with the polarizable continuum model (PCM) of water for the heterolytic cleavage of the C–N glycosidic bond, and the secondary process leading finally to the 1'-hydroxysugar and substituted uracil. Based on the calculated quantum chemical characteristics, the kinetics of hydrolysis was simulated for the three considered derivatives.

Our data indicate that a presence of substituent, having electron-withdrawing inductive effect, in the vicinity of the C–N glycosidic bond increases nucleoside propensity to hydrolysis. Therefore, despite favorable radiosensitizing characteristics DNA cannot be labeled with 6-iodo-2'-deoxyuridine in the cell.

**Acknowledgments:** Supported by the Polish National Science Centre under Grant No. 2014/14/A/ST4/00405 (J.R.).

## **Radiolysis of organic compounds under electron beam irradiation during radiation sterilization**

**Sergey Bazhukov<sup>1</sup>, Marina Pervova<sup>2</sup>, Irina Bazhukova<sup>1</sup>**

<sup>1</sup> Ural Federal University, Yekaterinburg, Russia

<sup>2</sup> Institute of Organic Synthesis of the Russian Academy of Sciences, Yekaterinburg, Russia

The analysis on the composition of radiolysis products of various organic compounds as a result of radiation processing by fast electrons is performed in the present work. The work was carried out on 14 samples of different materials with polyethylene packaging: polyethylene 40 Premium, Laminate 40, CMMS-35, CMMS-35 with adhesive technical layer, Medicaïs 54 with polypropylene, Medicaïs 54 with polypropylene coated with a sticky medical layer, Medicament 74 with viscose, SMMS pl.42, SMMS 35 Avgol, Medicare 23, Medicare 26, Medicare 3 (74) with viscose, Medicare 74 with polypropylene, Medicare 54 with polypropylene. These samples are used for manufacturing the disposable medical clothing and subjected to intense radiation exposure by electrons and bremsstrahlung during the process of radiation sterilization. The purpose of the work is to find out the source of the appearance of aromatic compounds in the final product, which negatively effect on the performance characteristics of sterile products. Control irradiation of the samples was carried out with resonance linear electron accelerator (Ural Federal University). Irradiation parameters were the following: electron energy is 9.5 MeV, electron beam current is 950  $\mu\text{A}$ , and absorbed dose in the samples is in range of 17.5-21 kGy. The analysis of the gas fraction in irradiated samples was carried out by gas and liquid chromatography with the plasma-ionization detector "Shimadzu GC 2010Plus".

The result of the study is the establishment of the source, which leads to appearance of volatile organic compounds as a result of radiation exposure by fast electrons.

## Regeneration of radiation-degraded extraction systems used in the reprocessing of spent nuclear fuel (SNF)

Zaiana Dzhivanova, Elena Belova, Mikhail Kadyko

A.N. Frumkin Institute of Physical chemistry and Electrochemistry RAS, Moscow, Russia

Modern methods of SNF reprocessing based on solvent extraction technology with a primary use as extractant solutions of TBP in hydrocarbon diluents. The constantly increasing depth of burn-up of reprocessed SNF leads to increase in radiation load on extractant, which leads to formation and accumulation of more radiolysis products in it, which worsen the hydrodynamics and selectivity of extraction process, as well as characteristics of fire and explosion hazard. An important role in formation of radiolysis products of extraction mixture is played by products of diluents radiation decomposition, especially short-chain hydrocarbons. Their derivatives present an increased danger, both in relation to uncontrollable chemical exothermic reactions – thermal explosion, and in relation to formation of a vapor-gas phase capable of ignition, because the partial vapor pressure of combustible liquid increases with a decrease in length of hydrocarbon chain.

The aim of investigation was to study different ways of regeneration of radiation – degraded system “30% TBP-Isopar – M”. The efficiency of regeneration methods was evaluated by such parameters as hydrodynamic characteristics, composition of degradation products and the lower temperature limit of flame propagation of samples before and after regeneration. Ionizing radiation of radionuclides was simulated by irradiation at linear electron accelerator. The extractant solution after contacting with 4.3 mol / l nitric acid solution was irradiated by accelerated electrons to doses of 0.5, 1 and 2 Mgy. Plates of copolymer with phenazine coloring agents were used for dosimetry. The composition of radiation degradation products before and after regeneration was determined by IR spectroscopy and gas chromatography. Regeneration of irradiated samples was carried out with solutions of sodium carbonate and bicarbonate, guanidine and methylamine carbonates, ammonium carbonate both by simple mixing in a separating funnel with a submersible stirrer, and by means of a separator with an upper separation chamber. In addition to regeneration solutions tried methods of bubbling in the separator and distillation. During the regeneration of the extractant irradiated in a cyclic mode, usual contact of the guanidine solution and methylamine carbonates equally remove impurities and quickly delaminate the organic and aqueous phases. During the regeneration of the irradiated extractant in continuous mode, all tested aqueous washing solutions with the use of a separator significantly reduce the concentration of low-boiling products. The lowest content of low-boiling products is observed after regeneration with sodium carbonate solutions. When bubbling, the total number of low-boiling products (with an exit time of up to 5 minutes), passing into the gas phase, is reduced by 10 times.

**Acknowledgments:** The work was partially funded by the Ministry of Science and Higher Education of the Russian Federation (topic № AAA-A16-116110910010-3).

## Radiation-thermal stability of extraction systems based on diamides of heterocyclic dicarboxylic acids in diluents F-3 and FS-13

Zaiana Dzhivanova, Elena Belova, Ivan Skvortsov

A.N. Frumkin Institute of Physical chemistry and Electrochemistry RAS, Moscow, Russia

Developed in 2001, the classic UNEX process consisted of the cesium, strontium, neptunium, plutonium, americium and rare earth elements (REE) combined extraction directly from high-acid (up to 6M HNO<sub>3</sub>) high-level waste or dissolved in 3M HNO<sub>3</sub> non-combustible high-level waste residues using an extraction system based on 0.08 M chlorinated cobalt dicarbollide (CCD), 0.01-0.02 M Ph<sub>2</sub>Bu<sub>2</sub>CMPO and 0.35-0.6 vol.% PEG-400 in polar diluent F-3. The disadvantages of the developed classical extractant of the UNEX process include the presence of phosphorus and sulfur-organic reagents in the system, which doesn't allow burning waste extraction solutions without the formation of additional solid waste sulfates or phosphates (CHON-concept). Partly to get rid of these shortcomings allow subsequent modification of UNEX-process that provides nitrogen-containing polydentate complexing agent, such as di(N-ethyl-4-ethylaniline) 2,2'-bidenten-6,6'-dicarboxylic acid (DYP-9), di(N-ethyl-4-foradile) 2,6-piridindikarbonovoy acid (Et(pFPh)of the DPA), di(N-ethyl-4-hexylaniline) 2,2'-bipyridine-6,6'-dicarboxylic acid (DYP-7) for extraction of TPE and REE in the organic phase, allowing for simple incineration of waste organic reagents (CHON-concept). However, their thermal and radiation stability has not been sufficiently studied.

For the comparative analysis of the interaction of components of extraction systems based on DYP-9, DYP-7 and Et(pFPh)DPA in diluents F-3 and FS-13 in emergency conditions, experiments were conducted using an autoclave and the dependence of the gas release parameters on the temperature and radiation dose.

It is shown that during the heating of both samples of diluents F-3 and FS-13 and extraction mixtures with nitric acid, oxidative processes occur, accompanied by gas evolution, but they don't have a pronounced autocatalytic character. In closed devices for non-irradiated two-phase systems, a noticeable gas release was observed at temperatures of about 110 °C, while it was not accompanied by significant exothermic effects. The recorded pressure values (18-23 atmospheres) during heating of irradiated samples in the autoclave were less than in the case of heating of extraction systems containing TBP under comparable conditions (up to 60 atmospheres); the achieved overheating of samples due to exothermic processes (4-10 °C) were significantly lower compared to extraction systems containing TBP (more than 100 °C). Thus, under external thermal influence, the studied extraction systems with diluents F-3 and FS-13, even in the case of radiation degradation and the difficulty of the output of technological blowers, including due to mechanical external influence on communications and equipment, will present a lower danger compared to the extraction systems based on TBP, used in practice.

**Acknowledgments:** The work is executed at financial support of Russian Scientific Foundation (project 16-19-00191).

## The correlation between radon in soil and indoor radon concentrations in houses in the City of Kalisz, Poland

**Sławomira Janiak, Henryk Bem**

State University of Applied Sciences in Kalisz, Kalisz, Poland

Radon is known to present a risk of lung cancer when it or rather its decay products are inhaled. Most of the radon (~60%) that enters indoor air comes directly from the soil, and this radionuclide can accumulate there to higher concentrations above 100 Bq/m<sup>3</sup>. Although the transfer of <sup>222</sup>Rn from soil to buildings depends mainly on the constructional features of the houses, investigations into its concentration in the soil are conducted worldwide to quantify that contribution to its final indoor concentration.

Recently, a new and fast method based on simple, direct absorption of the exhausted soil gas in a liquid scintillator has been elaborated for <sup>222</sup>Rn determination in soil gas. The method allows us to obtain result after 10 minutes of bubbling soil gas through the UltimaGold F scintillation cocktail. Using a portable BetaScout (Hidex) counter, such measurements can be done in the vicinity of existing or planned new buildings. The Kalisz area of the Greater Poland region has a relatively uniform geological structure. However, the measured radon in soil concentrations ranged from 2 to 10 kBq/m<sup>3</sup>. The observed indoor <sup>222</sup>Rn concentration in small two-story buildings in that area ranged from 25 to 180 Bq/m<sup>3</sup>. No correlation between radiation in soil and radon in the houses (on the basement level) was found. The investigation of the rate of radon transfer into two neighboring houses proved the great contribution that the construction type has on the resulting indoor radon concentration, especially for new energy efficient houses.

## $^{222}\text{Rn}$ and $^{226}\text{Ra}$ radionuclides in drinking water in the Kalisz Area of Poland

**Daria Mazurek, Sławomira Janiak, Henryk Bem**

State University of Applied Sciences in Kalisz, Kalisz, Poland

Most of the drinking water supplied in Poland comes from groundwater or surface sources, and the presence of natural radionuclides in it, except for tritium  $^3\text{H}$ , is a result of the interaction between the water and rocks. The aim of this study was to carry out a survey of  $^{222}\text{Rn}$  and  $^{226}\text{Ra}$  concentrations in the underground drinking water supplies located in the southern part of the Greater Poland region, in the Fore-Sudeten monocline tectonic unit. Both radionuclides  $^{222}\text{Rn}$  and  $^{226}\text{Ra}$  have relatively high dose factors for ingestion and should be monitored according to EU Drinking Water Directive 2013/51.

The 2 l water samples were collected directly from underground supplies and divided into two: 0.5 l and 1.5 l parts. To the 0.5 l sample in a glass flask, 20ml of a toluene-based liquid scintillation cocktail containing 8g/l butyl-PBD and 0.3 g/l dimethyl POPOP was added. After 5 min of vigorous shaking, the flasks were left for phase separation, and the toluene with extracted  $^{222}\text{Rn}$  was transferred to 20 ml scintillation vials. The activity of the eluted radon and its four decay products was measured in Beckman 3901 liquid scintillation counter. The detection limit of  $^{222}\text{Rn}$  for 60 min counting time was equal to 0.1 Bq/l. The second part of the sample – 1.5 l – was evaporated to 0.5 l in order to remove the unsupported  $^{222}\text{Rn}$ , and after adding 20ml of the scintillation cocktail, it was kept for 1 month to achieve a radioactive equilibrium between  $^{222}\text{Rn}$  and the mother  $^{226}\text{Ra}$  nuclide. Due to very low  $^{226}\text{Ra}$  levels, final activity counting was performed using the BetaScout low background scintillation counter with  $\alpha/\beta$  separation pulses mode with a low background of 0.1counts/.min in the  $\alpha$ -channel. The detection limit for  $^{226}\text{Ra}$  determination for 60 min counting time was 3 mBq/l

The measured  $^{222}\text{Rn}$  concentrations ranged from 4.4 to 12 Bq/m<sup>3</sup>, and the corresponding average annual effective dose from its ingestion was 1.2  $\mu\text{Sv}$ , while the average annual effective dose from inhalation of  $^{222}\text{Rn}$  escaping from water used for domestic purposes was  $\sim 12 \mu\text{Sv}$ ,

The  $^{226}\text{Ra}$  concentrations in the measured water samples were in the range of 4 to 36 mBq/l. The ratio of  $^{222}\text{Rn}/^{226}\text{Ra}$  activities in drinking water ranged from 15 to over 1300, and no correlation between these two activities was found. However, a weak positive correlation ( $r^2= 0.21$ ) between radon in water and radon in adjacent soil samples was observed.

## Radiation Induced Polymerisation and Crosslinking as an effective method for poly(olygoether methacrylates) smart materials synthesis

Krzysztof Piechocki<sup>1</sup>, Marcin Kozanecki<sup>1</sup>, Sławomir Kadlubowski<sup>2</sup>

<sup>1</sup> Department of Molecular Physics, Lodz University of Technology, Lodz, Poland

<sup>2</sup> Institute of Applied Radiation Chemistry, Lodz University of Technology, Lodz, Poland

Thermo responsive polymers based on poly(olygoether methacrylates) (POEGMAs) are regarded as promising biomaterials due to an abrupt and reversible Volume Phase Transition (VPT). Thermally induced VPT results from weakening of polymer-water and simultaneously the strengthening of polymer-polymer interactions and leads to sudden collapse of polymer network and to push out the water. This mechanism strongly accelerates release process and can be used to design hydrogel actuators, drug delivery systems and other smart materials. Due to biomedical applications, the radiation-induced methods of synthesis offering simultaneous product sterilization are extremely desired to prepare such materials. This project covers a comparative studies of materials obtained by 3 different methods:

1. One step Radiation Induced Polymerisation and Crosslinking (RIPC). In this case materials were obtained by irradiation of pure monomer by pulsed high energy (6 MeV) electron beam.

2. Combination of Atom Transfer Radical Polymerisation (ATRP) and Radiation Induced Crosslinking. Firstly, linear polymer chains were obtained by ATRP, next, polymer solutions were cross-linked by electron beam irradiation without any additional cross-linker.

3. One step ATRP. Polymerisation was performed in a presence of cross-linker (ethylene glycol dimethacrylate).

2-(2-methoxyethoxy)ethyl methacrylate and oligo(ethylene glycol) methyl ether methacrylates (MEO<sub>x</sub>MA) (Mn: 300, 500 and 950) were used as monomers.

The following properties of the products were analyzed: equilibrium swelling degree (by gravimetric method), VPT Temperature (thermo-optical analysis and differential scanning calorimetry – DSC). Raman spectroscopy was used to determine relation between hydration degree, side groups length and network density.

It was found that hydrogel properties depend on method of synthesis. Molecular mass of monomers (length of oligoether groups) have the biggest impact on properties of final polymer network: water sorption, T<sub>VPT</sub>, etc. The most promising results were found for polymers obtained by polymerisation of MEO<sub>x</sub>MA with Mn=500 and Mn=950. Synthesized networks can be used as skeletons for hydrogels and, in dry state, as self-composites. DSC and wide-angle X-ray scattering showed that the oligoether chains can form crystalline phase inside the network.

**Acknowledgments:** This project was supported by Polish National Science Center grants no. 2016/21/N/ST5/03078.

## **POEGMAs based smart drug delivery systems prepared by Radiation Induced Polymerization and Crosslinking**

**Krzysztof Piechocki, Marcin Kozanecki**

Department of Molecular Physics, Lodz University of Technology, Lodz, Poland

Stimuli responsive polymer hydrogels may be sensitive to physical (temperature, electrical or magnetic fields) and/or chemical (pH, ions, glucose, morphine and many other chemical compounds) stimuli. An abrupt, reversible transition under a small change in environmental conditions is the most demanding behavior of such systems. Recently, the special interest is focused on the thermo-responsive hydrogels exhibiting volume phase transition (VPT). They are synthesized from the polymers with lower or upper critical solution temperature in water and have been successfully applied in many fields, also as a carrier for controlled drug delivery systems. Thermally-induced VPT results from the weakening of polymer–water and simultaneously the strengthening of polymer–polymer interactions. These changes lead to sudden collapse of polymer network and to push out the water what accelerates the drug release.

This project is focused on an influence of polymer network density and concentration of selected non-steroidal anti-inflammatory drugs (aspirin, ibuprofen, naproxen) on VPT temperature of poly(2-(2-methoxyethoxyethyl) methacrylate) – PMEO<sub>2</sub>MA – hydrogels. The biocompatible, non-toxic, thermo-sensitive hydrogels based on PMEO<sub>2</sub>MA were prepared by Radiation Induced Crosslinking and Polymerization. Samples were irradiated at ambient temperature by a pulsed beam of fast moving electrons (electron energy 6 MeV) using an ELU-6 linear electron accelerator (Eksma, Russia) with 4 μs pulses sent at a frequency of 20 Hz (the dose per pulse was set as 5 Gy (the average dose rate = 100 Gy s<sup>-1</sup>). The network density was controlled by dose of radiation. After irradiation, products were conditioned at least 24 hours at room temperature to allow potentially slow post-irradiation reactions to occur. Next, samples were equilibrated in deionized water for at least 3 weeks at 7°C. Water was exchanged every 2 – 3 days to eliminate unreacted monomers, short polymer chains and clusters (nanogels and microgels). Finally, when a constant weight for the gels was achieved, the samples were freeze-dried and then loaded by selected bioactive compounds.

Obtained results show that VPT depends on crosslinking density of polymer network as well as on chemical structure and concentration of low-molecular substances inside the gel. It is also found that storage temperature does not impact on drug concentration inside the gel. Performed investigations showed that POEGMAs hydrogels are attractive materials for drug delivery system, and their properties could be easy controlled.

## Irreversible bacteriochlorophyll *a* degradation induced by visible light in methanol solutions

**Aleksandar Lazarević, Sanja Petrović,  
Jelena Stanojević, Dragan Cvetković, Jelena Zvezdanović**

University of Niš, Faculty of Technology, Leskovac, Serbia

Bacteriochlorophylls (BChls) are the photosynthetic light harvesting chlorophylls found in photosynthetic bacteria. While all pigments of anoxygenic photosynthetic bacteria are known as BChls, only three of them, BChls *a*, *b* and *g* are true BChls, that is, 7,8-*trans*,17-18-*trans*-tetrahydrophytytoporphyrins or their  $\Delta 8,8'$ -derivates. BChl*a* is the most widely distributed BChl and its photostability has been a matter of great interest, because of his light harvesting properties which have made them efficient sensitizers with the potential use in photodynamic therapy (PDT) and for the drug industry.

For this study, two methanol solutions were made – one with BChl*a* and the other with BChl*a* and lipid PL90 (Phospholipon® Phospholipid GMBH, Cologne, Germany), both with 0.025 mM of BChl*a*. The degradation of BChl*a* in two different mediums during VIS illumination treatment has been studied by absorption UV-VIS spectroscopy, using  $Q_y$  absorption band of BChl*a* as sensible indicator of detected changes and for kinetic analysis. Continuous illumination of BChl*a* solutions with VIS light (200-800 nm) were performed in hand-made cylindrical photochemical reactor equipped with symmetrically placed LED lamps at 10 cm distance from the samples (number of LED lamps was 60 com./m, distance between lamps 16 mm, light color “Pure White”, emitting angle 120° spherical). The total measured energy flux received by the samples was 14 W m<sup>-2</sup>. Time of irradiation ( $t_{irr}$ ) for both samples was 5 to 25 min. Absorption UV-VIS analysis were done on a Varian Cary-100 spectrophotometer, before and after illumination treatments.

According to obtained results, the continual light irradiation of BChl*a* in two different methanol mediums results in its irreversible degradation. The corresponding absorption spectra were changed, showing continuous drop in absorbance of  $Q_y$ -band ( $A_{Q_y,max}$ ) during the treatments. Bacteriochlorophyll *a* degradation induced by continuous VIS light, obeys first-order kinetics – results obtained from the kinetic analysis (from graphics  $\ln A_{Q_y,max} = f(t_{irr})$ ) showed no significant difference between two different samples in the degradation rate constant values. The degradation rate constants in methanol solutions for BChl*a* and PL90 + BChl*a*, were 0.03065 and 0.02969 min<sup>-1</sup>, respectively. The results showed that present lipid mixture hasn't significant effect on BChl*a* degradation process in methanol solutions.

**Acknowledgments:** This work was supported by the Ministry of Education, Science and Technological Development of the Republic of Serbia project 34012.

## Radiation induced drug release from PCL-PEO micelles

**Huanhuan Liu**

Delft University of Technology, Delft, Netherlands

Controlled drug release is of ultimate importance to decrease side effects and increase treatment efficiency for chemotherapy. In this work, we have investigated in possibilities to use radiation as a drug release trigger in combination with polymeric micelles. Depending on the type and energy of radiation the so-called Cerenkov light can be created which can be used to activate photosensitizers generating the very reactive singlet oxygen ( $^1\text{O}_2$ ) that is able to influence micelles and therefore possibly induce drug release. Here, we have tried to distinguish between radiation-induced release versus Cerenkov related effects. For this purpose, micelles composed of PCL-PEO (poly( $\epsilon$ -caprolactone)-poly(ethylene oxide)) have been either single loaded with the anticancer drug doxorubicin (DOX) or co-loaded with the photosensitizers chlorin-e6 (Ce6). Subsequently, the nano-carriers have been exposed to a  $\gamma$ -ray radiation source (i.e. Cobalt-60 source) delivering a well-controlled radiation dose, followed by determining the released drug and photosensitizer amounts. The results show that the Ce6-loaded and Ce6&Dox-loaded micelles exhibit a much more pronounced release as a function of radiation dose when compared to the micelles containing only DOX. The mechanism of this release has been further studied by evaluating the influence of different reactive oxygen species. The evaluation demonstrates that  $^1\text{O}_2$  has the most significant role in this release. Nevertheless, more studies are necessary to establish to what extent Cerenkov light contributes to the observed release in comparison to effects originating from ionizing radiation.

## Radiation reactions in polysaccharides: Crosslinking vs. scission

**Radosław Wach**

Lodz University of Technology, Institute of Applied Radiation Chemistry, Łódź, Poland

Irradiation of aqueous solution of either synthetic hydrophilic polymers or polysaccharides creates radicals on macromolecules, chiefly through indirect effect involving water-radiolysis products, which may cause scission of the chain or, oppositely, lead to formation of crosslinking bonds. The conventional modifications of polysaccharides by radiation were limited to reduction of molecular weight in order to facilitate further processing or induce specific biological activities. The scission of glycosidic bonds is predominantly responsible for the reduction in the molecular weight, whereas during irradiation of polysaccharides in an aqueous solution scission and crosslinking take place simultaneously. The possibility of polysaccharides crosslinking by radiation-initiation was demonstrated, firstly for water-soluble cellulose derivatives – high degree of substitution (DS) of cellulose with side chains accompanied by high concentration of the biopolymer in aqueous solution were found to be advantageous to obtain significant yield of insoluble fraction [1]. Other particular irradiation conditions might also facilitate crosslinking, such as appropriate pH or utilization of polysaccharides with unsaturated side-groups were reported and came into practice, to outweigh mainchain scission [2, 3]. Radiation method can be employed to circumvent disadvantages of classical methods to crosslink polysaccharides in order to form a network structure; therefore, it is especially suitable for manufacturing of hydrogels for biomedical applications. Moreover, if the dose applied for gel formation is of 25 kGy or more, the product that is being created may be sterilized simultaneously in situ, during its synthesis. In the present communication, a short review of current approaches to crosslinking of polysaccharides will be reported from the point of view of macroscopic properties and mechanism of the network formation.

### References

- [1] Al-Assaf, S.K.H. Gulrez, R. Czechowska-Biskup, R.A. Wach, J.M. Rosiak, P. Ulanski, Radiation modification of polysaccharides; in: *The radiation chemistry of polysaccharides*, Eds: S. Al-Assaf, X. Coqueret, K. Mohd Dahlan, M. Sen, P. Ulanski, International Atomic Energy Agency, ISBN: 978-92-0-101516-7, Vienna (2016)
- [2] R.A. Wach, B. Rokita, N. Bartoszek, Y. Katsumura, P. Ulanski, J.M. Rosiak, Hydroxyl radical-induced crosslinking and radiation-initiated hydrogel formation in dilute aqueous solutions of carboxymethylcellulose, *Carbohydrate Polym.* D112, 412 (2014), DOI 10.1016/j.carbpol.2014.06.007
- [3] K. Szafulea, R.A. Wach, A.K. Olejnik, J.M. Rosiak, P. Ulanski, Radiation synthesis of biocompatible hydrogels of dextran methacrylate, *Radiat. Phys. Chem.* 142, 115 (2018) DOI: 10.1016/j.radphyschem.2017.01.004



**Radiation  
Dosimeters**

**23**

## Electrical and photoelectrical properties of CdTe/CdMn(Fe)Te thin-film heterojunctions

Matanat Mehrabova<sup>1</sup>, Hidayat Nuriyev<sup>2</sup>,  
Huseyn Orujov<sup>3</sup>, Niyazi Hasanov<sup>4</sup>, Aybeniz Abdullayeva<sup>3</sup>

<sup>1</sup> Institute of Radiation Problems of Azerbaijan National Academy of Sciences, Baku, Azerbaijan

<sup>2</sup> Institute of Physics of Azerbaijan National Academy of Sciences, Baku, Azerbaijan

<sup>3</sup> Azerbaijan Technical University, Baku, Azerbaijan

<sup>4</sup> Baku State University, Baku, Azerbaijan

In this work, we have investigated the possibilities for the creation of photosensitive p-n heterojunctions (HJs) based on n-CdTe and p-Cd<sub>1-x</sub>Mn(Fe)<sub>x</sub>Te ( $x=0.08, 0.5$ ) epitaxial films. n-CdTe/ p-Cd<sub>1-x</sub>Mn(Fe)<sub>x</sub>Te thin film HJs were obtained in a vacuum  $1 \div 2 \cdot 10^{-4}$  Pa by molecular beam condensation method on glass substrates with a conductive SnO<sub>2</sub> layer, in a single technological cycle without violating the vacuum, with the use of an additional compensating source of Te vapor in the growth process by deposition of p-Cd<sub>1-x</sub>Mn(Fe)<sub>x</sub>Te solid solutions ( $d=1.5 \mu\text{m}$  thickness) on a glass substrate with a SnO<sub>2</sub> conductive layer ( $d=1.3 \text{mm}$ ), and then n-CdTe ( $d=6 \mu\text{m}$ ) evaporated on the p-Cd<sub>1-x</sub>Mn(Fe)<sub>x</sub>Te layer. Optimum conditions of obtain perfect HJs were determined: temperature of source was  $T_{sour}=1000-1200\text{K}$ , condensation rate  $v=14-16 \text{\AA}/\text{sec}$ , substrate temperature  $T_{sub}=640-670\text{K}$  for n-CdTe and  $v=18-20 \text{\AA}/\text{sec}$ ,  $T_{sub}=470-670\text{K}$  for p-Cd<sub>1-x</sub>Mn<sub>x</sub>(Fe)Te. Epitaxial films was growing in the (111) plane of a face-centered cubic lattice. It was defined, that thin films had a monocrystalline structure at a substrate temperature of  $T_{sub}=670\text{K}$ , but at  $T_{sub}=470\text{K}$  the polycrystalline structure.

Ohmic contacts was applied on the conductive SnO<sub>2</sub> layer on glass substrates by vacuum deposition by Ni of  $d = 2 \mu\text{m}$  thickness on the edge and on the n-CdTe layer from above.

To study the current-carrying mechanism in the HJs n-CdTe / p-Cd<sub>1-x</sub>Mn(Fe)<sub>x</sub>Te, dark VACs were investigated at room temperature. The VAC are asymmetric, the direct currents at displacement of about  $U=1\text{V}$  exceed inverse currents.

An investigation of photosensitivity spectrum showed that the CdTe / Cd<sub>1-x</sub>Mn<sub>x</sub>Te thin film HJs are sensitive in the wavelength range  $\lambda=0.5-0.9 \mu\text{m}$ .

The potentials of CdTe / Cd<sub>1-x</sub>Mn(Fe)<sub>x</sub>Te thin film HJs in detection of ionizing radiation were studied.

Thus, it is possible to create photosensitive CdTe / Cd<sub>1-x</sub>Mn(Fe)<sub>x</sub>Te thin film HJ, which can be used as photodetectors, photoconverters and detectors of ionizing radiation.

## **One numerical method for determining the absorbed dose of gamma and X radiation in the ZrO<sub>2</sub> dielectric within the MOS capacitor**

**Srboljub Stanković<sup>1</sup>, Aleksandar Jakšić<sup>2</sup>,  
Boris Lončar<sup>3</sup>, Dragana Nikolić<sup>1</sup>, Mirjana Radenković<sup>1</sup>**

<sup>1</sup> Vinča Institute of Nuclear Sciences, University of Belgrade, Belgrade, Serbia

<sup>2</sup> Tyndall National Institute, Cork, Ireland

<sup>3</sup> Faculty of Technology and Metallurgy, University of Belgrade, Belgrade, Serbia

At present, advanced microelectronics devices with Metal-Oxide-Silicon (MOS) structures are used to improve the functional characteristics of devices used in nuclear technology, radiation dosimetry and radiation protection in aerospace engineering, nuclear industry and radiotherapy equipment. Among other things, it is often the goal of new research to find new materials for the dielectric oxide such as of zirconium oxide (ZrO<sub>2</sub>) with higher dielectric constant (high-k) and testing its characteristics in an environment with radioactive radiation. The paper presents the application of a numerical method for the determination of the absorbed dose of gamma and X radiation in the dielectric thin layer of zirconium oxide, which is located in the structure of the MOS capacitor. The relation on the basis of the numerically calculated absorbed dose of radiation is obtained by using the theory of the physical transport of photons in a thin layer of dielectric. In doing so, it is necessary to know the spatial dependence of the photon flux of gamma or X-ray in a volume of the dielectric, as well as the values of the total mass attenuation coefficient and total energy absorbed mass coefficient for ZrO<sub>2</sub> as a radiation characteristic of the material from which is made a dielectric. Based on the results of our research, it can be concluded that ZrO<sub>2</sub> has satisfactory radiation characteristics as an alternative to the selection of dielectrics in MOS structures that are incorporated in dosimeters and radiation monitors.

## **Study of molecular mechanisms of radiochromic phenomenon in polycarbonate**

**Markéta Koplová<sup>1</sup>, David Zoul<sup>1</sup>, Vít Rosnecký<sup>1</sup>,  
Helena Štěpánková<sup>2</sup>, Václav Římal<sup>2</sup>, Josef Štěpánek<sup>2</sup>**

<sup>1</sup> Rasearch Centre Rez Ltd., Husinec-Rez, Czech Republic

<sup>2</sup> Faculty of Mathematics and Physics, Charles University in Prague, Prague, Czech Republic

The aim of this work is utilization of the polycarbonate for integrating dosimetry of high doses of ionizing radiation as a cheaper alternative to commonly used alanine dosimetry. We focused on molecular mechanisms of physical and chemical processes that cause color changes, on mapping of processes, which lead to regeneration of optical properties of the polymer and on changes of the optical density of the polymer after irradiation. Absorption optical spectroscopy, Raman spectroscopy and NMR spectroscopy were used in this study.

## Radiation, thermal and optical properties of PVA films containing arylazo pyridone dyes

**Slavica Porobić<sup>1</sup>, Milena Marinović-Cincović<sup>1</sup>,  
Dragana Jovanović<sup>1</sup>, Dušan Mijin<sup>2</sup>**

<sup>1</sup> Vinča Institute of Nuclear Sciences, University of Belgrade, Belgrade, Serbia

<sup>2</sup> Faculty of Technology and Metallurgy, University of Belgrade, Belgrade, Serbia

Films based on polyvinyl alcohol (PVA) containing different concentrations of some arylazo pyridone dyes have been introduced as plastic detectors for dosimetry. PVA was chosen due to its water solubility and the possibility to incorporate a variety of dyes.

The significance of arylazo pyridone dyes resides in their simple synthesis and wide application areas. The following dyes were used in optical data storage, laser technology, dye-sensitized solar cells, non-linear optics and biological systems.

The advantage of polymeric films based on arylazo pyridone dyes is a visual change of color after exposure to gamma radiation, making them easy to use. In addition, this form of dosimeters is cheap and easily portable.

Films containing arylazo pyridone dyes change the color when irradiated with  $\gamma$ -radiation at least up to 20 kGy. The color changes were confirmed spectrophotometrically.

All synthesized films were characterized by FTIR. Optical properties have been analyzed on the basis of reflection and excitation spectra.

Thermal degradation processes of PVA films containing arylazo dyes were investigated with thermogravimetric analysis (TGA), derivative thermogravimetry (DTG), differential thermal analysis (DTA) and differential scanning calorimetry (DSC).

## **Measurement of ambient dose equivalent $H^*(10)$ in the surroundings of nuclear facilities in Serbia and abandoned uranium mine in Kalna via OSL dosimetry**

**Aleksandra Sokić, Luka Perazić, Jovana Knežević**

Public Company “Nuclear Facilities of Serbia”, Belgrade, Serbia

Under the regulation of the Rulebook on Radioactivity Monitoring (Official Gazette RS 97/11 from 21.12.2011), it is necessary to measure ambient dose equivalent  $H^*(10)$  in the vicinity of all nuclear facilities. In accordance with this Rulebook, continuous measurements of said operational dose quantity are being carried out in the Public company Nuclear facilities of Serbia at Vinča site, Belgrade, in the surrounding of old reactor buildings RA and RB, as well as in the surrounding of the radioactive waste storage hangars H1, H2 and H3, at total of 34 measuring points. Additional measurements are being conducted on one measurement point in Kalna, at the location of abandoned uranium mine. These measurements are being carried out once a month. For that purpose, optically stimulated luminescence dosimeters (OSL dosimeters) made of  $Al_2O_3$  are being used. High sensitivity to ionising radiation of these passive dosimeters makes them suitable for measurement in both regular and accidental situations. This paper presents the dose levels measured on all points of interest in period between January 2016 and December 2017, with accompanied combined and expanded measurement uncertainty (with coverage factor  $k=2$ ), which is not greater than 33%. The purpose of this paper is to show that there is no significant increase in the level of radiation exposure, which is of particular importance to the environment and the population living around nuclear facilities in Serbia. This is also an indication that good radiological safety practice is being carried out within Public Company “Nuclear Facilities of Serbia”.

## The comparison of sensitivity of gafchromic EBT film types

Krzysztof Chelminski, Wojciech Bulski

The Maria Sklodowska-Curie Memorial Cancer Center, Medical Physics Department, Warsaw, Poland

**Purpose or Objective.** The aim of the research was to determine and compare sensitivity and the possibilities of using Gafchromic films in particular types of quality control in radiotherapy. The research concerned the suitability of particular types of films in dosimetry audits.

**Materials and Methods.** In the experiment, radiochromic Gafchromic films type EBT, EBT2 and EBT3 were used. The film sheets provided by the manufacturer in the format 8×10 inches were cut into rectangular samples with dimensions of 4×2 inches. FILMS were exposed to ultraviolet (UV) radiation present in sunlight. The gamma radiation of Co-60 and to X ray radiation from linacs. Analogue densitometer Victoreen 07-443 and two types of flat-bed scanners: A4 Epson Perfection V750 Photo and A3 Epson Expression 10000XL were used to assess optical properties of the films.

**Results.** The sensitivity of films to radiation can be defined in two ways: first, as the ratio of net OD increase in the film after exposure to radiation and the exposure time  $T$  (equivalent to absorbed dose  $D$ ), or in another sense, as the ratio of optical density increase  $\partial OD$  after infinitesimal short time  $\partial T$  of radiation exposure (or absorbed dose  $\partial D$ ) to which the film was subjected. In the latter approach the sensitivity of the film changes slightly with the increased OD. The comparison of the results of OD measurements obtained with the densitometer for particular Gafchromic films shows a decrease of the sensitivity to UV radiation of the EBT2 and EBT3 generation of films compared to the earlier EBT films. The shape of the characteristic curve for the historically first generation EBT indicates a higher sensitivity to the gamma radiation of this detector in relation to the successive EBT2 and EBT3 film types which were made to be less UV radiation sensitive. The results obtained when the flatbed scanners were in color mode indicate that there is no difference in the response of all three generations of films depending on the energy spectrum of megavoltage radiation. For all three types of films, the dependence of the PV signal value on the film orientation on the scanner BED is observed. There were not significant differences observed between the A4 and A3 scanners, however, there is a slight advantage of the larger model when scanning samples that absorbed higher dose values.

**Conclusion.** It is very difficult to assess the influence of film sensitivity to UV radiation in the spectrum of sunlight on the uncertainty of dosimetric measurements, due to the variability of conditions that can prevail in the laboratory, depending on the time of the day and the season, weather conditions, and habits and skills of the person performing measurement and analysis. Regardless of the influence of the film sensitivity to UV rays on the uncertainty budget, the exposure of the film should be limited to the minimum by appropriately storing films and avoiding accidental exposure during sample preparation, measurement and scanning.

## Simulation and measurements of 3D silicon detectors timing performance

**G. Kramberger<sup>1</sup>, V. Cindro<sup>1</sup>, D. Flores<sup>2</sup>, S. Hidalgo<sup>2</sup>, B. Hiti<sup>1</sup>, M. Manna<sup>2</sup>,  
I. Mandić<sup>1</sup>, M. Mikuž<sup>1</sup>, M. Mikuž<sup>3</sup>, D. Quirion<sup>2</sup>, G. Pellegrini<sup>2</sup>, M. Zavrtanik<sup>1</sup>**

<sup>1</sup> Jožef Stefan Institute, Ljubljana, Slovenia

<sup>2</sup> Centro Nacional de Microelectronica (IMB-CNM-CSIC), Barcelona, Spain

<sup>3</sup> University of Ljubljana, Faculty of Mathematics and Physics, Ljubljana, Slovenia

A silicon 3D detector with a single cell of 50x50 mm<sup>2</sup> was produced and evaluated for timing applications. The measurements of time resolution were performed for <sup>90</sup>Sr electrons with dedicated electronics used also for determining time resolution of Low Gain Avalanche Detectors (LGADs). The measurements were compared to those with LGADs and also simulations. The studies showed that the dominant contribution to the timing resolution comes from the time walk originating from different induced current shapes for hits over the cell area. This contribution decreases with higher bias voltages, lower temperatures and smaller cell sizes. It is around 30 ps for a 3D detector of 50x50 mm<sup>2</sup> cell at 150 V and -20°C, which is comparable to the time walk due to Landau fluctuations in LGADs. It even improves for inclined tracks and larger pads composed of multiple cells. A good agreement between measurements and simulations was obtained, thus validating the simulation results. Simulations were extended to larger cells of different shape in order to find an optimum detector for combined timing and position resolution.

## Smart Geiger Muller counter

**Stefan Ilić, Aleksandar Jevtić, Nikola Đikić, Goran Ristić**

Faculty of Electronic Engineering, University of Niš, Niš, Serbia

The design and development of a compact Geiger Muller counter with Android application that can be used as a personal dosimeter is presented. Android app is showing CPM, dose rate, absorbed dose and graph of radiation level for the last 30 minutes. It alarms user when higher radiation than normal is detected. Device has a buzzer and LE diode to indicate each count detected by Geiger tube. In case user is too busy to look at the app, it has also a LED Bar Graph, on the device, to show CPMs. The user can switch between two working regimes of a LED Bar Graph: CPMs or total dose. Maximum ratings of the device are investigated. Recorded data with GPS location are stored in a separate file for further analysis. One part of the City of Niš, in Serbia, was mapped for background levels of environmental radiation using recorded data.



**Radiation  
Effects**

**24**

## **An impact of electron-beam and laser irradiations on Ag nanoparticles stabilized by sodium tricitrate**

**Paulina Filipczak<sup>1</sup>, Piotr Chudobinski<sup>1</sup>, Szymon Bres<sup>1</sup>,  
Malgorzata Matusiak<sup>2</sup>, Slawomir Kadlubowski<sup>2</sup>, Marcin Kozanecki<sup>1</sup>**

<sup>1</sup> Department of Molecular Physics Lodz University of Technology, Lodz, Poland

<sup>2</sup> Institute of Applied Radiation Chemistry Lodz University of Technology, Lodz, Poland

The stability of silver nanoparticles (Ag NPs) gain an interest due to a broad field of their application including catalysis, medicine and pharmacy, electronics and optoelectronics, environment protection technologies, and others. Some of them require treating the NPs by radiation from various ranges of electromagnetic spectrum. In this work, the stability of aqueous dispersions of Ag NPs stabilized electrostatically by sodium tricitrate against laser and electron beam radiation was studied. The UV-Vis spectrophotometry, Dynamic Light Scattering and Transmission Electron Microscopy were used to control the changes induced in Ag NPs of different size and shape by laser as well as by electron-beam irradiations. Different laser beam wavelengths (457, 488 or 514.5 nm) and powers (up to 800 mW) were tested. In case of high energy electron beam (6 MeV) various doses and (from 1 Gy to tens kGy) and dose rates were used.

It was found that the nature and mechanism of size and shape changes in Ag NPs treated by various types of irradiation are different. Both laser as well as electron beam treatments result in narrower distribution of Ag NPs sizes. The effects induced by laser light strongly depend on the relationship between the maximum of the plasmonic absorption band and wavelength of laser light. In case of electron beam radiation small doses ( $\leq 100$  Gy) does not change the NPs immediately, contrarily to samples irradiated by higher doses. However strong post radiation effect is observed if the applied dose is small.

## Trapped-electron and trapped-hole centers in oxide scintillators

**Valentyn Laguta, Maksym Buryi, Martin Nikl**

Institute of Physics AS CR, Prague, Czech Republic

Charge carriers trapping phenomenon and related lattice defects in solid states are important tasks of the radiation physics. These tasks are especially actual for scintillating materials which are widely used as a convertor transforming the energy of ionizing radiation photons or high-energy particles into UV/visible light. Dielectric or semiconductor wide band-gap oxide materials of high degree of structural perfection are most suitable for such a purpose. They must accomplish the fast and efficient transformation of energy of incoming photons/particles in a number of electron-hole pairs collected in the conduction and valence bands, respectively, and their radiative recombination at suitable luminescence centers. However, before the radiative recombination, the migrating electrons and holes (eventually created excitons) can be trapped at a lattice defect or even self-trapped leading potentially to marked decrease of the scintillation performance. Therefore, monitoring of electron/hole trapping states in a scintillator material and revealing the nature of corresponding lattice defects is of crucial importance for further optimization of this entire family of scintillators.

It is the aim of this report to present selected results of Electron Paramagnetic Resonance and Thermally Stimulated Luminescence study of various point defects which participate in the processes of charge carriers transfer and capture in the family of practically important complex oxide single crystal scintillators based on lead molybdates [1], yttrium/lutetium garnets [2], yttrium/lutetium pyrosilicates and oxyorthosilicates [3]. Particular attention is paid to the most natural defects inevitably present or created by radiation in oxide materials, such as self-trapped electron and hole states (small polarons), anion and cation vacancies ( $F^+$  color centers), and antisite defects induced by structural disorder or natural nonstoichiometry of a material. Current understanding of the nature of charge trapping states and mechanisms of their creation in oxide scintillation materials will be discussed.

**Acknowledgments:** The support of the GA CR under project No. 17-09933S is gratefully acknowledged.

### References

- [1] M. Buryi, V. Laguta, M. Fasoli, et al., *J. Lumin.* 192 (2017) 767.
- [2] V. Laguta, M. Buryi, J. Pejchal, V. Babin, M. Nikl, *Phys. Rev. Appl.* 10, 034058 (2018).
- [3] V.V. Laguta, M. Buryi, J. Rosa et al., *Phys. Rev. B* 90, 064104 (2014).

## Point defect origin and local structure in LiCaAlF<sub>6</sub> single crystals

Maksym Buryi<sup>1</sup>, Valentyn Laguta<sup>1</sup>, Akira Yoshikawa<sup>2</sup>, Martin Nikl<sup>1</sup>

<sup>1</sup> Institute of Physics CAS in Prague, Prague, Czech Republic

<sup>2</sup> Institute for Materials Research, Tohoku University, Sendai, Japan

Large amount of ionizing radiation applications, especially the medical ones, for example, radiography and tomography, disease diagnostics and therapy require scintillating materials as efficient as possible with very high resolution.

Neutron radiography and tomography belong to non-destructive investigating techniques benefitting from the basically different characteristics of neutrons as compared to X-rays allowing extended penetrating abilities. Moreover, neutrons are sensitive to water and hydrogen-containing substances. However, lack of intense portable neutron sources and rather constrained spatial resolution of the detectors oppositely to X-rays leave the problem still open.

Activated with different rare-earth ions (e.g., Ce, Eu [1, 2], etc.), LiCaAlF<sub>6</sub> (LiCAF) crystals act as effective neutron scintillators (detectors) being highly transparent and non-hygroscopic. Co-doping of the Ce and Eu doped material with Na lead to even increased light yield [3, 4]. Neutron responses of the 3d-transition metal ions (Ti, V, Cr, Mn, Fe, Co, Ni and Cu) doped LiCAF have been studied relatively recently as well [5]. One way of the scintillation enhancement is to get rid of or suppress permanently existing and radiation-created defects of intrinsic (vacancies, interstitial ions) or extrinsic (accidental impurities) origin acting as charge traps. Therefore it is exceedingly useful to know the defect type and charge state, its local environment and thermal stability in order to eliminate or suppress it. With this aim, the undoped crystals of the LiCaAlF<sub>6</sub> were studied by electron paramagnetic resonance (EPR) technique. The obtained EPR spectra demonstrate the presence of two sufficiently strong signals which are composed of several lines creating super hyperfine structures (SHFS). One signal existed from the beginning whereas the second was created after the LiCAF sample exposure to X-rays at room temperature. Analyzing the signals g factors and SHFSs, the former was attributed to a many-electron impurity transition ion in either AlF<sub>6</sub> or CaF<sub>6</sub> octahedra. Oppositely, the irradiation-induced spectrum is produced by the molecular ion, the hole shared between two fluorine ions in the Al(Ca)F<sub>6</sub> octahedron in the vicinity of two Li cations (V<sub>k</sub> center). It is stable at room temperature.

**Acknowledgments:** The support of the CSF under project No. 17-09933S is gratefully acknowledged.

### References

1. Yoshikawa, A., et al., 2009, IEEE Trans. Nucl. Sci. 56, 3796-3799.
2. Yanagida, T., et al., 2011, Opt. Mater. 33, 1243-1247.
3. Yokota, Y., et al., 2011, Crystal Growth Des. 11, 4775-4779.
4. Yanagida, T., et al., 2011, Appl. Phys. Express 4, 106401.
5. Kawaguchi, N., et al., 2013, Radiat. Meas. 55, 128-131.

## On the phenomenological identity of radiation-induced effects in glassy chalcogenides under a prism of unified configuration-enthalpy model

**Oleh Shpotyuk<sup>1,2</sup>, Valentina Balitska<sup>3</sup>, Mykhaylo Shpotyuk<sup>4</sup>**

1 Department of Optical Glass and Ceramics, O.G. Vlokh Institute of Physical Optics, Lviv, Ukraine

2 Faculty of Mathematics and Natural Sciences, Jan Dlugosz University in Czestochowa, Czestochowa, Poland

3 Lviv State University of Life Safety, Lviv, Ukraine

4 Lviv Polytechnic National University, Lviv, Ukraine

Unified configuration-enthalpy model evolving conjugated configuration-coordinate and thermodynamic-enthalpy diagrams is developed to describe optical response in metastability of chalcogenide glasses (ChG) caused by combined physical ageing and high-energy irradiation. Within this approach, these glasses are supposed be stabilized in the ground state and temporary excited state, the former being presented by tightly interconnected metastable wells (i.e. rejuvenation-induced, irradiation-induced, physically-aged and deep crystalline-like ones) linked by thermally-activated over-barrier and tunneling through-barrier transitions.

Effect of high-energy  $\gamma$ -irradiation on ChG such as glassy As-S is reflected in vertical transitions of atomic sites into excited state followed by spontaneous non-radiative relaxation into irradiation-induced ground-glass sub-state. Thermodynamic enthalpy diagram linked with configuration-coordinate one allows complete parameterization of corresponding optical responses related to these states, defined in blue (bleaching) or red (darkening) shifts in the fundamental optical absorptions edge of As-S glasses. Thus, the phenomenological identity of “pure” radiation-induced optical changes can be revealed in ChG of multinary chemical compositions obeying competitive changes from many supplemented influences.

## The effect of UV irradiation on hydrolytic stability of urea-formaldehyde resins filled with thermally modified montmorillonite

**Suzana Samaržija-Jovanović<sup>1</sup>, Vojislav Jovanović<sup>1</sup>,  
Branka Petković<sup>1</sup>, Slaviša Jovanović<sup>2</sup>, Gordana Marković<sup>3</sup>,  
Milena Marinović-Cincović<sup>4</sup>, Jaroslava Budinski-Simendić<sup>5</sup>**

<sup>1</sup> University of Priština, Faculty of Natural Science and Mathematics, Kosovska Mitrovica, Serbia

<sup>2</sup> Trelleborg Wheel System, Business Unit Agricultural & Forestry Tires, Ruma, Serbia

<sup>3</sup> Tigar, Pirot, Serbia

<sup>4</sup> University of Belgrade, Institute of Nuclear Sciences Vinča, Belgrade, Serbia

<sup>5</sup> University of Novi Sad, Faculty of Technology, Novi Sad, Serbia

The hydrolytic stability of organic-inorganic nano-composites prepared by a two-stage polymerization of urea-formaldehyde resin (UF) filled with thermally activated montmorillonite (MMT) has been assessed before and after UV irradiation. The physical modification of MMT powder (type K10 with surface area 220 – 270 m<sup>2</sup>/g) was carried out by thermal treatment. The activated samples were designated as TA-K10 and the inactivated as NA-K10. The two types of urea-formaldehyde–MMT composites (UF/TA-K10 and UF/NA-K10) were synthesized. Obtained materials have been irradiated with different wavelengths of UV light (254 and 366 nm) and after that the hydrolytic stability was evaluated on the basis of free and liberated formaldehyde after acid hydrolysis. The free formaldehyde content in sample UF/TA-K10 that was irradiated was 0.60 % and it was smaller compared to the free formaldehyde content before irradiation (0.90 %). The content of the liberated formaldehyde from the modified UF composite which contains unmodified K10 was 2.04% compared to the cross-linked UF/TA-K10 where the content of the released formaldehyde was 2.82%. After UV irradiation of the UF/TA-K10 the content of the liberated formaldehyde decreased to 0.30% (for wavelength 254 nm) and 0.90 % (for wavelength 366 nm).

## Operational experience and performance with the ATLAS pixel detector at the large hadron collider at CERN

**Juan Antonio Garcia Pascual**

Chinese Academy of Science, Beijing, China

ATLAS is one of the four major experiments at the Large Hadron Collider (LHC) at CERN. It is a general-purpose particle physics experiment run by an international collaboration and is designed to exploit the full discovery potential and the huge range of physics opportunities that the LHC provides.

The tracking performance of the ATLAS detector relies critically on its 4-layer Pixel Detector, located at the core the ATLAS tracker. The ATLAS pixel detector consists of four barrel layers and a total of six disk layers, three at each end of the barrel region. The four barrel layers are composed of  $n^+$ -in- $n$  planar oxygenated silicon sensors at 33, 50.5, 88.5, and 122.5 mm from the geometric center of the ATLAS detector. The sensors on the innermost barrel layer (the insertable B-layer or IBL) are 200  $\mu\text{m}$  thick, while the sensors in the other layers are 250  $\mu\text{m}$  thick. At both ends of the innermost barrel layer, there are  $n^+$ -in- $p$  3D sensors that are 230  $\mu\text{m}$  thick. The innermost barrel layer pixels pitch is  $50 \times 250 \mu\text{m}^2$ ; everywhere else the pixels pitch is  $50 \times 400 \mu\text{m}^2$ .

It has undergone significant hardware and readout upgrades to meet the challenges imposed by the higher collision energy, pileup and luminosity that are being delivered by the Large Hadron Collider (LHC), with record breaking instantaneous luminosities of  $2 \times 10^{34} \text{ cm}^{-2} \text{ s}^{-1}$  recently surpassed.

The key status and performance metrics of the ATLAS Pixel Detector are summarised, and the operational experience and requirements to ensure optimum data quality and data taking efficiency will be described, with special emphasis to radiation damage experience.

By the end of the proton-proton collision runs in 2018, the IBL had received an integrated fluence of approximately  $\Phi = 9 \times 10^{14} \text{ 1 MeV n}_{\text{eq}}/\text{cm}^2$ . The innermost of the three outer layers (B-layer) has been exposed to about half the fluence of the IBL, and lower fluences for other layers.

The ATLAS collaboration is continually evaluating the impact of radiation on the Pixel Detector. In particular, signs of degradation are visible but are not impacting yet the tracking performance (but will): a trend of decreasing charge collection,  $dE/dX$ , occupancy reduction with integrated luminosity, under-depletion effects with IBL, effects of annealing that are significant for the innermost layers.

## Application of low energy electron beam for surface treatment of agricultural products

Wojciech Migdał<sup>1</sup>, Urszula Gryczka<sup>1</sup>, Sylwester Bułka<sup>1</sup>, Dagmara Chmielewska-Śmietanko<sup>1</sup>, Magdalena Ptaszek<sup>2</sup>, Anna Jarecka-Boncela<sup>2</sup>

<sup>1</sup> Institute of Nuclear Chemistry and Technology, Warsaw, Poland

<sup>2</sup> Research Institute of Horticulture, Skierniewice, Poland

Irradiation of agricultural products with ionizing radiation has about 100 years of history. The most popular is application of gamma irradiators. The increasing interest is also observed for application of high energy electrons as well as x-rays. New approach for irradiation of food and agricultural products is related to limited penetration of electrons having energy below 300 keV, which can be used for elimination of bacteria, molds and yeasts from surface of irradiated products. In the process where high energy electrons are used, the whole volume of food is irradiated. Since microorganism reside mostly on the surface of dry foods, nuts or seeds irradiation of external layer should be sufficient to eliminate microorganisms. The advantage of such solution is that low energy e-beam machines do not require thick shields and can be applied for in-line irradiation.

The most important parameter of the process is penetration of low energy e-beam, which can't be measured using traditional dosimetric systems. Presented study concentrates on determination of penetration ability of low energy electron beam by analysis of growth of irradiated seeds and onions. Spinach seeds, cabbage seeds and green onions were subjected to irradiation using a low-energy electron beam. Three energy levels were tested 180, 230 and 300 keV. The energy of the electron beam affects the range of the beam depending on the density of the irradiated product. To irradiate samples of plant materials, an electron beam emitted by the ILU-6 accelerator was used.

It was observed that irradiation with low energy electron beam can influence plant growth if irradiated with electrons having too high energy. In our experiments only electron beam of energy 300 keV had negative impact on plant growth.

**Acknowledgments:** The work was support by the IAEA under the CRP D61024 DEXAFI (POL19000) and by the Polish Ministry of Science and Higher Education (project Nr 3671/FAO/IAEA/2017/0).

## Effect of electron beam irradiation on paper-based materials

**Dagmara Chmielewska-Śmietanko<sup>1</sup>, Urszula Gryczka<sup>1</sup>,  
Wojciech Migdał<sup>1</sup>, Jarosław Sadło<sup>1</sup>, Kamil Kopec<sup>2</sup>**

<sup>1</sup> Institute of Nuclear Chemistry and Technology, Warsaw, Poland

<sup>2</sup> Warsaw University of Technology, Faculty of Chemical and Process Engineering, Warsaw, Poland

Paper as material based mainly on cellulose provides the excellent nutrient base for mould fungi. Therefore biodeterioration is the most common source of degradation of paper-based materials. Application of electron beam irradiation in paper-based objects preservation is very promising alternative for commonly used ethylene oxide treatment, which is toxic to human and environment. Moreover electron beam irradiation can be effectively applied for decontamination of biodeteriorated archives as well as for preventive conservation of large volumes of books in short time. However, advanced studies of material properties before and after radiation decontamination should ensure degradation monitoring and enable to determine appropriate irradiation dose, which will be effective in elimination of the microbiological decontamination as well as will be safe for the material. Therefore, many analytical techniques must be used in order to determine possible changes of mechanical, thermal, chemical and physical properties of paper-based objects irradiated with different doses.

In this study the correlation between electron beam irradiation doses and a change of some chemical, mechanical and thermal properties of different kinds of paper were established. Electron beam radiation inactivation patterns of different microorganisms present in different paper materials were studied as well.

The samples were exposed to electron beam irradiation using a 10 MeV-10 kW linear electron accelerator “Elektronika” and dosimetric analysis necessary for the proper realization of the process was performed with application of Riso B3 thin-film dosimeters as well as graphite calorimeters. A wide range of doses from 0.4 kGy up to 25 kGy were studied in order to determine safe and simultaneously effective dose for different papers decontamination with electron beam.

**Acknowledgments:** This work was supported by International Agency of Atomic Energy, Research Contract No. 18493 and by the Polish Ministry of Science and Higher Education, project “Electron beam for preservation of biodeteriorated cultural heritage paper-based objects”.

## Safety features of irradiated food

**Afrodita Ramos, Blagica Cekova**

MIT University – Skopje, Skopje, Macedonia

Irradiation of food underlines a process in which a controlled amount of radiation, usually below 10 kGy is used on a specific food type in order to increase the safety features of that food item. The sources of radiation that are used are: gamma rays (from the element Cobalt 60, or Cesium 137), from X-rays (that are a high energy stream of electrons from heavy metals), or electron beam (e-beam). The reasons for using radiation are as follows:

1. Prevention of illnesses caused by bacteria such as Salmonella and E.coli.
2. Preservation of the food by destroying the microbes that cause the spoilage.
3. Pest control on imported goods, usually but not necessarily from tropical regions.
4. Delay of the sprouting or ripening of the products in order to increase their longevity.
5. Sterilization of food intended for people with severely impaired immune system or people in specific conditions such as NASA astronauts who eat irradiated meat.

Is irradiated food safe to be eaten? The WHO, all of USA's food safety organizations have proclaimed that limited dosages of irradiation are safe to be applied onto food, however other countries and EFSA choose to strictly label those items in order to enable consumers to make an informed choice, considering the negative feedback of the consumers globally, when asked if they would buy irradiated food. According to research and experiments done, the radiation does not stay in the food, the nutritional value remains as it is, and in fact the USA's Centre for Disease Control and Prevention (CDC), on its page *Irradiation of Foodstates* that: *"there are no (other) significant changes in the amino acid, fatty acid, or vitamin content of food. In fact, the changes induced by irradiation are so minimal that it is not easy to determine whether or not a food has been irradiated."*

However, other research has shown that irradiation destroys the vitamins A, B1 and C as they are highly sensitive to even the smallest amount. Irradiation doubles the amount of trans fats in some foods such as beef and releases free radicals and binds with other chemicals to release toxins such as benzene. Furthermore the question is raised – if we had more sanitary and hygienic conditions in the slaughterhouses and factories for processing plant products, would we need to irradiate so many products? Finding a way to prolong shelf life while preventing the usage of more chemicals is an imperative goal in the sustainable production of food, and irradiation does pose as an answer; however the potential for development of cancerogenous cells in the human body is a huge red flag that has to be taken as the main argument against this solution.

## The effect of irradiation with accelerated electrons and gamma-rays on the oxidation state and structure of sodium-aluminum-iron-phosphate glasses

**Sergey Stefanovsky<sup>1</sup>, Olga Stefanovsky<sup>1</sup>, Michael Kadyko<sup>1</sup>, Jana Glazkova<sup>2</sup>**

<sup>1</sup> Frumkin Institute of Physical Chemistry and Electrochemistry RAS, Moscow, Russia

<sup>2</sup> Lomonosov Moscow State University, Moscow, Russia

The effect of 8MeV electron irradiation and gamma-rays from Co-60 source on the structure of anionic motif of the glasses in the series (mol.%) 40 Na<sub>2</sub>O, (20-x) Al<sub>2</sub>O<sub>3</sub>, x Fe<sub>2</sub>O<sub>3</sub>, 40 P<sub>2</sub>O<sub>5</sub> and iron oxidation state and coordination environment by Fourier Transform infrared and Mössbauer spectroscopies was studied. It has been shown that irradiation to a dose of 1 MGy does not appreciable effect on the type of bonds in the anionic motif of the glass network except possibly minor changes in coordination of aluminum and Fe(III) to Fe(II) ratio. The fraction of Fe(III) in octahedral oxygen environment was found to be 60-75% of total Fe and does not dependent from irradiation dose at up to 1 MGy.

## Radiation hardness estimation method of complex optoelectronic devices on YB:YAG laser with semiconductor laser pump

**Denis Ukolov<sup>1</sup>, Roman Mozhaev<sup>1</sup>, Maxim Cherniak<sup>2</sup>, Alexander Pechenkin<sup>2</sup>**

<sup>1</sup> National Research Nuclear University MEPhI, Moscow, Russia

<sup>2</sup> Specialized Electronic Systems, Moscow, Russia

The paper presents an example of componentwise radiation hardness assurance of optoelectronic components of solid state Yb:YAG laser. The crucial parameters selection for radiation hardness estimation, the measuring method of optical and electrical parameters and special features of radiation testing are described.

In high radiation levels environment optical parameters, such as output optical power, of laser systems may degrade over time depending on amount of total ionizing dose which can lead even up to operational failure of laser system. To prevent such result it is essential to evaluate its radiation hardness and determine the most radiation-sensitive elements and furthermore increase total radiation hardness.

The aim of the work is to justify the importance of “element-by-element” radiation hardness assessment of laser equipment to continuous and pulse ionizing gamma-radiation, neutrons and heavy charged particles.

The subject of the research is diode-pumped solid-state laser with spectral peak 1030 nm. The active medium of the laser is monocrystal of yttrium-aluminum garnet doped with ytterbium manufactured on a heat-conducting substrate with a mirror coating. The laser also contains an output-feedback mirror and pumping laser diodes. The pumping of active medium is carried out through specialized optic fiber into which the focused light emission with wavelength 940 nm is injected. The output mirror of the laser is made of ZrO<sub>2</sub>-SiO<sub>2</sub>.

The important stages of radiation tests are the determination of critical parameters of the “device under test”, preparation of test equipment, design and assembly of optical circuit. The main components of the laser susceptible to degradation under ionizing radiation are: active medium, pumping diode, output mirror and optical fiber.

The main parameters of active medium that degrade when exposed to ionizing radiation are: the lifetime of majority carriers in excited state, the absorption and luminescence spectrum and lasting generation efficiency.

The critical parameters of output mirror and optical fiber is the transmittance of optical radiation of the corresponding wavelength. Radiation induced color centers shifts the transmission spectrum of glass which affects the efficiency of the optical resonator and the pumping efficiency of active medium through the optical fiber.

An important parameter of laser diode is its output optical power, spectrum, forward voltage and current which can degrade under neutron and heavy ions irradiation.

The developed test-bench for parametric control of laser systems components has been successfully evaluated during radiation hardness researches.

The results alongside with schematics will be presented in full paper.

## The influence of network precursor ratio on the crosslinking and radiation resistance of hybrid elastomeric materials

**Slaviša Jovanović<sup>1</sup>, Jaroslava Budinski-Simendić<sup>1</sup>,  
Milena Marinović-Cincović<sup>2</sup>, Gordana Marković<sup>3</sup>, Vesna Teofilović<sup>1</sup>,  
Dejan Kojić<sup>4</sup>, Nevena Vukić<sup>1</sup>, Vojislav Jovanović<sup>5</sup>**

1 University of Novi Sad, Faculty of Technology, Novi Sad, Serbia

2 University of Belgrade, Institute of Nuclear Science Vinča, Belgrade, Serbia

3 Factory Tigar, Pirot, Serbia

4 University of Business Engineering and Management, Faculty of Engineering, Banja Luka, Bosnia and Herzegovina

5 University of Priština, Faculty of Natural Science and Mathematics, Kosovska Mitrovica, Serbia

Materials selected in nuclear processing plants are required to have radiation, thermal and chemical resistance. From experiments on different elastomeric seals materials it was assessed that after a high energy gamma treatment tremendous degradation of properties and compression set exist. Two common network precursors that are used in nuclear power plants are based on ethylene propylene diene rubber (EPDM) and chlorosulfonated polyethylene (CSM). Elastomeric materials based on CSM have good resistance to temperature extremes and chemicals but poor compression set and poor fuel resistance, which is limitation for its sealing application. Blending with other rubbers can improve these properties. *Polar* CSM rubber can interact with their active functional groups ( $-\text{SO}_2\text{Cl}$ ) via substitution or condensation reactions. Hydrocarbon origin of EPDM completely saturated chains (without none double bond that imparts an excellent resistance to ozone, weathering, heat, oxidation and polar fluids) are able to absorb more energy without cracking polymeric chain (thus it is classified as radiation-resistant). EPDM rubbers are used in radiation areas for wire coating materials and electrical cables, due to their good resistance to environmental effects. This work aims to the study the influence of network precursor ratio on crosslinking behaviour and radiation resistance of hybrid materials based on CSM/EPDM and high abrasion carbon black particles (iodine adsorption value 82 g/kg). Rubber compounds were prepared using two-roll mill at 40 °C to obtain sheets, which were pressed at 160 °C during 20 minutes at pressure of 16 MPa. Optimal crosslinking time was determined by moving die rheometer (type MDR2000). It was assessed that the optimum curing time of obtained materials increases with increasing content of CSM. The radiation of prepared hybrid materials was carried out using  $^{60}\text{Co}$  gamma source with the dose rate 10 kGy<sup>-1</sup> and different total absorbed dose (100, 200 and 400 kGy) at ambient temperature. For blends of two rubbers with dissimilar polarity, distribution of crosslink point can be non-equal through phases. Mechanicals properties and swelling properties were estimated for non-radiated and radiated samples. It was assessed that during radiation process, tensile strength, modulus and hardness and of prepared materials increased, but elongation at break decreased up to dose of 200kGy.

## **Possible role of intravascular hemolysis in the pathogenesis of oxidant stress after sublethal ionizing and non-ionising radiation dose effect**

**Anna V. Novikova, Viktor E. Novikov, Anna A. Oleshkevich**

Moscow State Academy of Veterinary Medicine and Biotechnology, Moscow, Russia

A dramatic change in the radiation environment or a sudden electromagnetic disturbance of the environment in most mammals is accompanied by stress. This can be considered as a non-specific reaction to the effect named. The anxiety stage of stress is accompanied by vasoconstriction. This leads to an increase in intravascular hemolysis. In this case the main factor of hemolysis is the erythrocyte's deformation stress. As a result, free oxygenated hemoglobin (Hb) appears in the blood plasma, and Hb-quantity exceeds the capabilities of the plasma hemoglobin detoxification system (haptoglobin, hematoxigenase, etc.). The question raised: Does this event lead to an increase in the level of reactive oxygen species (ROS) in plasma as promoters of oxidative stress?

There are two possible ways to form ROS. 1) heme iron oxidation. When hemi-iron is oxidized by hemoglobin, hemoglobin is converted to methemoglobin, and oxygen is reduced to the superoxide anion radical. 2) (hypothetical) formation of singlet oxygen in the dissociation of extra-erythrocyte hemoglobin. When oxyhemoglobin is deoxygenated, there is a possibility that oxygen is in the singlet state. However, in this case, an excess of heme redox-active iron appears in the plasma, regardless of the state of the released oxygen. This leads to the formation of ROS on the first named path. It should be noted that there are enough substrates in the blood for the intensification of lipid peroxidation (LPO). In other tissues, the development of processes for the intensification of the formation of ROS and the accompanying processes of LPO, should occur much later in time than in blood. Thus, the primary link of oxidative stress under the action of sublethal doses of ionizing radiation or a sharp electromagnetic disturbance of the medium (impulse) should be sought as a reaction of the circulatory system to the effect discussed.

To confirm the hypothesis, it is necessary to prove directly or indirectly the following:

1. Under the beam and immediately after irradiation, there is an intensification of intravascular hemolysis.
2. Increased intravascular hemolysis is accompanied by an increase in the level of ROS in the blood plasma.
3. Increased intravascular hemolysis is a non-specific response to radiation and, by its nature, is associated with the deformation stress of red blood cells.

If the hypothesis is correct, a new additional direction of the protector's search is opened. The search for protectors should be aimed at drugs that lower vasoconstriction during stress, as well as at increasing the rate of utilization (neutralization) of free hemoglobin and heme in plasma.

## **Nitrogen monoxide metabolites as the marker of acute radiation syndrome**

**Mikhail Ksendzuk, Marina Filimonova, Valentina Surinova,  
Alexander Filimonov, Tatyana Podosinnikova, Alina Samsonova**

A. Tsyb Medical Radiological Research Center – branch of the National Medical Research Center of Radiology of the Ministry of Health of the Russian Federation (A. Tsyb MRRC), Obninsk, Russia

Ionizing radiation affects various systems of organism. It is known that irradiation in doses that cause an acute radiation syndrome (ARS) can lead to the critical damage of bone marrow cells and complications, such as sepsis. Infections, including caused by ARS, activate inducible nitric oxide synthase (NOS), an enzyme catalyzing the generation of nitric oxide (NO) from L-arginine. In this regard, the estimation of the level of nitric oxide metabolites can be used as the marker of sepsis, caused by the ARS. It can also be used as the indicator of the effectiveness of radio modifiers based on nitric oxide synthase inhibitors.

The determination of nitric oxide and its metabolites levels in living organism is difficult to execute. Previously, there have been attempts to use such approaches as an indication of the NOS activity in radiobiology and other science, but widely used methods of NO determination have several serious disadvantages, therefore the search for new methods remains an urgent task.

In our work, we investigated the possibility of modifying the existing method for the determination of NO stable metabolites – nitrates and nitrites – to use more accurate electrochemical methods. In contrast to the widely accepted Griss method, the electrochemical methods allow to measure the concentration of nitrates and nitrites without the formation of azo dyes and spectrometry. We used the method of recovery nitrates to nitrites, but instead of spectrometry, we used the ISO-NOP 2mm ion-selective electrode (WPI, USA, Sarasota). The aim of our experiment was to assess the dynamics of the NO metabolites concentration in the liver of mice irradiated with the dose of 7 Gy at different stages of ARS.

According to the results of the experiment, a significant increase of the metabolites level was observed in the late stages of ARS.

The results obtained are confirmed by theory and consistent with the data received by other methods and other investigators. The new method is suitable for radiobiological research. The use of this method will allow to extrapolate experimental data to other species of animals and to humans.

## Activation of lipid peroxidation (LPO) is one of the universal effects of chronic radiation exposure

**Andrey Tugai<sup>1</sup>, Tetiana Tugai<sup>2</sup>, Viktor Zheltonozhsky<sup>3</sup>, Marina Zheltonozhskaya<sup>3</sup>, Olena Polischuk<sup>4</sup>, Leinid Sadovnikov<sup>3</sup>, Natalia Sergeichuk<sup>5</sup>**

1 D.K. Zabolotny Institute of Microbiology and Virology of the NASU, Open International University of Human Development 'Ukraine', Kiev, Ukraine

2 Open International University of Human Development 'Ukraine', D.K. Zabolotny Institute of Microbiology and Virology of the NASU, Kiev, Ukraine

3 Institute for Nuclear Research of the NASU, Kiev, Ukraine

4 National Technical University of Ukraine "Igor Sikorsky Kyiv Polytechnic Institute", Kiev, Ukraine

5 Open International University of Human Development 'Ukraine', Kiev, Ukraine

The study of the effect of chronic radiation doses in natural conditions on alternating micromycete generation is quite complex, difficult to solve, but extremely urgent task. The study of the responses of microscopic fungi, which for several generations have been exposed to chronic radiation, makes it possible obtain important data for understanding the mechanisms of formation of remote consequences irradiation at different levels of their hierarchical organization (from organisms to intracellular). In the literature, there are practically no data on the effect of chronic radiation on subsequent generations of micromycetes with radioadaptive properties. The purpose of the work was to study the contribution of lipid peroxidation processes to the implementation of adaptation in *Cladosporium cladosporioides* strains with radioadaptive properties compared to the control.

It was found that the content of primary metabolites of LP – diene conjugates in the control strain *C. cladosporioides* 4061 increased in exponential stationary growth phases, while in the strain with radioadaptive properties *C. cladosporioides* 4, their level was the same, and the increase was detected at the end of the stationary phase of growth. In the study of the content of secondary metabolites of LPO – malonic dialdehyde (MDA), reversed dependence of the strains examined was observed: linear increase in *C. cladosporioides* 4, and increase at the end of the stationary phase in *C. cladosporioides* 4061.

The effects of chronic irradiation in *C. cladosporioides* 4061 revealed an increase in the content of diene conjugates by 2 times in the exponential phase, and in the stationary phase, the increase did not exceed 125%. In contrast, *C. cladosporioides* 4 did not show a significant increase in the content of primary metabolites of LPO. In contrast, due to exposure to the *C. cladosporioides* 4061 control strain, the MDA level exponentially increased substantially and at the start of the stationary phase at 2.25 and 4.25 times, respectively. In the strain with radioadaptive properties, the increase in the content of MDA in the corresponding phases of growth was almost twice as low as 1.7 and 1.9 times.

Consequently, in the control strain *C. cladosporioides* 4061, the level of increase of primary and secondary metabolites of LPO for irradiation significantly exceeds that of *C. cladosporioides* 4 with radioadaptive properties, indicating that the latter has already developed resistance to the effects of small doses of chronic ionizing radiation.

## Age associated tritium vulnerability in postnatally developing Swiss albino mouse cerebellum

**Narendra Jain**

BBD Government College, Chimanpura (Shahpura) Jaipur, Rajasthan, Jaipur, India

Analyzing the energy situation on a total basis in a long term horizon, it is evident that nuclear energy may make a large addition to energy sources for many countries. Though, after the Fukushima Daiichi accident, this concept has suffered a big blow and serious efforts are under way to reduce the number of nuclear reactors under operation world over. With the development of nuclear power programs, an additional consideration outside the existing radiation protection framework has appeared and now apart from assessing the level of exposure, considerations with regard to the accidents which could release large inventories of radioactivity have become the main focus of attention. With the expansion of the nuclear power programmes, inventories of 'tritium' produced during such processes are bound to increase. Tritium production and release from nuclear detonations and thermonuclear reactors is enormously great and this may pose significant tritium management problems. Uptake studies of tritium have revealed that more tritium from tritiated water (HTO) accumulates in mouse brain as compared to the other organs of the body.

Swiss albino mice belonging to 1, 2, 4 and 6 weeks of age were injected with HTO at a dose 111 kBq/gm body weight. Initial Dose Rate (IDR) is defined as the rate at which the energy is imparted to unit mass of tissue. In the present investigation, when the animals were injected with a single 111.0 kBq/gm. body weight HTO, dose delivered has been calculated to be 0.0092 Gy/day or 0.92 cGy/day. The animals from each age group were autopsied on 1, 7 and 30 days *post-injection* and hence, qualitatively and quantitatively studied for age associated cerebellar vulnerability due to acute tritiated water exposure. In cerebellum, major cytoarchitectural changes occur mainly during the first three weeks after birth. This accounts for its high radiovulnerability and capability to repair the rendered damage during 1 week to 3 weeks of postnatal development, whereas at 4 and 6 weeks of age a tendency towards radioresistance is achieved. As the age advances relatively lesser damage post tritiated water exposure becomes evident. Hence, on the whole, tritium in the form of tritiated water renders appreciable damage on the postnatal development of mouse brain which warrants further investigation.

Recent reports justify that tritium has appeared as an occupational hazard mainly as tritiated water of high specific activity or as tritium gas. Most tritium is released into the environment as HTO, elementary HT or rarely as tritiated methane gas. Also, certain liquid effluents containing tritiated compounds may further constitute a peculiar risk as they are preferentially incorporated by living organisms. Tritium as a gas or as tritiated water can reach the body tissues of animals as it can be absorbed in either form by way of the skin or the lungs or it can also be ingested in the form of food as organically bound tritium (OBT) or as drinking water. Tritium gets fixed in the skin and hence, is transmitted to body fluids when skin is brought in contact with surfaces that have been exposed to tritiated H gas (HT or T<sub>2</sub>). OBT is formed in microorganisms, plants as well as in animals; Considerable information on transfer of HTO and OBT to milk and meat and on that to the growing organism has been obtained. Tritium in liquid effluents released in aquatic environments can come from several sources and occur in different physico-chemical forms. Certain organic compounds may constitute a particular risk due to their preferential absorption by aquatic microorganisms. As long as OBT is exchangeable with water, its behaviour may be unpredictable and the simulation with the way tritium will behave in different metabolic pathways face difficulty. Though, tritium exposure in the form of HTO has been considered not very toxic, yet the metabolism of tritium in mammals and man needs a careful evaluation when all forms of tritium have to be taken into account in terms of effects. For single generation studies, the course of tritium incorporation and its turnover is important, however, it is of less consequence in the case of multigenerational studies when the animals are chronically or continuously exposed to HTO. In such a situation, the maximum activity in the organism should remain constant. Looking into this fact, the present investigation has been designed to understand the behaviour of tritium with relation to the cerebellar architecture of Swiss albino mice following a single acute dose.

## New therapeutic strategy for medulloblastoma: $\mu$ S Pulse Electric Field exposure targeting cancer stem cells to promote radiosensitization

**Mirella Tanori<sup>1</sup>, Arianna Casciati<sup>1</sup>, Barbara Tanno<sup>1</sup>,  
Paola Giardullo<sup>2</sup>, Alessandro Zambotti<sup>1</sup>, Carmela Marino<sup>1</sup>,  
Caterina Merla<sup>1</sup>, Mariateresa Mancuso<sup>1</sup>**

<sup>1</sup> ENEA, Rome, Italy

<sup>2</sup> Guglielmo Marconi University, Rome, Italy

Medulloblastoma (MB) is the most common pediatric malignant brain tumor. Its conventional therapy consists of surgical resection followed by chemotherapy and radiotherapy that often involve severe neurocognitive deficiencies. Cancer stem cells (CSCs) seem to be candidates in the onset of the disease and constitute an endless reserve for the maintenance and progression of the tumor and it could be the reason of conventional therapy failure. Moreover, the quiescence state is the survival strategy of CSCs responsible for the later recurrence and relapses. Therefore, new therapeutic strategies are necessary to reduce not only long-term toxicity of radiotherapy or chemotherapeutic agents, but also to targeting specifically CSCs. The goal of this study is selectively target quiescent malignant CSCs and subsequently induce a differentiation process to sensitize them to radiotherapy treatment using appropriately modulated pulse electric fields (PEFs).

We started to characterize different MB cell lines in term of CSCs content. The D283 cells resulted a perfect model of MB SCs. They showed almost 100% of CD133 positive cells and this feature defined their high oncogenic potential and a major capacity to form neurospheres and to engraft in nude mice with respect to the other cell lines.

Exposure of living cells to PEFs is able to change the permeability of the cell membrane by modifying its molecular structure opening pores, causes the influx of ion permeation, inducing various cellular reactions, including signal transduction, stress response and cell death. Therefore, EF signal itself may lead to a multiple effect on the unhealthy cell target, thus achieving a potentiation of the anticancer therapy, but a crucial point involves the selective neutralization. To this aim different PEFs are been selected to be effective in D283 cells but not in Normal Human Astrocyte (NHA). In particular the  $\mu$ sPEF-3 (40  $\mu$ s 0.35 MV/m 5 pulses) exposure induced a different response in term of cell death and cell cycle perturbation. To provide deep insight into the mechanism that differentiates the response we focused our attention in cell cycle network as a molecular point of view, using the RT<sup>2</sup> Profiler PCR Arrays. The molecular analysis showed that  $\mu$ sPEF-3 induced the G2/M arrest via the up-regulation of GADD45a that could be crucial for the choice of the cell fate activating apoptosis, senescence or differentiation mediated by stress-activated p38 MAPK process.

Our results suggest that this new therapeutic approach could be suitable as pre-treatment to promote radiosensitization. Combined  $\mu$ sPEFs treatment with ionizing radiation exposure could represent an innovative strategy that will improve the clinical outcome.

**Acknowledgments:** This project has received funding from the European Union's Horizon 2020 research and innovation programme under grant agreement No 737164 Sumcastec.

## Radiation-induced cataract in *Ptch1*<sup>+/-</sup> mice: Exploring the role of age, dose, dose rate and genetic background

**Ilaria De Stefano<sup>1</sup>, Barbara Tanno<sup>1</sup>, Simona Leonardi<sup>1</sup>,  
Emanuela Pasquali<sup>1</sup>, Francesca Antonelli<sup>1</sup>, Paola Giardullo<sup>2</sup>,  
Arianna Casciati<sup>1</sup>, Mirella Tanori<sup>1</sup>, Gabriele Babini<sup>3</sup>,  
LDLensRad Consortium<sup>4</sup>, Simonetta Pazzaglia<sup>1</sup>, Mariateresa Mancuso<sup>1</sup>**

<sup>1</sup> Laboratory of Biomedical Technologies, Agenzia Nazionale per le Nuove Tecnologie, l'Energia e lo Sviluppo Economico Sostenibile (ENEA), Rome, Italy

<sup>2</sup> Department of Radiation Physics, Guglielmo Marconi University, Rome, Italy, Rome, Italy

<sup>3</sup> Department of Physics, University of Pavia, Rome, Italy

<sup>4</sup> LDLensRad: Towards a full mechanistic understanding of low dose radiation induced cataracts. Partners: Public Health England (Liz Ainsbury, PHE), Agenzia Nazionale per le Nuove Tecnologie, l'Energia e lo Sviluppo Economico Sostenibile (Mariateresa Mancuso, ENEA), Helmholtz Zentrum München (Joachim Graw, HMGU), Durham University (Roy Quinlan, DU), Oxford Brookes University (Munira Kadim, OBU), Chilton, United Kingdom

Cataract risk after ionizing radiation (IR) exposure is well established, but the increased cataract incidence after low-dose ionizing radiation has highlighted how little is still understood about the biological responses of the lens to IR. The EU project LDLensRad aims to answer this question. In particular, it aims to understand the impact of genetic background and age on the biological response of the lens to IR.

To elucidate these aspects, *Ptch1*<sup>+/-</sup> mice of 2 days and 10 wks of age, bred on two different genetic backgrounds (CD1 and C57BL/6J), were whole-body irradiated with 0, 0.5, 1 and 2 Gy of gamma-rays (<sup>60</sup>Co) at different dose rates (0.3 or 0.063 Gy/min). Quantitative analysis of the lens density by Scheimpflug analysis was carried out on each mouse on a monthly basis up to 18 mth post irradiation, in order to track the appearance and development of cataracts.

Results show that the genetic background hosting the mutation and the age at irradiation dramatically alters the individual risk for developing cataract. In fact, CD1-*Ptch1*<sup>+/-</sup> mice irradiated at 2 days develop cataract with high incidence and short latency, instead C57BL/6J-*Ptch1*<sup>+/-</sup> mice are completely resistant to cataract induction by radiation, suggesting that interactions between genetic and modifier factors underlie susceptibility to radio-induced cataractogenesis. Furthermore, adult irradiation does not increase cataract induction irrespective of genetic background on which *Ptch1* mutant mice are maintained.

To show miRNA-mediated regulation may be a mechanism responsible for incomplete gene penetrance in C57BL/6-*Ptch1*<sup>+/-</sup> mice, we also explanted lenses 24 hrs after exposure and assessed for miRNome analysis using Next Generation Sequencing. Our preliminary results show that genetic background produced significant differences in the deregulated miRNA lists. A lower number of significantly deregulated miRNAs, associated to slightly different molecular pathways, were identified following the different doses of ionizing radiation. Comparisons between identified miRNAs and pathways among the different conditions will be presented and discussed.

**Acknowledgments:** The LDLensRad project has received funding from the Euratom research and training programme 2014-2018 in the framework of the CONCERT [grant agreement No 662287].

## Effects of radiation damage in ATLAS Roman Pots (ALFA & AFP)

**Marko Milovanovic<sup>1</sup>, Maciej Trzebinski<sup>2</sup>, Michael Rijssenbeek<sup>3</sup>,  
Karlheinz Hiller<sup>1</sup>, Patrick Fassnacht<sup>4</sup>, Tomas Sykora<sup>5</sup>,  
Sebastian Grinstein<sup>6</sup>, Marco Bruschi<sup>7</sup>, Hasko Stenzel<sup>8</sup>**

1 DESY (Deutsches Elektronen Synchrotron), Zeuthen, Germany

2 Polish Academy of Sciences, Krakow, Poland

3 Stony Brook University, Brookhaven, NY, United States

4 CERN (European Organization for Nuclear Research), Geneva, Switzerland

5 Charles University, Prague, Czech Republic

6 IFAE (Institut de Fisica d'Altes Energies), Barcelona, Spain

7 INFN (Istituto Nazionale di Fisica Nucleare), Bologna, Italy

8 Justus Liebig University, Giessen, Germany

The ATLAS Roman Pots are a part of the ATLAS Forward detector system which consists of two subsystems, the ALFA (Absolute Luminosity For ATLAS) and the ATLAS Forward Proton (AFP) detector. ALFA was designed to determine the total proton-proton cross-section as well as the luminosity at the Large Hadron Collider (LHC) by measuring elastic proton scattering at very small angles, in a low luminosity environment, while the AFP is optimized for diffractive measurements and substantially improves ALFA coverage in a wide range of resonance mass. Together with the envisaged Time-of-Flight (ToF) system, AFP will also be able to conduct measurements at high instantaneous luminosities, by providing information on the diffractive vertex position.

The ALFA detector is based on scintillator fibers placed in Roman Pots close to the LHC proton beam at around 240m from the ATLAS Interaction Point (IP) on each side, while the AFP uses FEI4b 3D pixel based Silicon Tracker (SiT) placed at around 210m from the IP on both sides. To increase the physics sensitivity, the fibers and sensors have to be placed as close as possible to the proton beam (around 2-3mm). Thus, the system is required to sustain high radiation doses. Particularly challenging is the non-uniform nature of the dose distribution.

This poster presentation would shed a light on how these challenges are (being) mitigated and give an overview of the sustained radiation damage in both sensors and readout electronics of the ATLAS Roman Pots Forward Detector System.

## Radiation induced 3D structuring of chalcogenide glass thin films

Miroslav Vlcek<sup>1</sup>, Karel Palka<sup>2</sup>,  
Stanislav Slang<sup>1</sup>, Liudmila Loghina<sup>1</sup>, Anastasia Iakovleva<sup>1</sup>

<sup>1</sup> CEMNAT FCHT University of Pardubice, Pardubice, Czech Republic

<sup>2</sup> KOANCH FCHT University of Pardubice, Pardubice, Czech Republic

Chalcogenide glasses (CHGs) are extraordinary materials for photonics as they possess wide optical transparency window from VIS to far IR spectral region, high refractive index (2,0 – 3,2) and high optical nonlinearity. The weaker covalent bonds in CHGs cause significantly lower rigidity and lower softening temperatures relative to oxide glasses. It results in their sensitivity to various radiation, which can result either in changes of their optical properties and chemical resistance or to direct surface corrugation. All these phenomena can be exploited for fabrication of diffractive optical elements (DOE) in these materials.

In this contribution, we present our results of 3D micro- and nano-structuring of CHGs thin films as a result of radiation induced structural changes/mass transport. We demonstrate that the nature of the radiation induced phenomena is multifactorial. It depends not only on glass composition (in our case binary and ternary systems as As-S, As-Se, As-S-Se, Ge-S, Ge-S-Se, Ge-Sb-S), method of thin layers preparation (we applied classical vacuum evaporation method and spin coating) and their prehistory (e.g. thermal prehistory), but also on the type and intensity of interacting radiation (band gap or super-band gap radiation, electron beam) and conditions of the experiment (temperature, air/inert atmosphere etc.). We give evidence that exposure with suitable radiation significantly influences selectivity of consequent wet etching of CHG thin layers in various alkaline solutions and that in case of focused high energy laser beam exposure direct patterning of thin films is possible.

Various methods such as UV-VIS, Raman, IR, XPS, SEM, AFM were exploited for complex studies of radiation induced structure/properties changes and to propose possible mechanisms of different energy photons interaction with thin chalcogenide films. Examples of micro and nano structuring for fabrication of various DOE (gratings, Fresnel lenses, microlens arrays, etc.) in these high refractive and IR transparent materials are given.

**Acknowledgments:** Authors appreciate financial support from European Regional Development Fund-Project "Modernization and upgrade of the CEMNAT" (No. CZ.02.1.01/0.0/0.0/16\_013/0001829) and support from the grants LM2015082 and ED4.100/11.0251 from the Ministry of Education, Youth and Sports of the Czech Republic.

## The influence of pharmaceuticals on the ionization and excitation of molecules while exposed to ionizing radiation

**Galina P. Zhurakovskaya, Svetlana V. Belkina**

A.Tsyb Medical Radiological Research Center, Obninsk, Russia

Under the action of high-energy ionizing radiation, along with ionization of molecules and atoms by electrons, excitation is induced by UV light (Vavilov-Cherenkov radiation). The ability of cells to repair a certain portion of radiation damage under the action of visible light proves the existence of UV damage.

The purpose of this project is to determine the role of radiosensitizers and radioprotectors in the manifestation of the photoreactivation effect of cells after the action of ionizing radiation.

Bacterial cells of *E. coli* strain B<sub>s-1</sub>, which are hypersensitive to UV light were used. Cells were irradiated by gamma-rays of Co-60 in the presence of cisplatin (sensitizer) or a cysteamine (protector). In the post-radiation period, the cells were photoreactivated with visible light.

Photoreactivation of cells irradiated with ionizing radiation in the presence of cisplatin significantly influenced the final result: the photoreactivation process fully compensated for the sensitizing effect of the chemical, restoring damage and increasing survival to the level of survival observed after exposure to a ionizing radiation alone. The obtained data can be considered as evidence that the sensitizing effect of cisplatin is to contribute to the formation of additional damage not by ionization of molecules as a result of ionizing radiation, but by excitation causing UV damage. The presence of cysteamine protector under the influence of gamma-rays led to the loss of the cell ability to photoreactive radiation damage under the action of visible light in the postradiation period. As a result of the combined action of the protector and ionizing radiation, cell death is predominantly due to the ionization of molecules and there is practically no damage to the cells caused by excitation. In other words, cysteamine, protecting cells from radiation damage, primarily protects them from the action of ultraviolet light, as one of the components of ionizing radiation.

The detected effects showed how complex is the sequence of events leading to the development of radiation damage to the cell and how the excitation of molecules, which had been neglected for a long time, causes biologically significant effects.



**Radiation  
in  
Medicine**

**25**

## Clinical significance of radioimmunoassay (RIA) and immunoradiometric assay (IRMA) in endocrinology

**Mirjana M. Petrović<sup>1</sup>, Živorad N. Savić<sup>1</sup>, Katarina Ž. Savić<sup>1</sup>, Sofija Ž. Savić<sup>1</sup>, Aleksandra R. Vasiljević<sup>1</sup>, Dušanka R. Petrović<sup>1</sup>, Dragana D. Brakočević<sup>2</sup>, Danica M. Kovljanić<sup>2</sup>, Valentina S. Radunović<sup>2</sup>, Vanja Puletić<sup>3</sup>, Drina Lj. Janković<sup>4</sup>, Aleksandar A. Vukadinović<sup>4</sup>, Vojislav Antić<sup>1</sup>, Vladimir Jurišić<sup>5</sup>**

1 Clinical Centre of Serbia, Belgrade, Serbia

2 Health Center Vračar, Belgrade, Serbia

3 Health Center Kotor, Kotor, Montenegro

4 Vinča Institute of Nuclear Science, Belgrade, Serbia

5 University of Kragujevac, Faculty of Medical Sciences, Kragujevac, Serbia

Radiopharmaceuticals are compounds used in human medicine for the diagnosis of 95% and therapy of 5%. Radiopharmaceuticals are used by in-vivo and in-vitro in medicine. In-vitro application includes RIA methods (radioimmunoassay) in clinical laboratories. RIA methods are methods with bookmarks, i.e. the indicator molecule is marked with a radioactive isotope <sup>125</sup>J with a half-life of 60 days. RIA methods are the most sensitive quantitative and qualitative techniques.

A radioimmunoassay (RIA) is an immunoassay that uses radiolabeled molecules in a stepwise formation of immune complexes. Immunoradiometric assay (IRMA) is an assay that uses radiolabeled antibodies. It differs from conventional RIA in that the compound to be measured combines immediately with the radiolabeled antibodies, rather than displacing another antigen by degrees over some period.

RIA and IRMA are the most commonly used techniques which allow the measurement of a wide range of materials of clinical and biological importance, especially in endocrinology for estimation of hormones. These techniques have a significant impact on medical diagnosis due to the ease with which the tests can be carried out, while assuring precision, specificity and sensitivity. These techniques achieve sensitivity through the use of radionuclides and specificity that is uniquely associated with immunochemical reactions. They are largely used for measuring biologically active compounds present in low concentrations, such as hormones, proteins, drugs, microorganisms, etc.

The radioimmunoassay (RIA) method is employed to determine numerous hormones, enzymes, antigens, and drugs in very low quantities ( $10^{-12}$ – $10^{-9}$  M) in human plasma in order to assess various diseases. In RIA, the immunologic reaction between the antigen and the antibody is highly specific, and hence the method has high specificity. The accuracy of the method depends on various experimental factors and the specificity of the antigen–antibody reaction. The precision of RIA is affected by experimental errors in pipetting of reagents, chemical separation of the complex, and counting. IRMA is much more sensitive to RIA, which in some cases (e.g. in TSH) is very significant. Because of the use of monoclonal antibodies in the first phase of the reaction, this system has a much better specificity, which significantly reduces errors due to cross-reactions with other hormones.

## On the issue of control of equivalent doses of radiation for the eye lens for medical personnel

**Ekaterina Shleenkova, George Kaidanovsky, Stepan Bazhin, Vladimir Iliyn**

Saint-Petersburg Research Institute of Radiation Hygiene after Professor P.V. Ramzaev, Saint-Petersburg, Russia

The main effect of radiation of the eye lens is the radiation cataract. By data UNSCEAR risk of developing of a cataract was higher, than it was considered earlier. In this regard, the new standard of IAEA provides introduction of the new dose limit: an equivalent dose 20 mSv per year, average in five consecutive years (100 mSv in 5 years), and 50 mSv for any separate year was entered. The preliminary analysis of literary data shows that the new dose limit can be exceeded when carrying out a number of works with use of sources of ionizing radiation.

The staff of Laboratory of Radiation Control of Saint-Petersburg Research Institute of Radiation Hygiene after Professor P.V. Ramzaev investigated individual whole-body doses  $H_p(10)$  (position of the dosimeter over a protective apron and under a protective apron) and eye lens doses  $H_p(3)$  of personnel of X-ray surgical units of one hospital of St. Petersburg. Time of exposure was three months.

It was shown that in 42 cases from the 199th dose of radiation of the eye lens exceed 1.0 mSv, from them in 9 cases – 4.0 mSv, the maximum and minimum values are 0.1 mSv and 8.6 mSv respectively. At the same time, there are still exceptions caused, apparently, by the fact that the personnel during the work with sources of ionizing radiation not always used the dosimeter intended for measurement of doses of radiation of the eye lens.

Comparison of results of measurement of doses of radiation of the eye lens with doses registered by the dosimeters located over a protective apron shows that these doses are comparable in size and differ from each other not more than by 4 times.

## **Radiologic examination of urinary tract in children with special reference to ionizing radiation**

**Đurđica Milković, Danica Batinić**

Children Hospital Srebrnjak, Zagreb, Croatia

Radiologic imaging is valuable as a diagnostic tool in children with urinary tract diseases. However, it requires precise imaging protocols, sometimes there is need for sedation or general anaesthesia for longer procedures such as MRI, skilful healthcare personnel, expertise for evaluating the images, and most importantly it requires consideration for radiation exposure if ionizing radiation is being used. Children are more sensitive to radiation exposure than adults and have longer time ahead of them to manifest radiation-induced effects and injuries. Therefore, it is of great importance to reduce or minimise the radiation dose to children. The International Radiation Protection Commission (ICRP) of 1991 recommends the use of radiation and protection on principle ALAR (as low as reasonably achievable). Nowadays, ultrasound examination is the first method for imaging of urinary tract in children. There is no radiation exposure, but frequently further examination is required. Taking in account the incidence of vesicoureteral reflux in children, voiding cystourethrography (VCUG) is the next method. However, radiation dose is with VCUG high and in girls exposition of gonads is unavoidable. Fortunately, VCUG is increasingly replaced with ultrasound cystography. In past iv urography was used to display kidneys. However, it gives a high dose of radiation. Today iv urography is completely omitted, and replaced with MSCT urography. Special protocols for MSCT in children with decreased dose and time of exposure are developed. Whenever it is possible, better solution is MRI urography. The new modality of imaging with so-called functional MRI urography provides next to anatomical data kidney function, too.

## **Assessment of volume averaging effects in thimble ion chambers for flattening filter free photon beams**

**Francisco Cutanda-Henriquez, Silvia Vargas Castrillon**

Edinburgh Cancer Centre, Edinburgh, United Kingdom

This study describes a novel and straightforward method to assess volume averaging effects in thimble ion chambers when irradiated with flattening filter free (FFF). The use of FFF beams is increasing steadily, as they provide shorter beam on times in complex, modulated irradiations. This is particularly important when patient motion can affect the quality of the irradiation, but it also poses new challenges in absolute dosimetry.

In air measurements with standard equipment is all that is needed to perform the assessments: dose measurements at different, carefully controlled, source to chambers distances are compared. The magnitude of the effect depends on the distance, and it can be assessed after other effects are corrected for.

A Varian TrueBeam linear accelerator was used for this study. Measurements were carried out at distances ranging from 80 to 125 cm source to chamber axis distances (SAD), with flattened beams of 6 MV and 10 MV nominal energies, and FFF beams of 6 MV and 10 MV nominal energies. Two Farmer type ion chambers (NE 2571), and two small volume ion chambers (PTW 31015 PinPoint and PTW 31016 PinPoint 3D) were used with a Sun Nuclear PCE electrometer. Brass build up caps, equivalent to 2 cm of water, were used for all measurements. Variations of ion recombination, as dose per pulse changes with distance, were corrected for using the two voltage technique.

The range of the effect on measured dose of volume averaging has been estimated for 6 FFF (0.2% – 0.7%) and 10 FFF (0.6% – 1.5%) for the Farmer ion chambers, for the above measured range of SADs. The PinPoint ion chambers show negligible effects for 6 FFF and they range 0.1% – 0.3% for 10 FFF.

This method can be easily implemented as an additional test for ion chamber quality assurance. It should be possible to use it in the same way in Elekta linacs, although results could be different. This method could be included in the procedure for absorbed dose determination along with the spectral difference effect already described in the literature. The estimation of volume averaging effects allows Radiotherapy Physics departments to better assess the uncertainty of their calibrations for this type of non flattened photon beams.

## Evaluation of radiation dose at optimized protocols for some standard MDCT examinations in a large university hospital

**Darka Hadnađev Šimonji<sup>1</sup>, Olivera Nikolić<sup>1</sup>, Marijana Basta Nikolić<sup>1</sup>,  
Olivera Ciraj Bjelac<sup>2</sup>, Sanja Stojanović<sup>1</sup>, Mirela Juković<sup>1</sup>**

<sup>1</sup> Clinical Center of Vojvodina, Novi Sad, Serbia

<sup>2</sup> Vinca Institute of Nuclear Sciences, Belgrade, Serbia

**Purpose.** The goal of the research is to define the optimal examination protocol by multislice CT in diagnostics of certain body regions as well as to determine radiation doses and risks for patients both before and after protocol optimization.

**Methods.** This prospective study comprised 396 adult patients divided into groups according to body regions which have been scanned: I-unenhanced head CT, II-contrast enhanced head CT, III-chest CT, IV-abdominal and pelvic CT. In separate prospective studies groups for dose optimization have also been CT urography (40 patients) and sinus CT (50 patients). All studies have been conducted in two phases: in the first phase standard protocol for the scanned body region has been applied, and in the second phase CT examinations have been carried out according to the modified protocol (by changes of the exposure parameters such as mAs values, and in CT urography group tube voltage as well), with minimum requirements regarding the image quality.

**Results.** The results have shown that by optimal protocol selection in the sense of exposition parameters, it is possible to reduce significantly radiation dose regarding CTDI<sub>vol</sub> at unenhanced head CT examination for 7.5%, at contrast enhanced head CT examination for 7%, at chest CT examination for 40%, at abdominal and pelvic CT examination for 25%, at sinus CT examination for 52% and CT urography for 45%.

**Conclusion.** By selection of protocol in the sense of exposition parameters it is possible to reduce radiation dose significantly along with preserving image quality which is sufficient for adequate radiological image interpretation.

## Image quality and delivered dose in neuroradiological procedures

Monica Cavallari<sup>1</sup>, Laura Mantovani<sup>2</sup>, Loredana D'Ercole<sup>2</sup>,  
Nicoletta Paruccini<sup>3</sup>, Raffaele Villa<sup>4</sup>, Raffaella Soavi<sup>5</sup>

1 IRCCS Fondazione Policlinico San Matteo - Università degli Studi di Milano, Pavia, Italy

2 IRCCS Fondazione Policlinico San Matteo, Pavia, Italy

3 ASST di Monza – Ospedale San Gerardo-, Monza, Italy

4 Azienda Ospedaliero-Universitaria Maggiore della Carità Novara, Novara, Italy

5 USL Bologna, Bologna, Italy

**Purpose.** Analysis of brain interventional procedure from radiological equipment characterization to the clinical practice evaluation.

The aim is to assess the achieved level of optimization, considering different way of acquisition in term of image quality (IQ) and delivered dose.

**Material and Methods.** Three Italian centre (A, B, C) collected data related to 425 cerebral angiography and 234 cerebral embolization. Procedures were performed using Philips Allura FD 20 (monoplane system) in centres A and B and Philips Allura FD2020 (biplane system) in the centre C.

In order to evaluate image quality, images of a step wedge aluminium phantom into a 16 cm PMMA phantom were acquired; Low Contrast Detectability (LCD) was assessed using a Matlab program that automatically analyses images of the dedicated phantom to have a statistical evaluation of LCD. In the same asset the phantom input dose was measured, too.

Considering the results obtained, we analyse the clinical procedures to evaluate which settings could be optimized, in order to minimize patient dose. The procedures were performed using low-dose fluoroscopy (Low) and X-ray image subtraction (DSA).

**Results.** *LCD in Low fluoroscopy mode:* A's values are lower than B and C's ones. There isn't dose reduction related to the image quality's loss because the phantom input doses are comparable.

*LCD in DSA:* C shows the image quality index higher than A and B, with a great dose reduction (17%).

*Clinical practice in cerebral angiography:* centre B has fluoroscopy KAP- fluoroscopy time (FT) ratio and acquisition KAP over number of image (NI) values much higher than A's ones (fluoroscopy KAP/FT: 2.7 vs 1.3; acquisition KAP/NI: 0.9 vs 0.4). Detector and phantom input dose values do not justify these differences: the discrepancy between KAP values in the procedures is due to the different beam size. The acquisition protocols provided by the centres confirm the use of smaller FOVs in centre A (FOV 19-27) compared to centre B (FOV 27-37).

In fluoroscopy mode, C and B has the same FOV (27-37) but C lower KAP value (fluoroscopy KAP/FT: 2.7 centre B, 1.8 centre C). This is caused by the different numbers of pps used in the clinical practice (12.5 p/s in C e 15 p/s in B).

*Clinical practice in embolization:* C's fluoroscopy KAP is higher than A's ones, despite C has lower FT.

As for brain angiography, the difference is probably due to the use of larger FOVs in the centre C.

Air Kerma is unrelated from beam size so C has lower values, due to lower number of fps and low-dose modality in acquisition.

**Conclusion.** Optimization of interventional procedures should provide a characterization in terms of image quality of the different acquisition modality, which results into different patient doses in the clinic. Even if the analysis of clinical data and the optimization of interventional procedure are complex, they are very important for the reduction of patient dose.

## Possible use of CMOS image sensors in radioguided surgery with $\beta$ emitters

**Luisa Alunni Solestizi**

INFN, Perugia, Italy

A feasibility study about the employment of commercial-of-the-shelf CMOS image sensors in a real-time probe for radioguided surgery is proposed. The radioguided surgery (RGS) is a surgical technique that helps the surgeon to evaluate the complete resection of a tumoral lesion up to a millimetric resolution. This procedure makes use of a portable probe able to detect the emission of a radio-tracer preferentially taken up by the tumour. The background induced by the high penetration power of the gamma radiation is the main limiting factor of the current RGS. For that reason, the CMOS image sensors' detection capability of positrons and electrons in view of a  $\beta$ -probe prototype needs to be investigated. CMOS sensors have already shown, in our previous studies, high detection efficiency, high spatial resolution, and rejection capability of photons due to the thin thickness (down to a few microns) of their epitaxial layer. In this work, campaigns of measurement have been conducted on sources of different  $\beta$ -emitters, characterised by different activities and shapes. The performances of two CMOS sensors have been studied and compared: the MT9V011, featuring a sensitive surface of  $3.58 \times 2.69 \text{ mm}^2$  and a matrix of  $640 \times 480$  pixels and the MT9V115, with a surface of  $1.134 \times 0.854 \text{ mm}^2$  and a matrix of  $648 \times 488$  pixels. Several layer of copper of variable thickness have been interposed between source and sensor, and the same measurement configurations have been repeated using a photon spectrometer as detector. The aim of this campaigns was to distinguish the signals of photons and positrons, given the contribution of both annihilation ( $E=511 \text{ keV}$ ) and bremsstrahlung photons, and find an estimate of the positron flux detected by the sensor depending on the copper filter thickness. A pre-existent data-analysis framework, already validated on  $\beta$ - $\gamma$  sources, has been adjusted to optimize the discrimination capability between positrons and photons.

## New approach for prevention and treatment of radiation induced heart disease: Molecular hydrogen significantly reduces the effects of oxidative stress

Jan Slezak

Center of Experimental Medicine, Institute for Heart Research, Slovak Academy of Sciences, Bratislava, Slovakia

**Introduction.** During oxidative stress highly reactive hydroxyl and nitrosyl radicals can damage critical macromolecules such as DNA, proteins or membranes.  $\bullet\text{OH}$  radicals react with essentially any biological molecule present at the site of formation at a diffusion-controlled rate. Scavenging of free radicals may act preventively or therapeutically and such a unique substance appears to be molecular hydrogen ( $\text{H}_2$ ). Effects of  $\text{H}_2$  have been attributed to several major molecular mechanisms: a specific scavenging activity of hydroxyl radicals and peroxynitrite, alterations of gene expressions and signal modulating activities. Recently  $\text{H}_2$  is recognized as possible activator of Nrf2.

**Methods.** In experiments on Wistar rats, we studied the effect of  $\text{H}_2$  on oxidative stress of the heart and ATP formation in the mitochondria of the heart after inducing production of OH radicals by mediastinal irradiation of 10 Gy. Mitochondrial function was studied by measuring oxidative phosphorylation and Coenzymes Q concentration. Changes in translocation of left ventricular myocardium Nrf2 were studied using WB.

**Results.** Treatment with  $\text{H}_2$  provides significant reductions in levels of oxidative markers (MDA, 4-HNE), inflammation (TNF  $\alpha$ ) and markers of antioxidant status (GSH, SOD).  $\text{H}_2$  treatment increases concentration of Coenzyme Q in the tissue and in the mitochondria of the cardiac muscle and the stimulation of ATP production in the mitochondria of the myocardium via oxidative phosphorylation.

**Conclusion.** We demonstrated scavenging  $\bullet\text{OH}$  by molecular hydrogen by following high-molar-mass hyaluronan (HA) degradation in "in vitro" system. In the in vivo studies  $\text{H}_2$  was able to reduce oxidative stress.  $\text{H}_2$  offers antioxidant protection and decrease oxidative and inflammatory markers. It is suggested that  $\text{H}_2$  may act through stimulating Nrf2 and its translocation into nucleus thus promoting innate antioxidative enzymes and may exert anti-inflammatory and, anti-apoptotic effects. Thus  $\text{H}_2$  may represent a novel therapeutic strategy to mitigate oxidative stress and its consequences.

**Acknowledgments:** Supported by grants APVV-15-0376, VEGA 2/0063/18 and VEGA 2/0021/15.

## Activation of cyclotron construction elements

**Magdalena Długosz-Lisiecka<sup>1</sup>, Teresa Jakubowska<sup>2</sup>, Magdalena Zbrojewska<sup>1</sup>**

<sup>1</sup> Lodz University of Technology, Lodz, Poland

<sup>2</sup> Provincial Specialist Hospital, name of M. Kopernika in Łódź, Lodz, Poland

The medical cyclotron facility at PET-CT Laboratory in Provincial Multidisciplinary Center of Oncology and Traumatology in Lodz (11 MeV) is applied for the production of positron emitting radionuclides <sup>18</sup>F and <sup>11</sup>C. The pharmaceuticals labeled with these radioisotopes are used for positron emission tomography (PET) imaging.

This study aims to present the activation effects of irradiation cyclotron construction, during the <sup>18</sup>F or <sup>11</sup>C production. The <sup>18</sup>F target has thin circular foil composed of a metal alloy (Havar), that is highly activated by the proton beam and secondary neutrons. The silver target body is highly activated, also. In result several artificial radionuclides, activated in elements of cyclotron can impure target, during production <sup>18</sup>F or <sup>11</sup>C sessions, e.g. Mn-56, Co-56, Zn-65 or Cd-107 and Cd-109. Activities of several radionuclides in cyclotron construction elements have been estimated and control in FDG-F-18 purification process.

## Myocardial connexin-43 and PKC signaling are involved in adaptation of the heart to irradiation-induced injury: Implication of miR-1 and miR-21

**Narcisa Tribulova<sup>1</sup>, Csilla Viczenczova<sup>1</sup>, Barbara Szeiffova Bacova<sup>1</sup>,  
Tamara Egan Benova<sup>1</sup>, Branislav Kura<sup>1</sup>, Chang Yin<sup>2</sup>, Rakesh Kukreja<sup>2</sup>**

<sup>1</sup> Institute for Heart Research CEM SAS, Bratislava, Slovakia

<sup>2</sup> Virginia Commonwealth University, Virginia, United States

**Objective.** Intercellular connexin-43 (Cx43) channels are essential for electrical coupling and direct cardiac cell to cell communication to ensure heart function. Expression of Cx43 is altered due to stressful conditions and also affected by the alterations in extracellular matrix. We aimed to explore the effect of chest irradiation on myocardial expression of Cx43 and miR-1 which regulates GJA1 gene transcription for Cx43. Implication of miR-21 that regulates expression of extracellular matrix proteins and PKC signalling that may affect Cx43-mediated coupling was examined as well.

**Methods.** Healthy adult, male Wistar rats were irradiated with a single 25 Gray (Gy) dose on thorax. Six weeks later, the animals were anesthetized and hearts were excised. Left ventricular tissue was isolated for determination of Cx43 distribution and expression of Cx43, PKC-delta, PKC-epsilon, miRNA-1 and miR-21 using immunohisto-chemistry, western blotting and real-time PCR respectively.

**Results.** Western blot and real-time PCR analyses revealed that six weeks after the exposure of healthy Wistar rats chest to single irradiation of 25 Gy significant myocardial alterations were observed: 1) increase of total Cx43 protein expression and its functional phosphorylated forms; 2) suppressed levels of miR-1; 3) enhanced expression of PKC $\epsilon$  which phosphorylates Cx43; 4) increase of miR-21 levels; 5) increase of PKC $\delta$  expression. These results suggest that irradiation causes post-transcriptional regulation of myocardial Cx43 expression by miR-1 possibly through miR-21 and PKC signalling.

**Conclusions.** Findings suggest that single dose of irradiation has the potential to enhance myocardial intercellular communication that might be beneficial for the heart. It is challenging to investigate impact of single dose irradiation on heart function and susceptibility to arrhythmias in animals exhibiting cardiovascular risk factors, such as hypertension, diabetes or dislipidemia.

**Acknowledgments:** This work was supported by VEGA grants No 2/0076/16, 2/0159/19, 2/0063/18

## **Irradiation-induced cardiac connexin-43 and miR-21 responses are hampered by treatment with atorvastatin and aspirin**

**Barbara Szeiffova Bacova<sup>1</sup>, Csilla Viczenczova<sup>1</sup>, Branislav Kura<sup>1</sup>, Tamara Egan Benova<sup>1</sup>, Chang Yin<sup>2</sup>, Rakesh C. Kukreja<sup>2</sup>, Jan Slezak<sup>1</sup>, Narcisa Tribulova<sup>1</sup>**

<sup>1</sup> Institute for Heart Research, Center of Experimental Medicine, Slovak Academy of Sciences, Bratislava, Slovakia

<sup>2</sup> Division of Cardiology, Medical College of Virginia, Virginia Commonwealth University, Richmond, United States

Radiation of the chest during cancer therapy is deleterious to the heart, mostly due to oxidative stress and inflammation related injury. A single sub-lethal dose of irradiation has been shown to result in compensatory up-regulation of the myocardial connexin-43 (Cx43), activation of the protein kinase C (PKC) signaling along with the decline of microRNA (miR)-1 and an increase of miR-21 levels in the left ventricle (LV). We investigated whether drugs with antioxidant, anti-inflammatory or vasodilating properties, such as aspirin, atorvastatin, and sildenafil, may affect myocardial response in the LV and right ventricle (RV) following chest irradiation. Adult, male Wistar rats were subjected to a single sub-lethal dose of chest radiation at 25 Gy and treated with aspirin (3 mg/day), atorvastatin (0.25 mg/day), and sildenafil (0.3 mg/day) for six weeks. Cx43, PKC<sup>o</sup> and PKC<sub>o</sub> proteins expression and levels of miR-1 as well as miR-21 were determined in the LV and RV. Results showed that the suppression of miR-1 was associated with an increase of total and phosphorylated forms of Cx43 as well as PKC<sup>o</sup> expression in the LV while having no effect in the RV post-irradiation as compared to the non-irradiated rats. Treatment with aspirin and atorvastatin prevented an increase in the expression of Cx43 and PKC<sup>o</sup> without change in the miR-1 levels. Furthermore, treatment with aspirin, atorvastatin, and sildenafil completely prevented an increase of miR-21 in the LV while having partial effect in the RV post irradiation. The increase in pro-apoptotic PKC<sub>o</sub> was not affected by any of the used treatment. In conclusion, irradiation and drug-induced changes were less pronounced in the RV as compared to the LV. Treatment with aspirin and atorvastatin interfered with irradiation-induced compensatory changes in myocardial Cx43 protein and miR-21 by preventing their elevation, possibly via amelioration of oxidative stress and inflammation.

## Improved radioanalytical methods for quality control of [ $^{18}\text{F}$ ]NaF

**Mihon Mirela<sup>1</sup>, Ilie Simona<sup>1,2,3</sup>, Carmen Manea<sup>1</sup>, Chilug Livia<sup>1,4</sup>**

1 National Institute for Physics and Nuclear Engineering “Horia Hulubei”, IFIN-HH, Bucharest, Magurele, Romania

2 Extreme Light Infrastructure – Nuclear Physics, ELI-NP, IFIN-HH, Bucharest, Magurele, Romania

3 Doctoral School of Engineering and Applications of Lasers and Accelerators (S.D.I.A.L.A.), University Politehnica of Bucharest, Bucharest, Romania

4 Faculty of Applied Chemistry and Materials Science, University Politehnica of Bucharest, Bucharest, Romania

[ $^{18}\text{F}$ ]NaF is a radiopharmaceutical for diagnosis in Positron Emission Tomography (PET) as a bone imaging agent. Recently advanced in PET technology and the worldwide shortage of  $^{99\text{m}}\text{Tc}$ -radiopharmaceuticals led to the new interest in the use of [ $^{18}\text{F}$ ]NaF.

The objectives of this study were to optimize the methods used in determination of chemical and radiochemical purity of [ $^{18}\text{F}$ ]NaF to decrease the time of analysis. The analytical methods used in determination and quantification of radiopharmaceuticals impurities are high performance liquid chromatography (HPLC) and thin layer chromatography (TLC). Radionuclidic identity and purity are evaluated by gamma spectrometry. The bacterial endotoxins test is performed using Endosafe –PTS equipment.

Parameters of quality control (appearance, pH, half-life, radionuclidic identity and purity, chemical and radiochemical purity, bacterial endotoxins) were investigated to determine the purity and stability of the product. The analytical methods need to be fast and very accurate and complying with the quality standards of the usual pharmaceuticals. Complete quality control data for three batches of [ $^{18}\text{F}$ ]NaF was included in this work.

The HPLC method was found to be precise, accurate and specific assets recommending its use for determination of RCP. The proposed method was reproducible as the relative standard deviation of the peak area was less than 5%. The quality of the [ $^{18}\text{F}$ ]NaF meet the criteria specified in European Pharmacopoeia analytical method.



**Radiation  
Measurements**

**26**

## A study on preparation of HQ clathrate as gaseous radiotracer carrier

**Sung-Hee Jung<sup>1</sup>, Ji-Ho Yoon<sup>2</sup>**

<sup>1</sup> Korea Atomic Energy Research Institute, Daejeon, South Korea

<sup>2</sup> Korea Maritime University, Busan, South Korea

Radiotracers have been used widely in various industries ranging from refineries and petrochemical to steel and automobile. The selection of appropriate radioisotopes to be used as tracers is very important, and the procedure needs to consider physical and chemical characteristics of process fluids to be traced. In addition to them, the nature of radioisotopes should be carefully looked into in order to minimize environmental influence that radiotracers can cause during experiments.

Gaseous tracer is produced by irradiating target elements with neutrons in a research nuclear reactor. For safety reasons, radioisotopes with short half-life are preferred as tracers. Since it requires significantly long time to transport radiotracers from a radioisotope production facility to where a tracer investigation is to be taken place, however, gas target is normally pressurized in a quartz container for neutron bombardment. These pressurized containers should be guaranteed with its physical integrity during neutron irradiation, but it is almost impossible to produce them in the similar quality of physical strength. It's because a quartz ampoule is sealed by melting its inlet with high temperature flame while gas is liquefied by liquid nitrogen at the bottom. This uncertainty with gas containers seal status can make the radioisotope production procedure hazardous.

As a substitute of the traditional quartz ampoule for gas container, clathrate compound was brought to the attention. In this study, clathrate composite was prepared to hold Ar gas of up to several bars, and it was characterized to confirm its feasibility as gas tracer carrier in various conditions. From gamma radiation irradiation tests, the clathrate composite was found to be barely influenced by radiation environment.

The synthesized clathrates were examined with x-ray diffraction, in-situ high-pressure synchrotron XRD, Raman spectroscopy, and NMR in order to quantitatively characterize the samples. In addition, the gravimetric method was used to study Ar release kinetics as a function of the time as well as temperature dependent phase stability of Ar-loaded clathrates.

It's planned to irradiate the clathrate samples with neutrons in a research reactor, and to quantify the radioactivity that is produced. Furthermore, an optimal design dedicated to handling radioactive gas will be drawn and fabricated for a real test.

## Comparison of non-destructive nuclear forensics methods for analysis of nuclear material

**Jovana Nikolov<sup>1</sup>, Natasa Todorovic<sup>1</sup>,  
Andrej Vranicar<sup>1</sup>, Péter Völgyesi<sup>2</sup>, Éva Kovács-Széles<sup>2</sup>**

<sup>1</sup> University of Novi Sad, Faculty of Sciences, Novi Sad, Serbia

<sup>2</sup> Nuclear Forensics Laboratory, Academy of Sciences, Centre for Energy Research, Budapest, Hungary

Gamma spectroscopy method is widely applied in the analysis of samples for nuclear forensics. The main advantages of this method are that it is fast and non-destructive comparing to the other more precise techniques.

Nuclear Forensics Laboratory (NFL) of the Hungarian Academy of Sciences, Centre for Energy Research (MTA EK) has experience in nuclear forensics which activity started 25 years ago in Hungary. The bases of forensic research and investigation were mainly nuclear physics, gamma- and neutron measurements at the beginning. Several methods as age dating, determination of the isotopic composition and reprocessing characteristics of seized nuclear materials have been developed at MTA EK. Nuclear Physics Group (NPG) from University of Novi Sad has a long-term experience in gamma spectroscopy measurements and just recently started developing a methodology for nuclear material analysis. This paper will present the first results of the intercomparison of methods for uranium isotopic composition analysis used by those two laboratories. The main objective of this paper is to explore the possibility to use HPGe detectors in NPG together with “Multigroup  $\gamma$ -ray Analysis Method for Uranium” (MGAU) in order to be able to perform isotopic composition analysis and age dating of uranium samples. MGAU code will be used for precise determination of isotopic composition.

## Study of modulation properties of tungsten-based coded-aperture

Michal Cieslak<sup>1</sup>, Kelum A.A. Gamage<sup>2</sup>, James Taylor<sup>1</sup>

<sup>1</sup> Lancaster University, Lancaster, United Kingdom

<sup>2</sup> University of Glasgow, Glasgow, United Kingdom

The application of coded-aperture techniques for radiation imaging systems can be seen in various application fields, but the use of coded-apertures in mixed-field radiation detection in nuclear decommissioning remains largely unexplored. It is essential to understand the gamma-ray modulation properties of a tungsten-based coded aperture, in order to explore the suitability of coded-apertures for mixed-field radiation detection systems. In this paper, an investigation into the gamma-ray modulation properties of a tungsten coded aperture is presented. The aperture was designed using the mathematical principles of Modified Uniformly Redundant Arrays (MURA). Due to the complexity of the design and the small size of individual cells, the aperture was built using additive manufacturing methods. The gamma-ray field was produced by <sup>137</sup>Cs radioactive isotope at Lancaster University, UK. An organic plastic scintillator sample, which is capable of pulse shape discrimination, has been used to detect the gamma-ray field modulated by the tungsten aperture. The scintillator was energy calibrated using <sup>137</sup>Cs and <sup>22</sup>Na sources, before the first measurements of the modulated gamma-ray field were taken. The pulse shape discrimination performance of the scintillator was subsequently examined, using the mixed-field provided by <sup>252</sup>Cf. In this study, each of 169 coded aperture cells were investigated by collimating the modulated gamma-ray field of <sup>137</sup>Cs through a 25.4 mm thick lead supporting plate. The supporting plate has a single opening in the centre of the same dimensions as the single aperture cell 2.5 mm x 2.5 mm. The number of pulses detected for every aperture location was recorded in an array. The array was then used to create a two-dimensional image of the source, which was encoded through the coded aperture pattern. Finally, the image was decoded using deconvolution techniques to reveal the actual source location. The new results obtained in this study indicate that the gamma-ray modulation properties of the aperture are sufficient to create a useful image, despite the relatively small footprint and thickness of the coded aperture.

## Absorption ratio of treatment couch and effect on surface and build-up region doses

**Taylan Tuğrul**

Yüzüncü Yıl University, Medicine Faculty, Radiation Oncology Department, Van, Turkey

**Introduction.** In this study, treatment couch and rails dose absorption ratio and treatment couch effect on surface and build-up region doses were examined.

**Methods.** It is assumed that radiation attenuation is minimal because the carbon fiber couches have low density. Consequently, it leads the major dosimetric mistake. After the reference measurements were obtained at gantry angle  $0^{\circ}$ - $55^{\circ}$ - $305^{\circ}$ , these values were compared with opposed gantry angles ( $180^{\circ}$ - $235^{\circ}$ - $125^{\circ}$ ). The reason for use of gantry angle  $235^{\circ}$ - $125^{\circ}$  is that the beam center intersects with the couch rails. In additionally, results of the measurements were obtained for gantry angle  $0^{\circ}$ - $180^{\circ}$ . PDD curves were created with and without carbon fiber couch. In this study, Gerbi's method was applied for correction of PDD curves which were obtained in build-up region.

**Results.** The ratio of the carbon fiber couch dose attenuation was measured at different fields for 6-15 MV photons. The absorption ratio is between %3.4 and %1.22 when the beams intersect with couch rails. This ratio is much higher in small fields. The couch effect increased surface dose from %14 to %70 for 6 MV and from %11.34 to %53.03 for 15 MV.

**Conclusions.** As expected, dose attenuation effect of carbon fiber couch was seen when beams intersected with carbon fiber couch. When the effect of carbon fiber couch on surface and build-up region dose is examined, it is observed that the carbon fiber couch increases the dose on surface and build-up region. In additional, the maximum dose depth shifts towards the surface for all energy. The carbon fiber couch behaves like a bolus. Therefore, the effect of carbon fiber couch should be considered during treatment planning.

## Testing of RAM ION dosimeter in operational fields

Mariia Pyshkina, Michael Zhukovsky, Alexey Ekinin

Institute of Industrial Ecology UB RAS, Ekaterinburg, Russia

Recently published ICRP Recommendations No. 118 and IAEA General Safety Requirements No. GSR Part 3 set a new equivalent dose limit for exposure of an eye lens. Now all members of IAEA should bring their national regulation documents in line with current requirements and decrease equivalent dose limit for eye lens from 150 mSv up to 20 mSv for workers. Such a reduction of 7.5 times will lead to a situation when the action level for using individual dosimeter for exposure of eye lens should be nearly 2-3 mSv. Thus, many workers will be forced to wear personal eye dosimeter. Firstly, all workplaces should be sorted by the level of eye lens exposure and need of its monitoring. The exposure dose in the lens of an eye might be created by both weakly penetrating radiation ( $\beta$ -radiation) and highly penetrating radiation ('soft'  $\gamma$ -radiation). The contribution of highly penetrating radiation into exposure dose might be estimated with  $H^*(10)$ . It is necessary to determine workplaces where  $\beta$ -radiation makes the main contribution into a lens of eye exposure dose.

In this work testing of the RAM ION dosimeter in operational fields was performed. RAM ION is a battery operated, auto ranging, portable ion chamber survey meter designed for highly stable and accurate measurement of dose rates and an integrated dose of gamma, x-ray and beta radiation. The dosimeter allows measuring of  $H'(0.07, \Omega)$ ,  $H'(3, \Omega)$  and  $H^*(10)$  values, depending on a used cap. Measurements of ambient  $H^*(10)$  and directional  $H'(3, \Omega)$  and  $H'(0.07, \Omega)$  dose equivalents were done at workplaces, located on the territory of nuclear fuel cycle facilities. Also, dosimeter was testing in fields of beta radiation of  $^{90}\text{Sr}$ - $^{90}\text{Y}$  source and gamma radiation of  $^{137}\text{Cs}$  and  $^{241}\text{Am}$  sources.

Testing RAM ION in the field of gamma radiation was performed. No difference between measured values of  $H'(0.07, \Omega)$ ,  $H'(3, \Omega)$  and  $H^*(10)$  both for  $^{137}\text{Cs}$  and  $^{241}\text{Am}$  sources was obtained. The uncertainties of RAM ION readings in the gamma radiation field were in the range from -4% up to -10%. It means it does not have any statistical difference and is in measurement uncertainty. In case of testing RAM ION in the field of the beta radiation, the 'real' value of  $H'(d, \Omega)$  was calculated with Varskin 6.1. Ambient and directional dose equivalent were measured at about 30 workplaces, including reactor hall, room with spent fuel pool and other special technical rooms for working with equipment extracted from a reactor. Results showed that most part of obtained ratios  $H'(3, \Omega)/H^*(10)$  is in the range from 1.0 up to 1.5. It means in case of isotropic exposure and non-changing conditions  $H'(3, \Omega)$  might be estimated by  $H^*(10)$  and proportional factor. When the ratio is greater than 1.5, individual monitoring should be introduced.

**Acknowledgments:** This work was supported by the Ural Branch of the Russian Academy of Science Project 18-11-2-2.

## Radiation monitoring report from sailing around the Antarctic continent, along and south of the 60<sup>th</sup> parallel

**Magdalena Dlugosz-Lisiecka<sup>1</sup>, Marcin Krystek<sup>2</sup>, Michał Barasiński<sup>3</sup>**

<sup>1</sup> Technical University of Lodz, Lodz, Poland

<sup>2</sup> Geological Museum, Lodz, Poland

<sup>3</sup> Katharsis Jacht team member, all the world, Poland

Monitoring of the radiation during sailing around Antarctica south of the 60th parallel was first in research history. This region is still considered as one of the unpolluted regions in the world. It was a challenge – to circumnavigate Antarctica as close to the continent and within as short a time as possible. It was also a unique opportunity for scientific research. During the entire voyage, each 10 minutes sampling period, radiation monitor Gamma Scout acquire results of dose rate from the board of the Katharsis II jacht.

The average dose rate during the sailing around Antarctica south of the 60<sup>th</sup> parallel was  $92.1 \pm 9.5$  nSv/h. Similar value 90 nSv/h was measured in central Poland<sup>1</sup>. For comparison at PAPEETE-TAHITI\_987\_AGG\_CP location on the Pacific Ocean island gamma dose rate was 59 nSv/h, on the Atlantic Ocean island the location Fratel – SARA the monitored dose rate was 23 nSv/h, on the Indian Ocean island at location ST-LOUIS-LA-REUNION\_974\_AGG\_CP dose rate was 67 nSv/h. Radiation level in atmosphere at the Marambio Antarctic Base ( $64^{\circ} 13' S - 56^{\circ} 43' W$ ; 196 m a.s.l.) measured in 2015 by LIULIN3 type dosimeter was  $80 \pm 1$ . Taking into account various contribution of natural and artificial radiation levels at these places definitely different values of the gamma radiation was expected. Low natural radon ground level activities, low content of the artificial radionuclides at the sea level of the measurement around Antarctica suggest relatively low content of the gamma radiation in this region. So, why at sea level around Antarctica south of the 60th parallel the measured dose rate was average even 92.1 nSv/h. The possible reason is atmospheric ionizing radiations induced by Galactic and Solar cosmic rays. In this region dose rate values vary drastically due to the high altitude and the very low magnetic field.

### References

1. [www.paa.gov.pl](http://www.paa.gov.pl) – national network of dose rate monitoring.
2. <https://remap.jrc.ec.europa.eu/GammaDoseRates.aspx-radiation> – on line network for radiation monitoring JRC
3. Alba Zanini, Vicente Ciancio, Monica Laurenza, Marisa Storini, Adolfo Esposito, Juan Carlos Terrazas, Paolo Morfino, Alessandro Liberatore, Gustavo Di Giovan Environmental radiation dosimetry at Argentine Antarctic Marambio, Base ( $64^{\circ} 13' S, 56^{\circ} 43' W$ ): Preliminary results, Journal of Environmental Radioactivity 175-176 (2017) 149-157

## Random coincidences in the sum-peak method

**Tomas Nemes<sup>1</sup>, Dusan Mrdja<sup>2</sup>, Istvan Bikit<sup>2</sup>**

<sup>1</sup> Faculty of Technical Sciences, Novi Sad, Serbia

<sup>2</sup> Faculty of Sciences, Novi Sad, Serbia

For two step gamma cascade emitting radionuclides, the source activity can be obtained by spectrum data alone. At high count rates, random coincidence corrections must be considered even when the pile up rejection circuit is turned on. Starting from the count rate equations that consider random summing, a new equation for measurement of the activity is deduced. The results of the new formula are verified by Monte Carlo simulations.

## Ensuring the effectiveness of extensive EPR dosimetry study of combined radiation exposure

**Elena Shishkina<sup>1</sup>, Alexandra Volchkova<sup>2</sup>,  
Denis Ivanov<sup>3</sup>, Yurii Timofeev<sup>2</sup>, Bruce Napier<sup>4</sup>**

1 URCRM and ChelSU, Chelyabinsk, Russia

2 URCRM, Chelyabinsk, Russia

3 IMP and UrFU, Yekaterinburg, Russia

4 Pacific Northwest National Laboratory, Richland, United States

Environmental radioactive contamination in the Southern Urals occurred as the result of imperfections of the technology in the early period of production activities of “Mayak” (1949-1956). External human exposure resulted from environmental contamination with gamma emitters. In addition, radionuclide intakes by the population of contaminated areas occurred causing chronic internal radiation of bone tissues due to bone-seeking  $^{89,90}\text{Sr}$  as well as protracted internal exposure to short-lived isotopes and  $^{137}\text{Cs}/^{137\text{m}}\text{Ba}$  homogeneously distributed in soft tissues. Dosimetry of tooth enamel by electron paramagnetic resonance (EPR) was proposed as a method of retrospective dosimetry. Tooth enamel is the only biological tissue without living cells that is 98% calcium hydroxyapatite. Ionizing radiation induces stable radicals ( $\text{CO}^{2-}$ ) that may be detected by EPR spectroscopy. Thus, enamel is a unique individual biological dosimeter. EPR spectroscopy of tooth enamel is widely used for retrospective dosimetry for predominantly-external irradiation. Extensive EPR dosimetric study was performed from 1992 to 2014. The experience of this long-term study allows the formulation of the principles of optimal organization and implementation of large-scale EPR studies for the scenario of combined internal and external exposure. The basic methodological approaches for ensuring the effectiveness of extensive EPR dosimetry study of combined radiation exposure are as follows: information support of the study; a set of methods for unification and harmonization of measurement results; age criteria on sample exclusion (associated with the high accumulation of bone-seeking radionuclides entering the dental tissues during their calcification); a set of methods for assessing the concentrations of  $^{90}\text{Sr}$  in dental tissues and the calculation of internal doses; as well as the method for assessment of background doses.

## Determination of $^{210}\text{Pb}$ in water by Cherenkov counting

**Natasa Todorovic<sup>1</sup>, Jovana Nikolov<sup>1</sup>, Ivana Stojkovic<sup>2</sup>**

<sup>1</sup> University of Novi Sad, Faculty of Sciences, Department of Physics, Novi Sad, Serbia

<sup>2</sup> University of Novi Sad, Faculty of Technical Sciences, Novi Sad, Serbia

The analysis of  $^{210}\text{Pb}$  by Cherenkov counting is possible only through the detection of the Cherenkov photons produced by the daughter nuclide  $^{210}\text{Bi}$ , which reaches secular equilibrium with its parent nuclide. Here we present optimization and validation of a simple direct method for  $^{210}\text{Pb}$  screening in water via Cherenkov radiation detected by a liquid scintillation counter Quantulus 1220 without any chemical pretreatment. Cherenkov counting is a fast, reliable and non-destructive method for detecting high energy beta emitters in aqueous solution, but it is sensitive to color quench correction. The sample channel ratio (SCR) method has been applied to correct this effect. Various types of vials were tested and different efficiencies were obtained indicating the importance of the choice of vials. It is obvious that Cherenkov counting cannot compete with liquid scintillation counting as far as highest possible counting efficiency is concerned. However, if very high counting efficiencies are not necessary, determination of  $^{210}\text{Pb}$  by Cherenkov counting has the following advantages: samples may be counted directly in aqueous solution or in organic solvents; no fluor, fluor cocktails, or other compounds need be added, and thus the samples to be analyzed remain unadulterated and suitable for subsequent studies or analysis; a larger volume of sample may be counted in a 20-mL counting vial since fluor solution is not needed; there is no interference from other radionuclides that cannot produce Cherenkov photons in aqueous media.

## Determination of the Co-60 source activity by using the sum-peak method

**Simona Ilie<sup>1,3</sup>, Calin Alexandru Ur<sup>1,3</sup>, Octavian Sima<sup>2,4</sup>, Gabriel Suliman<sup>1</sup>**

1 Extreme Light Infrastructure – Nuclear Physics, ELI-NP, IFIN-HH, Bucharest, Romania

2 Horia Hulubei National Institute for R&D in Physics and Nuclear Engineering, Bucharest, Romania

3 University Politehnica of Bucharest, Bucharest, Romania, Bucharest, Magurele, Romania

4 Faculty of Physics, University of Bucharest, Bucharest, Magurele, Romania

The Extreme Light Infrastructure—Nuclear Physics (ELI-NP) is one of the three pillars of the Extreme Light Infrastructure Pan-European initiative. The main goal of the ELI-NP facility is the study of photonuclear physics and its applications.

ELI-NP, currently under construction in Magurele, Romania will host two major research systems. The first one is a very high intensity laser system, capable of delivering twin laser pulses of 10 PW. The second facility is an advanced high energy (gamma) photon source based on Compton back scattering of laser light on high energy electrons which will deliver a very intense gamma beam system with unprecedented bandwidth and spectral density.

The Gamma Beam System diagnostics of ELI-NP requires a precise determination of the gamma beam parameters up to 19.5 MeV. Part of the diagnostics will involve the use of the high efficiency HPGe detector for in-beam measurements. Knowledge of the detector full energy peak efficiency over the 0.2 – 19.5 MeV range is very important.

Usually, the efficiency of the detectors is assessed by making well controlled measurements of standard gamma-ray sources with known activity, but may appear situations when the activity of the source is unknown. In such situations it is very important to firstly determine the activity of the source using only the spectral data and secondly to determine the efficiency of the detector.

The sum-peak method allows for absolute activity measurements for point sources containing radionuclide with simple decay scheme similar to <sup>60</sup>Co emitting two coincident gamma-ray photons.

The advantage of this method is that the activity of gamma cascade emitting sources can be determined based only on the use of measured spectrum, without knowledge of the detector efficiencies. Most commonly, the method is applied to point-like sources measured in close geometry, which improves the statistics of the counts from the sum-peak.

The experimental values of activity obtained using the sum-peak method were calculated using measurements of a point-like source of <sup>60</sup>Co with a high-purity germanium detector (HPGe) with 150% relative efficiency from the new facility Extreme Light Infrastructure – Nuclear Physics, ELI-NP.

The obtained results will be presented in this work.

## LSC screening of wastewater samples

Ivana Stojković<sup>1</sup>, Nataša Todorović<sup>2</sup>, Jovana Nikolov<sup>2</sup>

<sup>1</sup> University of Novi Sad, Faculty of Technical Sciences, Novi Sad, Serbia

<sup>2</sup> University of Novi Sad, Faculty of Sciences, Department of Physics, Novi Sad, Serbia

Liquid scintillation counting (LSC) has gained popularity in environmental studies and monitoring for quantitative analysis of radionuclides. This paper explores the possibility of rapid LSC radioanalysis of wastewater samples collected in the vicinity of nuclear reactors or other water samples that arrive in the laboratory in the case of nuclear emergencies. Wastewater from nuclear power plants usually contains <sup>3</sup>H and <sup>14</sup>C in measurable activities, but can be contaminated also with a set of different beta-emitter radionuclides (<sup>90</sup>Sr, <sup>137</sup>Cs, and others).

Tritium analysis can be performed very accurately and precisely in the direct mixture of 8 ml of water and 12 ml of scintillation cocktail Ultima Gold LLT, which is well known in laboratory LSC practice. However, determination of <sup>14</sup>C content in water samples demands time-consuming chemical procedures and complex analytical equipment: gas proportional counting, LSC with either benzene synthesis technique or direct absorption of CO<sub>2</sub> etc. In the case of a nuclear accident, the necessity to detect elevated <sup>14</sup>C levels in water samples in short period of time has triggered an investigation of a possibility to quantify <sup>14</sup>C content without any chemical pretreatment of the samples.

We present an implementation and optimization of a direct method for the effective estimation of <sup>14</sup>C level in wastewater, investigating its limitation and the range of application. Our main concern was not to accurately quantify <sup>14</sup>C activity, but to detect in a simple and fast manner if water samples contain considerable <sup>14</sup>C activity or not, which would provide the advantages such as rapidity, low-cost, and simplicity of radioanalysis desirable in the case of nuclear emergencies. Its application is limited only to <sup>14</sup>C screening of samples with much higher <sup>14</sup>C activities than those of the environmental (surface and ground) waters. The method assumes mixing of the water sample with Ultima Gold AB scintillation cocktail, in the previously explored optimal water:cocktail volume ratio, optimal counting window selected, PAC (Pulse Amplitude Comparator) parameter adjustment, based on the highest FOM (Figure of Merit) value achieved, as well as detection efficiency and detection limit evaluated. The possibility to eliminate low-energy counts that would be generated from <sup>3</sup>H, and to estimate the contribution of other high-energy beta emitters to obtained results of <sup>14</sup>C content is presented as well. The presence of high-energy radionuclides can be detected and their contribution to calculated <sup>14</sup>C activity could be estimated in the high-energy region of spectrum via direct method for gross alpha/beta measurements. This screening test would provide gross beta activity of all other radionuclides excluding <sup>3</sup>H and <sup>14</sup>C.

Method's constraints, accuracy, and precision were considered from the obtained results of measurements of wastewater samples. Experiments were performed on Ultra Low-Level Liquid Scintillation Spectrometer Wallac 1220 Quantulus.

## Development of short-lived radioactive tracers for the description of processes influencing the migration of contaminants in the environment

**Hana Assmann Vratislavská, Jaroslav Šoltés, Pavel Kůs, Hana Kořenková**

Research Centre Rez Ltd., Husinec-Řež, Czech Republic

The increase in the amount of undesirable substances having a negative impact on health and the environment is due, among other things, to a number of technologies manufacturing products of everyday use. The migration of these substances in the rock environment is not sufficiently described and is problematic to be measured. Radioactive tracers are expected to be used to monitor such migration processes. The goal is to find short-lived radionuclides produced by neutron interactions with the target substance, in which neutrons do not produce long-lived radionuclides causing permanent rock contamination. The LVR-15 research reactor in Rez, Czech Republic is regularly utilized for nuclide production. The LVR-15 is a light water moderated, tank-type nuclear reactor operated with a thermal power of 10 MW. A list of perspective radionuclides was chosen to be studied as potential tracers of migration in rock specimens. For all calculations of expected activities of target chemicals to be irradiated the FISPACT-II software was utilized with neutron energy spectra standardly present in one of the reactor's vertical irradiation channels which were determined by means of the MCNP particle transport code. The radionuclide requirements are: chemical stability and purity of the target substance, a half-life between 5 hours and 3 days, an energy range of emitted gamma radiation from 60 keV to 3 MeV, and stable daughter radionuclides. A rapid drop in sample activity is an advantage of short half-life that allows the recyclability of samples or experimental sites for the further use of other tracers, allowing the description of different processes (sorption, anion exclusion, dispersion) for one type of environment. From the analyzed radionuclides ( $^{24}\text{Na}$ ,  $^{42}\text{K}$ ,  $^{64}\text{Cu}$ ,  $^{72}\text{Ga}$ ,  $^{76}\text{As}$ ,  $^{82}\text{Br}$ ,  $^{99}\text{Mo}$ ,  $^{140}\text{La}$ ,  $^{142}\text{Pr}$ ,  $^{198}\text{Au}$ ,  $^{166}\text{Ho}$ ,  $^{188}\text{Re}$ ,  $^{153}\text{Sm}$ ), the use of each of these as a radioactive tracer in the rocks is possible. However, the limitation occurs when a samarium is used, where radionuclides with long half-lives remain (e.g.  $^{151}\text{Sm}$ ,  $^{155}\text{Eu}$ ), which would cause permanent contamination in the case of accumulation. Using of hydroxides and oxides based chemical compounds is more advantageous for neutron activation than the irradiation of chloride forms according to analyzes. The highest efficiency of the screening cameras is shown for photon energies up to 200 keV, which limits the selection of the appropriate radionuclide to molybdenum, holmium, and rhenium according to the results of the pilot tests. The compounds of these selected elements will be irradiated to identify potential impurities in the next stage of the project.

## Thick target neutron yields: Experimental program in GANIL to measure the double differential neutron fluxes generated by the interaction of heavy ions with thick targets

**Manssour Fadil, Ngoc-Duy Trinh, Marek Lewitowicz**

GANIL, Caen, France

The neutrons are the major hazards in particle accelerator facilities. These neutrons are emitted by the interaction of the accelerated ions with different components of the accelerator (dipole, walls, beam-dumps...). The neutrons are emitted following a continuous spectrum that depends on several factors (nature of the incident particle, its energy, angle emission).

In order to quantify the hazard of these neutrons and, in consequence the necessary biological protection to be established in the facility we need to characterize the double (angle, energy) neutron flux generated by the interaction of the ion on thick targets. Some Monte Carlo codes (MCNP, PHITS, FLUKA) allow modelling these interactions and are able to calculate these neutron fluxes. But we often find major discrepancies between these models or between the models and the experimental data. So to accomplish these characterizations, we established an experimental program called TTNY in GANIL to measure the double differential neutron flux generated by the interaction of heavy ions with thick targets. Two measurement methods are used for the neutron detection: activation technique and Time of Flight technique. The measured spectra are compared to the simulated fluxes. The results presented in this work were obtained in the frame of PhD study (N-D. Trinh) accomplished in GANIL in 2018.

**Keywords:** Double differential neutron spectrum, activation, Time of Flight, Monte Carlo simulation, particle transport

## A study on the performance the CdZn<sub>x</sub>Te<sub>1-x</sub> radiation detectors grown by Vertical Gradient Freeze (VGF) technique

**Deniz Bender<sup>1</sup>, Rasit Turan<sup>1</sup>, Merve Genc Unalan<sup>1</sup>,  
Mustafa Unal<sup>1</sup>, Özden Basar Balbasi<sup>1</sup>, Ercan Yilmaz<sup>2</sup>**

<sup>1</sup> Crytsal Growth Laboratory, Department of Physics, Middle East Technical University, Ankara, Turkey

<sup>2</sup> Center for Nuclear Radiation Detector Research and Applications, Department of Physics, Bolu Abant Izzet Baysal University, Ankara, Turkey

Cadmium Zinc Telluride (CdZn<sub>x</sub>Te<sub>1-x</sub>) with Zn concentration of  $x = 10$  is a good candidate for detection of x-ray and gamma-rays due to its high atomic number and large bandgap. CdZnTe crystals for detector applications are commonly grown by Travelling Heater Method (THM) due to the advantages of high yield and uniform distribution of Zn ratio. In this work, we have investigated the use of VGF grown CdZnTe crystals in detector applications. VGF technique is faster and does not require any seed material, and may have a high single crystal yield. For this reason, it may be preferred over the THM technique under certain conditions. An x-ray or gamma-ray detector requires CdZnTe crystal with high resistivity and high  $m\text{-}\tau$  value to ensure a low the leakage current under high voltage applications which is needed to collect the electrons across relatively thick ( $> 3$  mm) body of the detector. For this reason, high-quality crystals with low surface leakage current should be used. The resistivity of CdZnTe crystals was shown to decrease with the amount of Cd vacancy which is a sensitive function of the growth environment. To reduce the Cd vacancy, it is usually doped with impurities like In and Cl which are introduced into the starting material prior to the growth process. Also, surface preparation and cleaning play an important role in device operation. For a low surface leakage current and a strong bonding with the metal electrode, the surface should be clean from contaminants like oxygen and carbon

We have studied the effect of doping and surface preparation of the crystal on the electrical properties of the CdZnTe crystals grown by VGF technique. We have shown that doping is extremely important in achieving high resistivity and high  $m\text{-}\tau$  material. The performance of the detectors having different doping levels and different surface properties were tested under x-ray illumination and found a strong correlation with doping level and surface properties. With these results, we have concluded The VGF technique is a promising crystal growth technique for detector applications.

## Improved approach for LSC detection of $^{35}\text{S}$ aiming at its application as tracer for short groundwater residence times

Michael Schubert<sup>1</sup>, Jürgen Kopitz<sup>2</sup>, Kay Knoeller<sup>1</sup>

<sup>1</sup> Helmholtz Centre for Environmental Research GmbH – UFZ, Leipzig, Germany

<sup>2</sup> Universitaetsklinikum Heidelberg, Heidelberg, Germany

Policy based decisions related to the management of groundwater resources necessitate a sufficient knowledge of mean groundwater residence times in the exploited aquifers. The data can be used for assessing (i) the volume of groundwater that can be sustainably abstracted, (ii) timescales of water-rock interaction processes that might influence the water quality, and (iii) the vulnerability of an aquifer to anthropogenic contamination. A powerful tool for investigating groundwater residence times is the application of naturally occurring radioisotopes as environmental tracers. The half-lives of the applied radioisotopes need to be in the same time range as the investigated processes. While  $^3\text{H}$ ,  $^{14}\text{C}$ , and  $^{36}\text{Cl}$  have already been commonly used in the past, general improvements in radio-analytical techniques brought about novel approaches that rely on application of  $^{39}\text{Ar}$ ,  $^{81}\text{Kr}$ , and  $^{85}\text{Kr}$  and thus an extension of the range of water ages that can be investigated. However, environmental radiotracers that allow studying groundwater ages below one year are still scarcely discussed in the literature. Innovative approaches that focus on this timescale include the application of  $^{222}\text{Rn}$  and  $^7\text{Be}$ . While its 3.8 days half-life limits the applicability of  $^{222}\text{Rn}$  for the dating of very young groundwater with ages of up to three weeks,  $^7\text{Be}$  with a half-life of 53.1 days covers potentially a time range of up to eight months. However,  $^7\text{Be}$  is very sorptive; the main part of the dissolved Be is held back by soil particles limiting its applicability as aqueous tracer. Another omnipresent natural radionuclide that is continually produced in the upper atmosphere by cosmic ray spallation (of atmospheric  $^{40}\text{Ar}$ ) is  $^{35}\text{S}$ . After its production it rapidly oxidizes to  $^{35}\text{SO}_4^{2-}$ , gets dissolved in the meteoric water and is finally transferred with the rain to the groundwater. Since its activity concentration in the groundwater starts to decrease as soon as it seeps into the ground, its 87.4 day half-life makes  $^{35}\text{S}$  a useful tracer for investigating groundwater residence times of up to 1.2 years. In contrast to beryllium,  $^{35}\text{SO}_4^{2-}$  is highly mobile in groundwater and hence not retarded by any mineral matrix. A challenge is however, that the concentration of  $^{35}\text{S}$  in rainwater may vary significantly even on short timescales of hours to days. Seasonal differences in rain intensity can also significantly affect the  $^{35}\text{SO}_4^{2-}$  activity of the rainwater. Thus the recording of extended time series of  $^{35}\text{S}$  in rainwater (input function) as well as the measurement of  $^{35}\text{S}$  in groundwater with a reasonably high frequency is compulsory for sound data interpretation. The objective of the presented study was to develop, test and present an improved LSC based method that allows the straightforward detection of  $^{35}\text{S}$  pre-concentrated from natural water samples that contain  $\text{SO}_4^{2-}$  concentrations of up to 1500 mg. The study aimed at the optimization of both LSC setup and measurement protocol.

## Use of contemporary diagnostic radiography methods in occupational diseases

**Elena Katamanova<sup>1</sup>, Elena Beigel<sup>1</sup>,  
Kseniya Panchukova<sup>1</sup>, Oksana Kalinina<sup>2</sup>, Evgeniya Zayka<sup>1</sup>**

<sup>1</sup> East-Siberian Institute of Medical and Ecological Research, Angarsk, Russia

<sup>2</sup> State Budget-Funded Educational Institution of Higher Vocational Education “Irkutsk State Medical University”, Irkutsk, Russia

Results of diagnosis of Occupational Fluorosis and Occupational bronchopulmonary diseases are presented in the paper. The aim was to determine the criteria for initial stage of skeletal fluorosis, and Multislice computed tomography significance for the diagnosis of severity of Chronic obstructive pulmonary disease (COPD) in individuals exposed to fluoride and dust. 145 aluminum industry workers were examined. One hundred five male exposed to fluoride compounds (average exposure time  $26.8 \pm 7.8$  years, average age  $55.4 \pm 5.0$  years,  $M \pm SD$ ) (group A) and age-matched 30 healthy male, who have no harmful working-environment factors in their workplaces, were enrolled in the study. Forty male patients with variable degree of occupational COPD – mild and moderate degrees – were in another group (group B) (the average age of  $51.04 \pm 6.9$  years,  $M \pm SD$ , work experience in production  $22.14 \pm 7.41$  years). Dual-energy X-ray absorptiometry (DXA) was performed by Lunar Prodigy Bone Densitometer and Multislice computed tomography of the lungs was done by an X-ray Computed Tomography “SOMATOM Definition 64”. The processing and statistical analysis was carried out with the program “Statistica 6.0”.

Based on the DXA and taking into account the T score bone density the criteria for initial stage of skeletal fluorosis were established – hyperostosis of the left radial bone, bone tissue density in the right radial and left tibia bones increase, and bone mineral density in the right radial bone and the lumbar spine increase.

Comparative analysis of the data of multislice computed tomography of the lungs showed structural changes in the lungs in 4 mild COPD patients (19%) and in 11 moderate COPD patients (57.9%) ( $p=0.0002$ ); the formation of bronchiectasis was observed in 1 (4.7%) and 3 (15.7%) patients, respectively ( $p = 0.01$ ); symptoms of emphysema were found in 1 (4.7%) and 8 patients, respectively (26.3%) ( $p = 0.0003$ ). Thus, the severity of COPD directly depends on the severity of clinical symptoms and degree of destructive changes in the lungs in the examined patients.

## Radiation survey during research reactor dismantling

**Iurii Simirskii, Alexey Stepanov, Ilia Semin, Anatoly Volkovich**

NRC, Moscow, Russia

In 2011, the Kurchatov Institute started to dismantle the MR reactor. 110 tons of equipment was taken down and 53 tons out of it represented radioactive waste with the total activity  $5.0 \cdot 10^{10}$  Bq. In 2013-2014 the equipment of 9 loop facilities was dismantled that vacated 47 basement premises. Dismantling of the equipment made it possible to reduce the equivalent dose rate in those premises to 0.01-0.03 mSv/h. Dismantling of in-core structures started in 2014. First of all the grid of the MR reactor fastening all the main reactor's parts removed. Next, 76 beryllium blocks of the reactor and 106 blocks of the graphite reflector were also removed. Spectrometric investigations of beryllium blocks showed that the main contaminating radionuclide was  $^{60}\text{Co}$ . Radioactive contamination of blocks removed from the active zone was in the range from 7.0 to 30.0 GBq. After removal of structural elements the lower reactor support was dismantled then in 2015 the MR reactor vessel was taken away. All the dismantling activities about the reactor's equipment and control mechanisms considered to be high-level waste were performed by the Brokk remotely controlled device.

In the same reactor hall there was a uranium-graphite reactor RFT stopped in 1962. In spring 2015 its dismantling began. 34 tons of irradiated graphite were removed. Graphite stacks were unloaded with the help of the Brokk remotely controlled device equipped with a multi-purpose clamshell capture. The dismantling of the RFT reactor vessel was made by a remote plasma cutting unit.

As a result of the MR and RFT reactors decommissioning, over 900 tons of equipment were dismantled and taken away for long-term storage and processing, 1400 cubic meters of solid and about 650 cubic meters of liquid radioactive waste were removed.

Now, the production premises undergo a radiation survey. Upon the results we will make decision about their further utilization. In all the rooms of the reactor building we measured the EDR values on a lattice of 0.5 m from distances of 0.1 m and 1.0 m and determined the flux density of  $\beta$ -particles. The value of the removed surface radionuclide contamination was determined by the method of smears that allows to estimate a possible degree of decontamination of the production facilities. Spectrometric analysis of over 400 smears was performed as well. Soil samples for spectrometric analysis (about 100 samples) were taken in all basements of the reactor building. If the specific activity of radionuclides in the soil exceeded the value of MSSA ( $10^4$  Bq/kg for  $^{137}\text{Cs}$  and  $10^5$  Bq/kg for  $^{90}\text{Sr}$ ) the soil was partially replaced. It was stated that mainly  $^{137}\text{Cs}$  and  $^{90}\text{Sr}$  caused the radioactive pollution.

## **$^{226}\text{Ra}$ in water measurement by non-Marinelli geometry and gamma spectrometry**

**Andrej Vraničar<sup>1</sup>, Nataša Todorović<sup>1</sup>, Jovana Nikolov<sup>1</sup>, Ivana Stojković<sup>2</sup>,  
Jan Hansman<sup>1</sup>, Branislava Tenjović<sup>1</sup>, Miloš Travar<sup>1</sup>, Miodrag Krmar<sup>1</sup>**

<sup>1</sup> University of Novi Sad, Faculty of Sciences, Novi Sad, Serbia

<sup>2</sup> University of Novi Sad, Faculty of Technical Sciences, Novi Sad, Serbia

According to the EU regulative (Euratom Drinking Water Directive 2013/51/EURATOM) all water intended for human consumption must undergo radiological analysis. Gross alpha/beta measurement is recommended for the first analysis. If the water sample has higher gross  $\alpha/\beta$  activity, a different kind of analysis must be done, where every radioisotope is checked separately. From past experience, it has been noticed that very often the main contributor to this higher activity is  $^{226}\text{Ra}$ . Due to this; accurately measuring  $^{226}\text{Ra}$  in water is of great importance. Most laboratories use Marinelli geometry for this purpose, because it provides great efficiency of detection, which is related to the large space angle that the sample holds, relevant to the detector. In this work, we introduced a new method for direct measurement of  $^{226}\text{Ra}$ , using regular cylindrical geometry on NaI and HPGe detectors, which is quick, efficient, simple and this geometry is usually available in most of the laboratories. A set of water solutions of  $^{226}\text{Ra}$  activity concentrations ranging between 0.05-50 Bq/l was made using  $^{226}\text{Ra}$  aqueous standard and measured overnight for a period of  $4 \cdot 10^4$  s. In the case of NaI detector, we aimed to test the effects of coincidence summing on the efficiency of detection. In addition, a new graphical method for determining the detection limit is presented. Using this direct method and without any water pretreatment, the acquired detection limit was 0.7 Bq/l and 1.6 Bq/l for NaI and HPGe detectors respectively. Taking into account the fixed detector parameters, these limits can be lowered with larger measurement times. Given the fact that the limit for activity concentration of  $^{226}\text{Ra}$  in drinking water is 0.49 Bq/l and detection limit of 0.04 Bq/l are set by EU regulations, this method can't be used for determining the activity of  $^{226}\text{Ra}$  in water intended for human use, but can be exploited for the case of higher activities or as a fast and effective screening method.

## The $^{210}\text{Pb}$ correction for the self-absorption effect in EFFTRAN and Angle software

**Miloš Travar, Jovana Nikolov, Nataša Todorović,  
Andrej Vraničar, Jan Hansman, Dušan Mrđa**

University of Novi Sad, Faculty of Sciences, Novi Sad, Serbia

Being able to accurately determine the efficiency of detection, in respect of having precise measurements of radioactivity, represents one of the main objectives of every gamma spectrometry laboratory. In this sense the following paper is focused on thorough study of the effect of self-absorption on and using naturally occurring radioactive isotope of lead,  $^{210}\text{Pb}$ , one of the  $^{238}\text{U}$  radioactive chain members, which found it's various practical purposes such as  $^{210}\text{Pb}$  sediment dating, calculation of the rate of soil erosion, being a valuable tracer for the behaviour of heavy metals in soil-stream-estuary systems, etc. In order to have efficient and adequate results in said techniques an accurate measurement of  $^{210}\text{Pb}$  activity must be obtained. The only gamma line of this radioisotope is on 46.5 keV, which by itself is quite weak and heavily affected by natural background in low energy region, thus making it hard to notice and detect. Due to this reason, the effect of self-absorption represents a major problem in accurate determination of it's activity concentration knowing it can in large proportion distort and interfere in the final results. Thankfully, this effect can be measured experimentally. This measurement demands that the laboratory has reference materials, which sometimes can be rather expensive. On the other hand the very contribution of the said effect can be obtained through modeling by using different software codes. The main objective of this paper is to calculate the effect of self-absorption using two different software, EFFTRAN and Angle, which are commercially available. It's also desirable to see how well is this effect incalculated within these programmes, which can be achieved through comparison of the final activity concentration of  $^{210}\text{Pb}$  given by these two programmes while knowing the exact value of activity concentration from the referent material measured on HPGe detector. The obtained results show that these methods can be implemented in daily practice with sufficient accuracy but with careful definitions of detector and sample characteristics. Being able to know the exact efficiency including all the effects that determine it is of crucial importance for future work and accurate results.

## ESR spectroscopy study of gamma irradiated dry yeast

**Ufuk Paksu, Birol Engin**

Dokuz Eylül University, Faculty of Science, Department of Physics, İzmir, Turkey

Electron Spin resonance (ESR) spectra of gamma irradiated dry yeast with doses between 0.5 and 10 kGy were studied. Un-irradiated dry yeast samples exhibited a weak singlet ESR signal at  $g=2.0058$ . However, irradiation produced an intensive singlet at  $g=2.0055$  with two shoulders at  $g=2.0140$  and  $g=2.0220$ . Dose-response curve of the radiation induced ESR signal at  $g=2.0055$  was found to be best described well by a sum of two exponential saturation functions. The stability of that radiation induced ESR signal at room temperature was studied over a storage period of 200 days. Progressive microwave saturation behaviors of ESR signals at room temperature were performed in the range of 0.01-50 mW. Also, the kinetic of the radiation induced signal at  $g=2.0055$  was studied in detail over a temperature range 313-373K by annealing samples at different temperatures for various times.

## Distribution of the gamma dose rate measured in 15 Portuguese thermal establishments

**Ana Sofia Silva, Maria de Lurdes Dinis**

Porto University, Faculty of Engineering; CERENA – Polo FEUP, Centre for Natural Resources and the Environment, Porto, Portugal

Natural radiation from external sources is variable worldwide and this is due mainly to high or low soil concentrations of radioactive minerals. In particular, high concentrations of radioactive minerals in soil have been reported in several countries such as Brazil, India, and China. The high variations in doses received by the public from natural sources results from the fluctuations of indoors concentrations.

In thermal spas, the exposure to natural radiation occurs mainly from radon dissolved in water, which may be released to the indoor air, and its solid decay products but also from external gamma radiation, although the radon exposure will be of much higher magnitude. Water supplies makes only a small contribution to the indoor radon concentration but can be the predominant source in areas where the radon content of groundwater is unusually high.

In Portugal, one of the tasks of the environmental radiation surveillance program is carried out through the Network of Continuous Monitoring of Radioactivity of the Environment (RADNET). Data from this network shows that the highest values for gamma radiation are registered on the northern and central areas of Portugal.

The objective of this study was to evaluate the indoor gamma dose rate in particular environments, such as thermal spas, and evaluate its contribution to the annual effective dose. For this purpose, a gamma dose rate assessment was carried out within 15 Portuguese thermal establishments, mostly located in the North-Centre region of the country, where both high and low indoor radon concentrations were previously registered.

The assessment was done using a Geiger counter equipment (GAMMA SCOUT® – GS3), able to measure  $\gamma$  radiation,  $\alpha + \beta$  and  $\alpha + \beta + \gamma$ . The equipment was used to measure the gamma radiation as *gamma dose rates* for an exposure period varying from 25 to 45 days.

The assessment focused on different treatment rooms of each thermal establishment: inhalation treatment rooms (ORL); thermal pool (TS); steam area room (SA) and it was carried out between 2011 and 2015. The moment of measurements for gamma dose rates was coincident with almost all measurements carried out for indoor radon concentration.

The measured data for gamma dose rates was statically studied for normality by applying two different tests: Chi-square test and Kolmogorov-Smirnov test.

The obtained data for indoor radon concentration was used to estimate the dose due to radon inhalation (internal dose) while the gamma dose rate registers were used to estimate the external exposure due to gamma irradiation exposure. The annual effective dose was then estimated by the combination of both doses.

The results show no abnormal or too high values detected for gamma dose rates in any situation and, therefore, the contribution of the external dose to the calculation of the effective annual dose is negligible. However, the Portuguese legislation (Decree-Law 222/2008) stipulates that professional activities, such as those that are developed in hydrotherapy treatments, may result in an annual effective dose higher than 1 mSv, and in these cases workers should be considered within an “existing exposure situation”. Depending on the values of the annual effective dose, workers are classified into two categories (A and B) and specific measures are previewed for each one of these situations.

The purpose of Directive 2013/59/EURATOM is to improve the radiological protection of workers who are or may be exposed to radiation, including workers who are exposed to natural radiation in the course of their professional activities, such as hydrotherapy treatments in thermal spas. Therefore, according to the legislation, measures should be taken to monitor and control the radiation exposure in these professional activities, such as (e.g.) : i) implementation of a monitoring system for the radiological protection of workers; ii) implement a radiological control plan for the facilities.

## Photoresist on thallium bromide crystals for gamma-ray detector fabrication

**Toshiyuki Onodera<sup>1</sup>, Keitaro Hitomi<sup>2</sup>**

<sup>1</sup> Tohoku Institute of Technology, Sendai, Japan

<sup>2</sup> Tohoku University, Sendai, Japan

This study reports electrode formation method by photoresist technique on thallium bromide (TlBr) semiconductor crystals for TlBr gamma-ray detector fabrication. TlBr crystals were grown by the travelling molten zone method and samples for photoresist were prepared from the grown TlBr crystals. After the surface treatment on the samples, conventional photoresist procedure consisting of coating resist solution, ultraviolet-rays irradiation and resist development were carried out to form mask patterns for electrode construction (3 mm diameters) on both side of the TlBr crystals (thickness of around 0.4 mm) by the vacuum evaporation method. Current-voltage characteristics and gamma-ray spectral response of the fabricated TlBr detectors were tested in order to evaluate the photoresist technique on performance of TlBr detectors.

## Dosimetric characterization of Methylthymol blue Fricke gel dosimeters using nuclear magnetic resonance and optical techniques

**Tariq F. Hailat<sup>1</sup>, Molham M. Eyadeh<sup>2</sup>,  
Khalid A. Rabaeh<sup>3</sup>, Balázs G. Madas<sup>4</sup>, Feras M. Aldweri<sup>5</sup>**

<sup>1</sup> Doctoral School of Physics, ELTE Eötvös Loránd University, Budapest, Hungary

<sup>2</sup> Physics Department, Faculty of Science, Yarmouk University, Irbid, Jordan

<sup>3</sup> Medical Imaging Department, Faculty of Allied Health Sciences, Hashemite University, Zarqa, Jordan

<sup>4</sup> Radiation Biophysics Group, MTA Centre for Energy Research, Budapest, Hungary

<sup>5</sup> Physics Department, Faculty of Science, Hashemite University, Zarqa, Jordan

Recently, a new radiochromic gel dosimeter based on the Fricke dosimeter with Methylthymol blue (MTB) dye in a gelatin matrix was introduced. The composition of MTB Fricke gelatin gel dosimeter was prepared and investigated using nuclear magnetic resonance (NMR) in terms of the spin-spin relaxation rate ( $R_2$ ) of hydrogen protons within the water molecule. The optical properties of MTB gel were also investigated using a spectrophotometric technique. The gel dosimeter presents a linear response for doses up to 20 Gy with ultraviolet visible (UV-Vis) spectrophotometry and 40 Gy with NMR. For a 0.1 mM MTB concentration and dose of up to 10 Gy, the sensitivity of the gel response analyzed by a spectrophotometer is 0.077 a.u. Gy<sup>-1</sup> at 620 nm with a linear coefficient of ( $r^2 = 0.998$ ), while the  $R_2$  sensitivity is 0.02 s<sup>-1</sup> Gy<sup>-1</sup> with a linear coefficient of ( $r^2 = 0.998$ ). By comparing the sensitivity of the Fricke-MTB dosimeter with the sensitivity of the Fricke-Xylenol orange (XO) dosimeter, the sensitivity of the Fricke-MTB dosimeter was higher. The absorbance and  $R_2$  dose sensitivity were dependent of the dose rate and photon energy beams, as observed over the range studied. The Fricke-MTB gelatin dosimeters can be scanned at higher wave lengths than the conventional Fricke-XO gelatin formulations.

## **Design and performance testing of the neutron detection module based on an inorganic scintillator for the neutron dosimetry**

**Seung Kyu Lee<sup>1</sup>, Sang In Kim<sup>2</sup>, Jungil Lee<sup>1</sup>, Insu Chang<sup>1</sup>,  
Jang-Lyul Kim<sup>1</sup>, Hyoungtaek Kim<sup>1</sup>, Min Chae Kim<sup>1</sup>**

<sup>1</sup> Korea Atomic Energy Research Institute, Daejeon, South Korea

<sup>2</sup> ARIM Science, Daejeon, South Korea

Recently, the neutron dosimetry is the most crucial issue as the increasing of the use of research facilities using an accelerator such as proton particle accelerators, BNCT facilities, and so on. In general, organic scintillation detectors using the liquid scintillators or a He-3 proportional detectors were used for the neutron measurements in the mixed fields of neutrons and gamma-rays. Since the organic scintillators have lower sensitivity due to the lower light output than inorganic scintillators and the H-3 detectors have a limited supply, there are many studies for neutron detectors to replace them. In this study, the neutron detection module using a Li-based inorganic scintillator has been designed and the separation sensitivity of the neutrons/gamma-rays was measured. In addition, the response functions for various moderated materials were calculated using Monte Carlo simulations for neutron dosimetry.

## **ISOCS measurements: A way to improve radioactive waste characterization**

**Alfonso Compagno<sup>1</sup>, Nadia Cherubini<sup>1</sup>,  
Maria Letizia Cozzella<sup>1</sup>, Alessandro Lago<sup>2</sup>, Luigi Lepore<sup>3</sup>**

<sup>1</sup> ENEA, Rome, Italy

<sup>2</sup> PE Consultant, Rome, Italy

<sup>3</sup> University of Rome La Sapienza, Rome, Italy

Radioactive materials are widely used in many different fields (medical, scientific research, industrial application, etc.) producing any kind of radioactive waste in terms of radionuclides included within the waste material and its physical and chemical characteristics. These radioactive wastes are conveniently stabilized in a suitable matrix to avoid its dispersion in the environment. The shape of those artefacts is usually a drum which can be incorporated into an additional barrier system to reinforce the confinement.

The radiological characterization is an essential step to plan the final disposal of the waste form. This operation has to be carried out with the all necessary technical precautions to preserve the safety of the exposed personnel and the environment, having care to generate results with sufficient accuracy and precision. The aim of this work is to propose a new procedure in using In-Situ Object Counting System (ISOCS) gamma spectrometry system to optimise the characterization of the waste drums providing reliable results and keeping the safety at acceptable level.

It is well known that a “one shot” measurement is rarely useful for the waste drum characterization, because of the inhomogeneity of the matrix. As to overtake this problem, ISOCS system has been combined with a portable rotating platform. The scope of the drum rotation is the simulation of the matrix homogeneity and uniformity of activity distribution, allowing to acquire -in a single measurement- enough data for the complete waste characterization.

In a laboratory setup, mock-up waste drums have been prepared. To simulate, as much as possible, real scenarios, waste drums have been filled with different materials: air; neoprene, and concrete. <sup>60</sup>Co, <sup>133</sup>Ba, and <sup>152</sup>Eu reference sources have been set in different positions inside each waste drum, as to test the proposed procedure.

The validation of data has been carried out by measuring the main gamma emissions from reference sources, considering the platform rotation speed, the use of different collimators coupled with the detector, and the efficiency calculation with different templates available within the ISOCS software.

## Monte-Carlo simulation of coincidence background spectrum of large-volume NaI(Tl) detector

**Dusan Mrdja<sup>1</sup>, Rade Marjanovic<sup>1</sup>, Kristina Bikit-Schroeder<sup>1</sup>,  
Istvan Bikit<sup>1</sup>, Jaroslav Slivka<sup>1</sup>, Sofija Forkapic<sup>1</sup>, Tomas Nemes<sup>2</sup>**

<sup>1</sup> Department of Physics, Faculty of Sciences, University of Novi Sad, Novi Sad, Serbia

<sup>2</sup> Department of Fundamentals Sciences, Faculty of Technical Sciences, University of Novi Sad, Novi Sad, Serbia

Different types of coincidence detection systems are widely used in the field of gamma spectroscopy in order to explore cosmic-rays induced process which can be of interest for deep underground experiments searching for rare nuclear processes or possible existence of dark matter particles. According to this, the qualitative and quantitative analysis of background events registered by detectors operating in coincidence mode is important. In this work we established the coincidence system of plastic scintillator and large volume (9"x9") NaI(Tl) annular detector and collected the corresponding background spectra, mainly induced by cosmic-ray muons. The spectra were acquired for two different position of plastic scintillator (axial and off-axis geometry) relative to NaI(Tl) detector. These spectra were collected within ground-based laboratory (~ 80 m a.s.l.) where the CR-muon flux is much higher than in underground environment, thus providing possibility to explore muon induced events with better statistics. In addition, we performed Monte-Carlo simulation of experimental setup, based on realistic energy and angular distribution of CR muons, and compared the obtained simulated results with experimental ones. Also, we showed that some features of coincidence spectra resulting in experiment as a consequence of pure geometrical characteristics of large volume NaI(Tl) annulus, are also visible in simulations. This was a good test of use of Geant4 simulation toolkit for exploration of CR muons interaction with different kind of materials.

## Monte-Carlo simulation of the MUCA imaging system

**Kristina Bikit-Schroeder<sup>1</sup>, Dusan Mrdja<sup>1</sup>, Istvan Bikit<sup>1</sup>,  
Jaroslav Slivka<sup>1</sup>, Gergő Hamar<sup>2</sup>, Gábor Galgóczi<sup>2</sup>, Dezső Varga<sup>2</sup>**

<sup>1</sup> Department of Physics, Faculty of Sciences, University of Novi Sad, Novi Sad, Serbia

<sup>2</sup> MTA Wigner Research Centre for Physics – High Energy Physics Laboratory, REGARD Group, Budapest, Hungary

The developed MUCA (MUon CAmera) system measures the cosmic muon induced secondary particles, while tracking the incoming muons in order to reconstruct the 3 dimensional image of the investigated object. In the last few years, the combined muon tracking system was operated in the nuclear physics laboratory in Novi Sad in collaboration with the WignerRCP of Budapest.

The first version of this equipment was very successfully used for muon imaging of organic structures, such as bones and soft tissue.

In the next phase, a larger 0.5m x 0.5m MWPC-based tracker has been added to the system, so now the system consists from this tracker above the object imaged, and the plastic scintillators detecting the secondary radiation created by muons in the object, while the smaller (0.25m x 0.25m) MWPC-based tracker is placed below the object.

In order to optimize this complex system for obtaining better image quality, Monte-Carlo simulations are necessary. Geant4 simulations were developed to understand the spectra of the muon induced secondary radiation. Material identification capabilities were tested via monoenergetic 2 GeV muons on several realistic targets.

The results of these simulations will be presented in this paper.

## Microdosimetry with a sealed mini-TEPC at the SOBP of CATANA

**Anna Bianchi<sup>1</sup>, Valeria Conte<sup>2</sup>, Anna Selva<sup>2</sup>, Paolo Colautti<sup>2</sup>,  
Alessio Parisi<sup>3</sup>, Brigitte Reniers<sup>4</sup>, Filip Vanhavere<sup>3</sup>**

<sup>1</sup> Belgian Nuclear Research Center SCK-CEN, UHasselt – Faculty of Engineering Technology – CMK – Nuclear Technology Center, INFN – Laboratori Nazionali di Legnaro, Mol, Diepenbeek, Legnaro, Belgium

<sup>2</sup> INFN – Laboratori Nazionali di Legnaro, Legnaro, Italy

<sup>3</sup> Belgian Nuclear Research Center SCK-CEN, Mol, Belgium

<sup>4</sup> UHasselt – Faculty of Engineering Technology – CMK – Nuclear Technology Center, Diepenbeek, Belgium

**Introduction.** Tumour treatments with protons and carbon ions are increasing worldwide thanks to both the favourable dose-depth distribution and the enhanced biological effect with respect to conventional radiotherapy.

The relation between the physical process and the biological effect has still to be established. Anyway, a detailed knowledge of the physical properties of the beam in depth would improve the final success of hadron therapy. A complete characterization of the proton beam radiation quality in terms of measurable physical quantities at the subcellular scale is necessary to improve treatment plans.

To this regard, microdosimetry is the suitable technique; it records the stochastic nature of the energy deposition process at a microscopic scale. The full microdosimetric spectrum gives a physical description of the radiation-target interaction. Tissue-Equivalent gas Proportional Counters (TEPC) are the reference devices for experimental microdosimetry.

**Methods.** A miniaturized TEPC (mini-TEPC) was developed in Legnaro National Laboratories (LNL) of the National Institute of Nuclear Physics (INFN) to cope with high-intensity clinical beams such as those employed in active-scanning beams. The cylindrical cavity has a diameter of 0.9 mm, as compared to the 12.7 mm of the Far West LET-1/2. Several microdosimetric measurements were performed over years, operating the detector in gas-flow modality in order to minimize the aging effects due to gas deterioration.

However, a sealed detector working in gas-steady modality would be a great improvement for its practical use in clinical environments by reducing the encumbrance of the set-up and avoiding the necessity of introducing the propane gas flow system in the treatment room.

A prototype of a sealed mini-TEPC was irradiated in the 62 MeV clinical proton beam of CATANA at the LNS of INFN, using a half-modulated SOBP already used to treat ocular melanoma.

**Results.** Following an appropriate procedure of cleaning and gas filling of the detector, several measurements were performed at different depths within the proton SOBP and at different beam currents.

Microdosimetric spectra were acquired repeatedly over time and they were found to be very well superimposable (both shape and mean values), highlighting the stability of the detector even in gas-steady modality.

The analysis is carried on both in terms of the shape of the microdosimetric spectrum and of the average quantities such as the dose-mean lineal energy and the frequency mean-lineal energy to be compared with dose and LET profiles.

**Conclusions.** The results of this measurement campaign will be benchmarked with Monte Carlo radiation transport computer simulations to confirm the possibility of using a sealed mini-TEPC as radiation quality monitor in therapeutic proton beams. Furthermore, the stability of the microdosimetric response even at high beam currents paves the way to the design of a new miniaturized TEPC that works in gas steady-modality.

## On the feasibility of dating the age of a nuclear incidental event by gamma-ray spectrometry of environmental samples

**Elio Tomarchio**

University of Palermo – Dipartimento DEIM, Palermo, Italy

The dating of a nuclear incidental event is an important element for the assessment of its environmental impact and radiation protection implications on the involved population. In this framework, a procedure has already been proposed to determine the age of a nuclear event by measuring through a gamma-ray spectrometric analysis the activity of two fission products in a small sample of uranium irradiated for a short time in a nuclear reactor [1,2]. However, It may be useful to extend the application of the above mentioned procedure for assessing the “timing of occurrence” of an incidental event considering other samples and in particular, by sampling and measuring environmental samples.

The aim of this work was to verify the feasibility of the dating procedure utilizing gamma-ray spectrometric measurements of environmental samples on various matrices as well as the applicability to cases where there are not enough information regarding sample characterization (as composition, sample density, measurement geometry, calibration parameters of the measurement system and so on).

The procedure, which involves the temporal analysis of the data of several measurements taken on a sample with increasing waiting times, was tested taking into account the results of the measurements related to the first irradiation of an UO<sub>2</sub> fuel pellet in the Research Nuclear Reactor AGN 201 “COSTANZA”, supplied with the University of Palermo, as well as those related to radioactive contamination following various nuclear events, as the Chernobyl or Fukushima accidents.

The analysis of the values of the activity ratios for different radionuclides (isotopes, isobars, etc.) has led to extremely comforting temporal results in the case in which the system can be considered isolated, for the irradiation modalities or its temporal evolution. More uncertainties characterize the evaluations related to samples of different origin and nature, in which the quantities may have been relatively modified due to the physical-chemical phenomena that have affected the reference matrices.

In conclusion, the method is largely applicable but attention must be paid to possible uncertainties caused by probable chemical-physical changes that may occur in a no-insulated sample originating from distant sites.

### References

- [1] – Nir-El Y., Applied Radiation and Isotopes, 60 (2004), 197-201.
- [2] – Nir-El Y., Journal of Radioanalytical and Nuclear Chemistry, 267 (2006), 567-573.

## Overview of recent nanodosimetric experiments with Jet Counter device

**Monika Mietelska<sup>1,2</sup>, Marcin Pietrzak<sup>1,2</sup>,  
Aliaksandr Bantsar<sup>2</sup>, Zygmunt Szepliński<sup>3</sup>**

1 Biomedical Physics Division, Faculty of Physics, University of Warsaw, Warsaw, Poland

2 National Centre for Nuclear Research, Otwock-Swierk, Poland

3 Heavy Ion Laboratory, University of Warsaw, Warsaw, Poland

New methods of radiotherapy using non-photon sources of ionising radiation are being introduced in last years to cure specific types of cancer. Unfortunately, the biological outcomes are much more difficult to predict for those new radiation modalities as it depends both on the type and energy of radiation. As the initiation of radiation induced damage is dominated by interactions occurring at the location of the DNA or within its vicinity knowing the distribution of such interactions is crucial to properly assess the biological effectiveness of radiation. For this reason, nanodosimetry, a new experimental field to investigate the particle track structure within radiosensitive biological targets, has emerged. Its crucial assumption is that initial physical effect changes into measurable biological outcome. Based on this hypothesis, nanodosimetry aims at establishing a new concept of radiation quality built on measurable characteristics of the particle track structure at the nanometre scale.

Four different nanodosimetric detection systems have been developed to date to measure the number of ionisations produced by the passage of single primary particle in nanometre-size targets comparable to a short segment of DNA molecule. One of them is the Jet Counter operated at National Centre for Nuclear Research, Poland. The overview of fundamental nanodosimetric concepts and recent Jet Counter experiments with carbon ions (U-200 cyclotron at HIL) and alpha particles (Am-241 source) will be presented.

## Survey of soil radioactive contamination in the basement premises of the reactor MR

**Alexey Stepanov, Iurii Simirskii, Nikolay Gromov,  
Ilia Semin, Vyachaslav Stepanov, Anatoly Volkovich**

NRC, Moscow, Russia

In 2011, the dismantling of the MR reactor was started at the Kurchatov Institute. 110 tons of equipment was dismantled, of which 53 tons were radioactive waste with a total activity of  $5.0 \cdot 10^{10}$  Bq. In 2013-2014 was dismantled equipment 9 loop facilities, from equipment released 47 the basement. Dismantling of the equipment makes it possible to reduce the equivalent dose rate in the premises to 0.01-0.03 mSv/h. Next step was a survey of soil radioactive contamination in these basement premises. Soil samples for spectrometric analysis (about 100 samples) were taken in all basements of the reactor building.

During dismantling of the pipes of radwaste sewage in the basement, leakage of liquid radioactive waste was found. In the samples taken from this pipes the elements of the fuel matrix was found. For soil samples taken at the leakage sites of radioactive waste, radiochemical analysis was made. Another criterion for radiochemical analysis was the detection of the radionuclide  $^{241}\text{Am}$  in the gamma-spectrum of the soil.

Concentrations of  $\gamma$ -radionuclides were measured by the spectrometric complex InSpector-2000 of the Canberra Company that included a semiconductor detector using HP Germanium GC-4018. The analysis of the  $\gamma$ -spectrum was made by the GENIE-2000 software. Concentration of  $^{90}\text{Sr}$  was detected by the scintillation  $\beta$ -spectrometer "Progress-beta", with the plastic scintillation detector BDEB-3-2U.

The concentrations of uranium and plutonium radionuclides in the soil samples were determined by alpha-spectra of the targets, prepared by the electrochemical method after radiochemical separation of the investigated samples. The alpha-spectra was obtained with the vacuum Alpha Analyst Integrated Alpha Spectrometer of the Canberra company with a semi-conductor passivated implanted planar silicon detector.

It was found that radioactive contamination of soil is formed mainly by  $^{137}\text{Cs}$  and  $^{90}\text{Sr}$ . The soil contaminations by alpha emitted radionuclides are negligible by activity and volume. In cases where the specific activity of radionuclides in the soil exceeded the value of MSSA ( $10^4$  Bq/kg for  $^{137}\text{Cs}$  and  $10^5$  Bq/kg for  $^{90}\text{Sr}$ ), it was partially replaced. This allows reducing the equivalent dose rate in the premises to  $\sim 0.8 \mu\text{Sv/h}$ .

## Investigation of light collection efficiency in plastic scintillators

**Kristina Bikit-Schroeder<sup>1</sup>, Dusan Mrdja<sup>1</sup>, Istvan Bikit<sup>1</sup>,  
Jaroslav Slivka<sup>1</sup>, Gergő Hamar<sup>2</sup>, Gábor Galgóczi<sup>2</sup>, Dezső Varga<sup>2</sup>**

<sup>1</sup> Department of Physics, Faculty of Sciences, University of Novi Sad, Novi Sad, Serbia

<sup>2</sup> MTA Wigner Research Centre for Physics – High Energy Physics Laboratory, REGARD Group, Budapest, Hungary

Plastic scintillators are widely used as anti-muon vetos for gamma spectrometry. Recently, we used plastic scintillators for the detection of secondary radiation induced by cosmic muons. The stability of the output signals from the plastic scintillators via the photomultiplier is not well known. Poor light collection will affect not only the amplitude of the output signal, but also the number of output signals because of the threshold in the amplifying stage. Thus, signals with smaller amplitude might be rejected, hence affecting the detection efficiency of the plastic scintillator.

The problematics of incorporating the light propagation inside plastic scintillator detectors in Geant4 simulations is one of the tasks considered in the paper. In order to quantify light collection efficiency of plastic scintillators, adequate experimental measurements were performed, and further compared with results of Geant4 simulations of this experimental setup. The issue of light propagation inside the scintillator was addressed by simulating the path of each individual photon inside the scintillators. For validation of the simulation results regarding light propagation, appropriate plastics calibration was needed in order to understand the light collection efficiency for each part of the scintillator. Hence, experimental spectra of plastic scintillators were recorded for several positions of Cs-137 and Am-241 sources along the plastic's surface, relative to the PMT position.

In this paper, the significance of incorporating light collection inside the scintillators on the results of simulation will be studied, relative to the simulations when only simple deposition of ionizing radiation energy in the scintillators is taken into account. Furthermore, the comparison between results of simulations and obtained experimental results will be presented.

## Analysis of radioactivity content in hard coal and products of coal combustion

Agata Walencik-Łata<sup>1</sup>, Danuta Smółka-Danielowska<sup>2</sup>

1 University of Silesia, Institute of Physics, Department of Nuclear Physics and Its Applications, Chorzów, Poland

2 University of Silesia, Faculty of Earth Sciences, Sosnowiec, Poland

Upper Silesia is one of the most urbanized and industrialized regions of Poland. In this region the majority of Polish hard coal is extracted and almost all mining plants of Poland are located. Hard coal is predominant energy source in Poland which is used in combustion, coking and other technological industrial processes, as well as for heating purposes in households. Literature data indicate low radioactivity content of hard coal. On the other hand combustion of fossil fuels leads to accumulation of radioisotopes in ash and emission of dust to upper atmosphere. In Upper Silesia high concentration of suspended particulates is noted. The aim of present study is to determine radioactivity content in hard coal, bottom and fly ash and products of coal combustion. The concentrations of  $^{232}\text{Th}$ ,  $^{226}\text{Ra}$ ,  $^{40}\text{K}$  were determined with the use of gamma spectrometer equipped with high purity germanium detector of 60.7 mm crystal diameter and Cryo-Pulse 5 Plus and electrically powered cryostat from Canberra-Packard. The measurements of  $^{234,238}\text{U}$  isotope activities were performed with the use of  $\alpha$  – spectrometer 7401VR (Canberra – Packard, USA) equipped with the Passivated Implanted Planar Silicon detectors with the surface area equal to 300 mm<sup>2</sup>. The wet-mineralization of samples was performed with the use of hot acids: HF, HNO<sub>3</sub>, HCl with H<sub>3</sub>BO<sub>3</sub>. Uranium was pre-concentrated with iron and co-precipitated with ammonia at pH 9. The separation of U was performed with the use of the anion exchange resin Dowex 1×8 (Cl<sup>-</sup> type, 200-400 mesh). Uranium can be used as environmental tracer and based on the  $^{234,238}\text{U}$  concentrations, uranium content and  $^{234}\text{U}/^{238}\text{U}$  activity ratios were calculated. The obtained results of radioactivity content in different samples will be presented and their impact on pollution of the environment will be discussed.

**Acknowledgments:** This work was partly supported by the National Science Centre, Poland (project: 2018/02/X/ST10/01540).

## **Application of remotely controlled collimated spectrometric systems in the works on dismantling the MR reactor and rehabilitation of the territory of NRC Kurchatov Institute**

**Vyacheslav Stepanov, Oleg Ivanov,  
Sergey Smirnov, Victor Potapov, Alexey Danilovich**

NRC Kurchatov Institute, Moscow, Russia

In NRC Kurchatov Institute since 2003 works on dismantling of the Mr Reactor and rehabilitation of the territory are carried out. Remote-controlled spectrometric systems were developed and used to map the distribution of radioactive contamination of the territory, premises and equipment of the reactor:

1. “Gamma-locator” is a spectrometric system, developed for remote radioactivity measurements using field radiometry methods. System consists of scanning head, CCD video camera, pan and tilt table, and controlling PC. The scanning head is a spectrometric detector, placed in collimated lead shielding. CsI(Tl) scintillator (volume ~80 cm<sup>3</sup>) coupled to Si PIN photodiode is used as the detector. This video camera represents a field of view (FOV) of the detector. A distance from the scanning head to the PC may be up to 200 meters. During activity for rehabilitation of the territory of temporal storage of radioactive wastes of Institute the gamma-locator system was used for remote measurements of radiological conditions. The data of measurements of gamma-field characteristics from different directions was used for calculation of dose rate. The use of gamma locator in rehabilitation works on the territory allows you to adjust the performance of work and plan protective measures that do not allow the increase of EDR above the control levels beyond the perimeter of the site of work.

2. The remote-controlled spectrometer system was used in the survey of technological rooms of the reactor. The system consists of a spectrometric collimated gamma-ray detector, color video camera and a control unit, mounted on a rotator, which are mounted on a tripod with the host computer. Two detectors are based on CsI(Tl) scintillator and a photodiode (with a volume of scintillator – 20 and 5 cm<sup>3</sup>) and a CdZnTe detector volume of 60 mm<sup>3</sup> may be used. The angle of view of the collimator is about 10 degrees. The instrument are controlled by operator from computer. Operator works at a safe position. The device was used to measure radioactive contamination in premises with a high level of EDR. The resulting maps of the distribution of contaminants in buildings and installations. According to the dose rate distribution map, the safest dismantling of the equipment was planned.

3. The upgraded remote-controlled spectrometric system with a 1500 m<sup>3</sup> CdZnTe detector was used to map radioactive contamination of the walls and floor of the reactor storage pool after dismantling the equipment and plating. The use of these systems has significantly reduced the radiation dose to the staff.

## Comparative assessment of individual doses of radiation of personnel in Russia and the European countries

**Stepan Bazhin, Ekaterina Shleenkova, George Kaidanovsky, Vladimir Iliy**

Saint-Petersburg Research Institute of Radiation Hygiene after Professor P.V. Ramzaev, Saint-Petersburg, Russia

To be convinced that the system of radiation safety in Russia functions properly, comparison of individual doses of radiation for the personnel of medical institutions was performed in Russia and a number of the European countries.

For the analysis and comparison of average doses, the following sources of information were used (data for 2013 and 2017):

- own database of Laboratory of Radiation Control of Saint-Petersburg Research Institute of Radiation Hygiene after Professor P.V. Ramzaev;
- reports of the Platform of the European Study on Occupational Radiation Exposure (ESOREX);
- Integrated State System for Doses Control and Registration database.

As a result of the analysis of the acquired information it is possible to draw a conclusion that results of Integrated State System for Doses Control and Registration database and own laboratory database are rather comparable while average effective annual doses for the European personnel differ by 2-3 times.

The main difficulties arise because of uncertainty in approach to the issues:

1. Record of doses is lower than the minimum level of registration (MLR);
2. Record of doses in the absence of the activity periods;
3. Processing of unexpectedly high doses;
4. Subtraction of doses of background radiation.

In the European countries officially there is a MLR of doses. Values below of this level are brought in registration records as zero.

Subtraction of values of doses due to a natural background from indications of the exposed individual dosimeters is not made. At small values of individual doses, subtraction of a natural background leads to errors in hundreds of percent. At doses over 1.0 mSv, background doses appear to be less, than an error of measurements of an individual dose and have no impact on the final result. Mean value of the dose caused by a natural background in St. Petersburg is about 0.7 mSv per year. If one subtracts this value from the average annual doses, then the results comparable to data of Slovenia will turn out and if one subtracts the mean European value MLR accepted equal to 0.4 mSv (0.1 mSv in a quarter), then the result will be comparable to data of Lithuania and Finland.

Thus all countries need to seek for creation of a uniform way of data recording for an opportunity carrying out future researches such as:

- assessment of the actual radiation of workers with the purpose to show its compliance to regulatory requirements and the fact that the used control measures allow to hold doses at reasonably achievable low level and that limits of doses are not exceeded;

- epidemiological and other researches of biological impact of ionizing radiation

## Influence of Mg codoping on carrier dynamics in GAGG:Ce scintillation crystals

**Gintautas Tamulaitis<sup>1</sup>, Saulius Nargelas<sup>1</sup>, Augustas Vaitkevicius<sup>1</sup>,  
Alberto Gola<sup>2</sup>, Alberto Mazzi<sup>2</sup>, Mikhail Korjik<sup>3</sup>**

<sup>1</sup> Vilnius University, Vilnius, Lithuania

<sup>2</sup> Fondazione Bruno Kessler, Trento, Italy

<sup>3</sup> Research Institute for Nuclear Problems, Minsk, Belarus

Fast luminescence response becomes one of the key parameters of scintillation crystals for radiation detectors to be exploited in medical imaging and high-luminosity high-energy physics experiments, where 10 picoseconds is the timing currently in target. Ce-doped garnet-type scintillators and, especially, gallium gadolinium garnet ( $\text{Gd}_3\text{Al}_2\text{Ga}_3\text{O}_{12}$ , GAGG) attracted considerable attention due to a good combination of high light yield and stopping power to gamma-radiation and neutrons, good matching of the emission spectrum with the sensitivity spectrum of the conventional silicon photomultipliers (SiMP), and competitive timing properties, which have been demonstrated to be improved by codoping.

To better understand the origin of the positive effect of the codoping, we studied the carrier dynamics in GAGG:Ce with and without codoping. We exploited optical pump and probe technique: the nonequilibrium carriers were excited by pump pulse, while the density of the carriers in free or trapped states and at the emission centers was probed by a delayed probe pulse. The technique exhibits three advantageous features: i) capability of selective excitation by selecting the excitation photon energy, ii) capability of following the kinetics of transient absorption due to nonequilibrium carriers in a wide spectral range, and iii) high time resolution limited just by the pulse width (200 fs in our experiments). The experimental results on carrier dynamics were compared with the results of our simulations based on the rate equations. The timing properties of the scintillators in conditions close to those in real operation were tested in our coincidence time resolution (CTR) experiments using SiPMs and a  $^{22}\text{Na}$  source providing 511 keV coincidence events.

We report that a substantial suppression of the slow rise component of the population of the lowest excited  $\text{Ce}^{3+}$  level acting as an emitting level in GAGG:Ce is achieved by codoping of the scintillator by divalent Mg even at codoping levels as small as 10 ppm. Carrier trapping has the main influence on the rise edge of the population of the emitting center in GAGG:Ce and is substantially suppressed by Mg-codoping. Fitting of experimental and simulated kinetics of the population of the excited  $\text{Ce}^{3+}$  levels show that the time of intracenter relaxation via  $5d_2$  to  $5d_1$  transition equals  $\sim 500$  fs. The disappearance of the slow component in the rise time of  $5d_1$  population correlates with the improved time resolution in CRT measurements. The full width at half maximum of 165 ps is demonstrated and is promising for further improvement.

## **Natural radiation background measured within the BSUIN (Baltic Sea Underground Innovation Network) project**

**Jan Kisiel**

Institute of Physics, University of Silesia, Katowice, Poland

Aim of the BSUIN (Baltic Sea Underground Innovation Network) project is to make underground laboratories (ULs) in the Baltic Sea region, which are usually built in mines, underground storage facilities or as tunnels for transportation, more accessible and attractive for innovation, business development and science. Converting such facilities to laboratory creates typically a lot of challenges, including a detailed description of natural radiation background. The goal of present study is to determine radioactivity content in rock and water samples using alpha, gamma and liquid scintillation spectrometry techniques. The radon concentration in air was measured with the use of the RAD7 semiconductor detector from DurrIDGE. The in-situ gamma spectra and neutron flux determination will be presented as well. The obtained results of natural radioactivity in a selected BSUIN UL will be discussed. Also the overall status of the BSUIN project will be given. The BSUIN project is funded by the Interreg Baltic Sea Region Program.

## **New results for the space radiation environment aboard the ExoMars Trace Gas Orbiter during the transit to Mars and in Mars orbit**

**Jordanka Semkova<sup>1</sup>, Rositza Koleva<sup>1</sup>, Victor Benghin<sup>2</sup>, Krasimir Krastev<sup>1</sup>,  
Yuri Matviichuk<sup>1</sup>, Borislav Tomov<sup>1</sup>, Tsvetan Dachev<sup>1</sup>, Stephan Maltchev<sup>1</sup>,  
Plamen Dimitrov<sup>1</sup>, Igor Mitrofanov<sup>3</sup>, Alexey Malakhov<sup>3</sup>, Dmitry Golovin<sup>3</sup>,  
Maxim Mokrousov<sup>3</sup>, Anton Sanin<sup>3</sup>, Maxim Litvak<sup>3</sup>, Andrey Kozyrev<sup>3</sup>,  
Vladislav Tretyakov<sup>3</sup>, Sergey Nikiforov<sup>3</sup>, Andrey Vostrukhin<sup>3</sup>,  
Vyacheslav Shurshakov<sup>2</sup>, Sergey Drobyshev<sup>2</sup>**

1 Space Research and Technology Institute, Bulgarian Academy of Sciences, Sofia, Bulgaria

2 Institute of Biomedical Problems of the Russian Academy of Sciences, Moscow, Russia

3 Space Research Institute, Russian Academy of Sciences, Moscow, Russia

ExoMars is a joint ESA – Roscosmos program for investigating Mars. Two missions are foreseen within this program: one consisting of the Trace Gas Orbiter (TGO), launched on March 14, 2016; and the other, featuring a rover and a surface platform, with a launch date of 2020. The science phase of TGO started in April 2018 when the satellite was inserted in its science circular orbit at about 400 km distance from Mars. We present recent results from measurements of the charged particle fluxes, dose rates, linear energy transfer spectra and estimation of dose equivalent rates in ExoMars TGO science orbit and comparison with the data obtained during the cruise and in high elliptic Mars's orbit, provided by Liulin-MO dosimeter of FRENDS instrument aboard TGO.

The average flux from GCR for April 16–November 30, 2018 in Mars science orbit is 3.01 and 3.11  $\text{cm}^{-2}\text{s}^{-1}$ , the average dose rate is 343.3 and 358.8  $\text{mGy h}^{-1}$ , the average dose equivalent rate is 1.56 and 1.63  $\text{mSv h}^{-1}$  in two perpendicular directions.

The dosimetric measurements in Mars' orbit demonstrate strong dependence of the charged particle fluxes of Liulin-MO field of view shadowed by Mars.

The obtained data show that during the cruise to Mars and back (6 months in each direction), taken during the declining of solar activity, the crewmembers of future manned flights to Mars will accumulate at least 60% of the total dose limit for the cosmonauts/ astronauts career in case their shielding conditions are close to the average shielding of Liulin-MO detectors – about 10  $\text{g cm}^{-2}$ .

In April–November 2018 in TGO Mars science orbit the flux is ~ 90%, dose rate is ~ 84%, dose equivalent rate is ~70% of that in February–March 2017 in high elliptic Mars's orbit.

The results are important for future manned mission to Mars radiation risk estimations.

A similar module, called Liulin-ML for investigation of the radiation environment on Mars' surface as a part of the active detector of neutrons and gamma rays ADRON-EM on the Surface Platform is under preparation for ExoMars 2020 mission.

## Neutron dosimetry at BINP using TLDs with LiF and portable devices

**Mikhail Petrichenkov, Vladimir Chudaev, Anatoliy Repkov,  
Vladimir Eksta, Nataliya Shamakina, Sergey Melnik**

BINP, Novosibirsk, Russia

The electron-positron colliders and accelerator based neutron source for boron neutron capture therapy (BNCT) at Budker Institute of Nuclear Physics (BINP) require to perform personal dosimetry and monitoring of controlled areas by using of certified means. Thermoluminescent dosimeters (TLDs) with Lithium Fluoride (LiF) are of this kind in Russia, but they have too high response to low energy neutrons. Fortunately there is “dosimeter of effective dose” method developed at Institute of High Energy Physics (IHEP, Russia), allowing correction of TLD response to neutrons. We have determined in experiments these correction coefficients for neuron field behind shielding of BNCT facility and in direct neutron beam. In addition, we compared the results behind shielding with data obtained from portable dosimeters MKS-1117M with BDKN-03 neutron detection unit and self-designed activation type neutron detector based on rhodium foil around Geiger counter placed inside ~12” polyethylene moderator. MKS-1117M with BDKN-03 have shown good agreement with TLDs after correction.

## Registration of gamma-gamma coincidences from Ba-133 decay

Nevenka M. Antović<sup>1</sup>, Nikola R. Svrkota<sup>2</sup>, Sergey K. Andrukhovich<sup>3</sup>

<sup>1</sup> University of Montenegro, Faculty of Natural Sciences and Mathematics, Podgorica, Montenegro

<sup>2</sup> Centre for Ecotoxicological Research, Podgorica, Montenegro

<sup>3</sup> National Academy of Sciences of Belarus, Institute of Physics, Minsk, Belarus

Man-made radionuclide  $^{133}\text{Ba}$ , with the main production mode – neutron activation:  $^{132}\text{Ba}(n,\text{g})^{133}\text{Ba}$ , but also  $^{133}\text{Cs}(p,n)^{133}\text{Ba}$ , has a half-life of around 10.5 y and decays to  $^{133}\text{Cs}$  by electron capture. It disintegrates dominantly to the two excited levels of  $^{133}\text{Cs}$  (~437 keV and ~384 keV), while the transitions to the other two excited levels and the ground state can be considered as minor. The  $^{133}\text{Ba}$  decay is followed by the emission of nine gamma rays, with energies in the range from 53.2 keV to 383.8 keV, and intensities – from 0.45% to 62.05%. The most intense two-fold cascade transition contains gamma rays: 356 keV (62.05%, from the excited level 437 keV to the excited level 81 keV) and 81 keV (33.31%, from the excited level 81 keV to the ground state of  $^{133}\text{Cs}$ ). Our research on coincident registration of gamma rays from the  $^{133}\text{Ba}$  decay using NaI(Tl) detectors (15 cm x 10 cm) working in different modes of counting has been started recently, and the first results are presented here. Calibration gamma standard solution (Eckert&Ziegler, 55.54 kBq on March 01, 2010) was used to determine detection efficiency of the gamma rays from Ba-133 decay with energy >200 keV by two NaI(Tl) detectors at an angle of ~180°. Registration of the 356 keV photopeak in the mode of double coincidences is particularly considered, as well as an overlapping of this peak and the peak created by the 383.8 keV gamma rays from the same decay (8.94%; from the excited to the ground state) – in the integral and non-coincidence mode of counting.

**Keywords:** Ba-133 decay, NaI(Tl), double gamma coincidences

## Quality assurance of gamma ray measurements with HPGe detectors used in radiopharmaceutical production

**Zbigniew Tymiński, Paweł Saganowski, Tomasz Dziel, Anna Listkowska,  
Edyta Lech, Ewa Kołakowska, Tomasz Ziemek, Daniel Cacko, Ryszard Broda**

NCBJ Radioisotope Centre POLATOM, Otwock-Świerk, Poland

Radioisotope Centre POLATOM, a part of National Centre for Nuclear Research is a one of manufacturers and distributors working for research, development and life sciences. The nuclear medicine and the radiopharmaceuticals are very important part of the interest. Since the radiopharmaceuticals have a significant impact on the human body all the isotopic goods applied in medicine have to conform to specifications under many headings i.e. must comply with European Pharmacopoeia standards.

To prove that products meet specific requirements the quality system should be implemented, among others, to the gamma-ray spectrometry. The measurement systems with HPGe detectors must meet several standards to fulfill the requirements of management system based on ISO 17025 by proper analysis routine and quality of results evaluated through inter-laboratory comparisons. The parameters of the measurement systems must be also optimized for the best possible response and monitored in quality control frame. The thresholds should be selected on the system for triggering warnings in case of deterioration of work. This work presents the experience gained by Gamma Spectrometry Laboratory from the use of methods applied for the radioactive impurities and activity measurements conducted using high pure germanium detectors and the GENIE-2000 software for many years.

## Study of luminescence properties of $Gd_3(Ga,Al,Sc)_5O_{12}:Ce^{3+},Ca^{2+}$ scintillating single crystals under UV and electron beam excitation

**Dmitry Spassky<sup>1</sup>, Sergey Omelkov<sup>2</sup>, Vitali Nagirnyi<sup>2</sup>, Nina Kozlova<sup>3</sup>, Nataliya Krutyak<sup>4</sup>, Alice Ukhanova<sup>4</sup>, Oleg Buzanov<sup>5</sup>, Mikhail Korjik<sup>6</sup>**

<sup>1</sup> Skobeltsyn Institute of Nuclear Physics, M.V. Lomonosov Moscow State University, Moscow, Russia

<sup>2</sup> Institute of Physics, University of Tartu, Tartu, Estonia

<sup>3</sup> National University of Science and Technology (MISIS), Moscow, Russia

<sup>4</sup> Physical Department, M.V. Lomonosov Moscow State University, Moscow, Russia

<sup>5</sup> Fomos-Materials, Moscow, Russia

<sup>6</sup> Institute for Nuclear Problems of the Belarus State University, Minsk, Belarus

The garnet scintillator crystals family  $Gd_3Al_2Ga_3O_{12}:Ce$  (GAGG:Ce) attracts increased attention due to the combination of high density, chemical stability, high light yield and good energy resolution [1]. Due to the superior scintillation properties, GAGG:Ce crystals are perspective for applications in a single photon emission computed tomography and environmental radiation monitoring. A drawback of the crystal is that beside a fast scintillation component of  $Ce^{3+}$  centers (~60 ns) slow components ( $\tau > 200$  ns) are present in the decay kinetics, which worsen the scintillation performance [1]. The most remarkable suppression of the slow decay components of scintillation was observed at co-doping of GGAG:Ce with Ca or Mg ions [2]. However, the co-doping suppressed also the scintillation light yield, which showed the necessity of additional studies for further improvement of the scintillation performance of GAGG:Ce.

Here we present the results of the study of the influence of partial substitution of Al and Ga cations by Sc on the structural and luminescence characteristics of GAGG:Ce and GAGG:Ce,Ca single crystals grown by the Czochralski method at the Fomos-Materials (Moscow, Russia). Such substitution leads to the decrease of the bandgap, which is associated with the low-energy shift of the states of conduction band bottom. It also causes the low-temperature shift of the thermal quenching threshold and the decrease of the activation energies of electrons traps. The luminescence thermal quenching is shown to be connected with thermal ionization of  $Ce^{3+}$  emission centers. Moreover, the introduction of scandium into GGAG:Ce allows the suppression of slow decay components. This effect is comparable to that obtained by Ca co-doping of GAGG:Ce crystals. However, it results also in the decrease of the light output under high-energy electron beam excitation. The afterglow of studied crystals strongly depends on temperature and is connected with the possibility of a gradual thermal release of charge carriers from traps.

### References

[1] Kamada et al, *Optical Materials*, **41** 63 (2015).

[2] Tyagi et al, *J. Phys. D: Appl. Phys.*, **46** 475302 (2013).

## Low-mass radiation-hard beam profile monitors for high energy protons using microfabricated metal thin-films

**Georgi Gorine<sup>1</sup>, Jacopo Bronuzzi<sup>1</sup>, Giuseppe Pezzullo<sup>2</sup>,  
Isidre Mateu<sup>2</sup>, Blerina Gkotse<sup>3</sup>, Maurice Glaser<sup>2</sup>, Didier Bouvet<sup>4</sup>,  
Alessandro Mapelli<sup>2</sup>, Federico Ravotti<sup>2</sup>, Jean-Michel Sallese<sup>4</sup>**

1 EPFL / CERN, Lausanne, Switzerland

2 CERN, Geneva, Switzerland

3 Mines ParisTech / CERN, Geneva, Switzerland

4 EPFL, Lausanne, Switzerland

At the CERN Proton Irradiation Facility (IRRAD), thousands of samples are yearly irradiated with a high-intensity 24 GeV/c proton beam extracted from the CERN Proton Synchrotron (PS) accelerator.

In order to precisely align the irradiation tables with the center of the Gaussian beam, custom made “mini” Beam Profile Monitors (miniBPM) are currently used. These pixelated particle detectors are realized by means of standard PCB fabrication techniques, composed of a stack made of six copper layers each ~15  $\mu\text{m}$  thick, and six 100  $\mu\text{m}$  thick Kapton isolation layers.

BPMs are continuously interacting with the high energy proton beam cumulating  $\sim 5 \times 10^{17}$  p/year. This sets challenges in terms of radiation hardness, and tradeoff between the overall mass of the detector, required to be robust enough for easy handling and installation, while being light enough to not degrade the beam and reduce its activation levels.

To satisfy these requirements and also allow measurements of different intensity and/or different particle beam energies, a new fabrication method is proposed in this paper. This is realized by employing microfabrication technologies using clean room facilities, giving the detector an increased radiation hardness and thinner sensitive areas.

Several types of microfabricated BPMs (microBPMs) were produced at the Center of Micronanotechnology (CMi) of the École Polytechnique Fédérale de Lausanne (EPFL), varying in substrate materials, deposited metal thickness, and interconnection techniques.

After fabrication, irradiation tests were carried out at IRRAD using different proton beam intensities and a lead ion beam. By comparing the signals obtained from the microBPMs with the currently used miniBPM, good agreement was found demonstrating that microBPMs are good candidates for a new generation of low-mass and radiation hard beam profile monitors.

In this paper a description of the fabrication techniques and the irradiation tests will be detailed, as well as the thoughtful discussion about possible improvements of these new fabrication concepts based on microtechnology which are aimed to be used in particle beam monitoring for medical applications and high energy physics experiments.

## **Development of polycrystalline chemical vapor deposition diamond detectors for radiation monitoring**

**Diego Sanz<sup>1</sup>, Harris Kagan<sup>2</sup>, William Trischuk<sup>3</sup>**

<sup>1</sup> ETH, Zürich, Switzerland

<sup>2</sup> Ohio State University, Columbus, United States

<sup>3</sup> University of Toronto, Toronto, Canada

The RD42 collaboration at CERN is leading the effort to use polycrystalline Chemical Vapor Deposition (CVD) diamond as a detector material in extreme radiation environments. During the last two years the RD42 group has succeeded in producing and measuring a number of devices to address specific issues related to use at the future High Luminosity Large Hadron Collider (HL-LHC) at CERN. We will present status of the development of polycrystalline CVD diamond detectors with emphasis on recent beam test results. In particular we present the latest results on radiation tolerance, measurements of charge collection in small 3D diamond devices and the development of a new polycrystalline CVD Beam Condition Monitoring system for use at the HL-LHC.

## Assessment of the occupational exposure of urologists during percutaneous nephrolithotomy surgical interventions

Vojislav Antic<sup>1</sup>, Olivera Ciraj-Bjelac<sup>2</sup>, Predrag Bozovic<sup>2</sup>, Otas Durutovic<sup>1</sup>

<sup>1</sup> Clinical Centre of Serbia, Belgrade, Serbia

<sup>2</sup> "Vinca" Institute of Nuclear Sciences, Belgrade, Serbia

Percutaneous nephrolitholapaxy (PCNL) is an endoscopic procedure that represents the method of choice for the need to shred and eliminate larger stones in the kidneys. The procedure is performed under fluoroscopy guidance, with presence of medical staff in the vicinity of patient couch which presents potential radiation protection concern. Assessment of the radiation exposure of the urologist who performs the procedure is an essential part of radiation protection arrangement. The objective of this work is to assess radiation dose for urologist in order to verify compliance with regulatory dose limits and to investigate need to occupations dose monitoring arrangements. Furthermore, in the particular case, the X-tube is above the patient's table, which brings higher dose compared with situation when it is bellow. Two consecutive 3 months long research was based on active personal dosimeters (APD) and passive, thermoluminescence dosimeters (TLD) use to assess whole body and eye lens occupational dose. During this period 77 interventions (conducted by two urologists) were performed. The average exposure measured using APD was 147  $\mu\text{Sv}$ , but doses varied from 24.5  $\mu\text{Sv}$  to 813  $\mu\text{Sv}$ . Using dedicated eye lens TLDs placed on left and right temple, the doses for the urologist were 3, 24 mSv and 3.43 mSv, respectively for first and 0.9 mSv and 1.03 mSv for second urologist. Whole body dosimeters worn over the apron showed a cumulative dose of 6.31 mSv and 0.54 mSv for two urologists, respectively. The presented results indicate that doses are below the regulatory dose limits; however, their magnitude requires caution and careful individual monitoring arrangements.

## A 2×32-format hybrid matrix high-speed XUV-detector

V.V. Zabrodskii<sup>1</sup>, S.V. Bobashev<sup>1</sup>, A.V. Nikolaev<sup>1</sup>,  
A.G. Alekseev<sup>2</sup>, P.N. Aruev<sup>1</sup>, E.V. Sherstnev<sup>1</sup>

<sup>1</sup> Ioffe Institute, St-Petersburg, Russia

<sup>2</sup> NRC "Kurchatov Institute", Moscow, Russia

The importance of high-temperature plasma direct ultrafast visualization system development is due to the need to study the behavior of the impurity in the scrape layer and radiation loss profile dynamics during the development of magnetohydrodynamic instabilities, having a time span of  $\mu\text{s}$ . Absorption of VUV, soft X-ray XUV, and HXR spectra [1] in optical window materials does not allow direct visualization of fast processes in plasma without the use of detectors placed just inside the tokamak. A 2×32-format hybrid matrix high-speed XUV-detector for high-speed detection of high-temperature plasma radiation profile is presented ( $E=1.. 10^4$  eV). The detector includes silicon XUV photodiodes, preamplifier, system of data digitizing and transmission from a tokamak with a frame for 2  $\mu\text{s}$  and continuous recording up to 4 seconds. The experience of using the previous 16×16-format hybrid matrix XUV detector model in tokamaks T-11M and Globus-M is taken into account when developing [2,3]. The results of SPD XUV photodiodes [4] absolute sensitivity calibration in a 1 – 60 000 eV quantum energy range are presented as well.

### References

1. ISO 21348 Definitions of Solar Irradiance Spectral Categories
2. "Investigation of the plasma jet penetration into the plasma on the Globus-M tokamak" A.D. Sladkomedova, A.N. Voronin, A.G. Alekseev, V.K. Gusev, G.S. Kurskiev, Yu.V. Petrov, N.V. Sakharov, S.Yu. Tolstyakov and V.V. Zabrodsky, *Physica Scripta*, Volume 93, Number 10, 2018
3. "Tomography diagnostic of plasma radiated power on the spherical tokamak Globus-M" A.D. Sladkomedova, A.G. Alekseev, N.N. Bakharev, V.K. Gusev, N.A. Khromov, G.S. Kurskiev, V.B. Minaev, M.I. Patrov, Y.V. Petrov, N.V. Sakharov, P.B. Shchegolev, V.V. Solokha, A.Y. Telnova, S.Y. Tolstyakov, V.V. Zabrodsky, 2018, *Rev. Sci. Instrum.*, v.89, 8
4. "Characterization of spatial homogeneity of sensitivity and radiation resistance of semiconductor detectors in the soft X-ray range" P.N. Aruev, Yu.M. Kolokolnikov, N.V. Kovalenko, A.A. Legkodymov, V.V. Lyakh, A.D. Nikolenko, V.F. Pindyurin, V.L. Sukhanov, V.V. Zabrodsky *Nucl. Instrum. Meth. Phys. Res. A* **603**, 58 (2009)



**Radiation  
Oncology**

**27**

## Radiation dose to the brain in postoperative radiation and impact on survival of patients with glioblastoma multiformae

Igor Stojkovski, Violeta Klisarovska, Petar Chakalaroski

Univ. Clinic of Radioth & Oncology, Skopje, Macedonia

**Introduction.** Purpose of this study is analyzing impact of irradiated brain volume on survival of patients with glioblastoma.

**Materials and methods.** Dosimetric analysis of treatment plan data has been performed on 70 patients with glioblastoma, treated with postoperative radiochemotherapy with temozolomide, followed by adjuvant temozolomide. Patients were treated with 2 different methods of definition of treatment volumes and prescription of radiation dose. First group of patients has been treated with one treatment volume receiving 60 Gy in 2 Gy daily fraction (31 patients) and second group of the patients has been treated with “cone-down” technique, which consisted of two phases of treatment: the first phase of 46 Gy in 2 Gy fraction followed by “cone-down” boost of 14 Gy in 2 Gy fraction (39 patients). Quantification of volume receiving 57 Gy and more and ratio between brain volume and has been done. Average values of both parameters have been taken as a threshold value and patients have been split into 2 groups for each parameter (smaller and larger than threshold value).

**Results.** Mean value for Volume V57 Gy was 593.39 cm<sup>3</sup> (range 166.94 to 968.60 cm<sup>3</sup>), Mean value for brain volume has been measured as 1332.86 cm<sup>3</sup> (range 1047.00 to 1671.90 cm<sup>3</sup>) and mean value for ratio of brain and V57Gy has been 2.46 (range 1.42 to 7.67). There was no significant difference between two groups for both V57Gy and ratio between brain volume and V57Gy.

**Conclusion.** Irradiated volume with dose more than 57Gy (“V57Gy) and ration between whole brain volume and V57Gy does not have any impact on survival of patients with glioblastoma.

## Reaction of peripheral blood's regulatory suppressor T-lymphocytes to components of chemoradiation therapy of Hodgkin's lymphoma

**Evgenija Kuzmina, Tatiana Mushkarina,  
Tatiana Konstantinova, Tatiana Bogatyreva, Ludmila Grivtsova**

A. Tsyb MRRC- branch of NMRRC Ministry of Health of the Russian Federation, Obninsk, Russia

Recent investigations suggest a prognostic role for regulatory T cells (Treg) in tissues of Hodgkin's lymphoma, correlating with poor overall survival both at diagnosis and in relapsed/refractory cases. But we have little observations whether chemotherapy and radiation influence at the level of peripheral blood regulatory T cells.

**Purpose of the study** – to investigate the reaction of peripheral blood Treg-cells for courses of ABVD chemotherapy and consolidation radiotherapy.

**Methods and materials.** 40 healthy donors and 20 patients with newly diagnosed Hodgkin's lymphoma were involved in a prospective study. 7 patients were in early (II stage) and 13 with advanced disease (III-IV stage). Examination of patients with Hodgkin's lymphoma treated according to the scheme of ABVD with the subsequent consolidation of radiation therapy, which was carried out to a dose of 20-30Gy. T-reg cells of peripheral blood defined as the phenotype CD45<sup>+</sup>CD4<sup>+</sup>CD25<sup>+</sup> CD127<sup>low/-</sup> population were examined using 6-colored flow cytometry method (FACSCanto II, BD). T-reg cells were counted at three time points: 1 – the initial baseline level, 2 – after 6-8 courses of ABVD chemotherapy, 3 – after consolidation of radiotherapy at the dose 20-30Gy. The leukocytes and lymphocytes level of peripheral blood was examined.

**Results.** Hodgkin's lymphoma develops on the background of inflammation: leukocytes quantity increased (average  $9.32 \cdot 10^9$  cell/L). Also noted relative and absolute lymphocytopenia (13.0% and  $1.45 \cdot 10^9$  cell/L, at normal 33% and  $2.0 \cdot 10^9$  cell/L).

**Initially**, during the Hodgkin's lymphoma, the percentage of suppressor Treg-cells is 1.5 higher than normal ( $M \pm SD$ ,  $5.15 \pm 2.65\%$  vs.  $3.69 \pm 1.69\%$ ;  $t=2.15$ ,  $p<0.05$ ). The absolute quantity was normal ( $0.033 \pm 0.028 \cdot 10^9$  cell/L vs.  $0.031 \pm 0.017 \cdot 10^9$  cell/L – donor level,  $p>0.05$ ).

**After 6-8 courses of ABVD chemotherapy** (2 timepoint) the percent of Treg-cells was almost twice higher that baseline ( $9.44 \pm 3.24\%$ ,  $t=6.65$  vs. donor level), while the quantity decreasing by 15% ( $0.028 \pm 0.020 \cdot 10^9$  cell/L) only.

**After consolidation of radiotherapy at the dose 20-30Gy** the percentage of Treg-cells remained at the level of the previous stage of treatment; 2.5 times higher than normal ( $9.13 \pm 4.0\%$ ,  $t=0.20$ ,  $p>0.05$ , compare 2 timepoint, ABVD chemotherapy). The absolute quantity of Treg-cells decreased 1.5 times compared to the quantity after courses of ABVD chemotherapy ( $0.019 \pm 10^9$  cell/L,  $t=1.42$ ,  $p>0.05$ , without statistically significant). But the difference was statistically significant compare baseline ( $t=2.7$ ,  $p<0.05$  for percent and  $t= 2.0$  for the absolute quantity).

**Conclusion.** Thus, analysis of suppressor Treg-cells dynamics during the treatment of Hodgkin's lymphoma demonstrated higher initial percent level and their chemoresistance to the used ABVD therapy. The sensitivity of Treg cells to subsequent radiotherapy consolidation at a dose of 20-30Gy was remained to it response level to chemotherapy.

## Combined immune and radiation therapy in the management of poor prognostic cancers

**Ioana-Carmen Brie, Maria Perde-Schrepler,  
Piroska Virag, Eva Fischer-Fodor, Olga Soritau**

Institute of Oncology Prof. Dr. I. Chiricuta, Cluj-Napoca, Romania

**Background.** Malignant melanoma (MM) and non-small cell lung cancers (NSCLC) are tumors that bear high mutational load and escape from the immune system surveillance. This explains their poor prognostic, with increased recurrence and high mortality rates. Immunotherapy (IT) is a promising treatment, targeting the immune checkpoint inhibitors (CPI). However, the clinical results of CPI blockade are still low meaning that, taken alone, they are far from being perfect predictive biomarkers.

**Objective.** The main objective of our research is to identify predictive biomarkers that could help in clinical setting to identify patients who are likely to benefit from IT alone and in combination with other therapies such as radiotherapy (RT).

**Material and method.** Two malignant cell lines (MM and NSCLC) co-cultured with blood mononucleated cells were treated with Nivolumab and radiotherapy. The effect of treatments on tumoral cells' apoptosis, percent of cytotoxic T lymphocytes and expression of immune checkpoint inhibitors CTLA4, PD-1 and PD-L1 were studied using immunocytochemistry and flowcytometry.

**Results.** In vitro irradiation with 4Gy induces increased apoptosis in tumoral cells, both alone and in co-cultures. PD-L1 expression is significantly decreased on Nivolumab treated tumoral cells, both irradiated or not. However, this expression increases in co-cultures. Cytotoxic T lymphocytes expressed lower CTLA-4, PD-1 and PD-L1 levels in Nivolumab- and irradiation-treated co-cultures as compared with non-irradiated ones.

**Conclusions.** Our data point towards a strong synergy between radiotherapy and immunotherapy in the killing of melanoma and lung cancer cells in vitro. An explanation is that radiotherapy acts as a trigger for increased immune destruction of tumors, through modulation of immune checkpoint molecules. This could change the classic paradigm of radiotherapy being just a loco-regional treatment in cancer.

## Radiation induced bystander effect – Pros and cons

Mateusz Bilski<sup>1,2</sup>, Karolina Brzozowska<sup>3</sup>, Kamila Masłowska<sup>3</sup>,  
Monika Bilaska<sup>4</sup>, Ludmiła Grzybowska- Szatkowska<sup>2</sup>

1 Nu-med, Center of Oncology Diagnostics and Therapy, Lublin, Poland

2 Center of Oncology of the Lublin Region St. John from Dukla, Lublin, Poland

3 Oncology Department, Medical University of Lublin, Lublin, Poland

4 Chair and Department of Oncological Gynaecology and Gynaecology, Lublin, Poland

**Introduction.** Current radiotherapy research focuses mainly on the immediate effects of radiation to targeted cells, tissues and organs. Little is known about similar effects to non-targeted cells, both located in the immediate vicinity to the irradiated cells or further outside of the field of primary irritation. The so-called “bystander effect” or “radiation induced bystander effect” (RIBE) refers to a multifaceted response of non-irradiated cells neighbouring the target tissue to signals and mediators released by the irradiated cells. Those effects include damage due to cytotoxicity, apoptosis and biochemical changes, as well as changes in translation, gene expression and cell proliferation. The end-effects can be both positive and negative, either aiding in therapy or inducing further unwanted damage in the course of treatment.

**Aim and methods.** The aim of the study was to analyse recent research regarding the bystander effect. Two independent researchers have searched the PubMed database for papers published in English, dated from 2015 to 2018. The abstracts were evaluated independently and in the event of disagreement, the third author reviewed the paper. We attempt to give a thorough summary of the current knowledge about the bystander effect, in particular the issues that are most likely to have a direct impact on clinical practice.

**Results.** Researchers tend to agree that the bystander effect is mostly induced by very low-dose radiation of alpha particles (mGy, cGy), as well as conventional therapy using gamma particles, both in low and conventional doses. No conclusive evidence exists with regards to the bystander effect and dose fractionation. A number of theories are proposed for the possible mechanisms underlying the bystander effect, though very little clinical evidence is readily available to back up the offered claims. The two mechanisms for cell signalling proposed by most authors are through gap junction intercellular communication (GJIC) and mediation through soluble factors. The latter include modulation via inflammatory and non-inflammatory cytokines, cell death factors, and free radicals that lead to oxidative stress. The study of Le et al. (2017) supports the role of exosomes in the bystander effect, while another study by Prevc et al. (2016) suggests that electroporation can induce bystander effect mediated by microvesicles. The signals induced can affect both nuclear and mitochondrial DNA of the neighbouring cells, as well as the cell membrane and some other organelles. Changes in gene expression for multiple types of RNA have been reported in a paper by Sokolov et al. (2018).

**Conclusions.** The bystander effect is a rare event in radiotherapy and the underlying mechanisms are still not fully understood. RIBE may have important clinical implications and this includes both localized and whole-body side effects. Some of those may aid in therapy while others increase the risk associated with radiotherapy exposure, including mutations, gene instability and second primary cancers. While most studies conclude a decrease in survival of non-irradiated cells, in some cases the effects can be quite opposite, with increased survival rates of bystander cells. Where the damage affects neighbouring cancer cells, the bystander effect can aid in overall therapy. Further research needs to be conducted on the latter with the emphasis on possible incorporation of bystander effect into clinical practice and its possible anti-tumour significance.

**Keywords:** Bystander effect, gene expression, gap junction intercellular communication

## High fraction doses for glioma treatment – An alternative for selected patients

**Mateusz Bilski<sup>1,2</sup>, Anna Rycyk<sup>3</sup>, Piotr Kozłowski<sup>2</sup>,  
Karolina Szymańska<sup>3</sup>, Ludmiła Grzybowska-Szatkowska<sup>2</sup>**

1 Nu-med, Center of Oncology Diagnostics and Therapy, Lublin, Poland

2 Center of Oncology of the Lublin Region St. John from Dukla, Lublin, Poland

3 Oncology Department, Medical University of Lublin, Lublin, Poland

**Introduction.** Gliomas are a group of central nervous system cancers that differ in terms of the brain cells from which they originate (astrocytes or oligodendrocytes). Glioma is considered a rare cancer because there are less than 6 in every 100,000 people each year. They account for 80% of all cancers of the central nervous system. In Europe, the largest annual rate of cancer is found. Survival of patients with glioblastoma multiforme is in most cases several months. Rarely, the patient is going through 5 years.

The gold standard of treatment is surgery. In fact, surgical resection with the widest possible, safe range is associated with a better treatment effect regardless of the glioblastoma subtype. The standard treatment in most patients is supplementary chemoradiation with temozolamide. The unsatisfactory results of the combined treatment of patients with high-grade brain gliomas justify the search for new, unconventional forms of treatment. In recent years clinical trials have been carried out in many centers on unconventional methods of fractionating the radiation dose. One of them is hypofractionation, i.e. irradiation with high fractional doses.

**Aim of the study.** The evaluation of the effectiveness of glioblastoma multiforme treatment by radiotherapeutic hypofractionation.

**Material and methods.** The aim of our study was to analyze published data on hypofractionated radiotherapy in glioblastoma patients. We searched Pubmed database, looking for papers published in English, from 2012 to 2018. We also reviewed the bibliography of retrieved articles. The abstracts were evaluated independently by two authors, and in the event of disagreement the third author reviewed the paper.

**Results.** From the research and assessment of time to disease progression (PFS) and the total time of survival of patients (OS) it results that support for treatment with hypofractionated radiotherapy extends the life of patients. The survival time without progression of the disease after using the hypofractionated radiotherapy in these centers ranged from 4.3 to 13 months. An important parameter to assess the safety of the treatment is the toxicity assessment. In more than half of cases, the toxicity of treatment was 0, which means that this type of radiotherapy is very well tolerated by patients.

**Conclusions.** The results of the conducted analysis suggest that the use of hypofractionated radiotherapy in the combined treatment of glioblastoma can be effective and safe. In some patients, it can be an alternative to conventional radiotherapy. However, it should be remembered that the most important prognostic factors in this disease are age, FPS and range of surgery (total or subtotal resection).

**Keywords:** Hypofractionation, radiotherapy, hypofractionated radiation therapy, hypofractionated radiotherapy, glioblastoma multiforme, glioblastoma, adjuvant therapy, adjuvant treatment, gray, toxicity

## Acute toxicity in standard treatment of cervical cancer

**Violeta Klisarovska, Petar Chakalaroski, Igor Stojkovski**

University Clinic of Radiotherapy and Oncology, Skopje, Macedonia

**Purpose.** Prospective evaluation of the acute toxicity caused by standard definitive treatment of cervical cancer – concurrent weekly cisplatin and External Beam Radiotherapy (EBRT) followed by high dose rate intracavitary brachytherapy (HDR BT).

**Methods and materials.** In this analysis were included 50 patients treated at one institution between June 2017 and June 2018. All patients were treated with 3D conformal chemo-radiation, with weekly Cisplatin 30 mg/m<sup>2</sup> for a maximum of 5 cycles. They received 50.4 Gy/28 fractions, 5 fractions per week of external beam radiation. In these patients dose optimization was done in order to achieve a tumor maximum dose (D<sub>max</sub>) around 105%. Various techniques were used for dose optimization which included the use of sub fields, adjusting the weightages, using wedges and the use of mixed energies. EBRT was followed by three fractions of HDR BT of 7 Gy each. Acute RTOG toxicity was assessed weekly during the treatment and 2 weeks post treatment.

**Results.** The median age of the patients was 51±11.3 years. All the patients (100%) completed EBRT; 42 patients (85%) of the patients received all 5 cycles of chemotherapy while 8 patients (15%) of the patients received 4 cycles of chemotherapy. The most predominant toxicity seen was gastrointestinal toxicity (radiation proctitis), diarrhea being the most common GI toxicity followed by vomiting. Neutropenia was the most common hematological toxicity: most patients had grade 0 and grade 1 toxicity. None of the patients had grade 4 toxicity while few had grade 2 and 3 toxicity. Radiation cystitis was observed in the majority of cases with a grade 0 and grade 1 toxicity, without the need for symptomatic therapy, only 2 patients have grade 3 toxicity with the need for therapy.

**Conclusion.** Acute toxicity appears as a result of the standard definite treatment of cervical cancer, but it is usually of low grade, easy to manage and does not disturb the general condition of the patient.

**Keywords:** Cervical cancer, 3D conformal, dose optimization, acute radiation toxicity

## Sinonasal intestinal-type adenocarcinoma

Özlem Mermut<sup>1</sup>, Esra Arslan<sup>2</sup>

<sup>1</sup> Health Sciences University, Istanbul Training and Research Hospital Department of Radiation Oncology, Istanbul, Turkey

<sup>2</sup> Health Sciences University, Istanbul Training and Research Hospital Clinic of Nuclear Medicine, Istanbul, Turkey

**Introduction.** Sinonasal intestinal-type adenocarcinoma (ITAC) is a rare neoplasm. The overall incidence of intestinal-type adenocarcinoma is less than 1% of all neoplasms and less than 4% of malignancies in the sinonasal area. Commonly presenting symptoms of ITAC are nasal obstruction and rhinorrhea. The tumor tends to be very locally aggressive. It is composed of growth patterns that resemble carcinomas or adenomas of intestinal origin or it may mimic normal histology of the intestinal mucosa. ITACs occur mostly in males in a wide age range with a mean around 50 to 64 years. The tumors are most often localized in the ethmoid sinus (40 %), nasal cavity (25 %) and the maxillary antrum (20 %). ITACs may spread to adjacent structures including the orbit, the pterygopalatine fossa, the infratemporal fossa and the cranial cavity. A remarkable association has been identified between long-term exposure to wood dusts and the occurrence of ITAC. Both ITACs and colorectal carcinomas express CK20, CDX-2, MUC2, and villin, while the presence of CK7 may be suggestive of ITAC. Surgery may be combined with radiotherapy. The behavior of ITAC is that of a high-grade malignancy.

**Case.** The patient was a 61-year-old man who had age and sex risks for sinonasal neoplasms, but no history of exposure to environmental carcinogens, such as leather or wood dust. In May 2017, the patient who had visual loss in the right eye and then in the left eye was admitted to the nasal congestion complaints. The patient, who was living outside of Istanbul, applied to the ENT clinic for further examination and treatment. Physical examination, he had bilateral proptosis and could not see the eyes. 15.10.2017/MRI: A mass of approximately 5.6x5.3 cm, with lobulated contouring, was found that filled the nasal cavity, infiltrated the lower and middle conchas, destroyed the nasal septum and the medial of the bilateral orbita. Mass causes extraocular muscles and the optic nerve to be pushed forward laterally.

With the effect of mass lesion pressure, both globes appear to be proptotic. No clear findings were found in favor of dural or cranial parenchymal involvement at this stage. Punch biopsy was performed in the nasal cavity mass. Diagnosis of intestinal type adenocarcinoma; KI 67: 60%; CK-7 and CK-20: Focal positive; NT-1: Positive in the stromal area. GIS research was recommended before primary acceptance. 12.10.2017/PET CT: Bilateral ethmoidal sinus and the sphenoid sinus filling the two maxillary sinuses, which are more prominent on the left, causing significant destruction of adjacent bone structures infiltrating the superior and middle nasal conchas, in the axial sections leading to destruction of the medial walls of the orbit, heterogeneous dense FDG uptake is observed in the mass lesion, which reaches 56x50x50 mm in the largest part (SUVmax: 11.24). Lymph node with pathological FDG involvement is not observed in cervical lymphatic stations. The focus of pathological FDG uptake in favor of distant metastasis is not observed. A total of 70 Gy of radiotherapy (35 frx. 200 cGy/day) was planned for the patient who was accepted as primary ITAC. When radiotherapy was applied to adaptive therapy, her eyes began to notice the light when his treatment was completed. 27.04.2018/PET CT: Hypermetabolic soft tissue lesion filling the nasal cavity, extending to the bilateral orbita, was observed in the current study, with no significant elevated FDG uptake in the calcification areas. (SUVmax: 10.38, before SUVmax: 11.24)

And adjuvant systemic (Cisplatin 60 mg / m<sup>2</sup> + 5-FU 1000 mg / m<sup>2</sup> (D1-7) continual infusion, every 21 days) chemotherapy was started. After 4 cycles of chemotherapy, 10.10.2018/PET CT: Partial metabolic regression was observed in the mass lesion, which contains common calcific areas filling the nasal cavity. (SUV max: 5.30, before SUV max: 10.38).

**Conclusions.** The behavior of ITAC is that of a high-grade malignancy. In a study of 213 ITACs, 50 % of patients developed recurrences, 8 % had cervical lymph node metastases, 13 % had distant metastases, and 60 % died of their disease. In our case the patient is still being followed without locally or distant metastasis.

## Pelvic insufficiency fracture (PIF)

Özlem Mermut

Health Sciences University, Istanbul Training and Research Hospital Department of Radiation Oncology,  
Istanbul, Turkey

**Introduction.** Pelvic insufficiency fracture (PIF) is a clinical condition observed after radiotherapy for pelvic malignancy up to 30% and in the first 1-2 years after radiotherapy (RT). With advanced radiological examinations, it is important to exclude the metastasis and to confirm the diagnosis. The most sensitive method is pelvic magnetic resonance imaging. Multidisciplinary management is needed in the diagnosis and treatment of PIF. Patients may have severe hip pain or completely be asymptomatic. This complication impaired the patient quality of life and physicians must be aware of that. This must be distinguished from bone metastasis.

**Case.** 57-year-old female patient. The patient underwent low anterior resection, with the diagnosis of rectum adenocarcinoma, stage T2N1bM0, lymphovascular invasion (+), 2+/24 lymph node. Radiotherapy was planned for the patient with capecitabine 2 \* 850mg / m<sup>2</sup>. For the pelvis, 28 fractions 180 cGy / day 5040 cGy, 3-D conformal radiotherapy was applied. RT was completed on 03.11.2016. At the first follow-up visit after 3 months, patient with back and right leg pain. MRG was performed to the patient. 23.04.2017/MRI: In the sacrum, T1A hypointense irregular signal changes in the medullary infiltration areas, secondary to radiotherapy, primarily show intense staining in postcontrast examination. In addition, increased contrast enhancement was observed in the focal area in the posterior right iliac bone. Metastatic involvement may be significant. PET CT was performed to the patient. No metastasis was detected in the PET CT. Pain palliation and bed rest recommended to the patient. The patient who had continued her disease-free follow-up one year later, 01.05.2018/ MRI: Bilateral sacrum 1/3 superior middle segment and right iliac crest, prominent in right inferior, coronal STIR sequence showed bone marrow edema and signal increase compatible with inflammation. Bilateral sacral insufficiency fracture was evaluated. In T1A series, there are superposed linear hypointense signal areas with marked edema on the right. 17.05.2018/ Bone Mineral Density (BMD) : Femur and lumbar osteopenia. In the control examinations of the patient without pain, 20.10.2018/MRI: Reconstruction findings were found in the bone structure due to radiotherapy. Signal deposition was observed in the oil-printed series which may be due to possible insufficiency fracture in the sacrum and sacroiliac joints. There was no difference according to the previous review.

**Conclusion.** Pelvic radiotherapy is one of the standard treatments, together with chemotherapy, for the management of gynaecological and gastrointestinal tumours. On MRI, PIF present an easily recognizable edema signal in contrast to metastases that disorganize the bone and form a real replacement tissue. Radiation-induced fractures are not associated with any invasion of adjacent soft tissues, which is commonly observed in the case of metastases. PIF should be management multidisciplinary. The biopsy of the patient with diagnosis of PIF is not recommended because of additional trauma. The osteoporosis status was available for only 9% of patients, although osteoporosis constitutes the leading risk factor for bone insufficiency fractures. In our case, there was no osteoporosis, but there was an osteopenia. RT-induced PIF is often seen as stable fractures and its treatment is conservative. Symptomatic treatments such as analgesics, life style changes (bed resting, vitamin D replacement, walker use) provided for 6-12 months. This case confirms that radiation-induced fractures can occur early (fifth months after treatment). Physicians must be carefully and knowledgeable about PIF. This will enable the patients to receive appropriate treatment.

## Monte Carlo simulations of radioembolization in various human organs

Adam Spyra

Nuclear Physics Division, Faculty of Physics, University of Warsaw, Warsaw, Poland

**Introduction.** Radioembolization tends to be one of the most perspective ways of treating several types of cancer. For about a decade now, it is successfully performed on liver tumours. It is a combination of brachytherapy, where a radioisotope (most commonly a  $\beta$ - emitter due to its appropriate range) is placed near the tumour, and an embolization, which is a method that uses microspheres to block the blood vessels near the neoplasm so it cannot absorb a sufficient amount of oxygen and nourishment, what causes a death of cancer cells. The radioembolization interfuze those two methods and uses radioactive microspheres. Moreover, it shrinks the volume of the lesion or even eliminates it.

The method is particularly effective when used on lesions that create their own vessel system. This mechanism is called angiogenesis and it helps tumour cells to multiply. From the oncological point of view, those blood vessels are ideal to apply radioembolization spheres into them.

**Motivation.** The radioembolization helped a lot of oncological patients to recover without using more invasive methods. Due to its very effective results, we decided to investigate if it could be useful in treating tumours located in organs other than liver. The studies can help in implementing a method that is already known and used to be performed on other neoplasm.

**Aim of work.** My work was focused on creating simulations in GATE software (based on a Monte Carlo method). Those simulations allow to estimate the dose distribution in a tumour tissue. By manipulating the source activity, type of isotope and time of irradiation, it is possible to calculate the optimal initial conditions that result with depositing a suitable dose in the tumour tissue.

The goal is to test some  $\beta$ - emitters like P-32, Sr-90 or Y-90 to find an ultimate half-life time of an isotope and a range of emitted electrons that meets our expectations. Results of my simulations will be verified with experimental data in a further part of the studies.

## Determination of optimal safety margins using image-guided radiotherapy for prostate cancer

Olena Safronova<sup>1</sup>, Tetyana Udatova<sup>2</sup>, Yaroslav Kmetuyk<sup>2</sup>

<sup>1</sup> Clinical Hospital, Kyiv, Ukraine

<sup>2</sup> Clinical Hospital "Feofaniya", Kyiv, Ukraine

**Background.** Prostate cancer is one of the most important medical problems facing the male population. Radiotherapy is one of the major methods of combined treatment for prostate cancer. Prostate cancer is radioresistant tumor and the total dose of radiotherapy should be increased. In this case a risk of complications is increased for surrounding organs. Intra- and inter-fractional motion of the prostate is a problem for the accuracy of dose delivery. This motion is the margin from clinical target volume (CTV) to planning target volume (PTV). But we can decrease these margins and reduce the dose for organs at risk (OAR) with the usage of cone-beam computed tomography (CBCT). The aim of this study is to determine the optimal margin from CTV to PTV considering of the motion of the prostate with usage of CBCT.

**Methods.** 102 patients with intermediate-risk prostate cancer were treated using three-dimensional conformal RT (3D-CRT) 76 Gy in 38 fractions (n=49) and using intensity modulated RT (IMRT) 70 Gy in 28 fractions (equivalently 79 Gy) (n=53). We provided the same algorithm: topometric CT-scans, contouring, planning and treatment. When we used IMRT, we judged the prostate position using CBCT before each daily fraction and changed the borders of the target volume depending on the soft tissue contours. We checked the pelvic bones using digitally reconstructed radiographs (DRRs) before each daily fraction using 3D-CRT. We calculated the safety margin by the van Herk equation.

**Results.** We have analyzed 2603 data CBCT and 559 DRRs so far. The average magnitude of shifts was  $0.5 \pm 0.31$  cm in anteroposterior direction for CBCT and  $1.14 \pm 0.24$  cm for DRR; in craniocaudal direction was  $0.55 \pm 0.20$  cm for CBCT and  $1.19 \pm 0.22$  – for DRRs; in laterolateral direction was  $0.54 \pm 0.14$  cm for CBCT and  $1.02 \pm 0.18$  cm for DRRs. We calculated the optimal margins from CTV to PTV with daily CBCT verification: 0.84 cm, 0.76 cm and 0.72 mm (respectively – anteroposterior, craniocaudal, laterolateral), without daily CBCT – 1.24 cm, 1.16 cm and 1.18 cm (respectively – anteroposterior, craniocaudal, laterolateral).

**Conclusions.** According to the survey the position of the prostate can alternate between 1.2 cm depending on the filling of pelvic organs. The implementation of daily CBCT verification in real time creates an opportunity to reduce margins from CTV to PTV to 0.8 cm. Image-guided radiotherapy with usage of CBCT guarantees the quality of dose delivery and decreases the dose for OAR.

**Keywords:** Prostate cancer, CBCT, image-guided radiotherapy

## Evaluation of radiation doses to organs at risk with application of 3D-conformal radiotherapy and intensity-modulated radiotherapy for treatment of patients with breast cancer

**Olena Safronva**

Clinical Hospital, Kyiv, Ukraine

**Background.** Breast cancer is one of the most important medical problems facing the female population. Radiotherapy is one of the major methods of combined treatment for breast cancer.

**Aim.** The aim of the study was to compare doses for the lung and the heart with the usage of 3D-conformal radiotherapy (3D-CRT) and intensity-modulated radiation therapy (IMRT) after breast-conserving surgery using the classic mode of fractionation.

**Material and Methods.** 75 patients with pT2N1M0 left breast cancer received adjuvant radiotherapy: 38 patients were treated with the usage of 3D-CRT (multiple, noncoplanar photon fields) and 37 patients were treated using IMRT. Total dose was 50 Gy in 25 fractions to the left breast and also 0.43 Gy in tumor bed and 2.0 Gy per fraction to total dose 46.0 Gy to the all lymph nodes, 5 days per week. Dose distribution: 95.0% isodose covered all CTV, max 103.0% in PTV. Radiation dose to organ at risk was analyzed according to report ICRU 62. Dose distribution was evaluated with homogeneity and conformity indices. Doses for the lungs and a heart were compared according to dose-volume histogram.

**Results.** The homogeneity index was  $0.16 \pm 0.020$  with 3D-CRT and  $0.13 \pm 0.016$  with IMRT, the conformity index was  $0.86 \pm 0.05$  with 3D-CRT and  $0.91 \pm 0.06$  with IMRT. V95 of PTV covered 96.8% for 3D-CRT versus 98.9% for IMRT, V105 of PTV was recorded 19.2% and 4.6%, respectively (U-test,  $p < 0.05$ ). V20 left lung was 19.9% and 25.3% with IMRT and 3D-CRT respectively (U-test,  $p < 0.05$ ). V30 heart received 31.0 Gy with 3D-CRT and 19.9 Gy with IMRT. Maximum dose for the heart was 48.3 Gy with 3D-CRT and 38.8 Gy with IMRT techniques (U-test,  $p < 0.05$ ). Median dose for the heart was 3D-CRT  $13.1 \pm 4.6$  Gy, IMRT –  $7.8 \pm 2.1$  Gy (U-test,  $p < 0.05$ ).

**Conclusions.** The use of the IMRT techniques enables more homogeneous dose distribution in target volume. The range of mean and maximum dose to the heart and V20 left lung was lower with the IMRT techniques in comparison with the 3D conformal radiotherapy. IMRT reduces irradiated volumes of heart and left lung in breast cancer patients treated on the left side.

**Keywords:** Radiotherapy, 3D-CRT, conformal radiotherapy, IMRT, breast cancer, organ at risk

## Organ wall as a superior volume in presenting the absorbed dose compared to the whole organ volume in intensity-modulated irradiation therapy-treated gynecological malignancies

**Petar Chakalaroski, Violeta Klisarovska,  
Igor Stojkovski, Lenche Kostadinova, Bojana Petreska**

University Clinic for Radiotherapy and Oncology, Skopje, Macedonia

**Introduction.** As external beam radiation therapy (EBRT) evolved from three-dimensional conformal radiotherapy (3D-CRT) to more sophisticated techniques like the intensity-modulated radiation therapy (IMRT) a question arose about the quantity of absorbed dose in the organs at risk (OAR), especially after many observations that directly linked the absorbed dose with tissue reactivity and the onset of late toxicity. IMRT and other modern techniques steep gradient opens a new chapter in hollow and tube-like OAR dose distribution, emphasizing the need for different dose presentation – the organ wall.

**Materials and methods.** All patients' primary targets received 30Gy in 15 daily fractions using IMRT technique. IMRT was used as a part of standardized radiotherapy treatment for gynecological malignancies.

In focus were bladder, rectum volumes of 30ccm and sigmoid volume of 10ccm.

**Results.** Average bladder whole organ volume was 208.32ccm (55.90-444.50ccm) and average bladder organ wall volume was 47.56ccm (21.10-87.00ccm). Average absorbed doses in 30ccm volume were 22.96Gy (12.16-27.89Gy) for the whole organ and 11.97Gy (10.37-12.98Gy) for the organ wall volume. Two patients had non-available dose values due to organ wall volumes smaller than 30ccm.

Average rectal whole organ volume was 81.32ccm (41.10-159.90ccm) and average rectal organ wall volume was 39.94ccm (27.60-61.00ccm). Average absorbed doses in 30ccm volume were 17.08Gy (9.95-20.19Gy) for the whole organ and 4.81Gy (0.37-10.97Gy) for the organ wall volume. One patient had non-available dose values due to organ wall volumes smaller than 30ccm.

Average sigmoid whole organ volume was 48.20ccm (29.40-68.60ccm) and average sigmoid organ wall volume was 27.82ccm (13.70-39.10ccm). Average absorbed doses in 10ccm volume were 26.67Gy (21.47-29.71Gy) for the whole organ and 22.33Gy (13.56-27.31Gy) for the organ wall volume.

**Conclusion.** Organ wall gives more precise and realistic view of different irradiated organ parts, its absorbed dose and dose distribution. Above results showed that there is a great absorbed dose difference between whole organ and organ wall volumes, most visible in rectal and bladder volume – in average 12.27Gy and 10.99Gy respectively. In sigmoid volumes absorbed dose difference was less pronounced – it averaged 4.34Gy. Dose differences, especially the 10+Gy dose difference paves the way to higher treatment dose escalations, thus giving potential for greater radio-biological effect that will provide better disease control and longer remissions.

**Keywords:** Intensity-modulated radiation therapy, gynecological malignancies, organ wall

## Protective effects of N-acetylcysteine on acute radiotherapy-induced cardiotoxicity in rats: An electrophysiological evaluation

Songül Barlaz Us<sup>1</sup>, Özden Vezir<sup>2</sup>, Ülkü Çömelekoğlu<sup>3</sup>

1 Mersin University, Faculty of Medicine, Department of Radiation Oncology, Mersin, Turkey

2 Mersin City Hospital, Department of Cardiovascular Surgery, Mersin, Turkey

3 Mersin University, Faculty of Medicine, Department of Biophysics, Mersin, Turkey

Radiotherapy (RT) is one of the commonly used methods of cancer treatment. During the RT treatment of malignant tumors found in thoracic cavity, mainly lung and breast, the heart is exposed to ionizing radiation. The risk of death increases in patients due to the emergence of diseases such as acute pericarditis, myocarditis, congestive heart failure, mitral and aortic valve insufficiency, fibrosis and rhythm disturbances in the communication system after irradiation due to ionizing radiation effect. These diseases are largely related to the increase of free radical production and the deterioration of the antioxidant defense system by the effect of ionizing radiation. Therefore, the use of antioxidant, anti-inflammatory agents may be important before or during treatment to reduce tissue and organ damage caused by radiotherapy. N-acetylcysteine (NAC) is an acetyl compound of L-cysteine with an active mercapto group. More recently, studies have demonstrated that N-acetylcysteine prevents oxidative damage, improves immunity, inhibits apoptosis and the inflammatory response and promotes the synthesis of glutathione in cells. This study aimed to investigate the protective effect of N-Acetylcysteine (NAC) on radiotherapy-induced cardiotoxicity in rats.

Thirty female Wistar Albino rats were used in the study. Rats were divided into four groups. Group I: Control group (n = 6), the rats in this group were injected (i.p.) with saline for 7 days. Group 2: NAC group (n = 8), the rats in this group were injected NAC at a daily dose of 240 mg / kg for 7 days. Group 3: RT group (n = 8), the rats in this group were injected with saline for 7 days and RT (20 Gy) was irradiated 1 hour after the last injection. Group 4: RT + NAC group (n = 8), the rats in this group were injected with NAC for 7 days and RT were irradiated 1 hour after the last NAC dose. To determine the acute effects of radiation on the heart 24 hours after RT, the electrical activity of heart was recorded using lead I. The signals were digitized with a 16-bit analog-to-digital converter at a sampling rate of 500 samples/s. Heart rate, QT interval and T wave amplitude were measured from ECG recordings.

Rats of the RT group presented significant decreased heart rate ( $p < 0.05$ ), but in the heart rate value, there were no significant differences in the NAC and RT+NAC groups compared with those of the control group ( $p > 0.05$ ). There were no significantly differences between control group and experimental groups for the QT interval ( $p > 0.05$ ). In the RT group, amplitude of T wave was significantly higher than the control, NAC and RT+NAC groups. These results can be indicator cardiotoxic damage.

The results of the present study showed protective effect for NAC on the heart. Further studies are needed to determine the mechanisms of this effect.

**Acknowledgments:** This study was supported by Mersin University (Project No: 2018-1-AP4-2712).

## Dosimetric results of two different planning systems for craniospinal irradiation with VMAT techniques

Serap Ketenci<sup>1</sup>, Ayşe Dağlı Değerli<sup>1</sup>, Funda Öztürk<sup>1</sup>,  
Mustafa Özer<sup>1</sup>, Tarık Sütçü<sup>1</sup>, Beste M. Atasoy<sup>1,2</sup>

<sup>1</sup> Marmara University Pendik Education and Research Hospital, Radiation Oncology Clinic, Istanbul, Türkiye  
<sup>2</sup> Marmara University School of Medicine Department of Radiation Oncology, Istanbul, Türkiye

**Aim.** We aim to analyse the dosimetric results of craniospinal irradiation with AAA and Monte Carlo treatment planning systems in our patients.

**Materials and Methods.** Six patients were chosen to make on the analyses from the database. Patients were planned in the supine position, with neck extended and, typically immobilized head and neck with a thermoplastic mask. The CT scanner used for this study was a General Electric Optima CT 580 and the scans were performed with 16 mm slice-thickness, scanned without a gap. For each patient treatment plans were constructed using the patient's planning CT dataset with VMAT technique. Different arc arrangements were used, with two or three isocentres, from four to six modulated arcs. To guarantee a smooth dose transition between isocentres were optimised defining an overlapping region between arcs of different isocentres. 6 MV photon energy and maximum dose rate of 500-600 MU/min were selected. Plans targeted the PTV to a total dose of 3600 cGy at 180 cGy per fraction. All treatment plans were generated on Eclipse treatment planning system (Varian Oncology Systems, Palo Alto, CA, v.11.0) and Monaco treatment planning system (v5.10.04) with an Elekta Synergy equipped. The Anisotropic Analytical Algorithm (AAA) photon dose calculation algorithm and The Monte Carlo Algorithm photon dose calculation algorithm were used for all plans.

**Results.** All results were summarized in Table 1. There was no difference observed in HI, CI, PTV90, PTV95, PTV107 and MU. However, lung V10 (24.53±14.18 vs 7.22±4.90, p=0.008), V5 (89.61±5.86 vs 31.26±18.53, p=0.000), Vmean (837.66±137.09 vs 429.50±154.17, p=0.000); both right and left kidney mean (R 1019.76±322.21 vs 324.00±63.37, L 977.78±316.41 vs 312.00±78.51, p=0.001); liver means (734.26±77.68 vs 498.33±161.16, p=0.012); body means (839.06±179.99 vs 500.16±110.99, p=0.001); right lens Dmax (655.70±90.55 vs 494.83±128.77, p=0.001), left lens Dmax (622.70±121.35 vs 482.83±89.18, p=0.033) were significantly different.

**Conclusion.** In our daily clinical practice, we irradiate our patient using two different planning systems. Therefore, low dose regions there was a significant difference observed in lung and kidney dosimetrics. Despite that, no optimization were in planning systems, statistical difference was observed in lung V10, V5, liver doses. In addition, an international guideline with dose constraints for CSI can be helpful essential to ensure comparable outcome between different centers.

## **Hadron radiation in cancer therapy**

**Dejan Trbojevic**

Brookhaven National Laboratory, Upton, New York, United States

Worldwide, cancer is the second cause of death after the cardiovascular diseases. There are many types of cancer treatments depending on the type of cancer. Most of the treatments are a combination of different methods: surgery, chemo-therapy, immuno-therapy, targeted therapy and/or radiation therapy, etc. The main reason of an exponential growth of the hadron cancer therapy facilities around the world is significant advantage with respect to the widely dominated X-ray radiation therapy. There are multiple methods in using the X-ray therapies like: Intensity Modulated Radiation Therapy (IMRT), 3D-CRT three-dimensional conformal radiotherapy, or the Image-Guided Radiation Therapy (IGRT) etc. The main difference between the hadron cancer radiation therapy and X-ray therapies is that the X-rays always completely propagate through the patient body while in the hadron (proton, light or heavier ions like carbon ions) most of the energy is deposited at the tumor where the “Bragg peak” is. In addition, there are unavoidable side effects of the X-ray treatments to the cardio-vascular and other internal organs affected by complete propagation of the X-rays through the body. This is especially critical in the case of children. The advantages of hadron therapies are recognized worldwide as the number of treatment facilities is growing exponentially. So far, a total number of the patients treated by the hadron therapy is larger than 200,000. The recent improvements and essential requirements of the hadron therapy facilities will be presented, with several author’s patent contributions in this field.

## A dosimetric comparison of single arc and double arc therapy in the treatment of high-risk prostate cancer with pelvic nodal radiation therapy

**Berrin Inanc**

University of Health Sciences, Istanbul Education and Research Hospital, Department of Radiation Oncology, Istanbul, Turkey

**Purpose.** To compare the dosimetric results of single and double-arc therapy in the treatment of high-risk prostate cancer with pelvic nodal radiation therapy.

**Methods and Materials.** Eleven high-risk prostate cancer patients were treated with prophylactic whole pelvic radiation therapy using a double-arc technique. The same patients were re-planned with single-arc technique. Radiotherapy was performed daily 2 Gy/fraction to 46 Gy for pelvic area, 58 Gy for prostate+seminal vesicle, 80 Gy for the prostate. The mean (Dmean), maximum (D max), and minimum (Dmin) dose of the planning target volume (PTV), conformity index (CI), homogeneity index (HI) and MU values and doses received by organ at risk (OAR) were compared

**Results.** Patients' age ranged from 57 to 76. Patients had prostate-specific antigen (PSA) scores ranging from 5.4-69. Dmax dose was higher in single-arc technique (84.30 Gy). HI was lower in double-arc technique (0.6). Dmax and HI were a statistically significant difference between the two techniques ( $p=0.019$  and  $p=0.003$ ). In terms of OARs, the rectum D25 and D35 doses were found to higher in single-arc techniques (55.98 Gy, 48 Gy). The differences in single-arc and double-arc comparison were statistically significant ( $p=0.016$  for both doses). Penil bulb mean doses were lower in the single-arc technique and this was statistically significant (37.10 Gy,  $p=0.012$ ).

**Conclusion.** In high-risk prostate cancer patients, double-arc technique resulted in favorable dosimetry when compared single-arc technique.

**Keywords:** High-risk prostate cancer, volumetric arc therapy, dosimetry, radiotherapy

## **Hyperthermic sensitization of tumour cells to radiation or chemicals: Optimization of the efficiency**

**Svetlana V. Belkina, Galina P. Zhurakovskaya, Olga A. Vorobey**

A.Tsyb Medical Radiological Research Center, Obninsk, Russia

A set of randomized trials have demonstrated the benefit of combining hyperthermia with modern cancer treatments, including radiation therapy and chemotherapy for treating a wide range of malignancies. Hyperthermia complements radiation and sensitizing effects occur through increased perfusion/tumor oxygenation and alteration of cellular death pathways. Multiply events can lead to the synergy between heat and drugs: heat damage to ABC transporters (drug accumulation), intra-cellular drug detoxification pathways and repair of drug induced DNA adducts. Optimization of combined interactions that provide maximum therapeutic impact can be achieved using the regularities of synergistic effects.

The purpose of the study was to adapt a previously developed mathematical synergistic model of cell survival to description of tumour progress and test it using the experimental data.

The model postulates that detected synergistic effect occurs due to the formation of additional efficient lesions arising from the interaction of sublesions induced by each of the applied agents. Those sublesions do not induce any registered damage when agents applied separately. The degree of synergy enhancement of the registered effect was determined by the synergy enhancement ratio (SER).

Experimental data published by other researchers were used to test the adapted model. It's necessary to stress that those researchers didn't use any mathematical model to predict the results of combined actions. The possibility to optimize and predict the malignant tumour and mouse melanoma cells sensitivity increase after ionizing radiation and hyperthermia or hyperthermia and Rhodamine was tested. The model forecast that hyperthermia doesn't enhance the other agent action by any temperature. The model predicts the value of SER depending on the duration of thermal exposure, its greatest value, and the condition under which it can be achieved. The theoretically predicted values of SER display good correspondence with experimental data in all cases. A possible mechanism of the displayed regularity is discussed.

Taken together, these results demonstrate the possibility to optimize and predict the results of synergistic interaction of two agents used in clinical cancer therapy on malignant tumour and mammalian cells was demonstrated.



**Radiation  
Physics**

**28**

## Ab initio calculations of electronic structure of defects in $\text{Cd}_{1-x}\text{Mn}_x\text{Te}(\text{Se})$ and impact of $\gamma$ -irradiation on optical properties of their epitaxial films

**Matanat Mehrabova<sup>1</sup>, Niyazi Hasanov<sup>2</sup>, Aygun Kazimova<sup>3</sup>, Aygun Hasanli<sup>4</sup>**

<sup>1</sup> Institute of Radiation Problems of Azerbaijan National Academy of Sciences, Baku, Azerbaijan

<sup>2</sup> Baku State University, Baku, Azerbaijan, Baku, Azerbaijan

<sup>3</sup> Ganja State University, Ganja, Azerbaijan, Ganja, Azerbaijan

<sup>4</sup> Azerbaijan University of Architecture and Construction, Baku, Azerbaijan

In the paper, we have considered the basic aspects of defective crystals, and discussed the electronic structure and optical properties of  $\text{Cd}_{1-x}\text{Mn}_x\text{Te}(\text{Se})$  SMS. In particular, we have systematically investigated the defects such as vacancy, interstitial atom, Frenkel pair in  $\text{Cd}_{1-x}\text{Mn}_x\text{Te}(\text{Se})$  by ab initio calculations. The defect formation energy has been studied.

We carried out Ab initio calculations in the framework of density functional theory (DFT) in Atomistix ToolKit (ATK) programme. The calculations are performed within the spin-polarized DFT and the Local Spin Density Approximation with regard to Hubbard-U correction potential ( $U=3.59\text{eV}$ ) on double zeta double polarized (DZDP) basis.

Ab initio calculations were used for electronic structure of the ideal and defective SMS  $\text{Cd}_{1-x}\text{Mn}_x\text{Te}(\text{Se})$ . ( $x=0.01-0.25$ ). It was calculated band gap, density of states, total energy, magnetic moments, number of electrons, Fermi levels, defect formation energies and threshold energies.

It was defined, that with an increase in Mn concentration in the  $\text{Cd}_{1-x}\text{Mn}_x\text{Te}$  SMS, band gap increases and lattice parameter decreases. Calculations for  $\text{Cd}_{1-x}\text{Mn}_x\text{Se}$  SMS shows, that with an increase in the Mn concentration, band gap decreases. It is determined that defects as vacancy, interstitial atom, Frenkel pair in SMS  $\text{Cd}_{1-x}\text{Mn}_x\text{Te}(\text{Se})$  leads to changing of band gap width, formation of magnetic moments around the defects and local levels in the band gap, shifting of Fermi level towards the conductivity or valence band, which are confirmed experimentally. Calculations of total energies showed, that in  $\text{Cd}_{1-x}\text{Mn}_x\text{Te}$  antiferromagnetic phase, and in  $\text{Cd}_{1-x}\text{Mn}_x\text{Se}$  ferromagnetic phase is more stable.

To compare the theoretical results with the experimental data  $\text{CdTe}(\text{Se})$ ,  $\text{Cd}_{1-x}\text{Mn}_x\text{Te}(\text{Se})$  epitaxial films were obtained on glass substrates in a vacuum  $(1,2)10^{-4}\text{Pa}$  by the Molecular Beam Condensation method. It was determined the optimal conditions for obtain of epitaxial films with perfect structure and clean, smooth surface, without the inclusion of second phase by using of additional source of Te vapor.

Absorption and transmission spectra of  $\text{CdTe}$ ,  $\text{Cd}_{1-x}\text{Mn}_x\text{Te}$  ( $x=0.07$ ) epitaxial films on glass substrates of  $d=22\mu\text{m}$  thickness and  $\text{CdSe}$ ,  $\text{Cd}_{1-x}\text{Mn}_x\text{Se}$  ( $x=0.03$ ) epitaxial films on glass substrates of  $d=1.3\mu\text{m}$  thickness have been studied. The band gap width for  $\text{CdTe}$  and  $\text{Cd}_{1-x}\text{Mn}_x\text{Te}$  ( $x=0.07$ ) epitaxial films correspondently were  $E_g=1.53\text{eV}$ ,  $E_g=1.62\text{eV}$  and for  $\text{CdSe}$  and  $\text{Cd}_{1-x}\text{Mn}_x\text{Se}$  ( $x=0.03$ ) epitaxial films were  $E_g=2\text{eV}$ ,  $E_g=1.72\text{eV}$ .

The studies of the effect of  $\gamma$ -radiation on the optical properties of studied epitaxial films showed that there occurs a change in the band gap width, absorption and reflection coefficients, which can be explained by the local levels in band gap due to the formation of defects.

## Collisions of low-energy helium cations with furan molecules

**Tomasz Wasowicz<sup>1</sup>, Marta Łabuda<sup>2</sup>, Bogusław Pranszke<sup>3</sup>**

<sup>1</sup> Department of Physics of Electronic Phenomena, Gdansk University of Technology, Gdansk, Poland

<sup>2</sup> Department of Theoretical Physics and Quantum Information, Gdansk University of Technology, Gdańsk, Poland

<sup>3</sup> Gdynia Maritime University, Gdynia, Poland

Collisions of He<sup>+</sup> and He<sup>2+</sup> cations with furan molecules were for the first time investigated utilizing collision-induced emission spectroscopy (CIES) and *ab initio* calculations. The interaction initiated the fragmentation of furan molecules. The measurements of the fragmentation spectra of furan for both cations were performed at different energies/velocities. In consequence, several excited products were identified by their luminescence. The recorded spectra also revealed significant variations of relative band intensities of these species with changes of the projectile and its velocity implying complex fragmentation mechanisms. The *ab initio* molecular calculations allowed us to show that in both impact systems this complexity of fragmentation was triggered by different collisional processes. In particular, our results demonstrate that an electron transfer from furan molecules to cations may appear in competition with the [He-C<sub>4</sub>H<sub>4</sub>O]<sup>+ / 2+</sup> temporary clusters formation prior to decomposition.

## Concept of clusters embedded in a crystal: Study of properties of point defects in xenotime and monazite containing actinides

Anatoly Titov, Iurii Lomachuk, Daniil Maltsev,  
Nikolai Mosyagin, Sergei Semenov, Leonid Skripnikov

B.P. Konstantinov Petersburg Nuclear Physics Institute NRC “Kurchatov Institute”, Gatchina, Russia

Capabilities of x-ray emission spectroscopy and other experimental methods in measuring properties of atoms-in-compounds as a way for non-destructive testing the physical-chemical state of heavy atoms are limited, first of all, by difficulties in interpretation of experimental data. Establishing a straight and unambiguous link between the measured characteristics and the effective states of an atom in a chemical compound (material) [1-3] by modeling its electronic structure has obvious perspectives in applications. However, this connection is still not well exploited due to the extreme cost of modern schemes of the relativistic study of materials and other systems of practical interest, particularly, if they contain actinides as regular atoms or as point defects. The numerical instability of theoretical estimates of the values of the chemical shifts etc., which are, e.g., up to six orders of magnitude smaller than the energy of x-ray transitions, is the main problem. It is shown in [1-3] that rather economical calculation of the values of the chemical shifts of X-ray emission spectra for heavy-element compounds can be performed using the embedded cluster model developed in our lab recently.

In the talk our results of the embedded cluster calculations of properties of point defects containing Th, U and vacancies in xenotime and monazite are presented and discussed. The calculations of the embedded cluster's electronic structure for these minerals are performed using hybrid DFT functional, pbeo, and the generalized relativistic effective core potential method [4].

### References

- [1] Y. V. Lomachuk and A. V. Titov, *Phys. Rev. A* **88**, 062511 (2013).
- [2] A. V. Titov, Y.V. Lomachuk, L.V. Skripnikov, *Phys. Rev. A* **90**, 052522 (2014); L.V. Skripnikov, A.V. Titov, *Phys. Rev. A* **91**, 042504 (2015).
- [3] A.V. Zaitsevskii, L.V. Skripnikov, A.V. Titov, *Mendeleev Comm.*, **26**, 307 (2016).
- [4] N.S. Mosyagin, A.V. Zaitsevskii, A.V. Titov, *Int. Rev. At. Mol. Phys.* **1**, 63 (2010).

## Quantum-chemical modeling of gadolinium endocomplexes with fullerenes

**Anna Zakharova<sup>1</sup>, Marina Bedrina<sup>2</sup>, Sergey Semenov<sup>1</sup>**

<sup>1</sup> Petersburg Nuclear Physics Institute named by B.P. Konstantinov of National Research Center, Gatchina, Russia

<sup>2</sup> Petersburg State University, Saint-Petersburg, Russia

To protect the body from the harmful chemical effects of heavy metal gadolinium when it used as a contrasting agent in the magnetic resonance imaging and radioactive gadolinium form when it used in radiotherapy, it is of interest the possibility of placing Gd into the inert cage of fullerene.

Using quantum-chemical DFT (U)PBE0 method, we calculated the equilibrium structural parameters, IR spectra, bond energies, dipole moments, atomic charges and spin populations for the endohedral gadolinium metallofullerenes: Gd@C<sub>60</sub>, Gd@C<sub>70</sub>, Gd@C<sub>82</sub>, Gd@C<sub>84</sub>, Gd@C<sub>90</sub>. Electronic states of these endocomplexes are characterized by the average square of the spin  $\langle S^2 \rangle = 20.04$  to 20.05 a.u. calculated with the predetermined quantum number  $M_S = 4$ ,  $\langle S^2 \rangle = 12.04$  to 13.01 a.u. for the states with the predetermined quantum number  $M_S = 3$ . In this study, we used the software package Gaussian09 [1].

The spatial extent of the endocomplexes and the displacement of the Gd atom relative to the center of the fullerene cavity  $C_{2n}$  increases in a series of  $2n = 60, 70, 82, 90, 84$ . As a result of the endoatom implantation, the maximum distance between the carbon atoms increases by a few tenths of angstrom. The dipole moments do not exceed 2.26 D. The summary spin population on carbon atoms for higher fullerenes is significantly smaller in absolute value than for Gd@C<sub>60</sub>, and distributed among a large number of carbon atoms. A small value of the spin density on each atom provides sufficient kinetic stability of the endocomplexes.

Due to the half-filled 4f shell of gadolinium, the endocomplexes have a high magnetic moment and therefore are of the great interest for magnetic resonance imaging.

### References

1. Frisch M.J. et al. Gaussian 09, Rev. D.01. Wallingford CT: Gaussian, Inc., 2013.

## Embedding a potential method for the cluster modeling of solids and its application to the study niobate minerals as actinide immobilization matrices

**Daniil Maltsev, Yuriy Lomachuk,  
Nikolai Mosyagin, Leonid Skripnikov, Anatoly Titov**

Petersburg Nuclear Physics Institute named by B.P.Konstantinov of NRC “Kurchatov Institute”, Gatchina, Russia

Tantalo-niobate structures, analogous to natural minerals of aeschynite and euxenite groups were proposed as host phases for immobilization of actinide fraction of nuclear waste [1]. For a detailed study of such structures, it is important to know the effective state of the substitute actinide atoms. However, available methods of solid-state quantum-chemical calculations are not accurate enough to yield reliable results in the cases of f- and heavy d- elements. Additional problems arise in cases of treating the substitute atoms as crystal defects. Thus, there is a demand in a so-called embedding potential method, which allows one to simulate the effective crystal environment in a limited cluster calculation. Such potential, if transferable, can have wide range of applications in modeling minerals with point defects.

In the talk, an application of our embedding potential approach to the fersmite crystal (mineral of euxenite group with formula  $\text{CaNb}_2\text{O}_6$ ) as a pure niobate representative is discussed. The embedding potential consists of “pseudoatoms” with modified parameters and pure electrostatic charges, both corresponding to original crystal atoms surrounding the central cluster, and the latter being fully treated by the quantum-chemical methods (DFT with PBE0 functional). The parameters of the embedding potential are partially derived from preliminary solid-state calculations and optimized to minimize total forces on the atoms of the central cluster. The resulting approach allows one to reproduce the crystal structure and electronic density in the vicinity of the central atom with sufficient accuracy for a single-center cluster. Additionally, it can be used to study effective state of the substitute actinide atoms, their chemistry and spectroscopy in a multicenter cluster approach.

### References

[1] W. L. Gong, R. C. Ewing, L. M. Wang, and H. S. Xie, Aeschynite and euxenite structure types as host phases for rare earths and actinides from HLW. *Mat. Res. Soc. Symp. Proc.* 412, 374 (1996).

## **Analytical model for calculating the energy spectra of neutron radiation produced in d-t reactions for neutron generators with gas-filled or vacuum neutron tubes**

**Renat Ibragimov, Natalia Khatina,  
Evgeny Klopikov, Svyatoslav Kolesnikov, Elena Ryabeva**

National Research Nuclear University MEPhI (Moscow Engineering Physics Institute), Moscow, Russia

As part of the work of registration the neutron generator radiation, it have been planned to create a model for calculating the neutron spectra of this generator in GEANT4. In the process of creating this model, a lack of the Geant4 was revealed, which consists in incorrect cross section values of the d (t, n)  $^4\text{He}$  reaction. In addition, it have been shown that Geant4 does not accurately take into account the slowing down of low-energy deuterium and tritium ions in the neutron generator target substance (this process has significantly affects on the properties of the final neutron energy spectrum at the target output).

In this work, we carried out an analytical calculation of the neutrons spectrum shape that produced in the d-t reaction in neutron generators, taking into account fluctuations of ionization losses and multiple scattering of d and t ions with the substance of the neutron generator target ( $\text{TiT}_2$ ). Only freely distributed information on the values of nuclear reaction cross sections, mass numbers of nuclei, etc., and the concerning free-to-use Clion program from JetBrains has used in this calculation.

In addition to the neutron radiation spectra, the diamond detector response spectra to the calculated d-t neutron radiation spectra have been also analytically obtained in this work. An algorithm for obtaining the response of a diamond detector to d-t neutron radiation with different calculation parameters: detector energy resolution, generator accelerating voltage, and neutron generator target material have been created.

The calculation results of using this analytical model have been compared with results that were carried out by other groups of scientists using simulation programs for the interaction of ions with matter (SRIM-2013), as well as using expensive and hard-to-reach software that usually used for modeling the interaction of ionizing radiation with matter (MCNP). The results analysis showed quite good coincidence of the data obtained with developed analytical model, with calculations that have been performed using specialized software. In the future, it is planned to use the developed analytical model for solving the problem of neutron radiation spectrometry in terms of obtaining the basic response spectra of a diamond detector to neutrons with an energy of about 14 MeV.

## Irradiation of cerium oxide nanoparticles by fast electrons

Irina Bazhukova<sup>1</sup>, Sergey Sokovnin<sup>2</sup>,  
Alexandra Myshkina<sup>1</sup>, Valentina Kasyanova<sup>1</sup>, Sergey Bazhukov<sup>1</sup>

<sup>1</sup> Ural Federal University, Yekaterinburg, Russia

<sup>2</sup> Institute of Electrophysics, Ural Branch of the Russian Academy of Sciences, Yekaterinburg, Russia

Cerium oxide (CeO<sub>2</sub>) nanoparticles present a promising object for various applications, including biomedical research [1-3]. The CeO<sub>2</sub> nanoparticles are characterized by a high oxygen nonstoichiometry [2]. The formation of oxygen vacancies leads to the reduction of cerium ions to the Ce<sup>3+</sup> state on the particle surface. Such property correlates with the catalytic activity of cerium oxide nanoparticles and is probably responsible for their biological activity [4]. The present work is devoted to the modification of CeO<sub>2</sub> nanopowders by fast electrons with the purpose of changing the Ce<sup>3+</sup>/Ce<sup>4+</sup> valence ratio on the nanoparticle surface.

CeO<sub>2</sub> nanoparticles were obtained by pulsed electron beam evaporation in the low pressure gas on NANOBIM-2 installation [5]. Irradiation of samples was carried out by an UELR-10-10S linear accelerator of electrons with 10 MeV electrons in two modes: the irradiation of nanopowders with the subsequent preparation of suspensions on their basis and the irradiation of directly prepared aqueous suspensions of nanoparticles. The study of CeO<sub>2</sub> nanoparticles was carried out using optical and luminescent spectroscopy.

The optically active defect centres responsible for the optical absorption in the UV region and the luminescence was observed. These defects are likely to have a nature associated with oxygen vacancies and associated Ce<sup>3+</sup> ions. The formation of these centres is primarily connected with the non-equilibrium conditions of the gas-phase synthesis of nanoparticles. The modification of CeO<sub>2</sub> nanoparticles by fast electrons leads to degradation of these centres and is manifested in a decrease of the optical density in the UV range and luminescence intensity with increase of radiation dose. The irradiation of the finished aqueous suspension in comparison with the irradiation of the nanopowder leads to a shift of the photoluminescence band to the long-wavelength part of the spectrum. The change of CeO<sub>2</sub> luminescence properties in this case could be explained by interaction of material with radiolysis products (solvated electrons, hydroxyl radicals) and reduction of Ce<sup>3+</sup> ions.

### References

- [1] S. Das et al., *Nanomedicine*, **2013**, *8*, 1483.
- [2] A.B. Sherbakov et al., *Biotechnology*, **2011**, *4*, 9.
- [3] C.W. Sun et al., *Journal of Solid State Electrochemistry*, **2010**, *14*, 1125.
- [4] V.K. Ivanov et al., *Chemistry Success*, **2009**, *78*, 924.
- [5] S.Yu. Sokovnin et al., *Engineering of Nanobiomaterials: Applications of Nanobiomaterials*, **2016**, *2*, 29.

## Computed gamma tomography of radioactive metallurgical and geological samples

**David Zoul<sup>1</sup>, Pavel Zháňal<sup>1,2</sup>, Ladislav Viererbl<sup>1</sup>,  
Antonín Kolros<sup>1</sup>, Milan Zuna<sup>3</sup>, Václava Havlová<sup>3</sup>**

1 Research Centre Rez, Ltd., Husinec, Řež, Czech Republic

2 Department of Physics of Materials, Charles University, Prague, Czech Republic

3 Nuclear Research Institute Rez, plc., Husinec, Řež, Czech Republic

A unique computed tomography apparatus was built and successfully tested in Research Centre Rez. The apparatus allows a three-dimensional view into the interior of low-dimension radioactive samples with a diameter up to several tens of millimeters giving a better resolution than one cubic millimeter and it is designed to detect domains with different levels of radioactivity.

Structural inhomogeneities such as cavities, cracks or regions with different chemical composition can be detected by using this equipment. To detect fine cracks inside small samples an ultrafine scan of the sample were carried out in the course of tens hours with a 0.5 mm longitudinal and transverse step and 18° angular step.

The study of intercrystalline permeability of granite for the purposes of the safety of deep deposition into geological formations allows for the description of migration processes taking place in the rock environment.

On a 3D scanner, geological samples are evaluated after the diffusion experiment where the sample is placed between two reservoirs with a suitable solution. The Intake Reservoir contains the radioactive tracer (<sup>134</sup>Cs), the Outlet Reservoir is inactive. The activity distributed along the sample axis is displayed, to examine the water permeability of the sample with appropriate radioactive salt.

3D analysis of the spatial distribution of the activity of the tracer in a geological sample after the realization of the diffusion experiment depict the propagation of tracer around the disturbance in the granite or the intercrystalline permeability of the intact granite.

## Investigation of charge multiplication in irradiated p-type silicon sensors designed for the ATLAS Phase II Strip Tracker

**Leena Diehl, Riccardo Mori, Marc Hauser,  
Karl Jakobs, Ulrich Parzefall, Liv Wiik-Fuchs**

Albert-Ludwigs-Universität, Freiburg, Germany

For the luminosity upgrade of the LHC commencing data taking in 2026, the ATLAS experiment will replace its Inner Detector with an all-silicon Inner Tracker (ITk).

To cope with the large increase both in instantaneous and integrated luminosity challenges, the novel p-type silicon sensors have been designed and their charge collection and electrical performance after high irradiation doses were evaluated. Furthermore, it is important to understand and predict the long-term evolution of the sensor properties.

During detailed studies on the annealing behavior of ATLAS12 strip sensors designed by the ITk Strip Sensor Working Group, the phenomenon of charge multiplication in highly irradiated or sensors appeared.

In this work, the results of a thorough investigation of this phenomenon with two types of ATLAS12 strip sensors irradiated with fluences between  $5 \cdot 10^{14}$  and  $2 \cdot 10^{15}$   $n_{eq}/cm^2$  are presented. Systematic charge collection, leakage current and electric field measurements have been carried out for several annealing temperatures between 23°C and 80°C to investigate the dependence on temperature and fluence. Additionally, the maximal amount of multiplication reachable was investigated as well as the stability, e.g. by keeping the sensors at high voltage for a long time.

The results showed that the amount of multiplication starts to even saturate the readout electronics for highly irradiated sensors.

## Application of Monte Carlo software for calculation of efficiency of semiconductor germanium detector

**Dragana Krstic, Dragoslav Nikezic**

University of Kragujevac, Faculty of Science, Kragujevac, Serbia

Gamma spectrometry is commonly used for measurements of activity concentration in samples from environment.

The high purity semiconductor germanium detectors (HPGe) are widely used for gamma spectrometry. In this work Monte Carlo MCNP software [1] is used to calculate an efficiency of gamma detector.

HPGe detector was based on an existing one at the Laboratory of Radiation Physics at the Department of Physics of Faculty of Science in Kragujevac. The physical detector an ORTEC GEM series coaxial HP-Ge detector was simulated with Monte Carlo MCNP code; only the capsule of detector was modeled with dimensions obtained from certificate.

In addition to theoretical calculation, the efficiency of the detector is determined experimentally. Detector calibration was done by MBSS2 calibration standard, where radioactive materials were homogeneously dispersed in silicone resin and placed in 450 mL Marinelli beaker.

Theoretical efficiency determination was performed using the MCNP software, using tally f8, which gives energy distribution of pulses created in a detector.

By comparing the experimental and theoretical values, a uncertainty of 5% was found, which confirms that MCNP can be used for most materials and different densities in the case of the known geometry of the source. The use of Monte Carlo software for calculation of efficiency is an effective method for avoiding the development of standards for certain types of environmental samples.

### References

- [1] X-5 Monte Carlo Team. MCNP—a General Monte Carlo N-Particle Transport Code, Version 5 Vol. I: Overview and Theory. Los Alamos, 2003. NM: Los Alamos National Laboratory; LA- UR- 03- 1987.

## Microwave absorbance properties of $\text{Fe}_3\text{O}_4$ +epoxy resin and $\text{Fe}_3\text{O}_4$ +bentonite/epoxy resin nanocomposites

Arif Maharramov<sup>1</sup>, Ulker Samedova<sup>2</sup>,  
Musa Nuriyev<sup>3</sup>, Mazahir Bayramov<sup>3</sup>, Amdulla Mekhrabov<sup>4</sup>

1 Azerbaijan National Academy of Sciences (ANAS) Institute of Radiation Problems, Baku, Azerbaijan

2 Center for Novel Materials and Devices, Science and Technology Park, Institute of Physics, ANAS, Baku, Azerbaijan

3 ANAS Institute of Radiation Problems, Baku, Azerbaijan

4 Center for Novel Materials and Devices, Science and Technology Park, ANAS, Baku, Azerbaijan

Polymer matrix, embedded with functional micro- and nano-particles, composites have attracted much interest due to their extensive applications in electromagnetic (EM) wave absorption, rheological performance, thermal and electrical conductivities, and various sensors or devices. An ideal EM wave absorber materials needs to have light weight, thin thickness, high EM wave absorption capability, broad width and tunable absorption frequency, and also multi-functionality. Polymer matrix composites have the benefit of easy process and preparation, several species of polymers such as epoxy resins, polyethylene terephthalate, and polyurethane with low price make the composite materials to be used extensively. There are mainly three types of EM wave absorbing materials according to the absorbing mechanisms, dielectric loss, magnetic loss and conductive loss materials.

In this study we present synthesis route of three polymer matrix embedded with magnetic nanoparticles composites:  $\text{Fe}_2\text{O}_3$ +epoxy resin and  $\text{Fe}_3\text{O}_4$ +epoxy resin nanocomposites and  $\text{Fe}_3\text{O}_4$ +bentonite/epoxy resin composite [1]. Epoxy resin (ED-20) was chosen for its excellent mechanical and antibacterial properties, chemical and thermal stability, low contractibility, and strong adherence. Nanoparticles of  $\text{Fe}_2\text{O}_3$  and  $\text{Fe}_3\text{O}_4$  are a kind of inexpensive, non-toxic and paramagnetic material and have potential applications in EM wave absorption. Microstructure of samples has been analyzed by means of Scanning Electron Microscopy (SEM) revealing that the average size of nanoparticles was about 20 nm. Bentonite clay and ferrite micro-particles (10-20  $\mu\text{m}$ ) were used as filler and thicknesses of synthesized composites were about 0.5 mm. Electrical properties of the samples were measured to establish the effect of nanoparticle sizes and volume fractions on the enhancement of electrical conductivities of samples. The frequency dispersion of dielectric permittivity of composite materials has been studied in the frequency range of 25-35 MHz. It is shown that  $\text{Fe}_2\text{O}_3$ +epoxy resin,  $\text{Fe}_3\text{O}_4$ +epoxy resin nanocomposites and  $\text{Fe}_3\text{O}_4$ +bentonite/epoxy resin composite exhibit enhanced dielectric properties as compared to samples with micro-size ferrite particles. The dielectric Cole-Cole semicircle analysis suggests that there are Debye relaxation processes in the synthesized composites, which have beneficial effect to enhance the dielectric losses.

### References

1. Samedova U. F., Nuriyev M.A., Bayramov M.N., Magerramov A.M., Mekhrabov A.O. Synthesis structure characterization and physical properties of  $\text{Fe}_3\text{O}_4$ +epoxy resin nanocomposites. Power engineering problems. 2017, Baku. No3, 39-45.

## Fragmentation of molecules into neutral high-Rydberg fragments after core excitation and core ionization using soft X-ray synchrotron radiation

**Tomasz Wasowicz<sup>1</sup>, Annti Kivimaki<sup>2,3</sup>, Robert Richter<sup>4</sup>**

<sup>1</sup> Department of Physics of Electronic Phenomena, Gdansk University of Technology, Gdansk, Poland

<sup>2</sup> Nano and Molecular Systems Research Unit, University of Oulu, Oulu, Finland,

<sup>3</sup> MAX IV Laboratory, Lund University, Lund Sweden

<sup>4</sup> Elettra – Sincrotrone Trieste, Trieste, Italy

Molecules, apart from the ordinary excited states, possess the long-living metastable states characterized by very long lifetimes. The states with the electrons excited to the high principal quantum number orbitals (high-Rydberg (HR) orbitals) having the energies below the first ionization potential (IP) can be classified as those long-living states. HR molecules may behave considerably different than molecules excited to the normal states. Thus, in order to probe reactivity of such molecules, their electronic structure and decomposition mechanisms, different spectroscopic techniques, including those utilizing synchrotron radiation, have been applied. In particular, the near edge x-ray absorption fine structure spectroscopy (NEXAFS) provides detailed information about the presence of specific bonds and interactions in HR molecules. In the present work, we have used NEXAFS combined with techniques of pulsed field ionization and ion time-of-flight spectrometry to investigate the gas-phase inner-shell excitation of different molecules as well as a new class of mechanism of the photon-induced fragmentation, namely photoelectron recapture into the high-Rydberg states.

## Repartition of the secondary particles contributions into the absorbed dose of proton radiation behind the Bragg peak in the presence of gold nanoparticles

Alexandr Belousov<sup>1</sup>, Vladimir Morozov<sup>2</sup>, Grigorii Krusanov<sup>3</sup>,  
Andrey Davydov<sup>2</sup>, Maria Kolyvanova<sup>2</sup>, Alexander Shtil<sup>4</sup>,  
Vladimir Klimanov<sup>2</sup>, Alexander Samoylov<sup>2</sup>

1 Faculty of Physics, Lomonosov Moscow State University, Moscow, Russia

2 State Research Center – Burnasyan Federal Medical Biophysical Center of Federal Medical Biological Agency, Moscow, Russia

3 D.V. Skobeltsyn Institute of Nuclear Physics, Lomonosov Moscow State University, Moscow, Russia

4 Institute of Gene Biology, Russian Academy of Sciences, Moscow, Russia

**Introduction.** Gold nanoparticles (GNPs) are promising in cancer research and practice. In particular, GNPs are interesting as a class of agents capable of enhancing the efficacy of radiation therapy of malignant tumors. The GNPs radiosensitization was observed upon exposure with various types of ionizing radiation, e.g., proton beams. Nevertheless, physical mechanisms of enhanced efficacy of proton irradiation by GNPs are not fully defined. The goal of the present study is to estimate the contributions into the absorbed dose of various primary and secondary particles formed upon interaction of the proton beam with GNPs-contrasted media.

**Materials and methods.** The Monte-Carlo calculations were performed using Geant4 software at the 'Lomonosov-1' supercomputer at Lomonosov Moscow State University. The irradiated with 150 MeV proton beam sample was a water phantom with five regions of interest, located in different positions on the Bragg curve, including one in the peak maximum itself, filled with 50 mg/ml uniformly distributed GNPs.

**Results and conclusion.** The addition of 50 mg/ml GNPs induced no changes of the absorbed dose. Presence of GNPs in the irradiated phantom did not significantly shift the depth position of the Bragg peak but re-distributed the contributions of secondary particles into the absorbed dose. The most pronounced changes were observed several mm behind the peak, that is, in the tail of the Bragg curve (fold increase): ~1.15 protons, ~1.6 recoil nuclei, >70 photons, ~0.65 electrons. It has also been established, that presence of GNPs caused a several-fold elevation of dose-average LET in the tail of the Bragg curve. Thus, one should be cautious about GNPs affecting the accuracy of proton dose delivery in view of potential damage of surrounding critical organs.

**Keywords:** Proton therapy, gold nanoparticles, Monte-Carlo calculation, Geant4, radiotherapy

**Acknowledgments:** This work was supported by the Ministry of Education and Science of the Russian Federation under Grant №14.W03.31.0020.

## **Auger electron spectroscopy studies at the National Physical Laboratory for medical applications**

**Giuseppe Lorusso<sup>1</sup>, Alberto Boso<sup>1</sup>, Peter Ivanov<sup>1</sup>,  
Ana Denis-Bacelar<sup>1</sup>, Andrew Pollard<sup>1</sup>, Hiroshita Haba<sup>2</sup>**

<sup>1</sup> NPL, Teddington, United Kingdom

<sup>2</sup> RIKEN, Wako, Japan

When an atom is ionized by removing an electron from an inner atomic shell, the residual atom is in an excited state. Atomic relaxation back to the ground state occurs rapidly via radiative (X-rays) and non-radiative processes involving emission of Auger electrons. Auger emitters hold great potential for future targeted radiotherapies. This is because Auger electron emissions, while low in energy, deposits energy in very short distances (comparable to the chromosome size).

Despite this great potential, only few Auger emitters have reached the clinical trial stage and none are presently licensed for clinical use. This is because of a number of open questions involving radiobiology, dosimetry, and the lack of robust decay data. At the National Physical Laboratory we have recently started a program of Auger emission probability measurements essential to assess the biological outcome of Auger emission and to validate theoretical models of atomic relaxation. Advancement in the field require improvement of detector technologies but most importantly of techniques to produce high quality radioactive sources that must consist of a single atomic layer of electron emitters, possibly deposited on a substrate made of a low-Z made material.

This contribution will present the recent efforts at the National Physical Laboratory in both directions, with a focus on the production and study of Platinum radioisotopes. Thanks to the large number of electrons emitted per decay, Platinum isotopes are among the most promising candidate for future Auger therapy.

## The $\text{TlPb}_2\text{Br}_{5-x}\text{I}_x$ system as potential detectors for X-ray and $\gamma$ -ray at ambient temperature

**Michal Piasecki**

J.Dlugosz University, Czestochowa, Poland

There is only limited number of semiconductor materials, which possess photodetector features for X-ray and  $\gamma$ -ray at ambient temperature. Such materials comprise wide-gap semiconductors ( $E_g$  equal to about 1.6 eV) with relatively high material constants as density, electrical resistance, average atomic number, the high values of the product  $\mu$  of carrier mobility  $\mu$  and lifetime  $\tau$  (a merit factor for the detector materials). More over, the process of synthesis these materials implies additional limits. Currently, the most known and commonly used materials are CdTe and  $\text{Cd}_x\text{Zn}_{1-x}\text{Te}$  (CZT). CZT detectors feature high energy resolution and stable operation at ambient temperature. On other side, despite decades of research, the spatial homogeneity of CdTe and CZT crystals is insufficient, particularly for larger size detectors applications. The technological difficulties in preparation of high quality telluride crystals of sufficiently large dimensions, significantly increases the cost of such detectors. Therefore, due to the growing demand, necessary miniaturization of devices, sustainability, supply power restriction, high mobility of devices, there is a strong need to look for alternative materials for detectors that do not require cumbersome and expensive deep cooling. For this reason, based on our previous experience and the analysis of the current state of knowledge regarding the relationship between detection properties and chemical composition and structure, we have obtained, as a result of investigation phase diagram of the  $\text{TlPb}_2\text{Br}_5 \leftrightarrow \text{TlPb}_2\text{I}_5$  section, a series of new crystal which we expect that possess promising X-ray and gamma ray detection capabilities at ambient temperature.

## Nanodosimetry: Estimating radiation damage to DNA with Monte Carlo track structure simulation

Heidi Nettelbeck<sup>1</sup>, Carmen Villagrasa<sup>2</sup>, Marion Bug<sup>1</sup>, Hans Rabus<sup>1</sup>

<sup>1</sup> Physikalisch-Technische Bundesanstalt (PTB), Braunschweig, Germany

<sup>2</sup> Institut de Radioprotection et de Sûreté Nucléaire (IRSN), Fontenay aux Roses, France

Initial DNA damage caused by ionising radiation can be estimated by means of track structure simulations with Monte Carlo codes. A common approach in these simulations is to substitute DNA material composition with liquid water owing to a lack of interaction cross section data for biological materials. Until recently, the physics models in Geant4-DNA (an extension of the Geant4 Monte Carlo toolkit) were only available for liquid water. While the approximation of using water to substitute DNA is considered sufficiently realistic down to the micrometric scale, inaccuracies may arise in track structure simulations involving detailed particle interaction. Densely ionising radiation (i.e. ions with an energy corresponding to their maximum stopping power) and low-energy electrons below 1 keV are of particular concern as these particles deposit a large fraction of their energy within volumes of a few cubic micro- or nanometres.

This work details a recent collaboration between IRSN and PTB, which led to the implementation of measured cross section data of DNA constituents in Geant4-DNA (version 10.4) [1]. An extension of this collaboration is the current implementation of nitrogen and propane cross sections for simulating radiation interaction in micro- and nanodosimeters, which operate with tissue-equivalent gases.

Recommended cross section data for track structure simulations of electrons and light ions in biological targets such as DNA [2-3], or in gaseous mediums (nitrogen or propane) [4] will be presented. Simulation results from using the cross sections of DNA constituents as opposed to those of water will also be shown. Finally, the procedure for estimating radiation damage to DNA by correlating the physical quantities obtained from track structure simulations with the yield of different biological endpoints will be discussed.

### References

1. Int. J. Model. Simul. Sci. Comput. 1, 157–178 (2010).
2. Radiat. Phys. Chem. 130, 459–479 (2017).
3. Phys. Rev. A 93, 052711 (2016).
4. Phys. Rev. E 88, 043308 (2013).



**Radiation  
Protection**

**29**

## Current state of medical diagnostic reference levels and possibilities for improvements in the Netherlands

Harmen Bijwaard<sup>1,2</sup>, Ischa de Waard<sup>1</sup>

<sup>1</sup> National Institute for Public Health and the Environment (RIVM), Bilthoven, Netherlands

<sup>2</sup> Inholland University of Applied Sciences, Haarlem, Netherlands

In 2012 Diagnostic Reference Levels (DRLs) were set in the Netherlands for 11 radiological procedures (X-rays and CT-scans), including 5 procedures for children, but excluding nuclear medicine and interventional radiology. These DRLs were intended as guidelines for radiation doses indicative of good medical practice. In 2013 research by the National Institute for Public Health and the Environment (RIVM) concluded that the DRLs were hardly used in the Dutch hospitals. From 2014 RIVM therefore carried out yearly DRL surveys in collaboration with universities of applied sciences. Here, the results of a meta-analysis are presented. This meta-analysis includes all DRL survey data from 2014-2017, as well as several side-investigations into DRLs for interventional radiology, nuclear medicine, and alternative DRL formulations for children.

From 2014 radiography students from three Dutch universities of applied sciences have performed comparisons of dose measures with the DRLs according to the formal procedure. These comparisons were carried out in the hospitals as a part of the internships of the students, supervised by local medical physicists. Every year approximately 10 to 20 hospitals participated on a voluntary basis (40 in total). Apart from that, several side-investigations were carried out into possibilities for new DRLs in Dutch clinical practice. These investigations included DRLs for fluoroscopy-guided interventional procedures and nuclear medicine (as these are currently lacking in the Netherlands), and alternatives for the DRLs for children (that are currently difficult to use in clinical practice).

The DRL comparisons show a consistent pattern of compliance of nearly all hospitals with their current values. However, the reported dose measures lie far below the DRLs, indicating that the DRLs need to be updated (ICRP recommends doing this every 3 to 5 years). The meta-analysis of four years of data shows no signs of a downward (or upward) trend in the reported doses from year to year. This allows for an approach in which data from several years are pooled to derive well-defined 75-percentile values that might serve as new DRL values, following ICRP guidelines that advocate national dose surveys for the derivation of DRLs. In addition, it is shown that *DRLs for children* could be formulated in terms of DRL curves. These curves (DAP against weight) would facilitate DRL comparisons for hospitals that receive relatively few children. Furthermore, preliminary investigations show that *for some interventional procedures* it seems feasible to define DRL values provided that these procedures are nearly complication-free. Finally, survey results indicate that for several *nuclear medicine procedures*, DRLs could be based on the activities prescribed by the national guidelines: the reported activities usually fall below the maximum values. Alternatively, one might use the 75-percentile values derived from the survey.

## **Modelling of a radiological incident in the intermediary storage of activated wastes from VVR-S nuclear research reactor decommissioning**

**Alexandru Pavelescu, Carmen Tuca, Radu Deju**

IFIN-HH, Magurele, Romania

As an outcome of decommissioning of the VVR-S nuclear research reactor from IFIN-HH, Bucharest significant amount of graphite and aluminium low and medium level active waste have to be intermediary stored in a safety manner. Due to legal aspects rationales these wastes cannot be finally stored in the existing National Geological Repository. In this respect the former Spent Fuel Building, located in the Reactor vicinity, was chosen for long term storage of the activated thermal column graphite and reactor vessel aluminium components. Currently the spent fuel was removed and repatriated in the Russian Federation, the fuel ponds were emptied and decontaminated for graphite storage. The aluminium is stored in dedicated stainless-steel containers located in the main hall of the same building. Despite all the implemented ALARA measures, there is a certain radiological risk for the workers and public due to potential ingestion of the radioactive aerosols released on 10 km radius from the storage building in an unexpected fire and/or explosion. For the assessment of the radioactive material atmospheric dispersion, dedicated calculation codes are used in order to insure a rapid interventional response (few hours). In our assessment we made use of Hot-Spot Health Physics code created by Lawrence Livermore National Laboratory (LLNL) which delivers results using a conservative deterministic approach. In case of the potential occurrence of a disruptive event a radiation dose intake and associated risks for workers and public members was estimated.

**Keywords:** Radiological incidents, dose intake, decommissioning, radioactive waste

## Clearance from regulatory control in Switzerland of CERN's radioactive waste

**Charlotte Duchemin, Matteo Magistris, Marco Silari, Biagio Zaffora**

CERN, Geneva, Switzerland

Clearance from regulatory control of potentially radioactive material is a regulated practice in several European countries bringing benefits to society and the environment. The cleared material can be recycled instead of being stored in repositories for many years, and its resale brings a return of investment when compared with its conditioning and disposal as radioactive waste. CERN produces a wide variety of potentially radioactive waste due to maintenance, upgrade and dismantling of accelerators and experiments. This waste is then eliminated according to a tripartite agreement between CERN and its Host States France and Switzerland: it is either disposed of in the national repositories of the Host States, or cleared from regulatory control in Switzerland. CERN, as an environmentally-aware research laboratory, is committed to limit the production of radioactive waste, sort it effectively and ensure safe disposal. In this context, a number of projects were conducted and are ongoing, starting from the decommissioning of LEP.

LEP and its four experiments were decommissioned in 2000-2001 to allow reusing the tunnel and associated infrastructures for the LHC. Most of the equipment (approximately 30,000 tons) was eliminated as conventional material for recycling, following an extensive study submitted to the French authorities. At that time, the superconducting radiofrequency (RF) system was kept for a possible future use, until a few years ago the decision was taken to dispose of it. In 2016 the CLEAR (Clearance of LEP Acceleration RF system) project was mandated to first study the feasibility and then clear from regulatory control the 71 modules (approximately 450 tons of material, mostly valuable metals). The project included a theoretical and experimental study to pre-characterize the materials on the bases of its radiological history, chemical composition, extensive  $\gamma$ -spectrometry measurements and radiochemical analyses, dose rate and contamination measurements, FLUKA Monte Carlo simulations and calculations with the ActiWiz code. The operational phase started in March 2017 and was completed in October 2017 with the elimination of 414 tons of material as conventional, representing 95% of the total.

Based on the same procedure including calculations,  $\gamma$ -spectrometry measurements and radiochemical analysis to determine the nuclide inventory, 30 tons of high purity copper cables removed over the past 40 years from accelerator tunnels and controlled and supervised radiation areas have been cleared at the end of 2017 through the ELISA (ELImination of Shredded cAbles) project. In 2018, clearance of the LEP vacuum chambers was undertaken; the project is currently ongoing and around 100 tons of aluminium and lead were sold as conventional material in November 2018.

The presentation will discuss the overall clearance procedure applied at CERN for the clearance of historical radioactive waste.

## **Radiological monitoring approach for dismantling of the fuel assembly separator from VVR-S nuclear research reactor**

**Radu Deju, Carmen Tuca, Monica Mincu**

IFIN-HH, Magurele, Romania

Present study is related to the radiological monitoring performed during dismantling operations of the fuel assembly separator from IFIN-HH VVR-S nuclear research reactor which took place in the second phase (2017 year) of the decommissioning project initiated in 2010. One of the main tasks consisted of ensuring of the suitable radioprotection measures for workers in order to avoid external and internal radiation exposure. The separator is an aluminium cylindrical vessel (650 mm diameter 850 mm height) located in the reactor inner vessel having both at the upper and lower side a grid with 52 locations for fuel assembly. Under the lower grid there is a welded plate provided with 51 coolant flow adjusting diaphragms (holes). The radiological monitoring consisted in dose rate measurements performed: i) inside of the inner vessel before separator removal; ii) inside of the inner vessel during the separator removal, including the external dose for the workers; iii) after separator removal; iv) during separator cutting; v) during the resulted radioactive waste management. Based on dose rates results, a selection of the adequate technology solution for separator dismantling as well as the proper radiological protection measures for the workers was implemented. In order to estimate and control the potential dose intake measurement there were also performed for the activity concentration in the air during the main steps of the dismantling process. The results of the radiological monitoring emphasize that despite of the external and internal exposure, the dose rates received by the working personnel were below the dose rate limits – 20 mSv/year (about 10  $\mu$ Sv/h considering that the working time is 2000 h/year) according to national legal provisions.

## **Terrorists and “dirty bomb”**

**Vlado Valkovic**

SAGITTARIUS Consulting, Zagreb, Croatia

For many years, those concerned with the spread of nuclear weapons worried more about their acquisition by nation-states than by terrorists. However, there is a real risk that sub-national groups will in the future acquire fissile material—particularly plutonium—and construct a nuclear explosive. The risk of nuclear terrorism carried out by terrorist groups should be considered not only in construction and/or use of nuclear devices, but also in possible radioactive contamination of large urban areas. The radiological material could be spread by radiological dispersal devices, RDD, i.e., “dirty bombs” designed to spread radioactive material through passive (aerosol) or active (explosive) means. There are a number of possible sources of material that could be used to fashion such a device, including nuclear waste stored at a power plant (even though such waste is not highly radioactive), or radiological medical isotopes found in many hospitals or research laboratories.

Immediate health effects from exposure to the low radiation levels expected from an RDD would likely be minimal. Probably, the best way to move these materials around the globe is by using sea containers. This is because sea container offers criminals the same benefits as those enjoyed by ocean carriers and shippers: efficiency and security.

## **PyActiWiz – A massively parallel scripting environment to calculate radionuclide inventories for radiation protection purposes**

**Chris Theis<sup>1</sup>, Fernando Pereira<sup>2</sup>, Helmut Vincke<sup>1</sup>**

<sup>1</sup> CERN, Geneva, Switzerland

<sup>2</sup> CERN, EPFL, Geneva, Switzerland

Nowadays, the calculation of nuclide inventories has become a fundamental tool in modern radiation protection. The use cases range from radiological material optimization over safety studies to waste characterization. Typically, either general purpose Monte Carlo particle transport codes are used or analytic codes like ActiWiz. Due to the analytic approach and the highly optimized and parallelized algorithms the latter offers calculation times in the order of fractions of a second to a minute even for highly complex cases. In contrast to common Monte Carlo based solutions this allows for doing large scale studies involving numerous variations of parameters in order to either determine for example envelope cases for waste characterization or for doing sensitivity studies. In order to do such studies a python based scripting interface has been developed which represents the calculation core of ActiWiz as a standard built-in python module. As a consequence, studies varying a multitude of different parameters can be carried out with a few tens of lines of codes and at the same time complemented with customized analysis functions. This framework in combination with ActiWiz has become a standard characterization tool at CERN, allowing for implementing state-of-the-art statistical analysis methods as well as big-data analysis algorithms that are sometimes applied to millions of individual simulations for a specific study.

## **Virtual biodosimetry laboratory as a small network for radiation emergencies**

**Nataliya Maznyk<sup>1</sup>, Franz Fehring<sup>2</sup>, Christian Johannes<sup>3</sup>,  
Tetiana Sytko<sup>1</sup>, Nataliia Bohatyrenko<sup>1</sup>, Wolfgang-Ulrich Müller<sup>3</sup>**

1 Grigoriev Institute for Medical Radiology of NAMSU, Kharkiv, Ukraine (IMR), Kharkiv, Ukraine

2 Institute for Radiation Protection of the BG ETEM and BG RCI (IfS), Cologne, Germany, Cologne, Germany

3 University Duisburg-Essen, Essen, Germany, Essen, Germany

Cytogenetic biodosimetry has been an important part of radiation accident countermeasures, both in occupational and public health fields. For radiation protection institutes, involved in radiation emergencies preparedness and response activities, international cooperation and networking became an excellent choice to solve biological dosimetry tasks.

We have established a small network bringing together the expertise from radiation protection and cytogenetic biodosimetry fields suggesting the concept of virtual cytogenetic biodosimetry laboratory. Several inter-comparison studies have been conducted in order to determine the best ways of communication, sample collection, sample processing, image and microscopy analysis and data protection.

The studies comprised in both in vitro experiments and in vivo pilot investigations with occupational exposure samples. The additional goal was to compare the data from scorers with various cytogenetic but non-biodosimetry background. In vitro studies where clinically significant doses were used demonstrated the moderate variability of cytogenetic data obtained by different network participants. In vivo studies in the low dose range provided information about the peculiarities of dose estimation depending on the number of images analyzed. It was shown that image analysis took three to five times less time than microscopy for the equal number of cells. The influence of software parameters on the data outcome as well as inter-scorers variability will be discussed for the low and high doses range biodosimetry.

The following steps for such a network are the elaboration of own dose-response curve for radiation induced chromosome aberrations and dealing with partial body exposure scenarios. Our recent activities are devoted to fulfilling these tasks.

We can conclude that virtual laboratory or small network gave enough flexibility to radiation protection institutions in building up biodosimetry service including accidental occupational overexposure. Considering our experience some requirements, including implementation of image analysis, study designs and further needs for network development will be discussed.

## **Biomarkers for assessing radiation injury identified using large animal model**

**Vijay Singh**

Uniformed Services University of the Health Sciences, Bethesda, MD, United States

Exposures to ionizing radiation, whether they are intended or unintended, are currently an undeniable reality and carry potentially catastrophic health consequences. Therefore, medical preparedness and countermeasures are critical security issues, not only for the individual, but for the nation as a whole. Identification of biomarkers for radiation exposure is an urgent need. We have identified several promising biomarkers for radiation injury and radiation countermeasure efficacy using hematology, cytokine/chemokine/growth factors, microRNA, proteomics, transcriptomics, metabolomics, and lipidomics using nonhuman primate (NHP) model.

We identified a unique signature of seven miRNAs that are significantly altered with irradiation in NHPs. A combination of three miRNAs (miR-133b, miR-215, and miR-375) can differentiate irradiated versus unexposed NHPs. We have also identified a 5-miRNA composite signature that has the potential to identify irradiated NHPs and predict their probability of survival. Our study revealed a highly dynamic temporal response in the serum lipidome after irradiation. Marked lipidomic perturbations occurred within 24 h post-irradiation along with increases in cytokines and C-reactive protein. Metabolomic study demonstrates that several metabolites are altered after irradiation, including compounds involved in fatty acid- $\beta$  oxidation, purine catabolism, and amino acid metabolism. We have also studied metabolites in exosomes of irradiated NHPs. Exosomal profiling enabled detection and identification of low abundance metabolites that comprise exosomal cargo which would otherwise get obscured with plasma profiling.

Our study demonstrates that the biomarkers discussed above will definitely help to determine the dose of radiation with which a victim is exposed during any radiation/nuclear scenario. MicroRNAs appear specifically promising since we have developed a classifier based on two miRNAs (miR-30a and miR-126) that can reproducibly predict radiation-induced mortality. Such biomarkers will also play an important role in studying the efficacy of promising radiation countermeasures under development following the United States Food and Drug Administration Animal Rule. Such biomarkers are important for drug dose conversion from animal model to human.

## Health protection measures for major radiation accidents

**Alexander Grebenyuk<sup>1,2,3</sup>, Alexander Starkov<sup>1</sup>,  
Olga Strelova<sup>2</sup>, Alexey Miliaev<sup>3</sup>, Kamil Mamedov<sup>1</sup>**

1 Pavlov First St. Petersburg State Medical University, St. Petersburg, Russia

2 St. Petersburg State Chemical and Pharmaceutical University, St. Petersburg, Russia

3 Research and Production Center "Special and Medical Equipment", St. Petersburg, Russia

Radiation accident is a situation in which there is an unintentional exposure to ionizing radiation or radioactive contamination. Radiation accidents are global disasters, presenting a serious danger to the life and health of the population, as well as the environment. Radiation accidents have been registered in many countries of North and South America, Europe and Asia, but the most global are accidents in Mayak Production Association (Russia), Chernobyl Nuclear Power Plant (Ukraine) and Fukushima Daiichi Nuclear Power Plant (Japan). These examples demonstrate the severity of radiation accidents and make it necessary to prepare in advance for the Health Protection and Medical Response.

The basis of the Health Protection doctrine is features of a medical situation at radiation environments: a large number of casualties and victims, all casualties will be contaminated and dangerous to the medical personnel. Besides, the medical support should be provided in the limited time, limited number of the medical personnel and the limited list of medicines, in condition of damaged infrastructure. On this basis, Health Protection support should be complex, medical care should be fast and should be provided in protected environments. Finally, medical personnel must be protected from contamination.

High danger of radiation accidents to people demands carrying out Health Protection measures. In a stage of preparedness and planning the actions directed to maintenance of radiation safety must be organize and carry out. Emergency response is usually divided into medical care on site (at the scene of the accident, more often for workers of nuclear facilities) and medical care off site (for emergency workers and the affected population). There are three levels of response for on-site and off-site actions: 1) first aid provided at the scene of the accident; 2) initial medical examination and treatment in a general hospital; and 3) complete examination and treatment in a specialized medical centre for treatment of radiation injuries. Specific health protection measures which have to be held at major radiation accidents will be discussed in the report.

## **Radon measurements in big buildings**

**Alain Niba Ngwa, Steffen Kerker**

Institute of Medical Physics and Radiation Protection, Giessen, Germany

The recently passed Radiation Protection Law in Germany deals for the first time at the legislative level with measures to protect against radon at workplaces and in public buildings.

Many jobs are in big buildings. In contrast to small buildings, there is no measurement protocol for big buildings that makes it possible to assess the radon situation of the building reliably and without much effort. According to the European Consortium for the Measurement of Radon in Big Buildings (RiBiBui) can such a measurement protocol be developed with research in the areas of fundamentals, simulations as well as experiments and data analysis.

In this paper the radon concentration of a big building is presented which was measured over a period of two years with the help of passive and active radon measuring instruments. In order to gain more information about the air movement and usage of the building, the carbondioxide concentration of the building was measured and analyzed. This helped in the interpretation of the course of the radon concentration in buildings. With this knowledge a measurement protocol for the measurement of radon concentration in big buildings could be created.

The obtained data are merged and analyzed for variances and dependencies. In addition, it is examined, how much the measurements can be shortened without losing any relevant information about its reliability.

Beyond one typical building, further buildings will be investigated and studies of other research institutions including this topic will also be looked on to obtain a wide possible range of buildings.

## **Development of an in-situ radioactivity screening method for building materials using XRF and radioactivity index**

**Mee Jang, Chang Jong Kim, Won Woo Choi, Jong Myoung Lim**

Korea Atomic Energy Research Institute, Daejeon, South Korea

There is always naturally occurring radioactive material (NORM) in nature. Natural radionuclides can be present in the products made by material containing NORM. NORM from byproducts of the general industrial process or the NORM industry can be partially recycled into building materials, which can increase radiation exposure to residents. For building materials containing NORM, internal exposure by radon as well as external exposure by gamma rays, may occur for residents. In order to meet the limits of external exposure standards and indoor air quality standards by radon, it is necessary to measure and evaluate the radioactivity concentration for the building material before the building is built. But precise analysis can be impossible for many materials because of time and budget. Therefore, it is necessary to screen the building materials in the field. For this purpose, in-situ radioactivity screening method was developed by taking into account the external exposure dose or the indoor radon concentration after the radioactivity concentration measurement by XRF. ED-XRF is a non-destructive analysis method that measures the concentration of an element by analyzing the characteristic x-ray generated from the sample after exciting the sample using x-ray. Also, this method has advantage simple sample preparation compared to other analytical methods and multiple elements analysis. Although all elements from Na-11 to U-92 are available for analysis, they have an advantage in analyzing light elements in terms of analytical sensitivity. In addition, X-ray fluorescence analysis has the advantage of being able to analyze regardless of the size of the sample, and since the surface analysis of a certain thickness is performed, the chemical pretreatment of the solid sample such as the building material is not required. Therefore, unlike alpha spectroscopy, LSC, and gamma spectrometry, which directly measure radioactivity, mass spectrometric methods such as ICP-MS and XRF can also be used to measure the radioactivity of radionuclides. After we measured the building materials using XRF, and then we can calculate the radioactivity using specific activity constant and abundance ratio. And then we calculated the radioactivity index and evaluated the criteria pass ability using index value and radium contents considering external dose and indoor air quality. As a result, we have developed a method and algorithm that can reduce the budget and time required for precise analysis and dose evaluation of the building material and judge the possibility of inadequate material in the field. Also we performed the preliminary test for some building materials using developed screening algorithm.

## Synthesis and adsorption properties of $\text{TiO}(\text{OH})\text{H}_2\text{PO}_4 \cdot \text{H}_2\text{O}$ titanium phosphate

**Marina Maslova, Lidia Gerasimova**

Institute of Chemistry and Technology of Rare Elements and Mineral Raw Materials, Kola Science Centre,  
Russian Academy of Science, Apatity, Murmansk Region, Russia

Selective properties of adsorption materials are largely determined by nature of their matrix and functional groups. From this point of view, titanium phosphates with dihydrophosphate group are of interest. Due to higher ion-exchange capacity towards the radionuclides compared to titanium hydrophosphates they are effective in the acid media and highly compatible with cement. New method of titanium phosphate synthesis of required composition has been developed. The effect of synthesis conditions on chemical composition and physicochemical properties of the final products, mechanisms of formation and transformations of solid phases has been studied. An adsorption capacity of the final products was studied and correlation between the synthesis conditions and the properties of new functional materials has been established. It has been shown that good adsorption properties of the products depends on occurrence of the main phase  $\text{TiO}(\text{OH})\text{H}_2\text{PO}_4 \cdot \text{H}_2\text{O}$  (TiP). This compound has a higher adsorption affinity compared to  $\text{Ti}(\text{HPO}_4)_2 \cdot \text{H}_2\text{O}$ . The best results in adsorption capacity of TiP were in relation to copper cation ( $5.5\text{--}8.5 \text{ meq}\cdot\text{g}^{-1}$  or  $175\text{--}270 \text{ mg}\cdot\text{g}^{-1}$ ). As for cations of s –metals, the titanium phosphate is shown higher selective towards divalent metals ( $\text{Sr}^{2+}$ ) than monovalent metals ( $\text{Cs}^+$ ),  $5.2\text{--}5.7 \text{ meq}\cdot\text{g}^{-1}$  v.s.  $1.2\text{--}1.4 \text{ meq}\cdot\text{g}^{-1}$ . TiP is selective for ppm levels of  $\text{Sr}^{2+}$  in seawater ( $K_d > 10^4$ ). Ion-exchanger also showed selectivity for  $\text{Cs}^+$  and  $\text{Sr}^{2+}$  in certain types of nuclear wastes, containing up to  $1\text{M NaNO}_3$  and low concentration Ca and K (not more than  $0.01\text{M}$ ). In this case the distribution coefficients are  $1.2 \cdot 10^3 \text{ mL/g}$  and  $4.6 \cdot 10^3 \text{ mL/g}$  for  $\text{Cs}^+$  and  $\text{Sr}^+$  respectively.

**Acknowledgments:** This work was financially supported by the Russian Science Foundation (RSF) according to the research project №17-19-01522.

## Ion-exchange behavior of titanosilicate ivanukite framework in relation to nuclear wastes treatment

**Lidia Gerasimova<sup>1</sup>, Marina Maslova<sup>1</sup>, Shchukina Ekaterina<sup>1</sup>, Anatoly Nikolaev<sup>2</sup>**

<sup>1</sup> Institute of Chemistry and Technology of Rare Elements and Mineral Raw Materials, Kola Science Centre, Russian Academy of Science, Apatity, Murmansk region, Russia

<sup>2</sup> Nanomaterials Research Centre of Kola Science Centre, Russian Academy of Sciences, Apatity, Murmansk region, Russia

Nano-porous titanosilicates (TiSi) are used as ion exchangers because of thermal and radiation stability, high selectivity, and fairly good adsorption properties. Their unique adsorption properties are due to tunable pore diameter and geometric parameters of the crystal lattice facilitating their selectivity to certain ions and molecules. These materials have high chemical stability and can be used for removal and safe storage of radioactive elements from nuclear wastes. Among TiSi family ETS-4 and ETS-10 are widely known and commercially available. A new promising ion-exchanger is ivanyukite  $\text{Na}_2\text{K}[\text{Ti}_4(\text{OH})\text{O}_3(\text{SiO}_4)_3] \cdot 7\text{H}_2\text{O}$  (NaIV). Its crystal structure is based upon a 3-dimensional framework of pharmacosiderite type and consists of main building blocks of four edge-sharing  $\text{TiO}_6$ -octahedrons interlinked by  $\text{SiO}_4$  tetrahedrons. The resulting framework has a 3-dimensional system of channels defined by 8-membered rings occupied by  $\text{Na}^+$  and  $\text{K}^+$  cations and  $\text{H}_2\text{O}$  molecules. Three atoms of  $\text{Na}^+$  and  $\text{K}^+$  per formula unit in ivanyukite-Na were found to be capable of ion-exchange and can be replaced by mono-, di-, and even trivalent cations. The substituted phases are water-free and very stable over a wide range of pH and high temperatures. So that NaIV can be used not only for the removal of radioactive and hazardous metals from waste solutions but also for immobilization into the stable titanosilicate matrix. The ion-exchange behavior of ivanukite towards  $\text{Cs}^+$  and  $\text{Sr}^{2+}$  has been studied. It was found that NaIV exhibits an extremely high affinity for radionuclides ( $K_D > 10^5$  ml/g) in solutions containing less than 1 M  $\text{NaNO}_3$ . For complex NPP solutions, uptake of  $\text{Cs}^+$  and  $\text{Sr}^{2+}$  decreases with increases of Na concentration and decontamination factor does not exceed 100 in 10 g/l Na solution. NaIV was also tested in real radioactive waste effluents from Fukushima NPP, Japan. According to results, ivanukite is an efficient  $\text{Cs}^+$  and  $\text{Sr}^{2+}$  ion-exchanger for treatment Fukushima nuclear wastes.

**Acknowledgments:** The reported study was founded by RFBR according to the research project 18-29-12039.

## Comparison of $^{90}\text{Sr}$ dose factors for active bone marrow of adult males and females

**Pavel Sharagin<sup>1</sup>, Elena Shishkina<sup>1</sup>, Evgenia Tolstykh<sup>1</sup>,  
Alexandra Volchkova<sup>1</sup>, Michael Smith<sup>2</sup>, Bruce Napier<sup>2</sup>, Marina Degteva<sup>1</sup>**

<sup>1</sup> Urals Research Center for Radiation Medicine, Chelyabinsk, Russia

<sup>2</sup> Pacific Northwest National Laboratory, Richland, United States

Improvement of internal dosimetry is an important task in the structure of epidemiological studies conducted of the population exposed to radiation in the southern Urals in 1950s. Wide areas of the Urals were contaminated as a result of the activities of the Mayak plutonium production facility. The radioactive contamination included bone-seeking beta-emitters such as  $^{90}\text{Sr}$  that contribute to doses to bone marrow. Previous studies showed the bone marrow doses for some proportion of the Urals population were found to be higher than 1 Gy. Therefore, great attention is paid to bone marrow dosimetry in the studies of Urals residents.

Dose factors (DFs) allow converting  $^{90}\text{Sr}$  specific activity in trabecular or cortical bone into dose rate in the active bone marrow (AM). The aim of the study is to evaluate the DFs for active bone marrow due to  $^{90}\text{Sr}$  incorporated in trabecular bone volume (DF (AM←TBV)) and in cortical bone volume DF(AM←CBV) for adult male and female.

For this purpose, the software “Trabecula” was used to generate representative bone models (phantoms) describing the shape and microstructure of the segments of 12 main hematopoietic bone sites of adults. DFs were calculated by simulating electron- photon transport in the media of male-specific phantoms. DFs were calculated both for population-average bone dimensions and for bone dimensions that vary within the range typical of individual variability. DFs were calculated with MCNP6.1 The dependences of DFs on model parameters were calculated and used for calculation of female-specific DFs.

11%. Male-specific dose factors were calculated as follows:  $\text{DF}(\text{AM}\leftarrow\text{TBV}) = 4.0 \cdot 10^{-11}$  Gy/s per Bq/g;  $\text{DF}(\text{AM}\leftarrow\text{CBV}) = 1.6 \cdot 10^{-11}$  Gy/s per Bq/g. Differences between male and female dose factors by no more than 11%.

## Compilation of available information on carbon-14 releases from different types of nuclear reactors

Evgeniy Nazarov<sup>1</sup>, Alexey Ekinin<sup>2</sup>, Alexey Vasilyev<sup>2</sup>

1 Ural Federal University, Ekaterinburg, Russia

2 Institute of Industrial Ecology of Ural branch of Russian Academy of Sciences, Ekaterinburg, Russia

Required condition for the normal operation of power plants is acceptable exposure or acceptable risk to human and environment. The benefits of the exploitation of nuclear materials and radioactive substances are always accompanied by negative consequences in the form of ionizing radiation and the intake of radionuclides into the environment. An important practical way to confirm the safe operation of nuclear power plants is radioactive discharges monitoring [1].

The majority of European NPPs have <sup>14</sup>C in their discharges monitoring program. Analysis of discharges from European NPPs shows that <sup>14</sup>C makes a significant contribution to the total activity of releases from NPPs with different types of reactor installations. The contribution to the effective annual dose of <sup>14</sup>C depends on the type of reactor installations and ranges from 5% for LWGR type reactors to 95% for PWR type reactors.

To estimate the release of <sup>14</sup>C into the atmosphere from nuclear power plants in Europe (68 plants), the specific indicator GBq/(GW·h) was calculated for each type of reactor facility according to IAEA classification [2]. The estimation was made according to the annual emissions of <sup>14</sup>C [3] and the energy produced by each NPP [2]. In calculating the median specific indicator was used, due to its greater resistance to rare abnormal values of releases. Separately, AGR type reactors, which are the second generation of GCR type reactors, and also VVER reactors, which are analogous to PWR, are considered. This distinction was made because of the significant difference in specific indicators.

Contribution of all nuclear power plants in the world to <sup>14</sup>C in the atmosphere for all time was calculated in comparison with other sources of <sup>14</sup>C (tests of nuclear weapons from 1945 to 1980 and receipts from natural sources). Conservative estimates without considering carbon migration in the environment showed that the contribution of nuclear power plants to the total <sup>14</sup>C activity in the atmosphere is less than 1%. The main source determining the activity of <sup>14</sup>C in the atmosphere over the last 70 years is the testing of nuclear weapons from 1945 to 1980.

**Acknowledgments:** This work was supported by the Ural Branch of Russian Academy of Science Project 18-11-2-2.

### References

1. IAEA. Environmental and Source Monitoring for Purposes of Radiation Protection. Safety Guide. – No. RS-G-1.8. – Vienna. – 2016.
2. IAEA official site. Power reactor information system. [Electronic resource] – link to website: <http://www.iaea.org/PRIS>
3. Official site of European Commission Radioactive Discharges Database for collecting, storing, exchanging and dissemination of information on radioactive discharges. [Electronic resource] – link to website: <http://europa.eu/radd/index.dox>
4. J. Garnier-Laplace and S. Roussel-Debet, // Carbon-14 and the environment. – IRSN. – Radionuclide fact sheet. – 2010.

## Dose assessment in decontamination process of hot cells from VVR-S nuclear research reactor under decommissioning

**Carmen Tuca, Alexandru Pavelescu**

IFIN-HH, Magurele, Romania

The paper presents the aspects regarding dose assessment and associated risks for the workers involved in the decontamination process of the Hot Cells from IFIN-HH VVR-S Nuclear Research Reactor in view of their dismantling. The decommissioning is the final step in the lifecycle of the nuclear facility after the operating completion and final shutdown. Reactor was operated between 1957 and 1997 at a nominal thermal power of 2MW. The main purpose was the radioisotope production also the research activities in physics, biophysics and biochemistry. The reactor decommissioning started in 2010 and will be completed in 2020. There are five Hot Cells used for radioisotopes production for medical ( $^{131}\text{I}$ ,  $^{99}\text{Mo}$  and  $^{198}\text{Au}$ ) and industrial applications ( $^{192}\text{Ir}$  sources for gamma-graphs and  $^{60}\text{Co}$  for furnaces) also for the radiochemical products manufacture. The main steps in the Hot Cells decommissioning consists of the clean-up (radioactive waste evacuation), radiological characterisation of the internal parts (e.g. the fixed equipment and stainless-steel lining), surfaces decontamination, internal parts dismantling and evacuation. After the radioactive waste evacuation, the Hot Cells doors were opened and dose rates measurements were performed inside in order to estimate the associated risk for the workers which performed hot cell decontamination. The risk assessment was made using ResRAD software developed by Argonne National Laboratory. The risk was determined to be relatively high, taking into account dose limit 20 mSv/year; 10  $\mu\text{Sv/h}$  for 2000 h work/year.

**Keywords:** Decommissioning, hot cell, radiological characterisation

## The level of patient doses in intraoral and panoramic radiography in Serbia

**Zoran Mirkov**

Serbian Institute of Occupational Health, Belgrade, Serbia

The purpose of this paper was to investigate patient doses in intraoral and panoramic radiography and establish diagnostic reference levels for this part of dental radiography in Serbia. Kerma area product (KAP) was measured in the case of 60 intraoral and 40 panoramic x-ray units. In case of intraoral radiography, measurements have been made for the molars of the upper jaw. Intraoral KAP measured values were between 8.4 and 260.1 mGycm<sup>2</sup> and panoramic KAP measured values were between 57.0 and 129 Gycm<sup>2</sup>. Local diagnostic reference levels for intraoral and panoramic devices in Serbia have been established. The data obtained in this study can serve as baseline data for comparison in subsequent tests that will include dose measurements for patients during exams which include cephalometric and CBCT x-ray units.

## Are there alternatives to nuclear power?

**Elimkhan Jafarov<sup>1</sup>, Haydar Piriye<sup>2</sup>**

<sup>1</sup> Institute of Radiation Problems of ANAS, Baku, Azerbaijan

<sup>2</sup> Azerbaijan Republic Armed Forces War College, Baku, Azerbaijan

Today people are facing dilemma. Thus, only oil, coal or natural gas are not enough to provide energy and get rid of ecological crisis, In addition, it causes excessive amount of carbon food print by burning oxygen in atmosphere (global warming), increase of frequency of acid rains, destruction of forests as well as formation, which affect the development and together living of beings.

There is no need oxygen for nuclear fuel. There is very little carbon foot print. Normal running process of a Nuclear Plant also provides maintenance of ecology. And heat and electricity energy cost little as well. In conclusion, nuclear fuel has unique artificial renewable characteristics. When the first nuclear power plant was launched in the Obninsk, Russia people thought it the safest kind of energy. But, the accidents, happened in the US Trimal Island, Chernobyl in Ukraine and Fukusima in Japan proved that nuclear enery is capable to cause tremendous hazard and danger. Even there is a risk in the nuclear power plant of modern technology whereto there are facilities of high security and control. In another word, no any reactor is insured from natural disasters.

In the end of the explosion of Block 4 of the Chernobyl NPP 7,4 tones of radioactive waste split around, and territories of Ukraine, Belarus and Russia was polluted. Hundreds of people suffered from radioactive affect and got psychological trauma. At early stages, pancreas cancer, leucosis as a disorder of function of spinal cord, later it emerged as cancer of lungs, breast, stomach and intestine. It is deniable that irradiation of sexual organs could cause more serious problems.

There are about 150 tones of nuclear fuel under the isolated Block 4 and even it is not possible to predict what might happen in the near future.

So what is the logic to build new nuclear plants or keep expired nuclear power plant run?

The Metsamor Nuclear Power Plant expired in 2005. There is no metal-concrete insulation corp of protection in order to prevent irradiation in case of an incident. The cover of the reactor got thinner through the exploitation period.

The Metsamor is located on a seismic mountainous zone and shortfall of water supply to cool it in case of an incident. Thus, this causes danger not only the countries of the region, but also it is a fact that it may cause a gloom day for Yerevan which is located 30 km far away.

What to do in this case?

## **Comprehensive study of environmental contamination at nuclear legacy sites in the Russian Far East**

**Sergei Akhromeev, Sergei Kiselev,  
Vladimir Shlygin, Tatyana Lashchenova, Natalya Shandala**

State Research Center – Burnasyan Federal Medical Biophysical Center of FMBA of Russia, Moscow, Russia

The purpose of this work is to improve regulatory supervision at the nuclear legacy sites – the former coastal technical bases of the USSR nuclear fleet in the Far Eastern region of Russia (Sysoyeva Bay, Primorsky Krai). Today, this site is used as a site for temporary storage of SNF and RW. There are some contaminated parts of the site and buildings requiring decommissioning. Currently, a regional center for the conditioning and long-term storage of radioactive waste (RCCLSW) is being created on the basis of the enterprise. During the RW conditioning operations, the remediation of areas and buildings contaminated due to past activities is planned. A village (Stary Dunai) is located 3 km from the site. A federal highway passes along the village used for the SNF transportation till 2013. Some emergencies (more than 20 years ago) resulted in contamination of local areas along the road in the residential sector, where remedial operations were carried out. The regulator solved two problems during the comprehensive monitoring studies. The first one was an overall risk assessment in respect to the local population. The second task was an integrated environmental assessment prior to the start of the RCCLSW construction project. The radiation situation in the village is generally characterized by background regional levels of gamma dose rate and the content of manmade radionuclides ( $^{137}\text{Cs}$  and  $^{90}\text{Sr}$ ) in the soil, local foodstuffs, and drinking water. Here, local excess of MPC (1.2 times) for heavy metals (As, Mn, Al) in underground drinking water was found. This fact may be due to background levels of metal content in the soils of the region and requires additional research. Based on a uniform risk methodology, the individual carcinogenic risks of public exposure ( $1.08\text{E}-06$ ) and chemical risks (from  $1.0\text{E}-4$  to  $5.0\text{E}-4$ ) were assessed. The technological site is characterized by the overall environmental contamination by manmade radionuclides ( $^{137}\text{Cs}$ ,  $^{90}\text{Sr}$ ,  $^{60}\text{Co}$ ) and chemicals (heavy metals, polycyclic aromatic hydrocarbons). Chemical environmental pollution of the technological site in comparison with the village area is characterized by a higher content of heavy metals both quantitatively and qualitatively (Tl, Cd, Mn, Pb in ground and waste waters, Cr, V, Zn, Pb, Cu, As in soils). A large amount of data was obtained; an electronic database of radio-ecological data was created. Statistical processing of the obtained data allowed obtaining average values for all monitored parameters, which were assigned the status of “background indicators” for each environmental media. Based on the data obtained, reference levels will be developed for this area, which will form the basis for the development of methodological documents for the state health and epidemiological surveillance during the work at the RCCLSW.

## Removal of radioactive contaminants incorporated in corrosion oxide film using decontamination foams

Wangkyu Choi, Seungeun Kim, Seonbyeong Kim

Korea Atomic Energy Research Institute, Daejeon, South Korea

Decontamination is one of the methods available for reducing radiation exposure. Chemical decontamination is based on the chemical dissolution of radioactive oxide films from the internal surface of system pipes and components of nuclear facilities. Foam decontamination process as one of the chemical decontamination methods has a potentially wide application in the removal of radioactive contaminants from large components with complex shapes or large area or large volume. The foam decontamination process has advantages such as easy operation by room temperature and small secondary waste generation, but it has disadvantage of relatively low decontamination factor (DF). In order to overcome this problem, it is suggested to introduce decontamination foam containing more aggressive chemical reagent and to enhance the stability of the foam to increase the contact time between the decontamination foam and the contaminated surface to be decontaminated. In this study, the removal performance of nickel ferrite ( $\text{NiFe}_2\text{O}_4$ ) and iron chromite ( $\text{FeCr}_2\text{O}_4$ ) films coated on the surface of stainless steel 304 as the model of fixed contamination was investigated using acidic reductive and oxidative decontamination foams, respectively. Decontamination foams used in this study were prepared by combining surfactants, silica nanoparticles, and chemical reagents such as inorganic acids containing  $\text{HNO}_3$  and/or HF, reductive HyBRID reagent composed of 50 mM  $\text{N}_2\text{H}_4$  and 0.5 mM Cu(II) with pH 3 adjusted by  $\text{H}_2\text{SO}_4$ , and oxidative reagent containing Ce(IV).

For the removal of nickel ferrite film coated on the stainless steel specimen at 500 nm thickness, the oxide film was completely dissolved within 3 hours by acidic decontamination foam mixed with 0.5 M  $\text{HNO}_3$  and 0.5 M HF, whereas only ca. 3% of the oxide film was dissolved during the same time period by strong acidic decontamination foam containing only 2 M  $\text{HNO}_3$ . Under the milder conditions of acidic and reductive decontamination foam, the nickel ferrite film hardly dissolved in the reductive decontamination foam containing only HyBRID reagent, whereas the oxide film completely dissolved within 3 hours not only in the acidic decontamination foam containing 0.5 M HF with pH 3 adjusted by  $\text{H}_2\text{SO}_4$  but also in the reductive decontamination foam composed of a mixture of 0.5 M HF and HyBRID reagent. The reductive decontamination foam containing HyBRID reagent has a much higher initial dissolution rate of oxide film than the acidic decontamination foam. On the other hand, iron chromite film with a thickness of 10 micrometer produced in an autoclave was completely removed within 3 hours by oxidative decontamination foam containing 0.2 M Ce(IV) as an oxidant, but almost not by acidic decontamination foam containing 2 M  $\text{HNO}_3$  or mixed with 0.5 M  $\text{HNO}_3$  and 0.5 M HF. It was found that the oxide film containing chromium can be removed by the oxidative decontamination foam while it was difficult to remove by the acidic decontamination foam.

## Regulatory supervision during decommissioning & dismantling of nuclear submarines in the Russian Northwest

**Sergei Kiselev, Vladimir Shlygin, Sergei Akhromeev, Tatyana Lashchenova, Renata Starinskaya, Tamara Gimadova, Julia Zozul, Natalia Shandala**

State Research Center – Burnasyan Federal Medical Biophysical Center of FMBA of Russia, Moscow, Russia

Since 1960, on the territory of the Gremikha village, the coastal technical base (CTB) of the Russian Navy functioned to carry out recharging water-water and liquid metal reactors. After the termination of the CTB operation in the 1980s, the infrastructure of the facility degraded for more than 10 years, resulting in the potential hazard of environmental contamination. Today this site operates as the site for temporary storage of SNF and RW. In the early 2000s, with international support, work began to bring the radiation situation into normal conditions, including the removal and transportation of SNF and RW to long-term storage facilities. The end-state of the site after the decommissioning and restoration of contaminated areas is to use it for industrial purposes. Currently, about 1200 persons live in the vicinity of the facility, and most of them work in the enterprise. In 2005, before the beginning of remediation, the specialists of the SRC-FMBC during their field work characterized the radiation situation in the vicinity of the facility and assessed threats of radiological risks. Currently, work has been completed on the removal of fuel assemblies for water-water reactors; emergency reactor installations have been eliminated; and work continues on the removal of fuel assemblies from liquid metal reactors of nuclear submarines. On-site there are contaminated areas for SRW storage and buildings requiring decommissioning. Taking into account the requirements of the IAEA, the regulator conducts independent studies of the radiation situation in the course of remedial activities. According to the survey of 2017-2018, there are some local soil contamination areas on-site.  $^{137}\text{Cs}$  and  $^{90}\text{Sr}$  with insignificant content of tritium (ground water at local areas) are the main manmade radionuclides in environmental media (soil, seawater, ground water, seaweeds and bottom sediments). No contamination of groundwater with manmade radionuclides was found, while MACs were exceeded for some heavy metals (groundwater – Cd and Tl, observation wells – Cd, Ni, Al, Mn, Zn). Chemical contamination of soil is heterogeneous; it is represented by the following metals: Pb, Ni, Cu, Zn, V, Cd and As. The similar distribution of metals is observed in the residential areas. To clarify the connection of chemical pollution with the past activities of the enterprise, the background values of metal concentrations in the region were assessed. The use of advanced methodological approaches to assessing the total exposure to chemical and radioactive material, based on a uniform risk assessment methodology, is an important aspect of regulatory supervision. In the residential area the radiation situation is characterized by background indicators of environmental contamination. To inspect the public health in the vicinity of the facility, basic medical and demographic indicators were studied.

## **Problems in meeting regulatory requirements related to the skin dose**

**Jozef Sabol<sup>1</sup>, Jana Hudzietzová<sup>2</sup>**

<sup>1</sup> Faculty of Security Management, PACR, Prague, Czech Republic

<sup>2</sup> Faculty of Biomedical Engineering, Kladno, Czech Republic

In accordance with the general recommendations of the International Commission on Radiological Protection (ICRP) stating that the dose limit for the skin dose in terms of the relevant equivalent dose is not supposed to exceed 500 mSv in a year. Since the actual equivalent dose has to be averaged over 1 cm<sup>2</sup> area of skin regardless of the area exposed, such a requirement is impossible to verify based on a routine monitoring relying on the reading of finger dosimeter. This dosimeter, usually a TLD, gives the information about personal dose equivalent at the depth of 0.07 mm but its position is generally not at the point where with maximum exposure. Averaging TLD reading over the prescribed area is also questionable. The paper is aimed at the assessment of the correction factors which would convert the TLD reading into the recommended quantity so that the compliance with dose limit could be confronted.

## The scavengers of reactive oxygen species TEMPOL and reactive nitrogen species cPTIO enhance chromosome aberrations induced by low-dose $\gamma$ -irradiation

Denis Komarov, Olga Komova, Viktoriya Gavrilova

Joint Institute for Nuclear Research, Dubna, Russia

There is significant evidence that, in living systems, the overproduction of reactive oxygen species (ROS) and nitrogen species (RNS) can damage DNA, proteins, cellular membranes and leads to tissue dysfunction. Ionizing radiation is a strong inducer of ROS and RNS. The SOD-mimetic TEMPOL and nitric oxide scavenger cPTIO were found to detoxify efficiently ROS and RNS, correspondingly, protecting cells from the mutagenic and cytotoxic effects of radiation. In the present study, we investigated the effect of these compounds on chromosome aberration induction in human breast carcinoma cells Cal51 exposed to  $\gamma$ -radiation at low and high doses. At high doses (1 and 2 Gy), treatment with TEMPOL resulted in an about twofold decrease in the *yield of aberrant cells*, which is in agreement with its declared properties. At the same doses of  $\gamma$ -exposure, the nitric oxide scavenger cPTIO had no effect on chromosome aberration yield compared with untreated and TEMPOL-treated cells. However, an inverse effect was observed at a low-dose irradiation (10 cGy). Both scavengers enhance chromosome aberration induction, and this effect was most pronounced when TEMPOL and cPTIO were used simultaneously. In this case, the frequency of chromosome aberrations increased more than 1.5 times. A measurement of the ROS level with CM-H<sub>2</sub>DCFDA-staining in cells exposed to this dose showed that in the presence of Tempol ROS yield increased rather than decreased. However, at the dose 1 Gy this compound efficiently detoxified ROS and it can explain pronounced protective effect of TEMPOL on chromosome aberrations induction which was observed at high doses. A pro-oxidant effect of nitroxides like TEMPOL was reported and ascribed to the formation of strongly oxidizing oxoammonium derivatives that can be responsible for its genotoxic effect at low doses of  $\gamma$ -irradiation. Hence, reactions with superoxide overproduced at high doses can reduce oxoammonium cation back to its respective nitroxide are anticipated to improve the antioxidative effect of nitroxides.

## Occupational health and safety considerations within CBRN area

**Dejan Vasovic<sup>1</sup>, Goran Janackovic<sup>1</sup>, Stevan Musicki<sup>2</sup>**

<sup>1</sup> University of Nis, Faculty of Occupational Safety in Nis, Nis, Serbia

<sup>2</sup> University of Defence, Military Academy, Belgrade, Serbia

Occupational health and safety represents a multidisciplinary scientific discipline connected with the safety, health, and welfare of the working people. Research of occupational safety and health aspects is a relatively recent scientific movement. Only the highly motivated and adequately educated professionals can be considered as well prepared to perform the all necessary functions on occupational health services facing all kinds of hazards associated with the CBRN activities, both within military or civil structures, war of peace-time, regular of emergency situations. The aim of this paper is to analyze the most prominent occupational health and safety issues related to the CBRN area, as well as to define the most appropriate occupational risk management procedures.

## **RAMESIS project aimed at supporting citizen monitoring network in the Czech Republic – Final report**

**Petr Kuča, Jan Helebrant, Irena Češpírová, Jiří Hůlka**

National Radiation Protection Institute (SURO), Prague, Czech Republic

The paper summarizes results achieved during solution of the RAMESIS project aimed at supporting of Citizen monitoring in the Czech Republic. The main accent was given to collaboration with schools and other selected institutions and the general public, resulting into establishing a national-wide Citizen Monitoring Network.

The support provided in the frame of the RAMESIS project covers development of equipment for fixed station based monitoring, selection of suitable equipment for mobile monitoring, and design and development of the web-based Central Application for data storage, processing and presentation of measured data.

Equipment for both types of monitoring as well as access the Central Application is provided to participating schools, institutions and public on a free-of-charge basis.

The presentation, follow-up previous presentation of the project progress given at the RAD 2018 conference, shows the final results of RAMESIS research project of the citizen monitoring networks in the Czech Republic and the future plans and perspectives for its progress and development.

**Acknowledgments:** The paper shows the final results of RAMESIS research project (ID: VI20152019028) supported by the Czech Ministry of the Interior in the frame of security research.<sup>8</sup>

## 30 years following the accident at the Chazhma Bay (Primorsky Territory): Environmental assessment of the contaminated areas

**Nataliya Shandala, Sergei Kiselev, Vitaly Starinskiy,  
Dmitrii Isaev, Yrii Belskih, Vladimir Shlugin, Alexey Titov**

State Research Center – Burnasyan Federal Medical Biophysical Center of Federal Medical Biological Agency, Moscow, Russia

The most severe radiation accident during the entire existence of the Russian nuclear fleet occurred on August 10, 1985, on the nuclear submarine, which was located at the pier of the shipyard in the Chazhma Bay (Primorskiy Krai, The Far East). During the refueling, one of the nuclear reactors, after the completion of the fresh fuel loading, a spontaneous chain reaction (SCR) occurred, accompanied by simultaneous release of radionuclides and aquatic and terrestrial contamination. The peculiarities of the spatial spreading of radioactive substances resulted from an accidental release led to local contamination of marine and terrestrial ecosystems. The present work, in a comparative aspect, presents the results of the radioecological survey of the contaminated area 30 years after the accident. The radio-ecological situation in the Chazhma water area is determined by the radioactive contamination of seawater, algae, benthic organisms and bottom sediments. The main artificial radionuclides are  $^{60}\text{Co}$  and  $^{137}\text{Cs}$  with minor  $^{235}\text{U}$  content. Gamma-spectrometric studies of the seabed helped to estimate the total content of manmade radionuclides in the bay water area and compare it with that over the first years following the accident. The terrestrial contamination is characterized by uneven distributions both of gamma dose rate and of radionuclide activities in environmental media along the accident track. Gamma dose rate varies from 0.05 to 0.55  $\mu\text{Sv/h}$ . The soil contamination with  $^{60}\text{Co}$  is observed predominantly in the surface layer (0-10 cm). The maximum value of the specific activity of  $^{60}\text{Co}$  reaches 5100 Bq/kg. The content of  $^{137}\text{Cs}$  varies from 0.1 to 88 Bq/kg and  $^{235}\text{U}$  from 0.8-35 Bq/kg. According to the results of measurements of the specific activity of  $^{60}\text{Co}$  and  $^{137}\text{Cs}$  in the soil on the trace of the accident, the ratio of the activities of these radionuclides varies over the wide range, which indicates both a different rate of radionuclide precipitation from the aerosol cloud at the time of the accident and the features of radionuclide disperse distribution. In the course of the studies, the features of the physical and chemical behavior of  $^{60}\text{Co}$  in real environmental media were first studied. Pollution of environmental media with heavy metals has been also carried out. The observed results allow to consider the Chazhma accident trace area as a unique site for radio-ecological studies of manmade radionuclide behavior (especially  $^{60}\text{Co}$ ) in real conditions. In summary, the current radio-ecological situation at the area of the Chazhma accident track is characterized by local excess of  $^{60}\text{Co}$  concentration in the surface layer of the soil without significant migration and accumulation of radionuclides in near-earth vegetation. Considering the levels of artificial radionuclides in the environmental media and limited access of the population in this area, the public doses are not the subject of concern.

## **Dose estimations for Chernobyl contaminations by UNSCEAR: Neglected lessons from cytogenetic studies**

**Inge Schmitz-Feuerhake**

German Society for Radiation Protection, Hanover, Germany

Numerous observations about congenital malformations, cancer and other radiation effects in the populations contaminated by Chernobyl fallout are not accepted by the World Health Organisation WHO and other international institutions because of the very low doses which were derived by physical considerations. They refer to estimations of UNSCEAR (United Nations Committee on the Scientific Effects of Atomic Radiation) which were updated in their report 2008. A basic assumption in their calculations is that among the nuclides with greater half-lives than some days, only the Cs-isotopes are volatile which have a very low dose factor for incorporation. "From mid-1986 onwards, internal exposure due to  $^{134}\text{Cs}$  and  $^{137}\text{Cs}$  in milk and meat were the most significant sources of exposure." Hot particles containing  $^{90}\text{Sr}$ , Pu-isotopes and  $^{241}\text{Am}$  were only considered to occur in distances up to 20 km. Except thyroid doses, the results for the mean effective doses in 1986-2005 are: evacuees 31 mSv, highly contaminated regions in Belarus, Russia and Ukraine 9 mSv, inhabitants of Belarus, the Russian Federation and Ukraine 1.3 mSv, inhabitants of Western Europe 0.3 mSv.

Several reports in the literature, however, show different results. We have compiled data about radiation-induced chromosome aberrations because they allow an assessment whether the physically derived value will grossly underestimate the true exposure. Some thousand persons have been investigated in the contaminated regions by cytogenetic methods that can be considered as random sample of the population living there.

For such comparison, we prefer the results about dicentric chromosomes in the lymphocytes. These aberrations can be regarded as radiation-specific. They are unstable, i.e., they leave the system with half-lives of about 1.5 years. But this effect causes, that the background rate remains low and is almost constant over the world (about 4 dicentric chromosomes in 10.000 metaphases of adults, 1 in 100.000 of children). Therefore, the method is very sensitive. The doubling dose is about 10 mSv for an acute and homogeneous whole body exposure. But even this method would show no significant elevation in a population if the average additional dose does not exceed a few mSv. Investigations were done in the surrounding regions of the exploded plant and in distant parts of Europe directly after the accident or some years later. These revealed that the rate of chromosome aberrations was much higher – by up to 2 orders of magnitude – as would be expected if the physically derived exposures were correct. A further finding was the occurrence of multiberrant cells which indicate a relevant contribution of incorporated alpha activity, i.e. contributions of nuclear fuel and breeding products.

## **Review of SAF CBRN equipment and personnel: Expectations, advantages and constrains**

**Stevan Musicki<sup>1</sup>, Sladjan Hristov<sup>2</sup>, Dejan Vasovic<sup>3</sup>**

1 University of Defence, Military Academy, Belgrade, Serbia

2 Serbian Armed Forces, Army Command, Nis, Serbia

3 University of Nis, Faculty of Occupational Safety, Nis, Serbia

In addition to civil structures, CBRN units of the armed forces play a key role in the CBRN management system. This is particularly important in the case of relatively small countries, where synergy is needed between the operational resources of civilian and military structures, which are, most often, very limited. The aim of this paper is to present the level of CBRN equipment of the Serbian armed forces and personal capacities advantages and constrains with particular regards to expectations, i.e. purposes defined by relevant national strategies, laws and by-laws as well as undertaken international agreements. The key finding shows that there is a permanent need of strengthening both technical and human capacities in order to achieve defined goals.

## **Study of environmental contamination and the health status of the population living in the vicinity of uranium legacy sites in the Central Asia countries**

**Vitaly Starinskiy, Nataliya Shandala, Sergey Kiselev,  
Alexey Titov, Anna Filonova, Sergey Ahromeev**

State Research Center – Burnasyan Federal Medical Biophysical Center of Federal Medical Biological Agency  
(SRC-FMBC), Moscow, Russia

The interstate target program “Reclamation of territories of states affected by uranium mining industries” provides for the remediation of two uranium legacy sites in Kyrgyzstan: Min-Kush and Kaji-Sai and one site in the Republic of Tajikistan – Taboshar. Within the first stage of work, the comprehensive assessment of doses to the population living in the vicinity of the legacy sites and in the reference areas was carried out.

The public doses due to the contribution of individual components of natural exposure: external gamma exposure, internal exposure due to ingestion of radionuclides via drinking water and foods and due to inhalation of radon decay daughter products – were assessed in this work.

It was established that the main contribution to the effective annual public dose was made due to inhalation of radon progenies. It was revealed that the public dose in the vicinity of the former uranium mines is significantly higher than in the reference areas, and reaches 12 mSv / year.

Recommendations how to improve the public health during the remediation process were developed. These recommendations will help to reduce the public doses.

## UV protection offered by textile fabrics

**Snežana Stankovic<sup>1</sup>, Dušan Popović<sup>2</sup>, Matejka Bizjak<sup>3</sup>,  
Ana Kocić<sup>1</sup>, Dragana Grujić<sup>4</sup>, Goran Poparić<sup>2</sup>**

1 Faculty of Technology and Metallurgy, University of Belgrade, Belgrade, Serbia

2 Faculty of Physics, University of Belgrade, Belgrade, Serbia

3 Faculty of Natural Science and Engineering, University of Ljubljana, Ljubljana, Slovenia

4 Faculty of Technology, Banja Luka, Bosnia and Herzegovina

It is common knowledge nowadays that prolonged exposure to ultraviolet rays (UVR) can be harmful for human health by inducing skin diseases such as acceleration of skin aging, photodermatitis and skin cancer, as well as the acute and chronic effects on eyes such as keratitis and cataracts. Therefore, the use of sunscreens and UV protective clothing has gained popularity. The safest protection is offered by clothing, even though the textile materials themselves undergo limited UV-induced degradation. The effectiveness of textile materials to protect from UVR is determined by fabric composition (fibre type), construction (open porosity, weight and thickness), and finishing treatments (dyes, chemical agents, UV stabilizers). UV protectiveness of textile materials is expressed as "UV protection factor" (UPF) which defines the protection efficiency of a fabric from the risks of UV radiation, similar to the sun protection factor for sunscreens. The higher the UPF value, the greater is the fabric's protection degree. Determination of UPF values is based on instrumental measurement of the UV transmission through textile materials and calculation of the ratio of the average amount of UV radiation emitted by the source to the amount transmitted through a sample of textile materials with an allowance for differing biologic effectiveness of the various wavelengths in UV radiation.

It is generally accepted that cellulose textile fabrics (cotton, viscose, flax) have low UV absorption capacity. On the other hand, cellulose-based textile materials are considered to be comfortable to wear (in the summer months especially) because of their excellent hygienic properties. Generally, dark colours provide better UV protection due to increased UV absorption. However, light pastel shades are preferable for using in warm weather. Therefore, the objective of this work is to develop cellulose-based textile fabrics with effective UV protection and keeping satisfied their comfort properties. The grey-state plain knitted fabrics were produced from cellulose fibres (cotton, hemp) and laboratory assessed in terms of comfort (air permeability, thermal properties) and UV protection properties. In vitro test method for UPF determination was done according to European standard EN 13758-1:2002 (Textiles – Solar Ultraviolet Protective Properties – Part I: Methods for Apparel Fabrics). According to the results obtained, the textile fabrics were evaluated and a fabric with the greatest potential in terms of investigated performances was chosen from the selected assortment.

## **A need for a simplified system in radiation protection**

**Jozef Sabol, Bedřich Šesták**

Faculty of Security Management PACR in Prague, Prague, Czech Republic

At present, too many radiation dosimetry and radiation protection quantities are in use where they cause some complications because of their complex definitions and difficulties to assess them by the measurements. In addition, radiation workers and even radiation protection officers find these excessive numbers of quantities hard to apply in practical situations. Another problem consists in correct interpretations of the dosimeter and radiation monitor readings. For a non-specialist in radiation protection it is usually tricky to distinguish among e.g. quantities such as the dose equivalent and equivalent dose or among factors like quality factor, radiation weighting factor, tissue weighting factor and RBE which are used in the definitions of the dose equivalent, equivalent dose and effective dose. The proposal presented in the paper is aimed at the simplification of the current system of radiation protection quantities relying mainly on directly measurable restricted number of quantities. At the same time, it is proposed to continue in refining further the present system, The results of their scientific work may be later taken into account in practice. One has to bear in mind that in radiation protection is more important to obtain reliable assessment of exposure based on modest monitoring resulted in some conservative approach rather than to try to apply scientific methods which cannot be readily implemented in practical conditions.

## **Nuclear safety and nuclear security – Integrated approach (PC NFS experience)**

**Milos Mladenovic<sup>1</sup>, Ivana Maksimovic<sup>1</sup>, Miodrag Milenovic<sup>1</sup>, Dalibor Arbutina<sup>2</sup>, Stevan Karimanovic<sup>1</sup>, Danijela Soldatović<sup>1</sup>, Nebojša Bilanović<sup>1</sup>**

<sup>1</sup> Public Company “Nuclear Facilities of Serbia”, Belgrade, Serbia

<sup>2</sup> Public Company, Belgrade, Serbia

Public Company Nuclear Facilities of Serbia (hereinafter PC NFS) is the only nuclear operator in the Republic of Serbia. It was founded in 2009 under the Law on Ionizing Radiation together with the Serbian Regulatory Body. PC NFS has continued all nuclear activities previously managed by Vinca Institute of Nuclear Sciences. Nuclear safety has strong tradition in PC NFS because of the experience of our employees in very complex activities and projects such as SNF repatriation in 2010. Nuclear safety culture principles are also fully implemented. Department for Development and Application of Nuclear Technologies has developed various techniques for nuclear material characterization, numerical calibration of detectors,...On the other hand, nuclear security is relatively new field even in the developed countries. PC NFS management recognized the importance of continuous improvements of nuclear security systems and founded Department for Nuclear Security which led to the situation where nuclear safety and security measures were treated equally important. In parallel with upgrading existing PPS, PC NFS has implemented self-assessment methodologies developed by the IAEA in order to enhance the nuclear security culture. The biggest issues recognized by the IAEA and other relevant institutions is to leave nuclear safety and security solely to the Departments directly involved in those fields, since all the employees has certain accountabilities in both nuclear safety and nuclear security. PC NFS has followed world best practices and put a lot of efforts in creating integrated nuclear safety/security system. This paper will provide our results and future plans in making strong and sustainable system.

## Study on plutonium in seawater collected around several nuclear power plants in China

Sixuan Li, Qiuju Guo, Youyi Ni

Peking University, Beijing, China

With atmospheric nuclear weapon tests and a series of nuclear accidents, plutonium as the most important transuranic element entered into the natural environment. The limited sources make Pu an ideal tracer for the radioactive contamination and even some geophysical processes. Its most recent application in the Fukushima nuclear accident offered people with a lot of information in the release, transportation and deposition of contaminants. Considering the role Pu could play in the response to a nuclear accident and the increasing development of nuclear power plants in China, there is a great significance for setting up plutonium database around these sites referring to the local Pu background level.

In this research, for the above purpose, 66 surface seawater samples from 11 coastal sites of nuclear power plants in China were collected and  $^{239+240}\text{Pu}$  activity concentrations along with  $^{240}\text{Pu}/^{239}\text{Pu}$  atom ratios would be measured by ICP-MS to investigate the current status of Pu in these areas. For each coastal site, 6 samples, one sample is some 80-liter seawater, in total were collected. Among them, 4 samples were located in a straight line, respectively 5km, 10km, 20km, 30km far from seaside. Another 2 samples were also collected at a distance of 30km but on the sides of that line. Preliminary experiments for the method validation have been carried out. So far the result shows that  $^{239+240}\text{Pu}$  activity concentration ranges from 0.70 to 14.42 mBq/m<sup>3</sup> and  $^{240}\text{Pu}/^{239}\text{Pu}$  atom ratio is in a range of 0.180-0.439. Based on the previous research on these sites, the possible origins of Pu in Chinese coastal seawater are concluded to be the global fallout and Pacific Proving Grounds which imported a large amount of Pu through the ocean currents to the Western North Pacific Ocean. But relatively large uncertainties in the result were also noted and need to be improved in our current study for the validity of conclusions. It is expected that a clear description on Pu distribution and variance in seawater of coastal areas in China can be given by our ongoing study, which can be help not only for setting up Pu background database of Chinese nuclear industry but also for a better comprehensive understanding on Pu issues in Western Pacific Ocean.

## **Radiation effects in occupationally exposed persons: Who cares for the adoption of the state of knowledge in compensation cases?**

**Sebastian Pflugbeil, Inge Schmitz-Feuerhake**

German Society for Radiation Protection, Hanover, Germany

Since the 1980-ies, there have been several extensive studies on occupationally exposed persons which showed increased cancer rates from exposures below the legal dose limits. The greatest number of persons was investigated in mortality studies of the project INWORKS which included 308,297 controlled workers of the nuclear industry of France, U.K., and U.S.A. The research was done on malign solid tumours by 9 international institutes and the first results were published in 2015. The mean accumulated colon dose (according to the reference dose of the atomic bomb survivors) was estimated to 25 mGy. This leads to an absolute mortality risk for solid cancer which is about 2-fold higher compared to the A-bomb survivors and about 4-fold compared to the risk figure of ICRP 103 of 2007 for occupational exposure. The latter recommendations are the basis for EURATOM Directive 59/2013 and had to be adopted by all members of the European Union.

The ICRP has up to now – in contrast to the evidence from occupational and other low dose-rate investigations – insisted in a DDREF=2 according to their thesis, that a high dose-rate exposure is more effective than a low-dose one, and in using the A-bomb survivor data as the main reference for risk estimation. On behalf of single cancer diseases they refer to the estimations of the report UNSCEAR 2006 which also considers the Japanese data to be the main source of knowledge. The report was an update of the one of 2000 and regarded some additional cancers (salivary gland, small intestine, rectum, pancreas, uterus, ovary and kidney as well as cutaneous melanoma). Since then, many details were published about single cancers and other diseases after occupational exposure and in liquidators of Chernobyl.

Members of our society were involved in many German cases (uranium mining, nuclear and medical workers, flight personnel, and military stuff who served in former Radar stations and was exposed by X-rays and radioactive paints). Apart from leukaemia, cancers of the lung, breast, and the gastric tract we noticed that most physicians, who are asked to evaluate cases, are not informed about the spectrum of possible distortions. Officially, referring to UNSCEAR 2006, the following cancers are assumed to be of very low radiation-risk: Non-Hodgkin lymphomas, chronic lymphocytic leukaemia, prostate, rectum, pancreas, myeloma, larynx; cutaneous melanoma. Testicular cancer is not at all listed. All these diseases were obvious in the mentioned cohorts. We made a compilation and will report on corresponding data from low dose exposures, which show that the doubling doses for chronic exposure lie in the range of 0.1 to 0.3 Sv.

## Measurement of long-lived radionuclide activity induced in target components of a cyclotron used for [ $^{18}\text{F}$ ]-[FDG] production

Elio Tomarchio<sup>1</sup>, Mariarosa Giardina<sup>1</sup>, Daniele Greco<sup>2</sup>

<sup>1</sup> University of Palermo – Dipartimento DEIM, Palermo, Italy

<sup>2</sup> Centro di Medicina Nucleare, Palermo, Italy

The evaluation of high activity induced in target components in using a medical cyclotron to produce positron-emitting radionuclides for PET (Positron Emission Tomography) diagnostic studies is one of important issue and involves radiation protection concepts when operators are engaged in maintenance and/or substitution of a target or its components.

Most of replaced target components are generally classified and stored in a Pb-shielded container in order to wait for their radioactive decay. However, after some years, it can be necessary to start with the removal of the oldest parts, for a temporary storage of the fresh activated ones. The feasibility of these operations and the waste final disposal depends on the level of activity achieved and in particular on the residual concentration of radionuclides.

In this work we perform a nuclide identification and activity evaluation of some activated target parts by high resolution gamma-ray spectrometry with various HPGe detectors.

The measurements were performed over a decay period of more than 10 years from extraction, which allows to identify radionuclides with different half-lives. In particular, measurements on some Havar foils, stripper foils and titanium parts of a target used inside an IBA CYCLONE 18/9 cyclotron, allow to evaluate the largest activity values related to the most important radionuclides produced by activation of the materials ( $^{51}\text{Cr}$ ,  $^{52}\text{Mn}$ ,  $^{54}\text{Mn}$ ,  $^{56}\text{Co}$ ,  $^{57}\text{Co}$ ,  $^{58}\text{Co}$ , ...) with half-life of 70-80 days, while radionuclides with higher half-lives ( $^{22}\text{Na}$ ,  $^{44}\text{Ti}$ ,  $^{60}\text{Co}$ ,  $^{207}\text{Bi}$ , .....) were detected in the same samples in measurements performed after a long time period.

In this way it is possible to evaluate in advance the activity level at a time period after the end of maintenance and establish the correct procedures for storage or disposal of waste

## Occupational exposures in the Centre for Nuclear Medicine, Clinical Centre of Montenegro

**Nikola Svrkota<sup>1</sup>, Jelena Popović<sup>2</sup>, Nevenka M. Antović<sup>2</sup>**

<sup>1</sup> Centre for Ecotoxicological Research, Podgorica, Montenegro

<sup>2</sup> University of Montenegro, Faculty of Natural Sciences and Mathematics, Podgorica, Montenegro

This paper deals with doses from occupational exposure to radiation from external sources in the Centre for Nuclear Medicine in Podgorica (Clinical Centre of Montenegro). Radiopharmaceuticals used as diagnostic agents in nuclear medicine in Montenegro are mostly ones containing Tc-99m, extracted in the Mo-99–Tc-99m generator. This radionuclide disintegrates mainly to Tc-99, with a half-life ~6 h, and the 140.5 keV gamma ray is the most intense (88.5%). In order to evaluate doses received by workers in the course of their work in *controlled areas* of the Centre, the ambient dose equivalent  $H^*(10)$  has been measured by the Canberra InSpector 1000 in the three main rooms. Dose rate equivalent  $H^*(10)$  ranged from 0.03 to 0.14 mSv/h. Individual monitoring was performed by the thermoluminescence dosimetry. The Thermo Scientific personal dosimeters were used to measure the personal dose equivalent  $H_p(10)$  and, for the first time in Montenegro, ring dosimeters – to measure the dose to the hands, i.e. the personal dose equivalent  $H_p(0.07)$ . After one month exposure, for five monitored workers,  $H_p(10)$  was found to be from 81 to 122 mSv, while  $H_p(0.07)$  – from 129 to 948 mSv. Obtained results are used to assess annual dose, and they are discussed in the light of the protection limits.

**Keywords:** Nuclear medicine, external radiation, dose equivalents

## **Analysis of the radiological risks associated with the installation, extraction, and long-time storage of the CASTOR detector at the CMS experiment**

**Anna Cimmino, Robert Froeschl, Heinz Vincke**

Radiation Protection Group, CERN, Geneva, Switzerland

In December 2018, the Large Hadron Collider (LHC) entered a two-year stop, the Long Shutdown 2 (LS2), during which the whole accelerator complex and detectors will be maintained and upgraded for the next data-taking period, starting in 2021, and also for the High-Luminosity LHC (HL-LHC) operation which will start operation after 2025. In particular, the Compact Muon Solenoid (CMS) experiment planned a complete replacement of its beam pipe. This has marked the retirement of the CASTOR detector.

CASTOR is an electromagnetic and hadronic tungsten-quartz sampling Cerenkov calorimeter located at the CMS experiment at the LHC. It covers the pseudorapidity range  $-6.6 \leq \eta \leq -5.2$ . This small-angle detector gives access to a broad physics program within and beyond the Standard Model. However, its location, very close to the beam pipe, means the detector is exposed to high radiation levels and poses a unique challenge from the radiation protection view point.

In October 2018, CASTOR was installed for a last data-taking period and subsequently removed at the start of LS2. This paper presents the work and dose planning, formulated for the installation and removal interventions. Ambient dose equivalent rates have been estimated by means of FLUKA Monte Carlo simulations for different cool-down times. Also, the impact of local shielding has been studied. All results were used to minimize dose to personnel without interfering with the job at hand and thus upholding the ALARA principle. Finally, activation of detector components and materials has been estimated. Results have been used to plan for its long time storage and eventual disposal in accordance with the Swiss legislation.



**Radiobiology**  
**30**

## Study of radioprotective properties of microbiological preparations EM-1 and EMX-Gold

Ihar Cheshyk, Natallia Puzan, Alexander Nikitin

State Scientific Institution "Institute of Radiobiology of the NAS of Belarus", Gomel, Belarus

**Objective.** We studied the effect of microbiological preparations EM-1 and EMX-Gold (EMRO, Japan) on the transport system serum albumin of white outbred male rats.

**Methods.** White outbred male rats (n=25), aged 10 months at the beginning of the experiment, were divided into the following groups (n=5 in each):

- Negative control (group 1);
- Positive control: the animals were exposed to a total external acute g-radiation; the accumulated dose was 2.0 Gy (group 2);
- EM-1: The animals were exposed to a total external acute g-radiation; the accumulated dose was 2.0 Gy. These rats got EM-1 as the addition to water during 14 days before the irradiation and during 30 days after the irradiation (group 3);
- EMX-Gold: The animals were exposed to a total external acute g-radiation; the accumulated dose was 2.0 Gy. These rats got EMX-Gold as the addition to water during 14 days before the irradiation and during 30 days after the irradiation (group 4);
- EM-1 + EMX-Gold: The animals were exposed to a single total external acute g-radiation; the accumulated dose was 2.0 Gy. These rats got EMX-Gold and EM-1 as the addition to water during 14 days before the irradiation and during 30 days after the irradiation (group 5).

Blood sampling for research was carried out on the 3<sup>rd</sup> and 30<sup>th</sup> day after the irradiation; it was done simultaneously in the control group.

The effect on serum albumin indicators was evaluated using a set of reagents, PROBE-Albumin (Russia), a spectrofluorimeter CM 2203 Solar (Belarus) and a published method [1]. The parameters measured were:

- Total albumin concentration (TAC) – quantity of albumin molecules;
- Effective albumin concentration (EAC) – quantity of unoccupied binding sites of albumin;
- Reserve albumin binding (RAB=EAC/TAC×100%) – reflects the degree of structural modification of the protein;
- Index of Toxicity (IT=TAC/EAC-1) – characterizes the filling of albumin centers by toxic ligands.

Analysis of the data was performed by using GraphPad Prizm 4.0. Statistical processing is made by using t-test at a significance level of  $p < 0.05$  and  $p < 0.01$ .

**Results.** After 30 days of receiving of microbiological preparations:

- The values of the total concentration of albumin were in the normal range for all analyzed groups;
- In the group "EM-1" the IT decreased by 77.5 % when compared to positive control;
- In the group "EMX-Gold" the IT decreased by 83.3 % when compared to positive control;
- In group "EM-1 + EMX-Gold" the IT decreased by 93.3 % when compared to positive control.

**Conclusion.** Tested microbiological preparations (EM-1 and EMX-Gold) contribute to a more rapid elimination of radiotoxins from the rat's body.

### References

- [1] Lopukhin Y., Dobretsov G., Gryzunov Y. Conformational changes of the molecule of albumin: a new type of reaction to the pathological process. Bull.Exp.Biol. 2000;130,7:4–8.

## Computational cell dosimetry for alpha-particle exposure by Monte-Carlo methods

**Tariq Hailat<sup>1</sup>, Emese Drozsdik<sup>1</sup>, Balázs Madas<sup>2</sup>**

<sup>1</sup> Doctoral School of Physics, ELTE Eötvös Loránd University, Budapest, Hungary

<sup>2</sup> Radiation Biophysics Group, MTA Centre for Energy Research, Budapest, Hungary

Most experiments in radiation biology are performed to estimate the relationship between some biological effects like DNA double-strand breaks (DSBs) or cell survival and radiation dose. While the difficulties of measuring the biological effects are well-recognized, less attention is paid to the problems of quantifying the radiation dose. It is particularly difficult in case of incorporated alpha-emitting radioisotopes. Some of the reasons are the followings: i) Alpha-particles have a very short range in water ( $\sim 100 \mu\text{m}$ ). Therefore the cell dose strongly depends on the distance between the cell and the location of the radioactive decay. ii) The energy deposition by alpha-particles is highly heterogeneous along the track. In the last  $10 \mu\text{m}$ , much more ionizations and much more damages occur than in the first  $10 \mu\text{m}$ . iii) Due to the densely ionizing nature of alpha-particles, 37% of cells do not interact with alpha-particles even if the average dose (over all cells) is 300 mGy, while a significant number of cells receive more than half Gy dose. iv) In case of incorporation of (or treatment of cell culture with) alpha-emitters, not only the administered radionuclide but also its daughter product may contribute to radiation dose.

However, due to the large number of decays, alpha-particles, and cells, radiation decay and alpha particle transport can be simulated by Monte-Carlo methods providing reliable estimation of cellular burdens like hit distribution (how many cells interact with a 0, 1, 2, 3, etc alpha particles) or dose distribution (how many cells receive a given dose) besides average dose. These distributions may also support the interpretation of biological effects: Why do we not see any DSBs in a large fraction of cells? What is the contribution of bystander signalling? For answering these questions, we have to know the fraction of non-hit cells. To perform such simulations, we only need the geometry, i.e. the size and shape of the cells in the culture, and the spatial distribution of radionuclides. If the latter is homogeneous, the concentration is enough. If we have more information about the intracellular and intercellular concentrations, we can take into account it (or if we do not know these concentrations, we can estimate it based on the DSB distribution and the Monte-Carlo simulations).

We applied Monte-Carlo methods for cell dosimetry for cell cultures irradiated with Am-241. We prepared a numerical model of the cell culture. We selected decay positions randomly in the source. The alpha-tracks are straight lines, their direction is uniform. We computed which cells are intersected by an alpha-particle, and how much energy is deposited in them. We simulated millions of decays in order to get good statistics for hit and dose distributions. These Monte-Carlo models can then be integrated with models of biological response, e.g. cell survival or DNA DSB induction.

## **Cytogenetic effects in lymphocytes of cancer patients with different tumor localizations on early and late stages of radiotherapy treatment**

**Nataliya Maznyk, Tetiana Sypko, Nataliia Bohatyrenko,  
Olena Sukhina, Irina Krugova, Viktor Starenkiy**

Grigoriev Institute for Medical Radiology of National Academy of Medical Science of Ukraine, Kharkiv, Ukraine

The estimation of the cytogenetic damages in peripheral blood lymphocytes of cancer patients is an important task in the development of radiobiological basis of radiotherapy.

The aim of study was to assess the cytogenetic effects in cultured lymphocytes of cancer patients following radiation treatment, depending on tumor localization.

Chromosome aberrations were analyzed in lymphocytes of 25 radiotherapy patients divided on three groups depending on tumor localization: with uterine body cancer, lung cancer and with head and neck cancer. Blood sampling was performed during  $\gamma$ -<sup>60</sup>Co radiotherapy or megavolt radiotherapy course on linear accelerator: before radiotherapy, after first fraction for all patients, after second fraction of radiotherapy and also at the end of a course for the most part of patients. Dose per fraction was 1.8 – 2 Gy.

It was shown the excess of chromosomal damage before treatment over spontaneous level in all groups of patients, regardless of tumor localization, and informatively of FPG- and Giemsa-staining to detect this excess was evaluated. The highest exceeding of spontaneous aberration frequency in the group of lung cancer patients was shown. During radiotherapy course the different pace of chromosomal and chromatid type aberrations accumulation in groups of patients with various tumor localizations was found. The monotonic increase of radiation-induced aberrations from beginning to end of treatment in patients with uterine cancer and lung cancer and less pronounced changes in these parameters in patients with head and neck tumors were demonstrated. The informativity of cytogenetic analysis to detect the partial body radiation exposure after the first and the second fraction of radiotherapy course were assessed. Different approaches to radiation cytogenetic effects interpreting will be discussed.

## “Out-of-target” effects in the murine hippocampus after partial body irradiation

**Soile Tapio<sup>1</sup>, Zohaib Nisar Khan<sup>1</sup>, Omid Azimzadeh<sup>1</sup>,  
Fabian Metzger<sup>2</sup>, Munira Kadhim<sup>3</sup>, Fiona Lyng<sup>4</sup>,  
Simonetta Pazzaglia<sup>5</sup>, Mariateresa Mancuso<sup>5</sup>, Anna Saran<sup>5</sup>**

<sup>1</sup> Helmholtz Zentrum München, Institute of Radiation Biology, Neuherberg, Germany

<sup>2</sup> Helmholtz Zentrum München, Research Unit Protein Science, Munich, Germany

<sup>3</sup> Oxford Brookes University, Department of Biological and Medical Sciences, Oxford, United Kingdom

<sup>4</sup> Dublin Institute of Technology, Centre for Radiation and Environmental Science, Dublin, Ireland

<sup>5</sup> Agenzia Nazionale per le Nuove Tecnologie, l'Energia e lo Sviluppo Economico Sostenibile, Rome, Italy

The contribution of systemic “out-of-target” effects to the risks of a long-term health detriment following exposure to radiation is largely unknown. Both protective and damaging effects have been described, and no information on a dose response relationship exists. The aim of this study was to elucidate direct and abscopal effects in the murine hippocampus after total body irradiation (TBI) or partial body irradiation (PBI), respectively.

Female C57Bl/6 mice were irradiated at the age of 80 days using TBI or PBI (lower third of the body) at doses of 0.1 and 2.0 Gy (X-ray). The control mice were sham irradiated. The hippocampi from all groups were collected after 2 weeks and 6 months and investigated using label-free proteomics and targeted transcriptomics. The number of activated microglia was investigated using Iba-1 staining.

The proteomics analysis at 2 weeks showed a significant upregulation of 11 proteins irrespective of radiation dose or location. Among these were NMDA receptor proteins GRIN1, GRIN2A and GRIN2B and cognition-related SHANK proteins 1, 2, and 3. Most of the differentially regulated proteins were involved in the synaptic long-term potentiation and CREB signalling. The proteomics-based prediction of induced neuroinflammatory signalling was confirmed by increased numbers of activated microglia in TBI and PBI hippocampus.

These data show that radiation effects are not restricted to directly irradiated tissues. Possible mediators of these “out-of-target” effects will be discussed.

**Acknowledgments:** The SEPARATE project has received funding from the Euratom research and training programme 2014-2018 in the framework of CONCERT under grant agreement No 662287.

## On formation of DNA double strand breaks after irradiation of human malignant cells with therapeutic proton and carbon ion beams

**A. Ristić-Fira<sup>1</sup>, O. Keta<sup>1</sup>, V. Petković<sup>1</sup>,  
G.A.P. Cirrone<sup>2</sup>, G. Petringa<sup>2</sup>, G. Cuttone<sup>2</sup>, I. Petrović<sup>1</sup>**

<sup>1</sup> Vinča Institute of Nuclear Sciences, University of Belgrade, Belgrade, Serbia

<sup>2</sup> Istituto Nazionale di Fisica Nucleare, Laboratori Nazionali del Sud, Catania, Italy

An important component of cellular processes that occur as a feedback to exogenous cytotoxic compounds used in cancer therapy is the DNA damage response (DDR). DDR is a signal transduction pathway that recognizes DNA damage and replication stress, thus regulating processes that are important for the future of the cell. Cellular mechanisms can be guided to undergo DNA repair, cell senescence or apoptosis. In this study the emphasis is given on the cellular DDR induced by ionizing radiation. Among the events that emerge after exposure to ionizing radiation, the DNA double strand breaks (DSB) represent critical lesions which can lead to genomic instability and cell death. Initial signaling events activate DNA DSB repair pathway that is either non-homologous end joining (NHEJ) being the major one or homologous recombination repair (HRR), restricted to S- and G<sub>2</sub>-phase of the cell cycle.

Phosphorylation of histone H2AX represents one of the first steps in the cellular response to DSB.  $\gamma$ -H2AX foci seem to have significant function in the activation of the DNA repair system of the cell. They are formed within seconds after the induction of DSBs, but since they are primarily rather small and difficult to visualize, they are usually examined 15 to 30 minutes later. Their number reaches maximum at ~ 60 min and then decreases. Dephosphorylation of  $\gamma$ -H2AX by protein phosphatase 2A facilitates DSB repair, thus reflecting the kinetics of the repair process. Therefore, the kinetics of appearance of  $\gamma$ -H2AX foci after irradiation of different human malignant cells, HTB177 non-small lung cancer cells, MCF-7 breast carcinoma and HTB140 melanoma cells, by proton and carbon ion beams is investigated. For proton beams the irradiation position is defined in the middle of the 62 MeV therapeutic (SOBP) Bragg peak. Irradiation positions for the 62 MeV/u <sup>12</sup>C ion beams are chosen as to obtain the linear energy transfer (LET) values that provide the highest cell killing efficiency both for the pristine and widened (SOBP) Bragg peak. The presence of DNA DSB in irradiated cells is analysed immunochemically using an antibody against  $\gamma$ -H2AX. Kinetics of the appearance of  $\gamma$ -H2AX foci is followed up to 24 h by Western blot and by immunocytochemical analysis via confocal microscopy. The  $\gamma$ -H2AX foci assay estimates the number of foci, thus allowing quantification of radiation response in individual cells. It also provides high DSB detection sensitivity by assessing DNA damage within biologically relevant range of radiation doses. Signal transduction pathways, related to DDR (DNA repair and different types of cell death), were assessed by tracking alterations in the expression of specific proteins that are involved in these processes (ATM, ATR, PARP,...). Changes of the cell cycle distribution of irradiated cells were also observed and cross analysed. The obtained data regarding DDR to different radiation qualities are important for improving radiation therapy.

## Radiobiological validation of the GEANT4-DNA simulation toolkit through evaluation of DNA DSBs

**I. Petrović<sup>1</sup>, S. Incerti<sup>2</sup>, V. Petković<sup>1</sup>, O. Keta<sup>1</sup>,  
G.A.P. Cirrone<sup>3</sup>, G. Petringa<sup>3</sup>, G. Cuttone<sup>3</sup>, A. Ristić-Fira<sup>1</sup>**

<sup>1</sup> Vinča Institute of Nuclear Sciences, University of Belgrade, Belgrade, Serbia

<sup>2</sup> Université de Bordeaux, CNRS/IN2P3, CENBG, Gradignan, France

<sup>3</sup> Istituto Nazionale di Fisica Nucleare, Laboratori Nazionali del Sud, Catania, Italy

Cellular response to radiation as a function of time is consecutively separated into the physical, chemical and biological stages. Radiation chemistry begins after ionization and excitation processes are completed. Formation of free radicals strongly influences biological processes leading to final cellular issue. In order to evaluate the primary outcome of radiation, known as direct effects, i.e. physics, radical scavengers such as DMSO or glycerol are used. This multidisciplinary approach is based on two research paths. On one side, the aim is to improve the GEANT4-DNA extension of the general purpose GEANT4 Monte Carlo simulation toolkit that is proposing a modern simulation platform of biological effects of radiation at the DNA scale. This platform has been extended in order to simulate accurately particle elementary interactions (including electron, photon, protons, hydrogen, helium and charge states, and a few ions) with liquid water. It also simulates subsequent water radiolysis, which can generate oxidative radical species causing most DNA damages for low LET (linear energy transfer) irradiation of cells. In order to predict direct and non-direct early damages on cellular DNA (single- and double-strand breaks, i.e., SSB and DSB) for the low (photons) and high LET (protons, carbons) radiation GEANT4-DNA was used to simulate realistic geometries of cells combined with physics and chemistry stages of this code. Realistic cell geometries comprise nucleus containing the whole human genome, implementing randomly oriented fragments of chromatin fibers in the B-DNA conformation in 3D space. This geometry is dedicated to predict direct DSBs obtained at different LET values from the described radiation fields (photons, protons and carbon ions). On the other side, simulated values underwent biological validation through quantification of the number of DSBs. The focus is based on the formation of phosphorylated H2AX ( $\gamma$ -H2AX) foci that appear at the damage sites of the cellular DNA very soon after irradiation. Their number is correlated to the number of DNA DSBs. To obtain experimental data for comparison with the results of GEANT4-DNA simulations, direct effects of irradiation on different human cancer cells (HTB177 lung carcinoma, MCF-7 breast cancer) were examined. DMSO and glycerol were used as free radical scavengers to diminish, if not exclude, oxidative stress in irradiated cells. Direct effects were followed through the formation of  $\gamma$ -H2AX. DSBs were detected in situ by immunocytochemistry, using confocal microscopy. Clonogenic assay was used to monitor cell survival after irradiation. The effects of irradiation were examined via changes in radiobiological parameters. This combination of experimental cellular irradiations and Monte Carlo simulations applying the GEANT4-DNA will allow us to validate this toolkit for radiobiology and potential therapeutic outcomes adapted to recent cancer treatment techniques, including hadrontherapy.

## The influence of accelerated 1 MeV electron beam on microbiological and organoleptic parameters of a chilled rainbow trout

**Ulyana Bliznyuk<sup>1</sup>, Valentina Avduhina<sup>1</sup>, Alexander Belousov<sup>1</sup>,  
Polina Borschegovskaya<sup>1</sup>, Alexander Chernyaev<sup>1</sup>, Irina Gordonova<sup>2</sup>,  
Victoria Ipatova<sup>1</sup>, Zoya Nikitina<sup>2</sup>, Felix Studenikin<sup>1</sup>, Dmitry Yurov<sup>3</sup>**

<sup>1</sup> Lomonosov Moscow State University, Moscow, Russia

<sup>2</sup> Russian Scientific Institute of Medical and Aromatic Plant, Moscow, Russia

<sup>3</sup> Scientific Institute of Nuclear Physics named by D.V. Skobeltsin, Moscow, Russia

Prolonging the shelf life of foods for health and wellbeing of people is an essential task these days. Considering such a trend, Russia is conducting food treatment research involving electron, gamma and X-rays radiation. Physics Department of Moscow State University in collaboration with Scientific Institute of Nuclear Physics named by D.V. Skobeltsin and Russian Scientific Institute of Medical and Aromatic Plant focuses on radiation treatment of agricultural food products including chilled fish. The purpose of the study is to examine the microbiological and organoleptic parameters of chilled rainbow trout after treatment with 1 MeV electrons during extended period of storage. To assess the microbiological parameters the trout was squashed, homogenized, and diluted in NaCl solution before putting it into sterile eppendorf tubes. To measure organoleptic properties the thinly sliced chilled trout was put in vacuum plastic bags. Samples were treated with 1 MeV electrons using Continuous Electron Beam Accelerator with the average beam power of 25 kW. The dose absorbed by samples was calculated using program code GEANT 4 which allows to simulate the flow of electron beam with different radiation parameters such as energy, spectrum and radiation field characteristics. All the samples were irradiated with 250 Gy, 500 Gy, 1 kGy, 3 kGy, 6 kGy. After treatment eppendorf tubes were stored in a fridge at the 3-4 degrees C. Every 3 days with in 15 days after irradiation fish homogenate was placed in thioglycolic solution to determine the quantity of viable cells. Control samples were examined using the same method. It was found that the quantity of bacteria and microorganisms in irradiated samples on the first day of research decreased with the higher radiation dose; the maximum quantity was observed in control samples. Further bacterial content in control samples was decreasing during 4 days and than on day 8 started to increase to exceed the initial content 10000 times by day 15. The quantity of bacteria in samples irradiated with 250 Gy and 500 Gy remained unchanged during first 11 days and started to decrease to reach 0 by day 15. The quantity of bacteria in samples irradiated with 1 kGy, 3 kGy and 6 kGy during the first 4 days decreased but than increased with in day 8 to 11 and began to decline by day 15. On day 15, bacterial content in all irradiated samples was 10 to 100 times lower to compare with control samples. Organoleptic studies compared visual properties, structure, smell and taste of trout after irradiation with those of control samples. It was found that treatment with 250 Gy and 500 Gy did not change organoleptic properties of trout; however, with the increase of radiation dose the difference between control and irradiated samples became more pronounced.

**Acknowledgments:** The reported study was funded by RFBR according to the research project N 18-016-00198 a.

## Human acute stress response to entry of cesium and strontium into an organism as a result of an unfortunate event in the manufacture

**Nely Metlyaeva, Valery Krasnyuk, Boris Kukhta,  
Vladimir Yatsenko, Vyacheslav Korenkov, Lyubov Yunanova**

State Research Center – Burnasyan Federal Medical Biophysical Center of Federal Medical Biophysical Agency, Moscow, Russia

A psychophysiological examination of a radioactive waste processing enterprise worker who suffered from a single ingestion of cesium-137 in the amount of about 2.5 annual income limit (AIL) and 90Sr in an amount less than AIL was conducted. Intake of  $^{137}\text{Cs}$  was determined on the basis of the results of direct measurements of its content in the body, carried out using HRM. Intake of  $^{90}\text{Sr}$  in the body was determined on the basis of the results of measuring its activity in the urine. The total effective dose of internal exposure accumulated for the first year from the moment of incorporation was 43 mSv, the contribution to it from  $^{137}\text{Cs}$  was 96%. The cesium content in the feces during the course of treatment with ferrocen and after its completion was almost at the same level (125-380 Bq/g). The dose of internal irradiation established by measuring the content of cesium 137 in the patient's body on HRM unit will be 20mSv during the complete elimination of cesium 137 from the body. The aim of the work is to assess the psychophysiological response of a person in the dynamics of the ingestion of cesium and strontium into his body as a result of an industrial accident. The indicators characterizing the patient's personality profile (MMPI) and character traits during the first examination (Cattell test), although they were within the upper limit of normal values ( $<70>30\text{T}$ -points), testified to the anxiety-depressive state of the individual (2-D scale-68.8% and 9-Ma scale-35.0%), mainly due to changes in the neurotic triad indicators and Cattell test scores in the form of dissatisfaction with the situation and their position in it (scale O-7.0), frustration intensity (scale Q4-7.0), anxiety (scale F1-6.1) in a person with a high level of intelligence (scale B-8.0), educated behaviors (scale N-6.0), capable of building behavior with regard to the requirements of the environment (Q3 scale -9.0), with good abstract-logical thinking and problem solving in the conditions of time deficiency (Raven test). Repeated examination revealed a positive trend with preservation of anxiety with a tendency to subdepressive state of the individual (scale 2-D-68.8% and 66.4% and scale 9-Ma-35.0% and 47.0%). The indices characterizing concern with the state of health, hypochondriacal tendencies (scale 1-Hs-50.0% and 33.5%), demonstrative behavior (scale 3-Hy-42.5% and 37.9%), law-abiding, emotional manifestations in immediate behavior (4-Pd scale-48.9% and 40.8%), sensitivity to shades of human relationships and nuances of the situation (5-Mf scale-65.4% and 59.0%), as well as an anxiety index, suspiciousness, self-doubt (7-Pt scale -50.8% and 48.7%). Evaluation of the time of a simple sensorimotor reaction (SSR-309.6 $\pm$ 60.7ms and 261.6 $\pm$ 38.6ms), a complex sensorimotor reaction (CSR-1448.0 $\pm$ 60.72 and 578.19 $\pm$ 95.44ms) and reaction on a moving object (RMO-1013.0 $\pm$ 66.0 and 1006.0 $\pm$ 43.5ms) in dynamics showed a lengthening of the reaction time during the first examination with subsequent positive dynamics.

## Reaction to gamma irradiation at in vitro studies of regulatory suppressor T cells ( $T_{reg}$ ) of healthy donors

Tatiana Mushkarina, Evgenija Kuzmina, Tatiana Konstantinova

A.Tsyb MRRC- branch of NMRRC Ministry of Health of the Russian Federation, Obninsk, Russia

**Purpose and task of this study** – to evaluate the sensitivity of regulatory suppressor T cells to gamma irradiation at the dose range of 2-8 Gy *in vitro*.

**Methods and materials.** The analysis of 6 samples of peripheral blood lymphocytes cultures from healthy donors aged 19 to 76 years. Mononuclear cells are divided on a ficoll-urografin density gradient ( $\rho=1.077$ ). For the evaluation of reaction of regulatory T-lymphocytes, the irradiation of cells was done with the teleirradiation gamma therapy device “Rocus M” with the dose equal to 2, 4, 8 Gy and the dose rate of 1.17 Gy/min. Unirradiated lymphocytes were used as a control sample. Lymphocytes were cultured in culture medium RPMI-1640, with addition of 10% fetal bovine serum, gentamycin – 400  $\mu\text{g/ml}$ , IL-2 (roncoleukin) – 100 ME/ml. The incubation of mononuclear cells was carried out for 1, 2, 3, 4 and 6 days in medium with concentration equal to  $1.0 \cdot 10^6$  cells/ml at 37°C. Regulatory T cells were evaluated with the multicolor flow cytometry with the FACS Canto II (BD Biosciences) by the phenotype of membrane molecules  $\text{CD45}^+\text{CD4}^+\text{CD25}^+\text{CD127}^{\text{low/-}}$  (monoclonal antibodies BD Biosciences).

Comparison of arithmetic mean values of the relative and absolute quantities of regulatory T cells depending of irradiation dose was made with using the univariate analysis of variance in the program “STATISTICA 8.0”.

**Results.** During the analysis of the data regarding the content of regulatory T cells in the total quantity of lymphocytes in the cultivation period (from 1 to 6 days) and with different irradiation dose (0, 2, 4 and 8 Gy), no statistically significant dynamics of percentage and absolute amount of that cells were found ( $F_{3/76df} = 0.22$ ;  $p = 0.88$  at the both cases). The mean value and standard deviation for all groups for relative ( $n = 80$ ) and absolute quantity ( $n = 80$ ) of regulatory T-cells were  $7.5 \pm 3.5\%$  and  $0.028 \pm 0.026 \cdot 10^9$  cell/l, respectively. This result could not be acknowledged as the final, because the collected material is not homogeneous enough.

**Conclusion.** Analysis of dose dependence of percentage and absolute amount of regulatory suppressor T-lymphocytes did not reveal the statistically significant dynamic at dose range from 2 to 8 Gy. However this data is preliminary, because in addition to irradiation, the results of studies during the research period were influenced by the time factor and the individual characteristics of the immunity of donors. Regarding the functioning of regulatory T-lymphocytes, the particular scientific and practical interest is the analysis of their correlations with the individual composition of cell populations of the immune system.

## Exosomes are communicators of prosurvival signals during radiation response

**Simone Moertl, Lisa Mutschelknaus,  
Michael Schneider, Omid Azimzadeh, Michael Atkinson**

Helmholtz Center Munich, Munich, Germany

Exosomes are small subcellular vesicles that are released from cells into all known body fluids. Once released by their donor cells exosomes are readily taken up by other (recipient) cells, where both the external membrane and internal cargo may have an influence on cellular functionality. However, neither the composition of exosomes, nor their biological functions are fully understood. Our aim is to investigate whether exosomes released from irradiated cells are able to modify the response of non-irradiated recipient cells, and if so to identify the exosomal components that mediate these effects.

Quantification of exosome release by particle tracking analysis showed that radiation increases exosome release in head and neck tumor cells as well as in several non-tumor cell models. By labelling the lipid and protein components of exosomes we were able to verify uptake and transfer of exosomal material from irradiated into non-irradiated cells (1). Moreover, radiation was able to modify the content of exosomes. We identified radiation-induced changes in both the microRNA and protein content in exosomes from cells of fibroblast, epithelial and endothelial origin (2).

In our head and neck tumor model we found that the recipient cell phenotype was altered by exosomes. Here we showed that the clonogenic survival of irradiated recipient cells increased when they were given access to exosomes from irradiated donor cells. This pro-survival action can be explained at least in part by an enhanced rate of radiation-induced DNA damage repair in the exosome-treated recipient cells. The ability of exosomes to sustain post-radiation survival was greater with exosomes harvested from irradiated donor cells compared to those from non-irradiated cells (1). In non-irradiated recipient cells we have observed that the exosomes from irradiated donor cells promote cell migration. Molecular data identified enhanced AKT-signalling, manifested through increased phospho-mTOR and MMP2/9 activity as an underlying mechanism (3).

In summary, our results demonstrate that exosomes contribute to the tissue-level radiation response through activation of a novel systemic communication pathway between irradiated and non-irradiated cells and tissues.

### References

- (1) Mutschelknaus L. et al (2016) *PLoSOne*, 11(3) e0152213
- (2) Yentrapalli R. et al (2017) *Int J. Radiation Biology*, 93(6) 569-580
- (3) Mutschelknaus L. et al (2017) *Scientific Reports*, 7:12423

## **Health study of industrial radiography of occupationally exposed workers**

**Fulger Ciupagea<sup>1</sup>, Nuta Niculaie<sup>1</sup>, Gabriela Rosca Fartat<sup>1</sup>, Constantin Ghioca<sup>2</sup>**

<sup>1</sup> Public Health Directorate, Bucharest, Romania

<sup>2</sup> AC RAD, Bucharest, Romania

This paper presents the health condition assessment of an occupationally exposed group compared to a control group of unexposed individuals. The health status was analyzed from medical surveillance records. The retrospective analysis of the results of medical examinations revealed no clinical symptoms or diseases caused by exposure to ionizing radiation. The cytogenetic tests and the analysis of lymphocyte subpopulations highlight a higher frequency of chromosomal anomalies in the occupational exposure group than in the control group.

## Effect of pre-sowing irradiation of chickpea seeds on the content of low molecular weight antioxidants under salt stress

**Elimkhan Jafarov, Mehriban Velijanova, Jamala Orujova**

Institute of Radiation Problems of ANAS, Baku, Azerbaijan

Despite the numerous research works conducted, the role of the small molecular components of the antioxidant defense system in stress conditions has not yet been clarified. That's why, the study of the defensive role of biologically active substances in the stress environment is both scientifically, and practically of great importance.

A part of our researches was aimed to study the activity of carotenoids, flavonoids and anthocyanin's, being the small molecule antioxidants, in various stress conditions. For this purpose seeds of chickpea (*Cicer arietinum* L.) plant were selected as the research object. The seeds were irradiated at 1, 5, 10, 50, 100, 200, 300 Gy doses. The irradiation process was carried out at the "RUXUND" irradiation facility with a  $^{60}\text{Co}$  source. In the first option the irradiated seeds were first cultivated in ordinary water, and in the second one, in various concentrated (1, 5, 10, 50, 100, 200, 300 mM) NaCl solutions. And in the third option of our experiments, ordinary (non-processed) seeds were cultivated in the above concentrated salt solution. Our goal was to find out the role of dry seeds' gamma radiation in their further adaptation to salt stress by comparing the results obtained from all the three options. As we know, in the usual case, plants can be exposed to only one, but a few stress factors in their surroundings. Some of them can be permanent and others may continue for a short time. For this reason, such scientific research works enjoy higher interest. Because when beings are exposed to more than one stressful factor, in their organisms the mechanisms called as cross adaptations are introduced. Studying these processes is one of the topical problems today.

According to our findings, the amount of anthocyanin's in chickpea plants cultivated at 5 and 10 mM concentrated salt solutions has decreased to about 7 times, and the amount of flavonoids to 3 times against the control. There is about 2 time growth in the concentrations of carotinoids amounts in the 1mM and 5 mM concentrations and up to 4 times in 10 mM. Our experiments discontinued because of the plants' interrupted development in further concentrations.

In the results of the experiments on gamma-radiated seeds, 1, 5 and 10 Gy – dosed flavonoids, anthocyanin's and carotenoids remained approximately equal to those ones in the control sample. In subsequent irradiation doses, the anthocyanin's amount decreased by 30% and the number of carotenoids on the contrary increased by 2.5 times against the control.

Finally, in the third option – in our experiments on radiated seeds cultivated in salt solutions, more effective results have been obtained in cross-combinations arranged by us with 5, 10, 50 mM salt solution and 5, 10 Gy radiated seeds.

## Microdosimetry investigations as a dosimetric tool to explore the radiation cellular mechanism

Coretchi Liuba, Gincu Mariana

National Agency for Public Health, Chisinau, Moldova

**Background of the study.** Microdosimetry is continually being applied in radiation protection and radiation therapy. Recently, nanodosimetry was proposed explicitly as a dosimetric tool to explore the radiation molecular mechanism to distinguish it from the microdosimetry, which is dedicated more to the cellular level. More than 3000 people from the Republic of Moldova participated in the work to reduce the consequences of the Chernobyl nuclear accident. About 2500 descendants of the first and second generation of participants in the work to reduce the consequences of the Chernobyl nuclear accident (PWRCCNA) live on Moldova territory. These children (second generation) receive healthcare at the Mother and Child Institute.

**Methodology.** The study included 33 children – second generation of the PWRCCNA and 50 children in the control group. The frequency of chromosomal aberrations and micronucleus and the structure of morbidity were studied. The susceptibility of individual cells to accumulate chromosomal mutations in children of PWRCCNA was studied by 2 classical cytogenetic analyses used: Study the frequency of chromosome aberrations (CA) and Micronucleus test (MT). Blood cell culture was performed on the standard RPMI medium. Using the Nikon microscope, 100-200 metaphases per patient were analysed to identify CA and 1000 binuclear cells – to identify micronuclei. The results of the CA study in children populations were compared with those investigated 20 years ago to monitor their evolution in dynamics.

**Results.** Individual evolution of CA was established. With regard to aberrations at the chromatid level (gaps, solitary fragments and interchange) and at chromosome level (pare fragments: interchange, dicentrics and rings) there was an essential growth. At the same time, “Abnormal Monocentric” types were previously recorded at a frequency of  $0.04 \pm 0.004$ , and in 2017 they were not detected, so they were eliminated. In contrast, new aberrations were recorded – “Interstitial deletion”, with a significant frequency of  $5.5 \pm 1.9$ . The micronucleus – biomarker assay, used as a dosimeter to estimate *in vivo* whole body exposure, in PWRCCNA descendants found that binuclear cell count was 68%, binuclear cells with 1 micronucleus – 20%, and 2 micronucleus binuclear cells – 12%. Compared to the control group, in the children (second generation) group of PWRCCNA predominated the disease: anemia, juvenile goiter, steno-vegetative syndrome, pancreatitis, reactive hepatitis, chronic gastro-duodenum & tonsillitis. The results show the susceptibility of the digestive, nervous and endocrine system to the studied group – considered target systems of ionizing radiation.

**Conclusions.** It is worth mentioning that “dicentrics”, “rings”, “gaps” aberrations are considered markers of ionizing radiation. The fact that their dynamic growth has increased significantly denotes that the children are a group with genetic risk for the Moldovan population and require constant supervision.

## Motility and chemotactic response of *Escherichia coli* mutant strains and gamma-irradiated cells

Kei Wakimura, Mikio Kato

Osaka Prefecture University, Sakai, Japan

*Escherichia coli* is a peritrichously flagellated bacterium that can swim in liquid medium by rotating its bundled flagella. We have shown previously that bacterial motility is robust against ionizing radiation (1-3) but chemotactic response to a repellent has been lost due to gamma-irradiation (4). To better understand the relationship of radiation damages to resultant behavior, we are examining the motility and chemotaxis of the single-gene knock-out mutants each of which lacks one of chemotaxis- and flagellar motor-related genes (obtained from Keio collection [Baba *et al.*, 2006, doi:10.1038/msb4100050]).

### References

1. Kato *et al.* (2012) Real-time observation of *Escherichia coli* cells under irradiation with a 2-MeV H<sup>+</sup> microbeam. *Appl. Phys. Lett.* **100**, 193702 .
2. Atsumi *et al.* (2014) Effect of gamma-ray irradiation on *Escherichia coli* motility. *Cent. Eur. J. Biol.* **9**, 909-914.
3. Wakimura and Kato. (2017) Motility of *Escherichia coli* after irradiation with gamma rays. *Radiat. Appl.* **2**, 230-232.
4. Wakimura *et al.* (2018) Loss of a negative chemotactic response in *Escherichia coli* after irradiation with gamma rays. In *Exploring microorganisms: Recent advances in applied microbiology* (A. Mendez-Vilas ed.), BrownWalker Press, pp281-285.

## Molecular dosimetry with gamma-H2AX Foci in MCF7 cells

**Jin Kyu Kim<sup>1</sup>, Mi Young Kang<sup>2</sup>, Jin-Hong Kim<sup>3</sup>, Seungsik Lee<sup>1</sup>**

<sup>1</sup> Korea Atomic Energy Research Institute, University of Science and Technology, Jeongseup, Daejeon, South Korea

<sup>2</sup> Chonnam National University, Kwangju, South Korea

<sup>3</sup> Korea Atomic Energy Research Institute, Jeongseup, South Korea

Despite safety measures and strict regulations, unplanned exposures or accidents may occur. Molecular detection of exposure dose implies different biochemical assays and is used to estimate the absorbed dose in the exposed cells or individuals. Ionizing radiation can induce DNA damage in cells. Upon DNA double-strand breaks (DSBs) induction, H2AX becomes rapidly phosphorylated at serine 139. This modified form, termed gamma-H2AX, is easily identified and serves as a sensitive indicator of DNA DSBs. Gamma-H2AX foci formation and its dose response was studied to setup suitable techniques to monitor cells or individuals exposed to radiation. Human breast carcinoma MCF7 cells were irradiated with 0, 1, 5 and 10 Gy of gamma-rays from a <sup>60</sup>Co source. Immunofluorescence staining was performed to score the number of radiation-induced gamma-H2AX foci in the cells after irradiation. The number of foci per cell 15 min after irradiation increased linearly with exposure dose. A linear dose-response relationship was established from the data. In case of 1 Gy irradiation, the number of foci gradually increased with time until 2 hours after irradiation. However, the number decreased down to the background value 24 hours after irradiation. The result indicated that the response of MCF7 cells to radiation as assessed by gamma-H2AX formation was similar to that of human peripheral blood lymphocytes. Detection of the foci is a possible approach to monitor DSBs or DSB repair kinetics in persons accidentally exposed to radiation and cancer patients during radiotherapy.

## Comparative evidence of meiotic rearrangements in gamma irradiated and virus infected tomato plants

Larisa Andronic

Institute of Genetics, Physiology and Plant Protection, Chisinau, Moldova

Meiotic process is a complex, multistep process developed in generative cells and involving spatial chromatin reorganization, chromosome pairing and molecular exchanges of DNA-strands, distribution of genetic materials between haploid gametes. In general, meiosis is highly conserved, although at same time, the most vulnerable to various factors.

For evaluation of meiotic division in tomatoes under viral pathogenesis and influence of gamma irradiation, as biological materials, were used the *Solanum lycopersicum* ( $2n=24$ ) cultivars: Fachel and Prizior. The experimental plants were infected at the stage of 3-4 leaves with Tomato Aspermy Virus (TAV) or Potato Virus X (PVX). In conformity with the objectives of the present study, the tomato plants at the developmental stage, corresponding to the microsporogenesis in flowers buds of second raceme, were exposed to gamma radiation in 20Gy dose ( $Co^{60}$  as source of radiation). The chromosomes behaviour in anaphase and telophase I and II was evaluated by aceto-carmin squash method.

Cytogenetic researches establish that the plants infection with TAV or PVX caused an increase in the percentage of aberrations per pollen mother cells (PMC). Thus, the percentage of CMP with aberrations increased in A-T I by 3.02 – 4.44 times in the Fachel variety and 3.92 – 3.65 times in the Prizior variety in the case of the VAT or VXC infection corresponding. The gamma irradiation conduct to the increase of the frequency of aberrant cells by 4.9 and 4.4 times in cv. Prizior and cv. Fachel. The impact of radiation was higher on first division in virus infected plants. In the second meiotic division, the solitary impact of gamma rays is about 60% lower. In the case of the combined influence of radiation and a virus, there is a similar tendency to decrease the abnormal CMP frequency in A-T II compared to the A-T I, but with a smaller magnitude. This effect is found for both genotypes and viruses.

The cytological study of meiosis revealed aberrations such as precocious and laggards chromosomes, bridges with or without fragments. Precocious and laggards chromosomes were observed more frequently in early anaphase and telophase in I and II divisions. Chromosomal or chromatid bridges with/without fragments often were noticed in tomatoes infected with alone TAV or in combination with radiation.

In virus infected plants it was found a significant increase of microsporocytes with two or more aberrations. At the same time, the irradiation of the infected material induced a decrease of CMP frequency ( $P \leq 0.01$ ) with multiple aberrations.

Application of ANOVA revealed that virus infection, like gamma rays, causes the meiosis disorders, reflecting to an effect dependent on virus (24 %) and radiation dose (22 %). The analyzed tomato genotypes (cv. Fachel and cv. Prizior), characterized by susceptibility to both viruses, showed a similar reaction to the microsporogenesis.

## The application of electromagnetic radiation in the development of *Polemonium caeruleum* varieties

**Alina Glazunova, Firdaus Hazieva**

Russian State Medicinal and Aromatic Plants Research Institute, Moscow, Russia

**Introduction.** Neurosis diseases become an important problem in health care. According to the World Health Organization's data, 1/3 of adult population of the developed countries takes sedative medicine, there are written out about 20% of recipes. The *Polemonium caeruleum* roots content terpenoid saponins, what have a sedative effect and useful for the treatment of neuroses diseases. However, a peculiarity of this plant remains poorly supported. The aim of research: studies of the electromagnetic irradiation effect on *Polemonium caeruleum* for use this method in the development of this plant variety for medicine production.

**Methods.** For irradiation of seeds, we used "IPA" ("Installation Process Activation") device. The effect of IPA based on the influence of powerful electromagnetic irradiation and active of ferromagnetic particles on investigated objects. Duration of irradiation: 10 seconds, 20 seconds, 60 seconds. Not irradiated plants were used as controlling variant. After irradiation, seeds were planted in the field. The soil of field characterized pH 5-6.

**Results and conclusions.** We analyzed the yield of roots, germination and germination energy of seeds, the weight of 1000 seeds, morphometric signs as plant height, length and width of the leaf, amount of stems. Duration of irradiation 60 seconds increases plant height, amount of stems, seed production and weight of 1000 seeds. Duration of irradiation 10 seconds increased amount of stems as well as irradiation 60 seconds. By the way, 10 seconds irradiation increases the energy of germination and increase yield of roots more than 60 seconds irrigation. Duration of irradiation 20 seconds did not have much effect.

## Gene mutations induced by gamma-rays in haploid and diploid yeast cells

**Natalia Koltovaya, Nadya Zhuchkina, Ksenia Lyubimova**

Joint Institute for Nuclear Research, Dubna, Russia

We study the biological effects induced by ionizing radiation in view of therapeutic exposure and the idea of space flights beyond Earth's magnetosphere. In particular, we examine the differences between base pair substitution induction by ionizing radiation in eukaryotic model haploid and diploid yeast *Saccharomyces cerevisiae* cells. Such mutations are difficult to study in higher eukaryotic systems for which typical studied events are chromosome rearrangements. In our research, we have used two approaches – specific mutations localizing in definite sites and spectrum of mutations localized in single gene. First approach composes from a collection of six isogenic haploid *trp5*-strains and 14 isogenic haploid and diploid *cyc1*-strains that are specific testers of all possible base-pair substitutions. These strains differ from each other only in single base substitutions within codon-50 of the *trp5* gene or codon-22 of the *cyc1* gene. In order to restore codon and revert to wild type the defined substitution is necessary. In second approach we use the *CAN1* gene (1.8 kbp) system. This gene code plasma membrane arginine permease, mutation confers canavanine resistance, which arose in single *CAN1* gene. Frequency of point mutations was linear function for dose-dependence in haploid and exponential in diploid cells irradiated by  $\gamma$ -rays. Different mutation spectra for two different haploid genetic *trp5*- and *cyc1*-assays and different mutation spectra for the same genetic *cyc1*-system in cells with different ploidy – haploid and diploid – have been obtained. These spectra compared with gene spectrum. We suggest that obtained differences reflect the depending on sequence context for haploids and different molecular mechanisms of mutations in haploid and diploid cells.

## Clustered DNA damage: A severe biological triggering effect with challenging detection

Zacharenia G. Nikitaki, Ifigeneia V. Mavragani,  
Spyridon A. Kalospyros, Alexandros G. Georgakilas

National Technical University of Athens, Athens, Greece

Ionizing radiation (IR) represents a major weapon in the treatment of cancer. It incites different types of clustered (complex) DNA damage like DNA double strand breaks (DSBs), single strand breaks (SSBs) and other non-DSB oxidative base lesions needed to be repaired simultaneously if possible (1). The difficulty of repair for these clustered DNA lesions is reflected by the great efficiency of IR to inhibit the growth of tumors by inducing cell cycle arrest and/or death or senescence to cancer cells.

The biological significance of clustered DNA damage is not only based on the difficulty encountered by the different DNA repair proteins that process these closely spaced DNA lesions, but also to the fact that several of these oxidatively-induced clustered DNA lesions (OCDLs) can be converted into de novo DSBs during repair. In addition, unrepaired OCDLs have been shown to be converted to chromosomal breaks and increase chromosomal instability (2).

Therefore, a better understanding of the mechanisms for induction and processing complex DNA lesions has been a major concern for the scientific community in the recent decades. In this presentation, we will provide latest updates in the challenging detection of clustered DNA damage, current techniques, as well as our novel adaptation for the calculation of the levels of damage clustering at the chromosome level, using fluorescence microscopy and protein colocalization methodology (3).

### References

- (1) A G Georgakilas, P O'Neill, and R D Stewart, *Induction and repair of clustered DNA lesions: what do we know so far?* Radiat Res, 2013. **180**(1): p. 100-9.
- (2) J M Hair, G I Terzoudi, V I Hatzi, K A Lehouckey, D Srivastava, W Wang, G E Pantelias, and A G Georgakilas, *BRCA1 role in the mitigation of radiotoxicity and chromosomal instability through repair of clustered DNA lesions.* Chem Biol Interact, 2010. **188**(2): p. 350-8.
- (3) Z Nikitaki, V Nikolov, I V Mavragani, E Mladenov, A Mangelis, D A Laskaratou, G I Fragkoulis, C E Hellweg, O A Martin, D Emfietzoglou, V I Hatzi, G I Terzoudi, G Iliakis, and A G Georgakilas, *Measurement of complex DNA damage induction and repair in human cellular systems after exposure to ionizing radiations of varying linear energy transfer (LET).* Free Radic Res, 2016. **50**(sup1): p. S64-S78.

## **Assessment of visual behavior and optomotor response of rats after irradiation with 5 Gy protons**

**Iurii Severiukhin**

Joint Institute for Nuclear Research, Dubna, Russia

In modern radiotherapy, it is important to pay particular attention to the possible risks to patient health and to monitoring radiation dose. When the patient's head is irradiated, there is a risk of damage to the visual system. Also, the correct functioning of the visual system is important for health and operator functions of astronauts. The present study will provide a better assessment of the risks for human during spaceflight and after radiotherapy. During the experiment, heads of rats were exposed to protons; the remaining animals were shamirradiated and used as control. To estimate the visual function, equipment was used, which included of a platform and display with visual stimulation. It is found behavioural alterations induced in rats by 5 Gy of 170 MeV cranial protons irradiation. Cranial irradiation of animals does not result in a statistically significant decrease in the optomotor response in rats. However, irradiation with protons leads to a decrease parameters of visual behavior at 90 days postirradiation. The presence of such differences when using visual stimulation with low contrast and the absence of differences when using a visual stimulus with high contrast may indicate a decrease in visual acuity in irradiated animals.

## Low-dose X-ray irradiation does not cause detrimental effects in the progeny of irradiated mesenchymal stem cells

**Andreyan Osipov<sup>1</sup>, Margarita Pustovalova<sup>1</sup>,  
Anna Grekhova<sup>2</sup>, Petr Eremin<sup>3</sup>, Natalia Vorobyeva<sup>1</sup>**

<sup>1</sup> State Research Center - Burnasyan Federal Medical Biophysical Center of Federal Medical Biological Agency, Moscow, Russia

<sup>2</sup> Emanuel Institute for Biochemical Physics, Russian Academy of Sciences, Moscow, Russia

<sup>3</sup> Russian Scientific Center of Medical Rehabilitation and Health Resort of the Ministry of Public Health, Moscow, Russia

Current uncertainties in measuring the health risks associated with exposures to low-dose radiation present a major scientific problem affecting various areas of human activities, such as radiological protection of the public and nuclear industry workers, safety of patients exposed to low-dose diagnostic procedures, space exploration and others. A special interest is given to the studies of the delayed low-dose radiation effects induced in the stem cells. Repair of low-dose induced DNA double-strand breaks (DSBs) has been hypothesized to be inefficient, potentially causing various malfunctions in the progeny of the irradiated stem cells, such as accelerated cellular senescence or malignant transformation. The aim of the present work was to study the  $\gamma$ H2AX and pATM foci (markers of DNA DSBs), cellular senescence and proliferation capacity changes in the progeny (up to 12 post-irradiation passages) of cultured human mesenchymal stem cells (MSCs) exposed to X-ray radiation at low- (80 mGy) and intermediate- (1000 and 2000 mGy) doses. Immunocytochemical methods and the senescence-associated  $\beta$ -galactosidase (SA- $\beta$ -gal) staining were used for the analysis. We show that cells exposed to low dose did not differ from the control non-irradiated cells at any time-point for all measured end-points. This was in contrast to cells treated with intermediate X-ray doses that showed changes that can be interpreted as detrimental. Thus, we recorded increasingly higher  $\gamma$ H2AX and pATM foci rates, suppression of proliferation and promotion of cellular senescence as the passage number increased in the progeny intermediate dose irradiated cells. Taken together, our results show that low-dose X-ray radiation do not lead to the delayed radiation effects associated with the cellular senescence and genome instability in the progeny of irradiated MSCs.

**Acknowledgments:** The studies were partially supported by the Russian Foundation for Basic Research grant #16-04-01810-a.

## Thyroid dysfunction of a child who was born after a radiological examination of its mother by oil-soluble iodinated contrast medium (Lipiodol)

**Tadashi Hongyo, Yukimitsu Sawai, Hirofumi Kuchino, Itsuki Seki, Kentaro Yamamura, Shota Hirose, Io Ishibashi, Yasuyuki Ueda**

Osaka University Graduate School of Medicine, Suita, Japan

**Introduction.** Lipiodol is widely used as a contrast agent, such as hysterosalpingography(HSG), cardiac catheterization, CT imaging, hepatic artery chemoembolization therapy (TACE). Although detailed studies have been conducted on renal disorder caused by iodine contrast agent, little attention has been paid to the influence of that on the thyroid gland.

Lipiodol, an oil-based iodinated contrast agent, is known to remain in the body for a long time after examination and treatment, and for example, in pregnancy after HSG, there are occasional reports suggesting that Lipiodol induces thyroid dysfunction not only to the mother but also the fetus and the newborn. However, since there are no known mouse models of Lipiodol-induced thyroid dysfunction, we examined the influence of Lipiodol on child's thyroid function in mice by administering Lipiodol to its mother.

**Materials and methods.** 12 week-old ICR female mice were intraperitoneally administered with Lipiodol once before mating or during pregnancy or after delivery, and the thyroid uptake rate of I-131 ( 74 kBq / mouse ) in their newborn mice was examined 24 hours after oral administration of I-131. The dose of Lipiodol used was either equivalent to that used in humans (0.2 $\mu$ L/g BW, iodine amount=96  $\mu$ g/g BW) or its 1/2 or 1/10 amount. Lipiodol was diluted with corn oil, and all were set to a total of 10  $\mu$ L/g BW. The same volume of corn oil was used as a control. When the offspring mice reached 4 weeks of age, serum TSH and FT<sub>4</sub> were measured by ELISA method. The number of mice in each experiment was 6 or more.

**Results and discussion.** When 0.2  $\mu$ L/g BW Lipiodol or its 1/2, 1/10 amount were administered intraperitoneally before pregnancy (5 days before gestation), thyroid uptake rate of I-131 in 5 day old infants was decreased to 24.4%, 24.0% and 58.7% compared to control, respectively.

When 0.2  $\mu$ L/g BW of Lipiodol was administered to mice during pregnancy (10th gestation) or immediately after birth, thyroid uptake rate of I-131 in 5 day old infant was decreased to 5.8% and 2.4% compared to control, respectively. There was no change in TSH level in infant mice at 4 weeks of age, but a significant decrease in FT<sub>4</sub> was observed.

This result suggests that the amount of Lipiodol used in examinations such as HSG should be kept as little as possible, and that thyroid function in children born after examinations using Lipiodol needs to be carefully observed.

## Modeling of chromosome aberrations induced in cells exposed to mixed beams of ionizing radiation

**Adrianna Tartas<sup>1</sup>, Maciej Gałeczki<sup>1</sup>, Mateusz Filipek<sup>1,2</sup>,  
Werner Friedland<sup>3</sup>, Andrzej Wójcik<sup>4</sup>, Beata Brzozowska-Wardecka<sup>1</sup>**

<sup>1</sup> Biomedical Physics Division, Faculty of Physics, University of Warsaw, Poland, Warsaw, Poland

<sup>2</sup> Heavy Ion Laboratory at the University of Warsaw, Warsaw, Poland

<sup>3</sup> Institute of Radiation Protection, Helmholtz Zentrum Munich, Germany, Neuherberg, Germany

<sup>4</sup> Department of Molecular Biosciences, The Wenner-Gren Institute, Stockholm University, Stockholm, Sweden

In the past, radiobiological experiments were typically aimed at studying the biological effectiveness of a particular radiation quality, such as alpha particles, in relation to low-LET photon radiation. However, since real radiation exposure scenarios frequently include major contributions of both alpha particles and photons, it is important to determine whether the response to this mixed beam exposure is greater than a simple sum of photon and alpha particle effects; moreover, this may help explain the possible mechanisms behind the observed reactions. Recent radiobiological experiments have studied DNA damage and repair in cells exposed to such mixed beams in order to find out whether the cellular response is different than that determined based on the assumption of additivity, but the results are not conclusive [1, 2].

In this work, the biological effects of X-rays, alpha particles and mixed beams were examined Monte Carlo simulations with the PARTRAC tools [3]. PARTRAC has been developed at the Institute of Radiation Protection in Neuherberg, Germany. It contains a set of related modules to perform calculations of ionizing particles track structures, overlaid with models of nuclear DNA, to assess the DNA damage and subsequent damage response processes in cells. Scoring of DNA end rejoining from different chromosomes provides simulated data on chromosomal aberrations and their types, such as dicentric chromosomes and translocations [4].

Calculations have been performed for X-rays, alpha radiation and for mixed beams that irradiated human peripheral blood lymphocytes. The results obtained from the PARTRAC code will be presented at the meeting in comparison to the experimental data from the experiment carried out at the Stockholm University described in [5].

### References

- [1] E. Staaf, M. Deperas-Kaminska, K. Brehwens, S. Haghdoost, J. Czub, A. Wojcik, Complex aberrations in lymphocytes exposed to mixed beams of Am-241 particles and X-rays, *Mutation Research* 756 (2013), 95-100.
- [2] E. Staaf, K. Brehwens, S. Haghdoost, J. Czub, A. Wójcik, Gamma-H2AX foci in cells exposed to a mixed beam of X-rays and particles, *Genome Integrity* 3 (2012) 8.
- [3] W. Friedland, M. Dingfelder, P. Kunderát, P. Jacob, Track structures, DNA targets and radiation effects in the biophysical Monte Carlo simulation code PARTRAC. *Mutation Research* 711 (2011) 28-40.
- [4] W. Friedland, P. Kunderát Track structure based modelling of chromosome aberrations after photon and alpha-particle irradiation. *Mutation Research* 756 (2013) 213-223.
- [5] E. Staaf, K. Brehwens, S. Haghdoost, K. Pachnerova-Brabcova, J. Czub, J. Braziewicz, S. Nievaart, A. Wójcik, Characterisation of a setup for mixed beam exposures of cells to Am-241 alpha particles and X-rays, *Radiation Protection Dosimetry* 151(3) (2012) 570-579.

## RBE of accelerated carbon ions and of neutron-produced heavy-charged particles in Chinese hamster cells

**Ekaterina Koryakina, Vladimir Potetnya, Marina Troshina,  
Maria Efimova, Raisa Baykuzina, Anatoliy Lychagin,  
Alexey Solovev, Sergey Koryakin, Stepan Ulyanenko**

A. Tsyb Medical Radiological Research Center, Obninsk, Russia

The accurate evaluation of heavy charged particles RBE is important for estimating cancer risks and the “biological” doses in the ion therapy. In the latter case it’s necessary to study the mechanisms of ions RBE variations in the spread Bragg peak, and, in particular, in its distal edge, where the maximal RBEs (because of particles with maximum LETs and short ranges, 2–5  $\mu\text{m}$ ) are observed.

The biological efficiency of accelerated ions  $^{12}\text{C}$  and slow heavy charged particles (SHCP) C, N, O was investigated on two Chinese hamster cell lines (CHO-K1, V-79) using cell surviving test.

Cell monolayers (CHO-K1) or suspensions (V-79) in the late stationary growth phase were irradiated with  $^{12}\text{C}$  ion beam (initial energy 454 MeV/u, U-70 synchrotron, IHEP, Protvino) in a water phantom either in the plateau region of the Bragg curve (dose-average  $\text{LET}_d$  11 keV/ $\mu\text{m}$ , doses of 1.0–8.5 Gy) or in the unmodified Bragg peak (120–140 keV/ $\mu\text{m}$ , 0.5–4.5 Gy). For inhibiting the repair processes cells were kept on ice between irradiation and replating. The effects of SHCP was studied by irradiating with 14.5 MeV neutrons cell monolayers through a glass Carrel flask bottom (1 mm) under the conditions of the secondary charged-particle equilibrium (CPE) absence. Under those conditions doses were 1–5 Gy, partial doses of protons,  $\alpha$ -particles, and C, N, O heavy recoils were 15 %, 30 %, 55 %, respectively,  $\text{LET}_d$  of SHCP was 460 keV/ $\mu\text{m}$ .

The results obtained showed that the survival curves for carbon beam were linear-quadratic in the plateau region of the Bragg curve and linear in the unmodified Bragg peak. There are no differences between monolayer and suspension results. RBE values of carbon beam in the plateau were 1.3–1.4, in the Bragg peak – 4.2. Dose curves of neutrons under the absence of CPE conditions were linear for both cell lines too, RBEs were 2.8.

To interpret the obtained efficiencies the complex spectra of all types of radiations need to be taken into account. 80 % of the dose in the Bragg peak is deposited by the primary ions  $^{12}\text{C}$  (LET of more than half of the ions was 60–200 keV/ $\mu\text{m}$ ), the others 20 % – by high energy (2–4 GeV) secondaries H, He, Li, Be, B with low LETs. So, the particles with LETs corresponding to the RBE maximum delivered quite half of the dose in the Bragg peak. As for SHCP experiments, approximately half of the dose is also formed by SHCP with  $\text{LET}_d \sim 460$  keV/ $\mu\text{m}$ .

Based on the dose composition of the radiation and on the assumption of the independent biological action of particles in the absence of CPE, the RBE value of the C, N, O heavy recoils was estimated to be 3.0–3.1. The higher RBE of  $^{12}\text{C}$  ions compared to RBE of the heavy recoils in the same LET range (50–1000 keV/ $\mu\text{m}$ ) may be explained by different  $\text{LET}_d$ : 120–140 keV/ $\mu\text{m}$  (maximal RBE) versus 460 keV/ $\mu\text{m}$  (RBE diminishing). It should be noted that the problem of possible synergism of the carbon beam radiation components in the Bragg peak remains unexplored and could also lead to differences in RBEs.

## **Dosimetric and radiobiological aspects of cell monolayer irradiation with 14 MeV neutrons in the presence and absence of proton equilibrium**

**Vladimir Potetnya, Ekaterina Koryakina, Marina Troshina,  
Nina Boldueva, Sergey Koryakin, Stepan Ulyanenko**

A. Tsyb Medical Radiological Research Center, Obninsk, Russia

Cell irradiation with 14 MeV neutrons in the absence of proton equilibrium allows to investigate radiobiological effects of light ions C, N, O with energies at the Bragg peak and behind it. The situation is close to that in the distal region of carbon ion SOBPs. We studied cell survival of two Chinese hamster cell lines, CHO-K1, V-79, and two bacterial strains, E. Coli Bs-1 and E. Coli WP2, irradiated with 14 MeV neutrons in the presence and absence of proton equilibrium. Mammalian cell monolayers in Carrel flasks were irradiated with neutrons either through a layer of Hank's solution under conditions of proton equilibrium (PE) or through a flask glass bottom (absence of PE). Bacterial cell monolayers were irradiated with neutrons either through polystyrene bottom of Petri dishes plus agar layer (PE) or through a 10  $\mu\text{m}$  thick mylar window plus 5 mm air gap (PE absence). Doses, particles energy and LET spectra with and without PE were estimated with the GEANT4.

Under conditions of proton equilibrium partial doses of protons,  $\alpha$ -particles, and C, N, O heavy recoils in the mammalian cells monolayer of 5  $\mu\text{m}$  thickness were 75, 13, and 11 %, respectively. In the absence of PE the doses changed to 18, 33, and 48 %, respectively. Protons and  $\alpha$ -particles originating in glass increased their partial doses in cells by "55 and "18 %. For a thinner bacterial cells monolayer of "1  $\mu\text{m}$  the partial dose of C, N, O heavy recoils in the absence of PE prevailed, being 79 % as compared to 5 % and 15 % of proton and  $\alpha$ -particles doses. Dose averaged LET values were about 100 keV/ $\mu\text{m}$  under PE conditions, 380 and 660 keV/ $\mu\text{m}$  in the absence of PE for 5 and 1  $\mu\text{m}$  thick monolayers, respectively.

RBE values of 14 MeV neutrons under conditions of PE were 2.1, and 1.7 for Chinese hamster cells CHO-K1 and V-79, respectively. For bacterial cells E. Coli Bs-1 and WP2 RBE were 0.6 and 1.2. In the absence of PE RBE values increased nearly twofold in the case of mammalian cells, 1.85 and 1.6 times, respectively. In the case of bacterial cells RBE in the absence of proton equilibrium increased slightly by only 5–10 %. It should be noted that RBE values for 14 MeV neutrons in the absence of PE are close to those of  $\alpha$ -particles with LET 115 keV/ $\mu\text{m}$ , which have the highest RBE as compared to all other particles. The results obtained point out on very high biological effectiveness of slow ions such as C and O with ranges < 5  $\mu\text{m}$  which cannot be predicted from the RBE-LET track-segment relationship. Slow ions track structure and elastic scattering mechanism may partly account for the revealed RBE difference of slow and fast particles.

## DNA damage in cancer cells exposed to beta radiation measured experimentally and modeled in Monte Carlo simulations

**Mateusz Filipek<sup>1,2</sup>, Beata Brzozowska-Wardecka<sup>1</sup>,  
Maciej Galecki<sup>1</sup>, Adrianna Tartas<sup>1</sup>**

<sup>1</sup> Biomedical Physics Division, Faculty of Physics, University of Warsaw, Warsaw, Poland

<sup>2</sup> Heavy Ion Laboratory, University of Warsaw, Warsaw, Poland

Radioembolization is one of the newest, non-invasive methods of cancer treatment. It consists in placing radioactive, spherical sources of microscopic size directly into the artery supplying the tumors with blood. The experimental setup is composed of two beta-radioactive sources Sr-90 placed in such a way to obtain a uniform distribution of the dose in the Petri dishes with prostate cells.

In this study the biophysical Monte Carlo code PARTRAC has been used [1]. It is a tool for calculating track structures of a variety of ionizing radiation acts and their biological effects. The number of single and double DNA strand breaks was simulated for prostate cancer cells exposed to beta radiation. At the same time the radiobiological experiments were conducted for human prostate cancer and normal cell line to perform the clonogenic cell survival assay. The ionisation and excitation pattern allowed to estimate the number of single strand breaks (SSB) and double strand breaks (DSB) affecting the survival of cancer cells. Additionally, the size of colonies has been investigated with a countPHICS software [2]. Further analysis of the colonies by measuring their size gives additional information, not incorporated in the clonogenic survival assay. The reduced colony size was observed for higher doses for both cell lines. Modeling the relationship between the DSB numbers and the energy deposits of the beta emitters within the cell and cell survival measurements provides primary results necessary to establish irradiation procedures in prostate radioembolization. The analysis may be exploited to create new cancer treatment method, which uses microspheric beta emitters.

### References

- [1] W. Friedland, M. Dingfelder, P. Kundrat, P. Jacob. Track structures, DNA targets and radiation effects in the biophysical Monte Carlo simulation code PARTRAC. *Mutat Res* 2011, 711:28–40.
- [2] B. Brzozowska, M. Galecki, A. Tartas, J. Ginter, U. Kaźmierczak, L. Lundholm. Freeware tool for analysing numbers and sizes of cell colonies. *Radiation and Environmental Biophysics*. <https://doi.org/10.1007/s00411-018-00772-z>

## **Pitfalls in isolation and characterisation of bone marrow extracellular vesicles mediating radiation-induced bystander effects in mice**

**Eszter Persa, Tünde Szatmári,  
Nikolett Sándor, Géza Sáfrány, Katalin Lumniczky**

National Public Health Center, Budapest, Hungary

Extracellular vesicles (EVs), membrane-bound packages containing amino acids, RNAs and lipids, are actively emitted by cells. Due to their role in cell-cell communication, they are taking part in several physiological conditions, additionally in stress response (e.g. ionizing radiation) and in cancerous state, as well. Isolation of EVs and characterization of them by flow cytometry are burdened with difficulties due to the size of the vesicles (50-500 nm) and their weak light scatter properties. However, knowing the phenotypic markers (expressed proteins) on the surface of EVs could give information about the cells they come from and furthermore about the aim of the emission.

The aim of our study was to work out a method for isolation of bone marrow EVs in appropriate amount and purity without cultivation and characterize them by flow cytometry.

0Gy and 3Gy irradiated CBA mice were used and EVs were isolated from bone marrow of both femurs and tibias. EV preparation was done by ultracentrifugation (UC) or Exoquick-TC solution (EQ) and further purification by G-25 sephadex columns. The amount and purity of isolated samples were measured by BCA assay and Western Blot analysis, respectively. EVs were labeled using specific antibodies and analysed by Cytotoflex cytometer.

According to the amount of isolated EVs and the purity of the samples, EQ method seemed to be better than UC, although the remaining PEG (from the EQ solution) could give a little bit more background during the cytometry analysis. Irradiation did not change significantly the amount and of EVs or the purity of EV samples. EVs isolated from irradiated animals looked to have more mature phenotype compared to control. A possible explanation would be the high radiosensitivity of bone marrow stem cells. Our future plans include examining which cells could take up these vesicles.

## Some aspects of nuclear-mediated pathway of radiation-induced apoptosis

**Tetiana Andriichuk<sup>1</sup>, Natalia Raksha<sup>1</sup>, Sergii Vakal<sup>2</sup>, Ludmyla Ostapchenko<sup>1</sup>**

<sup>1</sup> ESC 'Institute of Biology and Medicine', Taras Shevchenko National University of Kyiv, Kyiv, Ukraine

<sup>2</sup> Lab of Molecular Neuropharmacology, The Affiliated Eye Hospital of WMU, Wenzhou Medical University, Wenzhou, China

**Introduction.** The action of ionizing radiation, both directly due to damage of the nucleoprotein complexes, and an imbalance between the expression of a number of anti- and proapoptotic genes, leads to the activation of the nuclear-mediated pathway of programmed cellular death, apoptosis. DNA damage initiates coordinated response with the involvement of sensory, transducing and effector proteins that detect DNA defects and (upon low activity of reparation systems) initiation of apoptosis through activation of p53-dependent pathways.

**Goal.** To assess the level of DNA breaks and p53 protein in rat spleen lymphocytes after exposure to 1.0 Gy of X-ray radiation.

**Methods.** The experiment was carried out with white adult male rats with average weight of 150-170 g. IR was generated by X-ray apparatus RUM-17 (total dose of 1.0 Gy). Animals were sacrificed 30 min and 3 hr after the exposure, and spleen lymphocytes were isolated in Ficoll-Paque density gradient. Single- and double-strand DNA breaks were determined according to the method (Dmitrenko N., Andriichuk T.) The level of p53 was estimated using the "p53 pan ELISA" kit (Roshe Applied Science, Germany). Statistical processing was performed with IBM SPSS 22.0; data expressed as  $M \pm SD$ .

**Results.** The effect of ionizing radiation significantly affects the nuclear apparatus of rat spleen lymphocytes, which we have identified by accumulation of DNA breaks. Thus, irradiation of rats in a dose of 1.0 Gy causes an increase of single-strand DNA breaks in 3.2 and 2.2-fold, respectively, 30 min and 3 hr after radiation exposure. As for double-strand breaks in the nuclear DNA molecule of spleen lymphocytes, our study revealed 1.2 and 2.9-fold increase after irradiation (30 min and 3 hr respectively). DNA molecules damages result in a coordinated activation of the transduction signal pathways that are involved in the implementation of apoptotic cell death following the action of X-ray radiation. It should be noted that the increase of unrepairable single- and double-strand DNA breaks leads to the accumulation of the p53 protein, which plays a pivotal role in the induction of apoptosis. Our experiments have demonstrated certain increase in p53 protein level after ionizing radiation treatment.

**Conclusions.** These data are evidence of a hypothesis that in lymphoid cells the stabilization of p53 protein after X-ray exposure leads to the activation of apoptotic death, unlike in others, where the processes of cell cycle arrest and DNA repair are prevalent.

## Effect of radiation and temperature on the microbial community in the cooling water of a nuclear reactor

**Valérie Van Eesbeeck<sup>1</sup>, Ruben Props<sup>2</sup>, Mohamed Mysara<sup>1</sup>,  
Rob Van Houdt<sup>1</sup>, Pauline Petit<sup>3</sup>, Corinne Rivasseau<sup>3</sup>,  
Jean Armengaud<sup>3</sup>, Pieter Monsieurs<sup>4</sup>, Jacques Mahillon<sup>5</sup>, Natalie Leys<sup>1</sup>**

<sup>1</sup> SCK-CEN, Mol, Belgium

<sup>2</sup> Universiteit Gent, Gent, Belgium

<sup>3</sup> CEA, Grenoble, France

<sup>4</sup> VITO, Mol, Belgium

<sup>5</sup> Université Catholique de Louvain, Louvain-la-Neuve, Belgium

The BR2 nuclear research reactor consists of different watery environments, one of which is an open basin surrounding the reactor vessel. The water in this basin has a shielding effect on the radiation originating in the reactor core, where nuclear fission takes place during reactor operation. Remarkably, despite the ultra-high purity of the water due to constant filtering and deionization, combined with the high radioactivity exposure, microbial growth in these environments is not fully prevented. Indeed, several microbes appear to be able to survive and thrive in such conditions. Microorganisms identified in those environments thus provide a unique opportunity to acquire new insights into survival strategies and radiation-resistance mechanisms.

The objective of this work is to explore the bacterial communities present in the basin water of the BR2 nuclear research reactor. In order to accomplish this, the bacterial population was followed up over time during and outside reactor operation to monitor its dynamics in this unique, never-before-studied environment.

For the characterization and the follow-up of the bacterial communities, a 16S rRNA amplicon sequencing approach was adopted. Results from two long-term follow-up experiments highlighted a clear shift in the bacterial community profile during and outside reactor operation. Interestingly, the profiles for both experiments appeared to be quite similar, notwithstanding the fact that the two sampling campaigns were separated by a one-year interval. This indicates that the system is very robust.

During reactor operation, the bacterial community is mostly dominated by two OTUs that were taxonomically assigned to an unclassified Gammaproteobacterium and *Pelomonas*, respectively. During this phase, either one or the other becomes prevalent, or both are equally abundant. When the reactor goes into shutdown, the community clearly shifts to become dominated by an OTU assigned to *Methylobacterium*. This interesting finding can be explained by the change in physico-chemical parameters like flow rate, temperature and most importantly radiation that occurs when the reactor transitions from one phase to the other. In addition, exposure to radiation also causes the bacterial population to steeply decrease in number, before it can slowly recover during reactor shutdown.

To conclude, we have been able to shed some light on this unique system for the first time and thoroughly explored its dynamics. In a next step, we will further investigate the radiation resistance potential of some interesting isolated strains.

## Higher brain functions of the offsprings of irradiated animals

V. V. Panfilova, O. I. Kolganova, O. F. Chibisova

A. Tsyb Medical Radiological Research Center – branch of the National Medical Research Radiological Center of the Ministry of Health of the Russian Federation, Obninsk, Russia

The aim of the work was the experimental study of psychophysiological development of the offspring of the first and second generations of male rats, which were exposed to gamma radiation in non-sterilizing doses at different stages of spermatogenesis.

Male Wistar rats ( $F_0$ ) were irradiated at the gamma-ray unit ( $^{60}\text{Co}$ ) at a dose rate of 20.0 G/h, at doses of 0.2, 0.5, 1.0 and 1.5 Gy. To obtain the offspring of the first generation, they were mated with intact females at different intervals after irradiation (so that the germ cells irradiated at different stages of spermatogenesis participated in fertilization). Accordingly, the offspring of the first generation was divided into 4 experimental groups. The groups for further testing at the age of one month selected apparently healthy young and raised them to three months of age. The control group consisted of intact males and females who were in identical conditions with experimental rats. To obtain the second generation ( $F_2$ ) from irradiated males ( $F_0$ ), offspring from the first generation ( $F_1$ ) were mated with each other or with intact animals. Testing was conducted separately for groups of females and males.

Cognitive (memorial) brain function was assessed by the ability to generate and reproduction of the conditioned reflex of avoidance (URI). The experiments used a standard method of training rats in Shuttle-box. A special computer program developed in our laboratory was used to process the results.

It is established that acute gamma irradiation in non-sterilizing doses (0.2, 0.5, 1.0, 1.5 Gy) has a negative impact on the psychophysiological development of the offspring of the first generation of irradiated male rats, which is expressed in violation of the production, consolidation and subsequent reproduction of the conditioned reflex of avoidance.

Moreover, for the manifestation of hereditary effects of radiation effects on males, along with the absorbed dose of radiation, the stage of spermatogenesis at the time of radiation exposure is of fundamental importance.

According to our data, the dose of acute single gamma irradiation of 0.2 Gy is close to the minimum effective effect on the higher functions of the Central nervous system in the descendants of irradiated animals.

Signs of negative effects of irradiation on the second generation offspring from irradiated males, less pronounced than in the offspring of the first generation, were found.

The data obtained suggest that there is a summation of the negative effects of radiation in the second generation, if both parents are descendants of irradiated males.

## **Comparative study of DNA double-strand breaks formation in human mesenchymal stem cells exposed to organically bound tritium vs tritiated water, and X-rays**

**Natalia Vorobyeva, Oleg Kochetkov, Margarita Pustovalova,  
Anna Grekhova, Taisia Blokhina, Elizaveta Yashkina, Andrey Osipov,  
Dmitry Kabanov, Pavel Surin, Valeryi Barchukov, Andreyan Osipov**

State Research Center - Burnasyan Federal Medical Biophysical Center of Federal Medical Biological Agency,  
Moscow, Russia

Production of nuclear energy and the development of thermonuclear technologies has raised concern about the potential consequences of tritium compound exposure for human health. Tritium is hydrogen isotope and can be a part of water molecules (tritiated water, HTO) or organic molecules (organically bound tritium, OBT). HTO behaves as ordinary water in living cells and body. In contrast to HTO, OBT is non-uniform distributed in cells and tissues, which can lead to high microlocal doses and could be a source of serious damages of biological molecules including DNA. It is commonly assumed that the DNA double-strand breaks (DSBs) are the most crucial fate for the irradiated cells. Thus, inaccurately repaired DSBs may lead to cell death, senescence or cancer.

The aim of this work was to compare the DSB yields in cultured human mesenchymal stem cells exposed to OBT vs HTO or X-rays.

Potential transmission of the DNA lesions and mutations from the stem cells to the differentiated progeny requires thorough understanding of mechanisms of DNA damage and repair responses in the stem cells. The immunocytochemical analysis of the DSB repair protein ( $\gamma$ H2AX, 53BP1, pATM) foci was performed to estimate the DSBs yield. Cells were incubated with 50-800 MBq/L tritium compounds during 24-72 h.

It was shown the DSB yields after exposure to  $^3\text{H}$ -thymidine was 6.3-14.1 folds higher than after exposure to HTO. In a comparative study of the effect of HTO and X-ray radiation, it was shown that in the dose range of 3.78-60.26 mGy the relative biological efficiency of HTO was 1.5-2.0 folds higher compared to X-ray radiation. In summary, our results suggest that OBT produced a significant higher DSB yield than HTO equivalent do, while HTO gives a larger response than X-rays.

## Exposure of yeast cells with different repair efficiency to densely ionizing radiation

**Dariya Babina, Vladislav Petin, Victoria Panfilova**

A. Tsyb Medical Radiological Research Center – branch of the National Medical Research Radiological Center of the Ministry of Health of the Russian Federation, Obninsk, Russia

The understanding of RBE of densely ionizing radiation is very important and actual problem for several reasons. First, it is well known that half of the natural radiation dose caused by the action of  $\alpha$ -particles of radon and its decay daughter products. Second, understanding of RBE of densely ionizing radiation is very important in relation with analyzing the effectiveness of antitumor radiation therapy of high LET radiation - neutrons, protons and other heavy charged particles. Third, the assessment of the dangers of cosmic radiation with high LET radiation during long flights in the interplanetary space is also important.

The objective of this study is to obtain new experimental evidence for the role of cell recovery after radiation damage in the manifestation of the RBE densely ionizing radiation.

The work was performed with homozygous haploid and diploid yeast cells *Saccharomyces cerevisiae*: wild-type strains S288C (haploid, RAD), XS800 (diploid, RAD/RAD) and radiosensitive mutants XS774-4d (haploid, *rad51*) and XS806 (diploid, *rad51/rad51*), different from the parental strains only one mutation in a gene RAD51. As sources of radiation we used sparsely (gamma rays of  $^{60}\text{Co}$ , 20 Gy/min) and densely ( $\alpha$ -particles of  $^{239}\text{Pu}$ , 25 Gy/min) ionizing radiation. The dependence of RBE on the stage of cell growth, their ploidy and the ability to repair radiation damage to DNA was derived.

Based on the data obtained, it is concluded that the results obtained are consistent with the point of view that the RBE of densely ionizing radiation is determined not only by the probability of the primary damage production at the physicochemical stage of radiation interaction with cellular structures, but also by the cell ability to recover from sublethal and potentially lethal damage at biochemical stage of their fixation.

## Genetic diversity in *Plantago major* L. populations growing under conditions of radioactive and chemical contamination

Nadezhda Shimalina, Makar Modorov, Elena Antonova, Vera Pozolotina

Institute of Plant and Animal Ecology, Ural Branch of the Russian Academy of Sciences, Ekaterinburg, Russia

In the Southern Urals there are territories with different types of anthropogenic contamination. East Ural Radioactive Trace (EURT) was formed in 1957 after the accident at the Mayak Production Association. Roughly 74 PBq of radioactive substances were released into the environment. The zone of influence of the Karabash Copper Smelter (KCS) is located about 45 km from EURT. The main pollutants were sulfur dioxide and heavy metals.

The purpose of the research is comparison of the genetic diversity in *Plantago major* L. populations growing under conditions of radioactive or chemical contamination and on background territory.

Variability of 9 microsatellite loci was analyzed in 3 populations from EURT, and 3 from KCS zone, and 2 from background area. We tested two hypotheses: 1) genetic diversity in the *P. major* populations in the EURT zone is increased, since ionizing radiation is a mutagenic factor; 2) genetic diversity in *P. major* populations in the KCS zone is reduced due to the selection of metal-resistant organisms.

High level of inbreeding was revealed in all populations as a result of high rate of self-pollination of *P. major*. Despite the high level of inbreeding, the genetic diversity within the *P. major* populations is high enough. According to values of the mean and effective number of alleles per locus and the number of private alleles, genetic diversity in populations from the zones of chemical and radioactive contamination was lower than in background populations. Mantel test for isolation by distance between KCS and background populations showed that the roads are an important factor in the migration of plantain seeds.

The first tested hypothesis was not confirmed: the *P. major* genetic diversity in the EURT zone was lower than in the background populations, which possibly results from the reduced migration of seeds (genes) in EURT populations due to limited access of people to this territory. Probably, the frequency of radiation-induced mutations in plants with existing doses is not sufficient to compensate for the loss of genetic diversity resulting from isolation. The second tested hypothesis was confirmed: genetic diversity of *P. major* was decreased in the KCS zone, especially at the most polluted site. Despite the flow of seeds (genes) into the population is not limited, not all migrants are able to survive in conditions of high soil contamination. Thus, the reduction of genetic diversity in the *P. major* populations in zones of radioactive and chemical contamination (compared to background plots) occurs due to various reasons.

**Acknowledgments:** This study was performed within the frameworks of state contract with the Institute of Plant and Animal Ecology, Ural Branch of RAS.



**Radiochemistry**  
**31**

## **Ligands for extraction of actinides from alkaline high-level waste and from acidic used nuclear fuel. Theoretical and experimental studies of the effect of soft-donors in binding and extraction selectivity**

**Ingrid Lehman-Andino, Evgen V. Govor, Alexander N. Morozov, Alexander M. Mebel, Christopher J. Dares, Raphael G. Raptis, Konstantinos Kavallieratos**

Florida International University, Miami, FL, United States

The presence of minor actinides in used nuclear fuel is responsible for much of its radiotoxicity and heat generation. Actinide(An)/Lanthanide(Ln) separation processes via selective complexation and solvent extraction by designed soft S- and N-donor ligands can take advantage of the slight differences in relative hardness of An(III) vs. Ln(III), for achieving selective separations. Furthermore, the presence of actinides in the alkaline high-level waste at the Savannah River Site (SRS) has sparked interest in synthetic ligands that can be used together with calixarene ligands for combined coordination and extraction of Cesium, Strontium, and Actinides.

As part of our efforts in designing selective and strong extractants for Ln/An(III) coordination, soft-donor ligands containing sulfonamide, thioamide, pyrazole and/or pyridine sites that are derived from *o*-phenylenediamine or from dipicolinic acid, were synthesized and studied for complexation of f-elements by structural and spectroscopic methods. These frameworks allowed for comparative studies between ligands that contain the C=O vs. the C=S group: For example, while the O-donor dipicolinamide was shown to bind Ln(III) by UV-Vis and NMR in acetonitrile, the S-donor dithiopicolinamide ligand did not show any binding towards Ln(III). Yet the same dithiopicolinamide was shown to extract Am(III) vs. Eu(III) selectively from acidic solutions. Sulfonamide, hydroxysulfonamide, and pyrazole ligands that contain varying substitution patterns showed remarkable differences in Ln(III) complexation and fluorescence sensing capabilities, which show some variation along the Ln(III) series. Theoretical DFT calculations have provided remarkable insight in extraction selectivities, and have offered some explanation on the difference in spectroscopic properties observed. The role of ion-pairing and solvation in explaining these differences will also be discussed.

## Leaching behavior of Cs-137, Sr-90, Co-60 and Am-241 isotopes from native and radiation-degraded sulfur polymer concrete (SPC) composites

**Piotr Szajerski, Agnieszka Bogobowicz, Andrzej Gasiorowski**

Institute of Applied Radiation Chemistry, Lodz University of Technology, Lodz, Poland

Nuclear energy sector generates radioactive waste in various chemical and physical forms. Next to the most problematic high level radioactive waste (HLW), equal attention is paid to the separation and immobilization of low (LLW) and intermediate level waste (ILW). These wastes streams are generated as a result of the pellet-cladding interactions, thermal and radiation degradation and construction materials corrosion processes occurring in reactor core and followed by releasing radioactive contaminants into primary cooling circuit. Separation of radioactive isotopes from cooling media is a main goal of the continuous water purification processes. Resulting concentrated radioactive solutions, sludges and solid wastes must be subsequently immobilized in a safe and long-term stable waste forms.

Selection of the proper waste matrix material depends mainly on the chemical properties, physical form and activity of the radioactive waste to be disposed. In the case of low and intermediate level waste, very often asphalts, bitumens, polymeric resins and cementitious composites are used. Technologies used for radioactive waste immobilization are being continuously improved. One of such new group of materials being developed are mineral-polymeric materials based on sulfur polymers – sulfur polymer concrete (SPC). Sulfur polymer composites seem to be very attractive materials due to their properties: good mechanical behavior, very good properties of radionuclides retention and very low diffusivity within the SPC matrix.

In this work, the leaching behavior of SPC composites based on mineral fillers will be presented regarding immobilized Cs-137, Sr-90, Co-60 and Am-241 radionuclides – radioactive contaminants generated during nuclear power reactors operation. As a mineral fillers phosphogypsum, fly ash and lignite slag were used as the main radionuclides' immobilization phases stabilized by various continuous phase components – sulfur polymers. Experimental procedure was based on hot mixing (ca. 140°C) and pressing of sulfur polymer and mineral fillers with radioactive tracers. For the verification of immobilization efficiency of the prepared composites, and static IAEA long-term leaching test for solidified radioactive waste forms (ISO 6961:1982) was applied. Experimental results suggest good and satisfactory leaching behavior of fly ash- and slag-based SPC composites and much worse in the case of a phosphogypsum-based matrix. Minor effect is observed in the case of the application of a different sulfur polymer phase component. Next to the investigation of native SPC samples, radionuclides released from samples degraded releasing gamma and beta radiation in dose range 0-2.5 MGy. Results indicate comparable or slightly lower immobilization efficiency in radiation-modified SPC vs native samples.

**Acknowledgments:** This research project was supported by the Polish National Center for Research and Development (NCBR) under the Grant No.: GEKON1/O5/213122/26/2015.

## Sorption of U(VI) onto Mg-Al layered double hydroxides and oxides from aqueous solutions

**Sergey Kulyukhin, Igor Rumer, Elena Krasavina, Andrey Gordeev**

Frumkin Institute of Physical Chemistry and Electrochemistry, Russian Academy of Sciences, Moscow, Russia

The development of nuclear power engineering again becomes topical. At the same time, the human activity in this field results in certain release of radioactive substances into the environment. Therefore, the development of new materials for localization of radionuclides from various media, including liquid media, is an urgent problem. One of radionuclides whose recovery from aqueous solutions involves certain problems is U(VI). The complexing power of U(VI) in aqueous solution gives rise to certain problems with its recovery. To prevent migration of radionuclides, including U(VI), in the environment from the sites of their compact disposal, it is suggested to make antimigration barriers. Various minerals (bentonite, clinoptilolite, montmorillonite) are considered as materials for such barriers. In addition, various layered double hydroxides (LDH), e.g., hydrotalcite, green rust, etc., can be considered as materials for antimigration barriers.

The sorption of U(VI) from aqueous solutions onto LDH-Mg-Al intercalated with citrate, ethylenediaminetetraacetate, hexamethylenediaminetetraacetate, diethylenetriaminepentaacetate, and hexacyanoferrate(II) ions was studied. At the same time, since published data on the effect of different cations and strong complexing anions ( $\text{H}_2\text{EDTA}^{2-}$ ,  $\text{C}_2\text{O}_4^{2-}$ ) on the sorption of U(VI) on LDHs are lacking, we examined how different cations and anions present in aqueous solutions affect the sorption of U(VI) on various LDHs of Mg and Al. The above problems became the subject of this study.

Sorption of U(VI) from aqueous solutions of various compositions on layered double hydroxides (LDHs) of Mg and Al, and also on layered double oxides (LDOs) of Mg and Al was studied. Experiments on sorption of  $\text{UO}_2^{2+}$  carbonate complexes from aqueous solution on LDO-Mg-Al showed that  $[\text{UO}_2(\text{CO}_3)_3]^{4-}$  ions are weakly captured by LDH-Mg-Al formed by contact of LDO-Mg-Al with water. It is shown that U(VI) is efficiently sorbed from aqueous  $10^{-3}$  mol  $\text{l}^{-1}$   $\text{UO}_2(\text{NO}_3)_2$  solutions on LDH-Mg-Al with  $\text{CO}_3^{2-}$  and  $\text{OH}^-$  ions in the interlayer space. After 15-min contact of the solid and liquid phases,  $K_d$  of U(VI) exceeds  $5 \cdot 10^3$  ml  $\text{g}^{-1}$ . The use of microwave radiation allows not only acceleration of the synthesis of both LDH and LDO, but also preparation of compounds with high kinetic characteristics of the U(VI) sorption. The degree of U(VI) sorption from  $10^{-2}$  mol  $\text{l}^{-1}$  aqueous U(VI) solutions at a sorption time of 4 h and  $V/m = 50$  ml  $\text{g}^{-1}$  exceeds 99.0%.

## Adsorption of heavy metal ions onto titanium silicate

**Svyatoslav Vuchkan<sup>1</sup>, Ihor Syika<sup>1</sup>, Yuriy Kylivnyk<sup>2</sup>**

<sup>1</sup> Uzhgorod National University, Uzhgorod, Ukraine

<sup>2</sup> Institute for Sorption and Problems of Endoecology, Kyiv, Ukraine

This work is devoted to adsorption of HM ions onto novelty synthesized adsorbent titanium silicate Ti/Si. Titanium silicate was synthesized in the Institute for Sorption and Problems of Endoecology NAS of Ukraine. Pore radius and volume, surface area and other surface characteristics are investigated at the same institute.

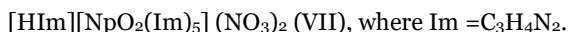
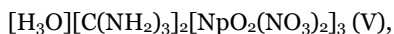
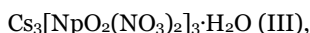
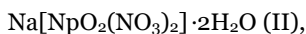
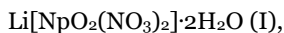
Adsorption ability of Ti/Si toward Zn<sup>2+</sup> and Sr<sup>2+</sup> ions is investigated at the Uzhgorod National University. Adsorption tests were carried out in batch studies and neutral pH. Residual concentrations of HM were investigated using complexometric titration. The preliminary studies show that Ti/Si adsorbed Zn<sup>2+</sup> ions better than Sr<sup>2+</sup> ions. The rate of the removal of Zn<sup>2+</sup> ions from water solutions is above 77.5% from 0.005M ZnSO<sub>4</sub> and 33.4% for Sr<sup>2+</sup> from 0.005M Sr(NO<sub>3</sub>)<sub>2</sub>. The investigations are still ongoing.

## Cation-cation interaction of $\text{NpO}_2^+$ ions in double neptunium(V) nitrate crystal complexes

Alexei A. Bessonov, Iraida A. Charushnikova, Alexander M. Fedosseev

A.N.Frumkina Institute of Physical Chemistry and Electrochemistry of the Russian Academy of Sciences (IPCE RAS), Moscow, Russia

Anionic nitrate crystal complexes of neptunoyl(V) have been synthesized and studied by single crystal X-ray diffraction. The cations of alkali metals from  $\text{Li}^+$  to  $\text{Cs}^+$ , as well as single charged organic cations guanidine  $\text{C}(\text{NH}_2)_3^+$ , tetramethylammonium  $\text{N}(\text{CH}_3)_4^+$  and imidazol  $\text{HIm}^+$  were used as outersphere cations. Crystal compounds of the following composition have been prepared in a form suitable for structural analysis:



It was found that cation-cation interaction (CCI) of  $\text{NpO}_2^+$  -ions occurs in the complexes with alkali metal cations (I – IV) and in the case of guanidine-cation (V). Square cationic nets are formed in the compounds (I) and (II), whereas trigonal-hexagonal ones are formed in (III – V). The size of the outer-sphere singly charged cation determines the type of cationic net. Large cavities in the structure with trigonal-hexagonal cationic nets are unsuitable for small alkali metal cations.

There is no CCI in the compound (VI) with the organic cation  $\text{N}(\text{CH}_3)_4^+$  in the outer sphere, due to the steric factor. The presence of large complex cations  $[\text{NpO}_2(\text{Im})_5]^+$  in the structure (VII) also prevents the formation of cationic bonds in the crystal.

A spectroscopic study of some of the synthesized crystalline compounds was also carried out in the course of the work. The influence of the structural features on the IR and electronic absorption spectra of crystals is noted.

## Application of nanocomposite sorbent SiEA-KNiFe in the process of water purification from radioactive isotopes

Dagmara Chmielewska-Śmietanko<sup>1</sup>, Marek Henczka<sup>2</sup>,  
Pavel Apel<sup>3</sup>, Oleg Orelovich<sup>3</sup>, Marina Gustova<sup>3</sup>

<sup>1</sup> Institute of Nuclear Chemistry and Technology, Warsaw, Poland

<sup>2</sup> Warsaw University of Technology, Faculty of Chemical and Process Engineering, Warsaw, Poland

<sup>3</sup> Flerov Laboratory of Nuclear Reactions, Joint Institute for Nuclear Research, Dubna, Russia

The total volume activity of water in the spent nuclear fuel basins is mainly determined by <sup>137</sup>Cs and reaches  $8.5 \cdot 10^8$  Bq l<sup>-1</sup>. The <sup>90</sup>Sr content did not exceed 20% of the <sup>137</sup>Cs content and other radionuclides (<sup>54</sup>Mn, <sup>60</sup>Co, <sup>85</sup>Kr etc.) are present in smaller amounts.

The <sup>137</sup>Cs is the product of uranium fission which is released to the cooling water from fuel cladding flaws. <sup>60</sup>Co is formed in the neutron activation reaction of corrosion products of reactor construction materials. All these radionuclides are very hazardous because of their long half-life time. Cesium easily bioaccumulates in human tissues, radiostrontium incorporates into bones and can lead to various bone diseases, including bone cancers. The <sup>60</sup>Co because of the high intensity emission of the  $\gamma$ -radiation is a serious threat for the personnel of the nuclear power plant. Therefore the removal of the radionuclides from nuclear wastewater is a matter of the great importance.

The objective of this study was the elaboration of the synthesis method of ion exchanger based on silica modified with metal hexacyanoferrate and ethanolamine. Obtained material is cesium-, strontium- and cobalt-selective adsorbent effective in purification of water solution as well as seawater from these radionuclides. Influence of different parameters (pH, temperature, initial concentration of radionuclide in the solution, contact time of phases) on adsorption kinetics was studied. Elaborated ion exchanger also exhibits good thermal, radiation and chemical stability. Examination of the morphology of the material with SEM method allowed to determine that aggregates of very small nanoparticles (~20 nm) create nanocomposite material of high porosity and high specific surface (162 m<sup>2</sup>/g). Very high distribution coefficient for radiocesium removal ( $K_d=10^4$ - $10^5$  ml/g) in water and seawater solutions together with beneficial physicochemical characteristics make these ion exchanger a promising technology for nuclear waste treatment.

**Acknowledgments:** This work was partially supported by the Polish Ministry of Science and Higher Education, project "New nanocomposite sorbent for different radionuclides removal". This research also was partially supported by the Cooperation Program between Polish Scientific Institutions and JINR (theme 04-5-1131-2017/2021, name of the program "New nanocomposite sorbent for different radionuclides removal").

## Adsorption of $Y^{3+}$ ions from aqueous solutions by neodymium-supported titanium dioxide

Hanna Vasylyeva<sup>1</sup>, Ivan Myroniuk<sup>2</sup>, Igor Mykytyn<sup>2</sup>

<sup>1</sup> Uzhgorod National University, Uzhgorod, Ukraine

<sup>2</sup> Vasyl Stefanyk Precarpathian National University, Ivano-Frankivsk, Ukraine

The relevance of the research of the adsorption of  $Y^{3+}$  ions is due to many factors: (a) yttrium isotopes together with other fission radionuclides can be in Nuclear Power Plant waste and spend nuclear fuel; (b) yttrium is a daughter radionuclide of strontium in a beta-decay chain. Together with Rare Earth elements, yttrium forms a group of YRE elements. Adsorption of YRE elements is investigated in several publications. For the adsorption of YRE elements, calcite, amorphous ferric hydroxide, amidoxime-hydroxamic acid polymer, cellulose –  $HO_2Sb_3$  nanocomposite, functionalized nano silica,  $TiO_2/La$  and some other adsorbents are offered. But the search for new adsorbents for the efficient removal of  $Y^{3+}$  ions from aqueous solutions is still ongoing.

This research is devoted to the adsorption of  $Y^{3+}$  ions from aqueous solutions by neodymium supported titanium dioxide ( $TiO_2/Nd$ ). Neodymium – the chemical element of atomic number 60, a silvery-white metal of the lanthanide series.

The dependence of the adsorption value of  $Y^{3+}$  ions onto  $TiO_2/Nd$  from time interaction, solution acidity and equilibrium concentration of yttrium ions was investigated. To experimental data four simple adsorption kinetic models were applied: Lagergren's PSF and PSS kinetic models, Elovich and intra-particle diffusion (Webber-Morris) kinetic model. The experimental isotherm of yttrium adsorption onto  $TiO_2/Nd$  was analysed using the Langmuir and Dubinin-Radushkevych equilibrium adsorption theory. Using D-R equation the Energy of adsorption was measured. The value of the adsorption Energy was found near 50 kJ/mol. The results were compared with the results of the adsorption of  $Y^{3+}$  ions onto samples of  $TiO_2$  without neodymium as well as with the previously described results of adsorption of  $Y^{3+}$  onto  $TiO_2/La$ .

It was shown that presence of neodymium in the  $TiO_2$  structure increases the adsorption of yttrium ions. We suppose that precipitation of  $Y(OH)_3$  or  $Y(OH)_2^-$  compounds on the surface of  $TiO_2/Nd$  is the dominant mechanism of adsorption.

## Plutonium and uranium concentration from sea water

Vladimir Kulemin<sup>1</sup>, Aleksandr Veleshko<sup>2</sup>, Sergey Kulyukhin<sup>1</sup>

<sup>1</sup> Frumkin' Institute of Physical Chemistry and Electrochemistry, Russian Academy of Science, Moscow, Russia

<sup>2</sup> Russian National Scientific Center, Moscow, Russia

The explosiveness of extraction technological processes in radiochemical industry is determined by the following main reasons: the interaction of an organic solution (extraction mixture) and degradation products with an oxidizing agent (nitric acid and metal nitrates); ignition of inflammable vapors and gases, including vapors of the diluent and the products of its radiation decomposition, radiolytic hydrogen, in mixtures with a gaseous oxidant. Ensuring the explosion safety of technological processes of radiochemical processing of nuclear fuel and high-level liquid waste requires systematic research to obtain information about the kinetics and mechanisms of interaction of nitric acid with the components of extraction systems, the qualitative and quantitative composition of the products of radiation destruction of technological media. Kinetic studies allow us to estimate the influence of various factors on the development of oxidative processes, as well as to determine the boundary conditions for the transition of oxidative processes to the thermal explosion mode. To solve the issue of ensuring the explosion safety of technological processes of radiochemical enterprises, it is necessary to have a number of characteristics of extraction systems, that allow to evaluate the process safety in the regulated conditions and in case of deviations from normal operation. Limit parameters are necessary to assess the probability of accidents and their consequences. The main characteristics to determine the possibility of a development of a thermal explosion, as applied to extraction systems, are: the maximum rate of heat and gas emission; the start temperature of the intense exothermic process; the total specific volume of the gaseous products of the oxidation process; thermal effect of interaction.

In 2018, on this subject were studied the extraction mixtures based on diamides of 2,6-pyridinedicarboxylic and 2,2'-bipyryl-6,6'-dicarboxylic acids in trifluoromethylphenylsulfone (FS-13) and meta-nitrobenzotrifluoride (F-3) diluents, considered for the fractionation of high level waste, in contact with 14 mol/L HNO<sub>3</sub>. The influence of pre-irradiation of mixtures with accelerated electrons on the kinetics of their oxidation is determined. Thermolysis of the mixtures was carried out in an autoclave at temperatures of 170°C and 200°C. Samples of the organic phase were irradiated at a linear electron accelerator UELV-10-10-C-70 (CCU PMR IPCE RAS) at a dose rate of 10 kGy/hour until reaching absorbed doses of 0.1, 0.5 and 1 MGy. It was shown, that by thermolysis of extraction mixtures, irradiated up to 1 MGy, conditions for the development of autocatalytic oxidation do not occur.

It was shown, that the main characteristics of fire hazard, which determine the mode of using a flammable liquid (excluding the ignition of the vapor-gas phase) for the FS-13 and F-3 diluents, are significantly higher than the maximum operating temperatures of conducting the technological operations of spent nuclear fuel regeneration. On the basis of the conducted research, we concluded that the use of heavy diluents in the regulated conditions of conducting the extraction process for the HLW reprocessing (UNEX process) will not lead to the ignition of air-vapor mixtures.

**Acknowledgments:** This study was supported by the Russian Science Foundation (project 16-19-00191).

## The products of radiolysis of extraction systems based on TODGA in 1-decanol with Isopar-M and TODGA in 1-nonanol with Isopar-M

**Elena Belova, Mikhail Kadyko, Yulia Nikitina, Ivan Skvortsov**

Russian Academy of Sciences, A.N. Frumkin Institute of Physical Chemistry and Electrochemistry RAS,  
Moscow, Russia

The utilization of high level waste (HLW) after the reprocessing of spent nuclear fuel is one of the main problems of the rapidly developing nuclear power industry. It is possible to reduce their amount by extracting actinides and long-lived products from SNF using extraction processes, in which not only the extractant that selectively extracts dangerous nuclides is important, but also a properly selected diluent that is resistant to high radiation doses. Due to the high acidity during the technological process of the reprocessing, in the extraction systems undesirable products can be formed that reduce the fire and explosion safety of the processes.

In the presented study, a qualitative and quantitative analysis of samples of the products of an extraction system was carried out with a promising extractant TODGA in Isopar-M diluent with the addition of 1-decanol or 1-nonanol, with saturation by 8 mol/L HNO<sub>3</sub> and without it. Irradiation was carried out up to 500 kGy.

For irradiated samples, unsaturated with nitric acid, the pattern of IR-spectra varies slightly with respect to similar non-irradiated samples. IR-spectroscopy was used to determine the formation of the main classes of products after radiation exposure: RCOOH, RCOR<sup>1</sup>, RCOOR. The presence of ketones, carboxylic acids and esters was proved by the coincidence of absorption bands by adding appropriate standards to irradiated samples, in a similar way the presence of organic nitrates (area 1646-1625 cm<sup>-1</sup>) and nitro compounds (1569-1539 cm<sup>-1</sup>) for samples, saturated with HNO<sub>3</sub>, was confirmed.

The results of chromatographic analyzes of irradiated samples did not reveal a significant increase in low-boiling products for both systems saturated with nitric acid and unsaturated samples. When ionizing radiation is applied to the extraction system based on 1-decanol, Isopar-M undergoes more destruction, and in the system with 1-nonanol disintegrates the alcohol itself. 1-Decanol is more resistant to ionizing radiation. According to the results of IR-spectroscopy, the radiation yields of nitro compounds, ketones and carboxylic acids were determined. While conducting a quantitative analysis, we used the standard procedure for constructing the calibration dependences of the light absorption on a sample of standards (the area of compliance with the Bouguer-Lambert-Beer law). By the method of potentiometric titration, we determined that the concentration of nitric acid in the extraction system with 1-decanol is lower than with 1-nonanol, both "before" irradiation and "after", which is consistent with the data on radiation yields. Thus, preliminary conclusions can be made, that extraction systems with 1-decanol showed themselves better at key stages of the analysis than systems with 1-nonanol. The most important is that 1-decanol is more resistant to ionizing radiation. The main products, formed by radiation exposure, were established. Fire and explosion-proof characteristics of the systems "Isopar-M - TODGA" with the addition of both alcohols during the tests do not significantly change.

**Acknowledgments:** This study was supported by the Russian Science Foundation (project 16-19-00191).

## An action towards food safety: Evaluation of chemical impurities in sugar by neutron activation analysis

**Maria Angela Menezes<sup>1</sup>, Paula Salles<sup>2</sup>,  
Márcia Sathler<sup>1</sup>, Hellen Oliveira<sup>1</sup>, Radojko Jačimović<sup>3</sup>**

<sup>1</sup> Nuclear Technology Development Centre/Brazilian Commission for Nuclear Energy (CDTN/CNEN), Belo Horizonte, Brazil

<sup>2</sup> FACSETE, Sete Lagoas, Brazil

<sup>3</sup> Jožef Stefan Institute, Ljubljana, Slovenia

Food safety covers the practice of measures to guarantee product quality from the field to the consumer table. The agents known as contaminants can be of a physical type (insects, glass, metals) or chemical (cleaning residues, chemical elements, pesticides) or biological (pathogenic microorganisms). Analytical techniques are suitable for identifying and quantifying the presence of inorganic elements in food that can be essential for human life or be a health risk. Depending on the chemical element and its concentration, the impact on consumer health can take many years to be observed due to the prolonged exposure to such elements at low levels. The considered environmental elements may be present in food from the field in which the food is grown and harvest. After these steps, the food is transported, stored, packaged, processed. The contamination may occur in all steps.

This paper is about sugar, a food considered safe that is consumed in several dishes and industrialized food (beverages, bakery, dairy, condiments and others). It is also used to stabilize large molecule active pharmaceutical ingredients in formulation, to strength tastes and aromas, to enhance color, flavor, bulk, texture, fermentation and preservation. Due to innumerable uses, it is relevant to evaluate chemical impurities mainly in white sugar, pure sucrose, available for consumption in bags of 3 to 5 g, in Brazilian public places without information about the place where the sugar was produced or to the origin of the sugarcane. It is important to mention that Brazil alone produces almost 52% of the world's sugar market.

The neutron activation technique was applied using the methodology to analyse larger samples, established at CDTN/CNEN, based on  $k_0$ -method. TRIGA MARK I IPR-R1 research nuclear reactor was used and the new spectral parameters were applied in the elemental concentration calculations. Elements – essential and non-essential - like As, Br, Fe, Ga, K, La, Na, Sb, Sc, Sm, Sr and Zn were determined in a large range of concentration. Among the determined elements, the Brazilian legislation, ANVISA, (National Health Surveillance Agency) establishes normative values only to As. Some samples presented As concentration higher than the values established by legislation.

**Acknowledgments:** FAPEMIG (Project PPM-00143-16), CNPq, CAPES, Department of Engineering/UFMG, CDTN/CNEN.

### References

- Kara R. Goldfein, Joanne L. Slavin. Why sugar Is added to food: Food Science 101. Comprehensive Reviews in Food Science and Food Safety, 2015 (<https://doi.org/10.1111/1541-4337.1215>)
- Salles, Paula M. B.; Menezes, Maria Ângela B. C.; Jačimović, Radojko; Campos, Tarcísio P. R. Journal of Radioanalytical and Nuclear Chemistry, v. 306, p. 1-9, 2015.
- ANVISA, Brazilian Health Surveillance Agency (1998) [www.anvisa.gov.br](http://www.anvisa.gov.br), Accessed: 9 Dec 2018

## Effects of gamma irradiation on cassava flour from Paraguay

**Juan F. Facetti-Masulli, Hector D. Colman**

Physics Department University of Asuncion Paraguay, Asunción, Paraguay

Cassava or *mandioca* (*manihot utilissima* Pohl) is a plant of Paraguayan origin. It is an agricultural commodity both of social and economic impact in the country. Its farming, by small producers in many cases, reached in the last years a considerable volume. In the population diet it is the most significant current source of carbohydrates.

Besides the advantages in food preparation of its derivatives, such as flour and starch, the large primary use as food or in industrial production, expanded its farming in the country. Currently, Paraguay is the second world largest exporter of cassava starch. And at last but not least cassava is likewise an important source for bio-fuels.

The present work shows results obtained in the irradiation of various cassava/*mandioca* flour samples with gamma rays from sources of Co-60. The work has a two-fold objective; the preservation of the material as well as the increase of its maltose content for enlarging the capacity of the irradiated flour to produce ethyl alcohol. Several kilograms of flour already sorted according their edible quality were used for preparing composite samples. Proximate analysis permits to classify them as of poor, as well as of low and good quality. The samples were irradiated at variable doses.

At low doses, the organoleptic properties do not change perceptibly, while at high doses they deteriorate. In regard to the acidity at low doses it does not vary significantly during the control/storage period but at high does acidity increases in such a period.

The maltose content also increases by the doses; in wheat flour, a slight increase was also observed. But in the case of manihot flour, the increase is very noticeable. These results are very important when the flour will be used for the production of ethanol. And since its content in total extractable carbohydrates (starch) is quite high, manihot flour is an excellent raw material for obtaining ethyl alcohol.

## Elemental composition of hair in individuals with sedentary lifestyle from Belo Horizonte, Brazil, analysed by ko-INAA

Paula Salles<sup>1</sup>, Márcia Sathler<sup>2</sup>,  
Cláudia Ferreira<sup>2</sup>, Maria Ângela Menezes<sup>2</sup>, Radojko Jaćimović<sup>3</sup>

<sup>1</sup> FACSETE, Sete Lagoas, Brazil

<sup>2</sup> Nuclear Technology Development Centre/Brazilian Commission for Nuclear Energy (CDTN/CNEN), Belo Horizonte, Brazil

<sup>3</sup> Jožef Stefan Institute, Ljubljana, Slovenia

The absorption of essential and non-essential elements by human body may change according to factors such as environmental exposure, sex, age and nutritional limits of the individual. Evidence of diseases in humans related to the ingestion of essential and non-essential elements points out the importance to study the interactions in the organism. One step of this kind of research is to identify the presence of those chemical elements in the human body. It can be done through hair, which is considered a "biological dosimeter". As a bioindicator, hair presents advantages because of its easy collection, transport, and storage.

The purpose of this study was to verify the concentration of chemical elements in hair from a sedentary group in Belo Horizonte, Brazil. The neutron activation analysis, ko-method, was applied analysing small and large samples, a new methodology established at CDTN/CNEN, Belo Horizonte, to multielemental concentration determination in hair. The TRIGA MARK I IPR-R1 nuclear reactor was used to carry out the ko-method and the new spectral parameters were applied in the elemental concentration calculations.

Among the twenty-seven hair samples analysed, the elements Au, Br, Na, and Zn were found to be common to all of them. It was attempted to compare the results obtained with similar studies performed in Brazil and abroad, using neutron activation analysis. It was verified, in this matrix, that nuclear technique was efficient to determine the presence of elements in hair.

**Acknowledgments:** Brazilian institutions: FAPEMIG (Project PPM-00143-16), CNPq, CAPES, Department of Engineering/UFGM, CDTN/CNEN.

### References

- Abdulla, M.; Chmielnicka, J. New aspects on the distribution and metabolism of essential trace elements after dietary exposure to toxic metals. *Biological Trace Element Research*, v. 23, n. 1, p. 25-53, 1989.
- Angerer, J.; Ewers, U.; Wilhelm, M. Human biomonitoring: state of the art. *International Journal of Hygiene and Environmental Health*, v. 210, n. 3, p. 201-228, 2007.
- Katz, S. A.; Katz, R. B. Use of hair analysis for evaluating mercury intoxication of the human body: a review. *Journal of Applied Toxicology*, v. 12, n. 2, p. 79-84, 1992.
- Mertz, W. The essential trace elements. *Science*, v. 213, n. 4514, p. 1332-1338, 1981.
- Zhang, H.; Chai, Z.; Sun, H. Human hair as a potential biomonitor for assessing persistent organic pollutants. *Environment International*, v. 33, n. 5, p. 685-693, 2007.
- Menezes, M. A. B. C.; Maia, E. C. P.; Albinati, C. C. B.; Sabino, C. V. S.; Batista, J. R. How suitable are scalp hair and toenail as biomonitoring? *Journal of Radioanalytical and Nuclear Chemistry*, v. 259, n.1, p. 81-86, 2004.
- Menezes, M. A. B. C.; Jaćimović, R. Implementation of a methodology to analyse cylindrical 5-g sample by neutron activation technique, ko method, at CDTN/CNEN, Belo Horizonte, Brazil. *Journal of Radioanalytical and Nuclear Chemistry*, v. 300, p. 523-531, 2014.

## Study of Tc(VII) ions reduction by diformylhydrazine in nitric acid solutions

**Konstantin Dvoeglazov, Ekaterina Pavlukevich,  
Lubov Podrezova, Tatyana Podimova, Yelizaveta Filimonova**

Bochvar High-Technology Research Institute of Inorganic Materials, Moscow, Russia

To reuse uranium as fuel of nuclear reactors, it is necessary to recycle irradiated nuclear fuel. During the recycling process, uranium is separated from the fission products, most of which are poorly soluble in tributylphosphate and do not cause any difficulties for the uranium hydrometallurgical purifying. Among the fission products there is technetium, which is formed in significant quantities. When dissolved in nitric acid, technetium transforms into the pertechnetate ion that is co-extracted in tributylphosphate with the uranyl ion and accompanies U until its back-extraction stage. To increase the uranium purification factor from technetium, it is required to select a reagent that could transfer technetium into a low-extractable form. Due to the pronounced oxidative properties of the pertechnetate ion, the most effective way is the selection of such reducing agent that is capable for the fast reduction of Tc(VII) to Tc(IV) or Tc(V). For such a process it is proposed to use diformylhydrazine – HCONHNHOCH.

The kinetics of  $\text{TcO}_4^-$  ions reduction by diformylhydrazine in the medium of nitric acid at the concentration from 0.5 to 1.5 mole/l was studied spectrophotometrically. Concentration of the reducing agent during the study was from 0.1 to 0.2 mole/l and a temperature of the solutions was changed from 30 to 49.6 °C.

Changes in the spectra were observed in the region of 350-800 nm, where according to various researchers' data there are characteristic peaks of the following technetium valence forms:  $\text{TcO}^{2+}$  and  $\text{TcO}^{3+}$ .

As experiments have shown the kinetics of technetium valence forms changing is complex. At the initial time an induction period was observed, and then began an active phase of interaction, which was characterized by an increasing in optical density of the solution. Then there was a slowdown in the optical density growth and almost immediately began its decreasing. Most likely, the optical density decrease was associated with the reverse oxidation of reduced forms of technetium.

To determine the quantitative characteristics of the transition rate of Tc(VII) into the Tc(IV) or Tc(V) forms a differential equation system was made and solved by the numerical technique. The selection of the reaction rate constants was carried out from the condition of optimal agreement between the experimental and calculated kinetic curves.

## Kinetics of Np(VI) and Pu(VI) reduction with diformylhydrazine in nitric acid

**Ekaterina Pavlyukevich, Konstantin Dvoeglazov, Polina Mitreas**

Bochvar High-Technology Research Institute of Inorganic Materials, Moscow, Russia

The search of new types of reducing agents for uranium separation from plutonium and neptunium in the hydrometallurgical reprocessing of spent nuclear fuel is currently relevant. One of the classes of reducing agents is organic derivatives of hydrazine. The rate of reaction with actinide ions such as  $\text{NpO}_2^{2+}$ ,  $\text{Pu}^{4+}$ ,  $\text{PuO}_2^{2+}$  changes due to the type of substituent group in the hydrazine molecule. To control the process of plutonium and neptunium stripping, it is necessary to know the dependence of the recovery rate on the concentration of the components in the technological solutions. Obtaining such information is the purpose of this work.

The kinetics of the reduction of Pu (VI) and Np (VI) with diformylhydrazine in an aqueous nitric acid solution was studied spectrophotometrically.

It was found that the reaction rate for ions  $\text{NpO}_2^{2+}$  and  $\text{PuO}_2^{2+}$  increases with increasing of reducing agent concentration and temperature and decreases with increasing of nitric acid concentration. The form of the kinetic equation for the reduction of  $\text{AnO}_2^{2+}$  to  $\text{AnO}_2^+$  with diformylhydrazine is the same for both types of actinide ions. It was found that the order of the reaction on the metal ion is 1, on diformylhydrazine 1.3, on nitric acid -1.5. The values of rate constants are significantly different. Under comparable conditions, the recovery rate of  $\text{NpO}_2^{2+}$  is in 220 times more than the recovery rate of  $\text{PuO}_2^{2+}$ . The activation energy for both reactions was determined.

## New Ti-Ca-Mg phosphate sorbents for removal of $^{137}\text{Cs}$ , $^{60}\text{Co}$ and $^{85}\text{Sr}$ from multicomponent liquid radioactive waste

**Andrei Ivanets<sup>1</sup>, Irina Shashkova<sup>1</sup>, Natalja Kitikova<sup>1</sup>, Artem Radkevich<sup>2</sup>,  
Tatiana Stepanchuk<sup>2</sup>, Marina Maslova<sup>3</sup>, Natalia Mudruk<sup>3</sup>**

<sup>1</sup> Institute of General and Inorganic Chemistry of NAS of Belarus, Minsk, Belarus

<sup>2</sup> Joint Institute for Energy and Nuclear Research – Sosny of NAS of Belarus, Minsk, Belarus

<sup>3</sup> Tananaev Institute of Chemistry – Subdivision of the Federal Research Centre «Kola Science Centre of the Russian Academy of Sciences», Apatity, Russia

Due to the intensive development of the nuclear industry, there is an increased interest in sorption technologies for the purification of liquid radioactive waste (LRW). Real LRW are multicomponent aqueous solutions of complex radionuclide composition that makes it promising to develop new materials characterized by high affinity to  $^{137}\text{Cs}$ ,  $^{60}\text{Co}$  and  $^{85}\text{Sr}$  radionuclides.

In this work, new Ti-Ca-Mg phosphate sorbents were obtained for the first time, allowing simultaneous removal of  $^{137}\text{Cs}$ ,  $^{60}\text{Co}$  and  $^{85}\text{Sr}$  radionuclides from multicomponent LRW. Synthesis of mixed Ti-Ca-Mg phosphates was carried out by the reaction of phosphatized dolomite ( $\text{Ca}_{2.65}\text{Mg}_3(\text{NH}_4)_{1.3}(\text{PO}_4)_4(\text{CO}_3)_{0.3}\cdot 6\text{H}_2\text{O}$ ) with aqueous solution of  $(\text{NH}_4)_2\text{TiO}(\text{SO}_4)_2\cdot\text{H}_2\text{O}$ , synthesized from the waste products of Apatite nepheline ores. Depending on the ratio of Ti/(Ca+Mg) in the reaction mixture of 0, 10, 20, 33, 60 wt.%, samples are designated as Ti0, Ti10, Ti20, Ti33, Ti60, respectively. Sorption properties was studied on the model multicomponent solution containing the radionuclides  $^{137}\text{Cs}$  ( $A_{\text{int.}}=5.5\pm 0.5$  kBq/L),  $^{60}\text{Co}$  ( $A_{\text{int.}}=5.0\pm 0.5$  kBq/L) and  $^{85}\text{Sr}$  ( $A_{\text{int.}}=5.5\pm 0.5$  kBq/L), at a ratio  $V$  (solution)/ $m$  (sorbent) = 250 mL/g. The distribution coefficients  $K_d$  ( $\text{cm}^3/\text{g}$ ) were calculated on the basis of experimental data.

The study of the porous structure of the obtained materials by the method of low-temperature adsorption-desorption of nitrogen showed that the synthesized Ti-Ca-Mg phosphates have a mesoporous structure (average pore size of 8-12 nm) with high values of specific surface area (100-200  $\text{m}^2/\text{g}$ ) and pore volume (0.27-0.37  $\text{cm}^3/\text{g}$ ). The effect of pH on sorption efficiency in the range of 2.0-11.0 was studied. It was found, that the samples of Ti-Ca-Mg phosphates provide high removal efficiency of  $^{137}\text{Cs}$ ,  $^{60}\text{Co}$  and  $^{85}\text{Sr}$  radionuclides in a wide range of pH=5.0-11.0. With an increase the Ti content in sorbents, there is a significant rising in the values of  $K_d$  for  $^{137}\text{Cs}$  and  $^{85}\text{Sr}$  radionuclides, while for  $^{60}\text{Co}$  there is a slight decrease in the sorption efficiency. Depending on the physical and chemical parameters, the sorbents exhibit selectivity with respect to different radionuclides: Ti60 ( $^{137}\text{Cs}$ ), Ti0 ( $^{60}\text{Co}$ ) and Ti10 ( $^{85}\text{Sr}$ ), for which the maximum values of  $K_d$  reach  $7.4\times 10^3$ ,  $9.0\times 10^4$  and  $2.0\times 10^4$   $\text{cm}^3/\text{g}$ , respectively.

The obtained data indicate the possibility of directed regulation of sorption and selective properties of Ti-Ca-Mg phosphates by changing their chemical composition, as well as the prospects of their practical application for the  $^{137}\text{Cs}$ ,  $^{60}\text{Co}$  and  $^{85}\text{Sr}$  removal from multicomponent LRW.

## Investigation of the natural radioactivity of the sediment samples from the area of Una River

**Mirza Nuhanovic, Mirza Nuhanovic,  
Nusret Dreskovic, Samir Đug, Narcisa Smječanin**

Faculty of Science, University of Sarajevo, Sarajevo, Bosnia and Herzegovina

It is indisputable that a certain number of radionuclides appear at different areas in nature. The occurrence of radionuclides in nature is a consequence of their crystallochemical and physicochemical properties, as well as the geological and hydrogeological characteristics of the examined areas. In this study, natural radioactivity of the tuff stones (sediments) from the river Una basins was examined. According to the available literature, evaluation of radioactivity of sediments from the area of Una river basins on the territory of B&H has not been conducted for more than fifty years. Tuff stones sampling was carried out at six locations: the upper course of Martin Brod, the lower course of Bosanska Otoka, the upper course of Strbacki buk 1 and 2, the lower course of Kostela 1 and 2. The activity concentrations of  $^{226}\text{Ra}$ ,  $^{232}\text{Th}$ ,  $^{40}\text{K}$ , and  $^{134/137}\text{Cs}$  and gross alpha-beta activity of the collected samples were evaluated. The activity concentration of the previously mentioned radionuclides was determined by the gamma spectrometric method, and gross alpha-beta activity was measured by gas-flow proportional alpha-beta counter. In the analyzed sediment samples activity concentrations for examined radionuclides ( $^{226}\text{Ra}$ ,  $^{232}\text{Th}$ ,  $^{40}\text{K}$ , and  $^{134/137}\text{Cs}$ ) varies in the range of 4.71-101.24 Bq/kg. Gross alpha and beta activity were between 54.52 and 188.78 Bq/L, respectively. After the analysis and interpretation of the obtained results and compared to the similar studies conducted on sediments samples from the rivers it is important to continue with this type of research.

## Experimental and theoretical study of gamma-radiolysis of diamides of N-heterocyclic acids promising for separation of trivalent f-elements

Vladimir Petrov, Anastasiya Smirnova, Petr Matveev,  
Artem Mitrofanov, Igor Rodin, Timur Baygildiev, Stepan Kalmykov

Lomonosov Moscow State University, Department of Chemistry, Moscow, Russia

One of the main methods for the separation of radionuclides in radiochemical technology is liquid extraction. Development of new extractants requires taking into account the effect of radiolysis on extractants particularly for the solutions with high activity of radionuclides. Experimental study of radiolysis requires a long time, special equipment, licensing and is not always possible in laboratory conditions or even at industrial sites. Thus, an important task is to develop *in silico* a theoretical model that allows predicting the radiolytic stability of extractants.

The objective of this work is a theoretical and experimental study of the stability under gamma irradiation of solutions of a series of ligands that are promising for the processing of high-level radioactive waste (HLW). The change in the extraction properties of extractants towards Am(III) and Eu(III) after irradiation up to absorbed doses 100 kGy was experimentally investigated. The composition of the radiolysis products was determined by the mass spectrometry with electrospray ionization. The theoretical part of the study is related to quantum chemical calculations and focused on the mechanism of radiolytic degradation of extractants. The calculations were performed by the DFT method (D3-B3LYP, MA-def2-TZVPP theory level).

Fukui indices were calculated. These parameters reflect the reactivity of compounds with respect to different types of reactions, as well as Mayer bond orders, which are used to evaluate the weakest chemical bonds in extractants. It was shown earlier [1] that this approach can predict the direction of the ligand degradation and possible radiolysis products.

The results of this study show the main features of the degradation processes under gamma-radiolysis and uncover the role of nitric acid in the enhancing the radiation stability of the extraction system.

**Acknowledgments:** This work was financially supported by Russian Foundation for Basic Research (grant No. 18-33-20179\_mol\_a\_ved).

### References

[1] Matveev P.I. et al. Testing a simple approach to radiolysis products in extraction systems. A case of N, O-donor ligands for Am / Eu separation // RSC Adv. 2017

## New pyridine-based phosphine oxides for liquid extraction of Am(III), Cm(III) and Ln(III)

**Petr Matveev<sup>1</sup>, Vladimir Petrov<sup>1</sup>, Nickolay Andreadi<sup>1</sup>, Natalia Borisova<sup>1</sup>, Gladis Zakirova<sup>1</sup>, Elena Belova<sup>2</sup>, Boris Myasoedov<sup>2</sup>, Stepan Kalmykov<sup>1</sup>**

<sup>1</sup> Lomonosov Moscow State University, Department of Chemistry, Moscow, Russia

<sup>2</sup> Institute of Physical Chemistry and Electrochemistry of Russian Academy of Sciences (IPCE RAS), Moscow, Russia

Phosphine oxide extractants are promising ligands that can be used in the extraction of rare earths and actinides. In this work we have investigated pyridine-based phosphine oxides.

We have investigated the extraction properties towards Am(III), Cm(III) and Ln(III) for the series of phosphine oxides in systems containing “0.001 mol/L ligand in nitrobenzene - an aqueous solution of 3 mol/L HNO<sub>3</sub>”. The results show that extractants with substituents with small volume have relatively high distribution coefficients *D*, and extractants with volume substituents have extremely small distribution coefficients. Calculations (DFT, B<sub>3</sub>LYP functional, basis def2-SVP) showed that the observed extraction efficiency correlates with the energy of ligand pre-organization. Meta-substituted phenyl phosphine oxides exhibit the highest selectivity in the separation of an Am/Eu pair. For the ligand with two phenyl substituents the extraction of curium(III) was studied in details, and it was shown that the separation coefficient of Am/Cm pair is 3.0-3.5 in this case.

The radiation resistance of this ligand towards external gamma irradiation was also investigated. It was shown that the ligand irradiated up to an absorbed dose of 350 kGy loses less than 10% of the extraction efficiency.

Thus, a new class of extractants shows moderate selectivity in the separation of Am/Ln and relatively high radiation resistance. However, further modification of the extractants is necessary to increase the solubility in weakly polar aliphatic solvents.

**Acknowledgments:** This work was financially supported by Russian Foundation for Basic Research (grant No. 16-13-10451).

## Study of radionuclide speciation in spent fuel pool model solutions

**Aliaksandr Zaruba, Artsiom Radkevich, Olga Korenkova, Nadzeia Voronik**

Joint Institute for Power and Nuclear Research – Sosny of the National Academy of Sciences of Belarus,  
Minsk, Belarus

At NPPs spent fuel is disposed to special at-reactor spent fuel pool after load out from the core. Water of spent fuel pool has complex chemical and radionuclide composition. Radionuclides get into water both from sediments at the surface of fuel assemblies and out of damaged fuel rods. Although the volume activity in water may be rather high radionuclides exist at trace concentrations ( $<10^{-7}$  mol/l) as chemical elements and their main state is pseudocolloidal. Pseudocolloidal species are formed by radionuclide sorption on secondary particles that always exists in solution, for example on corrosion products. Solutions containing such non-ionic species of radionuclides are treated by traditional ion-exchange method with decreased efficiency.

In this research the state of  $^{60}\text{Co}$ ,  $^{137}\text{Cs}$ ,  $^{85}\text{Sr}$  in trace concentrations was in solutions of  $\text{H}_3\text{BO}_3$ ,  $\text{KNO}_3$  and distilled water at different pH values and in the presence and absence of ferric ions, as corrosion products precursor. The methods of ultrafiltration and sedimentation at centrifugation were used for species separation.

It was shown that radionuclides have been rejected on membrane equally in boric acid solution at low pH value. At neutral pH decreased radionuclide retention is observed, but in alkaline pH range retention of radionuclide  $^{60}\text{Co}$  is increased. Sedimentation of radionuclides in low pH range at centrifugation is not observed. Likely, formation of radionuclides pseudocolloidal particles in boric acid solution at low pH is observed. The retention of  $^{60}\text{Co}$  on membrane and precipitation of  $^{60}\text{Co}$  at centrifugation is determined by formation of cobalt hydrolyzed particles in alkaline pH range. Commonly radionuclide cobalt species is changed at the addition of iron into studied solutions, it is rejected on membrane and it is precipitated at centrifugation at lower pH value.

Difference between retention on membrane and precipitation at centrifugation is explained by the sizes of formed pseudocolloidal particles.

## Gas-phase conversion of $UPd_3$ , $URu_3$ and $URh_3$ intermetallides into water-soluble uranium compounds

Iurii Nevolin<sup>1</sup>, Sergey Kulyukhin<sup>2</sup>, Vladimir Petrov<sup>1</sup>, Stepan Kalmykov<sup>1</sup>

<sup>1</sup> Lomonosov Moscow State University, Moscow, Russia

<sup>2</sup> Frumkin Institute of Physical Chemistry and Electrochemistry RAS, Moscow, Russia

One of the possible problems during reprocessing of the nitride spent nuclear fuel (SNF) can be uranium recovery from metallic phases with  $U(Pd, Ru, Rh)_3$  composition. The presence of these compounds was previously reported in the fast neutron reactors SNF. A promising solution for the head-end stage of nitride SNF reprocessing can be gas-phase processes of voloxidation (volume oxidation) and subsequent nitration (treatment with  $HNO_3$  vapor). The aim of this work was the study of the possibility of uranium recovery from  $U(Pd, Ru, Rh)_3$  using these processes.

The  $UM_3$  ( $M = Pd, Ru, Rh$ ) individual intermetallic compounds were synthesized by fusing simple substances in an arc furnace. Obtained compounds then were used as the imitators of the complex  $U(Pd, Ru, Rh)_3$  phase. The first stage of our work was addressed to the possibility of uranium recovery from  $UM_3$  by direct nitration in the “ $HNO_3$  (vapor)-air” atmosphere at the temperature 70–150 °C and the pressure 1.3–2 atm. The formation of water-soluble uranium compounds was observed in the case of  $UPd_3$ . No conversion of  $URu_3$  and  $URh_3$  into water-soluble uranium compounds was observed.

At the second stage of the work,  $UM_3$  compounds were oxidized in air, followed by nitration in an “ $HNO_3$  (vapor) -air” atmosphere. It was shown that the main oxidation products of  $UPd_3$  at 550–800 °C were  $U_3O_8$  and  $PdO$ . Oxidation at 800–1200 °C led to the formation of  $U_3O_8$  and  $Pd$  phases. The oxidation of  $URu_3$  at 550–800 °C resulted in the formation of  $RuO_2$  oxide. Uranium-containing phases were not observed. The oxidation products of  $URu_3$  at 800–1200 °C were  $RuO_2$  and  $U_3O_8$ . The nitration of the  $UPd_3$  and  $URu_3$  oxidation products resulted in the formation of water-soluble uranium compounds with a conversion degree of 60–100%. The conversion yield did not depend on the oxidation temperature. During the oxidation of  $URh_3$  at 550–900 °C, amorphous products were observed; individual phases of uranium and rhodium were not detected. Oxidation of  $URh_3$  at 900–1100 °C led to the phases of unknown structure. A further rise in a temperature up to 1200 °C results in  $U_3O_8$  and  $Rh$  phases. The degree of uranium conversion from the oxidation products of  $URh_3$  to water soluble compounds in a nitrating atmosphere strongly depends on the oxidation temperature. It reaches 100% only when oxidation products (after treatment at 1200 °C) were converted in the  $HNO_3$  vapors atmosphere.

Thus, we have demonstrated the fundamental possibility of uranium recovery into water-soluble compounds from intermetallic phases  $UM_3$  ( $M = Pd, Ru, Rh$ ) using a combination of voloxidation and gas-phase nitration processes.

## Exothermic processes in extraction systems during the reprocessing of spent nuclear fuel

**Elena Belova, Alexey Rodin, Georgy Thorzhnitskiy, Mikhail Kadyko,  
Zayana Dzhivanova, Ivan Skvortsov, Anton Smirnov, Yulia Nikitina**

Russian Academy of Sciences, A.N. Frumkin Institute of Physical Chemistry and Electrochemistry RAS,  
Moscow, Russia

The explosiveness of extraction technological processes in radiochemical industry is determined by the following main reasons: the interaction of an organic solution (extraction mixture) and degradation products with an oxidizing agent (nitric acid and metal nitrates); ignition of inflammable vapors and gases, including vapors of the diluent and the products of its radiation decomposition, radiolytic hydrogen, in mixtures with a gaseous oxidant. Ensuring the explosion safety of technological processes of radiochemical processing of nuclear fuel and high-level liquid waste requires systematic research to obtain information about the kinetics and mechanisms of interaction of nitric acid with the components of extraction systems, the qualitative and quantitative composition of the products of radiation destruction of technological media. Kinetic studies allow us to estimate the influence of various factors on the development of oxidative processes, as well as to determine the boundary conditions for the transition of oxidative processes to the thermal explosion mode. To solve the issue of ensuring the explosion safety of technological processes of radiochemical enterprises, it is necessary to have a number of characteristics of extraction systems, that allow to evaluate the process safety in the regulated conditions and in case of deviations from normal operation. Limit parameters are necessary to assess the probability of accidents and their consequences. The main characteristics to determine the possibility of development of a thermal explosion, as applied to extraction systems, are: the maximum rate of heat and gas emission; the start temperature of the intense exothermic process; the total specific volume of the gaseous products of the oxidation process; thermal effect of interaction.

In 2018, on this subject, were studied the extraction mixtures based on diamides of 2,6-pyridinedicarboxylic and 2,2'-bipyryl-6,6'-dicarboxylic acids in trifluoromethylphenylsulfone (FS-13) and meta-nitrobenzotrifluoride (F-3) diluents, considered for the fractionation of high level waste, in contact with 14 mol/L HNO<sub>3</sub>. The influence of pre-irradiation of mixtures with accelerated electrons on the kinetics of their oxidation is determined. Thermolysis of the mixtures was carried out in an autoclave at temperatures of 170°C and 200°C. Samples of the organic phase were irradiated at a linear electron accelerator UELV-10-10-C-70 (CCU PMR IPCE RAS) at a dose rate of 10 kGy/hour until reaching absorbed doses of 0.1, 0.5 and 1 MGy. It was shown, that by thermolysis of extraction mixtures, irradiated up to 1 MGy, conditions for the development of autocatalytic oxidation do not occur.

It was shown, that the main characteristics of fire hazard, which determine the mode of using a flammable liquid (excluding the ignition of the vapor-gas phase) for the FS-13 and F-3 diluents, are significantly higher than the maximum operating temperatures of conducting the technological operations of spent nuclear fuel regeneration. On the basis of the conducted research, we concluded that the use of heavy diluents in the regulated conditions of conducting the extraction process for the HLW reprocessing (UNEX process) will not lead to the ignition of air-vapor mixtures.

**Acknowledgments:** This study was supported by the Russian Science Foundation (project 16-19-00191).



**Radioecology**  
**32**

## The label method for the assessment of the technical feasibility waste management of the oil and gas industry

**S.V. Ostakh**

National University of Oil and Gas “Gubkin University”, Moscow, Russia

At present, the problems of the removal of natural radionuclides ( $^{226}\text{Ra}$ ,  $^{232}\text{Th}$ ,  $^{40}\text{K}$ ) from the layers and the formation of precipitation with their high content in the sludge products formed during the extraction and preparation of oil, face almost all oil and gas companies, both in Russia and abroad.

There is a whole complex of serious environmental problems due to the accumulation of large masses of sludge with a high content of natural radionuclides, which have variable ratios of heavy hydrocarbon components of different viscosity and composition, mineral impurities different in dispersion, composition and content in waste and a variable set of hazardous radionuclides, of different isotopic composition and concentration.

The generated toxic waste is stored in the sludge collectors. The only alternative way to solve this problem is the use of technologies of physical and chemical neutralization of waste with a controlled mechanism of appropriate reactions without violating their integrity. Radiation safety of neutralized waste is ensured with the permissible specific effective activity of natural radionuclides, which in the material does not exceed 370 Bq/kg. The complexity of waste assessment includes the determination of component and chemical composition, hazard class (toxicity), as well as routine radiological studies. As a “label”, diagnostic substance applies a stable isotope of carbon  $^{13}\text{C}$ . The labeled compound (test preparation) does not change the chemical properties of substances in the physical and chemical neutralization of waste. “Tags” are applicable for input control, process monitoring and periodic control. The proposed method will eliminate the uncontrolled spread and migration of radionuclides in the process of neutralization. The solution under consideration will provide a safe and significant reduction in the volume of accumulated waste.

## **Environmental studies of the radioisotope concentration in coal mine waste in Silesian and Lubelskie Province – Poland**

**Konrad Wysogład**

Maria Curie-Sklodowska University, Nuclear Methods Department, Lublin, Poland

The samples of soils and coal were taken in selected areas in Silesian and Lubelskie province. Dosimetric and gamma spectrometry were made. A significant accumulation of NORM isotopes from the Uranium, Actinium and Thorium series were found. The measurements showed the existence of radium anomaly in Upper Silesian Coal Basin.

## **Environmental risks for the freshwater ecosystem of the Yenisei River and health risks for humans**

**Lydia Bondareva, Nataliya Fedorova**

Federal Scientific Center of Hygiene named after Erisman, Mytischy, Russia

The area of the Krasnoyarsk Region is included into a number of regions where the population is influenced by adverse environmental factors. The Krasnoyarsk Region is a big unit of the Russian Federation which has a great economic potential including the fresh water supply – the river Yenisei; the environment determines the health of the nation, health economy in our environment. Due to this, in studying the stream flows of the particular parts of the Yenisei River each water object was considered as a unified specific water ecosystem which is also the human environment. The main components of this system were studied taking into account their interpenetration, interconnection, interdependence, and interaction.

The long-term monitoring of the state of the fresh-water ecosystem of the River Yenisei revealed the statistically reliable content of heavy metals (Fe, Zn, Cd, Cu, U etc.) in the water, bottom sediments, phyto- and zooplankton, and muscle mass of commercial fish consuming different types of food (benthos eaters, predators and herbivorous fish). The values of the indices of the ecological state of the Yenisei River were estimated to vary from 2.38 to 2.85 in the areas under study. A conclusion was made that the studied transects of the river Yenisei had a good ecological potential with a moderate level of ecological risks. The total index of risk for the water, taking into account the reference doses, amounts to 0.16 for the water, and to 0.47 for the flesh of commercial fish. The total index of risk for the population consuming fresh water and fish from the Yenisei River amounts to  $IR=0.63$ . The obtained value of the index is, in general, of no danger for the population health. Since the cancerogenic substances were not accurately revealed, we estimated non-cancerogenic nonthreshold risks. The non-cancerogenic nonthreshold risks for particular substances under consideration did not exceed the allowable level of 0.05 and were equal to 0.017. The estimation revealed that the ratio of developing reflectory-olfactory effects to the allowable value was equal to 0.01, and the ratio of the total noncancerogenic risk to the allowable level was 0.34. Here, the integrated indicator was 0.35, which did not exceed the regulatory level ( $\leq 1$ ). In general, the risks with regard to all the indicators analyzed did not exceed the allowable levels and did not require additional measures of regulating the water quality.

## Airborne uranium assessment by epiphytic lichen species in contaminated areas

**M. Radenković<sup>1</sup>, S. Milošević<sup>2</sup>, S. Stanković<sup>1</sup>, J. Joksić<sup>3</sup>, A. Onjia<sup>4</sup>**

1 Vinča Institute of Nuclear Sciences, University of Belgrade, Belgrade, Serbia

2 Municipality of Bujanovac, Bujanovac, Serbia

3 Directorate for Radiation and Nuclear Safety and Security, Belgrade, Serbia

4 Faculty of Technology and Metallurgy, University of Belgrade, Belgrade, Serbia

Natural uranium, consisting of  $^{238}\text{U}$ ,  $^{234}\text{U}$  and  $^{235}\text{U}$  isotopes is present in the environment in low concentrations especially in the atmosphere where it usually exists as a constituent of particulate matter submicron conglomerates suspended in the air. In the case of contamination, uranium may be present in the aerosol, being transferred to other areas by wind and again settled on the surface soil with possible migration into deeper layers or resuspension under certain meteorological conditions. Here results on the airborne uranium assessment based on the analysis of lichen species already present or transplanted into contaminated areas will be presented. With that aim, different *in situ* and transplanted epiphytic lichen species have been taken at selected locations in southern Serbia in the stage of existing contamination by depleted uranium, during the clean-up activities and afterwards, in all four seasons. Collected samples underwent analysis by sensitive nuclear analytical techniques. The INAA and ICP MS results are derived from  $^{238}\text{U}$  mass fraction while high resolution alpha-spectrometry gave results for each isotope expressed as specific activity concentration ( $\text{Bq kg}^{-1}$ ). Based on the isotopic ratios  $^{235}\text{U} / ^{238}\text{U}$  and  $^{234}\text{U} / ^{238}\text{U}$ , depleted uranium content was possible to distinguish from natural uranium in the samples. Results have shown that the sensitivity of the examined morphologically different lichen types and their ability to accumulate metals including uranium, strongly depend on metals' concentration in the air as well as on the age of lichens, properties of host species, chemical properties of particles, local climate conditions, exposure time etc. Epiphytic lichen species *Evernia prunastri* was found to be the most suitable bioindicator for the accumulation of uranium airborne particles. Concerning the uranium content, a significant difference in concentrations had been observed for different sampling phases, with maximum depleted uranium contribution during the clean-up activities. The variability in uranium concentrations was noticeable in relation to prevailing wind direction, position and distance of the sampling points. Having in mind the results obtained within the national radioactivity monitoring program 2011-2017, it may be concluded that for detailed airborne uranium assessment, a methodology such as biomonitoring with the application of sensitive nuclear techniques should be considered.

## The impact of high energy X-ray and $\beta$ -ray irradiation on the germination of rice seed

Hing Ming Hung

The University of Hong Kong, Hong Kong SAR, China

**Introduction.** Co-60 is widely used to investigate the effect of radiation on the germination of cereal seed for a long history. However, due to the low energy nature of the isotope, the effect of higher energy radiation in agricultural research is scarce. In this study, rice seeds were irradiated by high energy X-ray (Average: 5MeV) and  $\beta$ -ray (5MeV) produced by linear accelerator respectively and the germination parameters were recorded.

**Methods.** Rice sample was harvested 9 months before this study. Samples were divided into 11 groups, 100 grains each. During the exposure, samples were wrapped by water-equivalent bolus to facilitate dose build-up effect and irradiated at the doses 0Gy (Control), 60Gy, 120Gy, 180Gy, 240Gy and 300Gy by 5MeV X-ray (Average energy) and 5MeV  $\beta$ -ray respectively. All samples were then planted into glass well with a filter paper and incubated under 12h light and 12h darkness for 30 days. Seeds were considered to be germinated if roots were longer than 5mm. The length of root and sprout were measured daily.

**Results.** The germination rate at Day 10 for X-ray group was 100%(0Gy Control) and gradually dropped to 47%(300Gy). The same result was obtained for the root occurring rate. 100%(0Gy Control) of seeds developed a bud at Day 10 and dropped gently to 84%(300Gy). Those seeds that grew with a bud but without a root were considered not germinated, which accounted for 37%(300Gy). The overall survival rate at Day 30 was 98%(0Gy Control) and 36%(300Gy). In contrast to  $\beta$ -ray group, 46%(150Gy) of buds occurred at Day10 but all seed failed to develop a root. Thus, the germination rate was considered to be 0%(150Gy).

**Discussion and Conclusion.** The impact of higher energy radiation on germination was greater than that of lower energy. It was generally accepted by various studies that the reduction in germination rate was observed at >1kGy in Co-60 irradiation (1.33MeV) in rice seed while it was observed at a few hundred of Gy in this study. From the results, the effects of different radiation doses on germination were represented by the bud occurrence rate, the rate decreased with the increase of the radiation dose. It was found that the influence of high energy radiation on roots was more significant than that on buds in this study. The effects of high energy radiation on germination mainly affected the development of the root system.

Moreover, the impact of  $\beta$ -ray was greater than that of X-ray on rice seed germination. The germination rate terminated at 150Gy of  $\beta$  irradiation, compared with X-ray irradiation 79% at 150Gy. This can be explained by the difference in physical properties between the two types of radiations,  $\beta$ -ray is a charged particle while X-ray is an EM wave, the penetrating power of  $\beta$ -ray is weaker than that of X-ray, and hence the  $\beta$ -ray takes shorter distance to release their maximum energy. It is easier for  $\beta$ -ray to release ionizing power to produce radiobiological damage to the seed while X-ray photon may pass through the seed without ionization in tiny seed.

## RH control Cs<sup>137</sup> in fito-sanitary supervision

**Mihajlo Vićentijević<sup>1</sup>, Dubravka Vuković<sup>1</sup>, Vujadin Vuković<sup>1</sup>,  
Branislava Mitrović<sup>2</sup>, Dragan Živanov<sup>2</sup>, Jasna Kureljušić<sup>1</sup>**

<sup>1</sup> Scientific Institute of Veterinary Medicine of Serbia, Belgrade, Serbia

<sup>2</sup> Faculty of Veterinary Medicine, Belgrade, Serbia

Besides the regular veterinary-sanitary supervision the Laboratory for Radiation Hygiene, also carries out the phyto-sanitary control of foodstuffs of plant origin and animal feed. By determining the radiative state of the samples – identification of biologically important radionuclides and determining the level of activity – is created the possibility of a radiological and hygienic assessment of their use value, i.e. the degree of radioecological quality. The paper presents the results of the RH control of biologically significant radionuclides – Cs<sup>137</sup> in the 2015-2018 period in foodstuffs of plant origin, animal feed and their additives. The obtained results show that the activity of Cs<sup>137</sup> is within the background limits, which is below the prescribed limits prescribed by our Rulebook on the limits of the content of radionuclides in drinking water, foodstuffs, animal feed, drugs, objects of general use, construction material and other goods placed in transport, “Official Gazette of the Republic of Serbia”, no. 36/18. Nuclear accidents in Chernobyl and Fukushima remind us that RH control should be regularly implemented in order to ensure a high level of food safety for our population.

## The spatial distribution of radionuclides in the soils of the Urals contaminated from different sources

Ludmila Mikhailovskaya, Vera Pozolotina

Institute of Plant and Animal Ecology, Yekaterinburg, Russia

The contamination of the Urals region with long-lived radionuclides had been forming for a long time. Sources of pollution were global radioactive fallout from the atmosphere, gas-aerosol and liquid discharges of numerous industrial enterprises of the nuclear fuel cycle (regular or emergency), peaceful nuclear explosions, and storage facilities for nuclear waste. The most large-scale sources are the East-Ural Radioactive Trace (EURT), formed in 1957 as a result of the accident at the Mayak Production Association (PA Mayak) and the Techa river floodplain contaminated with liquid radioactive waste from this enterprise.

The purpose of this research is comparative study of the spatial distribution of  $^{90}\text{Sr}$  and  $^{137}\text{Cs}$  in the soils of the Ural region contaminated from various sources.

The studies were carried out in the zones of influence of the largest nuclear enterprises: PA Mayak and Beloyarsk NPP (BNPP), as well as outside these zones (background areas). It is shown that regional (Urals) background levels of radionuclide contamination ( $^{90}\text{Sr}$  1.6-3.0 kBq·m<sup>-2</sup>,  $^{137}\text{Cs}$  4.6-6.8 kBq·m<sup>-2</sup>) exceed the global background ( $^{90}\text{Sr}$  – 1.3 kBq·m<sup>-2</sup>,  $^{137}\text{Cs}$  – 2.2 kBq·m<sup>-2</sup>) characteristic for the middle latitudes of the Northern Hemisphere. Density of soil contamination in local sites of EURT and of the Techa river floodplain reach up to  $n \times 10^4$  kBq·m<sup>-2</sup> ( $^{90}\text{Sr}$ ) and  $n \times 10^3$  kBq·m<sup>-2</sup> ( $^{137}\text{Cs}$ ).

The distribution of radionuclides is determined by the landscape-geochemical features of the territory and depends on the type of industrial discharges (gas-aerosol or liquid waste). In cases of contamination by fallout from the atmosphere, a decrease of the radionuclides content and the  $^{90}\text{Sr}/^{137}\text{Cs}$  ratio were noted in the soils of geochemical conjugations on the banks of reservoirs in the direction of the flow vector. This can be explained by the self-cleaning processes of the submerged soils of the coastal zone, which are revealed in varying degrees for  $^{90}\text{Sr}$  and  $^{137}\text{Cs}$ .

In cases of liquid discharges of radioactive waste, a high content of radionuclides was formed in floodplain soils during the period of floods. The  $^{90}\text{Sr}$  inventory in floodplain soils are an order of magnitude and  $^{137}\text{Cs}$  is 2–3 orders of magnitude higher than at the watershed and coastal slopes. The  $^{90}\text{Sr}/^{137}\text{Cs}$  ratios decrease in the direction of the flow vector.

The depth of the vertical migration and the features of the distribution of  $^{90}\text{Sr}$  and  $^{137}\text{Cs}$  in the soil profiles have a similar character and are largely determined by the soil moisture regime.

**Acknowledgments:** This study was performed within the frameworks of state contract with the Institute of Plant and Animal Ecology, Ural Branch, Russian Academy of Sciences.

## Speciation of $^{226}\text{Ra}$ and $^{232}\text{Th}$ in Albic Stagnic Retisol

Dmitry Manakhov<sup>1</sup>, Elena Alekhina<sup>2</sup>, Denis Lipatov<sup>1</sup>, Sergrey Mamikhin<sup>1</sup>

<sup>1</sup> Soil Science Faculty of Lomonosov Moscow State University, Moscow, Russia

<sup>2</sup> Provimi Ltd., Moscow, Russia

Albic Stagnic Retisols are common in the taiga-forest zone among Albic Retisols, in weakly drained areas. They are formed during periodic waterlogging and alternation of reducing and oxidizing conditions, which consequent development of segregated ferrous nodules in the surface eluvial horizons, in which, in addition to Fe, such elements as Mn, Si and others are accumulate.

The studied soil is characterized by a strongly acidic reaction, a regressive-accumulative distribution of humus, an accumulative-eluvial-illuvial distribution of exchangeable cations, a high degree of base saturation. The concretions of the eluvial horizon accumulate more humus and exchangeable cations, compared with the soil mass. The value of hydrolytic acidity in the nodules is also higher.

The following fractions were sequential extracted from the soil: water-soluble (distilled water), exchangeable (1M  $\text{NH}_4\text{OAc}$ , pH=4.8), mobile (1M HCl), acid-soluble (6M HCl). Extraction the residue was performed by sintering with  $\text{Na}_2\text{CO}_3$ .

The distribution of the acid-soluble fraction of  $^{226}\text{Ra}$  in the profile is statistically significant ( $p = 0.05$ ) positively correlated with the content of exchange bases and the degree of base saturation. High positive correlation coefficients with  $\text{Ca}^{2+}$  and  $\text{Mg}^{2+}$  are also noted for the exchangeable fraction of  $^{226}\text{Ra}$ .

The availability of  $^{232}\text{Th}$  to plants and its migration mobility are significantly lower than  $^{226}\text{Ra}$ . The share of available (the sum of water-soluble and exchangeable fractions) and mobile fractions (the sum of water-soluble, exchangeable and own mobile fractions) for  $^{232}\text{Th}$  is 3-10 times less than for  $^{226}\text{Ra}$ .

In the eluvial horizon, nodules accumulate 1.1 times more of  $^{226}\text{Ra}$  and 1.5 times more of  $^{232}\text{Th}$ , than the soil mass. For  $^{226}\text{Ra}$  in nodules, an increase in the content of the water-soluble, exchangeable, mobile, and acid-soluble fractions is observed, with a decrease in the activity of the residue fraction. For  $^{232}\text{Th}$ , the content of mobile and acid-soluble fractions and the residue fraction increases, while the activity of water-soluble and exchangeable compounds decreases.

Therefore, with respect to  $^{232}\text{Th}$ , segregation concretions of the eluvial horizons of the Albic Stagnic Retisol act as a geochemical barrier, reducing its mobility in the soil profile. A significant part of  $^{232}\text{Th}$  is firmly fixed inside the crystal lattices of the newly formed well-crystallized minerals.

**Acknowledgments:** This study was supported by the Russian Foundation for Basic Research, project no. 18-04-00584 A.

## **Geological and non-geological aspects in the context of geological radioactive waste disposal**

**Liliana Petrenko**

Institute of Geological Sciences of the National Academy of Sciences of Ukraine, Kyiv, Ukraine

The problem of radioactive waste disposal occurs almost simultaneously with the beginning of the use of nuclear energy. In Ukraine, the use of nuclear energy began in the fifties of the last century. Radioactive waste (RW) is formed as a result of operations of the nuclear fuel cycle in the generation of electricity, as well as in other activities that use radioactive substances.

In Ukraine the activities to develop a deep geological repository (DGR) have been carried out since 1993. They are performed by Institutes of the National Academy of Sciences of Ukraine (NASU), Universities, State Specialized Enterprises of State agency for Management of Exclusion Zone (SAMEZ), the enterprises of the State Geological Survey (SGS), and by international organizations and consortia.

In recent years Ukraine has made significant progress in developing advanced safety case methodology for radioactive waste geological disposal. Results of preliminary safety assessments demonstrate suitability of crystalline rocks in the Chernobyl Exclusion Zone for waste geological disposal, as well as urgent necessity of detail field investigations (including drilling) within the promising areas. Disposal of the radioactive waste is a complex task. In addition to scientific geological studies, a significant part of the solution to such a task falls on legislation, work with the public, technical base and much more.

The purpose of this analysis is to distinguish scientific research from the tasks of other organizations and to demonstrate the complexity of creating a geological repository. This will serve as a benchmark for further scientific research for organizations involved in the disposal of radioactive waste.

## **Pb-210, Be-7 and Cs-137 in lichens, mosses and pine needles of the south of Western Siberia**

**Mikhail Melgunov, Kseniya Mezina, Boris Shcherbov,  
Yulia Vosel, Inna Zhurkova, Maksim Rubanov**

IGM SB RAS, Novosibirsk, Russia

According to studying of fruticose lichens, mosses and pine needles, an assessment of average concentrations of Pb-210, Be-7 and Cs-137 were calculated for the territory of the South of Western Siberia (Bq/m<sup>2</sup>).

For forest-steppe zone:

- Site I (May 2017, after full snowmelt): lichens – 571, 121, 6; mosses – 1178, 149, 12; needles – 49, 57, 5.

- Site II (May 2017, after full snowmelt): lichens – 964, 158, 16; mosses – 1233, 190, 43; needles – 45, 65, 5; (October 2017, before snow cover): lichens – 818, 280, 11.

- Site III (July 2017): lichens – 1733, 403, 31; mosses – 696, 236, 28.

For mountain-taiga and Alpine zones of Altai Republic (June 2017, Site IV): lichens – 1173, 487, 46; mosses – 1002, 504, 23; needles – 36, 103, 2.

The submitted data show nonuniformity of Pb-210 and Be-7 deposition in the territory of the South of Western Siberia both on absolute values, and on their accumulation in various components of a biogeocenosis. For a forest-steppe zone surface activity (Bq/m<sup>2</sup>) of Pb-210 in lichens considerably differ from those in mosses. In the site III it is nearly 2.5 times higher in lichens. In the sites I and II, located at a greater distance from Altai mountain system, the inverse ratio is observed: 0.8 – 0.5. In the mountain-taiga and Alpine zones Pb-210 concentrations in lichens is nearly 1.2 times higher, than in mosses. Unlike Pb-210, Be-7 surface activities in lichens and mosses are nearly equal. Lichen/moss ratios here are varied from 0.8 (site I and II) to 1 (site IV). Behavior of Be-7 in the site III is drastically different. Here, as well as in a case of Pb-210, beryllium concentration in lichens is nearly 1.7 times higher.

The Be-7 and Pb-210 activities ratio is quite informative indicator. Despite significant difference in absolute values, this indicator for lichens and mosses within one site has close values. Within the forest-steppe zone the Be-7/Pb-210 ratios in the lichens and mosses which were sampled in the spring period right after snow melting range from 0.23 to 0.13. This range can be considered inherited from the winter period. For the lichens and mosses which were sampled in the summer and late autumn the Be-7/Pb-210 ratios have higher values and vary in the range from 0.34 to 0.23. The highest values of the Be-7/Pb-210 ratios correspond to the lichens and mosses sampled in summertime in the mountain-taiga and Alpine zones – 0.42 to 0.5. Unlike lichens and mosses in young, annual needles there is dominance of Be-7. Within a forest-steppe zone the values of Be-7/Pb-210 ratios in needles are 1.16-1.44, in mountain-taiga – 2.9. Lower values of Be-7/Pb-210 ratios in lichens and mosses can be explained by effect of accumulation of Pb-210 due to its rather long half-life (22 years) and significant life time of lichens and mosses.

**Acknowledgments:** This study was carried out as a part of a governmental contract (Project 0330-2016-0011) with additional support by grant 17-05-41076 RGO\_a from the Russian Foundation for Basic Research.

## **Optimization of nutrient ratio in Hoagland solution to improve the capability of rapeseed (*Brassica napus* L) to decontaminate water from pollution of radioactive cesium isotopes in hydroponic condition**

**Fabio Girardi, Maria Letizia Cozzella, Donatella Ferri, Nadia Cherubini**

ENEA – Italian National Agency for New Technologies, Energy and Sustainable Economic Development,  
Rome, Italy

Phytoremediation is a process that uses plants to remove, transfer, or immobilize polluting substances and radionuclides from the contaminated soil, sediment, sludge, or water, and it is a useful method for treating large-scale low-level radionuclides contamination.

It is an in situ biological treatment method, which refers to the use of plants to reclaim the environment. It offers a great advantage in terms of cost compared to physical or chemical treatment. The effectiveness of one species for phytoremediation depends on its ability to tolerate the relatively high concentration of metals.

The aim of this work is to find the best ratio K/Cs to maximize the Cesium isotopes assumption of Rapeseed (*Brassica napus* L.) in contaminated water. To do that, *Brassica napus* plants have been grown in hydroponic condition using a modified Hoagland solution as growing medium.

Rapeseed has been selected for its well-known ability to accumulate high levels of Cs almost entirely inside biomass, producing oil with a Cesium low transfer factor suitable for the production of biodiesel.

Plants of *Brassica napus* will be grown in a hydroponic system and nourished with a type 1 Hoagland solution in which different amounts of CsCl have been added. The distribution of this element into the different part of the plants (roots, seeds, stem and leaves) and into the growing solution will be quantified through microwave plasma atomic emission spectrometer (MP-AES) measurements.

The proposed experiment aims at finding the best condition to increase the uptake of Cesium in Rapeseed plants changing, in the growing media, the concentration of the macronutrients. Strategy of using crop plants for phytoremediation is a promising approach, since this type of plants are easily cultivated and fairly fast growing.

## Measurements of natural radioactivity in soil of Buyukcekmece (Istanbul-Turkey)

Osman Günay<sup>1</sup>, Serpil Aközcan<sup>2</sup>

<sup>1</sup> Istanbul Okan University, Istanbul, Turkey

<sup>2</sup> Kırklareli University, Kırklareli, Turkey

The soil, rocks and minerals in the earth's crust contain naturally occurring radionuclides. These natural radioactivity (<sup>226</sup>Ra, <sup>232</sup>Th and <sup>40</sup>K) concentrations in the world vary from region to region and determine the level of background radioactivity in the world.

In this study natural radionuclide activity concentrations in soil samples from 5 different sampling stations in Buyukcekmece district of Istanbul have been measured using gamma spectroscopy (HPGe detector).

The activity concentrations of <sup>226</sup>Ra, <sup>232</sup>Th, <sup>40</sup>K in soil samples varied from 21.17 to 28.09 Bqkg<sup>-1</sup> with a mean of 25.52 Bqkg<sup>-1</sup>, 20.32 to 36.79 Bqkg<sup>-1</sup> with a mean of 27.62 Bqkg<sup>-1</sup> and 442.40 to 555.66 Bqkg<sup>-1</sup> with a mean of 497.36 Bqkg<sup>-1</sup>, respectively. The radiological hazards (radium equivalent activity (R<sub>aeq</sub>)), absorbed gamma dose rate (D), annual effective dose equivalent (AEDE) and excess lifetime cancer risk (ELCR) varied from 87.09 Bqkg<sup>-1</sup> to 125.80 Bqkg<sup>-1</sup>, 42.16 nGyh<sup>-1</sup> to 60.25 nGyh<sup>-1</sup>, 0.052 mSvy<sup>-1</sup> to 0.074 mSvy<sup>-1</sup>, 0.181\*10<sup>-3</sup> to 0.259\*10<sup>-3</sup>, respectively.

**Keywords:** Natural radioactivity, soil, Buyukcekmece

## The artificial isotope distribution in substrate–plant system: The design of rhizobox for laboratory and nature experiments

**Marya Kropacheva**

Sobolev Institute of Geology and Mineralogy SB RAS, Novosibirsk, Russia

The artificial isotopes distribution in “bulk soil – rhizosphere – plant roots – plants upper parts” system and hydrological regimes of floodplain biogeocenoses influence estimation are of significant interest of radioecology. One of the approaches to this problem is an experimental set up in laboratory and nature; correct design of a rhizobox is prerequisite for proper statement of the question.

The design of rhizobox developed by Youssef and Chino (1988) was used as a basis. With slight modification its design is widely used for laboratory and nature experiments (Youssef and Chino, 1988, 1989; Wang et al. 2002; Li et al, 2008; Neumann et al., 2009; Hafner et al., 2014; Koop-Jakobsen and Wenzhöfer, 2015), including experiments with plants, which, as our model plant (*Carex L.*), grew in morphologically and ecologically similar conditions and have similar root system structure (Luo et al., 2018).

The main issue was the selection of the rhizobox size. Our methods of determination of isotopes content ( $\gamma$ -spectrometry analysis and  $\beta$ -spectrometry analysis with radiochemical samples preparation) require quite large aliquot volume (50-200 g) for the methods' error minimization, and parallel measurements of several aliquots with following averaging of the results for minimization of random error because of irregularity in the isotopes' distribution in the substrate samples (Sukhorukov et al., 2000; Kropacheva et al., 2011). The original size of rhizobox provides 500 g of the substrate samples average mass, which is not enough for obtaining the right amount of aliquots. Our methods require 1000 g of substrate for one sample, which demands increasing the rhizobox size from 2300 cm<sup>3</sup> to 4000-4500 cm<sup>3</sup>. However, such increase of the volume may change the distribution pattern of the rhizosphere zones. The most logical way is to increase the width of the rhizobox. Aside from getting the necessary sample volume with minimum distortion of the distribution pattern of the rhizosphere zones, it will allow to conduct experiments on several plants put in side by side, which contributes to, first, random error minimization of individual plant metabolism differences, and, secondly, approximation to the natural vegetation conditions. Depending on the model of the hydrological regime (high flood, minimum flood, low water flow period), the income of water in the substrate will occur either through the open top, or from the one of the side compartments, or by drip from above. For the first two ways of the water income, the holes are designed at the bottom of the side rhizobox walls for removing the excess of water. For the nature experiment, the rhizobox design provides perforation not only in the middle compartment bottom, but also in the walls of side compartments for best interaction between rhizobox content and environment.

**Acknowledgments:** The work is done on state assignment of IGM SB RAS and is partly support by RFBR Grants 18-05-00953.

## Decision support system on radioactive consequences of wildfires in Chernobyl Exclusion Zone (Belarus)

**Alexander A. Dvornik<sup>1</sup>, Alexander M. Dvornik<sup>2</sup>, Sergey Gaponenko<sup>1</sup>, Natalia Shamal<sup>1</sup>, Raisa Korol<sup>1</sup>, Alesya Bardyukova<sup>1</sup>, Veronika Seglin<sup>1</sup>**

<sup>1</sup> Institute of Radiobiology of National Academy of Sciences of Belarus, Gomel, Belarus

<sup>2</sup> Gomel State University, Gomel, Belarus

Among natural emergencies, forest fires are one of the most harmful disasters. It is on a special interest for Belarus because of radioactive contamination. Resuspension of long-lived radionuclides with smoke aerosols during biomass burning can cause additional internal exposure for people in the area of fire. It also cause a big social and psychological stress.

The overall aim of the current research is to develop a special decision supporting system (DSS) based on the experimental data of long-lived radionuclides behavior in the air during forest fires, spatial information on fire risks and exposure dose prediction.

**Materials and methods.** The methodology is based on experimental data on long-lived radionuclides release during forest fires, mapping and modelling. It is also includes a programming methods.

The DSS is a decision supporting system called Forest Fire GIS Application. It is based on the MapWinGIS – a free and open source geographic information system programming ActiveX Control and application programmer interface (API) that can be added to a Windows Form in Visual Basic, C#, Delphi, or other languages that support ActiveX. To build Forest Fire application we used Borland Delphi environment.

**Results.** The level of forest fire hazard in Republic of Belarus is estimated by scale based on weather conditions. The scale includes five classes, where the first class is the most dangerous. We used forest fire hazard scale to estimated fire risks at contaminated areas.

The software complex Forest Fire GIS App allows to calculate the risk of fires in contaminated areas, the parameters of radionuclide transfer with smoke aerosols, additional exposure doses for firefighters and for population. Visualization of the results occurs using the GIS module MapWinGis. For the moment DSS Forest Fire GIS App performed by a demo version installation package for Windows OS.

**Conclusions.** DSS is a tool for all responsible authorities to reduce amount of wildfires at contaminated areas, and consequently, reduce a risks of additional internal exposure for firefighters, social and physiological stress.

The Forest Fire DSS is integrate all available spatial information on fire risks, mathematical models of radionuclides migration and exposure dose prediction, and potential threat of fire for nearest infrastructure.

The system addresses the problem of protection of fire fighters, local population and environment on different implementation levels such as administrative or regional levels.

## Estimation of radiation dose rate to fish occupying different ecological zones in water bodies within the Chernobyl Exclusion Zone

**Dmitri Gudkov<sup>1</sup>, Alexander Kaglyan<sup>1</sup>, Sergey Kireev<sup>2</sup>,  
Ludmila Yurchuk<sup>1</sup>, Vladimir Belyaev<sup>1</sup>, Alexander Nazarov<sup>2</sup>**

<sup>1</sup> Institute of Hydrobiology of the NAS of Ukraine, Kiev, Ukraine

<sup>2</sup> SSE "Ecocentre", Chernobyl, Ukraine

During 2012-2018 the characteristics of radionuclide concentration and absorbed dose rate of ionizing radiation for the common rudd (*Scardinius erythrophthalmus* L.), common roach (*Rutilus Rutilus* L.), perch (*Perca fluviatilis* L.) and Prussian carp (*Carassius gibelio* Bloch) from water bodies within the Chernobyl Exclusion Zone (CEZ) have been studied.

The main dose-forming radionuclides for fish in water bodies within the CEZ are <sup>90</sup>Sr and <sup>137</sup>Cs. The highest values of the specific activity of <sup>90</sup>Sr were found in fish of Glubokoye Lake (located at the left-bank flood lands of the Pripyat River) – 6460-30090 Bq kg<sup>-1</sup> (wet weight). By the average values of <sup>90</sup>Sr concentration, the studied species of Glubokoye Lake can be placed in the following series (Bq kg<sup>-1</sup>): Prussian carp (17220) > common rudd (15330) > roach (12390) > perch (9620). Specific activity of <sup>137</sup>Cs in lake fishes is recorded within 1590-31860 Bq kg<sup>-1</sup>. Average concentration of <sup>137</sup>Cs for different species fish from Glubokoye Lake form the following row (Bq kg<sup>-1</sup>): perch (7870) > common rudd (5860) > Prussian carp (3450) > roach (2650). Average specific activity of <sup>90</sup>Sr and <sup>137</sup>Cs for the common rudd from Dalyokoye Lake during the research period was 7460 and 2650 Bq kg<sup>-1</sup>, respectively. The fish of the Chernobyl NPP (CNPP) cooling pond were characterized by the following ranges of the specific activity of radionuclides: <sup>90</sup>Sr – 40-420; <sup>137</sup>Cs – 670-10900 Bq kg<sup>-1</sup>. The following values of radionuclide concentration are recorded for the fish of the Yanovsky Backwater: <sup>90</sup>Sr – 620-11660; <sup>137</sup>Cs – 430-6040 Bq kg<sup>-1</sup>. The ranges of specific activity of <sup>90</sup>Sr and <sup>137</sup>Cs for fish in lakes with background levels of radioactive contamination were 0.4-5.0 and 4.0-110.0 Bq kg<sup>-1</sup>, respectively.

The mean values of the absorbed dose rate for fishes of the CEZ during the research period were: for the common rudd – 6.5, 7.4 and 54.1 μGy h<sup>-1</sup> in Dalyokoye Lake, cooling pond and Glubokoye Lake, respectively; for the roach – 8.7, 17.4 and 67.3 μGy h<sup>-1</sup> in Yanovsky Backwater, cooling pond and Glubokoye Lake, respectively; for the perch – 7.8, 10.9, 66.4 μGy h<sup>-1</sup> in Yanovsky Backwater, cooling pond and Glubokoye Lake, respectively; for the Prussian carp – 16.9, 36.3, 84.5 in the cooling pond, Azbuchin Lake and Glubokoye Lake, respectively. For fish of reference reservoirs, the absorbed dose rate did not exceed 0.07 μGy h<sup>-1</sup>.

External irradiation of investigated fish species in standing water bodies is usually formed by <sup>137</sup>Cs, which is deposited in the bottom sediments of reservoirs. Thus, up to 80% of the annual dose of external irradiation of fish can be obtained in the winter period when located on the pits near or directly in the bottom sediments. The contribution of <sup>137</sup>Cs to the internal dose rate due to incorporated radionuclides in the tissues is 10-40%. Due to incorporation of <sup>90</sup>Sr in tissues about 60-90% of the internal dose rate of irradiation of fish is formed. Thus, in this period <sup>90</sup>Sr can be considered as the main radionuclide, which forms the internal dose of irradiation of fish in standing water bodies of the CEZ.

## Abnormalities of the postcranium skeleton of juvenile fish from lakes within the Chernobyl Exclusion Zone

Christina Ganzha<sup>1</sup>, Dmitri Gudkov<sup>1</sup>,  
Igor Abramiuk<sup>1</sup>, Vladyslav Pavlovsky<sup>2</sup>, Oleksandr Kaglyan<sup>1</sup>

<sup>1</sup> Institute of Hydrobiology of the National Academy of Sciences of Ukraine, Kyiv, Ukraine

<sup>2</sup> National Aviation University, Kyiv, Ukraine

Indicators of the diversity and occurrence of morphological abnormalities in the development of fish are a peculiar response to the force of both genetic and environmental factors. Skeletal disorders are one of the problems in the development of fish and they can affect morphology, growth and survival. The incidence of skeletal deformities can be used to evaluate and monitor the negative effects exerted on fish on the initial stages of its development. The research on the diagnosis of morphological anomalies, as well as the assessment of their diversity and occurrence of juvenile fish in the radioactive contaminated aquatic ecosystems of the Chernobyl Exclusion Zone (ChEZ) were not carried out.

The purpose of the study was to identify and evaluate the qualitative and quantitative characteristics of the main forms of abnormalities of skeletal development in juvenile fish from the most contaminated lakes of the ChEZ.

All specimens were cleared and stained for bone with alizarin red following the method of T. Potthoff (1984). Juvenile fish samples were represented by D<sub>2</sub>, G, and F stages. The study was conducted in Glyboke and Azbuchyn lakes within the ChEZ as a comparative study of fish from Pidbirna Lake near Kyiv City with background levels of radioactive contamination. The samples of the European bitterling (*Rhodeus amarus*) from lakes Pidbirna and Glyboke and sunbleak (*Leucaspis delineatus*) from lakes Pidbirna and Azbuchyn were studied.

The main radiation exposure for fish in the ChEZ water bodies is mainly formed by <sup>90</sup>Sr and <sup>137</sup>Cs. Absorbed dose rate for non-predatory fish in Glyboke Lake on the average depth was about 58 μGy·h<sup>-1</sup> in Azbuchyn Lake – 36 μGy·h<sup>-1</sup>. For fish from reference lake, the absorbed dose rate did not exceed 0.07 μGy·h<sup>-1</sup>

Among the observed anomalies in juvenile fish from Glyboke Lake, predominance of disorders of the structure of the elements of the caudal and abdominal sections was noted. Such anomalies as additional processes of neural arches, partial or total vertebral fusions, deformation of the last vertebra of the tail section, and also deformation of the ribs have been found. In the investigated specimens of juvenile *R. amarus* from reference lake no significant skeletal anomalies were detected. In the juvenile fish of Glyboke Lake, such anomalies as deformations of the last vertebra of the tail section (44%) and additional branches of the neural arch (36%) predominated.

In juvenile fish *L. delineatus* from reference lake anomalies were found in less than 15% of individuals. The anomalies such as deformation of the last vertebra of the tail section (36%) and additional processes of the neural arches (31%) were predominant in the fishes of Azbuchyn Lake, as well as significant deformations of the ribs (18%).

As a result of the research, four types of anomalies localized in two sections of the skeleton were diagnosed. The individual spectrum of anomalies did not exceed two anomalies per specimen.

## Atmospheric dispersion modeling of radionuclides around nuclear facilities in Serbia

**Vesna Radumilo<sup>1</sup>, Ivan Knežević<sup>1</sup>, Dalibor Arbutina<sup>1</sup>, Boris Lončar<sup>2</sup>**

<sup>1</sup> Public Company, Belgrade, Serbia

<sup>2</sup> University of Belgrade Faculty of Technology and Metallurgy, Belgrade, Serbia

Part of the monitoring of radioactivity around nuclear facilities in the Public Company “Nuclear Facilities of Serbia” implies the examination of the radiation field in the environment. This also includes mathematical modeling of dispersion of radionuclides emitted into the atmosphere. In order to assess the influence of nuclear facilities, air pollution dispersion model, developed in the Public Company “Nuclear Facilities of Serbia”, is used. This paper presents the results of the mathematical modeling in the first part of 2017, for the calculation domain 9.69 km to 5.62 km, as the graphical representation of the relative concentration fields for the location of nuclear facilities. The results of mathematical modeling show that there were no elevated values of concentration of radioactive pollutants in the terrestrial boundary layer of the atmosphere, in the specified period.

## Definition of air pollution

**Shafiga Topchiyeva<sup>1</sup>, Matanat Mehrabova<sup>2</sup>**

<sup>1</sup> Institute of Zoology of Azerbaijan National Academy of Sciences, Baku, Azerbaijan

<sup>2</sup> Institute of Radiation Problems of Azerbaijan National Academy of Sciences, Baku, Azerbaijan

The purpose of this work was a qualitative and quantitative assessment of atmospheric air pollution by heavy metals in order to study regional and local pollution of both air, soil and the waters of the studied area by environmental polluters during biomonitoring of biosphere pollution.

We studied samples of moss, soil and water (near Dashkesen region, Azerbaijan) to identify the bioindicator properties of moss and for bioindication of air, soil and water.

The concentrations of heavy metals were determined on an AgilentTechnologies 7500 SeriesICP-MS (7500cx) instrument using inductively coupled plasma mass spectrometry (ICP-MS, USA).

The content of heavy metals in samples of moss, soil and water, which amounted to samples of moss in mg / kg: Cr (28.5590), Mn (510.1783), Fe (16488.8129), Cu (14.9127), Zn (27.0134), Cd (0.1138 ), Ba (164.9149) and Pb (5.1229); for soil samples, Cr (15.1623), Mn (476.1827), Fe (12692.6514), Cu (12.2368), Zn (20.8277), Cd (0.1279), Ba (87.329) and Pb (4.2671), and in water samples the content is heavy metals ranged from: – Cr (0.1249), Mn (1.572), Fe (1.571), Cu (1.515), Zn (<0.0002), Cd (0.00315), Ba (19.23) and Pb (<0.0002), respectively.

## Natural and man-made aerosol activity observation at Moussala BEO

**Christo Angelov, Ilia Penev, Todor Arsov, Stefan Georgiev**

INRNE, BAS, Sofia, Bulgaria

The natural and man-made radioactivity of the air aerosols have been monitored at the Moussala Basic Environmental Observatory (BEO) on Moussala Peak (2925 m ASL) altitude for more than twelve years. The sampling techniques and radioactivity measurements involve pumping a volume of air (~15 – 20 000 m<sup>3</sup>) through a filter, than measuring the radioactivity in the filter by an HPGe detector. More than 1500 samples have thus been measured and analyzed. For most of the man-made radioactive isotopes, the minimum detectable activity is ~0.5 μBq/m<sup>3</sup>, or less. We thus have followed the seasonal fluctuations of <sup>7</sup>Be for several years. Interestingly, during the past 3-4 years, we observed a disturbed <sup>7</sup>Be distribution, namely, statistical fluctuations only, which we ascribe to a new climate dynamics established recently. In addition, the earliest and most detailed report on the arrival in South East Balkan peninsula of <sup>131</sup>I, <sup>134</sup>Cs and <sup>137</sup>Cs with air aerosols from Fukushima accident was provided by the team of Moussala BEO. The gamma-spectrometry analysis of the sample taken on Oct. 03, 2017, unexpectedly revealed the presence of the radioactive isotope <sup>106</sup>Rh. This isotope has never been observed in this region before. The most intensive gamma lines of <sup>106</sup>Rh were detected, namely, 511.8 keV, 621.8 keV and 1060.4 keV. Since <sup>106</sup>Rh has a very short half-life, it was logical to assume that its presence is due to the decay of <sup>106</sup>Ru, which, not being a gamma-emitter, was not identified in the gamma-spectra acquired. Latter the same isotope was found in some plants around the Moussala BEO. This isotope usually is used for medical purposes. So far, no credible explanation has been advanced of this isotope's appearance in the atmosphere in Moussala Peak vicinity. One of the probable sources could be an accident in a nuclear installation in Russia.

## **Determination of gamma-emitting radionuclides in soil sample for the purposes of proficiency test IAEA-TEL-2018-04 ALMERA**

**Marija Lekić<sup>1</sup>, Nataša Lazarević<sup>1</sup>,  
Nevena Zdjelarević<sup>1</sup>, Dalibor Arbutina<sup>1</sup>, Boris Lončar<sup>2</sup>**

<sup>1</sup> Public Company “Nuclear Facilities of Serbia”, Belgrade, Serbia

<sup>2</sup> Faculty of Technology and Metallurgy, University of Belgrade, Belgrade, Serbia

Proficiency test for members of Analytical Laboratories for the Measurement of Environmental Radioactivity Network (ALMERA) on the determination of gamma emitting radionuclides in soil sample was organized by International Atomic Energy Agency (IAEA) in 2018. Purpose of the proficiency test was to estimate analytical performance of participating laboratories. This paper presents results of gamma spectrometry measurements, simple procedures and techniques used for efficiency calibration standard preparation together with experimentally determined efficiency curve for used geometry and matrix material. Therefore, efficiency calibration standard has been prepared using certified mixed radionuclide standard solution which was incorporated into soil matrix material. Results of gamma-spectrometric determination of radionuclides in soil sample and analytical performance evaluation are discussed.

## Evaluation of genomic alterations in *Cladosporium cladosporioides* with radioadaptive properties

**Tetiana Tugai<sup>1</sup>, Lubov Zelena<sup>2</sup>,  
Andrey Tugai<sup>2</sup>, Olena Polischuk<sup>3</sup>, Natalia Sergeichuk<sup>4</sup>**

1 Open International University of Human Development 'Ukraine', D.K. Zabolotny Institute of Microbiology and Virology of the NASU, Kiev, Ukraine

2 D.K. Zabolotny Institute of Microbiology and Virology of the NASU, Open International University of Human Development 'Ukraine', Kiev, Ukraine

3 National Technical University of Ukraine "Igor Sikorsky Kyiv Polytechnic Institute", Kiev, Ukraine

4 Open International University of Human Development 'Ukraine', Kiev, Ukraine

The process of realization and unfolding of adaptive mechanisms to adverse environmental factors including ionizing radiation in microorganisms is still not completely understood. To study the directional growth of fungi to the radiation source, a number of model systems were created to evaluate the expression of effect and the dose of ionizing radiation at which it was observed. The performed analysis of the influence of ionizing radiation on soil microscopic fungi isolated from the Chernobyl Exclusion Zone showed that a significant number of studied fungi possessed radioadaptive properties involving both the ability to directional growth (positive radiotropism) and the stimulation of growth processes at small (1 Gy) and at high (800 Gy) doses of irradiation. The fungi with radioadaptive properties displayed changes of physiological and biochemical features although no morphological changes were detected. There were set up several hypotheses of the radioadaptation mechanism involving genetic alterations that facilitate the microorganism survival under irradiation treatment. Among them induction of DNA structural changes such as mutations, reorganization of nucleotide sequences and increasing of genomic polymorphism.

The present research was carried out as a comparative analysis between *Cladosporium cladosporioides* strain isolated from radioactively contaminated areas and displaying radioadaptive properties and *C. cladosporioides* strain isolated from the "clean" unexposed soil and not showing radioadaptive properties.

To assess genomic alterations that could promote radioadaptive properties genomic fingerprinting that is widely used for species identification and in the study of organisms' genetic diversity was carried out. Amplification with microsatellite primer M13 and DNA of two *C. cladosporioides* strains was performed. Results of comparative analysis between DNA-fragment profiles obtained in two strains it has been revealed the amplicon patterns consisting of five bands with size range 200 – 600 bp and they were the same for both strains. Thus, detection of identical DNA profiles generated by M13-PCR may assume involvement of epigenetic constituents in the adaptation mechanism to ionizing radiation.

## Beryllium-7 in six fish species from the Bay of Boka Kotorska

Ivanka Antović<sup>1</sup>, Nikola Svrkota<sup>2</sup>, Nevenka Antović<sup>3</sup>

<sup>1</sup> Department for Biomedical Sciences, State University of Novi Pazar, Novi Pazar, Serbia (\*Present address: Krupačka 1, Nikšić, Montenegro), Nikšić, Montenegro

<sup>2</sup> Centre for Ecotoxicological Research, Podgorica, Montenegro

<sup>3</sup> University of Montenegro, Faculty of Natural Sciences and Mathematics, Podgorica, Montenegro

The six fish species – gilt-head sea bream, hake, European seabass, golden grey mullet, leaping mullet and thinlip grey mullet – were analyzed on radioactivity due to cosmogenic Be-7. All the specimens had been collected in the Bay of Boka Kotorska, using the trawl net. The results presented in the paper are obtained in the period 2013–2015, and some of them – in 2018. Fish muscles (32), whole mullet individuals (6) and gastrointestinal systems (6) – were analyzed using the HPGe spectrometry, together with samples of seawater and *bottom* (containing sand, mud and mussels) from the same locality (Boka Kotorska Bay). In seawater, activity concentration of Be-7 was found to be 0.05 Bq/L, whilst in the bottom sample – 6.7 Bq/kg. The leaping mullet muscles showed the Be-7 activity concentrations less than 7 Bq/kg, European seabass:  $\leq 8.24$  Bq/kg, gilt-head sea bream and golden grey mullet:  $\leq 11$  Bq/kg, thinlip grey mullet:  $< 14$  Bq/kg, and hake:  $\leq 14.1$  Bq/kg. Whole mullet individuals showed higher activity concentrations of Be-7 (higher than 12 Bq/kg for leaping mullet and golden grey mullet), and particularly gastrointestinal systems (34.9 Bq/kg in the case of thinlip grey mullet). Concentration factors for Be-7 from seawater and *bottom* to fish are also calculated, as the ratio of its activity concentration in wet wt fish sample and in seawater, or in dry *bottom* sample. The highest factor for Be-7 from seawater was found to be 698 in the case of one thinlip grey mullet gastrointestinal system, which also showed the highest concentration factor from the *bottom* (5.21).

## Climate change reconstruction for modern warm period in north of Romania by using $^{210}\text{Pb}$ chronology

**Robert-Csaba Begy<sup>1</sup>, Daniel S. Veres<sup>2</sup>, Szabolcs Kelemen<sup>3</sup>**

1 Interdisciplinary Research Institute on Bio-Nano-Science, Babeş-Bolyai University, Cluj-Napoca, Romania

2 Romanian Academy, Institute of Speleology, Cluj-Napoca, Romania

3 Babes-Bolyai University, Faculty of Environmental Science and Engineering, Cluj-Napoca, Romania

Climate Variability became more visible and get a deal of attention in recent years. The late Holocene (last ca. 1400) encompasses some of the most striking variability events and/or alternations of climate that are claimed to be of importance in human history. These are the Dark Age Cold Period, the Medieval Climate anomaly, the little Ice Age and the Modern Warm Period. The Modern Warm Period (MoWP) is considered since the industrial revolution at 1850s, a warm shift has been predominant, and caused mainly by human-induced greenhouse gas emission, and characterized by fast glacial melt and extreme weather conditions, around the globe. The presented study has main goal to reconstruct the variation occurred in the climate in North part of Romania during the MoWP. The perfect environments for climate reconstruction are the peat bog accumulations which grow rate are directly correlated with climate variations. Four peat bog deposits was chose for investigation from Gutiiului Mountain (Maramures county, Romania). Peat samples were taken and (Loss of Ignition) LOI investigation was done for separation the organic material from the inorganic part. Radionuclide measurements ( $^{210}\text{Pb}$ ,  $^{226}\text{Ra}$ ,  $^{137}\text{Cs}$ , and  $^7\text{Be}$ ) were made by using gamma spectrometry with a HPGe Well-type detector. By using the  $^{210}\text{Pb}$  chronology each layer from the peat bog column was dated, and with organic material data the grow rates were calculated. The obtained grow rates reflects the changes between the humid and warm and dry could periods. In this moment the investigation is still in progress, final results will be present during the conference.

## Studies on the effects of land use changes on soil erosion and increased sedimentation using radionuclides

**Robert-Csaba Begy<sup>1</sup>, Szabolcs Kelemen<sup>2</sup>,  
Daniel S. Veres<sup>3</sup>, Timea Sandor-Nagy<sup>2</sup>**

1 Interdisciplinary Research Institute on Bio-Nano-Science, Babeş-Bolyai University, Cluj-Napoca, Romania  
2 Babeş-Bolyai University, Faculty of Environmental Science and Engineering, Cluj-Napoca, Romania  
3 Romanian Academy, Institute of Speleology, Cluj-Napoca, Romania

Vulnerability of the soil to human induced erosion processes varies in time and space depending on the climate, geology, type and term of land use. Scientific-based current state of knowledge on anthropic impact on forested areas in Romania is limited. For highlighting the environment erosion process and for reconstructing these processes for the recent past, aquatic sediments are the perfect environment.  $^{210}\text{Pb}$  dating method is a valuable tool for studying the sedimentation rates of lakes over the last 150 years. Variable sedimentation rates in lake catchments are indicative for changes in land use.  $^{210}\text{Pb}$  dating method has been previously applied for the quantification of the effects of land use in other international studies, but such an approach has not been attempted so far in our country. Based on our previous experience with  $^{210}\text{Pb}$  dating method as well as natural radioactivity in general, in the current proposal we will investigate lacustrine sediments from Retezat and Parang Mountains, Carpathian Mountains, as well as from Transylvanian lowlands. Sedimentation rates will be quantified by  $^{210}\text{Pb}$  method and radionuclides such as  $^{210}\text{Pb}$ ,  $^{137}\text{Cs}$  and  $^7\text{Be}$  will be used as tracers to highlight the effects of land use changes. Additionally, we propose a multi-proxy interdisciplinary approach which includes detailed geochemical and geophysical analyses of classic sediment input (XRF, magnetic susceptibility, LOI, trace metals) and detailed analysis of paleo-ecological proxies (pollen, micro and macro charcoal). This combined radiometric dating/multi-proxy approach surmounts limitations of the traditional approach of separate identification of the sediment components based on the sedimentation rate modification when only chronological proxies are used, leading to the development of a laboratory procedure and a mathematical model for identification, separation and quantification of the anthropic footprints from natural climate change forcing in sedimentation processes.

## Natural and artificial radionuclides in the soil of public parks and playgrounds in Kruševac, Serbia

**Milan Tanić<sup>1</sup>, Denis Dinić<sup>1</sup>, Željko Mihaljev<sup>2</sup>,  
Brankica Kartalović<sup>2</sup>, Marko Daković<sup>3</sup>**

1 CBRN Defense Centre, Kruševac, Serbia

2 Scientific Veterinary Institute, Novi Sad, Serbia

3 University of Belgrade, Faculty of Physical Chemistry, Belgrade, Serbia

Naturally occurring radionuclides are present in all environmental compartments ever since, while manmade radionuclides have been released in the environment through nuclear weapon tests and accidental events in recent times. High content of radionuclides in soil, either naturally occurring or anthropogenic, may be a significant environmental problem, leading to potentially increased radiation hazard for man. Children are especially susceptible to this environmental risk due to their specific hand-to-mouth behavior. Urban living greatly affects quality of life in cities, thus green spaces play an important role in maintaining environmental quality, human health and wellbeing, and became places where city residents spend a significant portion of their free time. Therefore, the knowledge of the content of the radionuclides in soils of areas designated for recreation, sports activities and children playing is of vital importance for the monitoring of environment radioactivity in urban areas and represent baseline for radiological risk estimation.

The specific activity of selected radionuclides was measured in soil samples collected from eighteen most frequently visited public parks, recreation areas and children playgrounds within the City of Kruševac, one of the largest cities and industrial centers in Central Serbia. The specific activity of <sup>232</sup>Th, <sup>238</sup>U, <sup>40</sup>K and <sup>137</sup>Cs were determined by gamma-ray spectrometry, using the HPGe detector. Mean values of specific activities were found to be 39 Bq/kg for <sup>232</sup>Th, 41 Bq/kg for <sup>238</sup>U, 353 Bq/kg for <sup>40</sup>K, and 5.9 Bq/kg for <sup>137</sup>Cs. Specific activities of natural radionuclides are in good agreement with average worldwide values, and values of <sup>137</sup>Cs specific activity are similar with results published for other regions in Serbia and neighboring countries.

Chosen sampling points were evenly distributed over the city area, so the obtained results could be used for the radiological risk estimation. External exposure outdoors mainly results from gamma radiation emitted by terrestrial radionuclides from <sup>238</sup>U and <sup>232</sup>Th series and radionuclide <sup>40</sup>K. Based on their specific activities, absorbed gamma dose rate in air, the annual effective doses and excess lifetime cancer risk were calculated. The total absorbed gamma dose rate varied between 38 nGy/h and 67 nGy/h. The mean value of 56 nGy/h suits well to the world average value. The mean value of annual effective dose was 68 μSv and 78 μSv for adults and children, respectively, which is very close to world average value published by UNSCEAR (70 μSv). The excess lifetime cancer risk fell in the range  $(1.6-2.9) \times 10^{-4}$ , with mean value of  $2.4 \times 10^{-4}$ , which is slightly lower than UNESCAR worldwide average ( $2.9 \times 10^{-4}$ ).

All calculated radiation hazard indices were lower than the recommended values. Therefore, it can be inferred that the soil in investigated green urban areas in City of Kruševac, does not pose any significant radiological threat to the residents.

## Effects of long-term irradiation on cytogenetic characteristics of the common roach (*Rutilus rutilus* L.) from water bodies within the Chernobyl Exclusion Zone

N. Pomortseva, D. Gudkov, A. Kaglyan

Department of Aquatic Radioecology, Institute of Hydrobiology, Kyiv, Ukraine

Cytogenetic studies of blood cells of fish allow us to identify the indicators for assessment of physiological status of organism while diagnosing and predicting of the fish pathology development under conditions of chronic impact of low doses of ionizing radiation.

Hematological parameters of peripheral blood of the roach (*Rutilus rutilus* L.) living in water bodies within the Chernobyl NPP (CNPP) Exclusion Zone (Lake Glyboke, Yanovsky Backwater and two parts of the CNPP cooling pond) have been studied during 2017, 2018. Mean values of the absorbed dose rate (ADR) for the roach during study period equalled to 8.7, 17.4 and 67.3  $\mu\text{Gy h}^{-1}$  in above water bodies, respectively. For fish from the reference lake the ADR did not exceed 0.06  $\mu\text{Gy h}^{-1}$ .

Analysis of the roach leucograms showed changes in ratio between different groups of leucocytes with increasing of absorbed dose rate. Decreasing of lymphocytes number and increasing of granulocytes and monocytes numbers have been discovered in dose range of 0.07–67.3  $\mu\text{Gy h}^{-1}$ . Quantitative analysis of leukograms indicated significant difference ( $p < 0.05$ ) not only comparing to the reference sample, but also between water bodies within the Exclusion Zone.

Evaluation of roach erythrocytes morphology identified that diversity of forms of red blood abnormalities cells increases with increasing of ADR. Specific pathomorphological changes were found in fish erythrocytes such as deformation of nucleus, vacuolized cytoplasm, pyknosis, microcytes, cytolysis, chromatinolysis, karyorexis, micronuclei and double-nucleus cells. Average number of damaged erythrocytes equalled to 27.5% in the mostly contaminated water bodies.

In range of ADR 0.07–67.3  $\mu\text{Gy h}^{-1}$  a significant ( $p < 0.05$ ) dose dependent increasing of the number of damaged erythrocytes was identified. The damages were the following: microcytes – up to 2.3% (with absence in the reference sample); pyknosis – up to 7.1 times (from 0.9 to 6.4%); cytolysis – up to 9.3% (with absence in the reference sample). Analysis of the roach blood showed that the main abnormalities in erythrocytes were pyknosis and cytolysis; those abnormalities had been found in species from all water bodies within the Exclusion Zone. The quantity of erythrocytes with mitosis pathology (micronucleus) increased from 0.9 to 1.2% in the ADR range of 14.63–67.26  $\mu\text{Gy h}^{-1}$ .

Average number of erythrocytes with structural abnormalities and mitosis pathology equalled to 14.3 and 0.2% in Yanovsky Backwater; 14.7 and 0.9% in Chernobyl NPP cooling pond (north-west part); 23.9 and 1% Chernobyl NPP cooling pond (north-east part); 26.1 and 1.4% in Glyboke Lake, respectively.

Therefore, increase of erythrocytes number with morphological abnormalities with ADR increase was characterized as dose dependent. This can testified the decrease of fish genetic stability under conditions of chronic ionizing radiation.

## Extraction of cesium, strontium and cobalt radionuclides by titanium phosphate adsorbents from NPP complex solutions

Vladimir I. Ivanenko, Roman I. Korneikov

Tananaev Institute of Chemistry – Subdivision of the Federal Research Centre “Kola Science Centre of the Russian Academy of Sciences” (ICT KSC RAS), Apatity, Russia

Sorption method is advanced technique for NPP liquid waste purification from  $^{134}\text{Cs}$ ,  $^{137}\text{Cs}$ ,  $^{90}\text{Sr}$ ,  $^{60}\text{Co}$  radionuclides. Inorganic adsorbents based on titanium(IV) hydrophosphates have a special interest. Their functional properties depend on chemical composition. The influence of the degree of hydration of titanophosphate adsorbents and their modification by transition metal cations have other electronegativity than titanium(IV) on the ion-exchange properties of the final products have been studied.

Modifying is based on creation of hetero-polynuclear associates from interaction of titanium(IV) and oxo-hydroxo-acido complexes of transition metals derived from different acidic-basic properties. The effect of chemical composition of the modified adsorbents on textural properties, ion-exchange capacity and ion-exchange constant has been investigated. It was found that for highly hydrated adsorbents an experimental ion-exchange capacity is close to theoretical calculated from content of functional  $\text{HPO}_4$ -group. Dehydration of the adsorbents led to decrease in ion-exchange capacity and increase in the ion-exchange constant. The effect of the adsorbed cation nature on the ion-exchange capacity and the ion-exchange constant was studied.

It has been shown that modified titanium-zirconium-phosphate adsorbent can be granulated without any binder agents forming mechanically and hydrolytically strong particles.

Elevation of ion-exchange process temperature results in increase of ion-exchange constant as well as uptake of low-hydrated cations. The ion-exchange process is described by intra-diffusion kinetics.

The increase in ion-exchange constant value can be explained by structural ordering of the titanium phosphate matrix during dehydration which is followed by polarization of ionogenic hydrophosphate groups and increases in the proton mobility. The affinity of adsorbed cations to titanium phosphate due to electrostatic interaction and polarization effects.

The modified adsorbents can be used for liquid radioactive wastes purification from radionuclides  $^{134,137}\text{Cs}$ ,  $^{90}\text{Sr}$ ,  $^{60}\text{Co}$  in present of high concentration of non-radioactive elements.

Heat treatment of spent adsorbents provides reliably immobilization of radionuclides in water-insoluble crystalline titanium phosphate matrix.

**Acknowledgments:** The research was carried out with the financial support of the Russian Science Foundation (Project No 17-19-01522).

## Natural radionuclides in soil and evaluation of their exposure in specific areas on the territory of Lithuania

**Milda Peciuliene<sup>1</sup>, Vaida Vasiliauskiene<sup>1</sup>,  
Vigilija Cidzikiene<sup>2</sup>, Dainius Jasaitis<sup>1</sup>**

<sup>1</sup> Vilnius Gediminas Technical University, Vilnius, Lithuania

<sup>2</sup> State Research Institute Center for Physical Sciences and Technology, Vilnius, Lithuania

The following three unique areas in Lithuania have been chosen for the research: Vilnius, Juodkrantė and Visaginas. Vilnius is the city with the largest population in the country which is dominated by an anthropogenic environment. Juodkrantė is characterized by a very clean environment; it is a recreation area located near the Baltic Sea and Curonian Spit which is included on the UNESCO World Heritage List. Juodkrantė has a natural environment and minimal urbanization. Visaginas is a special for the nuclear power plant (which is currently being decommissioned). It is the only nuclear power plant in the Baltic States built close to the border with Belarus on the shore of Druškiai Lake.

The specific activities of naturally occurring radionuclides  $^{232}\text{Th}$ ,  $^{226}\text{Ra}$  and  $^{40}\text{K}$  were determined experimentally in the soil samples taken from Vilnius and Juodkrantė districts and in the technogenic soil samples from the territory of Visaginas Nuclear Power Plant. Among all identified natural radionuclides, the highest level was that of  $^{40}\text{K}$ , i.e. the mean value was  $425 \pm 71$  Bq/kg, while the minimum level was that of  $^{232}\text{Th}$ , i.e. the mean value was  $3 \pm 1$  Bq/kg. The mean value of  $^{226}\text{Ra}$  specific activity was  $15 \pm 2$  Bq/kg. The contribution of the gamma radiation of each  $^{226}\text{Ra}$ ,  $^{232}\text{Th}$  and  $^{40}\text{K}$  (separately) on the external equivalent dose rate (EDR) was calculated. The EDR level in Vilnius city varied from 43 to 98 nSv/h. The highest EDR levels caused by gamma radiation were measured above asphalt surfaces, concrete surfaces and structures. The lower EDR levels were found in parks, above natural cellular surfaces. The EDR levels measured on the Curonian Spit varied from 22 nSv/h to 60 nSv/h. The lowest EDR levels were found on the beaches by the sea, in the sand dunes and above the forest cover. The higher levels have been measured in Juodkrantė, on the coast of the Curonian Lagoon since a major part of the coast of the Curonian Lagoon is covered by stone and special concrete embankments.

The EDR levels on the territory of Visaginas varied from 30 to 130 nSv/h. The wider distribution of the EDR values was potentially caused by the distribution of bulk soil and building materials within the research area. Having carried out the comparison with the EDR pollution on the other territories of Lithuania, it was found that the EDR level measured in Visaginas had varied within the limits of the environmental background level of Lithuania, and the measured specific activities of radionuclides are close to the measured specific activities of building materials found in other cities.

## Is there a health risk of radionuclides in drinking water from districts in Vojvodina?

Sanja Bijelović<sup>1,2</sup>, Nataša Dragić<sup>1,2</sup>, Emil Živadinović<sup>2</sup>,  
Tanja Likić<sup>3</sup>, Nataša Todorović<sup>4</sup>, Jovana Nikolov<sup>4</sup>

1 University of Novi Sad, Faculty of Medicine, Novi Sad, Serbia

2 Institute of Public Health of Vojvodina, Novi Sad, Serbia

3 Medical School, Novi Sad, Serbia

4 University of Novi Sad, Faculty of Sciences, Department of Physics, Novi Sad, Serbia

**Introduction.** In order to protect the human health from potential adverse effect of radionuclides, through drinking water, WHO recommended the determination of radionuclides concentrations in drinking water.

**Aim.** Identified trend of mean concentration of gross alpha and beta radioactivity in drinking water according to some district of region of AP Vojvodina, as well as the trend of the number of samples above the national limit value.

**Method.** In the six-year period (2013 – 2018), data of the concentrations of gross alpha and beta activity in drinking water from the territory of the three districts of AP Vojvodina (South Backa (SBD), Srem (SD) and South Banat (SBaD)) were analyzed. Cited districts are selected from the aspect of achieving a multi-annual continuity in terms of determining gross alpha and gross beta activity in drinking water. Total number of samples of drinking water in which it is determined gross alpha and gross beta activity by liquid scintillation counting technique in accredited laboratory of UNS was 141 in SBD, 140 in SD and 24 in SBaD. All samples, as well as samples with value below the laboratory limit value of gross alpha / beta activity (2%/68% in SBD, 1.4%/61% in SD and 4%/83% in SBaD) were analyzed with descriptive statistical method (average (determined deterministic), minimum, maximum and frequencies) and by linear trend regarding to average value for each examined year.

**Results.** During investigated period average value of gross alpha activity and gross beta activity was 0.06 Bq/l and 0.2 Bq/l in SBD, 0.12 Bq/l and 0.18 Bq/l in SD, 0.07 Bq/l and 0.25 Bq/l in SBaD, respectively. The value of gross alpha/beta activity in SBD, SD and SBaD ranged from <0.005/ <0.03 to 0.5/0.9 Bq/l, <0.006/ 0.028 to 1.2/0.94 Bq/l and from <0.005/ <0.03 to 0.26/0.18 Bq/l, respectively. The average annual gross alpha activity shows decreased linear trend in all district. Similar results show and average annual gross beta activity, except for SBaD. There was no exceeding national limit value for gross alpha and beta activity in SBD and SBaD. In SD there was exceeding national limit value for gross alpha activity in three samples in 2013, in two samples in 2014, and 6 samples in 2018, while there was no exceeding national limit value for gross beta activity.

**Conclusion.** Although there was decreasing trend of annual average gross alpha and gross beta activity in drinking water from several districts of AP Vojvodina, there was also increasing trend of samples with the exceeding national limit value for gross alpha activity in SD, which imply on possible risks for human health and necessity for continuous monitoring of drinking water.

**Keywords:** Drinking water, health, risk, radioactivity

**Acknowledgments:** The authors gratefully acknowledge the Provincial Secretariat for Higher Education and Science of the Autonomous Province of Vojvodina, Republic of Serbia for the financial support under the project "Radionuclides in drinking water and incidence of carcinoma in Vojvodina" No 142-451-2447 / 2018-01.



**Radiology**

**33**

## CT perfusion of endocranium

**Živorad N. Savić, Katarina Ž. Savić, Sofija Ž. Savić,  
Mirjana M. Petrović, Vladimir S. Radak, Srbislav S. Pajić, Vojislav M. Antić**

Clinical Center of Serbia, Belgrade, Serbia

For determining the functional efficacy of vascular structures of the brain parenchyma, one of the most successful diagnostic methods is perfusion CT. CT perfusion can be used to estimate collateral flow and estimates of cerebrovascular reserve, to estimate microvascular leaks in patients with intracranial neoplasms, for prognostic evaluation, and for monitoring the therapeutic response. The main limitation of CT is the risk of radiation, with frequent controls. Early detection of ischemia of non-contrast CT in the first three hours has a sensitivity of 15-20% and CT perfusion of 55-76%, while perfusion can separate the infarct into the penumbra zone. CT protocol for perfusion implies: a) non-contrast CT; b) depending on the apparatus, the coverage of the endocranium is on a single-slice 5mm; up to 80-120mm in 128-slice and 256 and over multi-slice can cover the entire endocranium; c) CT angiography with a 70 ml contrast medium and 20 ml of a physiological solution with a window from the aortic to the vertex and gives a velocity of contrast of 4-5 ml per second ; d) a post-contrast CT.

The parameter causality is represented by the formula:  $CBF = CBV / MTT$  where:

Cerebral blood flow - (CBF),

Cerebral blood volume - (CBV), and

Mean transit time - (MTT) (the most significant parameter)

The following illustration of the CT perfusion reconstruction was done: 160 slices of Toshiba CT Aquilion Prime in the Clinical Center of Serbia, Department of Emergency Radiology, for a 49-year-old patient, with view of the penumbra and ischemia.

Comparing CBV values in a circle, symmetrically, we notice the differences. If the value is 2.2-2.5 ml / 100 g or is 33% lower than the contralateral side, it is an ischemic core and if the difference is 33% it's for penumbra. Parameters are not the same for gray and white matter.

The CBF disorder value, if the rate on one side of 30 ml / 100 g / min is on a tissue that has a definite defect, and for tissues that are greater than 30 ml / 100 g / min, the possibility of having an infarct is 7%. Optimal CBF values vary from 14.1 to 35.0 ml / 100 g / min for penumbra and 4.8 to 8.4 ml / 100 g / min for infarction. As normal flow velocity values for the gray matter, values of 50-70 ml / 100 g / min and for a white matter of 20-30 ml / 100 g / min are taken. The use of the absolute CBF to define a penumbra in an acute stroke has two basic limitations. First, the threshold for penumbra can be different in gray and white matter, and second, even early after strokes, a low level of CBF below the penumbra limit can be partially reperfused and can irreversibly damaged the tissue, in which paradoxically low CBF is the result of a higher low metabolic activity.

If the MTT value is greater than 50% (> 5 seconds) on one side, it is an ischemic core, and if it's a penumbra, it's about 3-4 seconds healthy.  $MTT = CBV / CBF$  and this ratio is the same for both gray and white matter.

## Comparing kinetic imaging with conventional DSA -55% X-ray dose reduction in angiography

Milan Mijailović, Snežana Lukić

Clinical Center Kragujevac, Department of Interventional Radiology, Kragujevac, Serbia

**Purpose.** Kinetic imaging (KI) analyses pixel-intensity variations of an X-ray image series. Earlier findings indicate that KI of X-ray angiograms provide identical information to DSA, but with better signal to noise ratio. Therefore, using Kinetic imaging, the usual quality of DSA images becomes available at a lower x-ray dose.

**Materials and methods.** In the Clinical Center Kragujevac, Department of Interventional Radiology, we did a study comparing kinetic imaging with conventional DSA. The x-ray dose was reduced to maximum 0.12 mGy / frame instead of the factory setting's 2.8 mGy / frame (ALURA Philips) in the pelvic, femoral and the crural regions of 35 patients with elective angiography. We used the same contrast agent administration protocol as for the DSA and nonselective catheter position. DSA and KI images were calculated from the same series.

**Results.** Angiography specialist agreed that with 55% reduced radiation dose, the KI images were still diagnostically useful.

**Conclusion.** We can obtain fully diagnostic angiography images with 45% of the X-ray dose of the regular DSA using kinetic imaging.

**Keywords:** X-ray dose, DSA, kinetic imaging

## MR lower limb angiography, alternative to reduce radiation dose

Snežana Lukić, Milan Mijailović

Clinical Center Kragujevac, Department of Interventional Radiology, Kragujevac, Serbia

**Purpose.** To re-assess the use of Magnetic Resonance Angiography of lower limbs in our health board and compare with baseline the data gathered in 2011 and thus complete the audit cycle.

**Material and methods.** We performed a search of our Radiological Information System in Clinical Center Kragujevac, Department of Radiology over a 24 month period. For MRA requests, the clinical request information was read in order to assess whether MR was an appropriate in first line indication or what could have been performed instead. Accepted indications for MRA included poor renal function, acute limb ischaemia, femoral or popliteal aneurysmal disease, and the immediate post-operative period. Angiographies were done in MR AVANTO 1,5T Siemens.

**Results.** Between from 2012 and 2016 there has been an increase in the total amount of non-invasive lower limb angiography of 11%. In the period from 2016-2018 in Clinical Center Kragujevac, the proportion of MRA has dropped from 75%. Excluding the criteria for MR angiography: claustrophobia, pace maker, gangrene, prostheses with ferromagnetic properties.

**Conclusion.** There has been a proportional reduction in the use of DSA for the assessment of arterial disease of the lower limb which accompanies a huge increase in the total amount of non-invasive angiography. With year-on-year increases in total imaging volumes the ALARA principle and radiation stewardship becomes ever more important.

**Keywords:** MR angiography, lower limbs, reduced radiation dose

## The role of strain sonoelastography in evaluation of breast lesions - Physics, indications and diagnostic performance

Magdalena Radović

General Hospital "Euromedik", Belgrade, Serbia

**Introduction.** Sonoelastography is noninvasive, complementary, diagnostic technique that directly reveals soft tissue elasticity. Malignant breast masses are harder and show less strain compared to benign lesions following compression. Elasticity assessment consists of qualitative (Tsukuba elasticity score-TES) and semiquantitative evaluation (strain ratio between fat and lesion, SR).

**Objective.** To detect the diagnostic performance of the combined use of sonoelastographic scoring and strain ratio in differentiation of benign and malignant breast lesions with the histopathology as the standard reference and compare it with conventional sonography.

**Method.** A total of 128 breast lesions (73 malignant and 55 benign) in 125 women (mean age, 54 years, range 21-84 yrs) were enrolled in this one year prospective study, that was conducted in Clinical Center "Bezanijska kosa" in Belgrade.

Conventional US and sonoelastography (elasticity score "TES" and calculation of strain ratio "SR") were performed. B-mode images were classified according to the Breast Imaging Recording and Data System. The hardness was determined with 5-point scoring method and SRs of the lesions were calculated. Receiver operating characteristic (ROC) curves were performed and the cutoff point for differentiation of benign and malignant masses was detected.

**Results.** There was a significant difference ( $p < 0.001$ ) in the mean TES and SRs between benign and malignant breast masses. The area under the curve (AUC) for combination of ES and SR (0.874) was higher than for TES (0.863) and SR (0.820) alone. AUC for combination of B-mode US and TES (0.949) was higher than for conventional US (0.905) alone. A cutoff value of 4 for the TES when sensitivity and specificity were the highest (95% and 61.8%) allowed the best differentiation of benign and malignant breast lesions and sensitivity was 97.3%, and specificity 55.6%, when a best cutoff point of 4.27 for the SR was used.

**Conclusion.** The combined use of elasticity score and strain ratio of sonoelastography increased the diagnostic performance in distinguishing benign from malignant breast masses, but combination of sonography and TES had better diagnostic performance. Sonoelastography has demonstrated to be a promising, complementary, noninvasive technique to detect and evaluate breast lesions, and could potentially reduce the number of unnecessary biopsies.



**Radiopharmacology**

**34**

## 2-deoxy-2-[<sup>18</sup>F]fluoro-D-glucose glycoconjugates via oxime formation

**Boyan Todorov<sup>1</sup>, Iva Belovezhdova<sup>1</sup>, Outi Keinänen<sup>2</sup>, Anu J. Airaksinen<sup>2</sup>**

<sup>1</sup> Trace Analysis Laboratory, Faculty of Chemistry and Pharmacy, University of Sofia, Sofia, Bulgaria

<sup>2</sup> Radiopharmaceutical Chemistry, Department of Chemistry, University of Helsinki, Helsinki, Finland

Fluorine-18 glycosylation has become a useful tool for labeling compounds which are vulnerable to harsh reaction conditions. The introduction of a carbohydrate moiety can improve the bioavailability, in vivo kinetics, stability in blood, and accelerate clearance of biomolecules conjugated with sugar. <sup>18</sup>F-fluoroglycosylation can be achieved with several methods but it is most frequently used via oxime formation, reaction between aminoxy and carbonyl groups. [<sup>18</sup>F]FDG can be used as prosthetic group to radiolabel a wide variety of molecules by attaching an aminoxy functional group to the desired molecule. Automatization of such syntheses will reduce radiation burden and will provide the opportunity for use of GBq starting activities.

**Acknowledgments:** The present study was done within NSF "Ministry of Education and Science", project name: "Investigation on the possibilities of [4+2] cycloaddition for radiolabeling of bioactive molecules with <sup>18</sup>F-FDG by new bifunctional compounds".

## **Mechanisms of the implementation of damage to the functions of the small intestine in two generations of posterity of irradiated rats**

**Olha Storchylo**

Odessa National Medical University, Odessa, Ukraine

Interest in the effects of radiation on living organisms is not reduced. The consequences of irradiation of adult organisms are eliminated only in the 7-10<sup>th</sup> generation of their offspring. Therefore, the mechanisms for realizing the effects of irradiation of male rats on the functional activity of the small intestine of two generations of their offspring were analyzed. It has been established that nutrient hydrolysis systems are more sensitive to radiation than transport systems. Moreover, in the first generation of offspring, the effects of irradiation of the male precursor appear only for systems of hydrolysis of substrates of protein origin, and in the second generation for substrates of both protein and carbohydrate origin.



**Radiotherapy**

**35**

## **Development of inverse planning strategy using volumetric arc therapy for intensity-modulated radiation treatment for prostate cancer**

**Yong Nam Kim, Hyeong-min Joo**

Kangwon National University Hospital, Chuncheon-si, South Korea

When we consider the intensity-modulated radiation therapy (IMRT), the inverse optimization process requires a substantial amount of time. It is very effective to make a planning strategy, which considers a trade-off between target coverage/homogeneity and normal organ saving. This study intended to make an optimization strategy for IMRT planning for prostate cancer. A novel approach was proposed, which is based on the history of the optimization process, named “history-based optimization”. Firstly, we considered a step-by-step approach to obtain a clinically acceptable plan. In the first step, we obtained the best target coverage and homogeneity by using dose constraints of highest priority, regardless of the radiation damage of critical organs. In the next steps, the constraints of the critical organs were increased step by step, based on the dose volume histogram (DVH) data of the previous step. Considering a trade-off between the target coverage/homogeneity and the critical organs damage, we selected an optimal plan as the reference. As a novel approach, we deleted all the fluences of the reference plan and proceeded the optimization process with the constraints sets of the reference plan which had been obtained from the step-by-step approach. Both plans were compared with the DVH data and dose distribution. The ECLIPSE planning system was used. The planning performances were compared with the DVH data. It showed that the history-based optimization had the better plan quality in terms of the target coverage and homogeneity. The doses to the rectum and bladder significantly decreased in the plan with the history-based optimization method. Even though the dose to the left femur head increased, the magnitude is negligible in the sense of dose tolerance of the femur head. From this study, we developed a novel approach by employing a history-based optimization method for the inverse planning for the volumetric arc therapy for prostate cancer.

## The value of robust statistics in the analysis of linac quality assurance images

**Francisco Cutanda Henriquez, Silvia Vargas Castrillon**

Edinburgh Cancer Centre, Edinburgh, United Kingdom

Electronic Portal Imaging Devices (EPID) provide useful tools for the quality assurance of dynamic multileaf collimator (DMLC) performance through the acquisition of integrated images of complex DMLC irradiations. Picket fence and dynamic picket fence images are analysed by detection of landmarks (pickets). Linear fits of the leaf positions are used as the reference to assess deviations of individual leaves. As the reference values are found by this fit, faulty leaf performance could affect the reference values themselves. Robust statistical methods help overcome this difficulty.

Images have been acquired in 6 Varian linacs (TrueBeam and C-series) for a two-year period from tests plans provided by Varian for RapidArc quality assurance. Two of the linacs had high definition MLC, four of them Millenium MLCs.

The Python module Pylinac ([//github.com/jrkerns/pylinac](https://github.com/jrkerns/pylinac)) was used to extract picket positions from the images which were then the input for scripts written with R statistical software.

Robust central tendency measures, dispersion, tests and linear regression were used to fit robust models, providing measurements for gravity effect, MLC leaf accuracy and dynamic MLC delivery.

These methods provided high sensitivity analysis: it was possible to discriminate differences of 1 mm between picket fence results at different gantry angles, and 1 mm misplacements of the leaves. Yuen t-tests for two dependent groups were used ( $p < 0.05$ ) for this analysis.

Leaf fits based on trimmed means were consistent with the estimates obtained with robust linear models including all relevant variables (leaf pair, gantry angle, picket number).

This study shows Robust Statistics take advantage of all the information contained in the images, providing a sensitive and enhanced analysis of the tests. Leaf performance can be assessed neutralizing the effect of confounders like imager sag, gravity and accuracy of other leaf pairs. This analysis is fast and accurate. Its sensitivity and accuracy is independent of the result, as errors in a limited number of leaf pairs will not change results for the other ones.

## The cylindrical dosimeter for 3D verification of high-modulated radiation therapy plans

Andrey Vertinskiy<sup>1,2</sup>, Evgeniya Sukhikh<sup>1,2</sup>, Leonid Sukhikh<sup>2</sup>

<sup>1</sup> Tomsk Regional Oncology Center, Tomsk, Russia

<sup>2</sup> National Research Tomsk Polytechnic University, Tomsk, Russia

**Introduction.** The criterion for passing the radiation therapy plan is gamma index  $g(3\%, 3 \text{ mm}) \geq 95\%$  according to the AAPM TG-119 protocol. It was shown in that the use of  $g(3\%, 3 \text{ mm}) \geq 95\%$  criterium for several IMRTs and VMAT plans gives large systematic errors in the dose value compared to  $g(2\%, 2 \text{ mm}) \geq 95\%$ . The AAPM TG-119 protocol was changed by a new protocol AAPM TG-244 for the commissioning of the treatment planning systems for IMRT and VMAT and QA procedures. VMAT plans also need volume dosimetric verification.

The purpose of this work was to verify the Monaco plans for VMAT irradiation using a set of equipment of the dosimetric phantom ArcCHECK together with the SNC Patient and 3DVH programs at the Elekta Synergy accelerator according to AAPM TG-244, and to estimate the differences between the 2D and 3D calculations.

**Materials and Methods.** For the analysis, four radiotherapy VMAT plans for different localizations and fractional regimes were taken: head-neck (70 Gy/27 fraction), prostate (35Gy/5fraction), brain (60Gy/30fraction) and liver (30Gy/2 fraction).

All plans were created using planning system Monaco v.5.10.02. Dose delivery was carried out using Elekta Synergy linac. VMAT plan verification was done using cylindrical phantom ArcCHECK (Sun Nuclear) together with the SNC Patient and 3DVH software package.

**Results.** A technical malfunction of the accelerator diaphragm was detected with the help of the criterion  $g(2\% L, 2 \text{ mm}, TH = 5\%)$  using an example of a few irradiation plans, which could not be detected at milder values of the gamma index  $g(3\% L, 3 \text{ mm}, TH = 5\%)$ . Thus, the use of more stringent gamma-index criteria  $g(2\%L, 2 \text{ mm},)$  allows evaluation of distribution and finding out the nature of the systematic errors that can be missed by using “soft” criteria or 2D-verification of plans.

**Conclusion.** The use of 3D dosimetric evaluation with the help of the 3DVH program allows to proceed to more complex analysis of the results of verification of treatment plans. In this case, the value of the gamma index is only the first step to analyze the data obtained. The 3DVH software allows you to obtain a dose distribution in each voxel and patient contours, which makes it possible to analyze the DVHs. In this case, the conclusions on treatment plan passage should be based on the measured dose distribution for the target and the organs at risk.

## Accuracy of intensity-modulated radiation therapy treatment planning and delivery

**Dražan Jaroš, Goran Kolarević, Bojan Pavičar**

International Medical Centers Banja Luka, Member of Affidea Group, Banja Luka, Bosnia and Herzegovina

**Background/Aim.** The aim of this study was to verify the accuracy of the commissioning of intensity modulated radiation therapy (IMRT) treatment planning and delivery using the American Association of Physicists in Medicine Task Group 119 (TG-119).

**Methods.** TG-119 proposes test cases for testing the accuracy of the IMRT planning and delivery system. Each test includes target and normal structure shapes. For these test cases, we generated plans using 7 to 9 static sliding window IMRT fields. Dose optimization and calculations were performed using 6MV photons and Eclipse 13.6 treatment planning system (TPS). Each test includes specific dose goals. Prescription and planning objectives were set according to the TG 119 goals.

**Results.** Our planning results matched the results from TG-119. Point dose and fluence data used for comparison were within the acceptable limits.

**Conclusion.** Results obtained in this study were within the TG-119 recommendations for both plans and goals. It is helpful to test the treatment planning system capabilities in the preclinical stage and also to periodically check the system in the clinical stage. Using TG-119 test cases, one can eliminate accidents and incidents caused by TPS.

**Keywords:** Dosimetry, intensity modulated radiation therapy, quality assurance

## Comparison of 3D-CRT vs IMRT for anal cancer treatment planning

**Violeta Acovska, Dragan Nikolovski**

University Clinic of Radiotherapy and Oncology, Skopje, Macedonia

In radiotherapy, the most common techniques for treatment planning are three-dimensional conformal radiation therapy (3D-CRT) and intensity-modulated radiation therapy (IMRT). Both techniques provide acceptable dose distribution in planning target volumes (PTV's) and sparing of surrounding normal tissues or organs at risk (OAR's). The advantages of IMRT over 3D-CRT are in achieving better conformity of prescribed dose around PTV's and greater sparing of OAR's.

Anal cancer treatment planning is challenging for both treatment techniques because of complex shapes of PTV's including both inguinal lymph nodes. Also, the volume of the PTV and spatial correlation between PTV and OAR's poses big problems for anal cancer treatment planning.

At the University Clinic of Radiotherapy and Oncology (UCRO) in Skopje, Macedonia, in last 4-5 years IMRT technique has replaced 3D-CRT technique in treatment uses for complex cases in various localizations.

A comparison has been performed between plans for 11 cases of anal cancer (in last 2 years) calculated and treated in the IMRT technique and later recalculated in the 3D-CRT technique. A similar field setup for all 3D-CRT plans was used. A similar field setup and number of beams for all IMRT plans was used. An analysis of the dose-volume histograms (DVH's) and conformity indexes (CI) and homogeneity indexes (HI), as well as a comparison of the mean dose, maximum dose and DHV's for OAR's was performed.

The results show an improvement for CI values from interval 1.454 – 3.549 for 3D-CRT to 1.190 – 1.807 for IMRT; an improvement for HI values from interval 0.064 – 0.083 for 3D-CRT to 0.028 – 0.071 for IMRT; decrement of mean dose for bladder with IMRT technique between 4.56 Gy and 11.25 Gy; reduction of V<sub>45Gy</sub> for small bowel from 61.5 cm<sup>3</sup> to 291.4 cm<sup>3</sup>, reduction of V<sub>50Gy</sub> for femoral heads from up to 14.38% (3D-CRT) to 0% in most of the IMRT treatments, reduction of mean dose for genitals from 1.61 Gy to 8.59 Gy and reduction of V<sub>30Gy</sub> for genitals from 1.47% to 25.86%; decrement of V<sub>45Gy</sub> out of PTV from 1010.5 cm<sup>3</sup> to 1660.5 cm<sup>3</sup> and decrement of V<sub>95%</sub> from maximum prescribed dose out of PTV from 187.9 cm<sup>3</sup> to 1321.9 cm<sup>3</sup>.

The results of this comparison clearly give an advantage for IMRT technique over 3D-CRT technique for the treatment of anal cancer, despite the complex shape of PTV for anal cancer cases. This is why all anal cancer cases in the future will be treated with the IMRT treatment technique.

## Evaluation of tomotherapy HDA beam parameters

**Songül Barlaz Us, Eda Bengi Yilmaz**

Mersin University Faculty of Medicine, Department of Radiation Oncology, Mersin, Turkey

The helical tomotherapy is an image-guided intensity-modulated radiotherapy treatment technique. It is characterized by radiation delivery in which the patient is constantly translated through a continuously rotating radiation beam mounted on a slip-ring gantry. The aim of this study was to test beam parameters of tomotherapy and compare them with manufacturing settings.

In this study, Tomotherapy HDA, water phantom and ion chamber were used and percentage depth dose, transverse, and longitudinal beam profiles were measured on 1x40 cm, 2.5x40 cm and 5x40 cm fields, respectively.

According to measurement results, the percentage of maximum depth dose error was less than 2%, transverse profile Gamma index maximum and longitudinal profile gamma index maximum were less than 1%. These results were within limits and matched the AAPM TG-148 and the manufacturing values.

**Keywords:** Tomotherapy, beam profiles

## Proteomic signature of bone marrow-derived small extracellular vesicles in heart-irradiated radiotherapy model

**Hargita Hegyesi<sup>1</sup>, Nikolett Sándor<sup>2</sup>, Balázs Hornyák<sup>1</sup>, Szabina Mecsei<sup>1</sup>, Lilla Turiák<sup>3</sup>, Ágnes Kittel<sup>4</sup>, Géza Sáfrány<sup>2</sup>, Lóránd Bertók<sup>2</sup>, Edit I Buzás<sup>1</sup>**

1 Department of Genetics, Cell- and Immunobiology, Semmelweis University, Budapest, Hungary

2 National Research Directorate for Radiobiology and Radiohygiene, National Public Health Center, Budapest, Hungary

3 MS Proteomics Research Group, Research Centre for Natural Sciences, Hungarian Academy of Sciences, Budapest, Hungary

4 Institute of Experimental Medicine, Hungarian Academy of Sciences, Budapest, Hungary

As the incidence of breast cancer continues to rise, radiotherapy has emerged as the leading treatment modality. However, radiotherapy also increases the risk of coronary heart disease and cardiac mortality. In a chest-irradiated mouse model of cardiac injury, we investigated the effects of local irradiation. We found an increased lethality after 16 Gy irradiation, while radio-detoxified LPS treatment prolonged the survival significantly. By flow cytometry we demonstrated that upon the administration of radio-detoxified LPS, the number of bone marrow-derived endothelial progenitor cells increased in the bone marrow, and in particular, in the circulation. Furthermore, our mass spectrometry analysis showed that radio-detoxified LPS altered the proteomic composition of bone marrow cell-derived small extracellular vesicles (exosomes). Radio-detoxified LPS treatment induced a marked interferon-induced trans-membrane protein-3 (IFITM3) expression both in the cells of the bone marrow and in bone marrow cell-derived small extracellular vesicles. This is the first study to demonstrate that radio-detoxified LPS treatment induces an increased number of circulating endothelial progenitor cells in parallel with an attenuated radiotherapy mortality. Our results suggest that the transmembrane protein IFITM3, associated with bone-marrow-derived small extracellular vesicles, may provide a promising candidate biomarker of radiodetoxified-LPS effect, and may possibly find a place amongst strategies for evaluating regeneration potential of bone-marrow stem cells.

**Acknowledgments:** This work was supported by National Research, Development and Innovation Office NKFIH, Hungary, NVKP\_16-1-2016-0017.

## Study of nuclear fragmentation in particle therapy with the FOOT experiment

**Nazar Bartosik**

Istituto Nazionale di Fisica Nucleare (Sezione di Torino), Torino, Italy

In recent years, the Charged Particle Therapy has gained attention as a promising method for the treatment of deep-seated tumours. The most wide-spread technique is using a proton beam, while several facilities utilizing a carbon-ion ( $^{12}\text{C}$ ) beam are already operational in the world. Given that most of the charged-particle's energy is released in a localized region, characterized by the Bragg peak, the dose delivered to the surrounding healthy tissues is minimized. Nevertheless, secondary particles produced by nuclear interactions between the beam and patient tissues can pose an additional hazard that has to be carefully taken into account in clinical treatment plans.

In proton therapy, the fragmentation of the target is the main source of secondary radiation, represented by low energy and short range fragments produced along the proton path. In the case of the  $^{12}\text{C}$  beam, the projectile fragmentation generates a long range fragments that release dose in healthy tissues around the tumour. Understanding of these processes is one of the main goals of the FOOT (FragmentatiOn Of Target) experiment, an international project funded by the Istituto Nazionale di Fisica Nucleare (Italy). To overcome the great technical difficulties in detecting fragments traveling a few microns in the target, the inverse kinematic approach will be used by colliding a  $^{16}\text{O}$  or  $^{12}\text{C}$  therapeutic beam on graphite and hydrocarbons targets. The same configuration also allows to measure the projectile fragmentation of the mentioned beams using direct kinematics.

Current space programs focus on the exploration of the Solar system. For manned deep space missions, exposure to galactic cosmic rays is acknowledged as the main health risk. For risk assessment and mitigation, Monte Carlo or deterministic transport codes are commonly used to calculate organ doses through different shielding materials. The FOOT experiment will measure differential fragmentation cross sections of high-energy light ions in different shielding materials. These measurements are necessary to improve the accuracy of the transport codes.

The FOOT experiment is designed as a portable detector that can be easily transported to various facilities around the world for collecting experimental data with different beam conditions. The detector is designed to possess good particle identification capabilities for heavy fragments by measuring their trajectory, energy and time of flight, while the position and direction of the incident beam particle is measured by the beam monitor. For the measurement of light fragments all the subsystems after the beam monitor are substituted with an emulsion spectrometer, which measures the charge, energy and mass of the fragments.

The ultimate goal of the FOOT experiment is to measure differential cross sections of each type of fragments with  $\sim 5\%$  uncertainty for different beam-target combinations. In this work the final design of the experiment that will be presented together with the performance of its subsystems.

## **A dosimetric comparison between cyberknife and intensity/volumetric modulated techniques in stereotactic radiosurgery (SRS)**

**Marcello Serra<sup>1</sup>, Gianluca Ametrano<sup>2</sup>, Borzillo Valentina<sup>2</sup>, Rossella Di Franco<sup>2</sup>, Paolo Muto<sup>2</sup>, Maria Quarto<sup>1</sup>, Giuseppe Roberti<sup>1</sup>, Federica Savino<sup>1</sup>**

<sup>1</sup> Università degli Studi di Napoli Federico II, Napoli, Italy

<sup>2</sup> Istituto Nazionale Tumori IRCCS Fondazione Pascale, Napoli, Italy

Radiosurgery means the destruction of precisely selected areas of tissue using ionizing radiation. It was originally defined in the neurosurgery field as the delivery of a high radiation dose fraction stereotactically directed. Where stereotactically refers to the definition of a 3D coordinates system that enables accurate correlation between the virtual target localized by means of diagnostic images and the actual tumor position in the patient. Technological improvements have led to increased clinical adoption of SRS and have broadened its scope. In the last years the original concept of SRS expanded to include treatments comprising up to 5 fractions and has been applied in the treatment of pathology not localized in the head or spine, for example in the prostate cancer treatment, the SRS is widely applied. Therefore, today with SRS, the use of the SRS is intended together with the fractionated radiotherapy. This application has met large consensus in the medical community because they join the capability to destroy the target tissue preserving the adjacent normal tissue and the different sensitivity of the tumor with respect to the surrounding tissue of the total cumulated dose.

The most important device for the SRS planning is the CyberKnife (Accuray Inc., Sunnyvale, CA). It is a linear accelerator of 6 MV mounted on a robotic structure and an integrated image guidance system which acquires images of the patients during the treatment in order to track the actual position of the tumor despite movements due to respiration. The robotic arm has 6 degrees of freedom and 120 principal nodes, where it can assume 12 different directions, reaching 1440 different orientations, therefore a very high conformity of the tumor mass with sub-millimeter accuracy is reached, but at the same time, the healthy tissues are saved from useless radiation.

It is possible to obtain a similar dose delivery to the tumor by means of a LINAC using an Intensity Modulated Arc Therapy (IMRT) technique, or its direct technological evolution the Volumetric Modulated Arc Therapy (VMAT) technique. In the first case, the accelerator is equipped with a multileaf collimator made up of thin leaves which move independently and generate shapes that fit the treatment area, whereas in the second one the device continuously reshapes and changes the intensity of the radiation as the gantry moves around the body.

The exposed techniques present pros and cons; therefore, this study is aimed to compare the dosimetric results obtained by enrolling patients who received the treatment planned at the CyberKnife and re-planning them with the LINAC using IMRT e VMAT techniques with and without the rotation of the couch. The analysis was conducted by confronting the results on phantoms, DVH and by means the definition of opportune indices associated to the conformity, the dose gradient, the dose homogeneity and so on, in order to obtain the most performing solution for a given pathology.

## **Evaluation of the additional dose delivered to the patient during imaging procedures in image-guided radiotherapy through in vivo measurements: Preliminary results**

**Federica Savino<sup>1</sup>, Gianluca Ametrano<sup>2</sup>, Maria Quarto<sup>1</sup>,  
Marcello Serra<sup>1</sup>, Cecilia Arrichiello<sup>2</sup>, Leonardo Baldassarre<sup>3</sup>,  
Fabrizio Cammarota<sup>2</sup>, Giuseppe Roberti<sup>1</sup>, Paolo Muto<sup>2</sup>**

<sup>1</sup> Dipartimento di Scienze Biomediche Avanzate, Università degli Studi di Napoli "Federico II", Napoli, Italy

<sup>2</sup> Istituto Nazionale Tumori - IRCCS, Napoli, Italia

<sup>3</sup> LB - Servizi per le Aziende, Roma, Italy

The modern radiotherapy techniques allow to modulate the dose intensity to the tumor volume increasing the geometric accuracy of the radiant treatment and minimizing the risk of radiating the surrounding healthy organs. Accurate target localization is essential to quantify and correct the geometric changes that inevitably occur during radiotherapy treatment. This was made possible by the introduction of Image Guided Radiotherapy (IGRT), and the most common imaging modalities is the kV-Cone Beam Computed Tomography (CBCT), a radiological device that allows to acquire volumetric CT images, directly in the treatment room, before radiotherapy. The IGRT has rapidly been adopted as the standard of care to improve the geometric accuracy of patient positioning during radiotherapy reducing significantly reduce target positioning errors, therefore, enabling highly conformal treatments. However, the benefit of improved patient positioning comes at the cost of additional radiation dose, which in a high fraction regimen with daily imaging can lead to a total dose on the order of a gray or more.

The present work was carried out at the National Cancer Institute - IRCCS "G. Pascale Foundation" with the aim of developing a practical method for estimating the dose to the organs from kilovoltage cone-beam CT (CBCT) using available phantoms and dosimeters. Actually, the x-ray volumetric imager (XVI, Elekta Oncology Systems, Crawlwy, UK) is used to acquire volumetric images at the time of treatment. These images are then registered with the planning CT in order to determine the appropriate shifts of the treatment table required to properly align the patient. Currently, imaging dose is not accounted in radiotherapy treatment planning, and the aim of this study is to provide imaging dose data and develop guidelines for clinicians to make informed decisions regarding the risk and benefits of x-ray image guidance. A method of estimating CBCT organ doses from simple CT dose index (CTDI) phantom measurements would have excellent utility, allowing clinics to estimate organ doses from their own protocols quickly and easily. For these reasons, the additional dose delivered to the patient following the acquisition of volumetric CT images before or during the radiant treatment was evaluated. The CTDI parameter has been measured as a dosimetric index related to the dose absorbed by the patient undergoing the cone beam. A 100 mm pencil chamber and 16 and 32 cm diameter standard cylindrical Perspex CTDI phantoms were used to measure the cone-beam dose index (CBDI) and a weighted CBDI (CBDI<sub>w</sub>) was then calculated from these measurements to represent the average volumetric dose in the CTDI phantom. The evaluation of the dose delivered performed by TLD placed inside an anthropomorphic phantom will be also presented, using the data as a predictor of patient dose.

## **Stereotactic radiosurgery for small volume intracranial meningiomas: Plan quality**

**Irena Muçollari<sup>1</sup>, Artur Xhumari<sup>2</sup>, Aurora Aliraj<sup>1</sup>,  
Anastela Mano<sup>1</sup>, Gramoz Braçe<sup>1</sup>, Rejnardo Tafaj<sup>1</sup>, Ejona Lilamani<sup>1</sup>,  
Bledar Cullhaj<sup>2</sup>, Blerina Myzeqari<sup>2</sup>, Erald Karauli<sup>2</sup>**

1 University Hospital Center "Mother Teresa", Tirana, Albania

2 University of Medicine, Faculty of Medicine, Tirana, Albania

Meningiomas arise from the dural coverings of the brain and are the most common benign intracranial tumors. Surgical resections remain the preferred treatment. Stereotactic radiosurgery (SRS) and external-beam radiotherapy are being used increasingly for surgically inaccessible, recurrent, or subtotally excised tumors.

Stereotactic radiosurgery (SRS) treats brain tumors with a precise delivery of a single, high dose of radiation to a specific area of the brain in a one-day session. SRS treatment planning provides that a high dose of radiation is conformed closely to the 3D shape of the target volume with a rapid dose falling to surrounding normal tissue. Evaluation of SRS treatment plans quality realized for patients with small volume meningiomas at our department, in the period 2014 – 2017 will be presented. The parameters analyzed include conformity index and target dose-coverage. SRS treatment plans are realized using Integra XKnife Treatment Plan System (TPS), the Brown- Robert Wells (BRW) stereotactic frame and the linear accelerator Siemens Oncor with cones.

**Keywords:** Stereotactic radiosurgery (SRS), brain, meningiomas, dose, plan quality

## Adaptive radiotherapy in advanced nasopharyngeal carcinoma - Case report

**Lenche Kostadinova, Petar Chakalaroski, Marina S. Vukashinovic**

University Clinic of Radiotherapy and Oncology Skopje, Skopje, Macedonia

**Introduction.** Definitive radiation therapy in head and neck carcinoma, especially in advanced nasopharyngeal carcinoma, is the preferred treatment. During the course of radiotherapy, as a result of the shrinkage of primary tumor and nodal metastasis, alterations in the size, location and geometric of tumor and normal surrounding tissues occur.

Adaptive radiotherapy is a new approach in the treatment of head and neck carcinoma and can provide compensation in alterations which occur during radiotherapy by adaptively modifying the treatment plan during the radiation course.

**Material and Methods.** Adaptive radiotherapy was applied for the first time in Macedonia on a patient with advanced nasopharyngeal carcinoma with neck metastasis. After CT simulation was started with IMRT and concurrent weekly platinum chemotherapy. During the treatment because of shrinkage of neck metastasis more than 50 % two new CT scans were performed for resimulation and a new plan for IMRT was made.

**Results.** With this new adaptive radiotherapy technique we managed to achieve adaptation to anatomic and tumour volume or shape changes during the radiotherapy, better dose delivery and better normal tissue sparing especially to medulla spinalis.

**Conclusion.** Adoptive radiotherapy as a new standard in radiation therapy should continue to develop because it allows better treatment in advanced head and neck carcinoma by better dose coverage on the tumor and better sparing of normal tissues.

**Keywords:** Adaptive radiotherapy, nasopharyngeal carcinoma, adaptation



**Radon  
and  
Thoron**

**36**

## Low radon exhalation rate composites based on NORM residues

**Piotr Szajerski, Maciej Jura**

Institute of Applied Radiation Chemistry, Lodz University of Technology, Lodz, Poland

Current trends in production and materials reprocessing are focused on the development of the so-called zero-waste technologies, increasing the demand for the introduction of innovative schemes of materials flow and applications. Unfortunately, many by-products, residues and industrial waste materials are classified as the so-called NORM or TENORM materials and contain increased levels of natural radionuclides. Among these materials, in the multitude of industrial processes, the most common and produced in the highest amounts are phosphogypsum, mine tailings, metallurgical slugs, coal ash and slags or water purification residues.

Anytime NORM materials are used as components of building materials, increased radiological hazard must be taken into consideration. Three main radionuclides are usually monitored: K-40, Ra-226 and Th-228. Taking into account the concentration of these isotopes, gamma-rays as well as alpha-rays exposure can be estimated. The calculation model for alpha-rays exposure coming from Rn-222 and daughter isotopes (Po-218 and Po-214) assumes the complete release of radon gas being in equilibrium with Ra-226 parent. However, the real hazard from radon and its daughters can be significantly lower, if effective material fabrication technology is applied, slowing radon transport within material and decreasing the Rn-222 exhalation rate.

In this work we present an efficient approach, which allows for the preparation of mineral composites based on NORM materials (phosphogypsum, fly ash, slag) with a low radon exhalation rate. The proposed approach is based on the dry mixing of source materials in a powder form, pressing and high temperature sintering of the pressed samples. Measured aerial radon exhalation rates are ca. 10 times lower than for raw materials and are comparable or even lower than for building materials made of commonly used source materials. Next to the measurement of radon exhalation rates from the investigated materials, some other parameters were measured, as the compressive strength or chemical resistance in aggressive environments. Obtained results indicate interesting properties of these composites and a strong potential for their application in the building industry.

## Radon in Montenegrin schools and kindergartens – Preliminary results

**Perko Vukotic<sup>1</sup>, Ranko Zekic<sup>2</sup>, Tomislav Andjelic<sup>2</sup>,  
Nikola Svrkota<sup>2</sup>, Marija Bogicevic<sup>3</sup>, Aleksandar Dlabac<sup>4</sup>**

1 Montenegrin Academy of Sciences and Arts, Podgorica, Montenegro

2 Centre for Ecotoxicological Research, Podgorica, Montenegro

3 Primary School “Dr. Dragisa Ivanovic”, Podgorica, Montenegro

4 Centre for Nuclear Competence, University of Montenegro, Podgorica, Montenegro

In the framework of the national project MNE9005, funded by the International Atomic Energy Agency and the Government of Montenegro, radon was measured during the academic year 2016/17 (September – June) in all 519 buildings of the pre-university education in Montenegro - 376 buildings of primary and 51 of high schools, 81 kindergarten buildings, 4 buildings of resource centers and 7 of student dormitories. Radosys dosimeters (RSFV type) were placed in all classrooms, rooms occupied by children and educators' offices on the ground floor, and in some rooms on the first floor. The total number of dosimeters was 4078, of which 3793 were main and 285 duplicate (control) dosimeters. After the exposure period, 11.4% of them were lost or damaged.

Average 9-month radon activity concentrations were obtained for 3347 sampled rooms in 507 buildings. Mean value of radon activity concentration in them is 243 Bq/m<sup>3</sup>, while the corresponding value for 953 dwellings in Montenegro (national radon survey) is more than twice lower (110 Bq/m<sup>3</sup>). Average radon concentrations above of 300 Bq/m<sup>3</sup> are found in 23.3% of all sampled rooms in educational institutions and in 3.4% of all rooms they are above 1000 Bq/m<sup>3</sup>, whereas in the Montenegrin homes these percentages are 7.9% and 0.6%, respectively, which means 3 to 5 times lower.

Radon activity concentrations above 300 Bq/m<sup>3</sup> are measured in 223 buildings of educational institutions. In these buildings 1812 rooms were sampled and 779 (43.7%) of them have average radon concentrations higher than 300 Bq/m<sup>3</sup>. In 48 buildings there are rooms with radon concentrations above 1000 Bq/m<sup>3</sup> – among 425 sampled rooms 114 (26.8%) are of such kind.

It can be concluded that, on average, radon concentrations in educational institutions are significantly higher than in Montenegrin homes, which means that children and educators are significantly more exposed to the harmful effects of radon in them than at home (in equal durations of stay in them). This is due to the type of construction of educational institutions (usually spacious low-rise structures) and a relatively high average age of these buildings.

## The NRPI low-level continuous radon gas monitor for measurement below 1 Bq/m<sup>3</sup>

**Karel Jilek**

National Radiation Protection Institute, Prague, Czech Republic

In order to reduce the minimum detectable activity (MDA) of any measured  $\alpha, \beta, \gamma$ , radioactive sample to as low as possible, most worldwide laboratories and research centers need to also ensure a very low concentration of radon gas in ambient air. Since the activity concentration of atmospheric radon gas ranges from several Bq/m<sup>3</sup> to several tens of Bq/m<sup>3</sup>, there are required radon gas measurement instruments which are able to measure its activity concentration deeply below 1Bq/m<sup>3</sup> for the control of efficiency of any used radon gas suppression technology.

A continuous alpha spectrometric radon gas monitor, newly developed at the NRPI, allowing the measurement of atmospheric radon gas activity concentration with the MDA lower than 0.2 Bq/m<sup>3</sup> being adjusted on an hourly basis, its calibration and a radon gas suppression technology used at the NRPI will be introduced.

## **$^{222}\text{Rn}$ and $^{220}\text{Rn}$ exhalation rate and natural radionuclide content in different granites used in Serbia**

**Igor Čeliković<sup>1</sup>, Gordana Pantelić<sup>1</sup>, Ivana Vukanac<sup>1</sup>, Jelena Krneta-Nikolić<sup>1</sup>, Miloš Živanović<sup>1</sup>, Aleksandar Kandić<sup>1</sup>, Boris Lončar<sup>2</sup>**

<sup>1</sup> Vinča Institute of Nuclear Sciences, University of Belgrade, Belgrade, Serbia

<sup>2</sup> Faculty of Technology and Metallurgy, University of Belgrade, Belgrade, Serbia

Health hazard due to exposure to radon and its progenies in the indoor environment is confirmed by extensive epidemiological studies performed in Europe, Asia and America. World Health Organisation has identified radon as the second cause of lung cancer after smoking. The most important source of indoor radon after the soil subjacent to the building is building material. High concentration of  $^{238}\text{U}$  and subsequently  $^{226}\text{Ra}$  in building material could lead to high doses due to internal exposure to radon. On the other hand, a high concentration of natural radionuclides coming from  $^{238}\text{U}$  and  $^{232}\text{Th}$  series and  $^{40}\text{K}$  could lead to high external exposure as well.

Granites are a widely used building material, especially for decorative use. Depending on its mineral composition, granite could have a high concentration of natural radionuclides. In addition, depending on the surface finishes of granites, the radon exhalation rate could vary significantly. Therefore, the aim of this research is to investigate the exhalation rate of two radon isotopes  $^{222}\text{Rn}$  and  $^{220}\text{Rn}$  in different granites commercially available in Serbia, and to assess internal exposure to radon. Exhalation rate measurements were performed using the accumulation chamber method. Radon concentration in the chamber was continuously measured by an active SARAD RTM1688-2 device.

In addition, the activity concentrations of  $^{226}\text{Ra}$ ,  $^{232}\text{Th}$  and  $^{40}\text{K}$  in granites were determined using an HPGe detector. Radiological hazard due to exposure to granites was assessed by using different radiation hazard indices.

## Soil gas radon concentration and terrestrial radioactivity correlations in Afyonkarahisar

Hüseyin Ali Yalim, Ayla Gümüş

Afyon Kocatepe University, Afyonkarahisar, Turkey

Humans are exposed both to the natural radiation from the radioactive elements that have existed in the earth's crust since the formation of the earth and the high-energy cosmic rays, and to the artificial radiation from medical applications and sparrows after nuclear tests. The most important part in natural radiation affecting human beings is radon derived from terrestrial radioactive elements of uranium and thorium. Terrestrial radiation level is strictly related to the contents of thorium (Th), uranium (U) and potassium (K) in rocks originating from the soil in an area, and to the geological composition of the area.

The determination of natural background radiation levels is of great importance for all living things. In order to determine whether the living zone is healthy in terms of natural radiation, the concentrations of the radionuclides in the surrounding environment and the effects of radiation on all the living things must be known. In this study, it was aimed to determine the terrestrial background radiation ( $^{238}\text{U}$ ,  $^{232}\text{Th}$  and  $^{40}\text{K}$ ) level on the soil surface, and to evaluate the correlation between the Uranium and Thorium concentrations and the soil gas radon activity values in Afyonkarahisar city center. Moreover, annual effective dose the public is exposed to will be estimated.

## Indoor radon concentrations and related dose rates at the houses of Afyonkarahisar

Hüseyin Ali Yalim<sup>1</sup>, Ayla Gümüş<sup>1</sup>, Rıdvan Ünal<sup>2</sup>

<sup>1</sup> Afyon Kocatepe University, Afyonkarahisar, Turkey

<sup>2</sup> Uşak University, Uşak, Turkey

An indoor radon activity concentration survey has been carried out at 46 houses in the Afyonkarahisar province of Turkey using CR-39 passive nuclear track detectors four times during a one-year period. The measured values ranged from 21  $Bq.m^{-3}$  to 2494  $Bq.m^{-3}$ , whereas the calculated average values were in the range of 33.75  $Bq.m^{-3}$  and 1614.26  $Bq.m^{-3}$ . On the other hand, while the calculated annual geometric mean value was  $186.50 \pm 10.55 Bq.m^{-3}$ , it was  $136.07 \pm 8.76 Bq.m^{-3}$  when only the living areas of the houses were considered. The corresponding annual effective dose rates were obtained to be in the range of 0.53 and 25.45  $mSv.y^{-1}$ . The resulting annual effective dose equivalent calculated from the geometric mean was  $2.94 \pm 0.17 mSv.y^{-1}$  for the Afyonkarahisar province, while the annual effective dose in the living areas of the houses was obtained to be  $2.15 \pm 0.14 mSv.y^{-1}$ . According to the floor levels, the concentration value was found to be between  $86.60 \pm 7.80 Bq.m^{-3}$  and  $291.80 \pm 14.60 Bq.m^{-3}$ . The present results show an exponential decrease with the distance from the soil, having the correlation coefficient of  $R^2=0.988$ .

## Indoor radon survey in Hungarian kindergartens

**Anita Csordás<sup>1</sup>, Katalin Zsuzsanna Szabó<sup>2</sup>,  
Zoltán Sas<sup>3</sup>, Erika Kocsis<sup>1</sup>, Tibor Kovács<sup>1</sup>**

<sup>1</sup> Institute of Radiochemistry and Radioecology, University of Pannonia, Veszprém, Hungary

<sup>2</sup> Nuclear Security Department, Centre for Energy Research, Hungarian Academy of Sciences, Budapest, Hungary

<sup>3</sup> Social Organisation for Radioecological Cleanliness, Veszprém, Hungary

The main source of ionizing radiation in dwellings and workplaces is radon and its daughter elements. They are responsible for the highest part of the radiation dose that people are exposed to. The harmful effect of radon is most dangerous in the case of children.

In this study, kindergartens were chosen in several parts of Hungary. Three different regions with a different geological background were selected and 99 kindergartens were involved by volunteering themselves. Indoor radon concentration was measured in every kindergarten in every season for one year by discriminative SSNTD (Solid State Nuclear Track Detector). The detectors were placed on the ground floor in three rooms of each kindergarten near to the wall (maximum distance 15 cm). Heads of the kindergartens were interviewed and questionnaires were filled with relevant information about building characteristics e.g. usage and ventilation habits, building materials.

The annual average radon concentration was below 300 Bq/m<sup>3</sup> in each kindergarten, corresponding to the reference level in Hungary. Clear differences of radon concentrations were revealed in cases of different building characteristics, e.g. building material.

## A combined system for the measurements of aerosol size distribution

**Michael Zhukovsky<sup>1</sup>, Hyam Nazmy<sup>2</sup>,  
Mostafa Y. A. Mostafa<sup>2</sup>, Vladislav Semyannikov<sup>2</sup>**

<sup>1</sup> Institute of Industrial Ecology UB RAS, Ekaterinburg, Russia

<sup>2</sup> Ural Federal University, Ekaterinburg, Russia

Information on the size distribution of radioactive aerosols is important for the assessment of internal exposure in the case of inhalation in the respiratory tract. It is often not possible to have a priori information about the size distribution of radioactive aerosols. Typical sizes of radioactive aerosols are in the range of 1 nm to 10-20 microns. The size distribution of aerosols in such a wide range cannot be measured using any single measuring instrument. This is due to the fact that during the deposition of radioactive aerosols of various sizes, different physical principles take place: diffusion deposition, inertial deposition, impact, etc.

To measure the size distribution of radioactive aerosols in the entire possible range, a complex device operating on different physical principles was designed. The device consists of a twelve-stage diffusion battery, a five-stage cascade impactor, and a set of three analytical aerosol filters with known permeability functions. Diffusion battery allows to obtain data on the distribution of aerosols in the range of 1-50 nm, cascade impactor - in the range of 0.5-15 microns, and multilayer analytical filters in the range of 0.1-0.5 microns. The presence of a diffusion battery in front of the cascade impactor prevents diffusion deposition of ultrafine aerosols at the first stages of the impactor, which leads to false information about the presence of coarse aerosols in the atmosphere.

The system was tested in a radon box with an equivalent equilibrium radon concentration (EEC) from 1500 to 15000 Bq/m<sup>3</sup> and a concentration of aerosol particles from 2·10<sup>3</sup> to 2·10<sup>5</sup> cm<sup>-3</sup>. At low aerosol concentration, nearly 35-45 % of radon decay product activity connected with ultrafine particles with AMTD ~ 1 nm (so called unattached fraction). Additionally, a mode with a diameter of ~5-8 was registered. Larger aerosol particles were not caught by the cascade impactor and were deposited on the final filters. This shows that their size is less than 500 nm, which is in good agreement with the literature data. The <sup>218</sup>Po:<sup>214</sup>Pb:<sup>214</sup>Bi activity ratio was determined by Thomas technique. For the unattached fraction, this ratio was 1:0.33:0.05 and for the aerosol fraction, the activity ratio was 1:1.28:0.91. This shows that to interpret the results of the radon EEC measuring using a diffusion battery, a cascade impactor and analytical filters, the differences in the equilibrium shift between radon decay products should be taken into account. With a high concentration of aerosol particles created by an electronic cigarette, the unattached fraction is absent, however, the maximum activity is observed not at the cascade impactor, but at the finishing filters. This shows that this source of aerosols mainly generates medium-sized particles, and coarse aerosols in the smoke of an electronic cigarette are not significant.

## National radon survey in Moldova Republic

Coretchi Liuba, Bahnarel Ion, German Olga

National Agency for Public Health, Chisinau, Moldova

In order to obtain the first systematic data for indoor Radon concentrations, a pilot indoor Radon survey was conducted in the Republic of Moldova under a regional project of the IAEA (RER/9/094). The survey was performed during 2010-2015 in different districts of the country in the main Zones – South, Centre and North. The main purpose was to check the screening method protocols using the Radon meter RTM from the SARAD Company and to organize a national radon survey [1].

The survey indicated that the likelihood of a dwelling having elevated radon concentrations indoors was greatest in the north part of the country.

In 2001, the Government of the Republic of Moldova adopted Radon reference levels in the Regulation on Basic Norms of Radiation Protection, which sets the basic standards for protecting the health of personnel and the population in Moldova from harmful effects of ionizing radiation. The national reference level was set to a Radon concentration of 100 Bq/m<sup>3</sup> for new buildings and 150 Bq/m<sup>3</sup> for existing buildings (annually averaged), above which measures are required to be applied [2].

During the period 2018-2019, the IAEA MOL9007 project will be implemented in Moldova. Passive measurement Radtrak radon long-term measurement systems will be used in the national survey and only <sup>222</sup>Rn will be measured.

The survey will be population-based. The sample points will be divided into 200 detectors per regional district (n=10) according to a designed distribution scheme. A three-stage stratified sampling scheme will be used. The first stage included the stratification of districts to 10 regional centers of public health, which will be then subdivided in the number of districts with the regional Centre of Public Health, and each district will be subdivided in two strata of towns and villages. The number of detectors in each stratum will be determined proportionally to the population density.

The survey will be promoted and coordinated by Moldova's national laboratory, the National Agency of Public Health. The dwellings will be randomly selected by using a door to door approach. Survey participants will receive detectors together with an agreement, instructions, and questionnaires which will be completed during an interview to obtain the characteristics of dwellings.

We hope the survey will start in January 2019 and be finished in approximately April 2019. At the end of the survey period, the detectors will be collected by the regional health inspectorates from the Centers of Public Health and will be processed at the RADONOVA lab., Uppsala, Sweden.

### References

1. Bahnarel, I.; Coretchi, L.; Plavan, I.; Virilan, S.; Streil, Th. Control of public exposure to radon in the Republic of Moldova. INSJ, 2016.
2. National Fundamental Norms of Radiation protection (NFNRP-2000). 2001, Chisinau, Moldova Republic.

## Uncertainty evaluation in radon concentration measurement in soil using NAI detectors

**Gordana Pantelic, Ivana Vukanac, Jelena Krneta Nikolic,  
Milos Zivanovic, Igor Celikovic, Milica Rajacic**

Vinca Institute of Nuclear Sciences, Belgrade, Serbia

Radon is recognized as the second most important cause of lung cancer. Since a major influence on radon concentrations in dwellings originates from the soil beneath a house, it is important to analyze soil samples in the areas of interest.

Soil sample analysis is time-consuming and the focus of the presented study was to find the fastest method with small measurement uncertainties to obtain good quality results. Radon concentration in soil was measured by NaI(Tl) gamma spectrometer. The quality of the results depends directly on the soil sample preparation and the accuracy and precision of the measurements.

Contributions to the combined measurement uncertainty based on the equation for radon activity concentration calculation are identified. The components which were considered were uncertainties of: counting statistics, efficiency, samples weighting and measurement time. Each of these components contributes to measurement uncertainty, and it was necessary to evaluate the magnitude of each of them, as well as their influence on overall uncertainty.

The largest contribution to overall uncertainty comes from the detection efficiency and from counting statistics. As the radon concentration calculation is based on the net area obtained from 3 peaks (295 keV, 351 keV, 609 keV), a good definition of the peak area is the most important. For the net area determination, two different methods were used, one with the net area obtained from 3 peaks and the second method used the total sum of counts in all channels between 264 keV and 664 keV which means that all 3 peaks were included.

The obtained radon activity concentrations differ several percent between the two methods. Uncertainties for soil sample depend on the peak area method of determination. However, taking into account the measurement uncertainty and the difference between the two methods for the peak area determination, the total sum method produces acceptable results with less time and efforts.

## Long-term observation and analysis of atmospheric radon and its short-life progeny

Yunxiang Wang<sup>1</sup>, Lei Zhang<sup>2</sup>, Qiuju Guo<sup>1</sup>

<sup>1</sup> School of Physics, Peking University, Beijing, China

<sup>2</sup> State Key Laboratory of NBC Protection for Civilian, Beijing, China

It is known today that both radon and its progeny can be used as tracers in many research fields, such as studying the state of turbulence and the stability of the lower atmosphere, the origin and transportation of air mass, and the dynamics processes of aerosol deposition in local areas. To meet the needs of these studies, a relatively high sensitivity detection of concentrations of both radon and its progeny is required. Consequently, at the same time, long-term continuous sampling and measurements *in situ* are necessary.

In this study, a long-term observation of activity concentrations of both radon and its progeny has been carried out in Beijing. Continuous measurement has started in September 2016 for radon and January 2016 for radon progeny, respectively. An atmospheric radon monitor (ARM-Pin01, SairaTec) based on the Si-PIN detector and humidity control device and a step-advanced filter radon progeny monitor (RPM-SFO1, SairaTec) are adopted for continuous sampling and hourly measurement of radon and its progeny, respectively at the same site. The sensitivity of ARM-Pin01 is 15 cph/Bqm-3 for a 60-min cycle, and its lower detection limit is 0.3 Bqm-3 for a 60-min cycle. For RPM-SFO1, the filter is automatically rolled and stopped to collect progeny particles on a fresh filter at each interval. A 400 mm<sup>2</sup> PIPS detector is used, the sensitivity of the monitor is 50 cph/Bqm-3 for a 60-min cycle in a slow model, and its lower detection limit of EEC is 0.2 Bqm-3 for a 60-min cycle in a slow model. Both monitors are suitable to be installed in the outdoor environment for a long-term automatic measurement without any maintenance for at least one month. The analysis of all the data gathered is performed, and the results in detail will be given.

## Sample design for radon concentration investigation in Bulgarian caves

**Kremena Ivanova<sup>1</sup>, Zdenka Stojanovska<sup>2</sup>, Jana Djounova<sup>1</sup>,  
Bistra Kunovska<sup>1</sup>, Nina Chobanova<sup>1</sup>, Decislava Djunakova<sup>1</sup>**

<sup>1</sup> National Centre of Radiobiology and Radiation Protection, Sofia, Bulgaria

<sup>2</sup> Faculty of Medical Sciences, Goce Delcev University of Stip, Stip, Macedonia

As a very mountainous country, Bulgaria has a lot of caves, but only some of them are developed, managed and available for tourist visits. The main sources of radon are rocks and a high concentration can be measured in caves. Caves have been of interest because radon concentration in these environments may sometimes reach high values. A rather large number of investigations have been carried out all over the world, from the point of view of both researches on radon behavior in a cave environment and radiation protection. There are no systematic investigations of radon in the caves in Bulgaria in order to assess the health risk. The paper presents the sample design of the radon concentration survey in Bulgarian caves for the evaluation of the health risk of people. The sample design covers the method of selection, the sample structure and the plan for analyzing and interpreting the results. The method selected to define the representative sample corresponds to the following criteria: it covers all types of caves in different mountains in Bulgaria; it is consistent over time; it includes changes to the definition over time; it constitutes the selection of the sample design for the caves and organization of survey. The samples of caves are defined on the basis of mountains in Bulgaria in order for the definitions to remain constant over time. Groups of caves according to the mountains are: caves in Stara Planina, caves in Rhodope Mountains and caves in other mountains. The design of the samples of caves is built around a random selection from the most visited caves in Bulgaria. According public information, there are 65 of these caves. The calculated sample size for a confidence level of 95% and a margin of error of 30% is 10 caves. The numbers of samples have been weighed according to the percent of the caves in the groups with 5 per cent precision at 95 per cent confidence. The way of the selection of the sample and the measurement method is presented in the paper.

## The sampling frame definition of the buildings with public access to radon concentration surveys

**Bistra Kunovska<sup>1</sup>, Kremena Ivanova<sup>1</sup>, Zdenka Stojanovska<sup>2</sup>,  
Nina Chobanova<sup>1</sup>, Decislava Djunakova<sup>1</sup>, Jana Djounova<sup>1</sup>**

<sup>1</sup> National Centre of Radiobiology and Radiation Protection, Sofia, Bulgaria

<sup>2</sup> Faculty of Medical Sciences, Goce Delcev University of Stip, Stip, Macedonia

This study discusses the sampling frames of the buildings with public access to radon concentration surveys on the territory of Bulgaria in order to assess the health risk for the population. The sampling frame is the list from which the sample is selected, so the quality of the sampling frame affects the quality of the sample. The general list of different types of buildings with public access has been prepared in accordance with the list of the Ministry of the Regional Development and Public Works in Bulgaria and international experience in the field of radon investigation. The types of buildings with public access have been classified in nine general groups. These groups of buildings with public access are defined as follows: educational institutions; buildings for commerce and/or services; health and social care buildings; buildings in the field of culture; sports facilities; buildings in the field of transport; prisons; cult and religious buildings and post offices. Multicriteria analysis was applied to select the types of buildings in order to assess the health risk from radon exposure in buildings with public access. The main criteria for the analysis are: the probability of high radon concentration; time spent in building and the number of people accessing the place. For the purpose of the precise definition of the target buildings, it is necessary to ensure that all the places where the population could be exposed to radon are adequately covered. To define the whole list of the target buildings, the official available information has been used from: the Ministry of Education and Science for the schools and universities; Ministry of Health for the hospitals and polyclinics; Ministry of Culture for the theatres, cinemas and museums and the Ministry of Tourism for hotels, caves, etc.

**Keywords:** Radon concentration, buildings with public access, schools, hospitals, caves, Bulgaria

## Radon risk communication program for buildings with public access

**Nina Chobanova, Jana Djounova, Kremena Ivanova, Bistra Kunovska**

National Centre of Radiobiology and Radiation Protection, Sofia, Bulgaria

Radon risk communication program on the health effects of radon encounters many challenges and requires a variety of risk communication strategies and approaches.

This paper explores the channels used and discusses methods found to be most effective to the general population of radon exposure to different buildings with public access. It was demonstrated that different risk communication channels can be used to raise awareness amongst different stakeholder groups. The valuable lessons learned are discussed.

The radon risk communication program for buildings with public access we developed is based on the following principles: assessment of the public perception of risk, a set of core and understandable risk messages, identification of target audiences, and using comparisons (e.g. lung cancer due to radon compared to lung cancer from other sources) to clarify the risk associated with exposure to radon.

The article presents the main components of radon risk communication based on our experience of a national radon survey in homes, which are: sufficient messages, communication channels and assessing effectiveness. The investigated channels are: publications on websites, poster contests, radon distribution information materials, information day, advertisements on radio, television etc. To assess the effectiveness of raising awareness, we carried out public inquiries of different audiences.

**Keywords:** Radon, general population, building with public access, risk communication

## Influence of humidity on an electrostatic radon monitor with 16.8L volume

Yucai Mao<sup>1</sup>, Yunxiang Wang<sup>1</sup>, Lei Zhang<sup>2</sup>, Qiuju Guo<sup>1</sup>

<sup>1</sup> State Key Laboratory of Nuclear Physics and Technology, School of Physics, Peking University, Beijing, China

<sup>2</sup> State Key Laboratory of NBC Protection for Civilian, Beijing, China

Recently, an electrostatic radon monitor with a 16.8L volume chamber (Sairatec Inc., ARM-Pino1) has been developed. The positive polonium particles, produced by the decay of radon, can be collected on the surface of the detector in an electric field. And then with multi-channel analyzer, a high-sensitivity measurement of radon concentration can be achieved. However, research showed that a fraction of the positive polonium particles could be greatly affected by air humidity, especially for a monitor with a large volume chamber. To deal with this, a humidity-control system based on the Nafion membrane was developed. Through this humidity-controlling system, the influence of humidity on the sensitivity and electrostatic collection efficiency of the 16.8L chamber's radon monitor could be evaluated.

Results show that sensitivity of  $^{218}\text{Po}$  decreases from 9.63 to 2.68 cph/(Bq·m<sup>-3</sup>), and that of  $^{214}\text{Po}$  as well as  $^{218}\text{Po}$  decreases from 20.63 to 7.03 cph/(Bq·m<sup>-3</sup>), when the absolute humidity increases from 0.01 to 4.84 g/m<sup>-3</sup>. And the ratio between the ROI of  $^{214}\text{Po}$  and the ROI of  $^{218}\text{Po}$  increase from 1.14 to 1.62 with the increase of humidity. These results indicated that the effective collection efficiency of  $^{218}\text{Po}$  decreases from 31.86% to 8.86%, with the increase of humidity. The higher humidity, the higher the neutralization, which lead to a less positive  $^{218}\text{Po}$  collected and a lower collection efficiency as a consequence. However, the neutralized  $^{218}\text{Po}$  decay will also produce positive  $^{214}\text{Pb}$  as well as  $^{214}\text{Bi}$ , which then could be also collected on detector. So the higher humidity usually leads to a higher ratio between the ROI of  $^{214}\text{Po}$  and the ROI of  $^{218}\text{Po}$ .

## Determination of relative degassing rate of an extraction membrane based on a radon-in-water source

**Yunxiang Wang<sup>1</sup>, Lei Zhang<sup>2</sup>, Qiuju Guo<sup>1</sup>**

<sup>1</sup> State Key Laboratory of Nuclear Physics and Technology, School of Physics, Peking University, Beijing, China

<sup>2</sup> State Key Laboratory of NBC Protection for Civilian, Beijing, China

Measurement of radon-in-water is of great importance both in radiation protection and as a tracer in many other study fields. There are three commonly used methods for measuring radon in water, which are liquid scintillation counting (LSC), gamma spectroscopy and degassing. Among them, using an extraction membrane is one way to achieve the degassing process, which is simple to operate and suitable for long-term continuous measurement of radon-in-water concentration in situ. Based on the extraction membrane, a radon-in-water measurement system was developed, whose key parameter is the relative degassing rate of extraction membrane. In the present research, the experiment study on the determination of relative degassing rate of an extraction membrane is demonstrated.

A standard radon-in-water sample was made using a small polyethylene packet containing a Ra-226 source. When the source packet was put into the water sample, the radon concentration of water was found to increase linearly with time. The emanation power of the source packet was fitted to be 86.0 %, which can be used to estimate the radon-in-water concentration. When checked with the RAD7 monitor, the radon concentration of water sample can be determined. Based on the radon-in-water sample, combined with the extraction membrane and the RAD7 monitor, a determination system was set up to measure the relative degassing rate of a kind of extraction membrane under different radon-in-water concentrations. The relative degassing rate ranges from 91 % to 110 % and has an average value of  $97.1 \pm 7.3$  %, which shows that the relative degassing rate of an extraction membrane is stable and close to 100%.

## Statistical analysis of naturally occurring predictors affecting radon concentration in indoor air

**Robert Lakatoš<sup>1</sup>, Sofija Forkapić<sup>2</sup>, Selena Samardžić<sup>1</sup>,  
Kristina Bikit-Schroeder<sup>2</sup>, Dušan Mrđa<sup>2</sup>**

<sup>1</sup> Faculty of Technical Sciences, University of Novi Sad, Novi Sad, Serbia

<sup>2</sup> Faculty of Sciences, University of Novi Sad, Novi Sad, Serbia

Radon is a naturally occurring, radioactive noble gas derived from the decay of radium, which is part of the U-238 decay chain. In this investigation, CR-39 (nuclear track detector) was used to determine the yearly concentration of radon gas in indoor air. Soil samples were collected from the surface layer of the soil, close by the investigation room. The collected soil was desiccated and prepared for the spectroscopic (HPGe) and particle size (granulation) analysis. Particle size analysis was performed using MASTERSIZER 2000, a laser diffraction particle size analyser. Activity concentrations of radionuclides in soil were determined by a low-level gamma spectrometry method used on shielded HPGe detectors with maximal background reduction. Data for evaluation were collected over 14 investigation points. For the evaluation of the results, SPSS (Statistical Package for the Social Sciences) statistics were used. In order to predict the Radon-222 activity concentration in indoor air, standard regression analyses were performed with Radium-226 and Uranium-238 activity in soil, whereas the actual concentration of radon in indoor air was measured using RAD7 active device and soil granulation as predictors. From the linear correlation analysis between the average annual radon concentration and the actual radon concentration, it can be seen that they are not in significant correlation ( $p > 0.05$ ). However, the regression analysis shows that the actual indoor radon concentration, along with U-238 and Ra-226 concentrations in soil and the content of clay in soil, are statistically significant predictors for average annual radon concentration, confirming that the model is appropriate for predicting average annual radon concentration ( $p < 0.05$ , adjusted R square 0.684).

**Keywords:** Radon, SPSS, spectroscopy, granulation

## Correlation between indoor radon/thoron activity concentrations and gamma dose rates in Central Kosovo and Metohija

Ljiljana Gulan<sup>1</sup>, Gordana Milić<sup>1</sup>, Zora Zunić<sup>2</sup>, Bajram Jakupi<sup>1</sup>

<sup>1</sup> Faculty of Natural Sciences and Mathematics, University of Priština, Kosovska Mitrovica, Serbia  
<sup>2</sup> Vinča Institute of Nuclear Sciences, University of Belgrade, Belgrade, Serbia

Indoor radon/thoron concentrations and gamma dose rates were measured in thirty houses in rural areas of Central Kosovo and Metohija. The measurements of radon and thoron were conducted using an integral method with SSNTD CR-39 detectors, and gamma dose rates were measured using scintillation probe AUTOMESS, type 6150 AD-6/H. The detectors were placed at the distance of 20 cm from walls and at the height up to 2 m. Gamma dose rate measurements were performed in 3-4 positions in the room at the height of 1 m and then averaged in a single value. The arithmetic means of results were: for radon  $C_{Rn} = 674 \text{ Bq m}^{-3}$  (range from 48 - 1640  $\text{Bq m}^{-3}$ ) and for thoron  $C_{Tn} = 53 \text{ Bq m}^{-3}$  (range from NA - 635  $\text{Bq m}^{-3}$ ). The mean value of gamma dose rates in the measured interval from 95 - 268  $\text{nSv h}^{-1}$  was 131  $\text{nSv h}^{-1}$ . The Pearson coefficient of correlation between radon concentrations and gamma dose rates,  $r = -0.16$  indicates a negligible correlation, while the Pearson coefficient of correlation between thoron concentrations and gamma dose rates,  $r = 0.69$  denotes a moderate positive correlation.

## Case study of indoor radon measurements in one building

**Ljiljana Gulan, Gordana Milić, Biljana Vučković,  
Jelena Živković Radovanović, Boris Drobac**

Faculty of Natural Sciences and Mathematics, University of Priština, Kosovska Mitrovica, Serbia

This study was performed in order to get preliminary information of indoor radon concentrations inside an occupational building. Measurements were conducted in four basement workrooms with radon detector Airthings Corentium Home using the alpha spectrometric measuring method. The results of a short-term radon concentration (averaged from hour to hour), as well as long-term measurements (averaged daily) were read out every second day at the same time during one month. The detectors showed first results of measurements after 24 hours. The values of long-term indoor radon measurements in four workrooms were: 228 Bq/m<sup>3</sup>, 93 Bq/m<sup>3</sup>, 358 Bq/m<sup>3</sup> and 68 Bq/m<sup>3</sup>, while the values of short-term measurements spanned from: (113-326) Bq/m<sup>3</sup>, (46-191) Bq/m<sup>3</sup>, (315-634) Bq/m<sup>3</sup> and (21-105) Bq/m<sup>3</sup>, respectively. Besides radon potential (geology, permeability, local anomalies) and the quality of used construction materials, the noticeable differences in indoor radon concentration within the building are influenced primarily by different types of flooring. This includes various types of isolation from the ground: wooden floor, laminate, ceramic and vinyl tiles. We point out that ceramic tiles are a more efficient way for radon protection (stop the entering and accumulation in indoor space) than other types of flooring.

**PUBLISHER:** RAD Centre, Niš, Serbia  
Bulevar Nikole Tesle 17/12, 18000 Niš, Serbia  
[www.rad-centre.org](http://www.rad-centre.org)

**FOR THE PUBLISHER:** Prof. Dr. Goran Ristić

**YEAR OF PUBLISHING:** 2019

**EDITOR:** Prof. Dr. Goran Ristić

**COVER DESIGN:** Vladan Nikolić, PhD

**TECHNICAL EDITING:** Saša Trenčić, MA

**PROOF-READING:** Saša Trenčić, MA and Mila Trenčić, MA

**CD BURNING AND COPYING:** RAD Centre, Niš, Serbia

**PRINT RUN:** Electronic edition - 350 CDs (CD-R)

**ISBN:** 978-86-901150-0-6

The Seventh International Conference on Radiation in Various Fields of Research (RAD 2019) was financially supported by the Central European Initiative (CEI).

CIP - Каталогизacija y publikaciji  
Narodna biblioteka Srbije, Beograd

539.16(048)(0.034.2)  
57+61(048)(0.034.2)

**INTERNATIONAL Conference on Radiation in Various Fields of Research (7 ; 2019 ; Herceg Novi)**

Book of abstracts [Elektronski izvor] / Seventh International Conference on Radiation in Various Fields of Research, RAD 7, [RAD 2019], 10-14.06.2019 Herceg Novi, Montenegro ; [editor Goran Ristić]. - Niš : RAD Centre, 2019 (Niš : RAD Centre). - 1 elektronski optički disk (CD-ROM) ; 12 cm

Sistemski zahtevi: Nisu navedeni. - Nasl. sa naslovne strane dokumenta. - Tiraž 350.

ISBN 978-86-901150-0-6

a) Јонизујуће зрачење -- Дозиметрија -- Апстракти б) Биомедицина – Апстракти

COBISS.SR-ID 277775116



[rad-conference.org](http://rad-conference.org)

Silver sponsors



[www.ortec-online.com](http://www.ortec-online.com)



[www.h3dgamma.com](http://www.h3dgamma.com)